

# Contents

## **Welcome Lettet**

## **16<sup>th</sup> International Flight Inspection Symposium Agenda**

### **Certification of FIS**

Aspects Affecting Measurement Uncertainty of Flight Inspection Systems.....	1
A Suitable Quality Management System for Flight Inspection.....	5
Timing Synchronization and Uncertainty in Flight Inspection Systems.....	9
Results of Experiments of the R&S Receiver EVS 300 for VOR and ILS Flight Inspection.....	15
The Uncertainty Evaluation of Flight Calibration Parameters.....	27

### **Data Management**

Data Management.....	33
Ai-Sky.....	39
Integrity of Flight Inspection Data.....	53

### **GNSS**

Analysis on Flight Test Results of GBAS in China.....	67
Space Weather: It's Effect on GNSS, DGNSS, SBAS, and Flight Inspection.....	71
Study on flight inspection methods for GBAS.....	81
Flight Inspection of Performance Based Navigation Instrument Flight Procedure "A La Francaise".....	87

### **Flight Inspection Techniques**

Calibrating DME Coverage Predictions with Flight Inspection Measurements.....	105
Latest Achievements of Complex System Simulations for ATC-systems.....	117
On Robust Computation of Reference Datum Height.....	127
PC Based Simulation Tool to Evaluate Airfield lighting Systems.....	133
The investigation of the influence of snow upon Glide Slope.....	159
The Analysis and Solutions about GP Structure Problem in Flight Inspection on High Elevation Plateau Airports.....	169
Flight Inspecting Ground Based Augmentation Systems (GBAS).....	177
Current Issues in Flight Inspection Measurements.....	183
Portable Calibration System for Air Traffic Control Surveillance Radar.....	193
Method of Signal Assessment and Flight Inspection for DME/DME RNAV.....	199

### **Radio Frequency Interference**

Investigation of Terminal Area Distance Measuring Equipment Signal Interference.....	207
Airborne RFI Detection For China Civil Aviation(CFI).....	227

# Contents

How to make the airborne detection of RFI more efficient and more accurate.....231

## **Product Information**

Flight Validation Data Gathering and Evaluation Capabilities.....237

QA Document 9906, Volume 5, Flight Validation of Instrument Flight Procedures.....247

Flight Validation of Performance Based Navigation (PBN) Procedures.....261

Measurement sampling rates based on aircraft speed to accurately measure and  
characterize the guidance quality.....269

## **Expanded Role of Flight Inspection**

Improving Flight Inspection by process automation.....273

Necessities for Flight Inspecting ADS-B Signals.....281

ADS-B data evaluation supported by the flight tests in western China.....287

## **Operational Issues**

The Research of How to Reduce the Collision between Inspection Flight and  
Transportation Flight at the Busiest Airports.....291

Field Strength Versus Signal Strength.....295

How to save time and money on ILS Flight Inspection by using correct methods and input data.....303

Being Intolerant of Tolerances.....309

*16<sup>th</sup> International Flight Inspection Symposium  
Beijing, China  
21 – 25 June 2010*

“IMPROVING FLIGHT INSPECTION FOR NEXT-GENERATION TECHNOLOGY”

---

**OUTCOME OF SEMINAR  
ON TESTING OF NAVIGATION AND SURVEILLANCE FACILITIES  
AND VALIDATION OF FLIGHT PROCEDURES**

(Provided by the ICAO Asia and Pacific Office)

**SUMMARY**

A Seminar on the Testing of Navigation and Surveillance Facilities and Validation of Flight Procedures was organized by the ICAO Asia/Pacific Office held in Bangkok, Thailand from 5 to 7 August 2009. The Seminar was addressed by the leading global experts in the field. Recommendations developed by the Seminar were presented to the twentieth meeting of the Asia/Pacific Air Navigation Planning and Implementation Regional Group (APANPIRG/20) held in September 2009. They were also initially reviewed by the ICAO Navigation Surveillance Panel working group held in end of May 2010. This paper briefly reports on the outcome of the seminar and the actions taken by APANPIRG and Conventional NavAids and Testing Sub-Group (CNTSG) of ICAO Navigation System Panel (NSP).

**1. INTRODUCTION**

1.1 It is essential that the radio navigation aids are flight checked at prescribed intervals to meet the requirements of ICAO SARPs. Appendix Q of Resolution A36-13 adopted by 36th session of ICAO Assembly in 2007 emphasized that ‘... radio navigation aids shall be checked through regular flight testing.

1.2 In response to APANPIRG Conclusion 19/32, a Seminar on *Testing of Navigation and Surveillance Facilities and Validation of Flight Procedures*, was jointly organized by ICAO Asia/Pacific Regional Office and Aeronautical Radio of Thailand (AEROTHAI) in Bangkok, Thailand from 5 to 7 August 2009.

1.3 The Seminar was attended by 85 participants from 17 Administrations, ICASC, IFALPA and industry partners. Seminar discussed various issues related to the testing of navigation/surveillance facilities and validation of flight procedures.

1.4 Mr. Glenn Bissonnette, from flight Inspection Policy department, FAA & Executive Secretariat, ICASC and Mr. Gordon Young, GBAS Project Manager, Airservices Australia were the facilitators of the Seminar.

1.5 The presentations and papers for the Seminar and the summary report of Seminar is available at the following ICAO APAC website:

<http://www.icao.or.th/meetings/2009/nsfvfp/index.html>

## 2. DISCUSSIONS

2.1 Following Agenda Items were taken up for discussion during the seminar:

- 1) Performance Based Navigation (PBN) procedures: Flight procedure validation, database design, integrity, distribution, in-flight data recording and data sharing.
- 2) Ground and Air Calibration:
  - a) Ground maintenance of Conventional Navigation/Surveillance Systems: Evolution of maintenance techniques, remote maintenance, maintenance of records, protection areas (ILS).
  - b) Flight Inspection of Conventional Navigation Aids: evolution of flight calibration systems and techniques, data recording and maintenance.
  - c) Nav aids, SSR, Multilateration: performance monitoring and commissioning practices.
- 3) Change in ICAO Provision: New inclusions in Annex 10 and Doc 8071.
- 4) Satellite based systems: Maintenance, calibration and flight validation of GNSS systems (GBAS & SBAS), performance monitoring and data recording for investigation.
- 5) Regulator's Perspective: Regulators' role in validation/testing of navigation and surveillance systems.

2.2 Seminar was addressed by leading global experts in the field. In all 27 presentations were made and 2 Working Papers were presented to the Seminar. A visit to the Flight Calibration facilities of Aeronautical Radio of Thailand was organized during the seminar.

2.3 Recommendations made by the Seminar for the consideration of APANPIRG and the APANPIRG outcomes on the recommendations are provided as below. The result of initial review by CNTSG/NSP at its recent meeting held in May 2010 is also highlighted in the following paragraphs.

- 1) That, APANPIRG carries out a study to assess whether there is a need to develop guidance material for flight inspection/validation of ADS-B ground stations noting that ICASC technical group concluded that flight inspection of ADS-B is currently limited to coverage.

After a brief discussion on the issue, APANPIRG, through its Decision 20/47 tasked the ADS-B SITF with the study to assess the need for developing guidance material for flight inspection/validation of ADS-B ground station.

The Ninth Meeting of ADS-B Study and Implementation Task Force meeting scheduled to be held in Jakarta from 18-19<sup>th</sup> August 2010 will review this task and take necessary follow up actions.

- 2) That, ICAO – Navigation System Panel (NSP)
  - a) Consider developing guidance material on the use of DGPS as a position reference system for flight inspection Through its Conclusion 20/48 (a), APANPIRG invited ICAO to carry out a study to assess the use of DGPS as a positioning reference system for flight

inspection. The issue has since been taken up with ICAO HQ in October 2009. This issue was discussed in the ICAO Navigation Systems Panel (NSP) Working Group of the Whole Meeting held in Montreal from 17 to 28 May 2010 and the Conventional NavAids and Testing Sub-Group.

**- (CNTSG) meeting and it was decided that material on the use of GNSS for flight inspection will be considered in the next meeting of CNTSG scheduled in November 2010.**

- b) Review those areas of possible misinterpretations in ICAO Doc 8071 such as the ones shown in the Appendix A to the Seminar summary report and provide necessary guidance on the interpretation of the ICAO requirements in order to avoid inconsistency of interpretations and to harmonize application of ICAO standards and recommended practices.

**- CNTSG/NSP, while discussing the quoted possible misinterpretations, was of the view that for some of these observations, there was no scope for misinterpretation. For other cases, rectification action has already been taken but the amendments are yet to be published.**

- c) Review information on flight validation as contained in ICAO Doc 8071 Vol. II when the new Doc 9906 Vol. V becomes operational.

Through its Conclusion 20/48(d), APANPIRG invited ICAO to review information on flight validation as contained in ICAO Doc 8071 Vol. II consequent to new Doc 9906 Vol. V becoming applicable. Following the prescribed procedure, the issue was taken up with ICAO HQ through an Issue Form in October 2009.

**- On this issue, CNTSG/NSP agreed that the Group was working with the Secretariat to remove the overlap within the documents.**

- 3) That, ICAO coordinate for developing a template for flight validation report for PBN IFPs including RNP APCH procedures noting that ICASC is working on this to be included in the Flight Validation guidance manual (proposed Doc 9906 Vol. V). A sample template developed by Aerothai is available as Appendix B to the summary report of the seminar.

APANPIRG agreed with the recommendation and invited ICAO to develop templates for flight validation reports for PBN IFPs including RNP APCH procedures. An Issue Form, based on the Conclusion adopted was raised with ICAO HQ in October 2009.

**- CNTSG/NSP proposed that Flight Validation was to be removed from Doc 8071 and transferred to IFPP management. This proposal, hence was considered appropriate for the IFPP.**

- 4) That, States be urged to update the information in the Flight Inspection Catalogue and the new edition of the Catalogue be published by end of October 2009.

**- Updated Catalogue of Flight Inspection Units Asia and Pacific Regions was published in October 2009 as the Ninth Edition**

- 5) That, States be reminded of the contents of State Letter of ILS maintenance procedure as contained in Appendix C to the Summary Report of the Seminar.

APANPIRG, through its Conclusion 20/49 (a) reminded the States about the contents of State Letter AN 7/5-01/52 dated 11 May 2001 on ILS maintenance procedures. A State Letter dated 5 November 2009 was issued to this effect.

- 6) That, States consider to upgrade their FIS to include the flight inspection requirements of GNSS, Interference, ADS-B, Multi-lateration etc. as necessary.  
**- States were urged to consider upgrading their FIS to include the flight inspection requirements recommended through APANPIRG Conclusion 20/49 (c). State Letter dated 5 November 2009 was issued on the subject.**
- 7) That, ICAO be invited to provide guidelines for selecting GP reference point for flight inspection.

APANPIRG agreed with the recommendation and adopted Conclusion 20/48 (b) on this issue. Through an Issue form, the issue was taken up with ICAO HQ in October 2009. This issue was taken up for discussion in the NSP meeting held in May 2010 and

**- It was agreed that this is basically a measurement issue appropriate to Doc 8071 and it does not require any action within Annex 10. The issue is going to be discussed in the future NSP meetings.**

2.4 In Conclusion, the participants while appreciating the format and coverage of the seminar, called upon ICAO to organize similar seminars in future to encourage exchange of information on the subjects of testing of navigation/surveillance systems and validation of procedures. The Seminar thanked the presenters and appreciated the arrangements made by ICAO and AEROTHAI, the host for the seminar.

### **3. Action Recommended**

3.1 The participants at 16<sup>th</sup> International Flight Inspection Symposium are invited to note the outcome of the Seminar and the actions taken on those recommendations by the APANPIRG and follow-up action taken by the Conventional Nav aids and Testing Sub-Group (CNTSG)/ Navigation System Panel Working Group meeting held in Montreal from 17 to 28 May 2010.

-----

# Aspects Affecting Measurement Uncertainty of Flight Inspection Systems

## **Peter Thirkettle**

(On behalf of the ICASC)  
Navigation Specialist

Safety Regulation Group  
United Kingdom Civil Aviation Authority  
Aviation House  
Gatwick Airport South  
West Sussex  
RH6 0YR  
England

e-mail: [peter.thirkettle@caa.co.uk](mailto:peter.thirkettle@caa.co.uk)

Telephone: +441293768820

Fax: +441293573974

## **ABSTRACT**

Feedback received by the International Committee for Airspace Standards and Calibration (ICASC) from delegates at previous International Flight Inspection Symposiums, indicated that the flight inspection industry would like guidance on the certification of flight inspection systems. The Technical Group of the ICASC were tasked with providing the guidance on that subject. It soon became evident to the group that there are no recognised international standards or processes for the certification of flight inspection systems.

The only internationally recognised material applicable to flight inspection systems which could be considered a standard is the measurement uncertainty limits published in ICAO Doc 8071 'Manual of Testing Radio Navigation Aids' Volume 1 'Testing of Ground-Based Radio Navigation Systems'. [1] The Technical Group decided to scope the guidance material to only consider measurement uncertainty at this time.

## **PURPOSE**

This paper provides a report on the development of the ICASC guidance material on the "Aspects Affecting Measurement Uncertainty of Flight Inspection Systems". The guidance material is still being developed by the technical group and once it is mature it will be published on the ICASC website. The material presented in this paper is preliminary and may not represent the final content of the guidance material.

## **INTRODUCTION**

Flight inspection systems and aircraft used for flight inspection differ to varying degrees, however the parameters that need to be measured are generally the same. These parameters are typically those detailed in the various tables of ICAO Doc 8071. Each of the parameters detailed in Doc 8071 has an associated measurement uncertainty which needs to be demonstrated to be complied with to achieve correctly specified flight inspection results.

## **APPLICABILITY OF GUIDANCE MATERIAL**

The guidance material is intended for Regulators, Flight Inspection Organisations and Manufacturers to assist in understanding the aspects that can affect the measurement uncertainty of flight inspection systems.

## **SCOPE OF GUIDANCE MATERIAL**

The guidance material will discuss known aspects that may affect the measurement uncertainty of flight inspection systems.

The group also identified that configuration control is also important when stating that a flight inspection system is and remains compliant with the ICAO Doc 8071

measurement uncertainty limits. As such a discussion on configuration control will be included in the guidance material.

## **FORMAT OF GUIDANCE MATERIAL**

The Technical Group wanted the guidance material to follow a consistent format for each of the aspects identified. Firstly the aspect needed to be adequately defined so that all parties know exactly what is being considered.

The effect on the measurement uncertainty was then specified for each aspect.

The causes of the effect were then identified and discussed.

Finally, guidance is provided on possible solutions that either reduces the uncertainty or controls it within the limits prescribed in ICAO Doc 8071.

## **WHAT IS MEASUREMENT UNCERTAINTY**

Whenever you make a measurement there is always a doubt as to the value of the result. This doubt is what is termed as uncertainty.

A measurement uncertainty limit provides the dispersion of a measurement. This means that the value actually measured is highly likely to be within the measurement uncertainty limits.

## **MANAGING THE MEASUREMENT UNCERTAINTY BUDGET**

ICAO Doc 8071 provides uncertainty limits that need to be satisfied for each of the parameters that need to be measured by flight inspection. A flight inspection system can be designed to meet this value or efforts can be made to reduce the uncertainty to a level as low as possible.

The measurement uncertainty evaluation for flight inspection systems usually considers the errors of any contributing part. Where these errors are systematic it is possible to calibrate that part and as such reduce the contribution to the

uncertainty budget down to that of the calibrating test equipment.

Whilst it is normally good practice to reduce systematic errors through calibration when making any type of measurement, it is not always necessary for a system where an allowable budget is available and no real benefit is achieved by making such a reduction.

Whilst it is not always necessary to reduce the systematic errors it is necessary to know what they are, how they manifest themselves and how they contribute to the uncertainty budget. This may result in conditions where a contribution is acceptable or unacceptable depending upon conditions of the measurement. For example a receiver output may be acceptable at a temperature of 20°C but unacceptable at 21°C. A simple solution here would be to stop using the system at 21°C. Whilst this is an acceptable approach it may restrict the efficiency of the flight inspection.

## **CONTENT OF GUIDANCE MATERIAL**

The following provides a list of aspects that are currently being considered in the guidance material. Work is ongoing to identify and provide guidance on other aspects.

- Lever Arms
- Antenna Radiation Patterns
- Frequency Response
- Positioning (Surveying)
  - Aircraft Antennas
  - Ground equipment
- Time synchronisation
- Aircraft positioning (e.g. Flight guidance for measurement)
- Stability with temperature
- Cable Loss



The text below provides examples of the guidance material:

## **Antenna Radiation Patterns**

### **Definition**

Antenna performance when the aircraft is yawed or pitched.

### **Effect**

Systematic signal strength errors depending upon the amount of yaw or pitch of the aircraft.

### **Cause**

The receiving antenna radiation pattern is rarely uniform around the full 360 degrees. The measurement of the signal in space will be in a direct line between the ground antenna and the aircraft antenna. The signal in space will intersect the aircraft antenna depending upon the orientation of the aircraft. So the signal in space will be affected by different gain or loss depending upon where the signal in space intersects the aircraft antenna.

### **Error Reduction**

Errors can be compensated for by the flight inspection system if the antenna radiation pattern (which in theory is a calibration of the antenna) and the aircraft yaw and pitch are known. This compensation can be implemented by the use of look up tables in the flight inspection system.

The use of look up tables would not completely remove the uncertainty but may reduce it to an acceptable level. As with any measurement there remains an uncertainty, for example the following may still need to be considered:

- Resolution of the look up table
- Test equipment used for calibration
- Device used to measure pitch and yaw

### **Error Management**

It is possible that the errors from the radiation pattern are within the required measurement uncertainty value. As such the largest error from the radiation pattern

would need to be considered in the measurement uncertainty evaluation.

It is often the case that the error in certain parts of the pattern are larger than the required measurement uncertainty value. In this case it may be necessary to prevent the use of the results depending upon the amount of yaw or pitch. This may be through operating procedures, such as a setting a cross wind limit.

## **Stability With Temperature**

### **Definition**

Flight inspection system performance over a given temperature range.

### **Effect**

Systematic signal strength and / or DDM errors with different temperatures.

### **Cause**

The effects of errors with temperature on signal strength and DDM are normally associated with the analogue parts of the system. The processing stage may be affected by temperature, however as this is normally digital the effect would generally be loss of data rather than incorrect results.

Most analogue systems are designed to operate over a given temperature range. It is common in flight inspection systems to use modified commercial off the shelf receivers. The acceptable temperature range for navigation purposes of a commercial off the shelf receiver can be quite wide, however the output may not be sufficiently accurate for making flight inspection measurements over that same temperature range.

The temperature within an aircraft can vary significantly and over short periods of time depending upon the operating environments. e.g. Altitude, Location etc. This temperature change in the aircraft may affect the receiver temperature.

### **Error Reduction**

Errors can be compensated for by the flight inspection system if the receiver performance is established over a given

temperature range and the temperature of the receiver in the operational environment is known. This can be achieved by establishing a calibration graph for the receiver for different temperatures and by using temperature monitoring in the flight inspection system. One way of establishing a calibration graph for different temperatures is by performing the calibration in a temperature chamber.

Compensation can be implemented by the use of look up tables in the flight inspection system.

The use of look up table would not completely remove the uncertainty but may reduce it to an acceptable level. As with any measurement there remains an uncertainty, for example the following may still need to be considered:

- Resolution of the look up table
- Test equipment used for calibration
- Error and resolution of temperature monitoring device.

### ***Error Management***

The errors from the temperature graph may show that the measurement uncertainty value requirement is met. If this is the case then no compensation needs to be implemented within the Flight inspection System. The maximum error from the graph would need to be used in the measurement uncertainty evaluation.

It is possible that the equipment performs within the uncertainty limits in certain temperature ranges. In this case it would be necessary to limit the temperature range for which the receiver can be used to collect results. This may be implemented through operating procedures and / or temperature monitoring.

### **FURTHER WORK**

During the development of the measurement uncertainty paper several aspects were identified that may influence the quality of the results. Work has already started in developing similar guidance for the industry, this will also be published on the ICASC website. These aspects include:

- Propeller Modulation
- Filtering
- Field Strength in the Low frequency band
- Antenna Grounding and Bonding
- Algorithms
- Field Strength to Received Signal Level Conversion
- NDB Quadrature Error
- Dual sensor – comparison , voting , averaging

### **REFERENCES**

- [1] ICAO Doc 8071 - Manual on Testing of Radio Navigation Aids, Volume 1 - Testing of Ground Based Radio Navigation Systems

# A Suitable Quality Management System for Flight Inspection

## Introduction about ISO/IEC FDIS 17025---General Requirements for Competence of Testing and Calibration Laboratories

### Ms. Su Fenglan

Deputy Director  
Flight Inspection Center of CAAC  
23#, Tianzhu Road,  
Tianzhu Airport Industry Zone,  
Capital International Airport,  
Beijing,  
People's Republic of China  
E-mail: [Suf1@chinacfi.net](mailto:Suf1@chinacfi.net)



### Mr. Liu Tong

Deputy Director  
Development & Research  
Department  
Flight Inspection Center of CAAC  
23#, Tianzhu Road,  
Tianzhu Airport Industry Zone,  
Capital International Airport,  
Beijing,  
People's Republic of China  
E-mail: [ltzhsm@sina.com](mailto:ltzhsm@sina.com)



ensure the flight inspection quality.

Having consulted many quality management advisory service agency, we finally focused on the ISO/IEC 17025 system, which operated and managed in China by China National Accreditation Service for Conformity Assessment (CNAS).

### What is ISO/IEC 17025?

ISO ---the International Organization for Standardization

IEC---the International Electrotechnical Commission

**ISO/IEC 17025** is the main standard used by testing and calibration laboratories. Originally known as ISO/IEC Guide 25, ISO/IEC 17025 was initially issued by the International Organization for Standardization in 1999. There are many commonalities with the ISO 9000 standard, but ISO/IEC 17025 adds in the concept of competence to the equation. And it applies directly to those organizations that produce testing and calibration results. Since its initial release, a second release was made in 2005 after it was agreed that it needed to have its quality system words more closely aligned with the 2000 version of ISO 9001.

The standard was first published in 2001 and on 12 May 2005 the alignment work of the ISO committee responsible for it was completed with the issuance of the revised standard. The most significant changes introduced greater emphasis on the responsibilities of senior management, and explicit requirements for continual improvement of the management system itself, and particularly, communication with the customer

ISO/IEC 17025:2005 specifies the general requirements for the competence to carry out tests and/or calibrations. It covers testing and calibration performed using standard methods, non-standard methods, and laboratory-developed methods.

It is applicable to all organizations performing tests and/or calibrations.

### ABSTRACT

ISO/IEC 17025 Quality Management System has been widely applied in testing and calibration laboratories of various industries instead of ISO 9000 series for its virtue of detail technical requirements. This paper will describes how Flight Inspection Center of CAAC introduced ISO/IEC 17025 into its quality managements based on our experience and what benefits we have gotten from this effort.

### BACKGROUND

Being an important link, the purpose of flight inspection is to ensure flight safety. However, the quality of flight inspection is the most important base to realize this purpose.

With the rapid development of Flight Inspection Center of CAAC, we recognized a quality control system should be employed for such a large flight inspection institute, to

It separates all the requirements into two sections:  
Management Requirements  
Technical requirements

Management Requirements is very similar with ISO 9001 requirements, shown as following:

- Organization and management
- Quality system
- Document control
- Review of requests, tenders and contracts
- Sub-contracting of tests and calibrations
- Purchasing services and supplies
- Service to the client
- Complaints
- Control of nonconforming testing and/or calibration work
- Corrective action
- Preventive action
- Control of records
- Internal audits
- Management reviews

In addition to the management requirements, ISO/IEC specially established a set of requirements for technical to make quality control infiltrated into technical details. They include:

- General
- Personnel
- Accommodation and environmental conditions
- Test and calibration methods and method validation
- Equipment
- Measurement traceability
- Sampling
- Handling of test and calibration items
- Assuring the quality of test and calibration results
- Reporting the results

As every flight inspection technician knows, the activities of flight inspection is full of testing and calibrations, furthermore, some of flight inspection organizations directly named flight inspection as Flight Calibration. According to ICAO Document 8071 and Annex 10, all the flight inspection receivers/transceivers need to be calibrated in order to provide the accurate performance. We can give a name here to these activities ground calibration. And during the flight inspection, some of operations, such as LOC alignment inspection, can be considered as one kind of calibration while the ground facilities or signals can be considered as instruments or standard reference for normal flights, we can call them flight calibrations, and some other operations, such as identification check, can be thought as flight testing. In general, with the above features, flight inspection is fully a kind of laboratory activity.

To a technical industry as flight inspection, the detail technical management is more important for quality, and it can be provided by ISO/IEC 17025. It is just because of this reason that China Civil Aviation Flight Inspection Center decided to introduce ISO/IEC 17025 into the flight inspection as our quality management system Hereinafter we will introduce what we had benefited from experience of ISO/IEC 17025 management.

### Personnel

The laboratory management shall ensure the competence of all who operate specific equipment, perform tests and/or calibrations, evaluate results and sign test reports and calibration certificates.

According to this requirement, we redefined and refined our certification levels together their training program, certification procedures and conditions based on this requirement. The levels including:

- flight inspection trainee  
the one who is undergoing indoor training and simulation training
- assistant flight inspector  
the one who is in the period of actual flight inspection practice. The inspection system operation by assistant flight inspector should be supervised by an inspection instructor
- flight inspector  
the one who can independently operate flight inspection system and evaluate results
- authorized inspector  
the one who is certificated to give conclusion of flight inspection and sign the flight inspection report
- inspection instructor  
the one who can teach flight inspection lessons and give training to inspection trainee or instruct and supervise the operation of assistant inspector.

The required conditions and certificate standards are also defined in training course program and certification regulations

In order to make the technical personnel training systematized, BFIC created a dedicated section named Training Section in Safety & Technique Department last year, being responsible for all the technical trainings. Meantime, personnel technique management system including certificate management is also set up to improve the quality and skills of flight inspectors.

Besides inspector certificates, in other technical areas, such as system calibration and maintenance, the personnel performing these works is also required hold relevant certificate.

### Test and calibration methods and method validation

Most of the flight inspection institutions normally choose ICAO standards or FAA standards for their flight

inspection operation. But neither of these two standards can provide all detail instructions for every segment of flight inspection operations. So the inspection institutions should establish many detail inspection methods by themselves upon the understanding of ICAO or FAA standard. During the applying of ISO/IEC 17025, we reviewed all of our flight inspection methods, to find out existing references from ICAO or FAA documents, set up some of detail instructions for undefined area based on the detail conditions of China through issuing Technical Notices. Certainly, to ensure the scientificity and rationality and avoid mistakes, before any method being put in use, it should be analyzed and evaluated by specialist group, fully discussed and proved by Flight Inspection Technical Management Committee of BFIC following approving procedures.

Since there are many flight inspection methods for different facilities and different profiles, if more than one effective method can be used for same profiles, it will bring out different results, furthermore lead to bad quality of inspection. So a methods document management system have been created to ensure the uniqueness and validity of flight inspection methods.

Figure 1 shows the inspection flight procedures manuals of BFIC

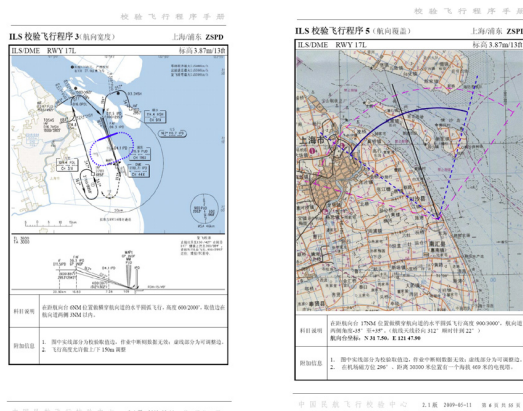


Figure 1 Inspection flight procedures manual example

### calibration items and testing items

ISO/IEC 17025 defined all laboratories into two basic types: calibration laboratory and testing laboratory. After discussing with ISO/IEC 17025 certification specialists, both sides reached a consensus that flight inspection is a kind of special comprehensive laboratorial activity since it includes both calibration and testing.

Based on above acknowledge, we separated all the flight inspection items into two parts: calibration items and testing items.

Calibration items are normally defined for those which need quantitative adjustment on inspected facility for optimization and balance of system based on inspection

results data.

Testing items are normally defined for those which do not need quantitative adjustment on inspected facility.

For example, items such as localizer alignment and path angle are defined as calibration items, which require adjustment if they are out of some allowed range even the value measured is in tolerance, however, the items such as polarization and identification are testing items which need only to check whether they are satisfied or in tolerance.

We also defined some interesting items as both calibration and testing item, such as the VOR bearing error and modulations which is also coincident with a hot topic in recent. During the calibration orbit check and reference radial check, as bearing error and modulations are defined as calibration items in these profiles, we normally require the facility maintenance make adjustment for optimizing the bearing error and modulations of the signals in space, and a stricter tolerance have to be applied to this item. But for airway radials and approach radials check, as the same signal parameters are defined as testing items, no adjustment will be made on facility even there is some places out of tolerance, instead, the segments of out of tolerance will be restricted.

### Estimation of uncertainty of measurement

A calibration laboratory or a testing laboratory performing its own calibrations, shall have and apply a procedure to estimate the uncertainty of measurement for all calibrations and types of calibrations. For a very long time, we haven't attached great importance to measurement uncertainty of our flight inspection systems. And now, with the knowing about ISO/IEC 17025, we realized how important this effort is.

We have separated our flight inspection items into two groups, calibration items which includes all the items needed facility adjustment and optimization, such as LOC course alignment, VOR alignment orbit, and inspection system calibrations; testing items which normally needn't make any farther optimization, such as identification check, enroute coverage.

During the estimation of measurement uncertainty, we compared the uncertainties we got based on tests and analysis with the uncertainty requirements in ICAO Doc 8071, and found that some of them even larger than ICAO standards, especially NAV receiver signal strength. The inbound signal strength is normally stronger than outbound, meanwhile, different AGC losses could be found corresponding to all different bearings relative to aircraft heading. After investigation, a conclusion about large uncertainty of NAV SS is that the different AGC losses is common for all inspection aircrafts, the reason of that is because aircraft body effect and antenna polar diagram variations. Additionally, the antenna feeder losses can also lead to AGC differences between different

inspection aircrafts.

In order to confirm the uncertainties fulfil the ICAO standards, we required the manufactory of flight inspection system provide enough information including data and polar variation diagram as well as compensation measures. Recently, all the data survey and compensation work has been done, the latest tests were shown that all the uncertainties of our systems have been fully fulfil ICAO standards.

From the estimation process of measurement uncertainty itself, we also make ourselves more clear about all the components of uncertainty which can affect flight inspection results, and of which, who is the main factor, with this benefit, it is easier for us to analyze inspection problems and deal with them.

### Measurement traceability

According to ISO/IEC 17025, all equipment used for tests and/or calibrations shall be calibrated before being put into service. From this viewpoint, flight inspection systems need much more accurate calibration based on accurate signal generator. Before applying of ISO/IEC 17025, as the accuracy foundation of flight inspection systems, some of our signal generator being used for inspection system calibration, had been sent to some calibration service center which we hadn't noticed neither their qualification, nor their calibration uncertainties of parameters. In theory, this could cause a big error and make inspection results unreal when all bad factors from various cycles were put together.

Learning from ISO IEC 17025, we recognized the importance of measurement traceability of flight inspection, and reset up our traceability system more clearly and directly to an authoritative institution. See figure 2.

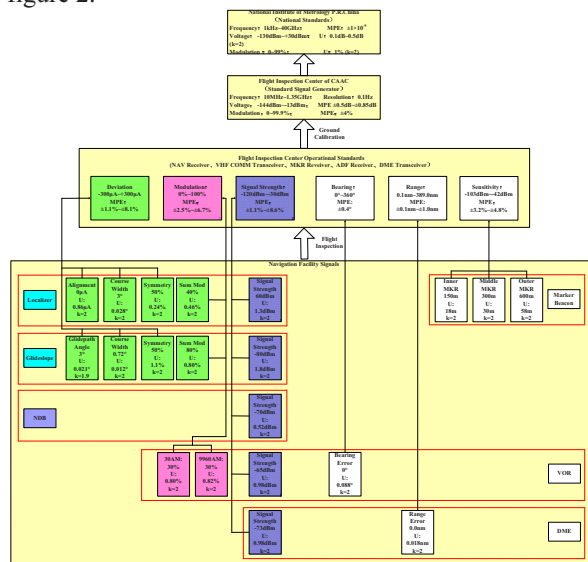


Figure 2 Traceability system flow diagram

### Assuring the quality of test and calibration results

The laboratory shall have quality control procedures for monitoring the validity of tests and calibrations undertaken. The resulting data shall be recorded in such a way that trends are detectable and, where practicable, statistical techniques shall be applied to the reviewing of the results. This monitoring can be planned and reviewed by participation in inter-laboratory comparison or proficiency testing programmes.

Generally, if ISO/IEC 17025 had been widely accepted by flight inspection domain as a standard quality control system, the inter-laboratory comparison should choose a relatively stable and comprehensive inspected object to carry out comparison, the purpose of it is to ensure the consistency of the results in the flight inspections which are carried out by different flight inspection organizations, make all the flight inspection organizations that participate in the comparison know their own accuracy status, and make the outliers timely find the trends that possibly exist and will lead to inaccuracy, so as to timely analyzes the reasons and carry out compensation.

Up to now, since BFIC is the only institution in flight inspection institution has passed qualification of ISO/IEC 17025 in the world, consequently, it is obviously not the best time for inter-laboratory comparison under such a condition as only one flight inspection institution existed. In this case, we also expect there would be more flight inspection institutions or organizations applying for and passing the qualification of ISO/IEC 17025, thereby maintaining the accuracy of flight inspection better and ensuring the quality of flight inspection.

Based on the existing conditions, BFIC decided to try its best to implement the inter-laboratory comparison. We carried out comparison for each inspection parameters between flight inspection aircrafts through test flights, in order to timely judge whether a outlier occurred and do our best to keep stable flight inspection accuracy.

### REFERENCES

ISO/IEC 17025:2005 -- General requirements for the competence of testing and calibration laboratories

ICAO Doc 8071

## Timing Synchronization and Uncertainty in Flight Inspection Systems

Title: Timing Synchronization and Uncertainty in Flight Inspection Systems

Author: Larry Brady, Airfield Technology, Inc. USA

---

### INTRODUCTION

Modern flight inspection systems use automated methods of collecting real time data from various sources. If all data are not satisfactorily synchronized, errors can occur which will contribute to the system measurement uncertainty. This paper describes some potential causes and effects of timing synchronization errors and methods to reduce and mitigate these errors.

### SCOPE

In FIS design, the effects of latency must be considered and eliminated in order to achieve time correlation of the position data and real-time parameters (from the avionics sensors). This is particularly critical in the evaluation of ILS structure and especially for the glidepath.

The use of GPS/DGPS<sup>1</sup> as the position reference for flight inspection has become commonplace throughout the world. In terms of accuracy, reliability and availability, GPS is much better for flight inspection than other methods including position-updated AHRS/INS<sup>2</sup>, laser trackers, or the ubiquitous theodolite. This paper focuses on timing synchronization in a flight inspection system which uses GPS as a position reference.

When using GPS as a position reference for flight inspection, a method is required to synchronize the GPS position data with the data from the other sensors in the Flight Inspection System (FIS). If not accounted for, latency and time skew between the GPS reported position and the other real-time sensors in the system would result in residual errors being indicated.

The uncertainty effects observed from improper timing synchronization are most noticeable when inspecting a glidepath on a day with turbulent wind conditions. Therefore this paper focuses on ILS glidepath inspections on a demanding day.

Although the discussion is limited to this scope, the concepts presented in this paper are applicable in general as well to other types of position reference equipment and navigation aids.

In a GPS-based FIS, the attitude and heading of the aircraft must be compensated for by the system software. Since the navigation sensor antenna and GPS position reference

---

<sup>1</sup> For simplicity GPS is used in this paper to designate the use of standard and/or differential GPS (DGPS).

<sup>2</sup> AHRS (Attitude and Heading Reference System); INS (Inertial Navigation System)

antenna cannot be physically located at the same point in 3-D space, a “coordinate transformation” must be accomplished to calculate the true position of the navigation sensor antenna (sometimes referred to as “antenna lever arms”). The attitude and heading data should also be used to compensate for antenna pattern effects. This information must also be time synchronized with the other data, but for simplicity it is not discussed further in this paper.

## BACKGROUND

A flight inspection system (FIS) collects data from numerous sources. In modern systems most of the data collected comes from various digital sub-systems. For the most part, all of the various sub-systems operate asynchronously.

In order to minimize the overall system measurement uncertainty, it is essential that time critical data from the avionics sensors are precisely synchronized with the position reference data. If the data are not satisfactorily synchronized, errors can occur which will contribute to the system measurement uncertainty.

A paper presented at the 2008 IFIS [1] provided an example showing the effects of an improperly synchronized GPS position reference. When the GPS referenced data was compared with manual theodolite tracking, the results seemed to indicate the theodolite provided better results, which clearly should not be the case in a properly synchronized system.

It should be noted that some flight inspection parameters are more dynamic and time critical than others. The most critical parameters are the primary aircraft guidance information (including ILS LLZ and GP deviation) and the FIS position reference data. These also tend to be the parameters which are the most dynamic.

## GPS RECEIVER TIMING CONSIDERATIONS

A finite, but variable, amount of time is required for a GPS receiver to calculate its position and quality information using the measured pseudoranges from each satellite used in the position solution. Following these calculations, an additional finite but variable amount of time also is required for the receiver to transmit the position and quality data to the FIS real-time computer. Historically, the GPS receiver manufacturers have specified these combined delays as “latency”.

Typical values for the latency of the high-end, survey-grade GPS receivers are on the order of 100 milliseconds. In the design of a FIS the effects of latency must be considered and eliminated in order to achieve time correlation of the position data and the avionics sensor parameters.

## SOURCES OF TIMING UNCERTAINTY

The sources of timing uncertainty are divided into two groups for this paper:



- Avionics Sensors
- Position Reference

The sources of timing uncertainty from both can be roughly generalized as follows:

- Processor “loop time”:
  - Sub-system control and monitoring
  - Calculation of data (ILS deviations, VOR bearing, GPS position, etc.)
  - Transmission of data to the outside world (in this case the FIS real-time Signal Processing Unit)
- Filtering delays

### AVIONICS DELAYS

If a “black box” avionics sensor is used in the FIS to calculate and transmit time-critical data, it will have a contribution to timing uncertainty which affects overall system uncertainty and must be considered.

Time-stamping is not an acceptable solution to the avionics delay issue if the internal sensor delay is still unknown. In general, time stamping is considered undesirable as a method of timing synchronization because of complicated software and data handling. In this method every sample must be re-calculated using interpolation methods following the flight inspection run.

A proven alternative is to use a method to measure the time-critical parameters externally from the avionics sensor using a method with insignificant timing uncertainty. This has been a very successful solution, with Digital Signal Processing (DSP) methods used successfully for more than 15 years.

### WHAT IS “REAL-TIME”?

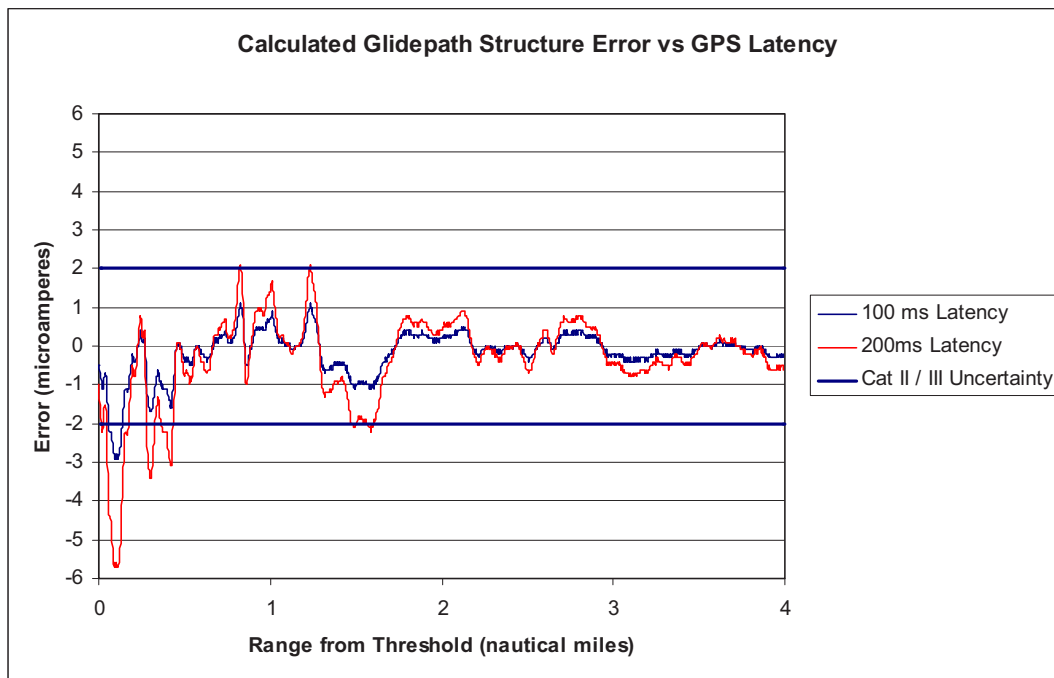
The term “real-time” as it applies to digital systems is a misnomer. It is impossible for any device that relies on a digital computer to truly operate in “real-time” since the microprocessor takes a finite amount of time to process its instructions. By “real time” it is meant that the amount of time required to process its required instructions is insignificant to the task at hand.

### NON-SYNCHRONIZED ILS GLIDEPATH EXAMPLE

In the paper “Current Issues in Demanding Flight Measurements Environments” presented at the 2008 IFIS, an example was given of errors due to what was apparently latency from a GPS receiver [1]. In the example, measurements using a theodolite seemed to provide better results than a DGPS system. It should be clarified that this would not be the case in a properly designed system.

To demonstrate the effects of improper time synchronization, an example graph is provided showing calculated glidepath structure error versus GPS latency. The following comments apply to the example.

1. The source data for this graph was recorded during an actual ILS approach on a windy day. This data was selected intentionally to represent demanding, real world conditions.
2. The source data is the output of the DGPS position reference system representing the aircraft deviation from the ILS glide path in microamperes.
3. The DGPS receiver position uncertainty was recorded and remained at an optimum level throughout the flight profile (1 cm horizontal and 2 cm vertical).
4. The effects of improper time synchronization were calculated by skewing each sample by 100 and 200 milliseconds.
5. The graph traces indicate the error between the skewed and true positions.
6. It should be noted that the error could correspond to avionics sensor latency, GPS receiver latency, or a combination.

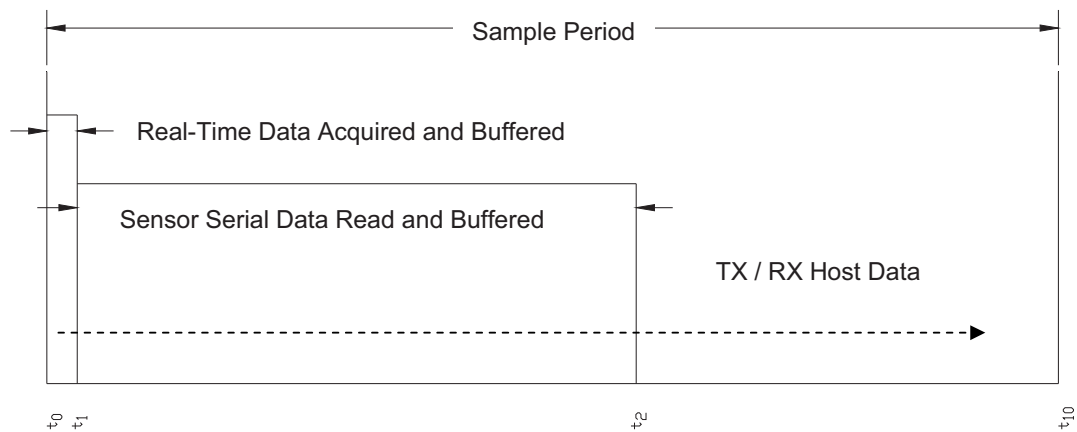


#### MITIGATION OF FIS UNCERTAINTY DUE TO TIMING SYNCHRONIZATION

It is possible to eliminate GPS time skew uncertainty error by synchronizing the FIS overall data acquisition timing with the GPS receiver position measurements.

If the FIS signal processing unit (the so-called “real-time” computer) is triggered by the DGPS receiver timing it can be ensured that the calculated GPS position is time correlated with the real-time data from the avionics sensors.

This methodology eliminates the possibility of errors due to latency in GPS receiver position calculation and data transfer.



FIS Timing Diagram

## CONCLUSIONS

Latency effects from the position reference or avionics sensors can produce significant residual errors. The residual errors are critical for evaluation of ILS structure and especially the glidepath.

Without proper time synchronization the magnitude of latency effects due to typical GPS receivers can exceed ICAO uncertainty limits during real operating conditions.

For an ILS, inspection uncertainty due to latency effects increases with the angular velocity of the aircraft relative to the measurement reference point. In real operating conditions this effect is seen as increased sensitivity as the aircraft approaches the threshold.

In FIS design, the effects of latency must be considered in order to achieve time correlation of the position data and real-time parameters from the avionics sensors.

Avionics sensors used for flight inspection must be carefully evaluated for latency effects.

Latency due to the avionics sensor can be eliminated in some cases by using external Digital Signal Processing (DSP) methods.

It is possible to eliminate the effects of position reference latency by synchronizing the FIS signal processing data acquisition to the GPS receiver.

#### REFERENCES

[1] “Current Issues in Demanding Flight Measurements Environments”, Dr.-Ing. Gerhard Greving, L. Nelson Spohnheimer, IFIS 2008.

[2] ICAO Doc 8071, Volume 1.

# RESULTS OF EXPERIMENTS OF THE ROHDE & SCHWARZ EVS 300 RECEIVER FOR VOR AND ILS FLIGHT INSPECTION

**Stéphane GARCIA**  
Flight Inspector  
Flight Inspection Service  
French DGAC/DTI  
Tél 00 33 5 62 14 55 96  
Email [stephane.garcia@aviation-civile.gouv.fr](mailto:stephane.garcia@aviation-civile.gouv.fr)



**Stéphane WATIER**  
Flight Inspector  
Flight Inspection Service  
French DGAC/DTI  
Tél 00 33 5 62 14 55 77  
Email [stephane.watier@aviation-civile.gouv.fr](mailto:stephane.watier@aviation-civile.gouv.fr)



**Philippe LABASTE**  
Laboratory  
Flight Inspection Service  
French DGAC/DTI  
Tél 00 33 5 62 14 55 95  
Email [philippe.labaste@aviation-civile.gouv.fr](mailto:philippe.labaste@aviation-civile.gouv.fr)



## 1 ABSTRACT

The Collins 51-RV4 is DSNA-DTI (French DGAC Technical Centre) "legacy" receiver. It's an old generation but high quality analogical VOR/ILS receiver, certified for airliners, modified to be a FI receiver by adding a connector to make available several voltages corresponding to flight-inspection parameters such as modulation depth. It's been used in DTI flight inspection systems for years: the

same RV4s used in our new **SAGEM CARNAC** Flight Inspection System were previously used in the **SAGEM "SMCV"** FIS in the end of the eighties.

Now it's time for us to think about replacing them, the EVS300 digital laboratory VOR/ILS/MKR receiver, designed to be a ground maintenance equipment, has been evaluated by DTI as a Flight Inspection receiver for more than 2 years, working together with the manufacturer **ROHDE & SCHWARZ** when it was still under development.

Several modifications have been done by manufacturer on our request. It was found satisfactory, with a much better accuracy than the RV4 (no need to use calibration tables, as the EVS300 is more precise than our IFR 2030 signal generator !) and much more features (separate Clearance and Course signal measurement while ILS is in normal condition, spectrum analysis, etc.). A large number of the same receivers have been bought by French DSNA/DTI (63) for the ground maintenance staff. SAGEM integrated it in its CARNAC Flight Inspection System.

The Honeywell RN34 is a new generation digital flight inspection receiver, designed from an aircraft equipment base. It's nearly the only dedicated FI receiver now available, except the receivers built or modified by FIS manufacturers for their own systems. It's one of the options SAGEM now proposes for CARNAC customers. This equipment was ground tested and integrated by SAGEM and then flight tested by DTI.

Following are some results of the DTI comparison of the RV4, RN34 and EVS 300, that took place during a routine ILS flight inspection.

## 2 ROHDE & SCHWARZ EVS 300



### Main characteristics

- Maximum precision in level measurement and modulation analysis.
- Portable equipment (low weight, weather protection).
- Measurement modes for ILS, VOR, Marker Beacon.
- Frequency Scan.
- FFT analysis.
- Oscilloscope mode.
- Support of R&S Power Sensors.
- GPS interface (NMEA, Ashtech ...).
- Internal Data logger.
- High temperature range.
- Operation time of 8 to 10 hours on battery power.
- Compliant to ICAO Doc. 8071 and Annex 10

It perfectly deal for dynamic runway measurements and flight inspections.

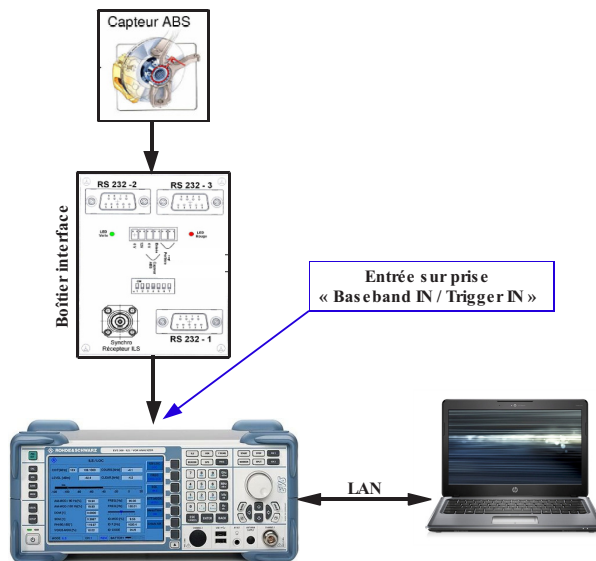
## 3 EVS 300 AND GROUND MEASUREMENT

### 3.1 Dynamic runway measurement

The Rohde & Schwarz EVS 300 is integrated in ILS maintenance vehicles to perform dynamic Runway measurement.



EVS 300 installed in an ILS vehicle



Vehicle installation diagramm

The external trigger (configurable) used for positioning is issued from the ABS car sensor.

A GPS can also be used for positioning information.

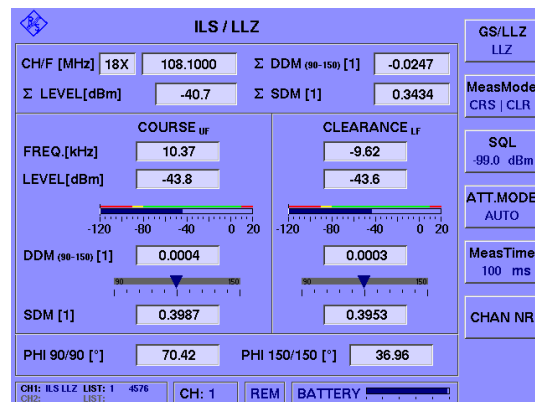
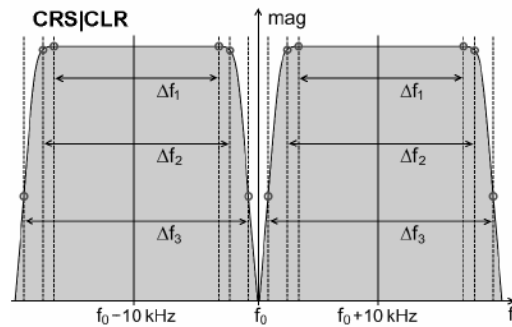
We connect to the EVS 300 an external GPS receiver via a second RS-232-C interface (NMEA 183, Ashtech format ...).

An exact location and time stamp appear with each block of measurement data.

### 3.2 Course/Clearance ratio measurement

Analysis of all important values like measurement of the phase relationship

between the two 90 Hz and 150 Hz signals are also performed with EVS300.



## 4 EVS 300 AND FLIGHT INSPECTION



Rohde & Schwarz EVS 300 and EB200 installed in the ATR 42

Parallel LLZ and GS measurement (with second signal processing card) are performed.

We measure all ILS parameters during runway approach with up to 100 Hz measurement rate.

We also perform VOR bearing and modulation measurements.

(Results will be presented in chapter 6).

There are also some interesting options that we used for jamming or interference detection:

## 4.1 Frequency Scan mode

70 to 350 MHz continuous scan.

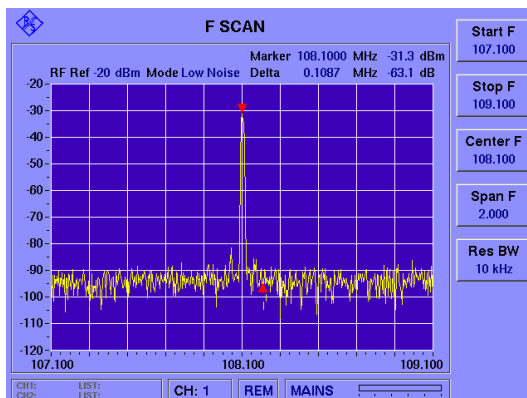
-120 dBm to +13 dBm input level.

clear/write, average, and peak hold trace functions.

bandwidth 30/10/3/1 kHz.

Marker and delta marker functions.

dynamic range of up to 100 dB.



Ideal for analyzing spurious signals in the ILS/VOR and communications bands.

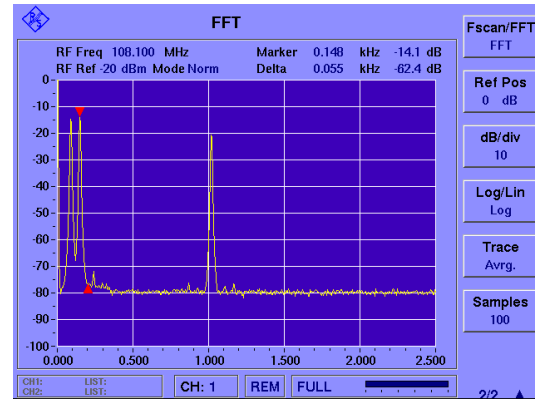
## 4.2 FFT analysis

Signal analysis of the demodulated RF signal or external baseband input.

Logarithmic or linear spectrum display;

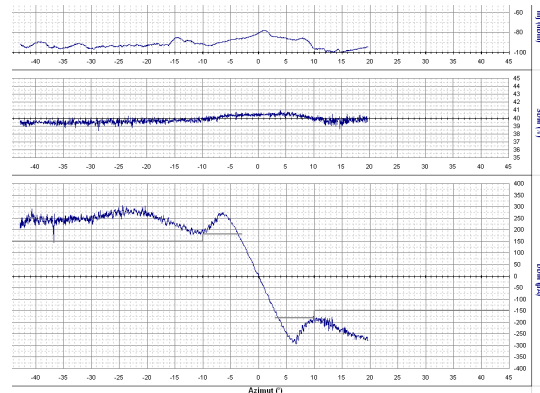
Hanning and flat top window functions.

Marker and delta marker functions.



Ideal for fast and easy analysis of harmonics and intermodulation products of ILS, VOR, and marker beacon signals

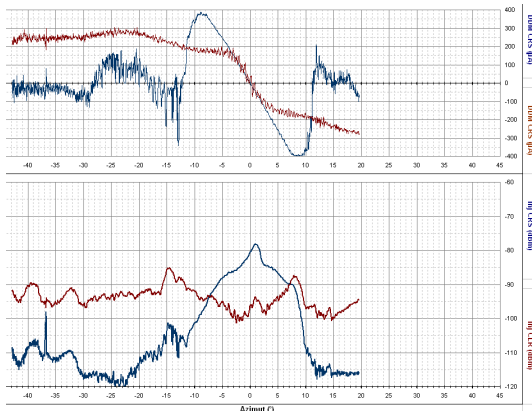
## 4.3 Simultaneous course / clearance mode



This case has been encountered in Cannes (Riviera) where the coverage was close to the tolerance at azimuths 10 and -10°.

It has been first suspected a problem in the course / clearance ratio.





It appears on the second measurement that the DDM clearance was too low.

These measurements have been performed without any impact on the air traffic in Cannes.

## 5 Filtering issues

RV4 DDM voltage passes through an analogical low-pass filter in the **SAGEM** FIS, before being digitalized. It's a Butterworth type 3<sup>rd</sup> order active filter, corner frequency  $F_c = 12\text{Hz}$ , value calculated to have the ICAO "time constant" (if it was a first order filter) for a measuring speed of 150kts.

RN34 DDM is internally filtered. Cut frequency and characteristics of the low-pass filter unknown of DTI (lack of documentation), it seems to be close to the one of the RV4 analogical filter referring to the curves.

EVS300 DDM is not filtered, output signals are raw data. A filtering has to be set up for an analysis of the results.

The first step is to find a first order filter which will make EVS 300 output signal comparable to RV4 or RN34 signal, "RV4 DDM like".

We chose a low pass filter, angular frequency  $\omega_c = 3 \text{ rd/s}$ .

In a second step a "MLS type" filter was chosen, as this kind of filter appeared to be more interesting than a first order filter.

### 5.1 CMN and PFE filtering

It's a first order filtering for CMN and a second order filtering for PFE.

- Command Motion Noise from a high-pass filter,  $\omega_c = 0.125 \text{ rd/s} * V_g / 140$  with  $V_g$ : Average Ground speed of the aircraft during measurement in knots

- Path Following Error from a low-pass filter,  $\omega_c = 0.125 \text{ rd/s} * V_g / 140$  with  $V_g$ : Average Ground speed of the aircraft during measurement in knots.

The PFE curve is to be compared to the error obtained from the filtered DDM of the other aircraft receivers

### 5.2 Use of CMN/PFE Filtering for VOR Course structure analysis

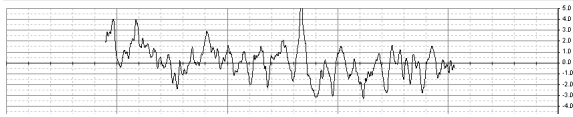
"Roughness, scalloping and bend are usually caused by reflection of the RF signal from terrain, trees, power lines, hangars, fences, ..."

"The character of the deviation can indicate the type of reflecting objects. A study of flight inspection recording and the surrounding terrain will often disclose the source of the course aberration."

"These conditions can occur alone or in any combination."

Application of bend or scalloping criteria is often difficult to clarify.

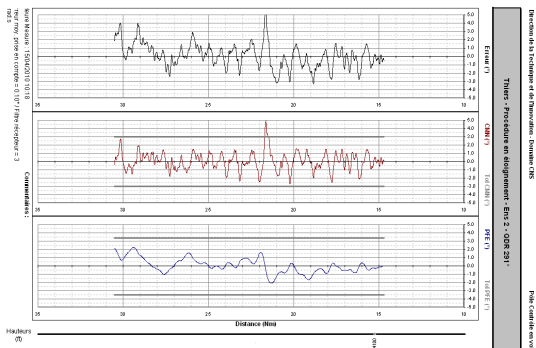
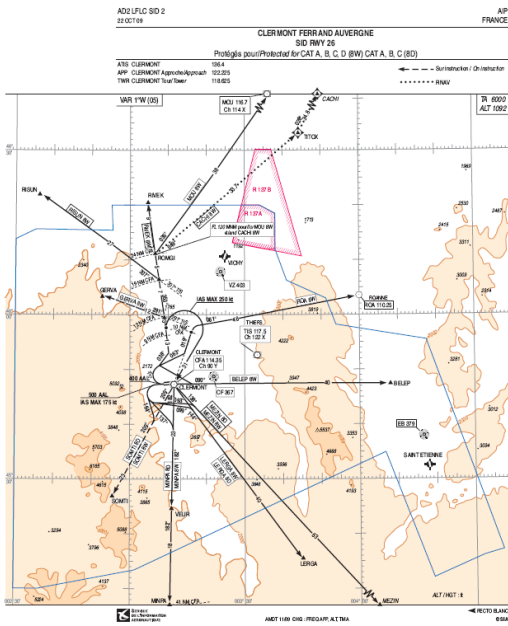
The analysis and the conclusions from one flight inspector to an other can be sometimes different.



To avoid these discrepancies and to impose our flight inspection conclusions on the radio navigation aid operators, we need an irrefutable tool.

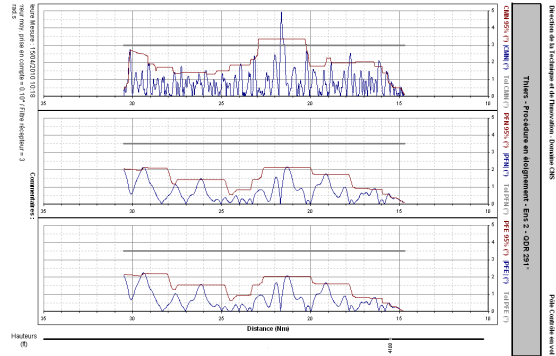
Examples of VOR in the centre of France in a mountainous area.

### Example course 1



Raw data, PFE and CMN

The course seems to be out of tolerances.

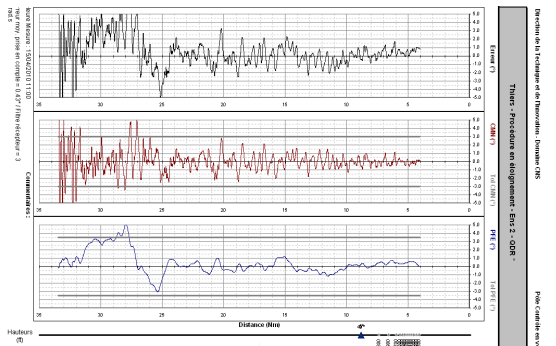
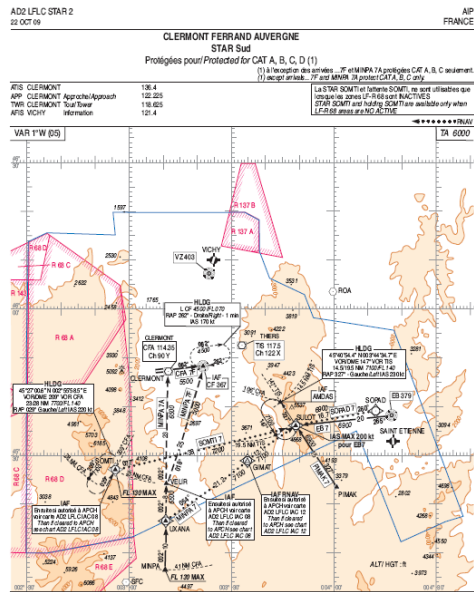


The same data with the 95<sup>th</sup> percentile criteria.

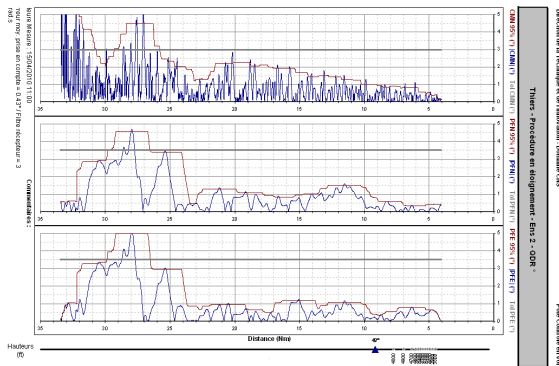
CMN is out of tolerances and PFE is in the limits.

The course is not OK

### Example course 2



Raw data, PFE and CMN



The same data with the 95<sup>th</sup> percentile criteria, PFE and CMN are out of tolerances, course is not OK.

### 5.3 95th percentile

The 95th percentile is a widely used mathematical calculation to evaluate the regular and sustained utilization of a network pipe.

Basically the 95th percentile says that 95% of the time, the usage is below this amount. Conversely of course, 5% of the time, usage is above that amount. The 95th percentile is a good number to use for planning so you can ensure you have the needed bandwidth at least 95% of the time.

There are three important factors to a percentile calculation:

#### Percentile number

A percentile basically says that for that percentage of the time, the data points are below the resulting value.

A 95th percentile says that 95% of the time data points are below that value and 5% of the time they are above that value. 95 is a magic number used in networking because you have to plan for the most-of-the-time case. Equivalent of the “2  $\sigma$ ” in a Gaussian distribution.

#### Data points used

A percentile is calculated on some set of data points. What those data points represent is significant to understanding the meaning of the percentile result. The sample rate indicates how accurate or forgiving the percentile is. The more frequent the sample rate, the more accurate and less forgiving the percentile will be.

#### Data set size

The data set size indicates the range of the values. In network percentiles, the data set is a period of time over which samples are collected.

Usually for any solid planning and trend determination, we need a reasonably large data set to cover the peaks and valleys of utilization. 40 seconds of samples is our typical data set, which represents approximately half a period of a bend.

**The PFE and CMN filtering and the 95th percentile are parts of the French regulation for validation of VOR, DME and soon TACAN.**

### 5.4 Air-Ground Correlation

Correlation of air and ground measurements records has allowed France to extend the interval between flight inspections.

Typical correlation activities begin with a confirmation that airborne and ground test equipment are operating within tolerances. Ground and flight test generators and receivers are compared. To have the same equipment used for ground and air measurement is a way to eliminate problems.

Ground equipment could be a spare in case of a main failure in the aircraft.

## 6 SOME RESULTS OF COMPARISON IN ILS

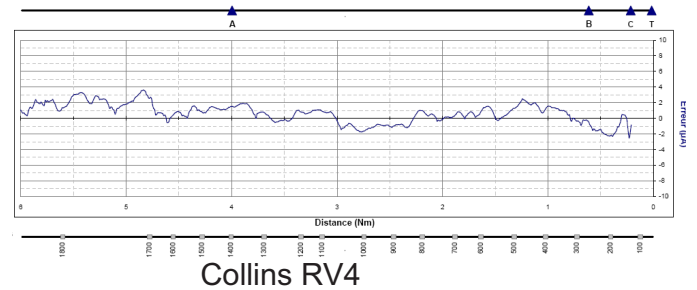
Here are some results of the DTI comparisons of the RV4, RN34 and EVS 300, that took place during a routine ILS flight inspection in Aurillac. The EVS DDM is not filtered, that's why the records shows much more details. A digital filtering (post processing) has to be done before comparing with RV4 or RN34. As the filtering introduces a delay that may be an issue for synchronising the position-fixing system (GPS) with the DDM, we choose to compute a raw error (CCP) using the raw DDM (CP), and then to filter the error, instead of trying to filter the DDM before computing the error.

The PFE curve is to be compared to the error obtained from the filtered DDM of the other receivers

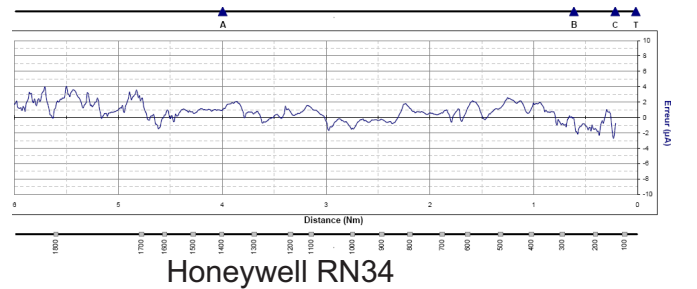
The sign convention on the curves is the one DSNA-DTI uses, opposite to ICAO one:  $DDM = M150 - M90$ .

RN34 DDM was used to compute a "real" DDM (i.e.  $M150 - M90$  instead of "normalized DDM"  $(M90 - M150) * 0.4 / (M90 + M150)$  obtained from the RN34). Otherwise the RN34 DDM shows a visible difference (compared to EVS300 or RV4) on the coverage curves were SDM is sometimes significantly different from 40% (LLZ) or 80% (GP).

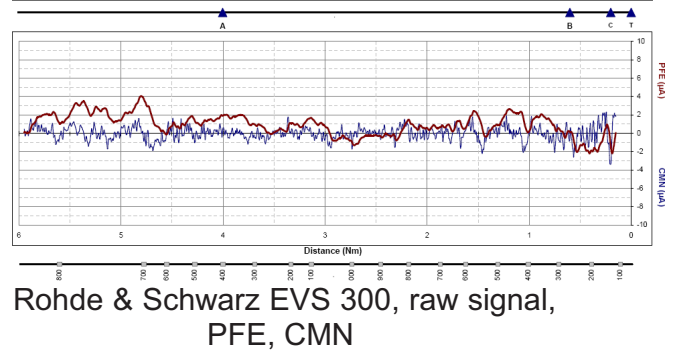
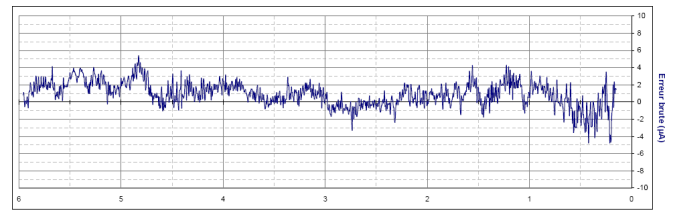
### 6.1 Aurillac 15 LOC AXIS



Collins RV4



Honeywell RN34



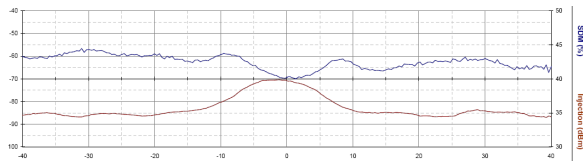
Rohde & Schwarz EVS 300, raw signal, PFE, CMN

#### Error between A-B Total Error

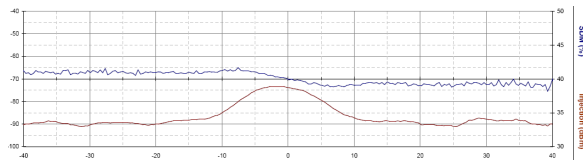
<b>RV4</b>	0.3 $\mu$ A	0.7 $\mu$ A
<b>RN34</b>	0.5 $\mu$ A	0.7 $\mu$ A
<b>EVS</b>	0.7 $\mu$ A	0.9 $\mu$ A

RV4, RN34 and EVS 300 PFE errors are similar.

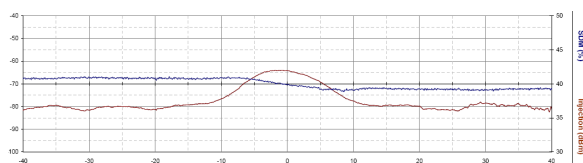
### 6.2 Aurillac 15 LOC Coverage



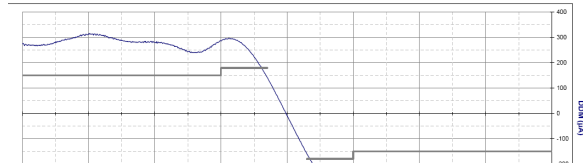
Collins RV4



Honeywell RN34



Rohde & Schwarz EVS 300



**EVS 300**    283    -265    286    -295

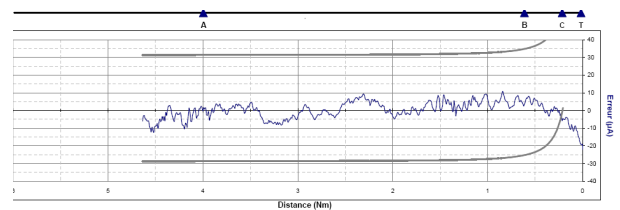
DDM from the 3 receivers is similar around the LLZ sector.

EVS300 and RN34 DDM and SDM (after computation of "raw" DDM M150-M90) are also the same in the coverage area.

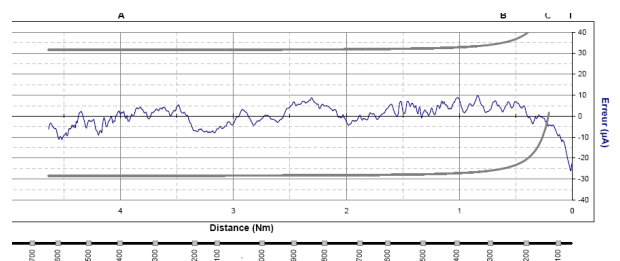
RV4 DDM and SDM are far from the other ones in the coverage area, this is a well known problem of the RV4 (It's precise only for DDM less than 200µA).

INJ (input level) have the same shape for the 3 receivers, with offsets due to a different wiring to the antenna (for the EVS300) and lack of calibration (for the RN34).

### 6.3 Aurillac 15 GLIDE AXIS

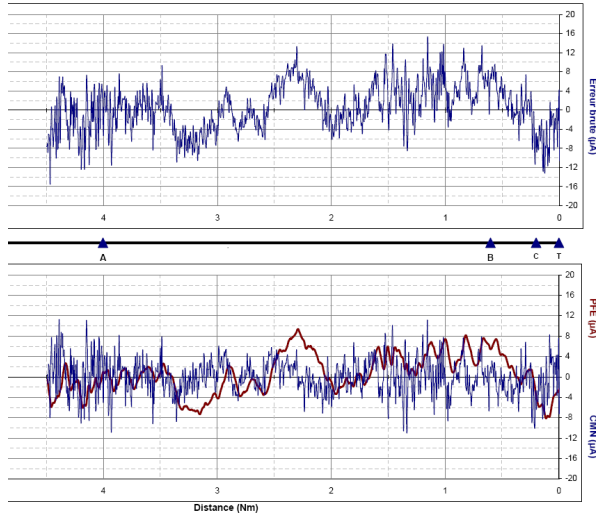


Collins RV4



Honeywell RN34

DDM at (µA)	-35°	35°	-10°	10°
<b>RV4</b>	267	-256	272	-275
<b>RN34</b>	276	-266	286	-298



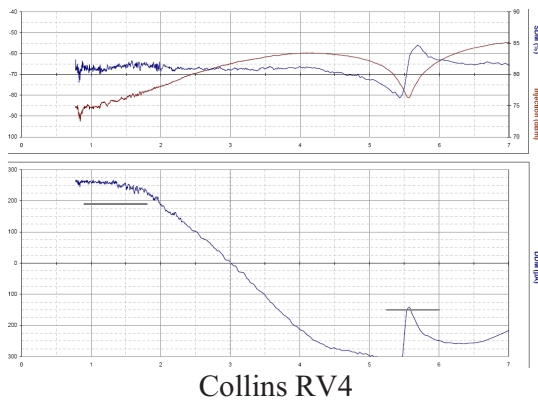
Rohde & Schwarz EVS 300, raw signal, PFE and CMN

**Error between A-B**

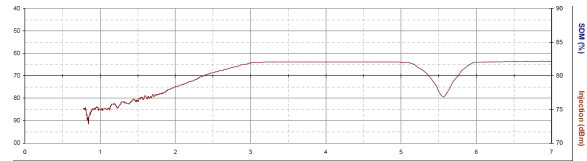
<b>RV4</b>	1.3 $\mu\text{A}$
<b>RN34</b>	1.5 $\mu\text{A}$
<b>EVS 300</b>	1.2 $\mu\text{A}$

RN34, RV4 and EVS300 PFE errors are similar.

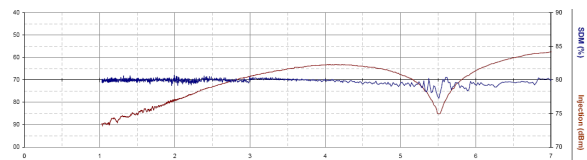
**6.4 Aurillac 15 GLIDE COVERAGE**



Collins RV4



Honeywell RN34



Rohde & Schwarz EVS 300

<b>DDM at</b>	<b>0.9°</b>	<b>1.4°</b>	<b>5.3°</b>
<b>(<math>\mu\text{A}</math>)</b>			
<b>RV4</b>	262	260	-319
<b>RN34</b>	267	265	-354
<b>EVS 300</b>	267	264	-359

EVS300, RV4 and RN34 DDM are similar in sector and below path area.

On high angles area, RV4 DDM differs from the other ones (same problem as for LLZ coverage).

On the antennae null angle (here 5.5°) the filtering of RV4 and RN34 DDM prevents from getting a curve similar to the EVS300.

In the case of the RN34, this even hides the pass-through of DDM below the 150 $\mu\text{A}$  template.



for DME and TACAN, to GPS receivers for trajectory and measurement, and to a guidance display (with ARINC 429-Ethernet converter connected to the Ethernet switch).



# The Uncertainty Evaluation of Flight Calibration Parameters

## Mr. Wang Lening

Development and Research  
Department  
Flight Inspection Center of CAAC  
23#, Tianzhu Road,  
Tianzhu Airport Industry Zone,  
Capital International Airport,  
Beijing,  
People's Republic of China  
E-mail: cfifzyjs@163.com



## Key words

Measurement Uncertainty Evaluation, Flight Calibration, Parameters..

## I Introduction

Accurate measurement, which implies the existence of standards of measurement, and the evaluation of uncertainties in a measurement process are essential to all areas of science and technology [1]. Measurement uncertainty consists of parameters which prevent the true and exact value of a measurement from being known.

Measurement uncertainty does not imply doubt about the validity of a measurement. On the contrary, knowledge of uncertainty implies increased confidence in the validity of a measurement result. The report of the measurement uncertainty for each measurement result is one of the most significant requirements for ISO 17025 Calibration Labs which is titled “General Requirements for the Competence of Testing and Calibration Laboratories” and has many of the same requirements as ISO 9000 but is more stringent in some specific areas.

The measurement uncertainty which called measurement error previously is the latest understanding and explanation in the area of error analyzing. Uncertainty is a consequence of the unknown sign of random effects and limits to corrections for systematic effects and is therefore expressed as a quantity. It is evaluated by combining a number of uncertainty components. The components are quantified either by evaluation of the results of several repeated measurements or by estimation based on data from records, previous measurements,

## Abstract

The most meaningful issue of a measurement practice is the estimation of uncertainty that must be associated with the result of a measurement so that it can usefully be employed in any technical, commercial, or legal activity. In the last years, many authors have dealt with the uncertainty evaluation in various fields of measurement and calibration, however, as we know, there is not any similar research on the Flight Calibration Parameters. This paper deals with the uncertainty evaluation for 20 calibration parameters of Flight Inspection Center of Civil Aviation Administration of China (CFI) which mainly employs the RVA-2 flight inspection systems. The rules for correctly estimating measurement uncertainty are going to be presented. After describing the key measurement model and the evaluation approach, the results obtained in a number of tests on actual measurement data are given. This paper shows that all the measurement uncertainties evaluated are within the values stated in Document 8071 by International Civil Aeronautics Organization (ICAO). The Conclusion and Further Work will be finally provided.

knowledge of the equipment and experience of the measurement.

Currently, there is not any systematic uncertainty evaluation for the flight calibration parameters in the whole area of flight inspection. For the purpose of accomplishing this task with high qualities, CFI has organized its technicians to compile the definition, inspection theory and calibration method for all the flight inspection parameters, analyzed the factors which could influence the inspection result uncertainty comprehensively, and formed the uncertainty evaluation documents for every calibration parameters.[2]

## II Method for Measurement

### Uncertainty Evaluation

#### Measurement equation

The case of interest is where the quantity  $Y$  being measured, called the *measurand*, is not measured directly, but is determined from  $N$  other quantities  $X_1, X_2, \dots, X_N$  through a functional relation  $f$ , often called the **measurement equation**:

$$Y = f(X_1, X_2, \dots, X_N) \quad (1)$$

Included among the quantities  $X_i$  are corrections (or correction factors), as well as quantities that take into account other sources of variability, such as different observers, instruments, samples, laboratories, and times at which observations are made (e.g., different days). Thus, the function  $f$  of equation (1) should express not simply a physical law but a measurement process, and in particular, it should contain all quantities that can contribute

a significant uncertainty to the measurement result.

An estimate of the measurand or *output quantity*  $Y$ , denoted by  $y$ , is obtained from equation (1) using *input estimates*  $x_1, x_2, \dots, x_N$  for the values of the  $N$  *input quantities*  $X_1, X_2, \dots, X_N$ . Thus, the *output estimate*  $y$ , which is the result of the measurement, is given by

$$y = f(x_1, x_2, \dots, x_N) \quad (2)$$

The uncertainty of the measurement result  $y$  arises from the uncertainties  $u(x_i)$  (or  $u_i$  for brevity) of the input estimates  $x_i$  that enter equation (2). Thus, components of uncertainty may be categorized according to the **method** used to evaluate them.

#### Standard Uncertainty

Each component of uncertainty, however evaluated, is represented by an estimated standard deviation, termed **standard uncertainty** with suggested symbol  $u$ , and equal to the positive square root of the estimated variance. The standard uncertainty can be categorized as **Type A evaluation** (method of evaluation of uncertainty by the statistical analysis of series of observations) and **Type B evaluation** (method of evaluation of uncertainty by means other than the statistical analysis of series of observations).[3]

#### Standard uncertainty: Type A

An uncertainty component obtained by a Type A evaluation is represented by a statistically estimated standard deviation  $s$ , equal to the positive square root of the statistically estimated variance  $s^2$ , and the associated number of degrees of freedom  $\nu$ . For such a component the standard uncertainty is  $u_A = s$ .

A Type A evaluation of standard uncertainty may be based on any valid statistical method for treating data. Examples are calculating the standard deviation of the mean of a series of independent observations; using the method of least squares to fit a curve to data in order to estimate the parameters of the curve and their standard deviations; and carrying out an analysis of variance (ANOVA) in order to identify and quantify random effects in certain kinds of measurements.

### Mean and standard deviation

As an example of a Type A evaluation, consider an output quantity  $A$  whose value is estimated from  $n$  independent observations  $A_k$  obtained under the same conditions of measurement. In this case the input estimate  $x$  is usually the **sample mean**

$$x = \bar{A} = \frac{1}{n} \sum_{k=1}^n A_k \quad (3)$$

and the standard uncertainty  $u_A$  to be associated with  $x$  is the estimated **standard deviation of the mean**

$$u_A = s(\bar{A}) = \left\{ \frac{1}{n(n-1)} \sum_{k=1}^n (A_k - \bar{A})^2 \right\}^{1/2} \quad (4)$$

### Standard uncertainty: Type B

In a similar manner, an uncertainty component obtained by a Type B evaluation is represented by a quantity  $u_B$ , which may be considered an approximation to the corresponding standard deviation; it is equal to the positive square root of  $u_B^2$ , which may be considered an approximation to the corresponding variance and which is obtained from an assumed probability distribution based on all the available information. Since the quantity  $u_B^2$  is

treated like a variance and  $u_B$  like a standard deviation, for such a component the standard uncertainty is simply  $u_B$ .

A Type B evaluation of standard uncertainty is usually based on scientific judgment using all of the relevant information available, which may include:

- previous measurement data,
- experience with, or general knowledge of, the behavior and property of relevant materials and instruments,
- manufacturer's specifications,
- data provided in calibration and other reports, and
- uncertainties assigned to reference data taken from handbooks.

### Combining uncertainty components

The **combined standard uncertainty** of the measurement result  $y$ , designated by  $u_c$  and taken to represent the estimated standard deviation of the result, is the positive square root of the estimated variance  $u_c^2$  obtained from

$$u_c^2 = u_A^2 + u_B^2 = u_A^2 + u_{B1}^2 \cdots + u_{Bn}^2 \quad (5)$$

### Expanded uncertainty

Although the combined standard uncertainty  $u_c$  is used to express the uncertainty of many measurement results, for the flight inspection application, what is often required is a measure of uncertainty that defines an interval about the measurement result  $y$  within which the value of the measurand  $Y$  can be confidently asserted to lie. The measure of uncertainty intended to meet this requirement is termed **expanded uncertainty**, suggested symbol  $U$ , and is obtained by multiplying  $u_c$  by a **coverage factor**, suggested symbol  $k$ . Thus  $U = ku_c$  and it is confidently believed that  $Y$  is greater than or

equal to  $y-U$ , and is less than or equal to  $y+U$ , which is commonly written as  $Y = y \pm U$ .

interval having a level of confidence greater than 99 %.

### Coverage factor

In general, the value of the coverage factor  $k$  is chosen on the basis of the desired level of confidence to be associated with the interval defined by  $U = k u_c$ . Typically,  $k$  is in the range 2 to 3. When the normal distribution applies and  $u_c$  is a reliable estimate of the standard deviation of  $y$ ,  $U = 2 u_c$  (i.e.,  $k = 2$ ) defines an interval having a level of confidence of approximately 95 %, and  $U = 3 u_c$  (i.e.,  $k = 3$ ) defines an

## III Our Uncertainty Evaluation and

### Results

CFI has made the measurement uncertainty evaluation for 20 main parameters in the area of flight inspection. The results are shown in the following table (Table 1), and the tolerances of uncertainty which is given by DOC 8071 are also displayed [4].

**Table 1 Uncertainty evaluation results**

Parameters	Standard Uncertainty	Expanded Uncertainty	Coverage Factor	Tolerance
Course alignment	0.43 $\mu$ A	0.86 $\mu$ A	2	3 $\mu$ A
Course width	0.014°	0.028°	2	0.04°
Course symmetry	0.11%	0.23%	2	1%
Course SDM	0.11%	0.22%	2	0.5%
Course field strength	0.82dB	1.6dB	2	3dB
Path angle	0.0065°	0.013°	2	0.0225°
Path width	0.0059°	0.012°	2	0.022°
Path symmetry	0.57%	1.1%	2	1.5%
Path SDM	0.17%	0.34%	2	0.5%
Path field strength	1dB	2dB	2	3dB
Marker coverage	9.4m	18m	2	20m
VOR field strength	0.49dB	0.98dB	2	3dB
VOR bearing error	0.044°	0.088°	2	0.6°
VOR 30 AM	0.40%	0.80%	2	1%
VOR 9960 AM	0.41%	0.82%	2	1%
VOR 30 FM	0.039	0.078	2	0.2
DME range error	16.44m	32.88m	2	40m
DME field strength	0.49dB	0.98dB	2	3dB
NDB field strength	0.26dB	0.52dB	2	3dB
PAPI angle	0.012°	0.024°	2	0.04°

Through the above results, we can see that the uncertainty value of every calibration parameter is within the tolerance from DOC 8071, and CFI owns the high-quality flight inspection technology and equipments.

#### **IV Conclusion**

This paper introduces the conception of uncertainty into the area of flight inspection. It presents the common method of measurement uncertainty evaluation for flight calibration parameters, and shows the results which CFI has evaluated. In order to improve our flight inspection quality, we will continue to do this research on other or new parameters.

#### **References**

- [1] L.Kirkup and R.B.Frenkel, “The importance of uncertainty in science and technology”, Cambridge University Press 0521844282.
- [2] “The measurement uncertainty evaluation criterion for CFI flight calibration parameters”
- [3] Uncertainty of Measurement Rults. <http://physics.nist.gov/cuu/Uncertainty/basic>.
- [4] “Manual on Testing of Radio Navigation Aids”.



# Data Integrity and the Gold Standard

William Geiser  
Manager, Aircraft Configuration  
Federal Aviation Administration  
Oklahoma City, Oklahoma  
Email: [william.r.geiser@faa.gov](mailto:william.r.geiser@faa.gov)

## Abstract

Controlling data from creation through publication is a challenging process. As technology advances, the ability to process all data electronically is possible. This process will provide the data integrity required to support SBAS and GBAS flight navigation.

Why is data integrity important? If the data for an instrument approach procedure is incorrect, the possibility exists for the aircraft to be flown by the aircraft autopilot to a position that may be unsafe.

Currently there is a significant amount of manual manipulation of electronic data which supports instrument flight procedures. This manual processing provides many opportunities to introduce errors.

The FAA has improved the data integrity by standardizing the data, automation, and workflows from which a procedure was created. This standardization includes new software for procedure development, the creation of digital procedural data in addition to the paper description of a procedure and digital distribution.

Working towards an electronic process has increased the importance of data integrity in the FAA organization. This awareness has reduced data errors and increased the organization's desire to automate the entire process as soon as possible. The concept of enter the data only once then move it to where it is used digitally, (CRC wrapped if needed) is the primary guiding philosophy to ensure data integrity.

Controlling instrument approach procedure data from creation to publication will reduce errors and provide a safer environment for the future of SBAS and GBAS flight navigation.

## Introduction:

What are data integrity and the Gold Standard? Data integrity, for the purposes of this discussion, is the assurance that each time aeronautical data is transferred, stored or retrieved it remains identical to when it was originated/created. The FAA's Gold Standard for instrument procedures is the process of creating an instrument procedure electronically from this data, and then controlling the process so this

data remains unchanged through flight inspection, charting and distribution.

There are additional, measures of data quality such as completeness, currency/timeliness, and accuracy as well a numerous approaches to assure data quality. The FAA considers these data quality considerations important and pursues them with vigor. However, this paper will focus on data integrity.

Why are data integrity and the Gold Standard important? How will this affect flight safety? The Gold Standard definition can be applied to different segments of this process, however the goal is to apply it to the entire process from start to finish. If the data is accurate prior to the creation of a procedure and it is controlled and not manipulated during the process, the value of the data increases significantly. This value increases because the flight crews who receive exactly the same data that procedure developer created has a product that matches the paper exactly and is known to be safe. As a result, the overall safety of each and every flight is raised to a higher level.

This paper will describe the entire process from start to finish. It will include the request of a new instrument procedure, its development/creation, how it's produced, scheduled, flight checked, charted and finally printed and distributed. In addition to the process description, the status of each will be identified with respect to the Gold Standard.

### **Instrument Flight procedure Request**

The initial request for a new instrument procedure is sent by a customer to the

Regional Flight Procedures Office (FPO). The FPO provides guidance on FAA instrument flight procedures development and maintenance functions. The FPO is the focal point to start the process for completing requests for new and revised instrument flight procedures. There are three FPOs within the United States located in Seattle, Washington, Dallas-Fort Worth, Texas, and Atlanta, Georgia.

The FPO answers questions related to general references, survey, airport data, environmental data, and funding to assist the FAA in support of an instrument procedure request. The FPO evaluates the effect of proposed obstacles through the Obstacle Evaluation and Airport Airspace Analysis (OEAAA) process to determine potential impact upon current and future instrument procedures.

The FPOs provide assistance in the collection and interpretation of airport and navigational aid data to ensure the most current and highest quality data is being used for procedure development, flight inspection and publication.

After the FPOs recommendations and feasibility study is completed, a request is sent to the Regional Aerospace Procedures Team (RAPT) for prioritization. When a procedure is ready to be created it is entered into the FAA's Procedure Tracking System (PTS). This system sends enroute requests to Silver Spring, Maryland and terminal requests to Oklahoma City, Oklahoma for development. This Gold Standard discussion will focus on terminal procedures.



## **Instrument Flight Procedure Development/Creation**

The FAA has a software application called Instrument Approach Procedures Automation (IAPA). This application is currently being used to design all instrument approach procedures. IAPA uses the Airport and Navigational Aid (AIRNAV) database and the Instrument Flight Procedures (IFP) fix database to create the new instrument procedure. The AIRNAV and IFP databases contain the most accurate and up to date information the United States has with respect to airports, navigational aids, fixes, and obstacles.

After the procedure is created, the data is manually entered into IFP Standard Instrument Approach Procedure (SIAP) database. This data is used by the IFP coder to create the ARINC 424 packets from the SIAP, FIX, and AIRNAV databases for the selected RNAV procedures. This application also has the ability to generate the selected FAA forms for the instrument procedure. This application is scheduled to be expanded to include all types of instrument flight procedure development including SIDs, STARs, ILS, VOR, NDB and etc.

In addition to expanding IFP, IAPA will be replaced in the future by the Instrument Procedure Design System (IPDS). This system will have the ability to automatically design the procedure in accordance with current directives, transfer the data to IFP, create the ARINC 424 packets, generate all the paper forms, and send the entire procedure to Flight Check electronically. The only item not scheduled to be completed by IPDS is the Terminal Publications Procedure (TPP) chart. The

charting tool is a separate process using Environmental Systems Research Institute (ESRI) geographic information systems (GIS) software. This entire process will finalize the requirements to meet the Gold Standard for instrument approach procedure development.

Currently we are finalizing the creation of RNAV procedures under the Gold Standard. This has been a challenging effort due to criteria changes, process changes, and the inclusion of the ARINC 424 code which will be loaded into the aircraft flight management system.

## **Instrument Flight Procedure Production**

The Production Integration Team (PIT) manages the production planning, administration, distribution, and coordination with Flight Inspection. In addition the PIT coordinates the procedure with charting to create the Flight Inspection Graphic (FIG) which is the rough draft of the approach plate.

The Aeronautical Navigation Services production plan is prioritized based upon risk assessment and contains a matrix that displays the priority as directed by the Regional Airspace and Procedures Team (RAPT)

These priorities are:

1. Procedures requiring amendment to correct a known safety deficiency.
2. Procedures based on newly installed or relocated navigational aids or airport runway/addition change.

3. Procedures which test or implement an FAA National Initiative.
4. Procedures at airports with no existing Instrument Flight Rule (IFR) approach.
5. Procedures providing a reduction in takeoff or landing minima.
6. Procedures which eliminate the requirement for a waiver or NOTAM.
7. Procedures providing flow improvement, more efficient routing, reduced Communication, or reduced coordination or complexity.
8. Procedures providing other benefits; i.e., compliance with new criteria or noise reduction.
9. Public use procedures not providing benefits of priorities 1 through 8.
10. Special and private procedures not providing benefits of priorities 1 through 8.

When all the documents have been collected and reviewed, the new, or amended, procedure is sent to the Flight Inspection Coordination Office (FICO) in both digital and paper formats.

The Navigation Database Services Team (NDST) receives the procedure from Quality Assurance (QA) and performs the manual process of validating all the 8260 forms against the ARINC 424 code. If the ARINC 424 code and forms don't match the procedure is returned for correction. If the code and paper match, the NDST creates a tailored file of new and amended instrument procedures and they are sent to Flight Inspection and Flight Inspection's avionics suppliers. The current suppliers are Collins and Universal Avionics. Collins and

Universal validate the code, combine it with a worldwide Jeppesen database, pack the data, and send it back to Flight Inspection electronically.

In addition to supporting Flight Check, the NDST produces two products; the National Flight Database (NFD) and the Digital Aeronautical Chart Supplement (DACS). These products are used both within the FAA to support the National Airspace System, and by other government and civil users.

The NFD is a data set, modeled to the Airlines Electronic Engineering Committee (AEEC), Aeronautical Radio Incorporated (ARINC) Navigation Data Base (NDB) international standard (ARINC 424). The NFD data can be used as the basis to support both Enroute and terminal navigation. Data elements included in the data set are; airports and heliports, radio navigation aids, fixes/waypoints, routes, airspace, standard instrument approach procedures, standard terminal arrival procedures and departure procedures.

The Digital Aeronautical Chart Supplement (DACS) is specifically designed to provide digital airspace data not otherwise readily available. The supplement is produced every 56 days, coinciding with the airspace cycle and includes Selected Instrument Approach Procedures, NAVAID and Fix Data. The DACS Change Notice is effective during the second half of the 56 day airspace cycle and is used to update the DACS. There is no Change Notice effective during the first 28 days of the Airspace Cycle.

## **Instrument Flight Procedure Scheduling**

The FICO takes delivery of the procedure and enters it into the Flight Operations Management Software (FOMS). FOMS is scheduling and tracking tool for all the procedures and NAVAIDs for the United States, its territories, and international locations which have a contract with the FAA. This software is used to create each weekly itinerary.

New and amended procedures are not scheduled until they have been processed and included in the custom database.

## **Instrument flight Procedure Flight Check/ Validation**

Each week, Flight Inspection takes delivery of a new custom database from Collins and Universal. When the new procedure is scheduled and shows up on an itinerary, the crew flying the new procedure reviews the code against the paper. If the review is satisfactory the crew flies the procedure by pulling it out of the custom database and flying it like any other certified procedure from the FMS.

The Mission Specialist (MS) which operates the Automated Flight Inspection System (AFIS) computer has previously loaded the new and amended procedures into the AFIS computer. While the pilots fly the new procedure from the FMS, the MS records and evaluates the data using the independent verification methods designed into the AFIS. This is where the real value of Flight Inspection is achieved. The AFIS

computer has the same electronic code that the NDST sent to Collins and Universal and this code is loaded directly into the AFIS.

When the procedure flies correctly, safely, and obstacles are not an issue, the procedure check is complete and signed off as meeting the Gold Standard.

## **Instrument Flight Procedure Charting**

The charting process is accomplished by our office in Silver Spring, Maryland. When the new procedure has been signed off by Flight Check, the next step involves updating databases prior to charting and distribution. All the procedure forms are sent to the National Flight Data Center (NFDC). The NFDC is another division within the FAA. The NFDC enters all the fixes into National Airspace System Resource (NASR) which is a database maintained by NFDC. This database generates a daily report of changes called the National Flight Data Digest (NFDD). NFDC also creates and issues Transmittal Letter (TL) every two weeks. The TL is the FAA's official document which enters the procedure into the Federal Register and makes it a legal document.

The new or amended chart is finalized by the Terminal Procedure and Chart Team and entered into the Consolidated Production Control System (CPCS). This system is a database which tracks all the new and current instrument flight procedure charts, including SIAPs, DPs and STARs, which are reviewed and finalized for the next chart cycle.

In addition to printing FAA civil procedures, the FAA also incorporates

all the Department of Defense (DoD) approach procedures. These procedures are merged and indexed with the FAA procedures.

### **Instrument flight Procedure Printing and Distribution**

Reproduction and Distribution (REDIS) provides replication and dissemination services for the Federal Aviation Administration (FAA) VFR charts. All IFR charts are printed by a local contractor. Printing and distribution are also completed in Silver Spring, Maryland.

The Reproduction Sub-Team provides prepress, printing, and finishing services. The production elements of the Sub-Team include production management, digital engraving, quality assurance, manual and digital imaging photography, litho-process plate-making, pressroom functions, and finishing operations. (Many aeronautical charts have a 28 day revision cycle and are printed on an extremely tight schedule to ensure they contain the latest changes).

The Distribution Sub-Team is responsible for the sale and distribution of FAA's aeronautical and NOAA's nautical charts and related publications to Government agencies, the public, and

approximately 450 Authorized FAA Chart Sales Agents. The Sub-Team's responsibilities include selecting and monitoring Authorized FAA Chart Sales Agents; determining print quantity requirements for charts and related publications; initiating print orders; and accounting and maintenance of customer mailing lists. The critical missions of the Sub-Team include the timely distribution of date-sensitive charts and publications and the maintenance and production of current information about inventory and revenue. The Sub-Team contracts for warehousing, order filling, and shipping.

### **Conclusion**

The process of creating a new instrument approach procedure is a long and complicated one. This process has the potential for many errors due to human interaction with the data. Automating the process and controlling the data will take the first step in maintaining data integrity. Constant review and validation of the process and software will provide a process from start to finish that will have achieved the desired Gold Standard. This Gold Standard will significantly reduce errors and provide a safer environment for the future of SBAS and GBAS flight navigation


# Ai-Sky data®

## IFIS-2010: Demonstration paper

---



Version V0R3 - 30 April 2010

	Company	CGx AERO in SYS
	Author (s)	Mohamed Ali MGALLES
	Responsible	Mohamed Ali MGALLES
	Project	Ai-Sky data®
	Reference	AIS_DS_IFIS2010_PAPER

**CONFIDENTIAL**

This document is composed of 15 pages.

# 1 PRELIMINARIES

---

## 1.1 Abstract

The life cycle of a procedure, from its design to its use in a real on boarded system, is dependent on the available means allowing the data transfer automation from the procedure designer point of view to the FMS integrated data one. These means have to guarantee data integrity and coherence but also to automatically check and pre-validate the produced data before their use on board. The demonstration proposed for the IFIS 2010 will be focused on Ai-Sky Data<sup>®</sup>, an aeronautical data management tool achieving these functionalities. Once the procedures have been designed using PANS OPS regulations (e.g. in GeoTITAN<sup>®</sup>), the procedure designers use Ai-Sky Data<sup>®</sup> to edit the information required for FMS interpretation of the nominal path (ARINC 424 coding). Ai-Sky Data<sup>®</sup> also displays the result in 2D (track view or profile view with DTM) or in 3D (in Google Earth for example). Used by data analysts, Ai-Sky Data<sup>®</sup> embeds consistency and aeronautical integrity checking tools, as well as format conversions. Because they are a gate from the world of procedure design to the actual integrated world of AIM, all these functionalities are an efficient asset for flight inspection. During the IFIS demonstration, a concrete example of these functionalities will be given with an RNP-AR procedure of LiJiang Chinese airport, designed by our procedure designers as part of the Chinese PBN implementation roadmap.

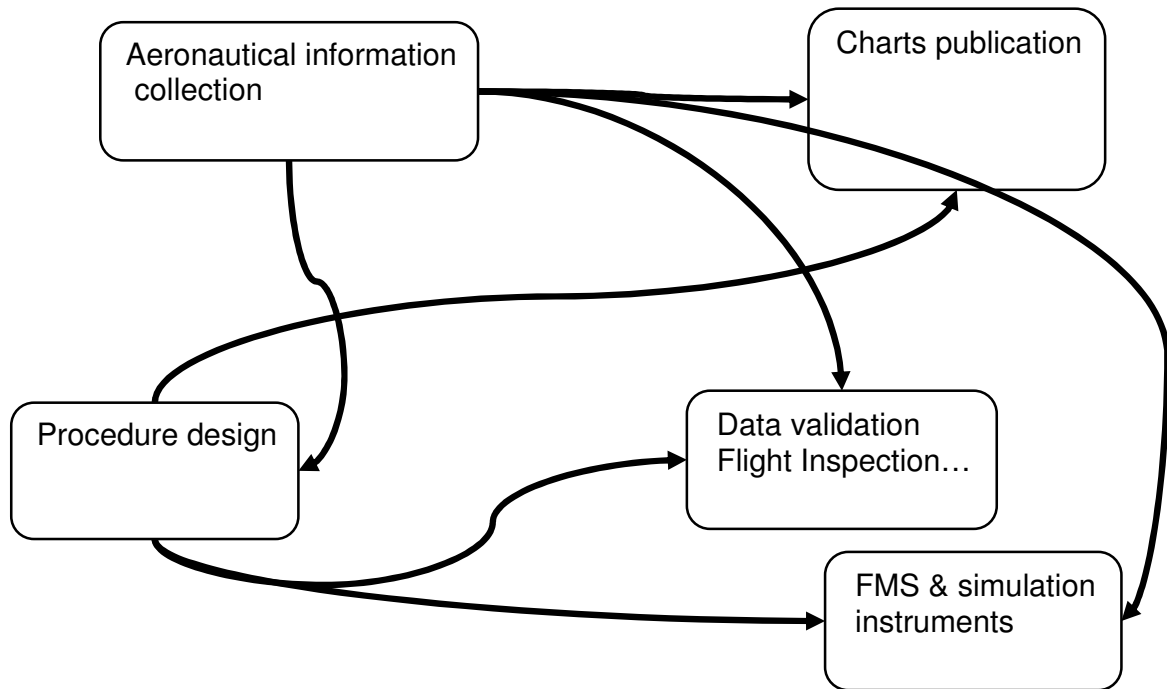
## 1.2 The need

In a few words, the major flight inspection usage need is data availability and exchange means. In fact, when the flight inspection is done the data is still a “fictive” one and not yet published. So it is not available for evaluation and analysis. The need difficulties can be classified as follow.

### 1.2.1 Data exchange chain

The aeronautical data exchange chain includes various actors with different points of interest and focus which introduces various divergences such as:

- The criticality definition: The data criticality and integrity is fully dependent on its usage. For example the range of a Navaid is critical data for a procedure designer and at the same time totally useless data in the charting task.
- The data management process: fully different data management and storage process.
- Data exchange: Non atomized data exchange process introduces a lot of manual data entry and modifications, which reduces the guarantee of data integrity.



### 1.2.2 Data interoperability

For validation and simulation, tools are missing the full aeronautical background data and especially theoretical average trajectories designed by the procedure designers in order to:

- Use them for simulation of noise and pollution propagation studies. Recently used by the IESTA simulator at the ONERA, France)
- Compare them to real flown trajectories for statistic and validation aims.

## 2 THE SOLUTION

---

### 2.1 The Basis

#### *2.1.1 Standard based*

Aeronautical data exchanges shall be based on worldwide used standards such as ARINC-424 (the FMS data definition format) and AIXM (EUROCONTROL aeronautical data exchange model). This eases interactions and communications between various tools and guarantees formats maintenance regarding the upgrades of ICAO recommendations.

#### *2.1.2 Exchanges control based automation*

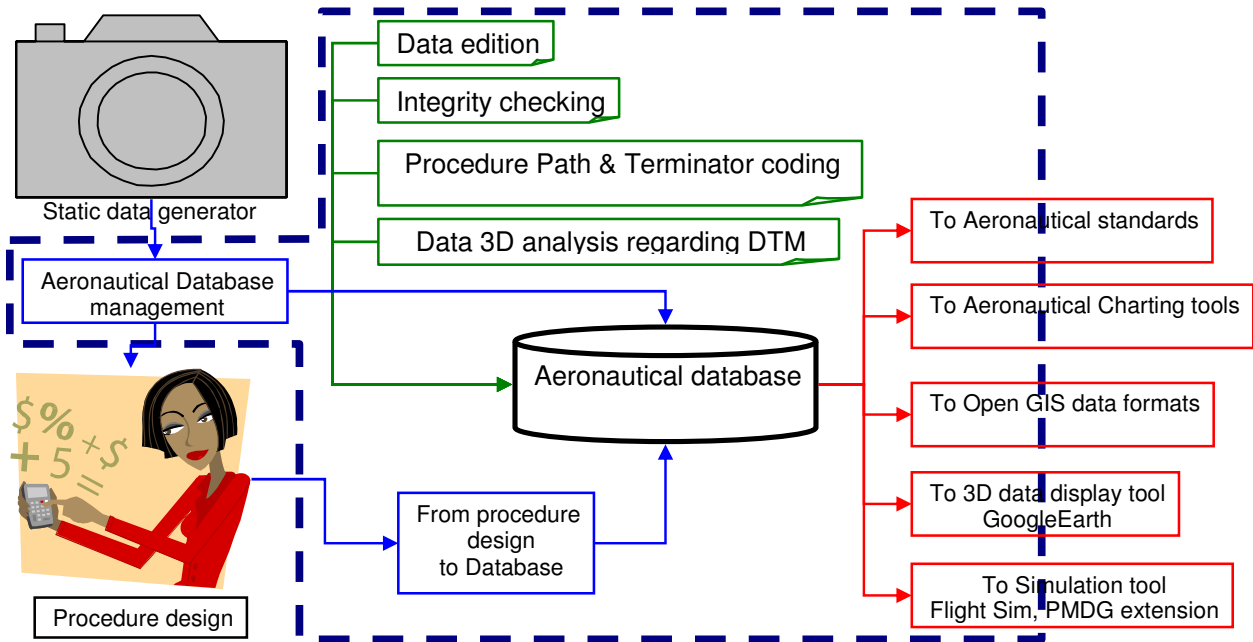
Data exchanges shall be fully automatized and control-based in order to ensure the integrity and coherence of data. This automation may use conversion report and CRC (Cyclic Redundancy Check) value control in order to check the data processing task.

#### *2.1.3 Database*

For fully inter-dependent tools using the same data under the same aspects like procedure design and charting tools, shall use a unique database in order to reduce the possible side effects of data exchange and transformations.



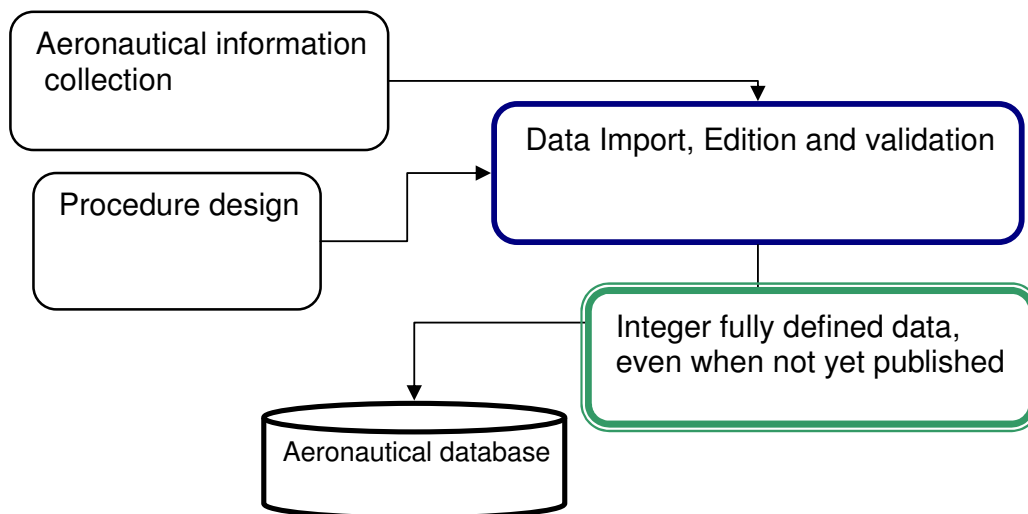
## 2.2 The workflow



### 2.2.1 Validating edition tool

In order to be able to create the not-yet-published data, a fully controlling edition tool shall be used. These controls shall be based on standards recommendations. This step enables users:

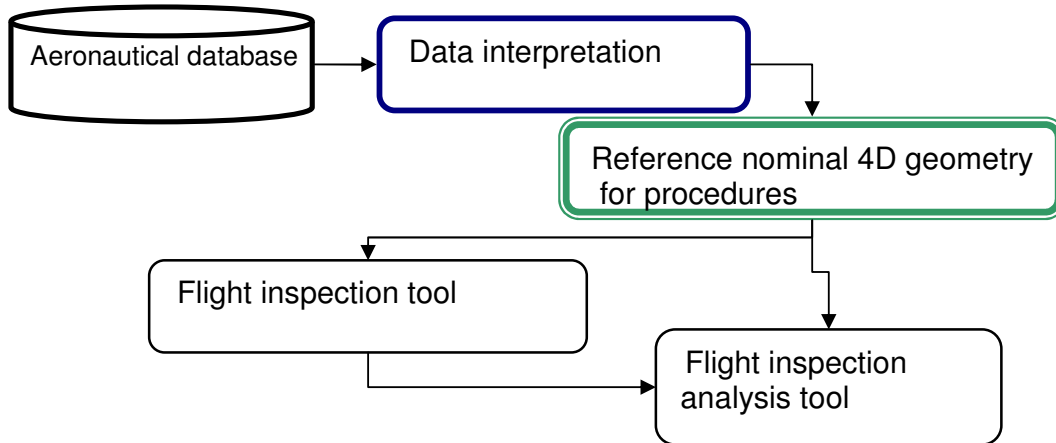
- To define their data based on worldwide used standards.
- To correctly edit and check the ARINC-424 coding of the procedures.



But this is still not sufficient: another need is to get the theoretical nominal trajectories in order to be able to compare them to ones flown.

### 2.2.2 Path & Terminators computing tool

This will result in an interpretation of the procedure definition, available using path and terminator. This function allows the construction of theoretical 4D nominal geometries.



## 3 THE TECHNICAL SOLUTIONS

---

### 3.1 Procedure design Software: GéoTITAN®

For more information please have a look at AIS\_GTT\_Leaflet.pdf

The ENAC PANS-OPS Unit has been known for years for its wide-ranging and exhaustive experience in procedure design, and also for its skills in training and information technology. This experience has been put to work in creating an expert software system: GéoTITAN®, a program which is entirely dedicated to assisting IFR procedure designers. GéoTITAN® belongs to ENAC, Ecole Nationale de l'Aviation Civile, the French Civil Aviation Academy of Toulouse, France.

GéoTITAN® is designed for the creation and management of flight paths and airspace entities. It enables IFR en-route and approach flight paths to be created, and provides modules for defining departure paths and RNAV procedures, including PBN procedures.

GéoTITAN® manages and displays all the useful information required to design flight paths with their associated protection areas, in a quickly way, with precision, and in compliance with ICAO DOC 8168-OPS/611.

Thanks to the automation of low-level tasks, the procedure designer can focus his/her attention on the important decisions of the analysis. The design process is under the designer's full control at all times, which guarantees reliable and coherent choices. The designer is never left alone: the exhaustive documentation reminds him/her of the regulation criteria and describes the manner in which GéoTITAN® calculates the protection areas. With GéoTITAN®, no protractors, rulers nor compasses are needed to design the flight paths but the processes and the logic are the same as those implemented in the manual method.

## 3.2 The aeronautical database management tool: Ai-Sky Data®

For more information please have a look at AiS\_SKD\_WhitePaper\_v1-9\_EN.pdf

### 3.2.1 Overview

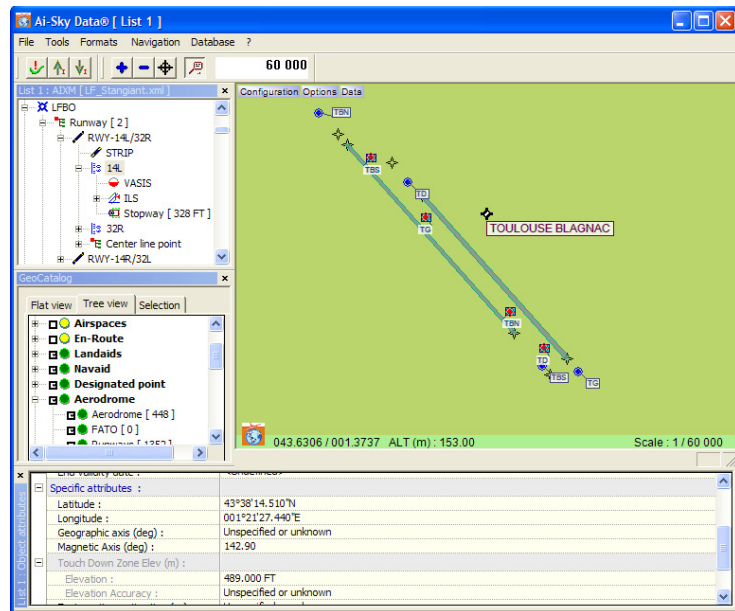
Ai-Sky Data® is an aeronautical data management software. It can provide the aeronautical information operators with a solution for aeronautical data processing, maintenance and exchange within different formats.

The temporal database also provides a data versioning system which permits the recording of the evolution of the information in accordance with its updates.

Ai-Sky Data® offers an aeronautical environment with a tree diagram display of the data as well as a user-friendly interaction and a symbology system which permits an intuitive use of the software.

The geo-referenced graphical viewer enhances the software ergonomics and enables a visual appreciation of handled data.

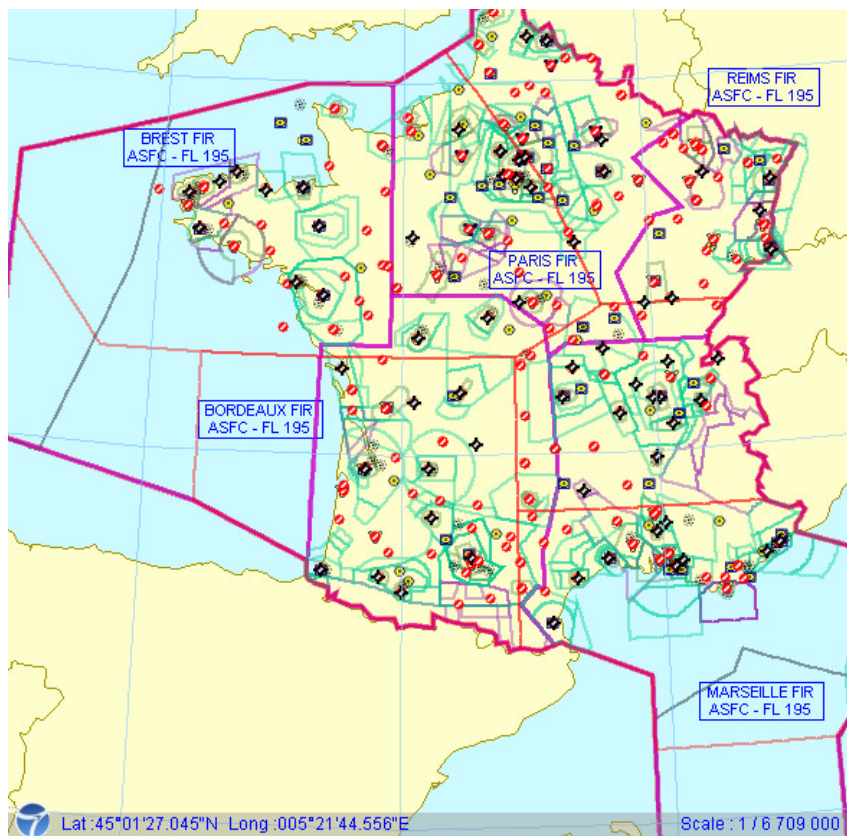
All data are displayed in a tree diagram system displaying the hierarchy, relationships and links between the aeronautical entities. The display is enhanced by aeronautical explicit and intuitive tree-structured symbols. The user can visualize all the attributes at any time.



### 3.2.2 Data formats pipeline

The software gives several management modules of various aeronautical data exchange formats, including:

- AIXM 3.3 & 4.5 import/export (5.x coming soon)
- ARINC-424 import
- ARINC-816 import (airport mapping database)
- DAFIF import
- GeoTITAN<sup>®</sup> import
- AIP-GIS Charting<sup>®</sup> connection
- Google Earth export
- PMDG/Flight simulator export



All these data can be stored in a remote or local database, with their associated temporal slots of validity. Ai-Sky Data<sup>®</sup> can display the life cycle of the aeronautical objects and all their evolutions since their creation. The OLC (**O**bject **L**ife **C**ycle) permits to automatically compare two different revisions of a same object.

### 3.2.3 Procedure path and terminators coding

**Ai-Sky Data® : Codage Procédure ARINC 424**  
 One or more NOT REQUIRED leg attribute(s) are indicated!

**Procédure : GNSS 33**

Type : IAP  
 Type de navig : R [Area Navigation (RNAV).]  
 Catégorie d'Av : AB [Categories A and B.]

**Aerodrome : LFOV**

AD administrat : <EMPTY>  
 Elévation : 330.000 FT  
 Mag Var (°) : 002°W

N° SEQ	PT	W/P ID	OverFly	MAP	HLD	TD	TDV	RMD ...	THE	RHO	OBD ...	TM/D...	ALT ...	ALT ...	ALT ...	SPD ...	VRT ...	N
10	IF	OV400																N
20	TF	OV406	Fly by								322.4...	5.000...		1500 ...	1500 ...	170 K...		N
30	TF	OV408	Fly by								322.4...	5.000...		1000 ...	1000 ...	170 K...		N
40	TF	RW33	Fly by								322.3...	4.830...		640 F...	640 F...	130 K...		N
10	IF	OV402																N
20	TF	OV406	Fly by								52.34...	5.000...		1500 ...	1500 ...	170 K...		N
10	IF	OV404																N
20	HM	OV404	Fly by		Y	L			052.0...	2039...	232.0...	5794...		1900 ...	1900 ...	170 K...		N
30	TF	OV406	Fly by								232.4...	5.000...		1500 ...	1500 ...	170 K...		N

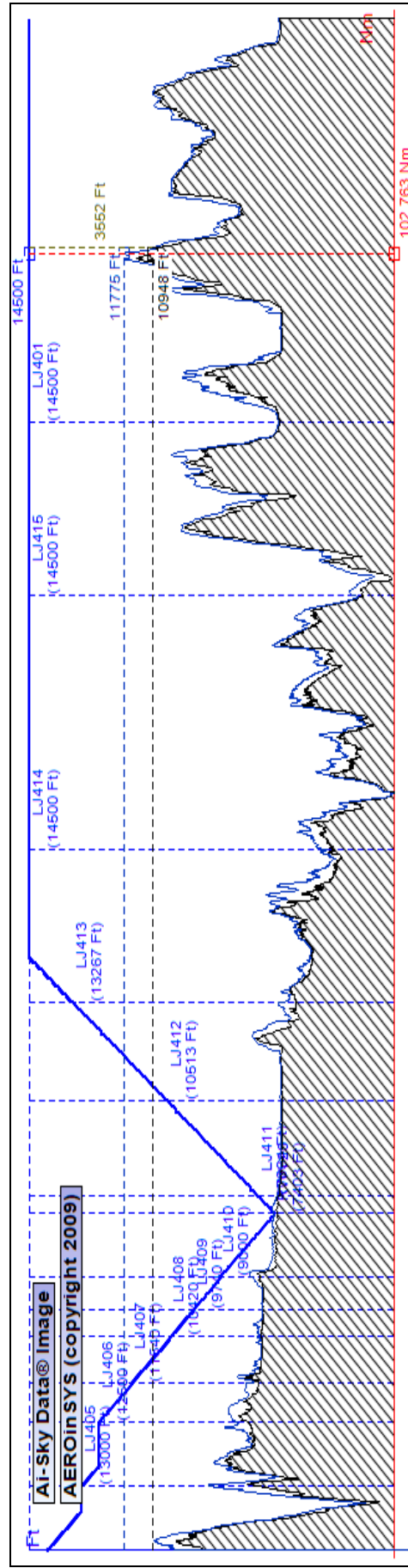
In the database the procedures are stored through Path and terminators (ARINC-424 coding).

Ai-Sky Data® permits the import of the procedures that have been designed with GéoTITAN® as well as an automatic generation of an ARINC-424 pre-coding of these procedures.

This pre-coding permits a first sequencing of the procedure segments, then completed by the edition module. Each intervention on the coding, through the editing module, is displayed in the geographical viewer, this one acting as a checking tool thus increasing the level of integrity of the coded procedure.

### 3.2.4 Procedure along track profile

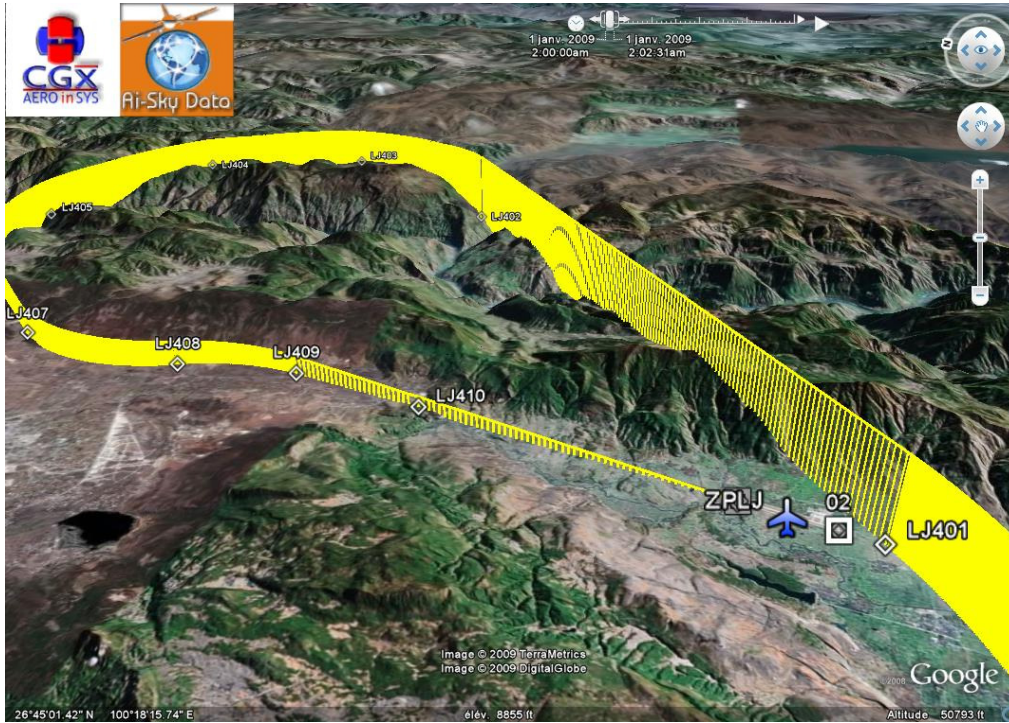
The along-track profile is based on a 3D procedure nominal geometry computation and an associated altimetric data (DTM). For RNP procedures, it computes also the protection area maximum altitude depending on the various procedure legs' RNP code.







### 3.2.6 Procedure 3D nominal geometry



The procedure 3D nominal geometry is made available in Open GIS formats (such as ESRI shape format) for any other software usage.

The procedures can be exported to Google Earth: the significant points and the 3D procedure nominal geometry are computed and displayed. The user can also export obstacles, airspaces, protection areas and RNP corridors.

### 3.3 The charting solution: AIP-GIS Charting

Please have a look at [AGC\\_Whitepaper\\_EN\\_v1-0.pdf](#).

### 3.4 The RAIM prediction Software: SAT4Flight®

The Procedure 3D nominal geometry is combined to a the new RAIM prediction solution SAT4Flight®.

[www.SAT4Flight.com](http://www.SAT4Flight.com): Quovadis ([www.quo-vadis.aero](http://www.quo-vadis.aero)) web service providing GPS RAIM prediction in PBN activities for Airlines, powered by SAT4Flight®. By combining US Coast Guards ALMANAC and NANU data with terrain data shadows, SAT4Flight® produces - in one dedicated service - prediction results for a single point or a single defined procedure as well as for a full airport, in departure and arrival configurations. If you are interested in accessing this service, please contact us at [sales@quovadisway.com](mailto:sales@quovadisway.com).

Please have a look at S4F\_QVS\_Fiche7-220210.pdf.

---

**End of document**

---

# INTEGRITY OF FLIGHT INSPECTION DATA

**Frank Musmann**  
Dipl. Ing.

Project Manager and System Engineer  
Aerodata AG  
Hermann-Blenk-Straße 34-36  
D-38108 Braunschweig, Germany

internet: <http://www.aerodata.de>  
email: [musmann@aerodata.de](mailto:musmann@aerodata.de)



## ABSTRACT

Flight inspection is a risk mitigation tool to ensure the use of a navigation aid is safe. It shall ensure that the probability of an aircraft accident caused by a faulty navigation aid is extremely remote. This safety level for navigation aids can only be achieved by periodic flight checks. According to the flight inspection results the navigation aid is adjusted, if required.

The overall process of getting flight inspection results is very complex. Many contributing factors can influence the correctness of the flight inspection result data, including databases, humans and equipment. Any error introduced by one of these sources typically propagates to the flight inspection result.

How can it be assured that the data measured by a flight inspection service is correct?

If these errors remain unidentified, they will be considered as characteristic of the navigation aid, thus requiring adjustment. This could even lead to adjusting a healthy navigation aid to out-of-tolerance conditions during flight inspection!

## PURPOSE

This paper addresses the main contributing error sources and provides solutions to improve the integrity of flight inspection results. Human factors as well as technical aspects are considered.

## BACKGROUND

Navigation aids shall provide safe navigation and landing of aircraft. Therefore navigation aids must be accurate and reliable to ensure the probability of an aircraft accident caused by a faulty navigation aid is extremely remote. As a risk mitigation tool Navaid Flight Inspection is conducted to ensure proper navigation aid performance in accordance with ICAO Annex 10 -[1].

The Navaids are adjusted according to the data measured by flight inspection. Flight Inspection Systems are designed to provide accurate measurements. But how reliable is this data? What are the most critical potential error sources influencing the integrity of the results determined by flight inspection.

## SUBJECT

For the analysis of integrity of flight inspection data one must distinguish between Accuracy and Integrity. The definition shall be as follows:

<b>Accuracy:</b>	The extent to which a measured value meets the actual value
<b>Integrity:</b>	The probability that a measurement is correct and free of undetected errors

**Table 1: Definitions**

Especially tasks carried out by human beings do not provide a high level of integrity. The following table lists the probability of errors caused by human action for different scenarios and will be referenced during this paper for estimation of error probabilities:

Description	Error Probability
General rate for errors involving high stress levels	0.3
Operator fails to act correctly in the first 30 minutes of an emergency situation	0.1
Operator fails to act correctly after the first few hours in a high stress situation	0.03
Error in a routine operation where care is required	0.01
Error in simple routine operation	0.001
Selection of the wrong switch (dissimilar in shape)	0.001
Human-performance limit: single operator	0.0001
Human-performance limit: team of operators performing a well designed task	0.00001

**Table 2: Human interface / Human Error -[3]**

According to Table 2, human tasks during flight inspection can be classified as “routine operation where care is required” or “simple routine operation”

For the analysis in this paper, we assume the flight inspection system has been designed properly, the software algorithms are correct and the accuracy of the system has been successfully verified. According to the definition this means the system provides sufficient Accuracy.

How about Integrity? What are potential sources of errors in a typical automatic flight inspection system?

**Contributing Errors:**

In a typical today’s flight inspection system one can identify the following contribution errors:

1. Incorrect Flight Path:  
The aircraft does not fly where the measurement shall be taken or variation of attitude affects the measurement
2. Incorrect Facility Database:  
The flight inspection database with Navaid coordinates and geometries is incorrect
3. Incorrect System Operation:  
The operator himself introduces errors by wrong run setup etc.
4. Incorrect Reference Position  
The position used as reference by the flight inspection system is wrong
5. Incorrect Receiver Data:  
The flight inspection receiver gives incorrect data
6. Incorrect Calibration Data:  
The calibration data applied to increase the accuracy of flight inspection receivers is incorrect thus introducing errors.

Any of these contribution factors leads to incorrect flight inspection data!

**1. Incorrect Flight Path:**

During a run the aircraft has to fly as accurate as possible on the desired calibration profile. Many of these profiles are hard to fly precisely by normal cockpit instrumentation since they are not supported by primary aircraft equipment (e.g. Offset Approaches, or Localizer crossings). This causes high workload for the flight crew. As a consequence of this the aircraft does not fly as intended with constant attitude.

This affects the measurements since the aircraft does not measure where the measurement is supposed to be done and field strength measurements suffer from variation of bank angle.

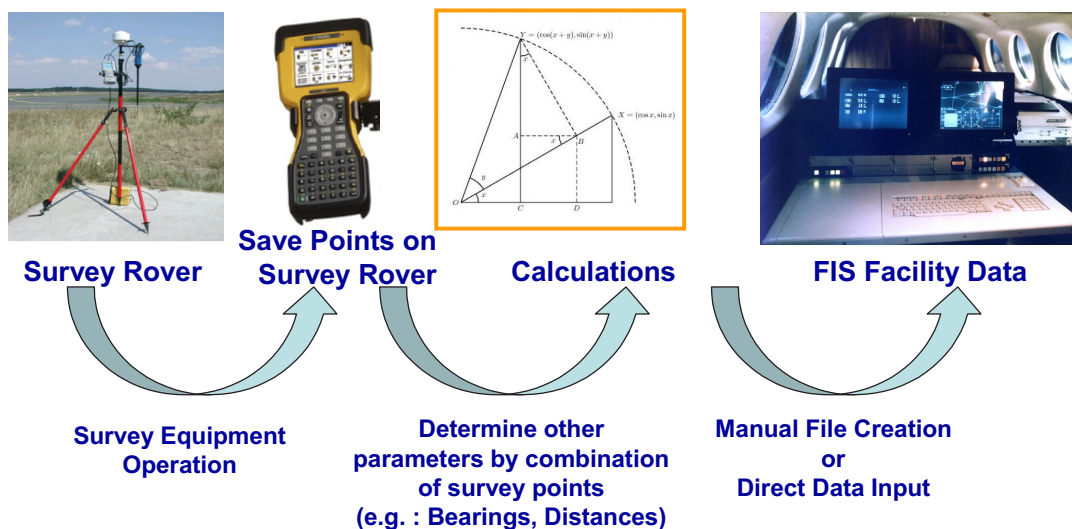
Incorrect Flight Path may also result from poor communication between flight crew and operator. A lot of information (information about the profile to fly) is typically shared by voice communication. This again leads to an increase of workload, and provides a high potential of errors by misinterpretation.

The probability of an error caused by incorrect flight path can be estimated following Table 2 to be:

**Probability of Incorrect Flight Path  $\approx 10^{-2}$**

**2. Incorrect Facility Database:**

Basis for the flight inspection facility database is a geodetic survey. Many human interactions make up this survey process: The survey equipment is manually initialized, locations are saved on the survey rover terminal. These coordinates are used in e.g. MS-Excel applications for calculation of bearings, distances or intermediate points. Afterwards the coordinates or values are entered into a file that can be read- or are directly entered to the flight inspection system. Many manual data handling steps are involved before this data reaches the flight inspection system.



**Figure 1: Typical Survey/Database Process**

The probability of an error caused by incorrect facility database can be estimated following Table 2 to be:

**Probability of Incorrect Facility Database  $\approx 10^{-2}$**

**3. Incorrect System Operation:**

A typical way how to operate the flight inspection system is to setup each run during flight before the measurement. In parallel the operator communicates via voice to the Navaid technician to inform him about measurement results (alignment, modulation etc.) and about how to configure the Navaid (alarm conditions, transmitter number etc). Misunderstandings may also occur by thinking in different units or perspectives (DDM vs.  $\mu A$  or left of centerline and fly-left).

These parallel tasks must be executed by a human being under stress conditions like:

- Time Pressure (Flight Plan, ATC clearance, fuel constraints, weather conditions)
- Hot or cold temperature
- Vibration
- Reduced oxygen partial pressure (non pressurized aircraft)

- Noise
- Limited workspace illumination

The probability of an error caused by incorrect system operation can be estimated following Table 2 to be:

**Probability of Incorrect System Operation  $\approx 3 \cdot 10^{-2}$**

**4. Incorrect Position Reference:**

Most automatic flight inspection systems used GPS in combination with a ground reference station to provide high accuracy. Many systems require a position initialization of the ground reference station (GPS-RTK). This position is manually entered to the ground station or recalled from previously manually entered data. During this process errors can occur very likely. Typical reasons are:

- Coordinates are entered with mixed up digits
- Wrong sign (N/S, E/W)
- Errors occur during format conversions  
(dd mm ss.ssss  $\leftarrow$   $\rightarrow$  dd mm.mmmmm)

Large errors can be identified by the operator if e.g. positioning crosschecks on threshold are performed, but require large effort for correction:

- Taxi back to the ramp
- Get to the Ground Reference Station again
- Re-Init the position
- Get back to the aircraft and try again

Smaller errors remain undetected and lead to wrong position reference.

Other reference position errors can be caused by GPS cycle slips. Sudden jumps in the position solution are the consequence when using GPS-RTK. This may not be expressed by any quality indicator (e.g. EPE).

The probability of an error caused by incorrect position reference when using RTK can be estimated following Table 2 to be:

**Probability Incorrect Position Reference  $\approx 10^{-2}$**

**5. Incorrect Receiver Data:**

The following error scenarios may affect the data integrity of the flight inspection receiver(s):

- Hardware failure
- Poor performance caused by environmental conditions  
(e.g. temperature)
- Error on analog interface

Dependency on environmental conditions and interface errors do affect only analog receivers. The error probabilities for the two types can be estimated as follows:

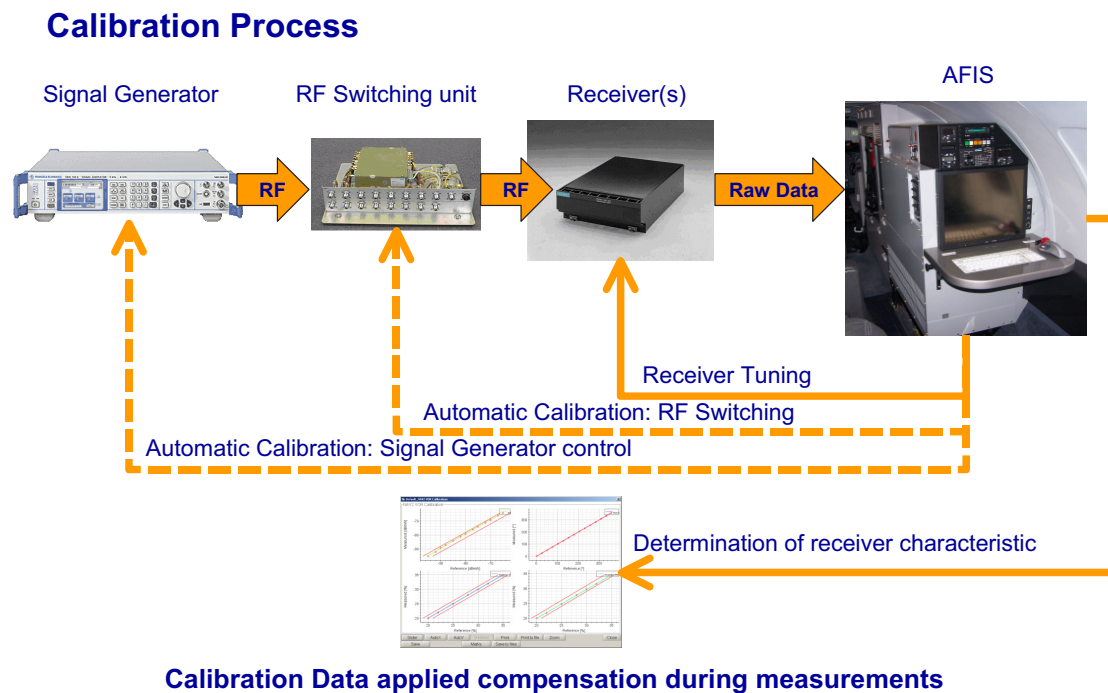
**Probability of Incorrect Receiver Data  $\approx 10^{-3}$  (analog receiver)**

**Probability of Incorrect Receiver Data  $\approx 10^{-4}$  (digital receiver)**

According to -[2] Flight Inspection Receivers shall be of highest quality. Digital flight inspection receivers compensate know effect internally. The use of analog receivers is therefore not recommended and not considered further in this analysis.

## 6. Incorrect Calibration Data:

Figure 2 shows the typical process of calibration:



**Figure 2: Typical Calibration Process**

As reference RF signals from a signal generator are provided to the flight inspection receiver. The characteristic of the receiver is determined through the measurement range of each parameter. This characteristic is applied by AFIS for compensation during measurements. The RF connection and signal generator steering during this process may be automatic (remote controlled by the FIS) or manual (manual antenna connection and manual signal generator setting).

Typical error scenarios during automatic calibration are:

- Equipment not at operational temperature (analog receiver)
- Signal Generator out of tolerance (a defect has occurred in between its own calibration interval)
- Abnormal signal loss due to defective RF cable

Additional during manual calibration process:

- Incorrect Signal Generator setting
- Cable loss of RF cable not considered correctly

Especially wrong signal generator setting during manual calibration provides a very high probability of error, since many signal generator settings are required for each reference point.

The error probability of incorrect calibration data can be estimated:

<b>Probability of Incorrect Calibration Data <math>\approx 10^{-2}</math></b>
---

**Resulting Error Probability:**

Based on the single error probabilities of the contributing error sources the probability of wrong flight inspection results can be determined. For small probabilities the following simplified equation may be used:

$$\text{Resulting Error Probability} \approx \sum_{i=1}^n \text{Error Prob. } i$$

(For small Probabilities)

**Equation 1: Resulting Probability**

**Probability of incorrect Flight Inspection Results (without improvement):**

The following table lists the probabilities of the contributing error sources without further improvements:

Error Scenario	Probability	Environment
Incorrect Flight Path	10 <sup>-2</sup>	Manually flown by pilots No FIS autopilot interface
Incorrect Facility Database	10 <sup>-2</sup>	Conventionally surveyed and manually entered facility data
Incorrect System Operation	3*10 <sup>-2</sup>	Manual system setup in flight before each run
Incorrect Reference Position	10 <sup>-2</sup>	RTK Solution, base station manually initialized
Incorrect Receiver Data	10 <sup>-4</sup>	Flight Inspection Receiver/Antenna system
Incorrect Calibration Data	10 <sup>-2</sup>	Typical Calibration Procedure

**Table 3: Error Probabilities (Without Improvement)**

According to Equation 1 the resulting probability can be calculated:

$$\text{Resulting Error Probability} \cong 7.01 \cdot 10^{-2} = 0,0701$$

**Equation 2: Error Probability Without Improvements**

This means for a Flight Inspection System without further improvements:

**“Seven out of hundred measurements are wrong!”**



## IMPROVEMENTS

It has been demonstrated, that the resulting probability of incorrect flight inspection data is approximately the sum of contributing probabilities. What can be seen from this in order to achieve a low resulting error probability (high integrity)?

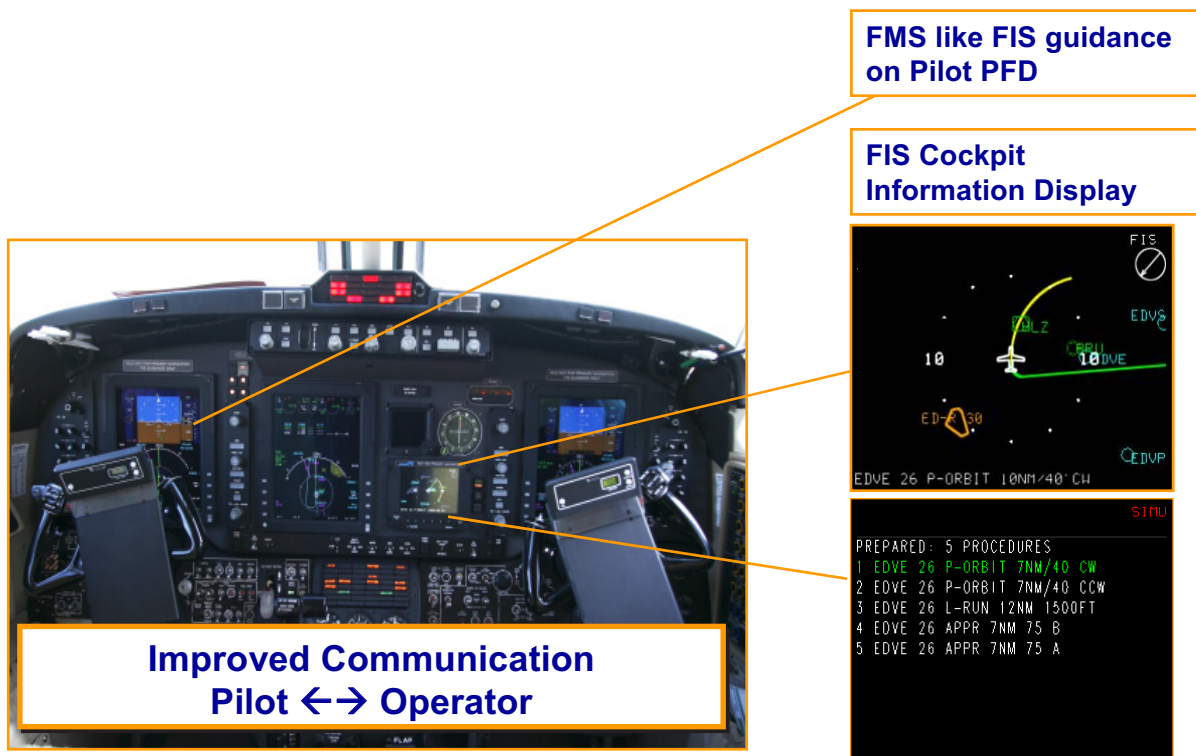
- It makes not much sense to improve just the error probability of one contributing error source (ideal: equal probabilities of contribution error sources)
- All contribution error sources must have an error probability approx. one order less than the maximum allowable resulting error probability

In order to improve the integrity of the flight inspection system the following means are available to reduce the individual error probability to be better than  $10^{-4}$  :

### 1. Improved Flight Path

The probability of measuring at a wrong flight track has been improved by:

- a) Improvement of communication between flight crew and AFIS operator by Cockpit Information Display
- b) Providing FMS-like FIS guidance on pilots instruments
- c) Provide autopilot coupling

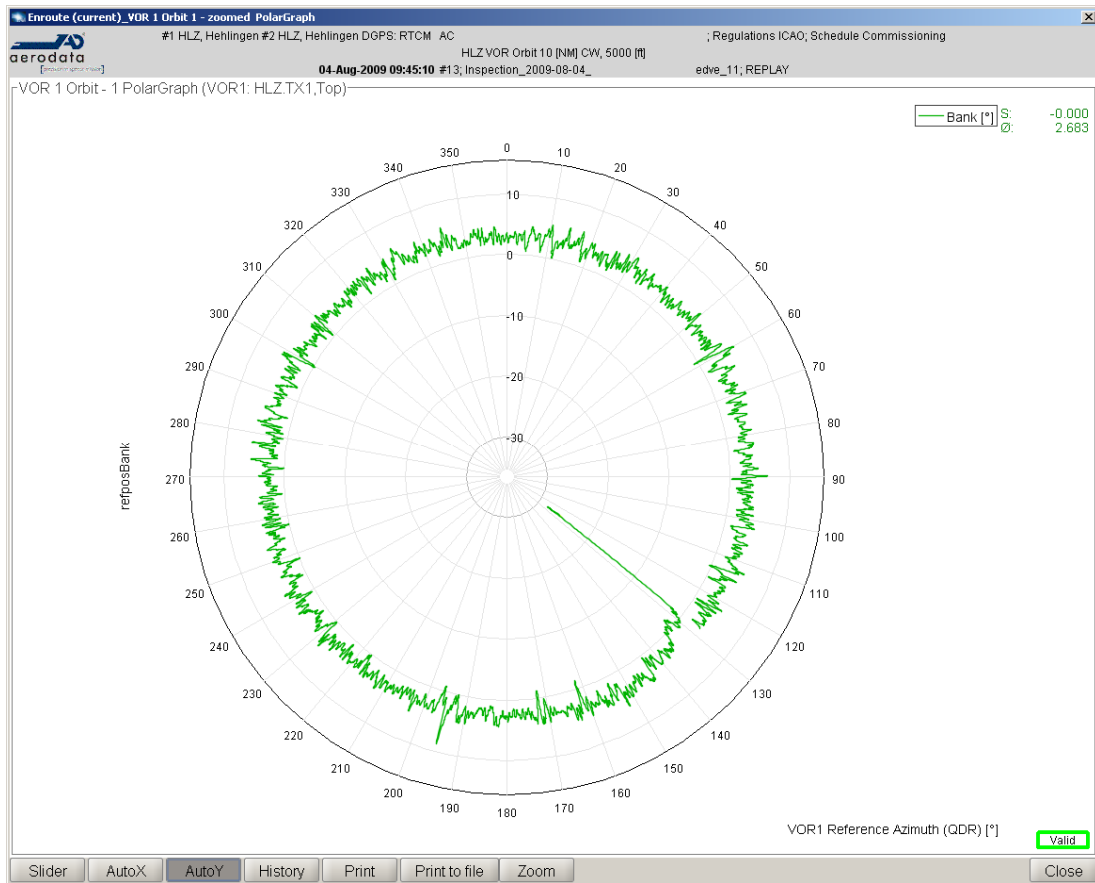


**Figure 3: Improved Communication between Pilot and Operator**

The FIS Cockpit Information Display shows the flight inspection aircraft in relation to the calibration profile on a Jeppesen based moving map. Alternatively all flight inspection runs prepared on AFIS can be displayed in text format which is intuitively to read. The positive effect of this display regarding error reduction has been confirmed by all flight inspection service providers using this feature.

Besides this positive effect on integrity, the FIS Cockpit Information Display further provides a reduction of aircraft operation costs, since it dramatically reduces the overall flight time required for calibration flights.

Precise flying of the flight inspection profile is supported by providing flight guidance on the pilot's Primary Flight Display (PFD). The pilot can select the FIS as additional navigation source like he selects his FMS. The AFIS controls the course pointer, lateral and vertical deviation as well as distance indication. The FIS waygenerator guides the pilot from the present position to the Start point of the flight inspection profile. At any time the autopilot can be coupled to the FIS guidance signals. This ensures the aircraft is fully established on the calibration profile when the start point of the measurement is reached. It further provides to fly all kinds of flight inspection profiles (including offset approaches or orbital flights) precisely with constant bank by autopilot:



**Figure 4: Constant Bank Angle during Orbital Flight (flown with FIS Guidance and Autopilot)**

Using the Autopilot for flying flight inspection maneuvers reduces stress and fatigue of pilots and frees resources for monitoring and crosschecks which again reduces the probability of errors.

By these features, the probability of incorrect measurements caused by an incorrect flight path can be reduced. The remaining probability can be estimated as:

**Probability of Incorrect Flight Path  $\approx 10^{-4}$   
(With Improvement)**

## 2. Improved Survey Process

The survey process can be significantly improved by:

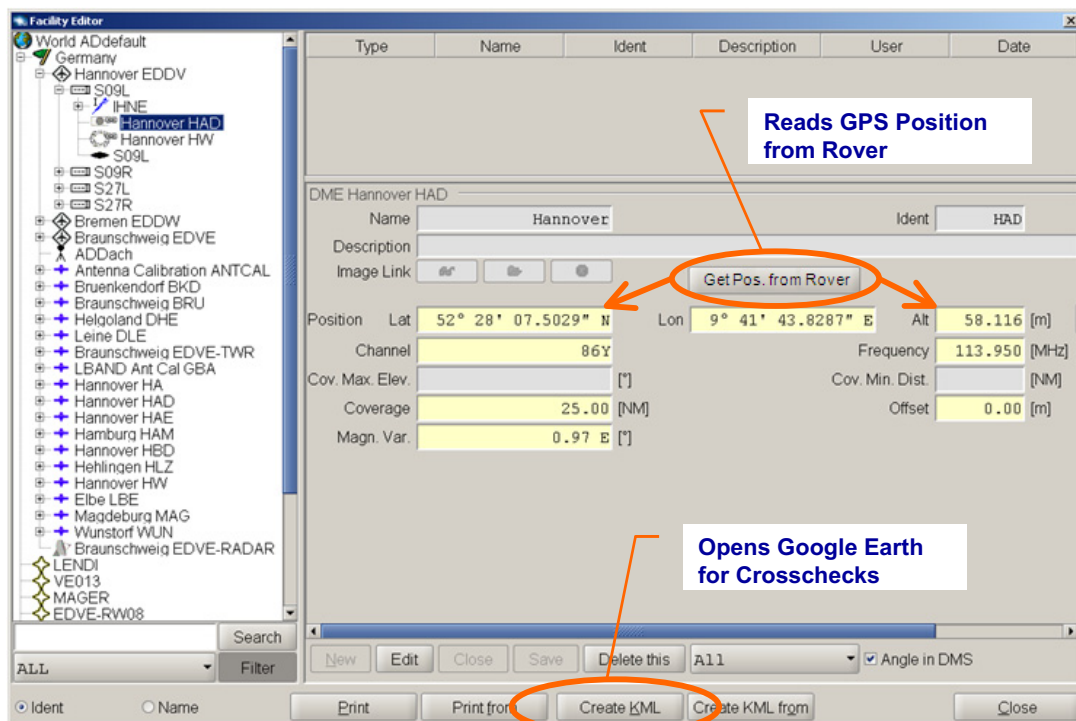
- a) avoid manual data handling and operation during the survey process.
- b) Provide database crosschecks tools
- c) Directly load survey data from survey rover to AFIS

A tablet PC with sunlight readable display and touch screen runs an easy to use software dedicated for flight inspection survey.



**Figure 5: Flight Inspection Survey PC**

Using a FI Survey PC one can directly create the database. When complete the file can be transferred to the AFIS on board the flight inspection aircraft without any manual data operation. The user interface of the software is intuitively to use similar to the AFIS database editor. This FI survey PC interfaces the rover GPS receiver and allows to directly save coordinates as e.g. as runway threshold or DME coordinates. It also provides tools to determine coordinates of points which are not directly accessible during survey.



**Figure 6: Flight Inspection Survey Software**

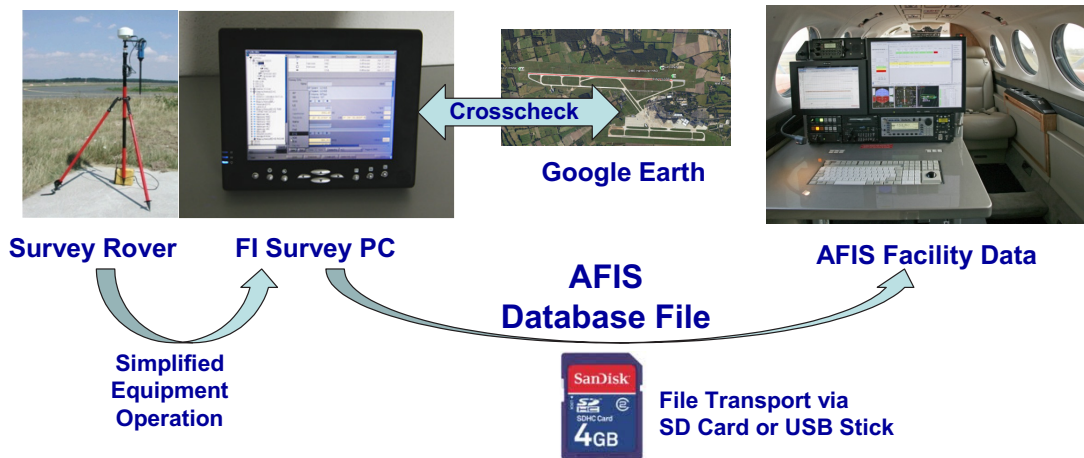
Once the database has been created in this way, it can be crosschecked using Google Earth (internet connection is not required since Google Earth can work offline as well).



**Figure 7: Database Crosscheck using Google Earth**

Errors caused by wrong survey equipment operation are easily detected.

After successful crosscheck the database file is directly transferred from the FI Survey PC to the AFIS on board the flight inspection aircraft. A checksum ensures that the file content is not altered.



**Figure 8: Improved Survey/Database Process**

The improved survey process described above avoids manual data handling and provides a reduced probability of errors. The remaining probability can be estimated as:

**Probability of Incorrect Facility Database  $\approx 10^{-4}$   
(With Improvement)**

### 3. Improved System Operation

The following improvements have been developed to reduce the probability of errors during system operation:

The AFIS system setup for the entire flight inspection mission is prepared on a office PC (laptop) before flight. This allows to setup the AFIS without being under time pressure or exposed to other environmental stress. The mission setup is transferred to the AFIS via USB memory stick or SD-memory card. Adaptation of the mission during flight is possible at any time in a drag and drop manner. This allows e.g. to rearrange the order of runs according to ATC clearances.

Once a mission for a facility has been prepared, it is crosschecked and archived. When the next calibration of this facility is required, the mission is just reloaded by AFIS. This avoids to setup the same mission every time again and again and reduces the probability of errors.

Using the FIS Cockpit Information Display (see Improved Flight Path) pilots perform also a crosscheck for each run.

Misunderstandings between AFIS operator and Navaid ground technicians are avoided by using a data downlink. The Navaid ground technician is provided with a portable data downlink station (laptop PC). The flight inspection data measured in flight is transmitted to the ground where the Navaid technician can monitor online flight inspection graphs and reports. The result of Navaid adjustments is directly visible to the technician. Results are available in different units like DDM,  $\mu A$  and degree to avoid confusion when ground technicians and flight inspectors are used to work with in different units.

The use of the above listed features/procedures allows to reduce the remaining error probability caused by incorrect system operation to:

**Probability of Incorrect System Operation  $\approx 10^{-4}$   
(With Improvement)**

#### 4. Improved Position Reference

In order to improve the integrity of the Position Reference System and for ease of operation the following improvements are recommended:

Instead of calculating GPS corrections at the ground reference station, the PDGPS ground station transmits just GPS L1 and L2 raw data to the aircraft. All calculations of GPS corrections are calculated on board of the flight inspection aircraft. By this technique no programming or position initialization of the ground station is required. The location where the PDGPS ground station is setup is defined by the operator on board the aircraft by selection out of the flight inspection database (refer to Improved Survey Process). The GUI filters the database and shows only the available PDGPS locations for the facility under inspection. This operation avoids to a high extend errors caused by position initialization. The remaining probability of an error during position initialization is reduced to  $10^{-4}$ .



**Figure 9: PDGPS Ground Reference**

The PDGPS Technology is designed to provide highest integrity. It has been proven that PDGPS is able to detect GPS cycle slips. It has been demonstrated that the probability of a false position reference caused by GPS cycle slips is less than  $10^{-7}$ .

**Probability of Incorrect Position Reference  $< 10^{-4}$   
(With Improvement)**

#### 5. Improvement of Calibration Process

The analysis of the calibration process has shown that there is a high potential for errors caused by the calibration process. Only if all elements of the calibration process are subsequently checked one can ensure that the accuracy improvement by application of calibration data works as intended.

Once the automatic calibration has been executed and the calibration data have been determined their integrity is checked by the Receiver Check:

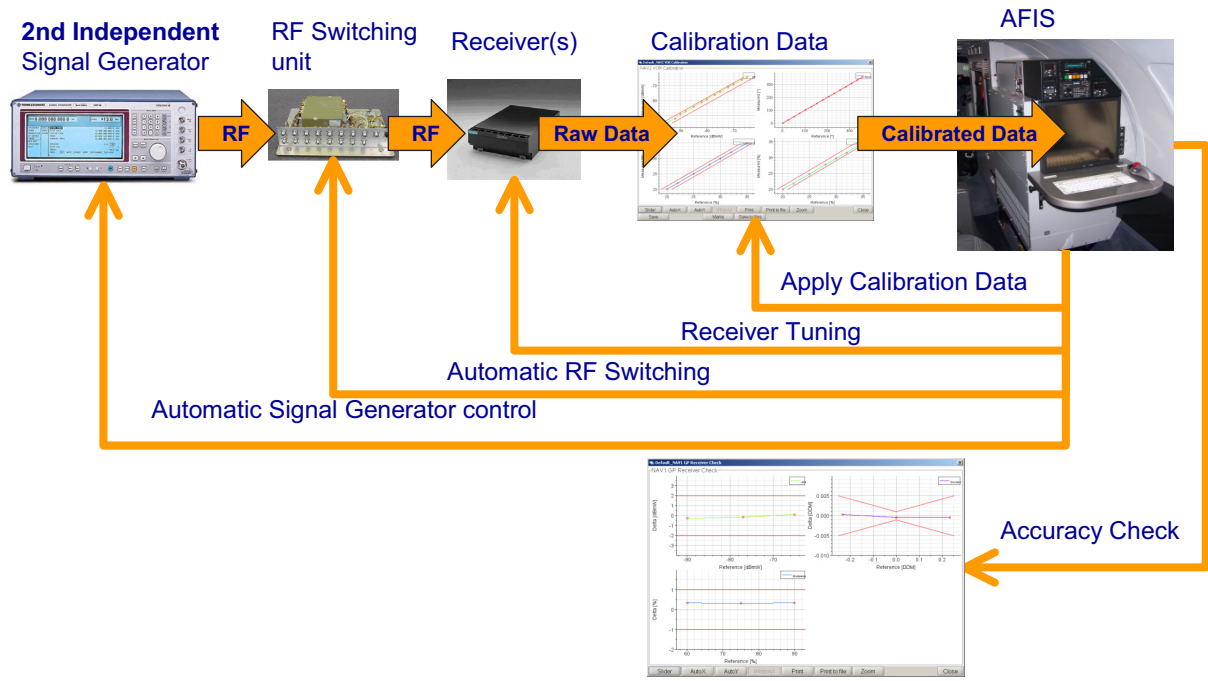


Figure 10: Automatic Receiver Check Process

The Receiver Check process is similar to the calibration process: A second independent signal generator is used as reference for this check. RF Signals are provided through automatic RF switching unit to the receiver. The receiver provides raw data output to which the calibration data (from calibration process) is applied for accuracy improvement. The output of this calibrated receiver data is now compared against the reference as commanded to the signal generator. The results of this check are provided to the operator in graphical and alphanumeric format.

A Receiver Check Report is created automatically which documents the actual system accuracy for quality management purposes. Automatic alerts appear if a tolerance violation occurs:

### Example of Error Detection:

#### Receiver Check Report:

**NAV1 GP**  
 Manufacturer: Honeywell AD  
 Model Number: AD-RNZ-850  
 Nickname: NAV1 GP  
 Serial Number: 077

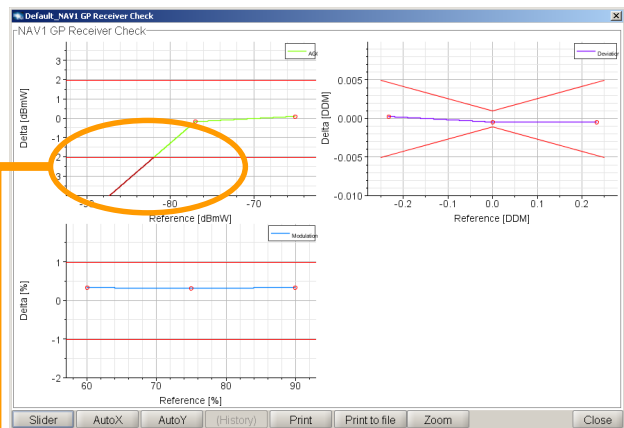
**Receiver Check Environment**  
 Cable Loss: -7.600 dBmV  
 Deviation: 0.000 DDM  
 Frequency: 332.000 MHz  
 Modulation Depth: 80.000 %  
 RF Level: -56.000 dBmV

**AGC**  
 Last Receiver check at 2010-04-29 14:47:54 UTC by Musmann

Reference [dBmV]	Measured [dBmV]	Delta [dBmV]
-90.000	-95.000	-5.000***
-77.000	-77.143	-0.143
-65.000	-64.867	0.133

**Deviation**  
 Last Receiver check at 2010-04-26 13:34:26 UTC by AD-Administrator

Reference [DDM]	Measured [DDM]	Delta [DDM]
-0.2330	-0.2327	0.0003



#### AFIS Alert Window:

No	Time	Last Time	Count	Text	Data	Ignore
1	14:52:44	14:52:44	1	Connection fail	Spectrum Analyzer (FSP)	<input type="checkbox"/>
2	14:52:46	14:52:46	1	Connection fail	Oscilloscope (TDS)	<input type="checkbox"/>
3	14:52:46	14:52:46	1	Startup complete		<input type="checkbox"/>
4	14:52:51	14:56:43	2	Receiver Check out of toleran...	NAV1 GP AGC	<input type="checkbox"/>

Figure 11: Receiver Check Reports

This process allows to check the real accuracy of the system and ensures high level accuracy, since the following error sources are identified:

- Signal Generator fault (by check with independent signal generator)
- Faulty RF Cable
- Fault in calibration data
- Receiver fault

**Probability of Incorrect Calibration Data  $\approx 10^{-4}$   
(With Improvement)**

**Probability of incorrect Flight Inspection Results (with improvement):**

Table 4 shows the integrity analysis of a flight inspection system providing the above described features for improvements.

<b>Error Scenario</b>	<b>Probability</b>	<b>Environment</b>
Incorrect Flight Path	$10^{-4}$	AFIS Autopilot coupling and Cockpit Information Display
Incorrect Facility Database	$10^{-4}$	Automated Survey Process
Incorrect System Operation	$10^{-4}$	Mission Preparation in Office, Crosscheck by Pilots, Navaid Technicians
Incorrect Reference Position	$10^{-4}$	PDGPS Position Reference
Incorrect Receiver Data	$10^{-4}$	Flight Inspection Receiver/Antenna system
Incorrect Calibration Data	$10^{-4}$	Automatic Calibration Procedure <b>and</b> Automatic Receiver Check

**Table 4: Error Probabilities  
(With Improvement)**

According to Equation 1 the resulting probability can be calculated:

**Improved Error Probability  $\rightarrow \cong 6.0 \cdot 10^{-4} = 0,0006$**

**Equation 3: Error Probability With Improvements**

## **Conclusions**

The data measured during flight inspection can be affected by the following potential error sources:

1. Incorrect Flight Path
2. Incorrect Facility Database
3. Incorrect System Operation
4. Incorrect Reference Position
5. Incorrect Receiver Data
6. Incorrect Calibration Data

Since each error source can lead to wrong results, a high level of integrity can only be achieved by improving the contribution errors sources to a common high integrity level.

Human beings involved in processes of the contributing error sources induce a high potential of errors due to the natural limit of human performance.

The integrity of a flight inspection system can dramatically be improved by the means described in this paper:

- FMS – like FIS Guidance with Autopilot coupling
- FIS Cockpit Information Display
- Mission Preparation in Office
- Data Downlink and Crosscheck by Navaid technician
- PDGPS Position Reference Technology
- Automatic Receiver Check

By these improvements the resulting integrity of the data measured by a flight inspection system can be improved by more than two orders of magnitude.

## **REFERENCES**

- [1] ICAO, Annex 10
- [2] ICAO, DOC 8071
- [3] Charles P.Shelton, “Human Interface/Human Error”



# Analysis on Flight Test Results of GBAS in China

Lin Bin<sup>1</sup>, Liu Kun<sup>2</sup>, Li Haijin<sup>2</sup>, Wang Xiaowang<sup>1</sup>, Zheng Jinhua<sup>1</sup>

(<sup>1</sup> 20th Institute of China Electronic Technology Group Company, XIAN, CHINA 710075)

(<sup>2</sup> Flight Inspection Center of CAAC, BEIJING, CHINA 101312)

(National Ministry of Science and Technology 863 Project, ID: 2006AA12A102)

## Abstract

As a new type precise approach and landing system based on satellite navigation system, Ground Based Augmentation System(GBAS) is greatly different with traditional ground-based radio precise approach and landing system on system architecture and application, therefore, flight inspection for GBAS system is also different with ground-based radio system on contents and methods for flight inspection. This paper presents the performance analysis of GBAS ground subsystem according to the flight tests results on several china airports, those flight tests were carried out by China Flight Inspection Center of CAAC. More, this paper also presents the inspection method and contents for those flight tests according to ICAO's standards on flight inspection. The analysis showed that GBAS system can meet the accuracy requirements for CAT I approach and landing navigation system, VDB signal coverage and data continuity also meet the test requirements.

## Introduction

In China , CAAC has started the feasibility study of GBAS in theories for a long time. In recent years, CETC20 focuses on the development of GBAS ground station adapted to China environment, and a GBAS ground station prototype has been installed in Linzhi airport for Research & Development purpose.

In the last two years, cooperating with China Flight Inspection Center of CAAC,

much work has been done on the flight inspection side. We carried out much more flight test at several airports in China to test the performance of prototype GBAS system due to the reason that navigation system's performance is changed with the constellation's movement. Different time range and different location's test will help us create the confident statistics on GBAS performance. The flight tests happened at Mianyang airport and NanChong airport, SiChuan province, ChiFeng airport, NeiMengGu Autonomous Region, HanDan airport, HuBei province and YinChuan airport, NingXia Autonomous Region. Approach times at different airports showed as following tables:

Tab. 1 Approach times at different airports and analysis result

Airport	Approaches
Mianyang	3
NanChong	10
HanDan	21
YinChuan	10
Total	44

## Data Processing Methodology

In this paper, the positioning result generated with RTK data from the airborne RTK receiver is considered as the true flight trajectory, and used to compare with the positioning result generated with MMR(GLS) data from the airborne MMR. When the RTK (truth) data and MMR (Test) data are prepared, it is necessary to time synchronize them and transform them to an appropriate coordinate system.

As the true data and MMR data may have different transmitting rate, and the movement in one second flight is more than 100 meters, to synchronize the time between RTK data and MMR data, during the processing, the true data should be cut and then interpolated to match the MMR data.

Although the true data and the MMR data are all based on X, Y, Z: WGS-84 Coordinate System, it also need to apply a coordinate transformation from X, Y, Z coordinates to E, N, U (East, North, Up) coordinates, because the data is generated by different airplane on different runways, the runways in different place have different FAS data, and not all the flights are in the same speed, for example, there are total 6 runways, including 1 runway in Mianyang, 1 runway in Nanchong, 2 runways in Handan and 2 runways in Yinchuan. As all the approaches are not performed on the same runway, to match the different approaches with different runways, the data should be transformed into an appropriate coordinate system, and processing with a uniform interval, 0.002nm in this paper. Each approach record is started at 6nm away from the threshold of the runway and its length is 7nm.

After above pre-processing, the true data and the MMR data are prepared for deeper analysis. The next step is the final statistical analysis, this statistical data includes the mean, two sigma and six sigma of the flights and plots. And then, the NSE (Navigation System Error), FTE (Flight Technique Error), and TSE (Total System Error) for all approaches are calculated. The NSE (Navigation System Error) is the difference between the Truth and MMR position data. The TSE (Total System Error) is computed by the error from the Truth flight path to the approach path. FTE (Flight Technique Error) is generated by the difference between the TSE and NSE. This error is due to the performance of the airplane

and the pilot. The Figure 1 is both Truth and MMR data of the 7<sup>th</sup> approach on 23<sup>rd</sup> runway in Handan. East axis is the approach path and (0, 0) is the runway threshold.

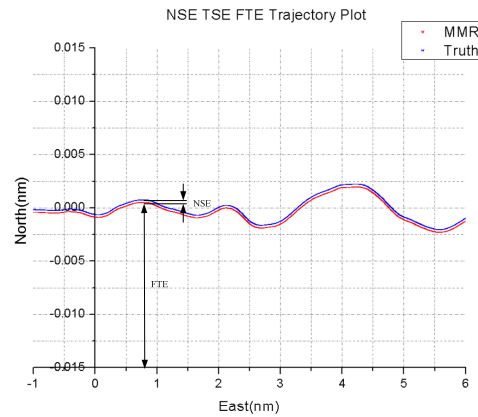


Figure 1 Illustration of NSE, TSE, FTE

## Result And Analysis

All the approaches are generated by 3 inspection airplanes of China Flight Inspection Center of CAAC on 6 runways in 4 different airports. The inspection airplanes are B3666, B3667 and B9330. There are 3 testers on the airplane for each test, one is responsible for airborne inspection platform, one is responsible for the flight control interface, and the other one is responsible for observing MMR data. During the test, the transmitted DGPS data of the RTK and GBAS station are derived from the same observing source. In addition, in some approaches, the pilots performed different operations for special test, such as approaches up or left/right the scheduled path for specific distance. In this analysis, approaches in such conditions are excluded.

All the flight data is input into and processed by self-programmed software. The Figure 2 and 3 are the flight test results of the approaches guided under GBAS signal. The Figure 2 is the lateral trajectory plots and the Figure 3 is the Altitude trajectory plots. The thin color lines are the individual guided missed approach paths. The black thick line is

the mean of all the flights. The red thick boundary lines represent the two and six sigma estimates of the data about the mean. After the trajectory plots, there are Illustration of NSE for all the Approaches, Figure 4 shows the lateral NSE trajectory and Figure 5 show the vertical NSE trajectory.

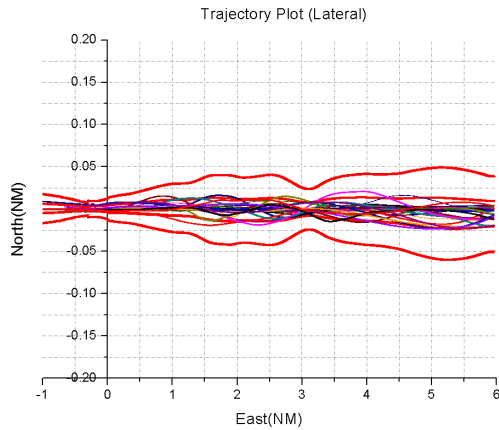


Figure 2 Lateral Trajectory plot

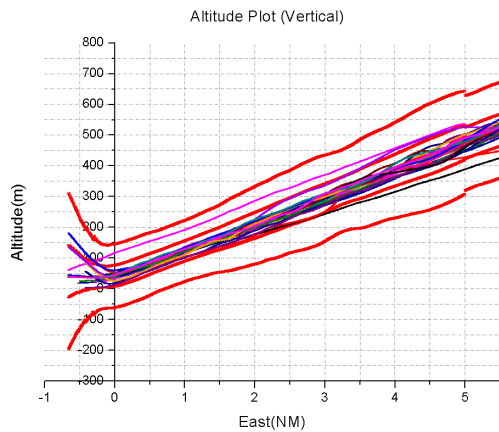


Figure 3 vertical Trajectory plot

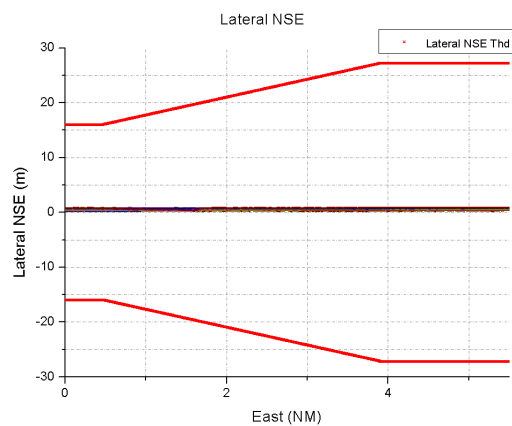


Figure 4 lateral NSE Trajectory

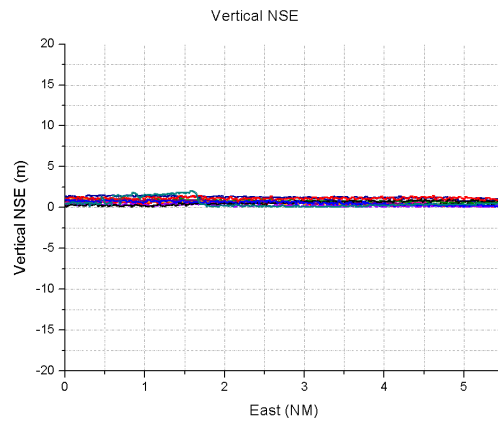


Figure 5 vertical NSE Trajectory

The result of the performance for the approaches are shown in the table 2.

Table 2

Distance to Threshold (meter)	Navigation Sensor Error(NSE)	
	Lateral Accuracy (meter,95%)	Vertical Accuracy (meter,95%)
0	0.56759	0.76945
874	0.56117	0.8549
1200	0.55733	0.84547
4200	0.58256	0.66406
7800	0.58831	0.76709

Except the above analyzed results, the condition of VDB signal strength and coverage is also very important for the performance of GBAS. As the requirement of the FAA-E-2937A, the minimum field strength shall not be less than 215 V/m (-99 dBW/m<sup>2</sup>) for a horizontally polarized signal and 136 V/m (-103 dBW/m<sup>2</sup>) for the vertically polarized signal.

Figure 6 shows the VDB signal strength and coverage in lateral, and Figure 7 shows the VDB signal strength and coverage in vertical. Due to the airborne devices, the signal strength showed in following figures can not be separated as horizontal signal strength and vertical signal strength, which is needed to improve for flight tests in the future.

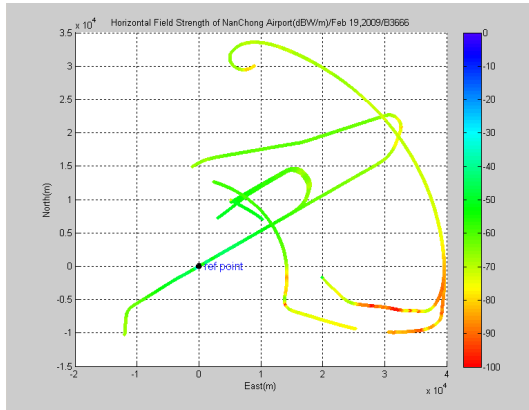


Figure 4 VDB signal strength in lateral

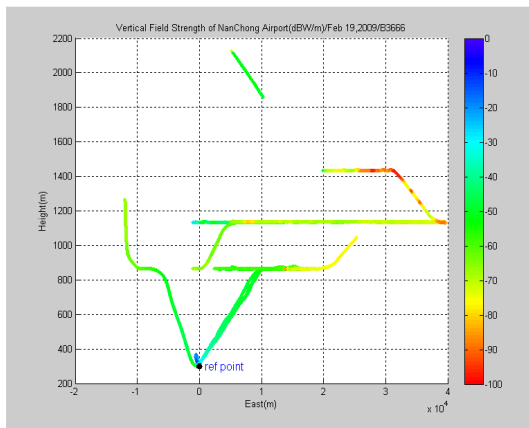


Figure 4 VDB signal strength in vertical

## Conclusion

The flight test described in this paper is the first time of the performance test for GBAS guided approaches in China, and the results are extremely significant. Through the process and analysis of the data generated from the test, the Approaches trajectory and the NSE, TSE, FTE trajectory are illustrated. The results show that the GBAS is able to provide information which can match the precision requirements of navigation for Category I Approaches. This indicates that the GBAS can support safer and more valuable techniques for the final area navigation. And, this technique has lower cost and more convenient than the current techniques.

## References

[1] "Flight Test Results of a MOPS Compliant LAAS System to Provide

Guided Straight and Curved Path Departures and Missed Approaches", ION GNSS 18th International Technical Meeting of the Satellite Division, 2005.  
 [2] "Preparation for GBAS at Braunschweig Research Airport — First Flight Test Results", ION NTM, 2006  
 [3] "Flight Test Results of an Integrated Wideband-only Airport Pseudolite for the Category II-III Local augmentation system", IEEE, 2002.

# Space Weather: It's Effect on GNSS, DGNSS, SBAS, and Flight Inspection

*J. David Powell, Aero/Astro Dept., Stanford University, Stanford, CA*  
*Todd Walter, Aero/Astro Dept., Stanford University, Stanford, CA*

## Abstract

Space weather, primarily the ionosphere, produces the largest GNSS errors. This paper reviews the ionosphere's effect on satellite ranging measurements and discusses how the effect is accounted for in receivers. In addition, the variations in the ionospheric delay will be discussed along with historical ionosphere delay data on normal days as well as some of the solar storm days with the highest variations. Scintillation, a highly random anomaly of the ionosphere, will also be discussed and data presented that demonstrates the effect of this phenomenon. These two ionospheric effects will then be examined in terms of their effect on differential GNSS, a common system used by many flight inspection agencies worldwide. The performance of the FAA's WAAS during normal and anomalous ionospheric periods will also be presented. Finally, the 11-year ionosphere cycle will be discussed along with the implications on GNSS. Widespread use of GNSS for aviation has largely occurred during a relatively quiet time in solar activity; however, we are now emerging from that quiet period and the time of maximum solar activity is expected to occur around 2013 with likely increased ionospheric effects. Flight inspection activity may be affected; therefore, it will be prudent for flight inspectors to monitor ionospheric activity to ensure the integrity of their data.

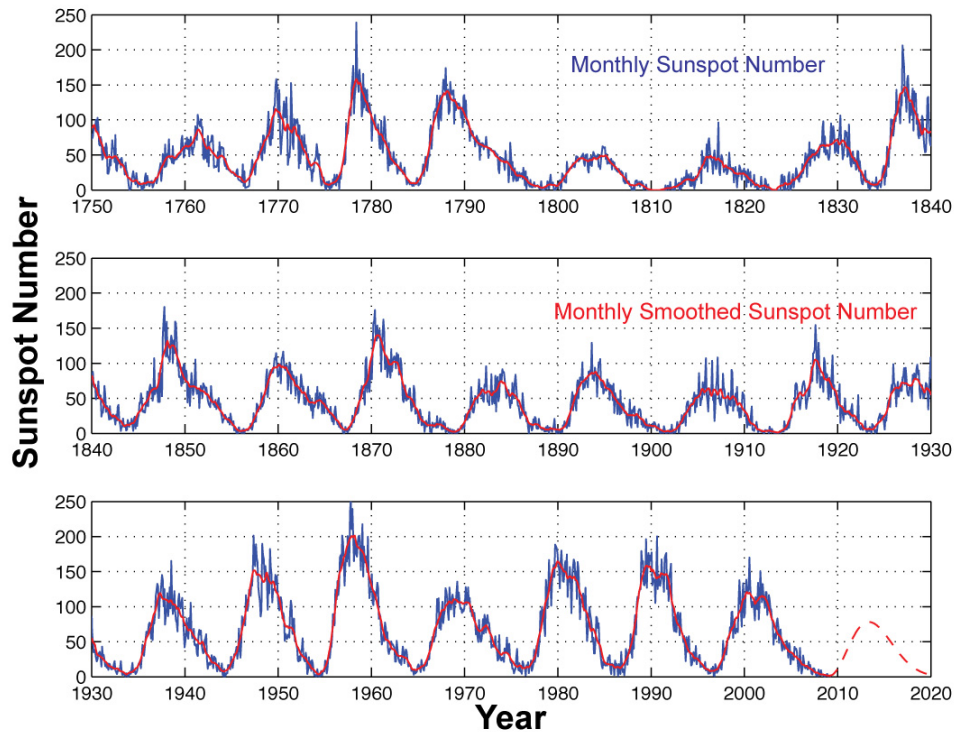
## Introduction

*Space Weather* has been in the news because of the possibility of intense solar activity damaging power grids and communications, thus causing trillions of US\$ worth of damage. Efforts are being undertaken to improve our ability to predict these events [1]. Likewise, the phenomenon can also have an effect on GNSS accuracy. Most of the GNSS transmissions are through the vacuum of space where they are not affected by solar activity; however, they are affected as they pass through the ionosphere during approximately the last 1000 km before reaching the earth. The signals travel at the speed of light (299,792,458 m/sec) through space, but are slowed slightly by varying degrees as they pass through the ionosphere. Both normal and unusual solar activities produce variations in the effect of the ionosphere on GNSS signals. Ionospheric models are used to remove as much of the variability as possible, but there are random components that create errors in the position fixes. We use the term *Space Weather* here to describe the GNSS navigation error sources that occur due to the ionosphere. There is also some signal delay in the troposphere; however it is small and not significantly affected by solar activity so it will not be addressed in the paper.

The paper will first discuss the magnitude of ionospheric delays and its variation over time, both over short time frames and over the centuries. This will be followed by an explanation of how the various types of GNSS receivers deal with ionospheric issues. Finally, the impacts on flight inspection activities will be assessed.

## Characteristics of the Ionosphere

The ionosphere's effect on GNSS range measurements is highly variable. During a low solar activity period it would typically cause vertical (zenith) range measurement delays between 1 m at night to 5 – 10 m during the day. During peak periods of solar activity, the delay can vary between 1 m at night to 100 m during the early afternoon [2]. Perhaps even more important from a navigation or flight inspection perspective is that there can be large spatial gradients in the ionosphere's effect on range measurements. Depending on the type of receiver used, the gradient could cause significant position errors. In addition to range measurement errors, there can also be *scintillation*, which can cause power fades of 30 dB-Hz that typically last a few tenths of a second [3, 4]. Figure 1 illustrates the solar cycle history for the last 250 years. It is a plot of the *sunspot number*, which has been observed by astronomers over the centuries. It has been determined in more recent history that the variability of the ionospheric delay is highly correlated with the sunspot number.



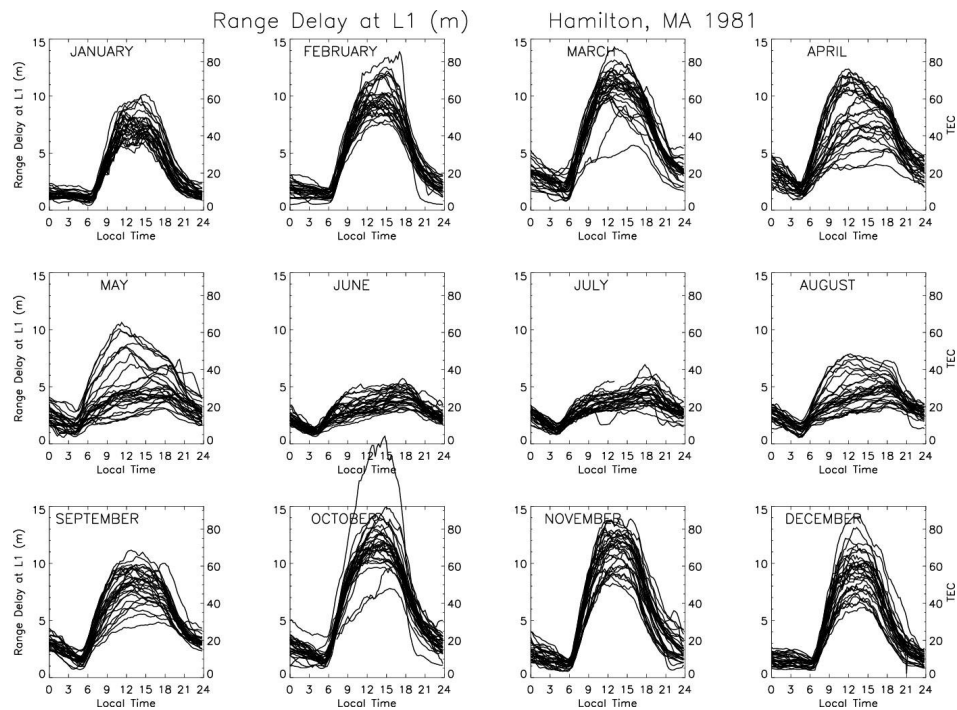
**Figure 1. Sunspot Observations [5]. Current data and projections can be obtained from [www.swpc.noaa.gov/SolarCycle](http://www.swpc.noaa.gov/SolarCycle)**

There are a number of observations to be made from Fig. 1: 1) “Solar maximums”, on average, occur every 11 years, but the period has varied by as much as 4 years. 2) The average sunspot number at the peak of the solar cycle has varied by a factor of 2. 3) We are now (2010) very near the low point in solar activity and the next solar maximum is predicted to be one of the lower ones and arrive around 2013 – 2014. However, there is not universal agreement on these predictions nor have prior predictions always been accurate. 4) Even when the average (red line in Fig. 1) sunspot number is relatively low, there can still be monthly peaks (blue) and daily bursts that greatly exceed the average. Those monthly and daily variations are reduced during the solar minimum periods.

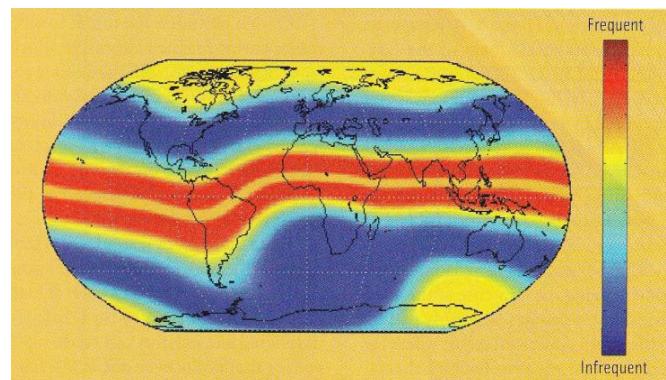
During solar maximum periods, the increased solar activity causes the sun to send out bursts of high energy x-rays and protons that increase the density and thickness of the ionosphere. This activity also increases the electron content of the ionosphere which directly contributes to changes in the range measurements from GNSS satellites.

Figure 2 shows the effect of the ionosphere on *zenith* range measurements (i.e., those from satellites directly overhead) through the daily cycle during the solar maximum period in 1981. Note the pronounced daily effect that is highest slightly after noon local time. Also note the large variations from month to month during this solar maximum year and, for some months, the large variations from day to day (e.g., April, May, and October).

*Scintillation* acts in a very different way and at different times of the day. Its effect is worse at or near solar maximum years due to increased high energy emissions from the sun, just like the range error measurements discussed above. However, with scintillation, the effect is to reduce the received power and phase coherence of the GNSS signals which can cause a loss of lock on the signal for short periods. The loss of lock results in no GNSS measurement, as opposed to the range measurement errors previously discussed. The frequency of these disturbances varies greatly based on the distance from the geomagnetic equator as shown in Fig. 3.



**Figure 2. Measured ionospheric zenith delays during the 1981 solar max period in Massachusetts [8]**



**Figure 3. Scintillation map showing the frequency of disturbances [3]**

Fortunately, the effect of scintillation is minimal throughout much of North America, Europe, Northern Asia, Australia, and New Zealand; however, much of South America and the equatorial regions in Africa and Asia will be affected much more severely than other parts of the world. During periods near solar maximum years, the red areas in Fig. 3 will experience intense scintillation on the order of 100 days per year while the dark blue areas less than 10 days per year [3]. Unlike the range errors that occur during the daylight hours, scintillation mostly occurs during a time shortly after sunset, which is illustrated in Fig. 4 for a specific time of day.

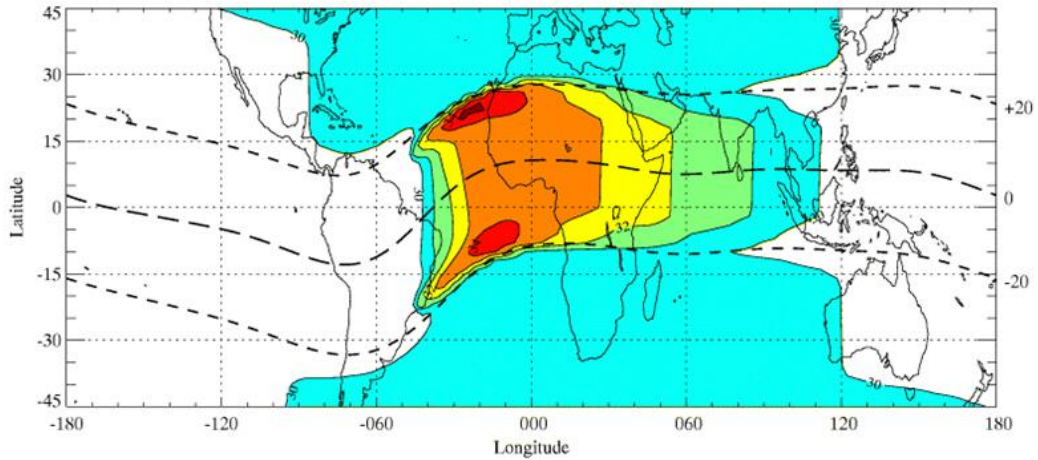


Figure 4. Scintillation map showing intensity for a specific time of day. [6]

Figure 5 illustrates the significant difference between normal, healthy GNSS signals and those that are affected by scintillation. It demonstrates why receivers are susceptible to loss of lock during severe scintillation periods.

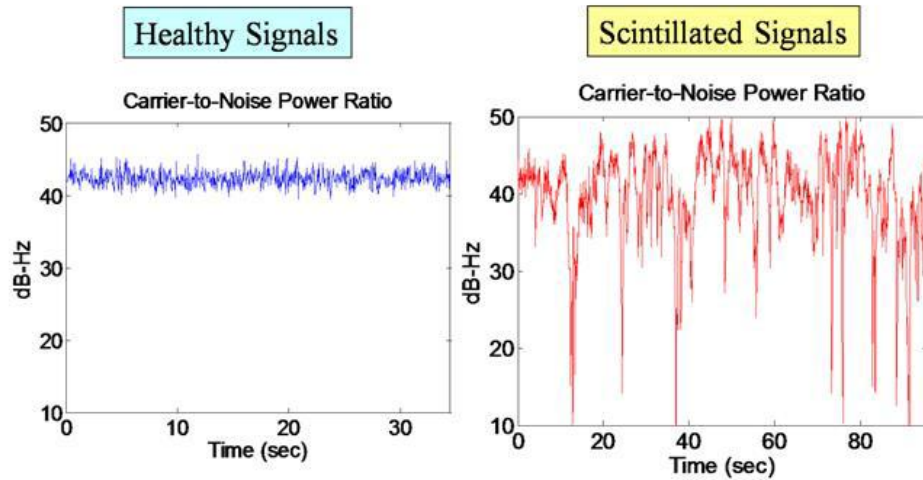


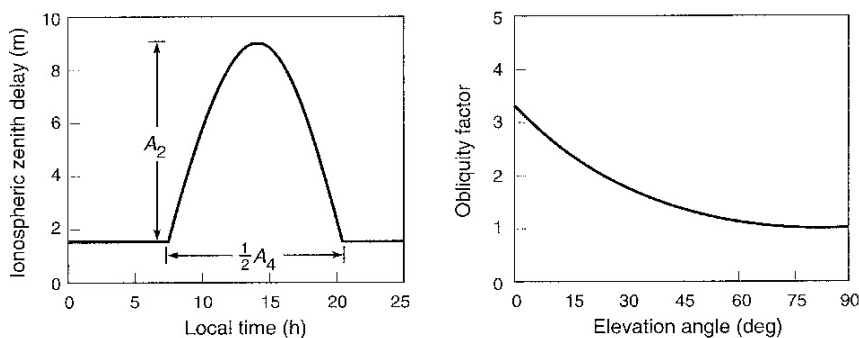
Figure 5. GPS Signal-to-noise power ratio for healthy and scintillated signals [4,7]

## Mitigation of Ionospheric Ranging Errors

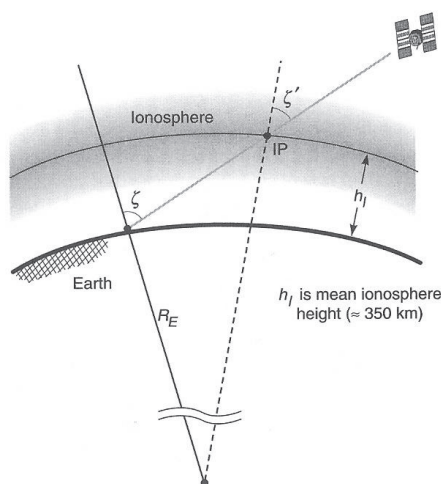
Current aviation GPS receivers use a model of the ionospheric effect on range errors in order to reduce the navigation error as much as possible. The model used is shown in Fig. 6 (a). It was developed by Klobuchar [8] and is essentially a fit to the data such as that shown in Fig. 2. The parameters  $A_2$  and  $A_4$  are adjusted by the GPS master control station for the best fit to ionospheric conditions. Information is broadcast to the users daily so those parameters can be determined based on the expected ionospheric activity and the user's latitude. The function in Fig. 6(a) represents the zenith delay for a satellite that is directly overhead the user. However, most range measurements are not from satellites



directly overhead; therefore, the zenith delay is adjusted by a *obliquity factor* to account for the longer propagation path through the ionosphere. Figure 7 depicts the geometry and shows why the obliquity factor in Fig. 6(b) increases for low elevation angles.



**Figure 6. (a) Klobuchar ionosphere zenith delay model, (b) Obliquity factor [2]**



**Figure 7. Ionosphere geometry effect on the obliquity factor [2]**

This model has been estimated to reduce the uncompensated ionospheric zenith delay by about 50% [2]. However, as can be seen by the delay variations shown in Fig. 2, there can be significant error remaining in spite of the use of the Klobuchar model. At mid latitudes, the remaining zenith error can be up to 7 m during the day during nominal solar maximum periods, and as high as 30 m during severe solar disturbances. For actual range measurements from the satellites, these errors could be a factor of 3 higher if derived from low elevation satellites, as can be seen from Fig. 6(b).

Aviation receivers manufactured to date rely solely on the L1 frequency (1575.42 MHz) being broadcast from the GPS satellites. The satellites also broadcast an L2 frequency (1227.60 MHz) which is primarily designed for use by the military. This second frequency is utilized by many non-military receivers in order to provide further mitigation of the ionospheric errors. However, the L2 frequency is not part of the internationally accepted spectrum for civil aviation nor is the signal designed for civilian use; therefore, it cannot be used for civilian navigation purposes. Many of the GPS receivers used in flight inspection do make use of this second frequency, so it is instructive to review the benefits of using a *dual-frequency* (L1 & L2) receiver.

When the GNSS signals reach the ionosphere, they are changed slightly from the speed of light in a vacuum due to the presence of charged particles. The amount of speed change depends on the frequency of the wave. Therefore, a receiver that can receive both signals is able to deduce the effect of the ionosphere by comparing the two simultaneous

range determinations and attributing the difference to ionospheric effects. Thus, the ionosphere delay can be essentially removed with an error less than a meter with no modeling required.

Furthermore, the GPS signals are made up of a carrier (at 1575.42 MHz) and a superimposed code (at 1 MHz). The code is said to *spread* the bandwidth of the GPS signal. In fact, the overall signal occupies the radio spectrum from approximately (1575.42 – 1.00) MHz to (1575.42 + 1.0) MHz. The speed change is different for the signal components near (1575.42 – 1.00) MHz than the signal components near (1575.42 + 1.00) MHz. The net effect is to change the relationship between the code and carrier in the combined signal. This is commonly referred to as *code-carrier divergence*. It is so named, because the code goes more slowly than the speed of light and the carrier phase is advanced relative to the speed of light. (Since the carrier phase does not carry any signal power, this does not mean that any signal power is going faster than the speed of light.) However, code-carrier divergence can be a factor when using carrier smoothed code algorithms in single frequency receivers. Furthermore, code-carrier divergence can be used to estimate the ionospheric delay [9] in single frequency receivers and is being utilized in some DGPS reference receivers as will be described in the next paragraph. No commercial aviation receivers currently use this process to reduce errors due to the ionosphere.

Another method of mitigating the errors due to ionospheric variations is to use Differential GPS (DGPS). These systems are used widely throughout the world for many applications because they remove many of the errors in the system, not just those due to the ionosphere. For DGPS systems, no error from the ionosphere will result if the user is located at the same site as the reference receiver. However, if the user has a single-frequency receiver and is some distance from the reference site, any spatial gradient in the ionospheric delay will create an error that grows with the distance from the reference site. An ionospheric gradient on the order of 1ppm (or 1mm/km) is typical for a quiet solar period in the mid latitudes such as that shown in Fig. 8. Therefore, the error due to the ionosphere would be 10 cm at 100 km from the reference under these quiet conditions. However, under the solar storm condition on 20 November 2003, gradients of the zenith delay on the order of 300 ppm were observed [10] in the mid latitudes which would result in a zenith ionospheric error of 6 m at 20 km from the reference site. In addition, it has been estimated [11] that the worst worldwide ionospheric gradient that might occur is around 500 ppm, most likely during a solar maximum period. However insufficient data exists for the equatorial regions to be sure that this is a reasonable upper bound worldwide. Given this estimate, for a user with a single-frequency DGPS receiver, the worst possible range error would be approximately 10 m at 20 km from the reference site. Note that these maximum error estimates are based on receivers using “raw” or unfiltered range measurements. In the Ground Based Augmentation System (GBAS) discussed below, reference and airborne receivers apply 100 seconds of carrier smoothing to range measurements and thus incur additional error due to the impact of code-carrier divergence on the smoothing filter. Since code and carrier-phase measurements are affected by equal but opposite amounts, the range error due to divergence can be approximated as twice the smoothing time constant times the user velocity times the ionospheric spatial gradient. For an aircraft moving at 70 m/sec and a maximum gradient of 500 mm/km, this divergence effect can add as much as  $2 \times 100 \text{ s} \times 0.07 \text{ km/s} \times 0.5 \text{ m/km} = 7$  additional meters of ranging error to the error created by reference-to-user separation. The possibility of such large errors is partially responsible for the slow adoption of the GBAS for CAT III use. GBAS is being implemented now for CAT I use and is susceptible to ionospheric delay errors at several kilometers from the reference receiver antenna under extreme solar storm conditions. The ground reference receivers for GBAS are single-frequency receivers; therefore, they are not able to directly measure the ionospheric delay. However, they are able to utilize the code-carrier divergence phenomenon described above to monitor the ionosphere’s behavior and to provide warnings when the observed temporal gradients are excessive.

On the other hand, many other DGPS systems consist of dual-frequency user and reference receivers, many of which are Real-Time Kinematic (RTK) Systems [2]. Use of a dual-frequency receiver essentially eliminates any significant ionospheric error no matter what the gradient is. The RTK systems primarily use the carrier phase measurements; therefore, their errors are typically at the cm level providing they have determined the correct integer number of carrier wavelengths between satellite and receiver. The process of determining the correct integers is referred to as Ambiguity Resolution (AR) and can typically be accomplished with a very high probability of success. However, during severe ionospheric storms, the probability of a successful AR determination has been shown to drop to 78% [12].

Satellite-Based Augmentation Systems (SBAS) are also differential GNSS systems. The FAA’s Wide Area Augmentation System (WAAS) is now in operation in North America, the Japanese Multifunction-transport Satellite Augmentation System (MSAS) is in operation around Japan, and the European Geostationary Navigation Overlay Service (EGNOS) will become operational by 2011. SBAS for other parts of the world are in the planning phase. These systems have dual-frequency reference stations spread over the coverage area. The continental U.S. has 25 reference stations that are roughly 600 km apart. Figure 8 shows the measured ionosphere delay information depicted by the colored bands. The reference station measurements of the ionospheric delay are used to map the information into a grid with points that are 5

deg apart in latitude and longitude over the continental U.S., which are then transmitted to users via Geostationary satellites along with corrections for satellite ephemeris and clock errors. Real time values of these ionosphere grid points are updated every few minutes and can be viewed at the FAA’s website [13]. This scheme has been shown to yield total system errors smaller than 1 m in horizontal and 2 m vertical 95% of the time [14].

WAAS protects integrity by guaranteeing that the vertical position error will not exceed a Vertical Protection Level (VPL). VPL is calculated by users based on the user’s satellite geometry and error bounds transmitted by WAAS. A real time display of VPL can also be seen from the FAA’s website [15] and typically shows a VPL of 20 to 30 m for Canada, U.S., and Mexico. This VPL level is sufficient to support a “LPV200” approach, which provides precision landings with a 200 ft Decision Height (DH). However, during high solar activity the ionosphere has large gradients that cannot be represented well by the coarse grid representation [16]. WAAS transmits this fact to the users, thus some types of flight operations become unavailable during very high solar activity periods over portions of the coverage area. An example of the ionospheric delay measurements during a severe solar storm are shown in Fig. 9. It shows the substantially larger ionospheric delays and gradients in the southeast portion of the U.S., which would have prevented acceptable VPLs for precision approaches. Note that the zenith ionospheric delay varied from about 1 to 25 m over short distances in Fig. 9 vs. 1 to 8 m over much longer distances for the normal solar day in Fig. 8.

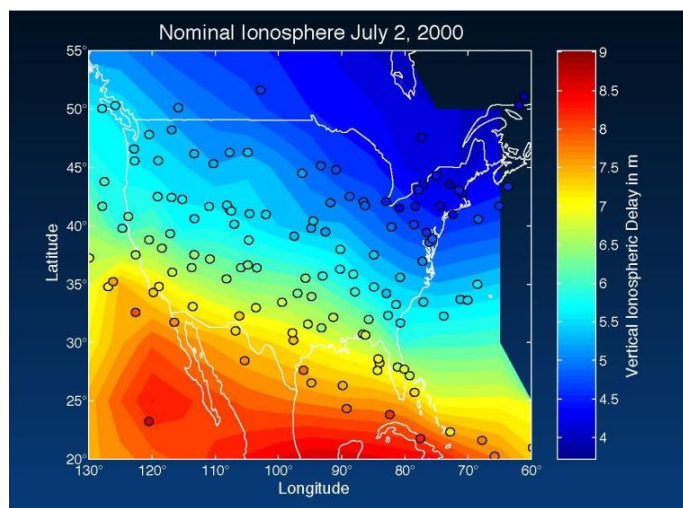


Figure 8. Mid latitude zenith ionosphere delay during quiet solar activity [17].

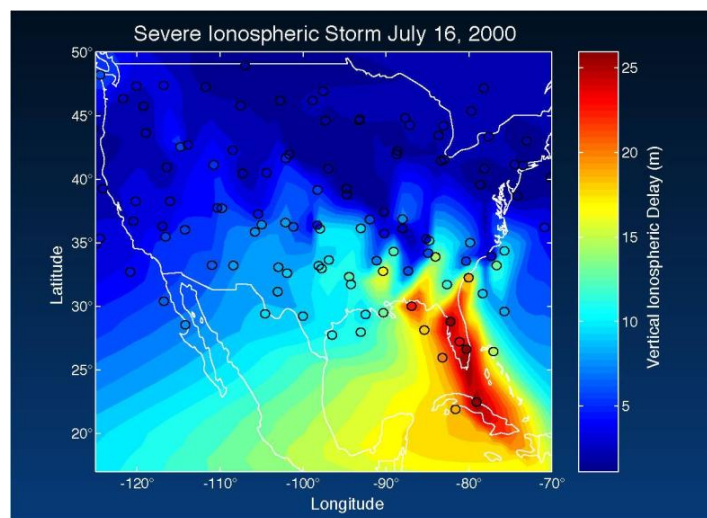


Figure 9. Mid latitude zenith ionosphere delay during severe solar activity [16,17].

Scintillation effects are less easily mitigated. None of the systems described in this section were designed to improve the ability of receivers to maintain lock through severe scintillation. The phase-lock loops in receivers have filtering time constants designed for normal ionospheric conditions. These time constants are selected to balance the need to maintain lock through vehicle accelerations with the need to smooth out range measurement noise. Scintillation severe enough to cause loss of lock occurs primarily in the equatorial and arctic regions (red and yellow bands in Fig. 3) and only for a few hours after sunset; therefore, receivers have been primarily optimized to operate in scintillation-free environments. However, as GNSS adoption becomes more widespread, more effort is being placed on how to also optimize performance during severe scintillation. It is possible to couple inertial navigation information to the receiver tracking loops to enhance the ability to perform precision landing operations in equatorial regions during severe scintillation [7].

There are improvements to GNSS on the horizon that will also mitigate the effects of ionospheric variations. The European GNSS (Galileo) is nearing deployment. Galileo will have two civil frequencies at L1 and L5 (1176.45 MHz), which will encourage the development of aviation GNSS receivers that rely on two frequencies. These receivers can essentially eliminate ionospheric variations as a source of error. Contracts have been awarded to deploy the Galileo satellites with a scheduled completion by 2014 [18]. Also, GPS launched its first satellite with L5 in March 2009 and will continue deploying satellites with both L1 and L5 as current on-orbit satellites are replaced. The current plan is for a sufficient number of GPS satellites to be on orbit in 2018 [19] to enable a user to have enough satellites in view with both L1 and L5 for a reliable, dual-frequency navigation solution. Given that manufacturers develop and certify dual-frequency receivers and that users replace their existing single-frequency GPS receivers, errors due to the ionosphere will essentially be eliminated for both GPS and Galileo users. The most likely scenario is that receiver manufacturers will produce multi-constellation receivers designed to receive dual-frequency (L1/L5) signals from both Galileo and GPS with an availability timed to coincide with the advent of the first operational dual-frequency constellation. Russia and China also have GNSS constellations being deployed; however, their plans to transmit civil dual-frequency positioning signals worldwide for aviation users are less clear.

## Ionospheric Effects on Flight Inspection (FI)

Ionospheric delay errors potentially affect flight inspection in two ways: 1) errors in the system used to determine the true position of the FI aircraft, and 2) errors in the aviation receiver used to determine the navigation signal while performing FI of a GNSS approach procedure.

First considering the truth systems, four different systems are used: (a) dual frequency RTK systems with a reference site installed at the airport, (b) DGPS code-based systems with dual-frequency receivers, (c) DGPS systems using single-frequency airborne receivers, and (d) INS-based systems with biases removed via single-frequency un-augmented aviation GPS receivers, radar or laser altimeters, and runway threshold cameras.

**(a) RTK systems** have essentially no errors from the ionosphere due to their dual-frequency receivers, providing that they have converged to a correct set of phase ambiguities. As pointed out on page 6, there can be a 22% chance of Ambiguity Resolution (AR) failure during severe solar storm days. On days when convergence failures are encountered, the FI aircraft would have to return to the inspection site on another day with less solar storm activity or use another method to obtain the true position. The AR determination procedure will report a failure to determine the ambiguities in most cases. If flight inspection is carried out in the early evening hours during severe solar storms, and especially near equatorial or polar regions (the red and yellow areas in Fig. 3), scintillation may cause a loss of lock in the RTK receivers, thus necessitating a repeat, perhaps at a different time of day. In fact, this phenomenon could pose difficulties for any of the GPS-based truth systems. The severe storm days can be determined in advance to some degree by monitoring the sun's activity which is reported almost daily by SpaceWeather.com [20]. SpaceWeather.com will also issue email alerts of space weather anomalies upon request. Longer term measurements and predictions are offered by the U.S.'s National Oceanic and Atmospheric Administration (NOAA) [21]. It is interesting to note from the NOAA data that the average sunspot number for July 2000, the month during which the severe storm shown in Fig. 9 occurred, was 170 whereas from Fig. 2 we see that the average monthly sunspot numbers from 2004 to the present have remained below 100. On the other hand, the average sunspot number for October 2003 was 65, whereas the sunspot number for a severe storm on 30 October 2003 was 330! However, the sunspot number for 20 November 2003 was 114, the same day that produced the extreme ionospheric gradients discussed above. The predictions from 2010 to 2020 are that the monthly average sunspot numbers will remain below 100. Nevertheless, severe storms can still occur even with low sunspot numbers as evidenced by the 30 October 2003 and 20 November 2003 examples. So it would be prudent for flight inspectors to monitor the solar activity on a daily or weekly basis, not just during the predicted solar max years from 2013 to 2014. The website: [www.spaceweather.com](http://www.spaceweather.com)

provides a range of measurements reporting on the sun's activity, including the probability of severe activity of the earth's magnetic field. The reported probability of a severe storm on 20 November 2003 was 20% while the probability reported for 30 October 2003 was 70%. During quiet solar periods, the reported probability of a severe solar storm is typically below 5%. Another measure of ionospheric disturbances is the *Kp Index* [22]. It is also correlated with magnetic disturbances due to solar activity and current data is available from NOAA [23].

**(b) DGPS with dual-frequency airborne receivers** and a reference site at the airport are not susceptible to range errors due to ionospheric variations, severe storm or not. Code-based receivers do not require AR; therefore, they do not experience the higher chance of initiation failure during severe storm periods that RTK systems do. As mentioned in the paragraph above, DGPS systems would be exposed to a loss of lock possibility due to scintillation for a few hours after sunset, especially in equatorial and polar regions.

**(c) DGPS with single-frequency airborne receivers** could experience ionospheric delay errors due to the gradient as described on page 6. We saw that zenith gradients of 300 ppm have been observed and that such a gradient could result in range measurement errors of 6 m at 20 km from the reference site. Larger gradients are possible, especially in equatorial and polar regions during severe solar storm conditions, which would result in larger range errors. Here again, it would be prudent for flight inspectors to monitor the actual solar activity on a daily or weekly basis as discussed in (a) to alert them to possible severe ionospheric delay variations.

**(d) INS-based systems**, when aided by non-GPS measurements only, would not be affected by any ionospheric effects. However, when aided by a single-frequency, aviation GPS receiver without SBAS capability, the receiver would not be able to correct for ionospheric delay variations and could exhibit large ranging errors (10 m or more) during a severe solar storm. A certified aviation Receiver's Autonomous Integrity Monitoring (RAIM) algorithm would most likely detect the errors and display that information to the flight inspector, but the flight inspection would need to be repeated.

The second area of FI that could be affected by space weather is the flight check of a GNSS-based approach. These flight checks are done to assure the flyability of the approach design, the accuracy of the database for the approach, and the quality of the VHF data link for GBAS installations. Here the flight inspector needs to be aware that the aviation receiver may be experiencing larger errors than typical during severe solar storms. The pilot would be given an alert if the protection levels were exceeded, whether it be a RAIM, SBAS, or GBAS-based approach. However, that does not preclude abnormal GNSS errors that are within the protection levels required for the approach being flight checked. Again, it would be prudent for the flight inspector to monitor solar activity on a routine basis.

Once the dual-frequency GNSS constellations are operational, probably by 2020, and flight inspectors are equipped with dual-frequency airborne equipment, ranging errors due to severe solar activity will no longer be an issue. Due to the frequency diversity, loss of lock due to scintillation in the equatorial regions may also be reduced. However, the correlation of scintillation across L1 and L5 is not yet known but is believed to be high; thus relatively little improvement can be expected at present.

## Conclusions

Space weather can potentially have a significant effect on the accuracy and usability of GNSS flight inspection on rare occasions. Variability in the signal delay through the ionosphere has been shown to be correlated with the sunspot number which has exhibited an 11 year cycle over the last 250 years. We are currently (2010) in a quiet period of solar activity; however, a more active solar period is expected in 2013-2014. Severe solar disruptions that materially affect the ionospheric delay, and thus GNSS accuracy, are more likely to occur during the approaching solar maximum, but they could occur during any part of the solar cycle. Flight inspection systems mitigate the ionospheric errors in varying degrees, with a code-based, dual-frequency DGPS system being the most robust. RTK systems are generally the most accurate, but they may have difficulty determining the correct carrier phase integer ambiguities during severe solar activity. The least accurate are systems depending on single-frequency airborne receivers with no augmentation from reference receivers located near the facility being inspected. Flight inspectors are encouraged to routinely monitor the current solar activity on [www.spaceweather.com](http://www.spaceweather.com) and/or [www.swpc.noaa.gov](http://www.swpc.noaa.gov) in order to be alert to the possibility of severe ionospheric activity during the days and times at which flight inspections are conducted.

## Acknowledgements

The authors gratefully acknowledge the FAA AVN for their support of this effort. Special thanks go to Per Enge and Sam Pullen for their contributions as well as to other colleagues at Stanford University and members of the ICASC.

## References

- [1] Balwin, E., “Predicting Solar Storm Arrival at Earth”, *Astronomy Now*, April 2010 issue. Also see: <http://www.astronomynow.com/news/n1004/14sun/>
- [2] Misra, P., and Enge, P., *Global Positioning System*, 2<sup>nd</sup> Edition, Ganga-Jamuna Press, Lincoln, MA, 2004.
- [3] Kintner, P., Humphreys, T., and Hinks, J., “GNSS and Ionospheric Scintillation: How to Survive the Next Solar Maximum”, *Inside GNSS*, July/August 2009.
- [4] Seo, J., T. Walter, T.-Y. Chiou, and P. Enge, “Characteristics of deep GPS signal fading due to ionospheric scintillation for aviation receiver design,” *Radio Sci.*, 44, July 2009. <http://waas.stanford.edu/pubs/index.htm>
- [5] Walter, T., and Powell, J. D., “Ionospheric Influence on GPS”, Presented at FAA GPS Workshop in Bangalore, India. April 22-24, 2002. Also, [http://sidc.oma.be/sunspot-index-graphics/sidc\\_graphics.php](http://sidc.oma.be/sunspot-index-graphics/sidc_graphics.php)
- [6] Northwest Research Associates, creators of the WBmod scintillation model.  
See: [www.nwra.com/ionoscint/wbmod.html](http://www.nwra.com/ionoscint/wbmod.html)
- [7] Chiou, T., “Design of a Doppler-Aided GPS Navigation System for Weak Signals Caused by Strong Ionosphere Scintillation”, PhD Dissertation, Aero/Astro Dept., Stanford Univ., March 2010. <http://waas.stanford.edu/pubs/index.htm>
- [8] Klobuchar, J., “Ionospheric Effects on GPS”, in *Global Positioning System: Theory and Applications*, Vol I, B. Parkinson, J. Spilker, P. Axelrad, and P. Enge (Editors), AIAA 1996 Publication, pp 485-515.
- [9] Kim, E., Walter, T., and Powell, D., “GNSS-based Flight Inspection Systems,” Presented at International Flight Inspection Symposium, Oklahoma City, June 2008. <http://waas.stanford.edu/pubs/index.htm>
- [10] Zhang, Godwin, Lee, Jiyun, Datta-Barua, Seebany, Pullen, S., and Enge, Per, Low-Elevation Ionosphere Spatial Anomalies Discovered from the 20 November 2003 Storm,” in Proceedings of the ION Institute of Navigation National Technical Meeting, San Diego, CA, January 2007. <http://waas.stanford.edu/pubs/index.htm>
- [11] Pullen, S., Murphy, T., Harris, M., Saito, S., and Yoshihara, T., “Standard Threat Model Used in GAST D Ionospheric Monitoring Validation,” ICAO Navigation Systems Panel (NSP) Meeting, WBW/WP 29, Montreal, Canada, November 10 – 20, 2009.
- [12] Wielgosz, P., Kashani, I., and Grejner-Brzezinska, D., “Analysis of Network RTK with Weighted Ionospheric Corrections Under Severe Ionospheric Storm,” presented at ION Annual Meeting, Cambridge, MA, June 27-29, 2005.
- [13] [http://www.nstb.tc.faa.gov/RT\\_WaasSIGPStatus.htm](http://www.nstb.tc.faa.gov/RT_WaasSIGPStatus.htm)
- [14] “WAAS Performance Analysis Report,” April 2010 available at <http://www.nstb.tc.faa.gov/reports/waaspan32.pdf>
- [15] [http://www.nstb.tc.faa.gov/RT\\_VerticalProtectionLevel.htm](http://www.nstb.tc.faa.gov/RT_VerticalProtectionLevel.htm)
- [16] Walter, T., Rajagopal, S., Datta-Barua, S., and Blanch, J., “Protecting Against Unsourced Ionospheric Threats,” Beacon Satellite Symposium, Trieste, Italy, 2004 <http://waas.stanford.edu/%7Ewww/papers/gps/PDF/WalterBSS04.pdf>
- [17] Walter, T., and Powell, J. D., “SBAS Ionospheric Correction & Confidence Bounding”, Presented at FAA GPS Workshop in Bangalore, India. April 22-24, 2002.
- [18] <http://europa.eu/rapid/pressReleasesAction.do?reference=IP/10/7&language=en>
- [19] [http://www.faa.gov/about/office\\_org/headquarters\\_offices/ato/service\\_units/techops/navservices/gnss/waas/news/media/FirstL5\\_GPS\\_SV\\_LE\\_040709.pdf](http://www.faa.gov/about/office_org/headquarters_offices/ato/service_units/techops/navservices/gnss/waas/news/media/FirstL5_GPS_SV_LE_040709.pdf)
- [20] <http://www.spaceweather.com/>
- [21] <http://www.swpc.noaa.gov/SolarCycle/>
- [22] [http://son.nasa.gov/tass/magnetosphere/ob\\_kp.htm](http://son.nasa.gov/tass/magnetosphere/ob_kp.htm)
- [23] [http://www.swpc.noaa.gov/rt\\_plots/kp\\_3d.html](http://www.swpc.noaa.gov/rt_plots/kp_3d.html)

*International Flight Inspection Symposium (IFIS), Beijing, China, June 21 – 25, 2010*

## Study on Flight Inspection Methods for GBAS

Zheng Jinhua<sup>1</sup>, Liu Kun<sup>2</sup>, Li Haijin<sup>2</sup>, Lin Bin<sup>1</sup>, Wang Xiaowang<sup>1</sup>

(<sup>1</sup> 20th Institute of China Electronic Technology Group Company, XIAN, CHINA 710075)

(<sup>2</sup> Flight Inspection Center of CAAC, BEIJING, CHINA 101312)

(National Ministry of Science and Technology 863 Project, ID: 2006AA12A102)

### ABSTRACT

Now there are many navigation methods in the civil air traffic. But the civil air traffic has increased tremendously during the last decade, and this steady rise will increase in the future. Ground Based Augmentation System (GBAS) is one of those newer navigation systems, which should help the global traffic solving those conflicts. GBAS is a ground-based augmentation system to base the Global Position System (GPS), which uses the differential technique to compute a single correction for each satellite. The single correction includes all common errors between a local reference and users, aircraft will receive the correction through data link and calculate precision position. This system has the high possibility of supporting Category III precise approach and landing by improving precision, integrity, continuity and availability.

This paper summaries the institution and the testing of GBAS in China. We have set up a GBAS station in LinZhi airport, and have actualized the ground testing in 2008. The flight testing activities have been actualized six times in 2009. Intention of this paper is to present a proposal and provoke discussion about the methods of GBAS inspection in the ground testing and flight testing.

### INTRODUCTION

This section provides a discussion of the GBAS and how GBAS is used to augment GPS position performance. The whole augmentation system includes satellites subsystem, ground subsystem and airborne

subsystem.

The satellites subsystem is GPS. Now there are 31 useful satellites in space. Although the satellites are monitored by the control segment, the requisite user alarm, warning functionary typical of navigation, approach, and landing systems is not provided. So, ground subsystem must provide integrity information and leading information for airborne subsystem.

The ground subsystem is referred to as the LGF. The LGF mainly includes the reference GPS receivers, the data processor, the VDB transmitter and the VDB receiver. The GBAS ground subsystem receives satellite ranging signals and calculates ground monitored differential corrections and integrity information for each satellite in view. A VHF data broadcast transmits these and other pertinent data such as approach path information to the airborne subsystem. The coverage volume typically extends to 20NM near the runway centerline.

The airborne subsystem can receive and process the satellite ranging signals and VDB signals, to compute and output a differentially-corrected position solution, deviations relative to a desired reference path, distance information, and approach alert annunciations. Now Multi-Mode Receiver (MMR) has realized the performance of the airborne subsystem. In addition to the integrity information broadcast by the VDB, the airborne subsystem also employs Receiver Autonomous Integrity Monitoring (RAIM) as a means of GPS ranging signal fault detection on the airborne side. Airborne subsystem

outputs are formatted to interface with other aircraft equipment used to support the particular operation. For example, deviation outputs are provided to aircraft displays and/or navigation systems.

## ENVIRONMENT OF THE GBAS INSPECTION

The LGF receives satellite ranging signals and calculates ground-monitored differential corrections and integrity information for each satellite in view. A VDB transmitter broadcast these and other pertinent data such as approach path information (FAS) to the air subsystem. The airborne subsystem encompasses the aircraft equipment used to receive and process the satellite ranging signals and VDB receiver, to compute and output a position corrected differentially, deviations relative to a desired reference path, distance information, and appropriate alert annunciations. There is difference in conducting the testing of the traditional groundbased navigation aids and satellite navigation.

Unlike ground-based navigation aids, for which system accuracy is measured during flight testing activities, GBAS accuracy assessments must be accomplished on the ground, due to the variation of satellite geometry over time. The testing of GBAS is not possible to be done in a short period of time. It means that the testing of accuracy of the GBAS is mostly statistical and it is ground testing, because flying with the aircraft for several hours for flight testing of the equipment is not pragmatic solution. The primary purpose of ground testing is to ensure that the GBAS ground subsystem meets the requirements of ICAO Annex 10 in terms of system performance and monitor operation. And flight tests are used to confirm procedure design, final subsystem alignment, GNSS signal reception, and data link reception

within the coverage volume. So, the GBAS inspection includes ground testing and flight testing.

So, in order to complete GBAS inspection, we shall develop the testing system (see figure 1). The testing system contains ground subsystem and airborne subsystem. And the LGF in ground subsystem generates differential corrections, integrity information and FAS data, to broadcast this information to the air subsystem by VDB transmitter. The MMR in airborne subsystem receive the VHF signal and GPS signal, then to provide precision flight path deviation guidance to the aircraft during the final approach and landing phase of flight. Through 422 serial port and 429 bus interface, the data processor receive the position information, VDB coverage information, broadcast SIS integrity data, FAS data broadcasted and satellites information to calculate precision position.

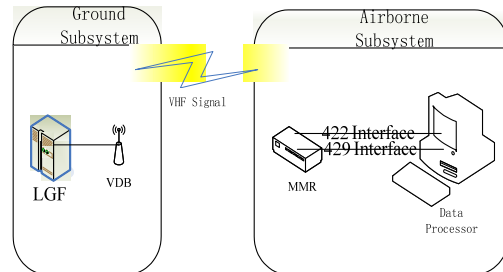


Figure 1. GBAS Inspection System

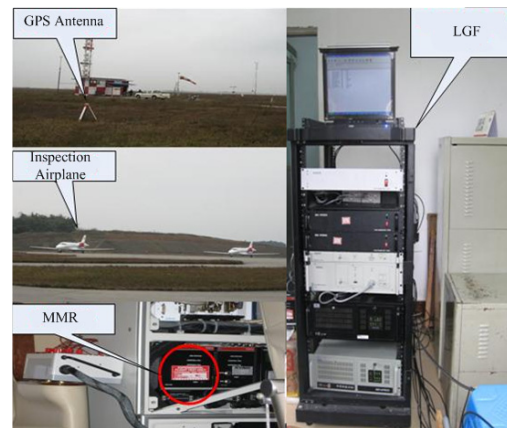


Figure 2. GBAS Inspection in NanChong Airport, China

## GROUND TESTING METHODS

First, we must get the precision position



of MMR's GPS antenna through RTK difference devices. The primary purpose of ground testing is to ensure that the GBAS ground subsystem meets the requirements of Annex 10 in terms of system performance and monitor operation. Unlike ground-based navigation aids, for which system accuracy is measured during flight testing activities, GBAS accuracy assessments must be accomplished on the ground, due to such factors as the statistical nature of satellite signals and their variation over time. Some ground testing activities can result in the GBAS ground subsystem radiating a signal in space that is not compliant with the Annex 10 SARPS. To reflect this, the equipment should be administratively removed from service and its status properly published prior to the start of testing, and the "Message Block Identifier" field of each radiated message should be set to "Test".

The ground functional test is intended to confirm that the overall position domain accuracy is satisfactory, using a receiver independent of the GBAS ground subsystem. It is not intended to provide a statistical confidence level of the position measurement. To make the position measurement, place a GBAS receiver at a precisely-surveyed position free of significant multipath, and collect at least three independent samples at intervals of at least 200 seconds. When we keep on collecting data, the inspection airplane must hold still above parking apron. The horizontal and vertical errors of each of the samples should meet the tolerance. If this tolerance is exceeded, first confirm that the measurement was done properly and that the multipath environment is clean. If necessary, repeat the measurement at other precisely-surveyed positions to determine whether it is the GBAS accuracy or the measurement location that is flawed.

The position accuracy measurement

model is

1.  $(Lon_0, Lat_0, H_0)$  is a precisely-surveyed position. Where,  $Lon_0$  is Longitude,  $Lat_0$  is latitude, unit is degree ( $^{\circ}$ ),  $H_0$  is altitude, unit is meter (m).

2.  $(Lon_i, Lat_i, H_i)$  is independent samples position. Where,  $Lon_i$  is Longitude,  $Lat_i$  is latitude, unit is degree( $^{\circ}$ ),  $H_i$  is altitude, unit is meter(m).

**Calculate lateral position precision:**

Step1: Calculate lateral distance between samples and base position:

$$\Delta_i = \sqrt{[(Lat_i - Lat_0) \times 60 \times 1852]^2 + [(Lon_i - Lon_0) \times \cos(\frac{Lat_0 \times \pi}{180}) \times 60 \times 1852]^2} \quad (1)$$

Step2: Calculate the mean of the  $\Delta_i$ :

$$\Delta = \frac{\sum \Delta_i}{n} \quad (2)$$

Step3: Calculate standard deviation  $\sigma$ :

$$\sigma = \frac{\sqrt{(\Delta_i - \Delta)^2}}{n - 1} \quad (3)$$

Get lateral position precision:

$$\kappa_{lateral} = \Delta + 2\sigma \quad (4)$$

**Calculate vertical position precision:**

Step1: Calculate vertical distance between samples and base position:

$$\Delta H_i = H_i - H_0 \quad (5)$$

Step2: Calculate the mean of the  $\Delta H_i$ :

$$\Delta H = \frac{\sum \Delta H_i}{n} \quad (6)$$

Step3: Calculate standard deviation  $\sigma$  :

$$\sigma = \frac{\sqrt{(\Delta H_i - \Delta H)^2}}{n-1} \quad (7)$$

Get vertical position precision:

$$\kappa_{vertical} = \Delta H + 2\sigma \quad (8)$$

### FLIGHT TESTING METHODS

Flight tests are used to confirm procedure design, final segment alignment, GNSS signal reception, and data link reception within the coverage volume. The airborne GBAS equipment used for the flight test should meet the applicable standards required for the procedure being tested. There are situations that may require modifications to the flight test receiver that could invalidate the certification, This may require special consideration or certification for instrument flight conditions use. This receiver may be used for all required checks. In some cases, it may be desirable to acknowledge and suppress GBAS alerts, warnings, and flags for the purposes of completing required checks.

As it is mentioned in Doc 8071, Chapter 4, flight tests of GBAS are required under the following circumstances:

- a. Prior to commissioning on each runway served and for each approach.
- b. Whenever interference is reported or suspected and ground testing cannot confirm elimination of the source of interference.
- c. As a result of a procedure modification or the introduction of a new procedure.
- d. Whenever changes occur to the

GBAS configuration such as the location of the GBAS ground subsystem antenna phase-center, the location of the data link transmit antenna, or the system database.

e. Whenever site changes such as new obstructions or major construction occur that have the potential to impact GNSS signal reception and data broadcast transmission.

f. Following certain maintenance activities.

Field Strength that received by MMR has been mentioned in Doc 2937. For Horizontal Field Strength, the minimum field strength shall not be less than 215 V/m (-99 dBW/m<sup>2</sup>) for a horizontally polarized signal, the maximum field strength shall not be greater than 350 mV/m (-35 dBW/m<sup>2</sup>) for a horizontally polarized signal. And for Vertical Field Strength, the minimum field strength shall not be less than 136 V/m (-103 dBW/m<sup>2</sup>) for the vertically polarized signal, the maximum field strength shall not be greater than 221 mV/m (-39 dBW/m<sup>2</sup>) for the vertically polarized signal.

According to above requirement, we have actualized three flight testing methods:

#### 1. Arcs Flight

Fly an arc  $\pm 10$  degrees across the extended final approach segment course at 37 km (20 NM) from the FTP/LTP. Fly an arc  $\pm 35$  degrees across the extended final approach segment at 28 km (15 NM). The arc can be flown in either direction. A  $\pm 35$  degree arc at 20 NM may be flown in lieu of the  $\pm 10$  degree 37 km (20 NM) and  $\pm 35$  degree 28 km (15NM) arcs. Confirm minimum field strength requirements are met at the lowest vertical coverage limit. And Fly an arc 360 degrees orbit across the extended final approach segment at 23 NM at an altitude of 2000 ft.

#### 2. Level Flight

Fly at the upper height of the required

coverage volume (e.g. 7 degrees minimum, 3000 m (10000 ft) HAT) from the outer limit of coverage to less than 24 km (13 NM) (for 7 degrees), and at an altitude of 2000 ft beginning at 39 km (21 NM) (corresponding to the lowest vertical coverage limit of 0.9 degrees) to within 4.6 km (2.5 NM) for each runway end served. Confirm minimum field strength requirements are met on both level runs.

### 3. Approach Flight

Intercept the glidepath and fly to an altitude of 30 m (100 ft). When the coverage is required to be extended down to 3.7 m (12 ft) above runway surface, the maximum and minimum field strengths should be confirmed to the touchdown point. If the signal level is unsatisfactory prior to glidepath interception, altitudes may be raised incrementally to coincide with the lower limit of the coverage volume.

Through 422 serial port, We record VDB power level outputted from MMR. And according to DO-253, message failure rate should be measured in flight testing. The airborne subsystem shall achieve a message failure rate less than or equal to one failed message per 1000 full-length application data messages.

Figure 3 shows the VDB signal strength and coverage in lateral. Figure 4 shows the VDB signal strength and coverage in vertical.

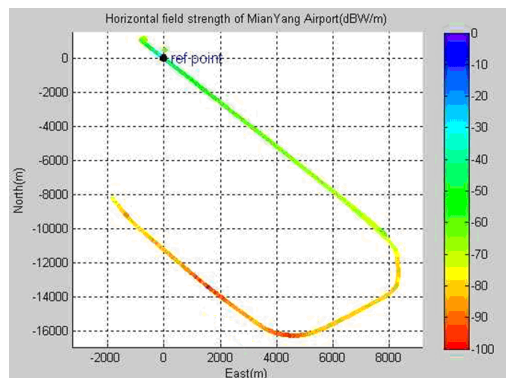


Figure 3. Horizontal field strength of MianYang Airport, China

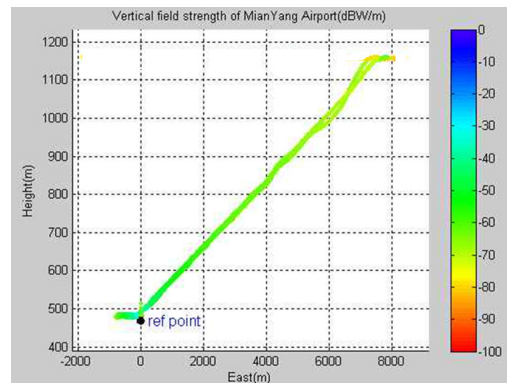


Figure 4. Vertical field strength of MianYang Airport, China

In flight testing, the RTK positioning result from the airborne RTK receiver is considered as the true flight trajectory, and used to compare with the positioning result generated with MMR data from the airborne MMR. According to the position accuracy measurement model, we should get position accuracy in flight testing. Figure 5 shows approaches trajectory plots in horizontal. Figure 6 shows approaches trajectory plots in vertical. Figure 7 shows total trajectory plots in Handan Airport flight testing.

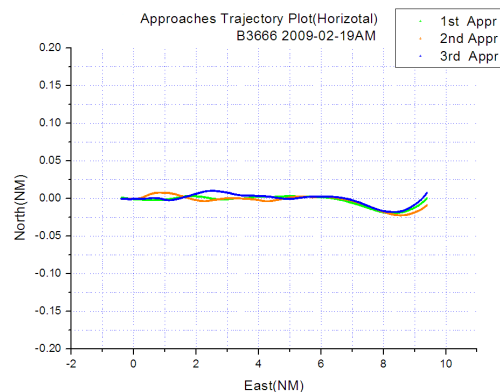


Figure 5. Approaches Trajectory Plots in Horizontal

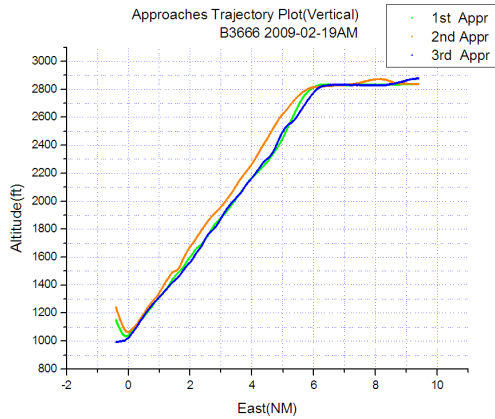


Figure 6. Approaches Trajectory Plots in Vertical

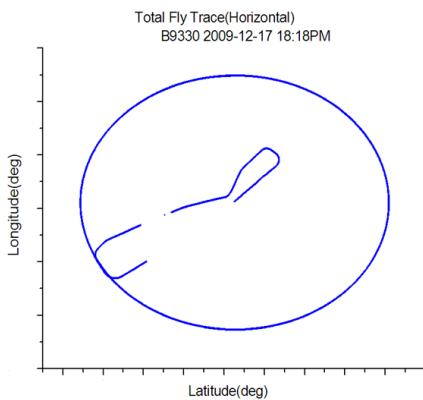


Figure 7. Total Trajectory Plots in Handan Airport, China

## CONCLUSIONS

The flight testing activities in this paper have been actualized six times until 2010. We have discussed about the methods of GBAS inspection in the ground testing and flight testing. Through these methods, we can get the performance of the GBAS. The testing results show that the GBAS is able to provide performance which can match the precision requirements of navigation for Category I Approaches. In the future, we will search the flight programs and inspection programs that suit GBAS service.

## REFERENCES

[1] ICAO, October 2004, NSP WGW Report/Attachment L-Doc8071 GBAS,

Chapter 4, Ground Based Augmentation System (GBAS).

[2] RTCA, December 9, 2004, Minimum Aviation System Performance Standards for the Local Area Augmentation System, Document Do-245A.

[3] RTCA, December 16, 2008, Minimum Operation Performance Standards for GPS local area augmentation system airborne equipment, Document Do-253C.

[4] 14th IFIS, June 16, 2006, GBAS Testing – Practical Considerations, by Saso Andonov.

[5] 15th IFIS, April, 2008, Initial Federal Aviation Administration Flight Inspection Criteria for Precision Instrument Approach Procedures Supported by the Local Area Augmentation System, by Michael F. DiBedetto, Dan G. Burdette.

[6] FAA, April 17, 2002, Category I Local Area Augmentation System Ground Facility, Specification FAA-E-2937.

[7] RTCA, December 16, 2008, GNSS-Based Precision Approach Local Area Augmentation System Signal-in-Space Interface Control Document, Document Do-246D.

# FLIGHT INSPECTION OF PERFORMANCE BASED NAVIGATION INSTRUMENT FLIGHT PROCEDURE “A LA FRANCAISE”

**Franck BUFFON**  
Sales Manager  
Flight Inspection Systems and NCS products  
Sagem DS  
Tél : + 33 158 124 177  
Email [franck.buffon@sagem.com](mailto:franck.buffon@sagem.com)



**Philippe LABASTE**  
Laboratory Manager  
Flight Inspection Service  
French DGAC/DTI  
Tél :+ 33 562 145 595  
Email [philippe.labaste@aviation-civile.gouv.fr](mailto:philippe.labaste@aviation-civile.gouv.fr)



**Florence JACOLOT**  
Laboratory Expert  
Flight Inspection Service  
French DGAC/DTI  
Tél : + 33 562 145 534  
Email [florence.jacolot@aviation-civile.gouv.fr](mailto:florence.jacolot@aviation-civile.gouv.fr)



## 1 ABSTRACT

Before RNAV based procedures, Flight Inspection role was to verify the compliance of the means, i.e. the radiated signals, to the SARPS (ICAO Annex 10) on any area where the radio navigation system could be declared usable.

Now with the PBN implementation, Flight Inspection needs also to ensure that RNAV paths are correctly defined before publication.

Flight Inspection of Performance Based Navigation procedures using ground facilities or satellites has become an issue of concern in the last few years for Air

Navigation Providers. The documentation available, both recommendation and requirement based, that covers this subject is diverse and at the same time not detailed enough to determine the flight inspection operations.

The purpose of this paper is not to list all the documents published within the international environment but to introduce an overview of the French rules (interpretations and differences) and practical experiences of carrying out Procedures Inspections and highlight some particular points.

## 2 FRENCH FLIGHT INSPECTION SERVICE

### 2.1 ORGANISATION

The DTI “Direction de la Technique et de l’Innovation” (French “Direction Générale de l’Aviation Civile” Technical Centre) Flight Inspection Unit (CNS/CEV) attached to the Communications, Navigation and Surveillance domain, is the unit responsible for this activity.

Flight inspection is carried out in partnership with the SEFA “Service de l’Exploitation et de la Formation Aéronautique” (the aeronautical operations and training service), which operates the flight inspection aircraft.

All the flight inspection aircrafts are equipped with automatic flight inspection systems provided by Sagem.

The flight inspectors are authorised by the ESARR 5 European regulations to perform flight inspections.

### 2.2 FLEET



King Air Beech 200



ATR 42

### 2.3 FLIGHT INSPECTION SYSTEM

Dedicated aircraft with specific equipments in the cabin, with Sagem CARNAC Flight Inspection System:

- To acquire, record, process and visualise in real time the signals to be analysed.
- Multi-purposes and very accurate trajectography system
- Detection and Localization of RF interference jamming capability
- « Independence » of the FIS from the cockpit.
- Flight inspectors have deep knowledge of the features of the radiated signals.



Sagem CARNAC FIS for B200

## 2.4 AIRCRAFT GUIDANCE



Calibration display for guidance

For radio navigation systems inspection, interface with pilots is through a dedicated EHSI fed by the FIS.

For RNAV procedures, the aircraft navigation equipments are used (FMS or GPS)

A connection between the FIS and the Beech 200 autopilot is under test and will be integrated in late 2010.

## 2.5 FRENCH FIS TRUTH REFERENCE SYSTEM

VP D-GPS Truth Reference System (better than 10 cm accuracy on 3 axes) is used for assessment of the true position to be compared to the radio navigation or RNAV procedure under verification.

## 3 APPLICABLE REGULATIONS TO RNAV PROCEDURES

### 3.1 ICAO DOC 8071 VOL II- MANUAL ON TESTING OF SATELLITE-BASED RADIO NAVIGATION SYSTEMS

- Guidance on extent of testing and inspection normally carried out to ensure that the radio navigation systems meet the SARPS in ICAO annex 10 (not a SARPS itself)

- Vol II provides guidance on the flight inspection of GNSS-based procedures:

- What to check,
- How to check (aircraft, equipment and methodology),
- Expected results

► ***Validation of the GNSS Signal in Space is not a task allocated to Flight Inspection, considering the moving GPS constellation***

### 3.2 EUROCONTROL GUIDANCE MATERIAL FOR THE FLIGHT INSPECTION OF RNAV PROCEDURES (2005)

Extracts from doc 8071, Instruments flight procedures, applicable to all procedures

“When the State can verify, by ground validation, the accuracy and completeness of all obstacle and navigation data considered in the procedure design, and any other factors normally considered in the flight validation, then the flight validation requirement may be dispensed with”:

- a) Verify the obstacle that serves as the basis for computing the minimum altitude in each segment of the IAP.

► ***Only “commented” by Flight Inspection, performed on paper, and if any abnormal situation, verified by Airlines Flight Inspection(\*)***.

- b) Evaluate aircraft manoeuvring areas for safe operations for each category of aircraft for which the procedure is intended.

► **Only “commented” by Flight Inspection, performed on paper, and if any abnormal situation, flight evaluated by Airlines Flight Inspection(\*)**.

- c) Review the instrument procedure for complexity of design, and evaluate the intensity of the cockpit workload to determine if any unique requirements adversely impact safe operating practices. Check for correctness of information, propriety and ease of interpretation.

► **Assessment done by Flight Inspection, while flying the procedure for commissioning**.

- d) If appropriate, verify that all required runway markings, lighting and communications are in place and operative.

► **Only “commented” by Flight Inspection, performed on paper, and if any abnormal situation, verified by Airlines Flight Inspection (\*)**.

**(\*) .Airlines Flight Inspection (AFI)**

This French body (Organisme du Contrôle en Vol) within the French DGAC verifies, by ground or in flight inspections, that the aircraft’s operating regulations are respected.

It also controls the qualifications of the aircrew, flight crew and cabin crew.

It proceeds to the initial assessment at the creation of a new airline or during the training of new aircrews allocated to a new type of aircraft.

It’s totally independent of the DTI/CNS/CEV Radio Navigation Aids Flight Inspection.

**3.3 FRENCH LAW: DECREE OF 28/08/2006 AMENDED IN 2008 FOR P-RNAV**

- a) Regulation on procedures for departure, arrival, holding, and approach and associated operational minima and charts,

- b) For RNAV GNSS, DTI/CNS/CEV is only requested **to check that there are no permanent RF Interferences along the procedure under commissioning**.

- c) For RNAV1, Flight Inspection is requested to perform **an assessment of the infrastructure (DME coverage), which might be supported by in-flight validation**.

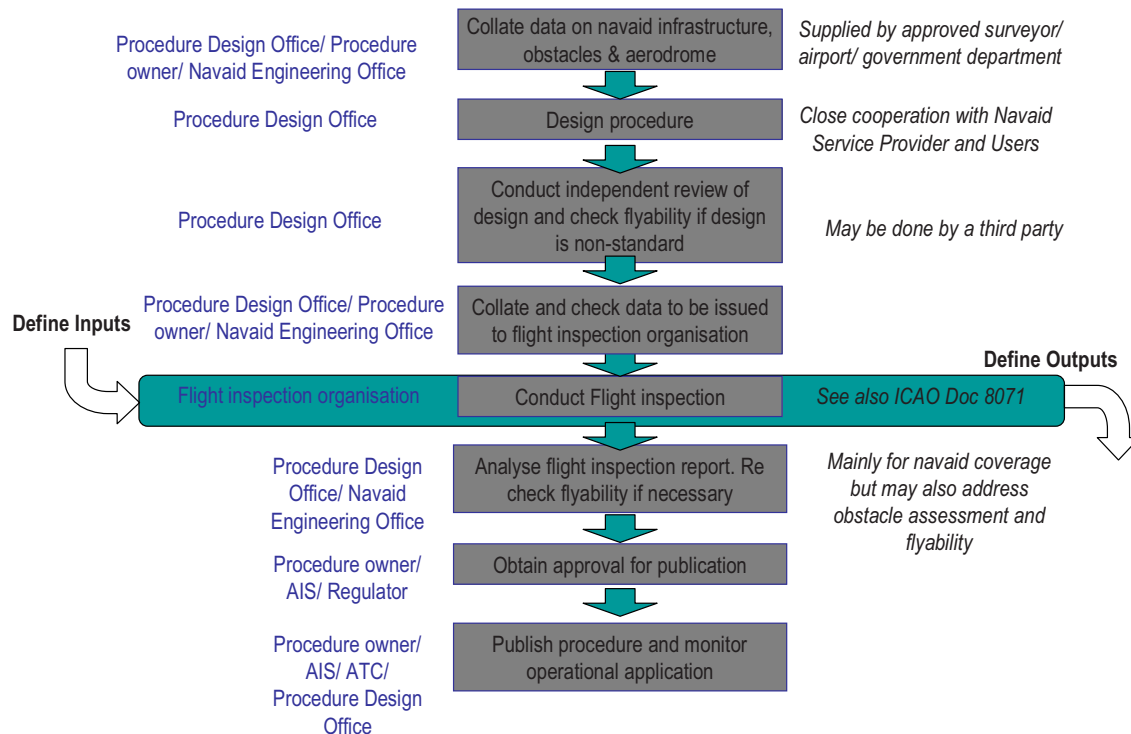
- d) Charts obstacles/ Flyability of the procedure is not assigned to Flight Inspection but to Airlines Flight Inspection(\*), however flyability assessments are performed by our pilots during the Flight Inspection and “commented” on the FI report.

**3.4 DSNA LPV SAFETY CASE**

PSSA (Preliminary System Safety analysis) has identified an important role assigned to DTI Flight Inspection: **FASDB verification**, as a mitigation mean to prevent some of the hazards identified (further detailed in LPV Flight Inspection paragraph).



## 4 PROCEDURE DESIGN PROCESS AND FLIGHT INSPECTION



## 5 PRINCIPLES OF RNAV FLIGHT INSPECTION

Because GNSS is available on a worldwide basis, not much needs to be done in terms of infrastructure assessment.

We just assess that the interference environment is satisfactory for the planned procedures.

We have two ways of accomplishing this:

- We can during our annual High Altitude VOR Flight Inspection Campaign (see paragraph 7 of DTI Presentation : **Results of experiments of the R&S EVS300 receiver for VOR and ILS Flight Inspection**) record the L1 band using the DTI tool Melba and a Rohde & Schwarz EB 200 receiver ( See paragraph 5.2.6).

- Also, the reference trajectography during the annual High Altitude VOR Flight Inspection Campaign is based on GPS receivers using L1 and L2 band. Any GPS interference on L1 (or L2) band would be reported by the aircraft positioning system and a specific flight could be later performed to characterise the interference.

## 6 PRINCIPLES OF RNAV1 FLIGHT INSPECTION

### 6.1 REMINDER

Two Navigation Aids or Sensors are concerned: GNSS and DME/DME. DME/DME is a back-up to GNSS and primary for « old » aircraft – it is estimated by Eurocontrol that 29% of P-RNAV aircraft fleet is not GNSS capable -.

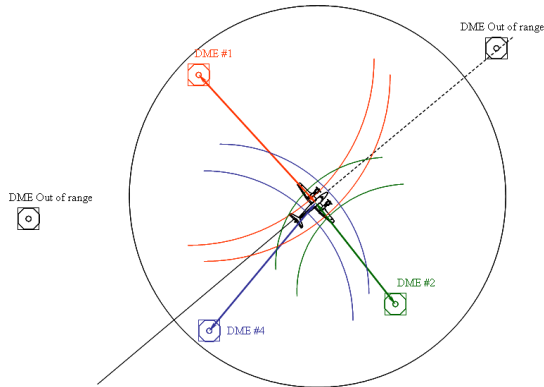
In addition to traditional applications, avionics have been developed that can interrogate multiple DME enabling determination of aircraft position:

- B-RNAV ±5Nm 95%
- P-RNAV (RNAV1) ±1Nm 95%

**Each combination of navigation aid needs to be assessed and inspected**

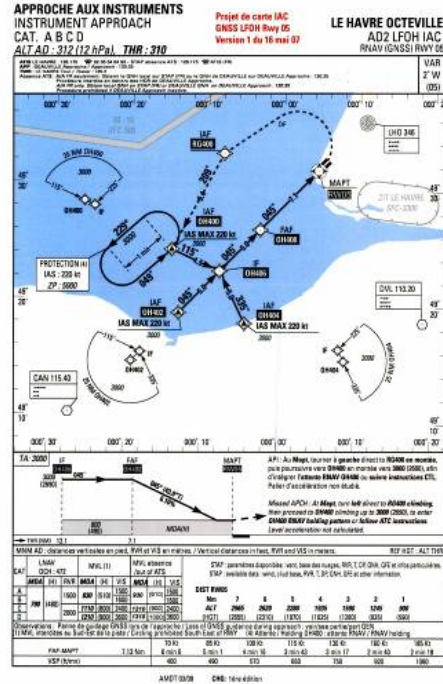
### 6.2 RNAV1 DME/DME

There is nothing yet in Doc 8071. An add to PBN Manual: “Navigation Infrastructure Assessment in Support of PBN” describes the general requirements to apply.



#### 6.2.1 Collation of necessary Data

The Flight Inspection Service receives all the necessary information from the procedure designer. These procedure data include the approach chart and the path descriptor (path terminator, all waypoints coordinates, and any vertical profile restrictions (minimum climb gradients, minimum crossing altitudes, speed categories ...), offset, direct-to or other operational requirements ...



Approach chart

Table for data integrators

REPERES Fixes	IDENTIFICATION Identification	COORDONNEES Coordinates	CODAGE PROPOSE Proposed coding	STATUT Status
IAF	GIMAT	45°29'07.7" N - 003°35'03.6" E	IF	Fly By
IAF	NIGLO	45°50'56.7" N - 003°49'23.6" E	IF	Fly By
IAF	RIMOR	46°01'21.8" N - 003°28'47.8" E	IF	Fly By
	LC402	45°39'20.5" N - 003°33'05.2" E	TF	Fly By
	LC403	45°49'49.2" N - 003°37'20.6" E	TF	Fly By
IF	LC406	45°49'14.0" N - 003°31'09.9" E	TF	Fly By
FAF	LC408	45°48'33.5" N - 003°24'06.6" E	TF	Fly By
MAPT	MAPT1	45°47'23.32" N - 003°12'05.40" E	TF	Fly Over
MATF	LC410	46°05'39.7" N - 003°15'03.4" E	DF	Fly By
MATF	ARSOM	46°08'14.0" N - 003°25'11.0" E	TF	Fly By
MAHF	RIMOR	46°01'21.8" N - 003°28'47.8" E	TF	Fly Over

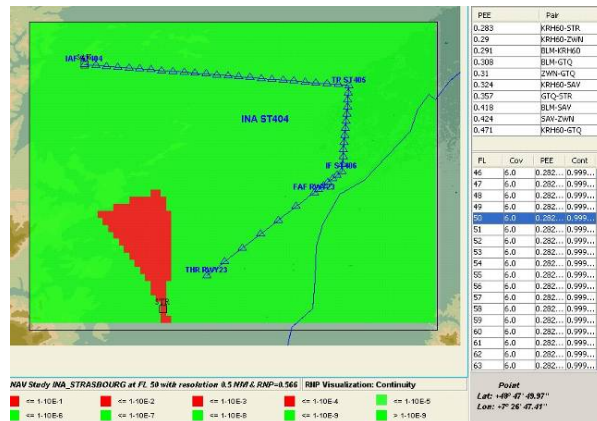
Path descriptor

#### 6.2.2 Infrastructure assessment

The first phase consists of a simulation of projects for RNAV routes using a DME coverage forecasting tool based on the use of 3D terrain databases, and on modelling of the propagation of the DME radio electric signals. The COVERNAV product, developed by the Spanish firm INECO, has been selected by DTI.

The simulation indicates, for each point of the procedure, the DMEs within line of sight and the pairs of DME that can be used for navigation.

It also indicates critical DMEs. A DME is considered «critical», if its loss results in the disappearance of all the pairs of DME that are essential to maintain the P-RNAV capacity, when this is based on DME/DME. The program makes calculations based on the EUROCONTROL recommendations.



This receiver (as the Honeywell) when used in directed scanning mode can't get an accurate field strength measurement by automatic gain control voltage calibration. AGC lock status and system reply efficiency are used as indicators of potential problem areas.

EDS 300 from ROHDE&SCHWARZ is scheduled in 2010 to be included within the Sagem CARNAC FIS as DME receivers.

EDS 300 can track 10 DME with field strength measurement. It can also be used for TACAN calibration.

Additionally the EDS 300 has a capability to characterise and identify the causes of propagation distortions. It's able to analyse the DME pulses automatically. This task has to be done actually by observing the base band pulse video.

The second phase is the in flight evaluation of the coverage. A flight inspection could be decided to measure DME coverage. The objective is to limit the flight inspection hours. The FI equipment has the capability to record multiple DME simultaneously and accurately.

The FI will confirm the signal in space compliance with ICAO Annex 10, the accuracy and field strength of individual DME facilities supporting R-NAV and see if the initial assessment made by the software tool has been confirmed or if any unforeseen effects have been discovered.

### 6.2.3 Capabilities of the flight Inspection System

“...It's recommended to use a flight inspection system with the capability to record multiple DME signals simultaneously and accurately...”

Our Flight Inspection bench using Sagem CARNAC Software is equipped with two Collins DME 442 receivers or with Honeywell DME receivers.

Six DME can be checked simultaneously using two Collins 442.

### 6.2.4 Inputs to Flight Inspection System

The procedure is flown on the centreline.

We consider that the Flight Inspection of the totality of the procedure is not necessary if the number of DME is more than sufficient in a particular airspace.

According to experts experience and evidence some Flight Inspection can be omitted.

Required:

- Identification of critical DME's
- Intended procedure (WP data and position of DME's)
- List of DME's that are part of the procedure design
- Identification of facilities that are to be used outside of their currently Defined Operational Coverage volumes

Desirable:

- Predicted coverage of DME's to be inspected
- Consideration of expanded service volumes
- List of restrictions applicable to the DME's under inspection
- Review of existing DME Flight Inspection records

The Flight Inspection System will determine all combination of DME pairs at each point usable by FMS ( 3NM < Distance < 160NM, Angle < 40° ) and calculation of RNAV 1 parameters (accuracy, continuity) by evaluating the substended angle ( 30°-150° ), calculating the PEE ( < 0.86 ) and identifying the critical DMEs..

Toulouse take-off PROCEDURE INPUT

Procedure Number: 0

0 -> large template (100Nm)  
1 -> template IAWP, 2 -> template IWP  
3 -> template FAWP, 4 -> template MAWP

Procedure Name		Toulouse take-off		GNSS Category		RNAV DME	
WPTS	TRIP	Flight level	Temp. Ver	Name	Distance	Bearing	Int
Wpt01	DER32	FO	504	1	0		
Wpt02	TOU	FB	1000	1	1	Initial	3.29 322.00 Int 3.29 -0.00 321.84 -0.16
Wpt03	BO322	FB	2200	1	1	inter 1	6.00 336.00 Int 6.00 0.00 335.19 -0.81
Wpt04	BO323	FB	6400	1	1	inter 2	21.00 0.00 Int 21.31 0.31 359.06 -6.34
Wpt05	FISTO	FO	10500	1	1	fin SID	20.00 0.00 Int 20.11 0.11 359.05 -21.95
Wpt06		FB	0	0	0		0.00 0.00 Int 0.00 0.00 0.00 0.00
Wpt07		FB	0	0	0		0.00 0.00 Int 0.00 0.00 0.00 0.00
Wpt08		FB	0	0	0		0.00 0.00 Int 0.00 0.00 0.00 0.00
Wpt09		FB	0	0	0		0.00 0.00 Int 0.00 0.00 0.00 0.00

Sagem FIS Interface Procedure Input

WAY POINT INPUT

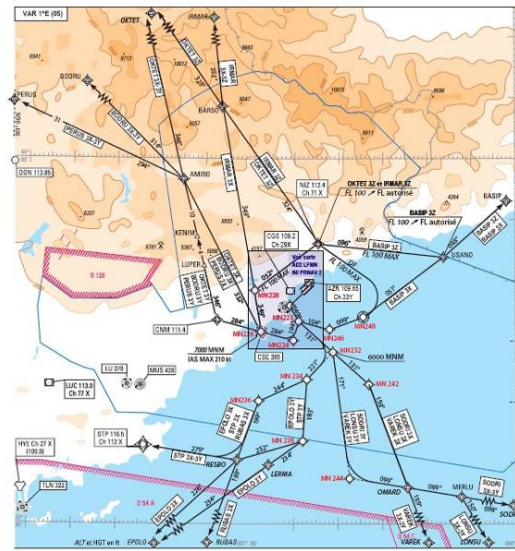
Country: \*  
Way Point Identification  
Way Point Name: BO322  
Country: FRANCE  
Way Point Coordinates  
Latitude: 43.771253333 N  
Longitude: 1.250870556 E  
Altitude: 0.00 (feet)  
Data format: deg.dddssssss, deg'min.dddssss, deg'min'sec.ddd

Mise a jour du: 11/05/2010

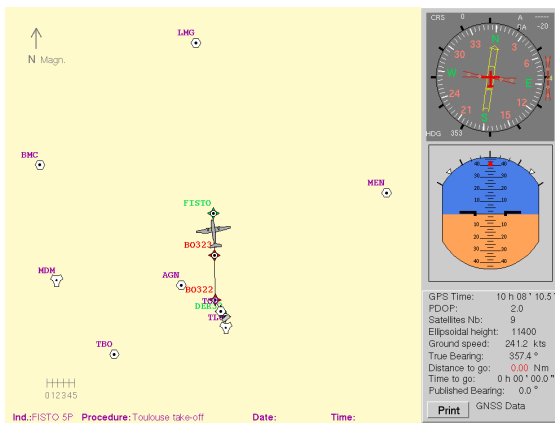
Sagem FIS Interface Way Point input

AD2 LFMN SID PRNAV 2  
xx aaa xx

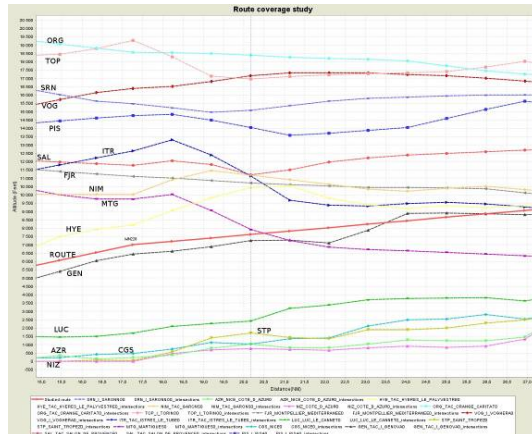
NICE COTE D'AZUR  
SID PRNAV RWY 23L/R  
(Protégés pour CAT A, B, C, D)



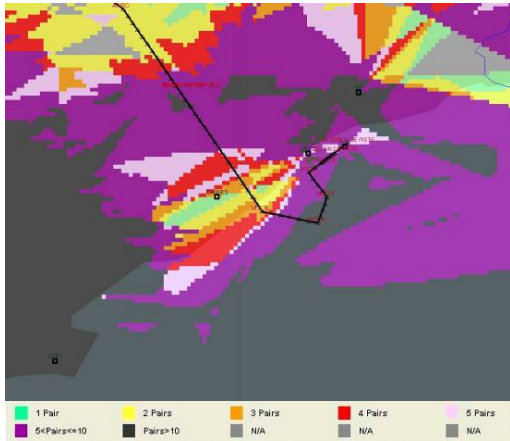
Nice (French Riviera) PRNAV SID STAR



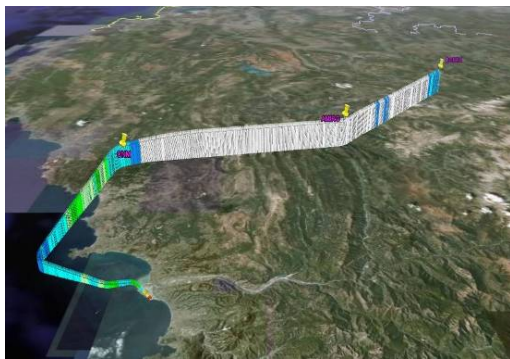
Sagem FIS Guidance Interface



Results of simulation, coverage of the different DME on a SID in Nice area



Results of simulation in Nice (French Riviera) area on a SID



Results of flight Inspection in Nice area on a SID using Google earth representation

### 6.2.5 Flight inspection procedure data

The data issued from the procedure designer are received at step one, path descriptor and chart.

The list of DME facilities to be flight inspected is prepared and communicated to the flight inspection organisation, including any specific factors to be considered.

These data need to be available together with the same input data that were required for the assessment performed with the modelling tool (including the path definition and the vertical profile ...).

#### Two policies confront one another:

The flight inspection can be performed after the design or after the coding.

- If the procedure is flown after the coding, the reference procedure is present in the

FMS data base and the FI can use the FMS for the guidance. In case of any problem, all the process has to be re-done which is not efficient in timing and financial terms.

- If the procedure is flown after the design, and before the coding and the publication, the reference procedure has to be determined.

This solution seems to be more consistent and coherent with our policy of flight inspection.

**The French policy is to flight inspect the procedure before the coding.**

There are no data in the FMS data base concerning the Reference procedure.

Approach chart and path descriptor only are available.

With a basic design with TF, DF or IF as for most of DME/DME procedures, the Waypoints and the Fly By or Fly Over are entered manually in the aircraft FMS or GPS and the procedure is flown using the autopilot.

The procedure coded by the providers could be slightly different from the one calibrated, 0.1 or 0.2 NM of difference around the waypoints. The result won't be affected.

It's nevertheless important to have the same reference procedure for the ground simulation and the calibration flight in order to have true comparison of results.

With a more complicated path descriptor, using turns or RF for example and with LPV and RNP as accurate as RNP 0.15, the reference procedure as to be identical to the one coded latter by database providers.

We use for this purpose AI Skydata software from CGX which will generate data for the aircraft guidance and the simulation tool.

This software is normally used for procedure design. We just use a sub function of the software to obtain the reference procedure as a sequence of points defined with latitude, longitude and height.

The reference procedure can be secured in ARINC 424 or in Excel format for example.

Latitude (deg)	Longitude (deg)	Altitude (ft)
26.2115416667	100.281969444	15700
26.2131813423	100.281811211	15651.8653943
26.2148210175	100.281652972	15603.7307886
26.2164606921	100.28149473	15555.5961829
26.2181003661	100.281336482	15507.4615773
26.2197400396	100.281178231	15459.3269716
26.2213797125	100.281019975	15411.1923659
26.2230193849	100.280861714	15363.0577602
26.2246590568	100.280703449	15314.9231545
26.2262987281	100.28054518	15266.7885488
26.2279383988	100.280386906	15218.6539432
26.229578069	100.280228628	15170.5193375
26.2312177386	100.280070345	15122.3847318
26.2328574078	100.279912058	15074.2501261
26.2344970763	100.279753767	15026.1155204

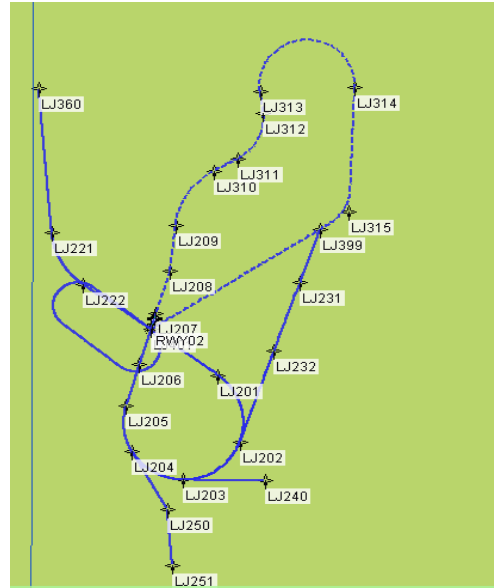
The sampling step, distance between two points, can be set-up.

This file can easily be used for guidance, calculation, comparison ...

It will be used for simulation tool and for flight inspection.

The simulation and FI results in f(x) can be easily compared and superimposed.

Also in post processing we can obtain a layout of the procedure and of the aircraft path.

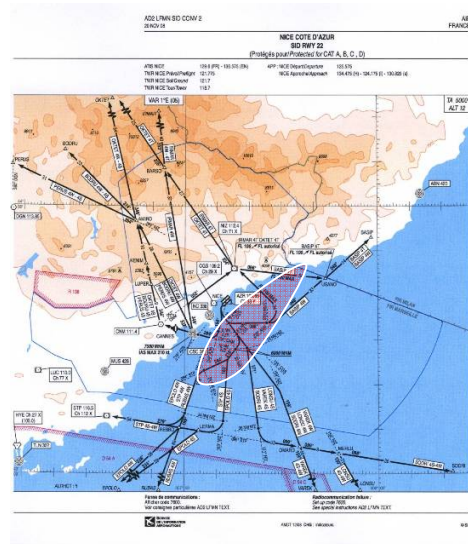


### 6.2.6 GNSS L1 Interference detection

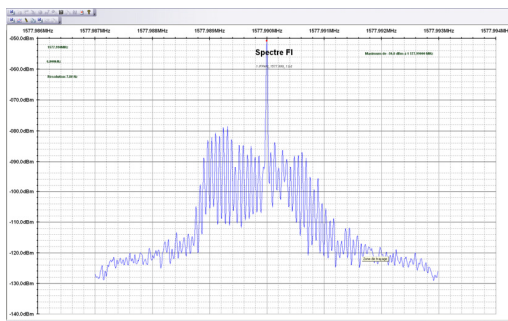
For the Detection and Localization of RF interference jamming FI capability, we use a ROHDE&SCHWARZ EB 200 receiver and a dedicated DTI Software called MELBA to record L1 Band. Melba software has been presented in Toulouse IFIS in 2006.



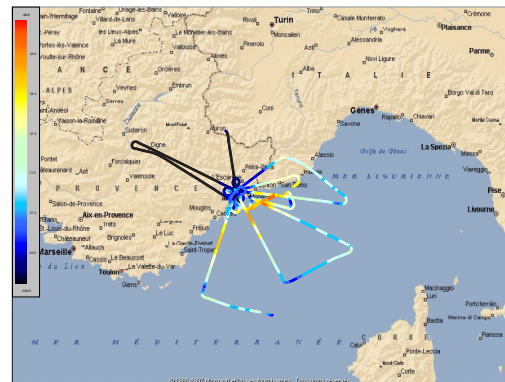
Rohde&Schwarz EB200 Receiver



Volume of GPS L1 jamming



Example of GPS L1 jamming monitored using MELBA Tool in Djibouti around an US military base.



Jamming localisation using Melba tool



An other example of L1 jamming in the vicinity of Nice (French Riviera)

Flight Inspection can check GNSS performances when flying the procedure but it does not guarantee that performances are always met over time.

Compliance to ICAO SARPS are ensured by ground recordings.

### 6.3 RNAV1 GNSS

We just have to assess that the interference environment is satisfactory for the planned procedures.

This can be accomplished by a variety of means, through specific ground or airborne interference equipments or by reviewing existing recordings (see paragraph 5.0).

## 7 PRINCIPLES OF RNP APCH FLIGHT INSPECTION

### 7.1 RNP APCH WITH LNAV MINIMA (NPA GNSS)

#### Extracts from doc 8071, RNAV GNSS (NPA)

“Flight testing/inspection of the GNSS signals-in-space is not required. Flight test is concerned with:

- Validation of RNAV instrument flight procedures.

▶ **Limited for DTI to flyability assessment.**

- Verification of adequate GNSS signal reception for the specific procedure.

▶ **GNSS signal reception is recorded along the procedure.**

- Testing for interference. (*idem decree 28/08/2006*).

▶ **Either check of number of satellites received versus satellites availability prediction or dedicated Interference monitoring system (MELBA).**

Note: IRU can also be used by aircraft but is not part of flight inspection

#### RNAV Verification

Chart publication includes :

The chart and the RNAV path descriptor.

#### → Verification on the ground:

Waypoints / Segments / Distance / Alignments Correctness and Consistency are verified according to existing airport ground references.

#### → Verification during flight inspection:

Using FMS, the pilot follows the procedure (coded as previously) and compares with chart and with external environment.

All arrivals are flown till the MAP.

### 7.2 RNP APCH LNAV/VNAV MINIMA (BARO VNAV)

No such procedure has been implemented yet in France.

We have no specific regulation concerning these flight inspections.

### 7.3 RNP APCH LPV

#### 7.3.1 Extracts from doc 8071, SBAS

“Flight-testing/inspection of the GNSS and SBAS signals-in-space is not required. Flight test is concerned with:

- Validation of RNAV instrument flight procedures.

▶ **Limited for DTI to Flyability assessment.**

- Verification of adequate SBAS support for the specific procedure.

▶ **GNSS and SBAS Signal reception recorded along the procedure together with indication of appropriate accuracy.**

- Testing for interference. (*idem decree 28/08/2006*).

▶ **Either check number of satellites received against satellites availability prediction or dedicated Interference monitoring system (DTI tool MELBA).**

- + **Adequacy and integrity of the FAS DB to the procedure**

#### 7.3.2 FASDB criticality as viewed by DSNALPV Safety File

FAS Datablock is considered as a **critical piece of data** (wrt ICAO Annex 15) since an error in these data can lead to catastrophic event.

▶ Specific data processes must be set up from the very beginning of the procedure design to the integration into the aircraft navigation System.



Within this loop, **flight inspection has been identified as a Risk Reduction Mean** (to reduce probability of occurrence of FE) :

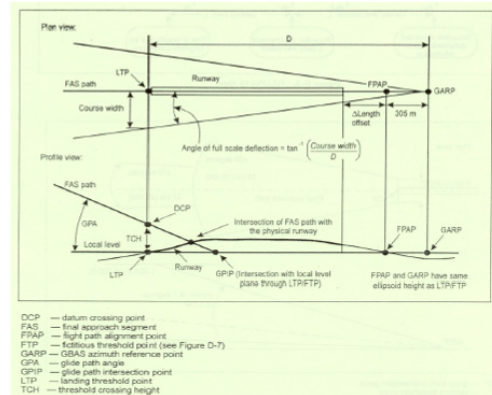
- **As the ultimate detection mean for procedure design error**, (by flying the procedure using the FASDB and chart elements that will be delivered to the DB providers).
- **Against FASDB data corruption/alteration** : FASDB is internally protected by its CRC, but as long as it is a binary file **non human readable**, handling error can still exist and leads to wrong binary file being sent and not detected because its CRC is correct.

### 7.3.3 Principle

Ground (office) preparation: checking FASDB content

- Check of the CRC included in the FASDB using the Eurocontrol tool.
- FASDB Way Points consistency check
  - QFU with existing ILS:
    - Comparison of the coordinates of the WP of the FASDB with the runway and ILS WGS 84 coordinates, published runway azimuth, and doc 8168 rules for FASDB construction.
  - QFU without existing ILS:
    - Comparison of the coordinates of the WP of the FASDB with the runway WGS 84 coordinates, published runway azimuth and doc 8168 rules for FASDB construction

### 7.3.4 FASDAB content

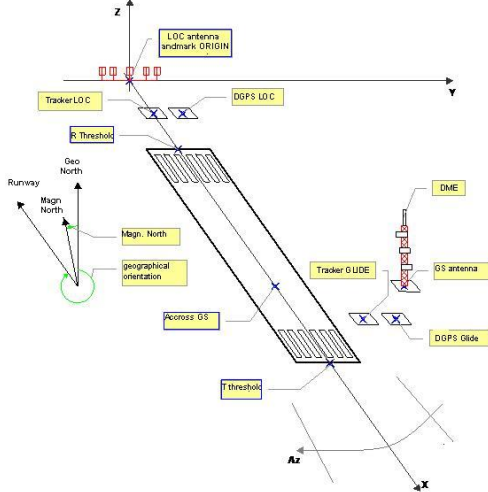


Operation Type:	0
SBAS Provider:	1
Airport Identifier:	LFLC
Runway:	26
Runway Direction:	0
Approach Performance Designator:	0
Route Indicator:	Z
Reference Path Data Selector:	0
Reference Path Identifier:	E26A
LTP/FTP Latitude:	454718.3185N
LTP/FTP Longitude:	0031114.4545E
LTP/FTP Height (metres):	372.3
FPAP Latitude:	454705.1260N
Delta FPAP Latitude (seconds):	-13.1925
FPAP Longitude:	0030900.4790E
Delta FPAP Longitude (seconds):	-133.9755
Threshold Crossing Height:	15.00
TCH Units:	1
Glidepath Angle (degrees):	3.0
Course Width (metres):	105.00
Length Offset (metres):	48
HAL:	40.0
VAL:	50.0
Calculated CRC Value:	AB8761C6

### 7.3.5 WGS 84 Data Base

The WGS 84 Data Base hosted and maintained at SIA (French Procedure Designer) has been developed for more than 15 years.

We've used intensively this DB for the flight inspection of the conventional radio navigation aids (ILS, VOR ...), especially since our truth reference is DGPS based. Flight Inspectors are used to manipulate landmarks and WGS 84 coordinates, which makes the transition to LPV and FAS DB quite similar.

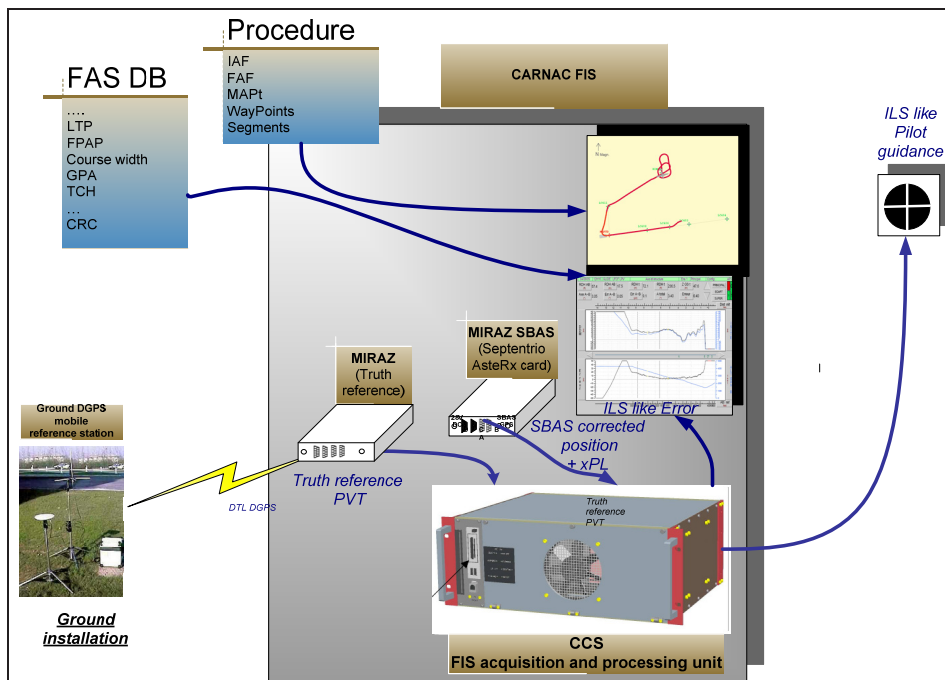


Typical reference data base for an ILS.

### 7.3.6 Flight Inspection System, Installation

Inputs to the Flight Inspection System are:

- The FASDB collated from procedure designer.
- The procedure collated from procedure designer and coded using CGX Skydata software



Three different GPS receivers are used for SBAS procedure flight inspection:

- SBAS receiver (used for LPV flight inspection to rebuild an ILS like DDM)

Based on an OEM card:

- GPS L1 + SBAS (+ Galileo)
  - 24 channels, among which up to 3 SBAS channels
  - SBAS corrected position calculation according to DO229c (TSO C145b/146)
  - Real Time provision of Protection Levels (HPL/VPL) in SBAS positioning mode
  - RAIM computations
- 
- GPS receiver (used for LNAV flight inspection)
    - Based on a Navigation GG24 card
    - 24 channels
    - Can be forced to GPS L1 only
    - RAIM computations according to TSO C129
- 
- D-GPS receiver (truth reference)
    - Dual frequency carrier phase tracking receiver
    - 12 channels
    - Z tracking technology
    - Real time carrier phase differential in RTK/RTCM/DBEN proprietary format
    - Provides 1cm accuracy real time position in ASCII format

These receivers are not MOPS compliant receivers due to:

- The unavailability of the procedure encoded by a data coder by the time of the flight
- The need to access specific data, xPL, ...
- EGNOS is still broadcasting ( till july 2010 ? ) a permanent DO NOT USE flag for SoL operations.

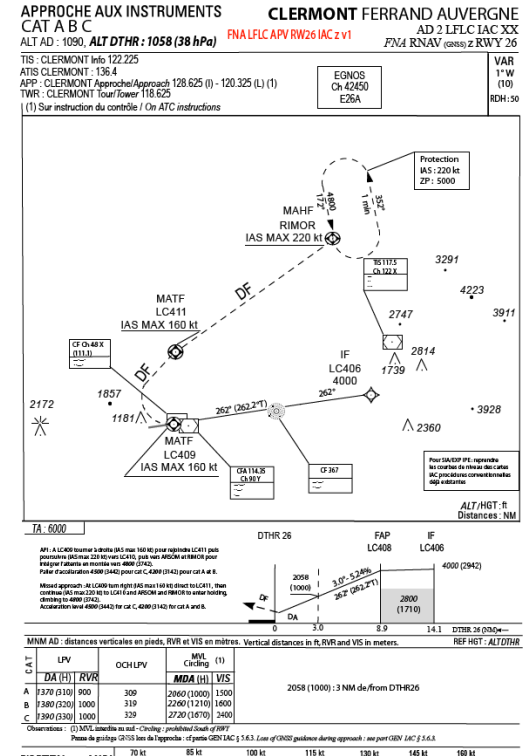
### 7.3.7 Flight Inspection Operations

We perform three different measurements:

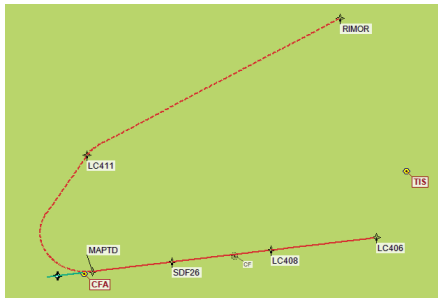
- Taxi on Runway
- Fly the procedure in the axis. FASDB has to lead us right over the runway; altitude and distance have to be consistent with the chart at 1000ft.
- Fly the horizontal sector  
We fly no R/L offset approach, the structure xPL can change from an offset flight to another. We consider more interesting to fly a crossing sector.

The CGX AI Skydata software is used to determined the reference procedure and in post processing to superimpose reference procedure and aircraft path in vertical and horizontal plans.

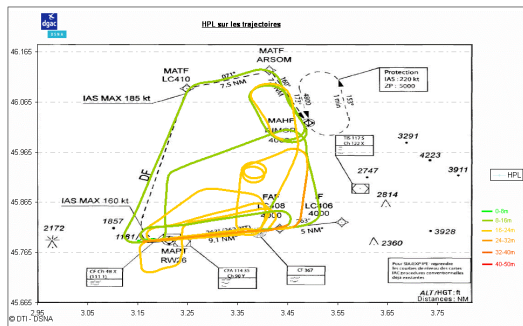
### 7.3.8 Results



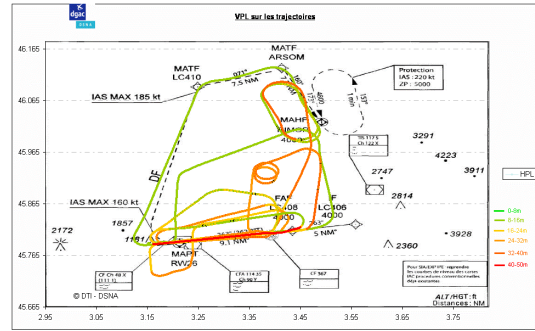
Clermont-Ferrand LPV Procedure Chart



Procedure Clermont-Ferrand as coded with CGX AI Skydata in CARNAC

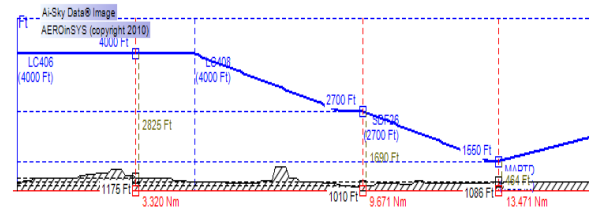


Result of Horizontal Protection Level 8 runs performed



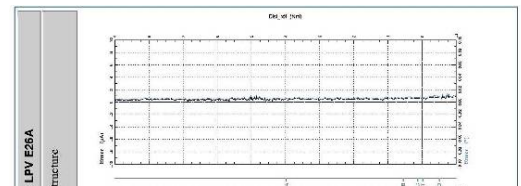
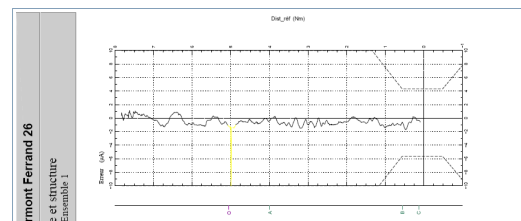
Result of Vertical Protection Level, 8 runs performed

FASDB has leaded us right over the runway; altitude and distance are consistent with the chart at 1000ft.



Vertical aircraft path and procedure superimposed with ground relief using CGX AI Skydata in post processing.

### 7.3.9 Accuracy of LPV guidance in comparison with ILS



## **8 PRINCIPLES OF RNP AR APCH FLIGHT INSPECTION**

A test in coordination with Air France airline should take place in Bastia (Corsica) soon.  
We have no specific regulation concerning these flight inspections now.

## **9 CONCLUSION**

PBN Flight Inspections in France are today limited to RNAV1 GNSS/DME-DME and RNP APCH (LNAV and APV/LPV).

The French Flight Inspection Service must comply with the international and national regulations.

Some potentially contradicting or confusing points have been noticed.

We are, within the DSNA (French CAA), working towards a more appropriate and pragmatic regulation for the definition of the PBN procedure's flight inspection.

Thus, the Sagem CARNAC Flight Inspection System and the associated software functions are ready for new features of RNP flight inspections, including RNP APP-AR.



# Calibrating DME Coverage Predictions with Flight Inspection Measurements

## **Gerhard E. Berz**

Navigation Infrastructure Focal Point  
EUROCONTROL  
B-1130 Brussels, Belgium  
E-mail: [gerhard.berz@eurocontrol.int](mailto:gerhard.berz@eurocontrol.int)

## **Valeriu Vitan**

Senior Navigation Expert  
EUROCONTROL  
B-1130 Brussels, Belgium  
E-mail: [valeriu.vitan@eurocontrol.int](mailto:valeriu.vitan@eurocontrol.int)

## **Dr. Jochen Bredemeyer**

Head of Research  
FCS Flight Calibration Services GmbH  
D-38108 Braunschweig, Germany  
E-mail: [brd@flightcalibration.de](mailto:brd@flightcalibration.de)

## **Wietze Oenema**

Senior Navigation Expert  
EUROCONTROL Experimental Center  
F-91222 Bretigny-sur-Orge, France  
E-mail: [wietze.oenema@eurocontrol.int](mailto:wietze.oenema@eurocontrol.int)

## **ABSTRACT**

With the implementation of Performance Based Navigation (PBN), infrastructure suitability analysis for Distance Measuring Equipment (DME) is becoming increasingly important. This requires a new level of collaboration between navigation engineers, flight inspectors and procedure designers. Additionally, the use of software coverage prediction tools based on terrain data is critical to optimize flight inspection. However, this requires a detailed understanding of the limitations of software prediction tools. Recent flight inspection measurements at the limit of DME coverage were collected to understand these limitations.

The paper gives an overview of the performed analysis, addressing the interaction between software predictions and flight inspection. The flight inspection measurements were recorded passively using a dedicated receiver and recorder. The receiver measurements were corrected for the antenna factor, such that they represent a true field strength measurement. These measurements were then compared with corresponding terrain based coverage predictions. The understanding derived from this analysis will serve to guide the use and development of the software prediction tool. The paper summarizes the lessons learned from this effort with a view to give guidelines on how to optimize flight inspection of

infrastructure supporting Area Navigation (RNAV) procedures.

## **INTRODUCTION**

The recently introduced chapter 3.4 of ICAO Doc 8071 [1] describes the need to conduct flight inspection especially for terminal area RNAV procedures, and to balance these activities with a complementary software tool. The use of such tools aims first to optimize the flight inspection, such that the right set of DME's can be inspected in an efficient manner. This is often essential as most current flight inspection systems have only a limited number of DME interrogators, requiring several runs for a single RNAV procedure – which may be difficult to accommodate in a busy terminal area from an operational point of view. However, a second aim of using a software coverage prediction tool is also to try to avoid the flight inspection completely, trusting in the accuracy of the prediction. Given this understandable desire in the current cost constrained environment, it is important to understand the quality and limitations of such coverage predictions. Consequently, EUROCONTROL, the European Organization for the Safety of Air Navigation, is investigating this subject with the aim to provide guidance on how to find a correct balance between simulation and testing. Guidance material on the overall assessment process has already been published [2].

The software tool that has been used for this work is called DEMETER. A number of other, commercial tools exist as well. DEMETER has just been through a major upgrade, specifically with a view to integrate simulation and flight test activities. More information on this tool can be found on [3]. These tools all use terrain databases to conduct a line of sight coverage calculation. The quality of the coverage prediction is a relatively complex relationship between the actual terrain shape, the quality and resolution of the available terrain data, and a number of propagation, calculation and sampling issues. Thus it is not a simple matter to determine the accuracy of those predictions analytically. However, using flight inspection to provide calibration points is not a simple matter either. First, determining coverage boundaries due to terrain shading through an accurate measurement of achieved field strength near the Annex 10 [4] limit is not trivial, as has been discussed in a previous paper [5]. Second, actually collecting such data at relevant points, often far out in coverage where typically no historical records exist, can easily become economically prohibitive.

A passive recording approach has been used to collect such flight inspection data. While this has made a significant amount of data available, the next challenge is to sort that data and to filter it in a way that meaningful comparisons can be made. This paper will describe this process and show some initial results. More work is still needed to come to more conclusive results.

### **SOFTWARE COVERAGE PREDICTION ISSUES**

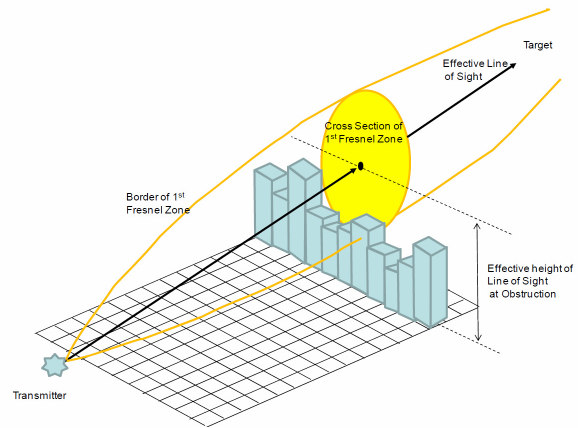
The quality and resolution of available terrain data has significantly improved in recent years. This includes freely available data, such as from the NASA Shuttle Radar Topography Missions (SRTM), while commercial sources deliver even more accurate and continuous coverage, but typically only on a regional level. For the purposes of this work, the focus is on the use of terrain data that meets the Digital Terrain Elevation Data (DTED) Level 1 standard, providing elevation postings every 3 arc seconds (roughly 90m). While this is a great improvement over the formerly best freely available 30 arc second data (roughly 1km point spacing), it is still at the limits of what is suitable for terminal area (low altitude) coverage predictions. Furthermore, in a number of cases some additional processing is needed even for good DTED 1 data, as it may contain voids that need to be filled. A more detailed description of terrain data related issues can be found in [6].

Another critical piece of input data is the station height. While current Aeronautical Information Publications (AIP) indicate antenna height, this is only required to the nearest 30m, resulting in errors up to  $\pm 15m$ . This can cause significant errors when trying to relate an antenna

height in meters above mean sea level (AMSL) to its height over terrain, because relative accuracy between the antenna and terrain is more important than absolute accuracy. While this information can easily be obtained by a site visit and a lookup of the database terrain height at the beacon location, it is not generally available.

### **Fresnel Zone and Effective Obstacle Height**

The level of sophistication necessary in software modeling to accurately predict radio frequency propagation at DME frequencies is very significant, both in terms of algorithm complexity and requirements for input data. Typically, it is not worthwhile to do this for applications such as DEMETER, since more dedicated software packages exist and because the additional effort is not justified by a corresponding gain in accuracy (given the general absence of the required input data). Nonetheless, in the context of geometrical coverage prediction it is appropriate to consider Fresnel zone effects. An initial study of the subject has been conducted, showing a few issues relevant to coverage prediction. This was done by applying the rule that for sufficient signal-in-space propagation, 60% of the area of the first Fresnel zone needs to be unobstructed, while applying this to a number of terrain and obstacle scenarios. Figure 1 shows the interaction between terrain and the first Fresnel zone radius at a given distance, illustrating its impact on effective obstacle height.

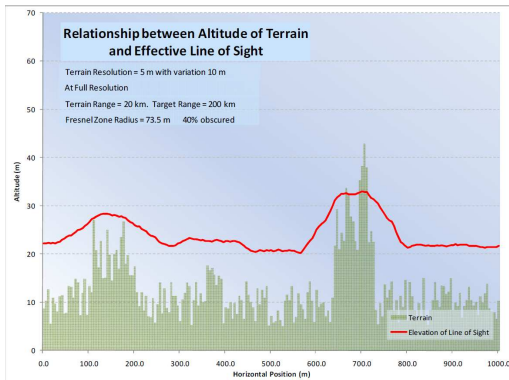


**Figure 1: Fresnel Zone, Terrain and Effective Obstacle Height Interactions**

The figure above demonstrates that the “effective height” of an obstacle, depending on the terrain surrounding it, can be higher than the actual terrain height. When applied to various samples of terrain data, plots such as contained in figure 2 can be generated. The analysis shows that in general, the effective height of terrain or obstacles for line of sight propagation is slightly above the terrain levels – this height will vary with “terrain noise” (roughness) and



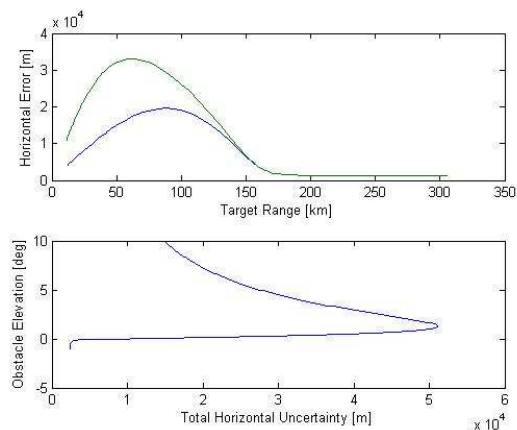
the respective distances between the terrain and the beacon and the aircraft receiver. It can also be seen that narrow obstacle spikes (a tower in this case) are insignificant while an obstacle in general has an effect that is wider than the obstacle itself.



**Figure 2: Effective Terrain Height using Fresnel Zone Criteria**

### Geometric Version of the Near-Far Problem

Another analysis looked at the sensitivity of coverage prediction to height errors. While the coverage plots are presented as a map on a flat screen, the calculations are carried out for a specific aircraft height, e.g., the map-plot represents a surface on an approximate sphere. Furthermore, the elevation angles between the transmitter of the beacon and the aircraft receiver that interact with terrain are shallow – often even below zero degrees. Figure 3 shows the result of an analysis that was performed to look at a worst case geometry using height errors that are considered possible. The obstacle under consideration was 10m high, with a bias error of 5m and an error slowly increasing with distance (up to 20m at a 200km range). The obstacle was moved along the distance between the transponder and the interrogator to see what the impact would be for a given prediction altitude, in this case 2000m above the transponder.



**Figure 3: Worst Case Geometric Multiplier Effect**

The horizontal error plot above shows the impact of a vertical obstacle error on the horizontal prediction, both to the near side (obstacle higher than assumed) and to the far side (obstacle lower than assumed), the far errors being greater in magnitude. From the lower plot it can be seen that the most critical elevation angles are around 1 degree. This is due to the geometric interaction between the line of sight and the earth curvature. In this scenario, the worst case obstacle is at 357m from the beacon with a corresponding elevation angle of 1.6 degrees. This means that shallow angles and relative errors at close ranges can create the most significant prediction errors. While the latter is obvious, the sensitivity to shallow angles is surprising. This is bad news for the average clean site and for terminal area predictions, where the chosen altitudes and ranges are common. However, as will be seen later when looking at flight inspection results, the sum of error variables seems to balance out somewhat, since the errors seen in the real data are not that dramatic.

### Calculation Methods and Sampling Issues

Coverage prediction is essentially a polar matter, looking out over the terrain at little increments of azimuth. On the other hand, terrain data is available in a Cartesian format. This requires some conversion between the two systems, causing a variety of sampling issues. DEMETER calculates coverage by taking “cake slices” of terrain data from the beacon to determine visibility-limiting summits along that sector. At the beginning of the sector (near the station), the terrain data rectangles are much too big, e.g., more data than necessary is being considered. This leads to overlaps from one azimuth increment to the next, distorting the true size of close-in obstacles. At the far end of the sector, too many terrain data cells fit the width of the sector, such that a single narrow peak can incorrectly dominate the overall height within that azimuth increment.

Another concern resulting from terrain data resolution issues is calculation efficiency – while it is desirable to use the highest resolution terrain data available to ensure the best possible prediction in the near field, this causes significant calculation overheads in the far field. DEMETER’s smallest calculation increment is 0.3 degrees of azimuth and 500m or sector length. One new feature that was introduced to optimize terrain data handling is the ability to use mixed levels of terrain data resolution, from DTED level 0 to level 2 (1 arc second data). Even if DTED 2 data is not widely available, it can be re-sampled from local survey sources using some reasonably priced off-the shelf software packages, allowing local optimizations near the beacon sites.

Finally, there is also the question of what earth radius to use. It is commonly held that a four thirds earth radius is appropriate for radio line of sight. However, in some cases and depending on atmospheric conditions, DME propagation may be closer to optical line of sight. Without using propagation tools it is not possible to settle this question analytically. This was another reason for collecting flight inspection data, to see what values would most closely match reality.

### **Coverage Prediction Issues Summary**

While the basic approach of terrain data based coverage prediction seems straightforward, a number of complexities make it difficult to produce generic statements such as given a certain level of DTED, accuracy will be x. First of all, the terrain data needs to allow the identification of the relevant constraining summit for a given azimuth with reasonable accuracy, in particular of the relative geometry. This needs to take full account of the sampling issues mentioned above. A further complication is then added by Fresnel zone aspects, which may modify the apparent height of terrain features. Once these questions can be settled analytically, the achievable accuracy is a function of the individual obstacle geometries, which vary with each azimuth. This means that each individual coverage plot can have widely varying prediction accuracies along its periphery. The next sections of this paper discuss the efforts to collect data to verify these aspects.

### **FLIGHT INSPECTION DATA RECORDING**

One objective of the work was to obtain data on DME reception in flight at low costs. This could be achieved by installing a recording system operating in the background in a flight inspection aircraft, carrying out recording during the regular flight inspection activity. Therefore, no project-specific flight testing costs arose. This is a major factor to achieve a low cost of this study, in view of the cost of a flight testing hour which is usually in the order

of several thousand Euros, depending on the type of aircraft used.

FCS carries out flight inspections in the terminal areas as well as for en-route systems in Germany, Austria and Switzerland. This geographical range provides data on a wide cross section of DME installations in a variety of terrain environments. Data recording also took place during ferry flights.

### **System Architecture Considerations**

The DME recording unit is part of the SISMOS (Signal-in-Space Monitoring System) equipment family and is a specially designed RF receiver covering all DME (and TACAN) channels. It contains one physical recording channel which can be instantaneously switched from one frequency to another. Its main purpose is to detect all DME pulses above Minimum Tracking Level (MTL) of a certain channel on the video baseband (e.g., time domain) while preserving all data of the DME channel’s multipath propagation activity for later post-processing analysis.

In the selected channel there may be numerous pulses apart from the selected DME, for example those emitted by air-to-air TACANs. A major advantage of the system’s time-lag free channel switching feature is the fact that data of a selectable number of DME beacons can simultaneously be recorded without any loss of data. The benefit of such a recording facility is also described in [5].

The system’s firmware contains information on all DME facilities in the area of operation, the data being stored in a comprehensive hash table. The real-time algorithm during flight uses a hash function to efficiently map the current WGS84 position gained from the local GPS receiver to a number of associated DME facilities.

### **Mode of Operation**

SISMOS / DME is a fully autonomous facility which is connected to aircraft power (28V DC), to a spare L band antenna and to a GPS antenna to obtain the momentary, rough position and the GPS pulse per second as the main time reference for synchronisation. Additionally, the precise flight path and aircraft orientation is derived from the regular Flight Inspection System (FIS) installed in the FCS flight inspection aircraft. Furthermore, SISMOS is connected the aircraft’s ARINC suppression bus to obtain dead time information from airborne L band emissions from on-board avionics systems (DME, SSR). Once the system is running, it is designed to function without manual intervention. A liquid crystal display provides system active status information, as well as usage of the internal hard disk which is directly controlled by the firmware.

As a consequence of the continuous operation during e.g. a one week flight inspection mission, very large files are generated. They contain a sequence of GPS time-stamped video data referenced to the selected channel.

### **Mission Planning and DME Beacon Selection**

If there are no special requirements, the recording system is active during any ferry and mission flights and will select the DME channels according to the standard hash algorithm: A comprehensive data base of all DME/TACAN facilities is structured as a matrix against WGS84 longitude and latitude. One single matrix value is a pointer to a list of the DME beacons at the border of their operational coverage which will then be recorded for a certain minute roll call period. Since the aircraft moves, the roll call list will be continuously updated. The hash table (matrix) must be computed and loaded in the recording system before the missions starts. This causes the system to record some 50% of all German DME/TACAN facilities during a single ferry flight from Braunschweig to Munich.

The tuning approach described above depends on the Designated Operational Coverage (DOC) declared by the Air Navigation Service Provider (ANSP). Other tuning strategies, such as defining specific regions for particular terminal airspaces with a group of associated DME have also been considered, but not yet implemented. This “special region” strategy would need to be coordinated with mission control in order to activate the airspaces relevant for a specific week’s mission. Another modification being envisaged is to only switch to a new channel once a specific DME has been fully lost, rather than actively switching to a new channel depending on the lat/lon position of the aircraft.

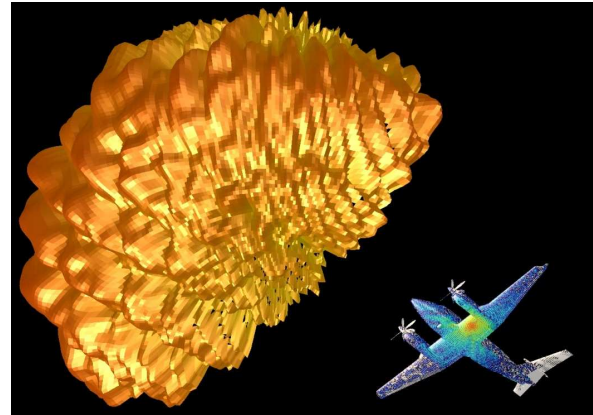
### **Post Processing of Recorded Data**

Collected data can be analysed in various, generic ways. At first, the most important task is to perform a time-synchronized data fusion between the SISMOS/DME data and flight path gained from the FIS.

### **Traceability of Measured Levels to Field Strength (e.g. dBV/m, dBW/m<sup>2</sup>)**

In traditional flight inspection the role of the aircraft antenna embedded in a dynamic airborne platform is underestimated. A simple correction value usually serves to compute the “field strength” from the received receiver level. In fact, things are much more complex. The effective antenna factor cannot be treated as a scalar but must be a 4-dimensional vector. A complex radiation diagram of a bottom-mounted L band antenna of a Beech Super King Air B300 is shown in figure 4. The aircraft orientation angles pitch, roll, heading must be taken into consideration to pick out the relevant gain value which is

also frequency-dependent. The determination of the antenna cable complex S parameters in context with the selected antenna factor are a prerequisite to derive the correct momentary field strength.



**Figure 4: Front-orientated gain of an L band antenna in 3D view**

FCS has invested significantly to validate the antenna installed performance of their flight inspection aircraft by means of major computer simulation and additional validation and reference measurements. This project was carried out in cooperation with EADS of Bremen (simulation facility) and the German National Institute of Metrology (PTB). Papers [7, 8] provide an overview of this work.

### **ANALYSIS APPROACH**

Coverage is achieved when the DME ground facility provides a signal in space of at least  $-89\text{dBW/m}^2$ . While UHF propagation mostly follows radio line of sight, actual receiver performance will vary. The amount of margin depends also on the location, range and shape of the obstructing obstacle. A prediction based on pure geometrical calculations knows nothing of the RF propagation budget. Thus it is not a straightforward process to compare terrain data based coverage predictions that are essentially of a binary nature (inside / outside of coverage) with recordings of field strength.

For all flight data positions, the theoretically expected field strength can be calculated, using either a standard free space propagation link budget, or by using a model such as IF77 (the model normally used by ICAO and ITU in propagation and compatibility studies of navigation systems). Both methods require making some assumptions of typical installation parameters, such as cable losses and antenna gain patterns. Once these comparisons are established, it is reasonable to assume

that any recorded values that are significantly lower than the theoretical values are due to terrain attenuation. However, given the various noise levels present both in the predictions and the recordings, insufficient time was available as of the time of this writing to drive this analysis to relevant conclusions.

The approach that was adopted for the analysis presented here was to reduce the problem to a binary comparison. If the recorded field strength is below the minimum level, but inside software predicted coverage, then the prediction was considered to be optimistic. On the other hand, if the recorded field strength was above the minimum level, but outside predicted coverage, then the prediction was considered conservative. In the remaining two other cases, the prediction is correct. This simple comparison still suffers from a data noise issue – peaks and troughs in the field strength data make it difficult to say when and where the  $-89\text{dBW}/\text{m}^2$  boundary has been crossed. To address this, a five second filter has been used, e.g., only if the field strength is below the minimum level for five seconds, then the recording is considered as out of coverage (and vice-versa for in-coverage values).

Another problem in sorting through large amounts of data is to identify relevant trajectories. The DEMETER horizon tool was used to do this. By calculating the elevation angle from the respective beacon, and comparing them to the terrain horizon profile seen by that beacon, relevant pieces of flight data can be extracted. Those trajectories were further parsed into pieces at common altitude ranges, since DEMETER does predictions for a specific altitude. The coverage prediction of a specific altitude was then exported as a shape-file, to permit numerical comparison with the flight inspection data, e.g., to generate histograms for both optimistic and conservative predictions and get a feel for the associated error magnitudes.

The same type of analysis would also be possible in the vertical domain, by importing the trajectory into DEMETER as an RNAV procedure. However, as this requires re-sampling of the trajectory down to a reasonably low number of artificial procedure points, this has not yet been carried out.

## INITIAL FINDINGS

The planning and constraints of our activities did not permit finalizing the analysis in time for the IFIS. Consequently, these results need to be considered as preliminary. The goals of the analysis are as follows:

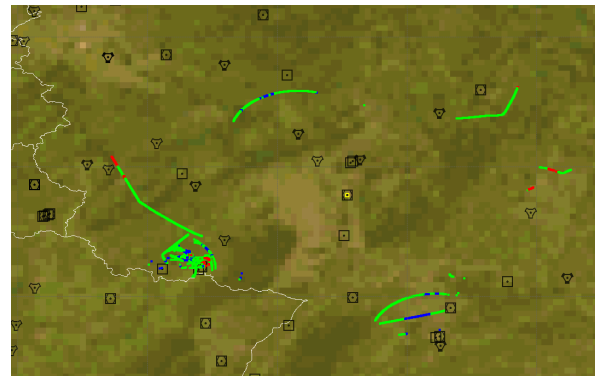
- 1) Establish an analytical link between the relevant input factors and the achievable coverage

prediction accuracy, validated through measurements.

- 2) Use this link to provide guidance on what levels of terrain data, and which calculation and algorithm settings are most appropriate for a given scenario.
- 3) Provide guidance on what other optimizations (algorithm, analysis process) are most effective to improve prediction accuracy and confidence.

The data analysis results are not sufficiently clear yet to provide significant answers to meet the stated goals. This work will be further matured in the coming months. On the one hand, the flight data recording process (tuning strategy) needs to be further optimized. On the other hand, further analysis is needed to try and establish the desired links.

Figure 5 shows the trajectory data that is available for the Ried DME, located in West / Central Germany near Luxemburg. The green lines represent correct predictions, while the blue ones are conservative and the red are optimistic. In the context of using these predictions for PBN infrastructure assessment, optimistic predictions unfortunately represent the more significant problem than conservative ones. The navaid symbol that is highlighted with a little yellow point is the Ried DME. Despite the massive amounts of data collected in terms of Mega Bytes, the data still seems rather sparse spacially, with the Ried example being one of the facilities with the most relevant data. Data has been collected from 137 facilities spread across Germany and Switzerland.

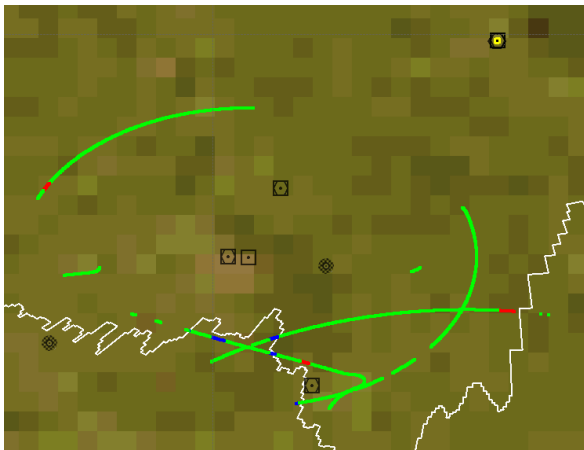


**Figure 5: Trajectory Data for the Ried DME**

The coverage prediction contours are not shown on this summary plot, because the flights go through a range of altitudes - showing all coverages would clutter the picture too much. In general, the coverages seem to match better with a k-factor of 1, e.g., a normal earth radius. For a k-factor of 1.33, 4/3 earth radius, the coverage contours

simply move further out, yielding more optimistic results. While this may be correct given the UHF wavelengths of DME pulses, the data overall is too sparse to draw any firm conclusions.

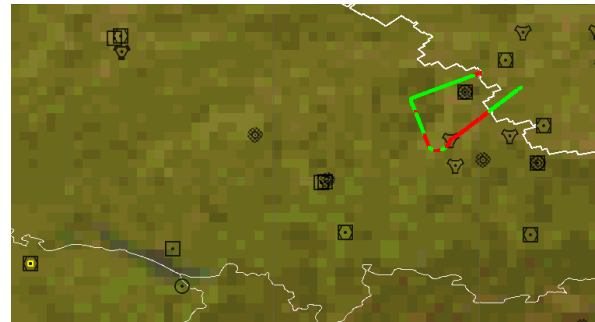
When looking at the trajectories in more detail, a number of fairly good results are present in the data. One such example is Bayreuth, a terminal facility in Bavaria. It should be noted that in most of these cases, it was necessary to remove the DOC as a coverage constraint – a constraint that is normally imposed when doing assessments for RNAV procedures. Some Bayreuth trajectories are shown in figure 6. They have been flown at or near 5000ft AMSL, and the white contour is the corresponding coverage prediction. With the exception of a small red segment on the very left (west) of the picture, no significant mismatches are apparent. However, there are also some gaps in the trajectories where it is reasonable to assume that the aircraft actually flew and that the signal strength was below the minimum tracking level of the receiver – the red tracks only apply when there is recorded data. Strictly speaking, these would need to be colored red (optimistic) as well. However, it needs to be remembered that despite calibrating out the 3D antenna gain patterns, the receiver is still subject to signal dynamics as the aircraft goes through attitude changes.



**Figure 6: DME Bayreuth Coverage at 5'000ft AMSL**

The strong azimuth dependence of the prediction errors can also be inferred from figure 6. Making the coverage prediction contour match the actual data is not just a matter of scaling the overall contour further out or further in – in some cases it would need to be pulled in while in others it needs to be extended. This can also be seen in figure 7, where the prediction contour seems to be right in that something happens, but unfortunately in the wrong sense. The example is from DME Zurich East in Switzerland, the actual flight path being over southern Germany near Lake Constance. One may be tempted to

think that this example is quite a bad prediction. However, considering the far distance from the facility and the fact that the receiver continued tracking the signal while the software prediction knows nothing of RF signal levels, it does not seem so bad.



**Figure 7: DME Zurich East Coverage at 25'000ft AMSL**

Confronted with these results, the questions invariably turn to try and identify what the underlying causes are for the inaccuracies. This requires a more refined analysis both on the propagation side and on the geometric side. While these sorts of investigations have not yet advanced sufficiently for presentation, some preliminary observations on the geometric side are shown here. While this was a priority because of the ongoing DEMETER tool development, it is also because these methods have not gotten much attention in the past, while RF propagation aspects through modeling such as IF77 and Fresnel zone consideration are more developed. This is evident from the availability of corresponding tools.

Turning back to the Ried DME example, the geometric analysis capabilities of DEMETER can be shown, using some trajectories at and near 6000ft AMSL, South-East of the beacon, as an example. In this case, good signal reception is available outside of geometric coverage (this time indicated by red lines). The DEMETER plot in figure 8 shows the tracks and the corresponding line of sight coverage contours in the upper half of the screen. The lower half shows the already mentioned horizon tool, which is a terrain data generated visibility horizon showing elevation angles against 360 degrees of azimuth. The horizon tool is linked to the coverage plot, in that the blue circle (showing as an ellipse due to map projection) and its radial correspond to the vertical line on the coverage plot. Using this reference, it can be seen that the high peaks on the station horizon are responsible for the coverage limitations east of the beacon. The coverage plot additionally shows the summits resulting from the coverage calculation. The light blue points correspond to negative screening angles, while the yellow points refer to elevations between zero and two degrees. Looking at the highlighted radial to the southeast, it can be seen that the

optimistic coverage tracks are due to terrain summits between 0,5 and 1 degree of elevation, at a fairly close range to the facility. The terrain features having an impact on coverage can now easily be identified as the Zwingenberg and Felsberg mountains at ranges between 5 and 7 NM from the DME. A next step could be to further

verify the elevation angle profile for the relevant azimuths using local data. DEMETER permits a variety of options to deal with cases when there are mismatches between the real and the calculated elevation profile. Using such processes, the coverage predictions can be further optimized.

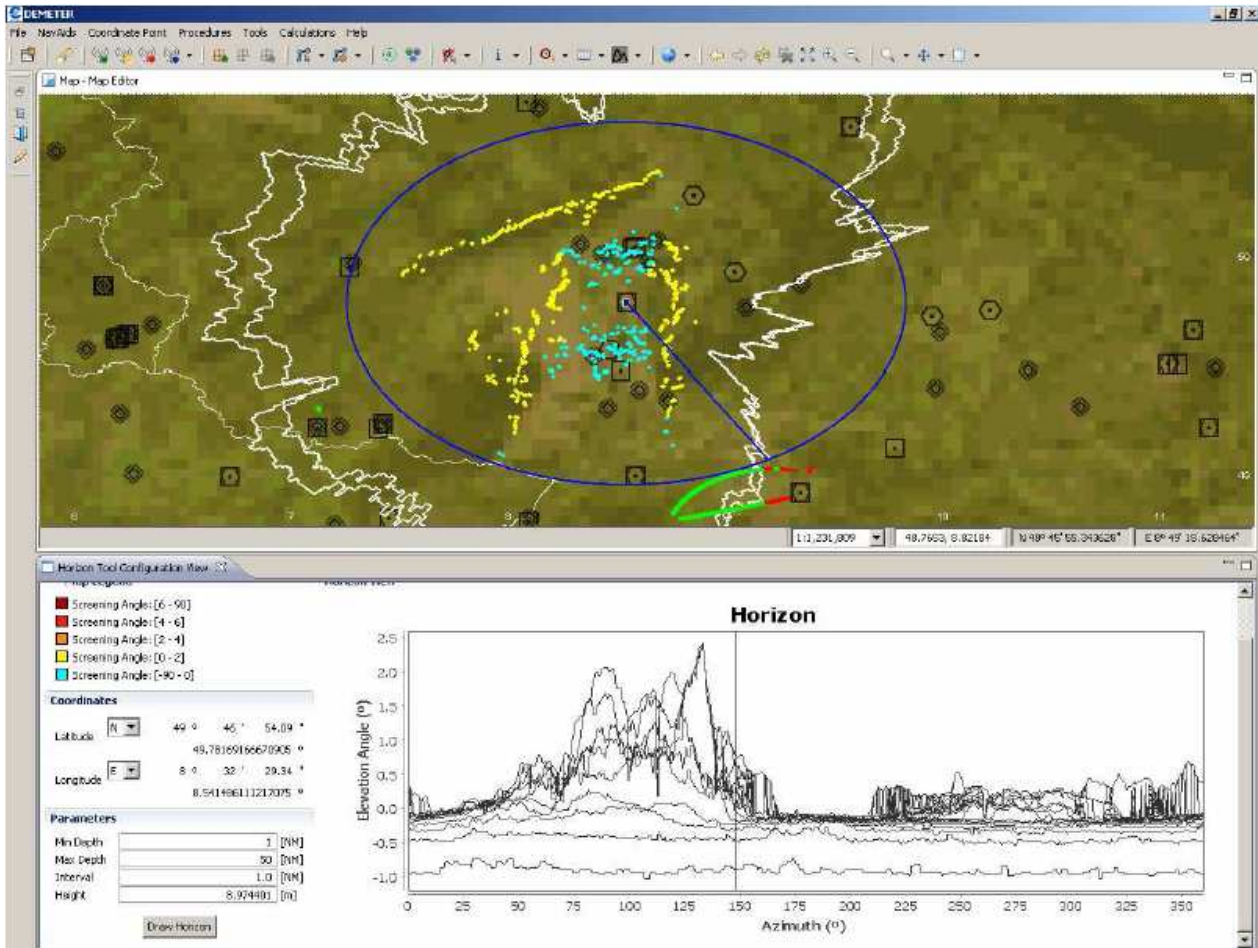


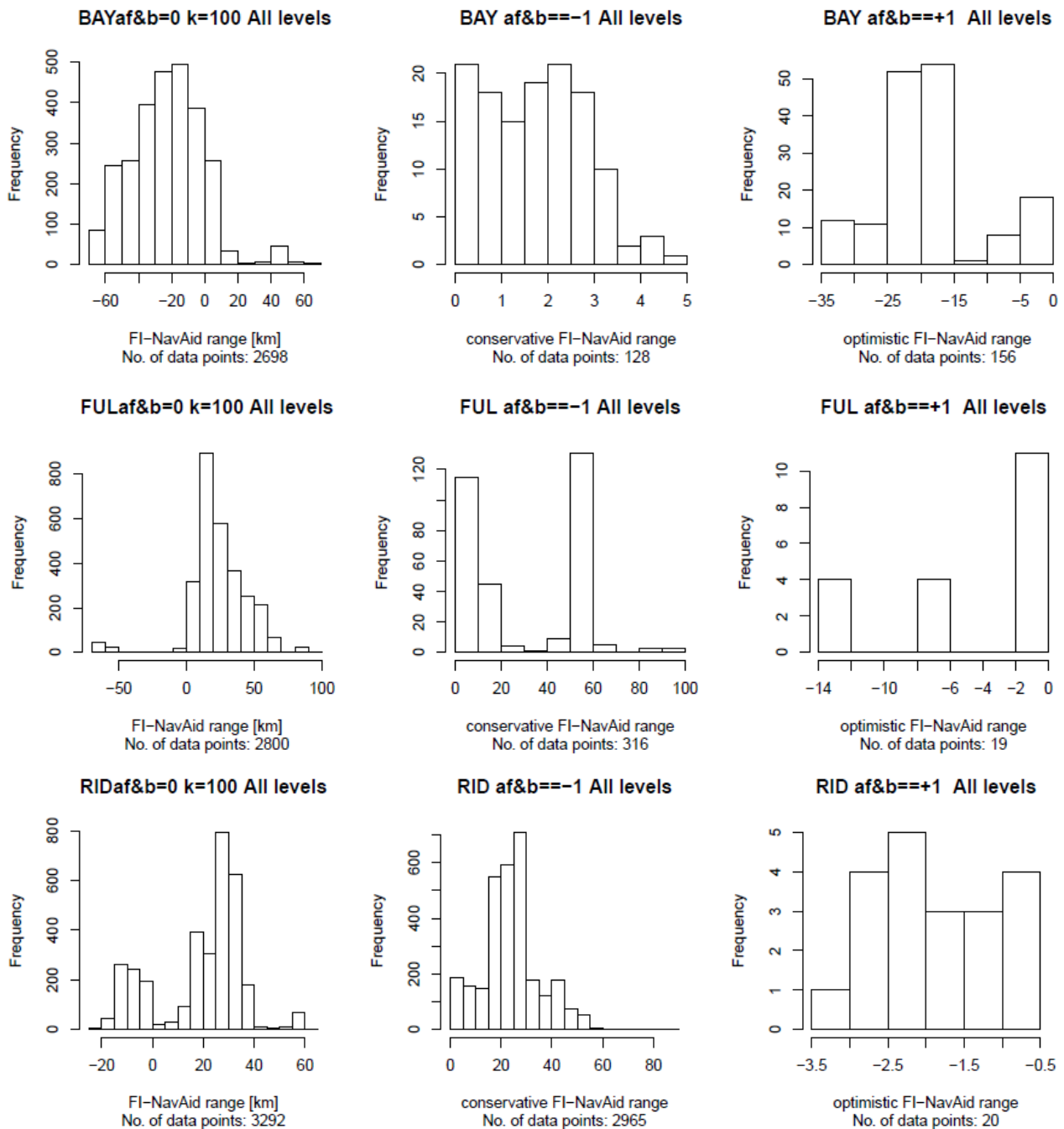
Figure 8: DEMETER Horizon Tool and DME Ried Coverage at 6'000ft

### Some Quantitative Results

While the benefits of visualization capabilities of such Geographic Information Systems (GIS) are evident, it is also a labor intensive matter. Consequently, some histograms were generated to see what sorts of range prediction errors are visible in the data, to try and tie back to the original objectives of the data analysis. Figure 9 shows these results for DME Bayreuth, Fulda and Ried. The histogram on the left shows the number of data points where the flight recordings match the coverage prediction, e.g., minimum field strength is exceeded inside coverage

and not achieved outside of coverage. The horizontal scale is given in kilometers from the coverage prediction boundary, giving a somewhat “inverse” idea of the radial distribution of points. The second (center) histogram presents the conservative data point distribution, e.g., those that are outside of predicted coverage where reception was still above minimum field strength. The third (right) histogram shows the optimistic data, e.g., points that are below minimum field strength but inside coverage. Despite the apparently high number of samples for these three facilities, it has to be remembered that they

still represent a highly random and sparse sampling of the individual facility coverage.



**Figure 9: Flight Inspection Data Histograms in Relation to Predicted Coverage for DME Bayreuth (BAY), Fulda (FUL) and Ried (RID)**

While it is good news that the large majority of data points is in the “correct” histograms on the left, that

appears to run into significant limits when considering the center/conservative histogram for Ried. However, the

Ried histogram was generated taking into account the formally declared DOC of 60NM, and additional sectorization limitations down to 40NM. Figure 5 on the other hand was generated with an artificially chosen DOC of 80NM, giving more positive results and illustrating the importance of considering the impact of both the DOC and the k-factor. Nonetheless, in the case of Fulda for example, range prediction errors easily exceed 60km. The level of optimism is luckily more restrained, with the majority of cases for these three facilities being limited to under 25km.

The analysis shows that terrain data based coverage prediction is far from being an exact science. While many predictions are quite accurate and normally conservative, it is also important to recognize that excessive conservatism is not good either: navigation signals should be made available as far as possible both for the benefit of aircrew and passenger safety and to minimize the need for investments in navigation facilities.

## **CONCLUSIONS**

This paper has shown that it is possible to apply a passive data recording process (low cost) to collecting good quality coverage data in locations that are normally too far away from the beacon for dedicated inspections, and to use that data in verifying terrain-data-based coverage predictions. While much of this process can be automated through the development of appropriate tools, there still remain manual interactions in interpreting the visualized data, especially when trying to identify probable causes for any mismatches. Despite the overall promise of the approach, significant issues remain, not only simply because of the large number of variables on the analytical side but also in terms of process: despite enormous amounts of collected data, any conclusions at this point rely too much on spotty observations, limiting their relevance. Consequently, the data recording and analysis process needs to be further improved to enable a more targeted analysis. More dedicated flight tests may be needed to provide a comprehensive baseline analysis.

The two hypothesis that have garnered some initial support are that a k-factor of 1 (optical line of sight) may be more appropriate and that the coverage azimuths with the greatest vulnerability to errors are those with shallow and close-by terrain summits. What concerns tying the results back to the original objectives, e.g., creating at least an approximatively deterministic relationship between input variables and achievable prediction accuracy, the analysis has not progressed sufficiently. The only thing that can be clearly concluded for the purpose of guiding infrastructure assessments is that while coverage predictions using the best generally available data (DTED Level 1 and maximum processing resolution of

DEMETER) are generally conservative, they can easily be several nautical miles off from actual coverage.

The above conclusion underlines the need for software prediction studies to work in close cooperation with flight inspection activities. While it may be possible to offer RNAV procedures based on coverage predictions alone especially at higher altitudes, this can only work if sufficient flight inspection experience exists in a given area and with a given facility. The new DEMETER software is built on this premise and facilitates the importing and integration of flight inspection data to enable direct comparisons with terrain based predictions. This supports the process of using the software to first identify relevant DME's to flight inspect for a given RNAV procedure, and then build up the database with both simulated and actual results to obtain a comprehensive airspace and navigation service picture, in close cooperation between the air navigation service provider and the flight inspection organization.

## **RECOMMENDATIONS**

EUROCONTROL is supporting the implementation of performance based navigation. The PBN concept builds on a process of matching navigation infrastructure with the operational needs in terms of airspace organization, in line with the ICAO PBN Manual [9]. For much of European airspace and especially terminal areas, efficiencies can be gained by aligning arrival and departure routes with the most efficient airspace organization possible. In many cases this means that there is a need to provide P-RNAV (RNAV-1) service in the terminal area to fairly low levels, often posing a challenge for DME/DME navigation service. In line with current strategies, DME/DME is a recommended back-up service to GNSS, in particular for Air Transport users. In order to avoid excessive investments in DME infrastructure optimizations, it is desirable to drive the capabilities of coverage prediction to higher level of fidelity. This requires the availability of corresponding verification data, which in many cases is difficult and expensive to obtain. Consequently, flight inspection organizations are invited to:

- continue improving their multi-channel DME measurement capabilities (note that conventional scanning DME avionics are normally insufficient for this purpose);
- make any relevant coverage data available to EUROCONTROL for further analysis.



## **FUTURE WORK**

The upgrade of DEMETER and the associated analysis capabilities have just been finalized. Over the coming months, a validation phase will continue to analyze coverage prediction quality and study individual cases further, also by using additional tools. Additional flight inspection data collection and ultimately further upgrades to DEMETER algorithms are a possible outcome of these activities, but have not yet been decided.

## **ACKNOWLEDGEMENTS**

The authors and their organizations would like to thank DFS and skyguide, Air Navigation Service Providers of Germany and Switzerland, respectively, for the information and assistance provided. Some of the theoretical analysis has also been supported by Mr. M. Perry of Largs, Ltd.

## **REFERENCES**

- [1] ICAO, Manual on Testing of Radio Navigation Aids. Doc 8071, Volume I: Testing of Ground Based Radio Navigation Systems, 4<sup>th</sup> Edition incorporating Amendment 1, October 2002.
- [2] EUROCONTROL, Guidelines for P-RNAV Infrastructure Assessment. Eurocontrol-GUID-0114, Edition 1.2, Brussels, 16 April 2008
- [3] [www.ecacnav.com](http://www.ecacnav.com), Tools Section
- [4] ICAO, Aeronautical Telecommunications. Annex 10 to the Convention on International Civil Aviation, Volume 1, Radio Navigation Aids, 6<sup>th</sup> Edition, July 2006.
- [5] Berz G., Bredemeyer J.: Qualifying DME for RNAV Use. Proceedings of the 15<sup>th</sup> International Flight Inspection Symposium, 23-27 June 2008, Oklahoma City, USA.
- [6] Vitan, V: DEMETER Terrain Data and Associated Processes. Working Paper on Infrastructure Agenda Item 5.2 of the 11<sup>th</sup> Eurocontrol Navigation Subgroup Meeting, Brussels, 27-28 April 2010.
- [7] Bredemeyer J., Battermann S., Garbe H., Ritter J.: Antenna Installed Performance of a Flight Inspection Aircraft. Proceedings of the International Symposium on Precision Approach, 5-6 October 2004, Munich, Germany.
- [8] Bredemeyer J., Kleine-Ostmann T., Schrader T., Muentner K.: Airborne Field Strength Monitoring. Advances in Radio Science, Kleinheuerbacher Berichte Bd. 5, U.R.S.I., 2007
- [9] ICAO, Performance-Based Navigation Manual. Doc 9613, 3<sup>rd</sup> Edition, 2008



# Latest Achievements of Complex System Simulations for ATC-systems - Actual Examples and Flight Inspection

**Gerhard Greving**  
 NAVCOM Consult  
 Ziegelstr. 43  
 D-71672 Marbach / Germany  
 Tel.: +49 7144 862560  
 E-mail: [navcom.consult@t-online.de](mailto:navcom.consult@t-online.de)



## ABSTRACT

All modern ATC-systems, i.e. navigation, landing and surveillance systems, are based on the transmission and reception of radio signals. These can be distorted by large objects in some distance to these ground based systems or subsystems. The level of distortions and the potential mitigation measures have to be analyzed and defined in advance, before the applied new buildings are realized and before the distorting objects appear in the coverage volume of these systems. The analysis of these suspected distortions is the task of the discussed system simulations in the course of the application of these “buildings” or objects, such as terminals, hangars, cranes, wind turbines or the appearance of large aircraft such as the A380.

These objects tend to be larger and more complex in terms of size, shape and structure. The simulation results must be sufficiently accurate and must be reliable to the extent possible. It is obvious that only advanced state-of-the-art methods and simulation procedures combined with the realistic signal processing can meet these general requirements. Compromises for fast computer time versus accuracy and reliability of the results are disputable. Modern advanced system simulations are reliable in general if the adequate methods and tools are applied accompanied by the adequate knowhow.

This paper continues a major number of papers on this subject by the author dating back more than a decade. In this paper, they are put into the historical context. An update is given on the latest methodology and on most recently achieved results. Examples are discussed which have a link to ground or flight check measurements.

## INTRODUCTION SYSTEM SIMULATIONS

Many systems in the fields of navigation, landing, radar and communications rely on the transmission and reception of radio signals. However, these systems are never operating in free space without distorting objects.

A typical general system in its operating environment is shown in Fig. 1 comprising also a distorting scattering object. The basic system simulation flow and the impact parameters are shown in Fig. 2. It is highlighted that the simulations may have risk, safety and economic impacts. On the other hand a well based knowhow on all related fields and experience is the presumption of a reliable system simulation. Errors may occur in all steps of the simulation (Fig. 3). These have to be minimized by the adequate knowhow and experience on how to perform the system simulations.

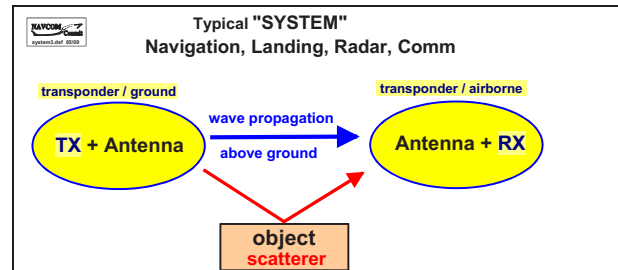


Fig. 1: Typical system in question

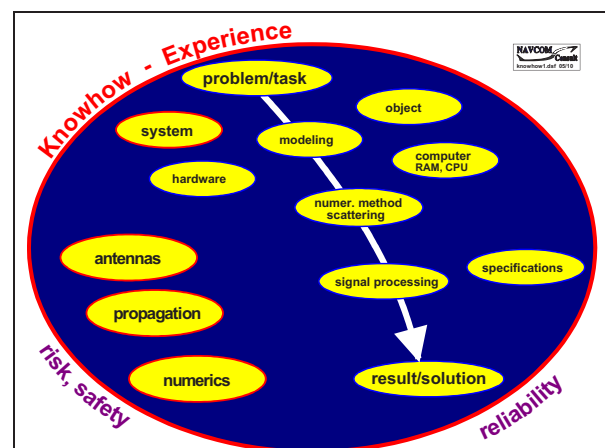


Fig. 2: Basic signal flow of a system simulation, relevant aspects

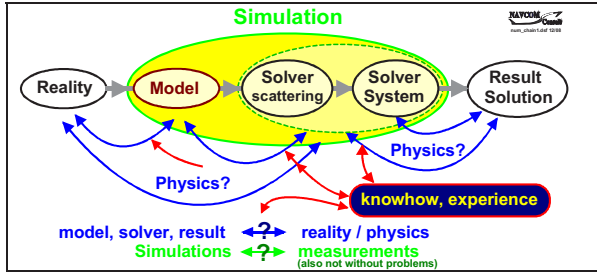


Fig. 3: Error sources in the simulation flow

Fig. 4 shows a schematic of systems and distorting objects on and around an airport. The classical and modern systems operate typically in the frequency range between 500kHz and 6GHz. A typical variety of distorting objects, such as hangars, control towers, cranes, wind turbines, fences, aircraft can be seen and also the ground itself in the wave propagation (Fig. 5). These objects have to be analyzed for a variety of different nav aids, landing and surveillance systems (Fig. 6). Often a hybrid approach is needed where different methods and also the wave propagation aspects are taken into account, such as in the case of “humped runways” (Fig. 7) in combination with objects and aircraft. The recent dramatic progress of the system simulations for increasingly complex objects has been supported by available numerical methods from the electromagnetic field and also by the availability of faster and remarkably more powerful computers in terms of speed, memory and multi CPU.

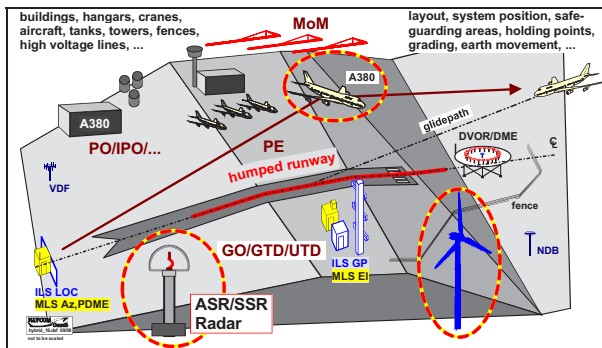


Fig. 4: Schematic airport scenario with systems associated antennas and distorting scattering objects

### Modeling and Analysis for System Simulations

Numerical system simulations are required and carried out today for the analysis of distortions on navigation or radar systems by scattering objects in advance. This means before the “distorting objects” appear or before the system has been installed on a particular site.

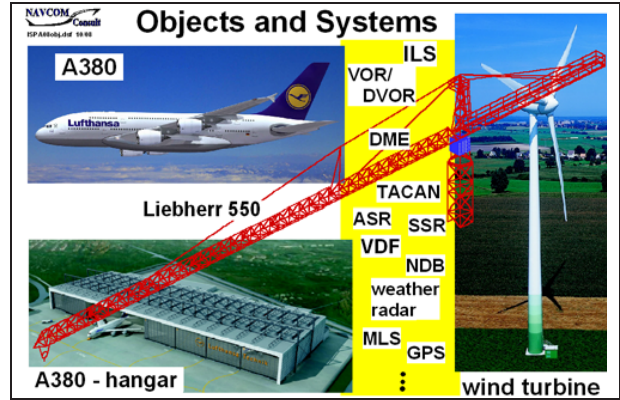


Fig. 5: Actual examples of complex 3D objects threatening the systems

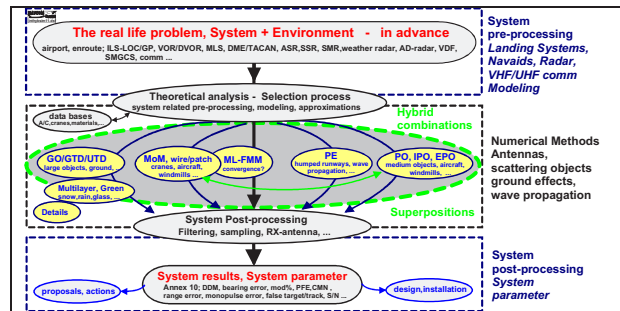


Fig. 6: Detailed flow chart of the system simulations (IHSS Integrated Hybrid System Simulations)

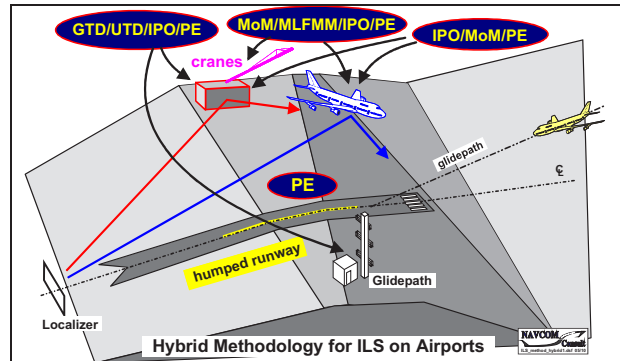


Fig. 7: Actual examples of complex 3D objects and hybrid methodology

The appearance of large objects in close distances to the systems due to the need to handle the growing air-traffic, boosts the need for accurate and reliable general system simulations in order to avoid unnecessarily strict safeguarding which may reduce the airport capacity. The “distorting objects” can be (Fig. 5, Fig. 7) of a wide variety and combinations, e.g.

- Buildings, hangars, terminals, skyscrapers, tanks;
- High voltage lines, tower cranes, transmitter towers, fences;

- Wind turbines, transmitter towers;
- Aircraft, e.g. A380, B747, A340-600 etc. or
- Non-flat ground such as “humped runway”, natural terrain and vegetation.

The real physical object has to be modeled for the analysis in the simulation procedure. The “computer model” is a “translation” of the reality and must reflect the relevant physical effects of the physical object with respect to the considered system.

The system itself has to be modeled as well by the

- **Signal generation** (antennas, signal format)
- **Signal processing, signal evaluation** (antennas, receiver, filtering, sampling). The type and concept of the signal processing depends on systems and also on the actual problem as will be shown below for the VOR/DVOR case if the distorting objects are very close to the system.

The result of the simulation process (Fig. 3, Fig. 4) of the distortions has to be at the end the so-called “system parameter”. The specified quantity which is the purpose and intention of that considered system, is e.g.

- DDM (Difference of Depth of Modulation) for ILS used for the guidance of the aircraft
- Bearing error for VOR/DVOR, TACAN, NDB
- Range error for the DME etc.

The simulated results are “raw data” in the first step. In certain system-cases a specified filtering is applied, e.g. for ILS the DDM by a low-pass-filtering procedure.

### **System simulations; Numerical Methods; Historical aspects**

System simulations depend on the numerical methods for the scattering analysis and the available computers. The first application of the simple GO geometrical optics (“ray tracing”) is long time ago. Johannes KEPLER developed telescopes with the manually processed ray tracing methods as long ago as the 17<sup>th</sup> century. The original PO (“physical optics”) was invented by KIRCHOFF already in the 19<sup>th</sup> century. Many system simulations and also public tools still rely on this simple Kirchhoff-approach which has its well-known limitations, such as neglecting the scattering at the rims of finite screens and yielding wrong results for grazing angle incidence. The latter aspect is important for the analysis of aircraft and its tail fin [13] on parallel TWY.

Many improvements of the GO-method have been developed, namely the GTD by KELLER and the later UTD/UAT. The simple PO was improved by the rim scattering components – named PTD and by other features such as the Fock-currents and shadowing mechanism resulting in the IPO which is not rigorous strictly

speaking, but a good approximation of the rigorous solutions if suitably applied.

The rigorous methods are the solutions of integral equations, namely the MoM (“method of moments”) which was introduced by HARRINGTON [1] as long ago as in the 1970s last century. Recently, its iterative variant the MLFMM (“multi level fast multipole method”) has been introduced which has the problem of the convergence often practically.

The author started to apply the GTD/UTD and to publish the 3D system analysis of ILS GP and buildings, as well as the 3D IPO and the 3D MoM for multiple cranes and the 3D MLFMM subsequently also for antennas on FI-aircraft. So a long extensive experience and knowhow has been gained in the course of more than a decade for each of applications.

The definition of the computer model and the selection of the related adequate numerical method for the analysis of the scattering depend in an iterative interaction process on a number of factors and parameters. By this, it is an important and critical optimization process. It may seem to be straight forward to select the numerical method for the analysis of the scattering according to the characteristics of the object or model and not vice versa. The basic idea of the IHSS approach (Fig. 6) is to take into account all the factors in order to find the best suited and physically realistic model and the related best adapted method(s). The method can be a single one or a hybrid combination (Fig. 7).

Due to theoretical, physical and practical reasons, other classes of powerful numerical methods have not been implemented and applied for the system simulations by NAVCOM, namely the family of finite discretization methods, the finite elements FE-, finite integration FI- and finite difference FD-methods.

### **ACTUAL EXAMPLES OF SYSTEM SIMULATIONS**

System simulations do have the objective and background to analyze and predict the performance of a system in advance due to the impact of objects or environmental conditions. Other objectives may deal with the design and positioning of system antennas and with the layout design of airports.

A lot of cases and examples have been analyzed by the author in the course of the years since about the early 1990s and has been published in the past on IFIS conferences and other conferences and in magazines. Some of the earliest publications may be highlighted where the referenced topics have been discussed extensively:

- 1994, 1996 [4], [5]  
3D analysis and design of ILS GP by GTD/UTD
- 2000 [6], [7], [8]  
Single and large groups of up to 40 cranes on airport for ILS;  
Analysis of B747 by MoM for ILS

Analysis of wind turbines on nav aids  
Hybrid methodology by combining different methods

- 2002 ff [9] - [18]  
Antennas on aircraft; analysis by MoM/MLFMM  
First analysis of A380 (IFIS 2002)  
Large windfarms and nav aids and radar etc.

Three selected recent cases are discussed in the following which require the full range of methodology and newly developed signal processing.

**A340-600 and roll-off from RWY**

On busy airports the rolling off/on and taxiing aircraft pose a threat to the performance of the ILS-guidance signal for the (next) landing aircraft. Many scenarios for potential distortions are encountered (Fig. 8) and have been analyzed systematically.

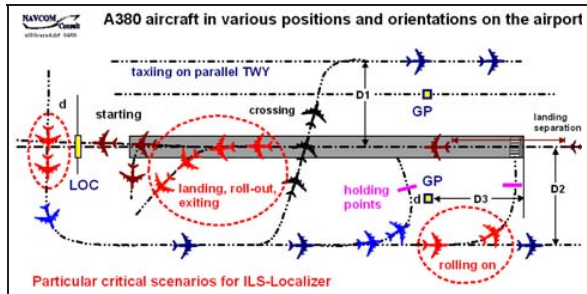


Fig. 8: A380 aircraft as a potentially distorting object in different scenarios on the airport; on the runway, on the taxiways, rolling on/off, crossing runways etc.

A recent case for an A340-600 (Fig. 9) has been analyzed where actual measurement details (Fig. 11) could be reproduced by a full MoM analysis only.

Fig. 10 shows the hybrid solution for the hybrid IPO/MoM analysis and also the full MoM-results. The leading minor measured DDM-peak appeared only in the full MoM-analysis. It was also found that for this aircraft, the tail is not the dominant part as often anticipated generally for aircraft.

**A380-800 rolling off from RWY**

The case of rolling-off A380-800 has been published several times by the author. The following analysis example demonstrates that the maximum amplitude of the DDM-distortions depend on the position of the observation point (i.e. FI-aircraft) on the glidepath. This is in particular the case if the position of the observation point, i.e. the next aircraft, is relatively close to the THR. This is relevant for the ongoing discussions of the critical/sensitive areas.

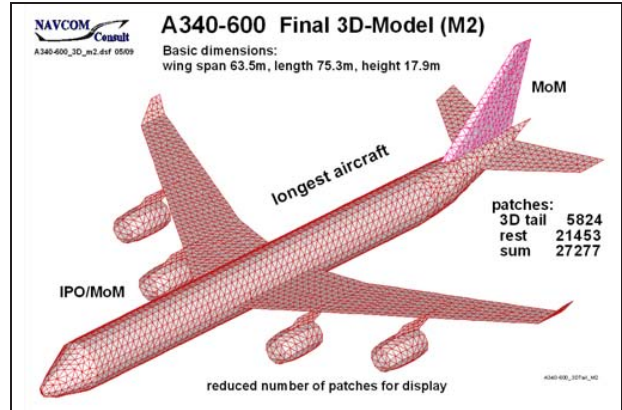


Fig. 9: 3D-model of an A340-600

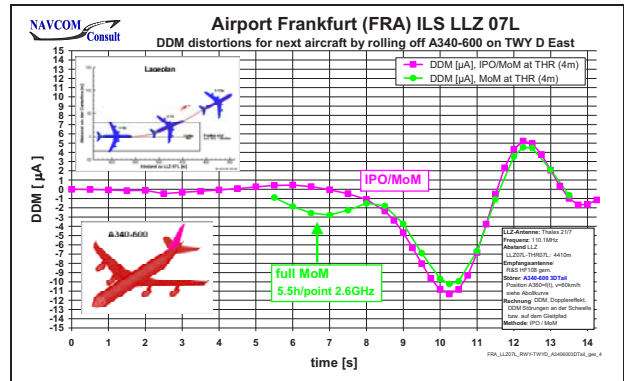


Fig. 10: DDM-distortions of an A340-600 rolling off; comparison of hybrid IPO/MoM with full MoM

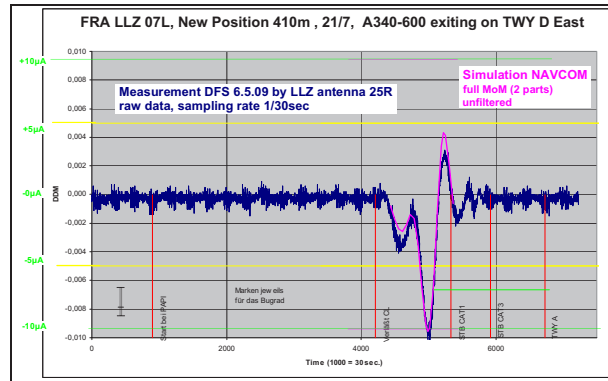


Fig. 11: Measured and simulated DDM-distortions of an A340-600 rolling off; simulations full MoM

Fig. 12 shows the 3D-models of the A380-800, B747-8F and the C130 used for systematic simulations using the hybrid numerical analysis (IPO/MoM) for ILS LOC and GP for a new CATIII ILS installation.

Fig. 13 shows the DDM-distortions for a high performance wide aperture ILS-Localizer where the A380-800 rolls off at around 600m distance. The fixed observation points are on the glidepath at distances from 1nm to

10nm. It can be seen that the CATII/III is violated if the next aircraft is at a distance of 2nm. That is probably often the case in daily operation. At a distance of 4nm, the specs are met for this case easily.

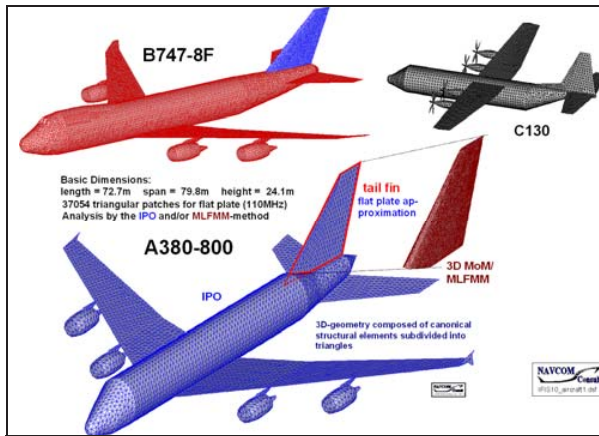


Fig. 12: 3D-models of aircraft ; A380-800, B747-8F, C130

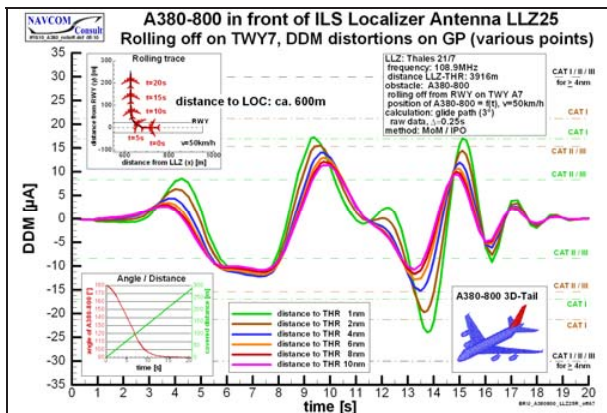


Fig. 13: DDM-distortions of a A380-800 rolling off; various observations points on glidepath

A generally good agreement between simulations and measurements has been presented on several conferences (e.g. [14], [18]).

### VOR/DVOR distortions by objects in the nearfield; wind turbines

The VOR-system is prone to distortions by scattering objects. The classical theory assumes that the distorting objects are in a relatively far distance to the VOR/DVOR-antenna and, by that, can be treated approximately as a point-scatterer which has a scattering pattern.

If the objects are large and close to the VOR/DVOR, such as for VOR/DVOR on airports, the standard simulation schemes fail and exhibit wrong results. First the scattering process itself is incorrect and the signal processing

scheme by applying “simple formulas” for the bearing error fails. In addition to the results shown on the last IFIS /14/, systematic simulation results are shown in the following for the CVOR and DVOR due to wind turbines

The general applicable approach presented for the VOR/DVOR treats the object as part of the VOR-antenna and processes a spectral analysis of the rotating antenna pattern. By that, almost arbitrary objects at arbitrary distances can be analyzed, such as aircraft close to a DVOR on an airport. By this approach, the general basics of the signal processing of amplitude modulation for the VOR and of frequency/phase modulation for the DVOR are taken into account.

The 3D-models of the VOR and DVOR antennas are shown in the Fig. 15 and 16 for the application of the MoM.

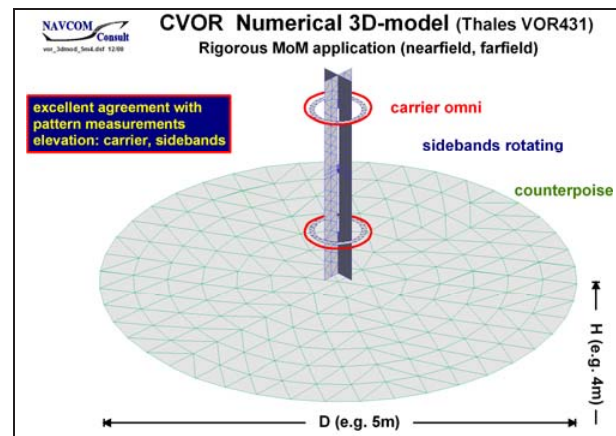


Fig. 14: Realistic 3D-model of the CVOR-antenna

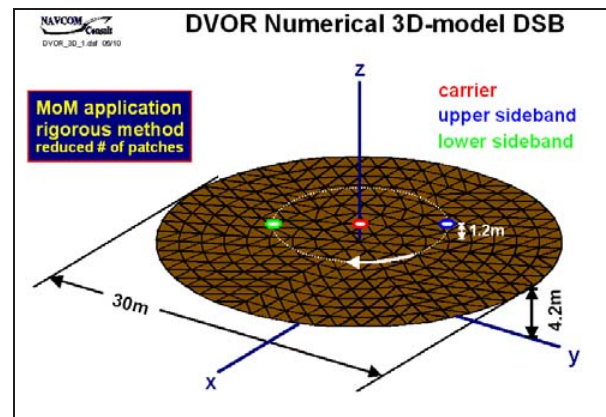


Fig. 15: Realistic 3D-model of the DVOR-antenna

A 3D-model of a large wind turbine E82 is shown in Fig. 16. The model is fully metallic as a worst case, taking into account also the environmental heavy rain condition for non-metallic parts. The model consists of a large number of triangular patches, representing the geometrical 3D-form and its electrical scattering properties.

It is suspected sometimes that the bearing error would depend very sensitively on the direction of wind and on the position of the rotating blades. Fig. 17 shows a systematic variation of the direction of the wind and of the rotor position in steps of  $15^\circ$  each. The bearing error simulation has been done in a  $\pm 60^\circ$  sector up to 100km and in a height of 2000ft. It can be clearly seen (Fig. 17) that the worst case bearing error per set of parameter is relatively smooth. This fact holds basically as well for the DVOR for a different set of parameters (Fig. 18).

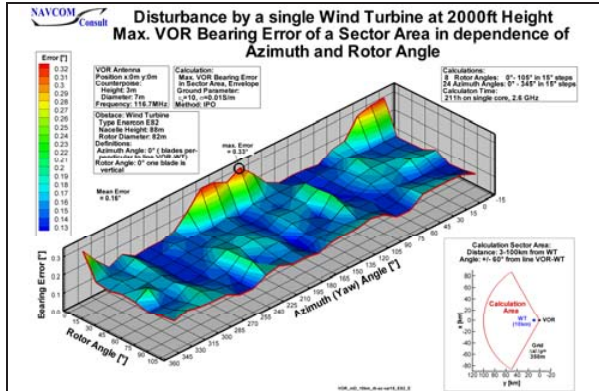


Fig. 17: VOR bearing error by a wind turbine E82 in 10km distance; 2000ft, sector  $\pm 60^\circ$ , up to 100km

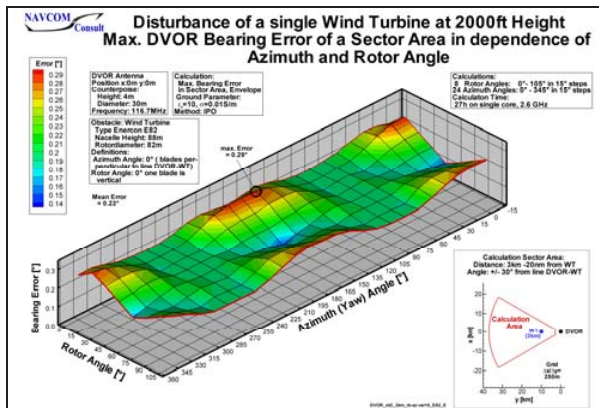


Fig. 18: DVOR bearing error by a wind turbine E82 in 3km distance as a function of wind direction and rotor position; height 2000ft, sector  $\pm 30^\circ$ , radius 20nm

Significant and identifiable measured bearing error results are not available for wind turbines for comparison and verification purposes.

However, the methodology and the software can be verified safely by other cases for which clear and unique bearing errors are available by flight check. A particularly difficult 3D-case is shown in Fig. 18 (photo) and Fig. 19 (3D-model). A large silo complex is located in the mutual nearfield of a DVOR. The standard bearing error theory is not applicable. The adequate 3D-modeling and the new spectral analysis are applied instead. However, Fig. 20 shows a remarkably good agreement between the flight

check results and the simulations, despite the large complex buildings and the near-field conditions where standard simulation techniques fail.

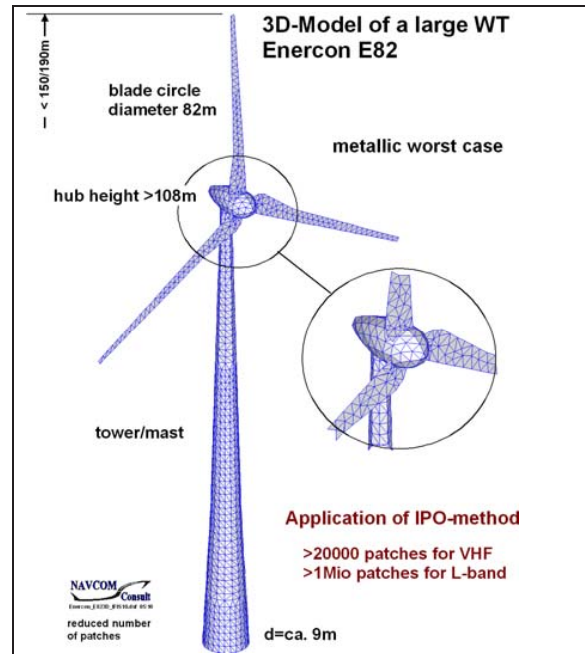


Fig. 16: Realistic 3D-model of a large wind turbine E82

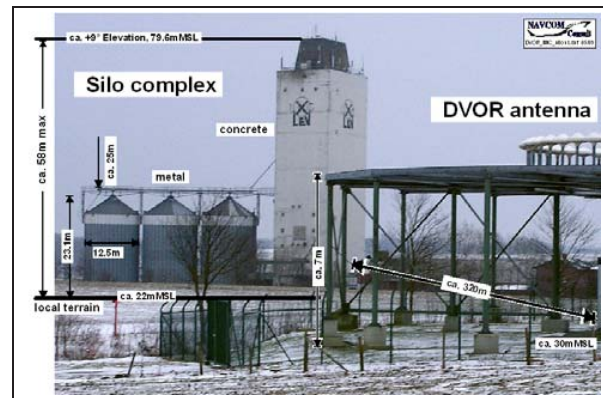


Fig. 18: Silo complex in a distance of 320m only to a DVOR

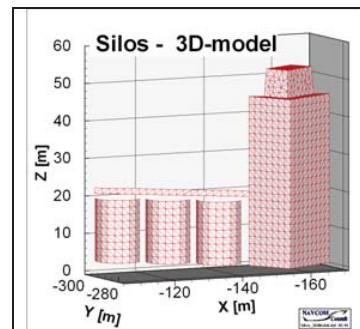


Fig. 19: 3D-model of the building complex (see Fig. 18)



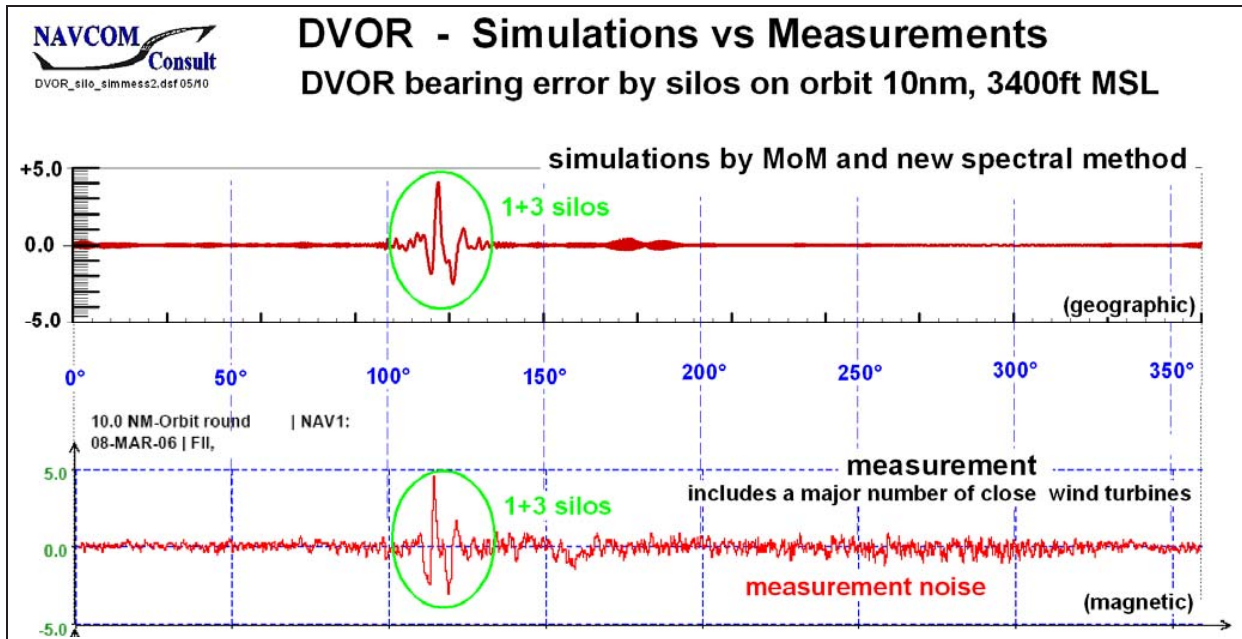


Fig. 20: Comparison of simulations and flight-check measurements for the silo complex (see Fig. 18 and 19)

### Field amplitude simulations and FI measurements

The (minimum) field strength for the ILS subsystems is specified in ICAO Annex 10 [3] as shown in Fig. 21 for the ILS Localizer. It is indeed a particularly difficult task to measure sufficiently accurately the absolute field strength (Fig. 22) in space by aircraft. Often large differences, i.e. in the order of 6dB, are recorded by different FI-measurements for the same installation or for type measurements between installations.

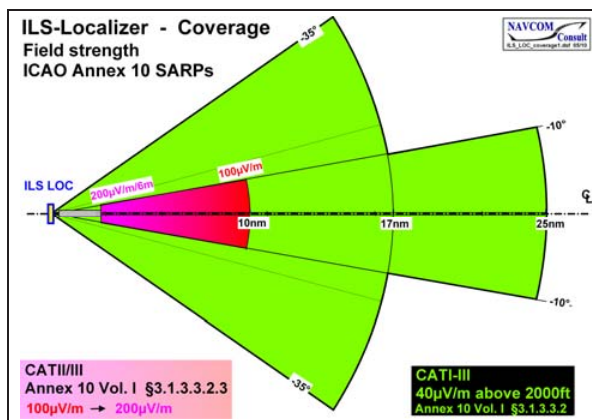


Fig. 21: Coverage and field strength specifications ILS Localizer

ICAO Annex 10 [3] defines the field strength or the power density while ICAO DOC 8071 defines the voltage at 50Ohms at the input of the receiver. It seems to be a

straight forward task to determine and calibrate the “conversion factor” or “antenna factor”. This factor is defined for “free space” conditions, i.e. a locally “plane wave” condition.

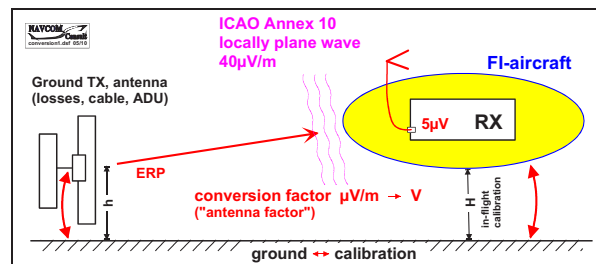


Fig. 22: Field strength measurements FI; conversion factor

The “conversion factor” is tried to be determined by a “calibration” which can be carried out practically only above ground. The ground is a distortion factor for the field generation ( $40\mu\text{V/m}$  plane wave) and for the antenna pattern of the aircraft installation. The aircraft is part of the antenna. From a theoretical point of view it is very difficult to achieve a certain absolute accuracy, i.e. an accuracy of e.g.  $\pm 1\text{dB}$ . A reasonable estimate is a best accuracy of  $\pm 3\text{dB}$ .

In contrast, the modern simulation capabilities offer an improved highly reliable solution by calculating the absolute field strength of an antenna under reasonably modeled conditions, i.e.

- known TX-power and known losses yielding the radiated power

- spherical curved earth with average material parameters
- application of the method of parabolic equation PE after pre-calculating the “launching” field with the MoM. A highly effective wave absorber is simulating free open space radiation conditions.
- calculations for 17nm and 25nm distance and 2000ft height.

Fig. 23 shows the absolute azimuthal patterns (course, clearance) of a common wide aperture Localizer antenna above flat ground.

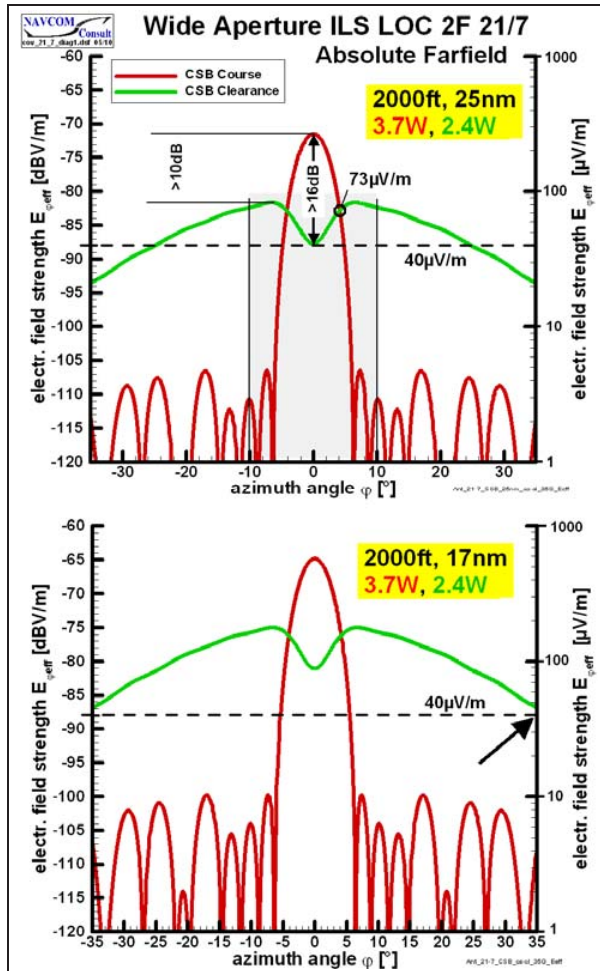


Fig. 23: ILS Localizer azimuthal antenna pattern course/clearance (modern wide aperture 2F antenna)

Fig. 24 shows the wave-propagation PE-analysis where the achieved absolute field strength of  $40\mu\text{V/m}$  at  $\pm 35^\circ$  is iteratively computed for a radiated power of only 2.4W for the LOC-clearance-CSB-antenna. Typical clearance transmitters do have an output power of 25W. Hence, it is clearly shown that a certain amount of maximum total losses of about 10dB can be tolerated in order to meet the ICAO specs easily and safely. The variations between

different FI-measurements and also relative to the straight-forward simulations according to state-of-the-art methodology must be considered to be calibration problems and/or “different calibrations”.

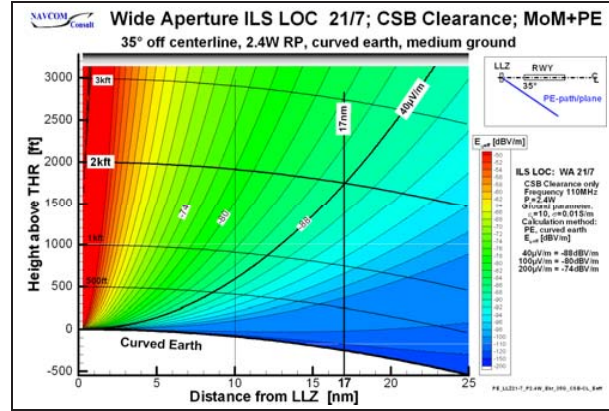


Fig. 24: Field strength simulation by hybrid MoM/PE application; ILS LOC clearance CSB at  $35^\circ$  for 2.4W radiated power

## CONCLUSIONS AND RECOMMENDATIONS

The presented state-of-the-art system simulations consist of the modeling of the system, the distorting object and the signal processing. It has been shown that by the integration of the applicable most advanced numerical methods even complicated and very complex 3D-cases can be simulated reliably and accurately by the IHSS-scheme. However, the numerical effort and the modeling have to be optimized on a case by case basis to achieve the results in an acceptable time frame and with an acceptable resource requirement, i.e. available high performance modern PCs (or work stations). However also, approximate, mostly fast methods and tools are no longer justified driven by the previously valid need for simplicity and short run times.

The status and achieved progress have been demonstrated for several challenging system cases, the A380 related to ILS, special VOR/DVOR scenarios and wind turbines. The demonstrated progress made is the general applicability for large 3D objects of curved surfaces or hybrid structures and for small near field distances of the objects to ILS and VOR and other systems.

Simulations and measurements show a good agreement to that extent that effects observed in the flight check could be verified and explained. The achieved results by the advanced generally applicable methods also show to have powerful capabilities. The demonstrated progress does allow a complementary cooperation with the flight check or may substitute the flight check in certain cases.

The final recommendation is to apply state of the art methodology and hybrid simulations for the reliable site

dependant determination of minimized safeguarding areas on airports as well as en-route.

### ACKNOWLEDGEMENTS

The numerical simulations have been carried out by Mr. W.-D. Biermann and M. Mundt of NAVCOM Consult.

### REFERENCES

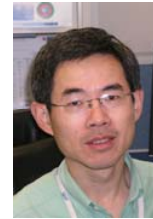
- [1] Y .T: Lo, S. W. Lee, *Antenna Handbook*, Chapman & Hall, New York 1996, Vol. I chapter 4 (see related references)
- [2] BOROVIKOV, KINBER Geometrical Theory of Diffraction, IEE, London 1994; chapter 6: GTD or physical optics?
- [3] ICAO, July 1996, International Standards and Recommended Practices, Annex 10 to the Convention on International Civil Aviation, Volume 1, Radio Navigation Aids, 5th Edition
- [4] G. Greving, Computer aided site analysis and site adapted installation - Efficient commissioning of landing systems, 8th IFIS International flight inspection symposium, Denver USA, June 1994
- [5] G. Greving, Aspects of operation and flight check of ILS under difficult site conditions, IFIS96 (International Flight Inspection Conference) , Braunschweig, June 1996
- [6] G. GREVING, Numerical system-simulations including antennas and propagation exemplified for a radio navigation system, AEUE (International Journal of Electronics and Communications), Vol 54 (2000), No. 3, pp. 1-7
- [7] G. GREVING, Numerical analysis and flight check of difficult sites, , 10<sup>th</sup> International Flight Inspection Symposium IFIS 98, Seattle 1998, Proc. pp.38-46
- [8] G. GREVING, Hybrid-Methods in Antennas and 3D-Scattering for Nav aids and Radar System Simulations, AP2000 Millenium Conference on Antennas & Propagation, Davos, Switzerland, April 2000
- [9] G. GREVING, Recent Advances and New Results of Numerical Simulations for Nav aids and Landing Systems, 11<sup>th</sup> IFIS International Flight Inspection Symposium, Chile 2000, Proc. pp. 172-181
- [10] G. GREVING, Latest Advances and Results of Complex Numerical Simulations for Nav aids and Landing Systems, 12<sup>th</sup> IFIS International Flight Inspection Symposium, Rome/Italy 2002, Proc. pp. 152-162
- [11] G. GREVING Advanced Numerical System Simulations for Nav aids and Surveillance Radar - The Verification Problem, 13<sup>th</sup> IFIS, June 2004, Montreal/Canada, pp.173-186
- [12] G. GREVING, System Simulations for Navigation and Radar Applications Based on Sophisticated Numerical Hybrid Scattering Analysis, MAPE 2005 in Beijing/China August 2005
- [13] G. GREVING, W.-D. Biermann, Theoretical Aspects and Numerical Solution of Scattering from Objects under Grazing Angle Incidence - The A380 and the Aircraft Tailfin; 37<sup>th</sup> EuMW, Munich October 2007
- [14] G. GREVING, N. Spohnheimer, Current Issues in Demanding Flight Measurement Environments; 15<sup>th</sup> IFIS; Oklahoma/USA, June 2008
- [15] G. GREVING, The Electromagnetic Scattering within System Simulations for Distortions of Navigation, Landing and Radar Systems, URSI GA, Chicago, August 2008; (Invited Paper)
- [16] G. GREVING, Hybrid Numerical Scattering Field Analysis Embedded into Simulations of Complex Radio Based Systems - Examples, Capabilities and Limitations; ICEAA 2009, Torino September 2009
- [17] G. Greving, W.-D. Biermann, R. Mundt Numerical A&P Analysis Integrated into System Simulations for Radar and Navigation, ISAP 2009, Bangkok; October 2009
- [18] G. GREVING, On the Advanced Simulation of Distortions for Navigation, Landing and Radar Systems - Modern Methods, Cases and Results; IAIN 2009, Stockholm October 2009



# On Robust Computation of Reference Datum Height

## Cheng Zhong

Aviation System Standards  
The Federal Aviation Administration (FAA)  
P.O. Box 25082, Oklahoma City, OK 73125, USA  
Tele: +1 405 954 5388  
[Cheng.Zhong@faa.gov](mailto:Cheng.Zhong@faa.gov)



## Derek A. Blackford

Aviation System Standards  
The Federal Aviation Administration (FAA)  
P.O. Box 25082, Oklahoma City, OK 73125, USA  
Tele: +1 405 954 6616  
[Derek.A.Blackford@faa.gov](mailto:Derek.A.Blackford@faa.gov)



**Abstract**— FAA Order 8240.47C provides for the determination of the reference datum height (RDH) by means of the computation of a best fit straight line (BFSL) in instrument landing system (ILS) Zone 2 projected down to the runway and intersecting the vertical plane containing the threshold. The current algorithm for computing the BFSL uses a least squares (LS) method which is optimal for signals contaminated with Gaussian noise. This technique, while sound, can be sensitive to glide slope structure in Zone 2. Alternative numerical method using adaptive linear regression or a robust statistical method may prove beneficial for compensating for the effects of structure on the computation of the BFSL. Since glide slope structural effects are not inherently Gaussian and vary significantly with environmental conditions, methods based on adaptive linear regression and robust statistics are being evaluated to determine their benefits in the computation of RDH. These methods produce similar results to the current BFSL algorithm when analyzing signals contaminated with Gaussian noise but perform better when the noise is distributed with a heavy tail.

**Keywords**—reference datum height; best fit straight line; threshold crossing height; adaptive linear regression; robust statistics, FAA Order 8240.47C

## I. INTRODUCTION

The research on threshold crossing height (TCH), reference datum height (RDH), and achieved reference datum height (ARDH) has been very active over the years. A number of papers were presented in the past ten years in the International Flight Inspection Symposia (IFIS) [1]-[8]. Most recently, the United States (US) Federal Aviation Administration (FAA) Aviation System Standards tasked Ohio University to conduct two research projects: (1) Validation of the best fit straight line (BFSL) algorithm used in the automatic flight inspection system (AFIS) for an instrument landing system (ILS) [9]; (2) Assessment of the effectiveness of the RDH/ARDH evaluation methodology for the ILS glide slope [10]. These parameters (TCH, RDH, ARDH) are not only critical to an ILS, but also one of the characteristics of instrument flight procedures (IFP)

for US's wide area augmentation system (WAAS) and local area augmentation system (LAAS)<sup>1</sup> [11].

While the definitions of TCH, RDH, ARDH seem to be clear qualitatively (to be reviewed in Section II), computation varies depending on the methods employed. As mentioned in [9][10], prior to the publication of the first version of FAA Order 8240.47 [12] in 1983, there was no distinction between the computed and measured TCH for ILS. In order to overcome the dilemma that certain glide slopes were “out of tolerance” simply because of the computed TCH while in practice the flight inspectors were able to fly them safely, FAA issued Order 8240.47 to analyze the glide slope performance based on flight data in two particular segments<sup>2</sup> -- Zone 2 (between 4 nautical miles (nm) Point A and 3500 feet (ft) Point B), and between 6000 ft and Point C along the approach path, and applied the BFSL algorithm to compute the RDH and ARDH, respectively. Thus, TCH and RDH/ARDH are usually not one and the same. A short history account of the activities leading to FAA Order 8240.47 can be found in [9][10]. Revision C of this order [12] is the most recent version, which was published in March 2001.

Because of the simplicity of BFSL, it has been routinely employed during the commissioning flight inspection both in the US and internationally<sup>3</sup>. However, several people [2][7] [10] have observed that issues exist when applying BFSL to compute RDH. Courtney and Quinet [7] observed that “Analysis shows reference datum height can be affected by the magnitude and location of the glide path structure roughness.” Similarly, Edwards and DiBenedetto [10] stated that “One of

<sup>1</sup> The two systems are the US implementations of the International Civil Aviation Organization (ICAO) space based augmentation system (SBAS) and ground based augmentation system (GBAS), respectively.

<sup>2</sup> All distance are relative to the runway threshold.

<sup>3</sup> Greving and Spohnheimer [3] also proposed a periodic flight check and evaluation of TCH.

the problems with the RDH calculation is that the computation is affected by aberrations in the glide path which are far from the threshold.”

In this paper, we revisit the BFSL method and give a mathematical explanation of the above observed phenomenon. We also identify the different usage of BFSL based on different aiming points (AP). Finally, we use several robust methods for computing the BFSL.

The rest of the paper is organized as follows. In Section II, we review the definitions of TCH, RDH, ARDH, and AP. In Section III, we review the BFSL method, introduce a new form for the calculation of a straight line that passes through the origin, which is often neglected. We also introduce another linear regression method based on least absolute deviation (LAD). In Section IV, we present an alternative method [13] to the BFSL. In Section V, we present numerical results. Finally, we conclude the paper in Section VI.

## II. DEFINITIONS

### A. TCH

The TCH is a height determined by airport geometry assuming an ideal transmission and a known glide slope point of origin. However, due to terrain undulations and reflective surfaces on the airport facility that produce multipath conditions, the actual threshold crossing height may be different from that computed assuming ideal conditions.

### B. RDH

The RDH is a height above the runway threshold at which a line fitted to glide path measured data in Zone 2 and projected down to the runway would cross the runway threshold. This is an estimation of TCH. As mentioned in Section I, this technique for determining the RDH is sensitive to structure the further away from the runway threshold one goes within the zone of investigation. This problem will be explored in Section IV.

### C. ARDH

The ARDH is a height above the runway threshold at which a line fitted to glide path measured data between 6000 ft and Point C and projected down to the runway would cross the runway threshold. This is another estimation of TCH. ARDH can still suffer from some of the problems encountered by fitting a line to data generated in Zone 2; however, since the data used in the computation of ARDH is closer to the runway threshold, the effects are less severe.

### D. AP

The AP is a location which is programmed into the AFIS from which glide path measurement results are referenced. The aiming point may not be coincident with the glide slope origination point [12].

## III. SIMPLE LINEAR REGRESSION

### A. Least Squares Regression Line

Regression analysis is a set of data analysis techniques which examine functional relationships among a given set of variables. There are various kinds of regression models [14]. By a simple linear regression model, we mean the data set  $\{(x_i, y_i), 1 \leq i \leq n\}$  are related by

$$y_i = \beta_0 + \beta_1 x_i + \varepsilon_i, \text{ for } 1 \leq i \leq n \Leftrightarrow \mathbf{y} = X\boldsymbol{\beta} + \boldsymbol{\varepsilon}, \quad (3.1)$$

where

$$X = [\mathbf{I}_n \ \mathbf{x}] = \begin{bmatrix} 1 & x_1 \\ 1 & x_2 \\ \vdots & \vdots \\ 1 & x_n \end{bmatrix}, \mathbf{y} = \begin{bmatrix} y_1 \\ y_2 \\ \vdots \\ y_n \end{bmatrix}, \boldsymbol{\varepsilon} = \begin{bmatrix} \varepsilon_1 \\ \varepsilon_2 \\ \vdots \\ \varepsilon_n \end{bmatrix}, \boldsymbol{\beta} = \begin{bmatrix} \beta_0 \\ \beta_1 \end{bmatrix}, \quad (3.2)$$

$\varepsilon_i$  is a random variable representing disturbance or error. Because  $\{(x_i, y_i), 1 \leq i \leq n\}$  represent data, (3.1) can be regarded as fitting the equation (here it represents a line) to data. More specifically, it is to find  $\boldsymbol{\beta}$  that minimizes the discrepancy (also called the error function) between  $\mathbf{y}$  and  $X\boldsymbol{\beta}$  in a certain measure. Among all the different measures, the sum of squares  $\varepsilon_i^2$ , i.e., the square of  $L_2$  norm  $\|\boldsymbol{\varepsilon}\|^2$

$$\sum_{i=1}^n \varepsilon_i^2 = \|\boldsymbol{\varepsilon}\|^2 = \|\mathbf{y} - X\boldsymbol{\beta}\|^2, \quad (3.3)$$

is most often used. Minimizing (3.3) (with respect to  $\boldsymbol{\beta}$ ) is called the ordinary least squares (OLS) or least squares (LS) method, which leads to the following normal equations

$$X^T X \hat{\boldsymbol{\beta}}_{OLS} = X^T \mathbf{y}. \quad (3.4)$$

where the superscript  $(\cdot)^T$  represents the transpose of a vector or a matrix. The solution  $\hat{\boldsymbol{\beta}}_{OLS}$  is called the LS estimate of  $\boldsymbol{\beta}$ . It is trivial to show that

$$\hat{\boldsymbol{\beta}}_{OLS} = \begin{bmatrix} \hat{\beta}_0 \\ \hat{\beta}_1 \end{bmatrix} = \frac{1}{n \left( \sum_{i=1}^n x_i^2 \right) - \left( \sum_{i=1}^n x_i \right)^2} \begin{bmatrix} \left( \sum_{i=1}^n x_i^2 \right) \left( \sum_{i=1}^n y_i \right) - \left( \sum_{i=1}^n x_i \right) \left( \sum_{i=1}^n x_i y_i \right) \\ n \left( \sum_{i=1}^n x_i y_i \right) - \left( \sum_{i=1}^n x_i \right) \left( \sum_{i=1}^n y_i \right) \end{bmatrix}. \quad (3.5)$$

With  $\hat{\beta}_0$  and  $\hat{\beta}_1$ , the LS fitted equation is

$$\hat{y} = \hat{\beta}_0 + \hat{\beta}_1 x, \quad (3.6)$$

where the fitted values are  $\{\hat{y}_i = \hat{\beta}_0 + \hat{\beta}_1 x_i\}$  for  $\{x_i, 1 \leq i \leq n\}$ .

Eq. (3.6) represents a straight line, which is called the least squares regression line or BFSL for the data set

$\{(x_i, y_i), 1 \leq i \leq n\}$ .  $\hat{\beta}_0$  and  $\hat{\beta}_1$  are known as intercept (with the y-axis) and slope (of the regression line), respectively.

### B. Least Squares Regression Line Passing through Origin

Sometimes, it is known that the true relation between  $x$  and  $y$  is linear (represented by a line passing through the origin) because of the subject matter or other physical considerations. For example, if we choose the AP of the glide slope as the origin of the coordinates, the BFSL is in fact a no-intercept model.  $\beta$  in (3.1) is now a scalar and the model becomes

$$y_i = \beta x_i + \varepsilon_i, \text{ for } 1 \leq i \leq n \Leftrightarrow \mathbf{y} = \beta \mathbf{x} + \boldsymbol{\varepsilon}. \quad (3.7)$$

It should be emphasized that we cannot simply let  $\hat{\beta}_0 \equiv 0$  in (3.5) and obtain  $\hat{\beta}_1$  because it will lead to incorrect results. Instead, we should apply the same LS procedure to the model in (3.7), which gives

$$\hat{\beta} = \frac{\sum_{i=1}^n x_i y_i}{\sum_{i=1}^n x_i^2}. \quad (3.8)$$

The least squares regression line without intercept is

$$\hat{y} = \hat{\beta} x. \quad (3.9)$$

### C. Discussions

The desire on behalf of flight inspectors is to determine the effective glide path being radiated by a glide slope transmitter. Linear regression in this case refers to any statistical approach to fitting a line to a data set. If the line placed through the data set causes a certain discrepancy measure between them to be minimal, then the line is considered to be the *best fit straight line*. Although FAA Order 8240.47C [12] states that this line is to be determined using the OLS method and is called BFSL, we argue that the more appropriate name in this case should be least squares regression line and that BFSL should not be tied solely to OLS. In addition, we find that the name BFSL seldom appears in books on linear regression. However, because the term BFSL is so well-known to the flight inspection community, we follow the current convention.

The general form of discrepancy measure mentioned above is the  $L_p$  norm

$$\| \mathbf{y} - X\boldsymbol{\beta} \|_p^p = \left( \sum_{i=1}^n |y_i - (\beta_0 + \beta_1 x_i)|^p \right)^{\frac{1}{p}}, \quad p = 1, 2, \dots \quad (3.10)$$

LAD and OLS correspond to  $p = 1$  and  $p = 2$ , respectively.

The method of using OLS to determine the parameters (cf. (3.5)) that describe the line fit to a data set is guaranteed to minimize the error function defined in (3.3). However, some underlying assumptions are made in the use of OLS [15]. If  $X$  in (3.2) has full rank, and  $E\{\boldsymbol{\varepsilon}\} = 0$ ,  $Var\{\boldsymbol{\varepsilon}\} \equiv E\{[\boldsymbol{\varepsilon} - E\{\boldsymbol{\varepsilon}\}][\boldsymbol{\varepsilon} - E\{\boldsymbol{\varepsilon}\}]^T\} = \sigma^2 I_n$ , then  $\mathbf{c}^T \hat{\boldsymbol{\beta}}_{OLS}$  is the unique estimate with minimum variance, i.e., the best linear unbiased

estimate (BLUE) of  $\mathbf{c}^T \boldsymbol{\beta}$ , where  $\mathbf{c}$  is a column vector [16]. If we further assume that  $\varepsilon_i$  is normally (Gaussian) distributed,  $\hat{\boldsymbol{\beta}}_{OLS}$  is also maximum likelihood (ML) estimate of  $\boldsymbol{\beta}$  and has an easily derivable probability distribution with a slue of inference tests on  $\hat{\boldsymbol{\beta}}_{OLS}$  [16]. The discussions and examples based on data for glide slope can be found in [15].

In the collection of glide path data, there may be instances where the effective error in the data set is not truly of a Gaussian nature; or the majority of errors are Gaussian, but some follow a different pattern or no pattern at all. It is well known that OLS estimates can be very sensitive to departures from normality. A classic example [17] is that just 2 bad observations (from normal distribution  $N(\mu, 9\sigma^2)$ ) in 1000 standard normal observations (from normal distribution  $N(\mu, \sigma^2)$ ) suffice for LAD to be more efficient<sup>4</sup> than OLS method.

### D. Least Absolute Deviation Regression Line

Among the numerous methods for robust regression, LAD regression is considered to be the simplest one. LAD regression seeks to minimize the sum of the absolute values of the residuals, i.e., the  $L_1$  norm

$$\hat{\boldsymbol{\beta}}_{LAD} = \arg \min_{\boldsymbol{\beta}} \sum_{i=1}^n |y_i - (\beta_0 + \beta_1 x_i)|. \quad (3.11)$$

It is less sensitive than OLS to unusual values of  $y_i$ . It should be noted that the LAD regression does not have a closed-form solution, and the solution itself is not unique. In the following, we present an iterative algorithm.

If we let  $\beta_i^{(k)} = y_i - \beta_1^{(k)} x_i, 1 \leq i \leq n, k = 0, 1, \dots$ , then (3.11) is  $\sum_{i=1}^n |\beta_i^{(k)} - \beta_0|$ . It follows that for fixed  $\beta_1^{(k)}$

$$\beta_0^{(k)} = \text{Median}\{\beta_i^{(k)}\} = \text{Median}\{y_i - \beta_1^{(k)} x_i\}, \quad (3.12)$$

minimizes (3.11). To obtain  $\beta_1$ , set the derivative of (3.11) with respect to  $\beta_1$  to zero,

$$\sum_{i=1}^n \text{sgn}(y_i - (\beta_0 + \beta_1 x_i)) x_i = 0, \quad (3.13)$$

where

$$\text{sgn}(x) = \begin{cases} -1 & \text{if } x < 0 \\ 0 & \text{if } x = 0. \\ 1 & \text{if } x > 0 \end{cases} \quad (3.14)$$

If we replace  $\beta_0$  in (3.13) by  $\beta_0^{(k)}$  in (3.12), we can solve the nonlinear equation (3.13) for  $\beta_1^{(k+1)}$  using root-finding methods with bisection method being the simplest one. The

<sup>4</sup> In statistics, an estimator is called efficient if it best estimates the parameter of interest in a certain measure.

iteration process is repeated until  $|\beta_1^{(k+1)} - \beta_1^{(k)}|$  is within a certain tolerance. Methods based on linear programming or ML are also available, see [18] and references therein.

#### IV. ROBUST STATISTICS AND ADAPTIVE LINEAR REGRESSION

##### A. Leverage, Outlier, and Influence

Since the 1960s, robust statistics [17] has emerged as an alternative approach to classical statistical methods, which produce reliable parameter estimates and inference not only when the data follow given assumptions exactly, but also when the data deviate from model assumptions.

Several concepts which are basic and relevant to the discussion of robust statistics are given here. A univariate outlier is an observation of a particular variable that is atypical in terms of being far from the bulk of the data. If the univariate outlier is in terms of the  $y$ -value, it is a regression/vertical outlier, or simply called outlier. If the univariate outlier is in terms of the  $x$ -value, it is a leverage point. The further  $x_i$  is from  $\bar{x}$ , the sample mean of  $\{x_i, 1 \leq i \leq n\}$ , the greater its leverage. A point is influential if excluded from the analysis, the regression estimates change substantially.

##### B. Effects of Glide Slope Structure on Line Fitting

The glide slope signal being evaluated produces angular deviations from the glide path and not linear deviations. As such a 0.1 degree angular error at 1000 ft from the point of origination would only produce a vertical error of 1.75 ft while that same 0.1 degree angular error at 4 nm would produce a vertical error of 42.4 ft. This intrinsic feature will cause the same angular deviation to have considerably more impact the further one moves away from the signal origination point.

Also the effects of deviations on the computation of a straight line can be seen to cause changes in the computed RDH. Figure 1 demonstrates how deviations at Point B, Zone 2 midpoint, and Point A affect the slope of the line being fitted to the data using an OLS method. Some caused a lower than expected RDH and some higher even though all deviations were below the glide path. This counter intuitive result is intrinsic in the method used to compute BFSL and the subsequent extrapolation beyond the data field to compute the RDH. The line will tend to rotate around the centroid of the data set used as the basis for the computation of the BFSL if the outliers are towards the ends of the data set. If the deviation is near the centroid of the data, it may cause more of a translation up or down versus a rotation. Figure 1 only demonstrates the effects of a consistent linear deviation (an outlier) and not the angular deviation discussed above.

Because of these effects to line fitting caused by outliers, the RDH will be lower if the outliers are between the centroid of the data and the runway threshold. The RDH will be higher if the outliers tend to be further out than the centroid of the data.

Figure 1 is illustrative of computing a BFSL using the standard OLS technique. If the BFSL is computed assuming

the line must pass through the point of signal origination, no outlier deviation below the expected glide path would cause a rise in RDH calculations.

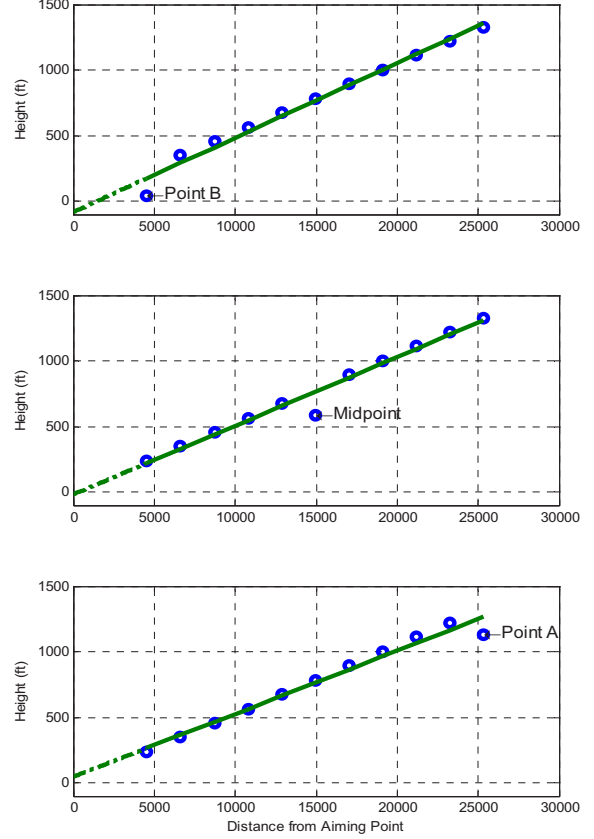


Figure 1. Effects of Outliers on OLS-based BFSL Determination.

In fact, the above phenomena can be easily explained mathematically. For a fixed value of  $i$ , consider  $x_i$  to be fixed in  $\{(x_i, y_i), 1 \leq i \leq n\}$ . If we write the slope of the OLS regression line  $\hat{\beta}_1$  in (3.5) as a weighted sum of  $y_i$

$$\hat{\beta}_1 = \frac{\sum_{i=1}^n (x_i - \bar{x})(y_i - \bar{y})}{\sum_{i=1}^n (x_i - \bar{x})^2} = \sum_{i=1}^n w_i y_i, \quad (4.1)$$

where the sample mean of  $\{(x_i, y_i), 1 \leq i \leq n\}$  are

$$\bar{x} = \frac{1}{n} \sum_{i=1}^n x_i, \quad (4.2)$$



$$\bar{y} = \frac{1}{n} \sum_{i=1}^n y_i. \quad (4.3)$$

and

$$w_i = \frac{x_i - \bar{x}}{\sum_{l=1}^n (x_l - \bar{x})^2}, \quad (4.4)$$

with

$$\sum_{l=1}^n w_l = 0, \quad (4.5)$$

we observe that the further  $x_i$  is from  $\bar{x}$ , the larger  $w_i$  becomes and the greater influence the corresponding  $y_i$  has on  $\hat{\beta}_1$ . On the other hand,  $x_i = \bar{x}$  has no influence on the calculation of  $\hat{\beta}_1$ . Therefore, we conclude that different data points have different influence on the slope of the LS regression line.

The one issue characteristic in the usage of BFSL for RDH/ARDH is that RDH/ARDH has to be estimated by extrapolation of a statistical model obtained from the measured data not at or near the runway threshold. As is known in linear regression analysis, the standard error of prediction is given by [14] (2.37),

$$\sigma(\hat{y}_{TH}) = \hat{\sigma} \sqrt{1 + \frac{1}{n} + \frac{(x_{TH} - \bar{x})^2}{\sum_{i=1}^n (x_i - \bar{x})^2}}, \quad (4.6)$$

where

$$\hat{\sigma} = \frac{1}{n-2} \sum_{i=1}^n (y_i - \hat{y}_i)^2, \quad (4.7)$$

and

$$\hat{y}_{TH} = \hat{\beta}_0 + \hat{\beta}_1 x_{TH}. \quad (4.8)$$

Eq. (4.6) shows that the standard error of prediction increases the further the value  $x_{TH}$  (runway threshold) is from the centroid  $\bar{x}$  of the measured data (Zone 2 for RDH, and 6000 ft to Point C for ARDH). Therefore, care should be taken in employing the obtained linear regression line for prediction far outside the range of the measured data.

### C. Adaptive Linear Regression

Generally speaking, robust estimates involve highly nonlinear optimization, which are computationally intensive. Described here is a method which is simple and effective. Recently, Maity and Sherman [13] proposed an adaptive linear regression method (ALR), which is a linear combination of OLS and LAD to achieve small mean square error for a broad range of error distributions. The solution  $\hat{\beta}_{ALR}$  for (3.1) is obtained by

$$\hat{\beta}_{ALR} = \lambda \hat{\beta}_{OLS} + (1 - \lambda) \hat{\beta}_{LAD}, \quad (4.9)$$

where the weight  $\lambda \in [0, 1]$  could be chosen to reflect the error distribution. For light-tailed<sup>5</sup> distribution, more weight is on OLS; for heavy-tailed distribution, more weight is on LAD. The choice of  $\lambda$  is not unique, two examples are

$$\lambda(\kappa_{ALR}) = \begin{cases} 1 & \text{if } \kappa_{ALR} \leq 3 \\ \frac{3}{\kappa_{ALR}} & \text{if } \kappa_{ALR} > 3 \end{cases}, \quad (4.10)$$

or

$$\lambda(\kappa_{ALR}) = \begin{cases} 1 & \text{if } \kappa_{ALR} \leq 3 \\ \left(\frac{3}{\kappa_{ALR}}\right)^2 & \text{if } \kappa_{ALR} > 3 \end{cases}, \quad (4.11)$$

where  $\kappa_{ALR}$  is the kurtosis computed by

$$\kappa_{ALR} = \frac{1}{2}(\kappa_{OLS} + \kappa_{LAD}), \quad (4.12)$$

and the kurtosis of data  $\{x_i, 1 \leq i \leq n\}$  is defined as

$$\kappa = \frac{\sum_{i=1}^n (x_i - \bar{x})^4}{(n-1)S^4}, \quad (4.13)$$

where  $S$  is the sample standard deviation. It should be emphasized that the kurtoses  $\kappa_{OLS}$  and  $\kappa_{LAD}$  in (4.12) are computed based on the residuals of their respective estimates.

## V. NUMERICAL RESULTS

In order to illustrate our findings, we perform simulations under the same assumptions as those in [10], i.e., the terrain and the runway surface are assumed perfectly flat and in the same plane. The initial aiming point is the origin of the  $x$ - $y$  coordinates. In addition, the original electronic data generated by flight inspection have been converted to quantities such as distance to threshold (or distance to AP) and height above runway surface (or height above the horizontal plane where AP is located). The conversion can be done by the procedure in [9].

In [10], the authors reported an issue that an aberration in the glide path (peaks at 20  $\mu A$  below) between 3 nm and 4 nm, which results in RDH of 66.0 ft, an out-of-tolerance value, the AP being raised by 12.38 ft, and unrepresentative low BFSL and average angles after the adjustment. We apply ALR, LAD, and a robust statistical method. The results are shown in TABLE I. TABLE II lists the results when the same aberration pattern occurs 2080 ft closer to the runway threshold. From the two tables, we find that ALR improvement over OLS will be more significant when the aberration is high leverage. ALR with (4.11) weighting gives better results than that by (4.10). However, it is cautioned that when the error distribution is light-tailed, the reverse is true. The robust method based on iteratively reweighted LS with the bisquare weighting function [17] also gives good RDH although more complex in computation.

<sup>5</sup> The light-tailed and heavy-tailed are relative to the tail of normal distribution.

TABLE I. AP ADJUSTMENT AND RDH BY VARIOUS METHODS WHEN THE ABBERATION OCCURS AT 3.66 NM TO THE THRESHOLD

Methods	AP Adjustment (ft)	RDH (ft)
OLS	12.38	66.00
LAD	6.54	60.72
ALR with (4.10)	11.51	65.21
ALR with (4.11)	10.76	64.54
Robust	10.60	64.41

TABLE II. AP ADJUSTMENT AND RDH BY VARIOUS METHODS WHEN THE ABBERATION OCCURS AT 3.32 NM TO THE THRESHOLD

Methods	AP Adjustment (ft)	RDH (ft)
OLS	6.34	60.43
LAD	4.67	59.01
ALR with (4.10)	6.10	60.22
ALR with (4.11)	5.89	60.05
Robust	0.00	54.98

Figure 2 shows the RDHs computed by various methods when there is an instantaneous vertical deviation indicator (VDI) blip of  $100 \mu A$  fly-down in Zone 2. The simulation setup here is the same as that in [10], i.e., Zone 2 is divided into 100 equally spaced points. Point "1" is at Point A and Point "100" is at Point B. The  $100 \mu A$  excursion is stepped, one point at a time, through the field of 100 points in Zone 2 while the remaining 99 points have  $0 \mu A$  values. For comparison purpose, we also draw the curve generated by the OLS method, which is Figure 18 of [10]. The nominal RDH value is 54.98 ft. Again it is shown that the methods suggested in this paper are less sensitive to course structure excursion and to where the excursion happens.

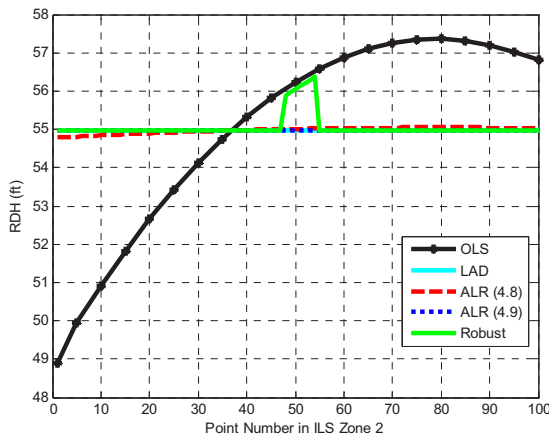


Figure 2. Effect of Migrating Course Structure Excursion on RDH.

## VI. CONCLUSIONS

We suggest that OLS will continue to be used. ALR is a compromise between simplicity and statistical efficiency. We do not recommend blind use of this method, but rather recommend it as a diagnostic tool to complement and explain the unusualness when OLS is not satisfactory. In addition, more sophisticated robust statistical methods may be used if the computational complexity and time constraint are not of concern.

## REFERENCES

- [1] U. Buchheim, "Methods of computing glidepath characteristics in modern flight inspection systems," 11<sup>th</sup> International Flight Inspection Symposium (IFIS), 2000.
- [2] G. Greving and L. N. Spohnheimer, "Problems and solutions for ILS category III airborne and ground measurements – European and US views and perspectives," 11<sup>th</sup> IFIS, 2000.
- [3] G. Greving and L. N. Spohnheimer, "Problems and solutions for navaid airborne and ground measurements -- Focus on receiver sampling and TCH," 12<sup>th</sup> IFIS, 2002.
- [4] I. Ferencz, "Harmonisation between calculated value of the ILS reference datum height and flight inspection results," 12<sup>th</sup> IFIS, 2002.
- [5] M. Wills, "Threshold crossing height - A fresh perspective," 12<sup>th</sup> IFIS, 2002.
- [6] H. Renouf, "RDH / TCH issues," 13<sup>th</sup> IFIS, 2004.
- [7] S. D. Courtney and D. A. Quinet, "Techniques to change glide path reference datum height (RDH) without relocating the ground facility," 14<sup>th</sup> IFIS, 2006.
- [8] L. Brady, "Glide path flight inspection geometric reference point and recommendations for international standards," 14<sup>th</sup> IFIS, 2006.
- [9] D. A. Quinet, "Validation of the automatic-flight-inspection instrument-landing-system best fit straight line application," OU/AEC 07-10TM-15689/0005-1, Avionics Engineering Center, Ohio University, Aug. 2007.
- [10] J. S. Edwards and M. F. DiBenedetto, "Assessment of the effectiveness of the RDH/ARDH evaluation methodology for the ILS glide slope," OU/AEC 08-21TM15689/0006-1, Avionics Engineering Center, Ohio University, Dec. 2008.
- [11] M. F. DiBenedetto, "Re-assessment of the necessity of flight inspection as the means for validation of final approach segment (FAS) data that define precision approach procedures supported by satellite-based technologies," OU/AEC TM09-07/80000/06-1, Avionics Engineering Center, Ohio University, Nov. 2009.
- [12] FAA Order 8240.47C -- Determination of Instrument Landing System (ILS) Glidepath Angle, Reference Datum Heights (RDH), and Ground Point of Intercept (GPI), Federal Aviation Administration, Mar. 1, 2001.
- [13] A. Maity and M. Sherman, "On adaptive linear regression," *Journal of Applied Statistics*, vol. 35, no. 12, pp. 1409-1422, Dec. 2008.
- [14] S. Chatterjee and A. S. Hadi, *Regression Analysis by Example*, 4<sup>th</sup> ed. Hoboken, NJ: John Wiley and Sons, 2006.
- [15] C. Zhong, "Flight inspection airborne processor application (FIAPA): analyses of selected formulas and algorithms," D09-009 (Release 02 D01W), Aircraft Maintenance and Engineering Division, Aviation System Standards, FAA, Apr. 2010.
- [16] G. A. F. Seber and A. J. Lee, *Linear Regression Analysis*, 2<sup>nd</sup> ed. Hoboken, NJ: John Wiley and Sons, 2003.
- [17] P. J. Huber and E. M. Ronchetti, *Robust Statistics*, 2<sup>nd</sup> ed. Hoboken, NJ: John Wiley and Sons, 2009.
- [18] Y. Li and G. R. Arce, "A maximum likelihood approach to least absolute deviation regression," *EURASIP Journal on Applied Signal Processing*, vol. 12, pp. 1762-1769, Sep. 2004.

## PC Based Simulation Tool to Evaluate Airfield Lighting Systems

*David A. Quinet*  
*Senior Program Engineer*



*Avionics Engineering Center*  
*228 Stocker Center, Ohio University*  
*Athens, Ohio 45701, USA*  
*Email: [quinet@bobcat.ent.ohiou.edu](mailto:quinet@bobcat.ent.ohiou.edu)*

## PC Based Simulation Tool to Evaluate Airfield Lighting Systems

### Abstract

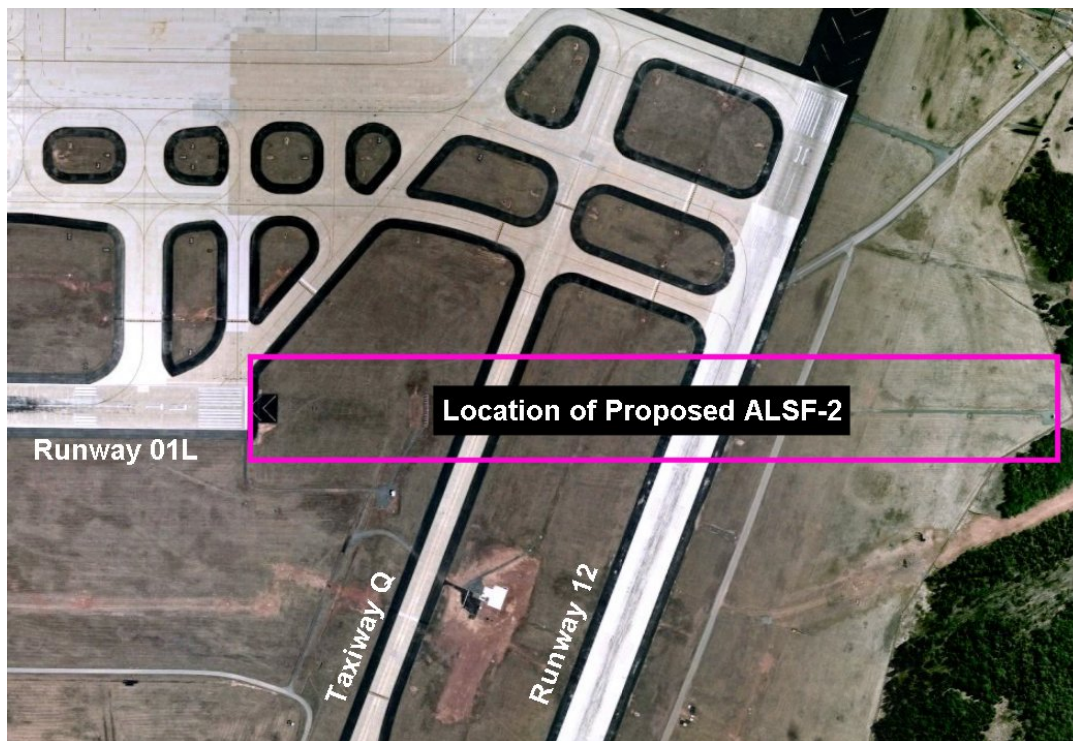
Computer Simulation tools have been used to evaluate guidance signal degradation for Navigation and Landing Systems for over 35 years. Electromagnetic theories are heavily dependent on complex computations to 1) generate the Radio Frequency (RF) propagation signals, including the directed and reflected signals, 2) process the composite signals through receiver processing and 3) apply accepted tolerances to the predicted guidance signals. Due to the complexity of the algorithms; initial simulation tools were developed on main-frame computers with little or no graphics capability.

With the advent of the personal computers which have excellent graphics capability, the navigation simulation tools have been ported over to the personal computer. This also has allowed for development of a simulation tool for airfield lighting systems. The Ohio University lighting tool was developed to assist with modifications to a newly installed ALSF-2 at Washington Dulles Airport (IAD) to support a new Category III approach for the 4<sup>th</sup> runway. A taxiway and runway required the approach lighting system to have non-standard spacing and heights which resulted in an abnormal visual cue along the approach. The simulation program was used to determine the optimum heights to reduce this abnormality.

The simulation tool has implemented all airfield lightening system (domestic & international) including MALSR, ALSF-2, PAPI, REILS and runway lights (edge, touchdown, centerline). Other features allow the user to define the viewing location and observation point. Objects can be placed near or within the light planes to determine if blockage occurs.. In addition, user defined flasher sequences and rates are possible. Approaches to the runway showing the airfield lightening systems, user selected, can be saved to a video file (.AVI). This paper documents the 1) simulation tools features, 2) example uses for the simulation tool and 3) a case studies;

## Development of the Airport Lighting Model

In 2007, the Avionics Engineering Center at Ohio University was asked to provide aerial videographic evaluation support to Washington Dulles International Airport (KIAD) regarding an ALSF-2 installed on Runway 01L. The ALSF-2 was configured using flush-mount and non-standard stem heights to accommodate Runway 12/30 and taxiway Quebec that crossed in front of the 04 threshold (see Figure 1) These changes to the light plane created some visual anomalies on the approach to Runway 01L. Figure 2 is a screen capture from the video data collected during that flight evaluation.

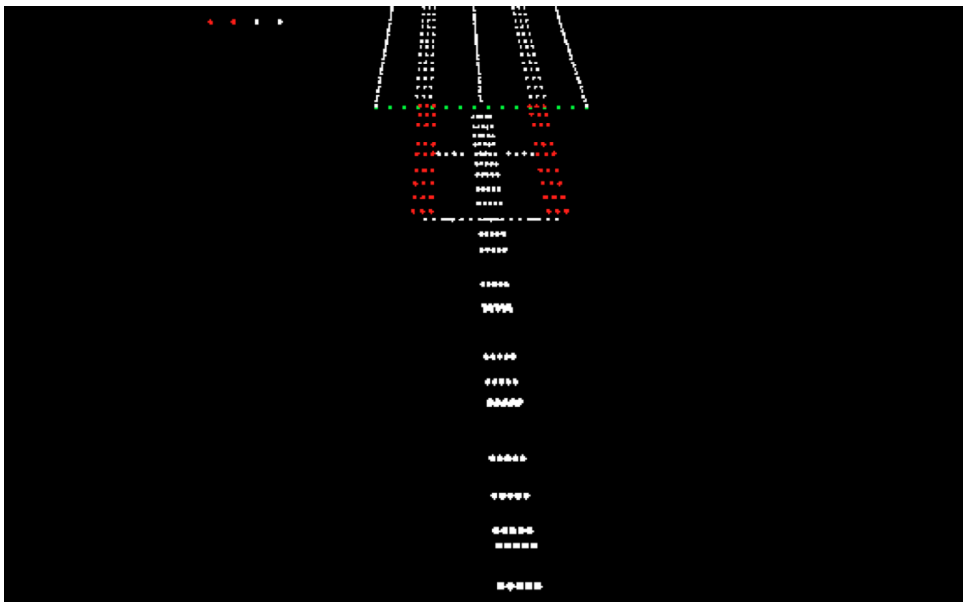


**Figure 1. Location of Proposed ALSF-2 on Runway 01L at KIAD**



**Figure 2. ALSF-2 As Installed on Runway 04 at KIAD**

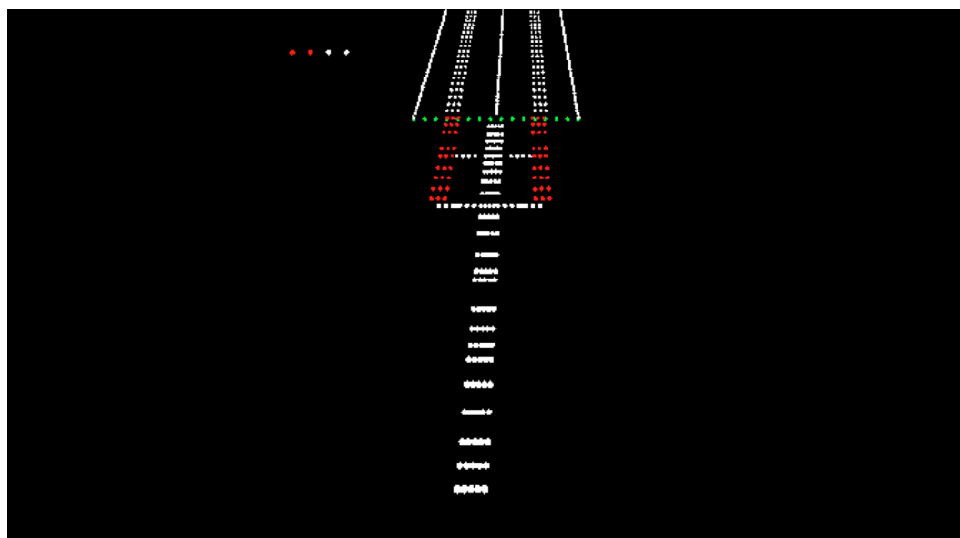
The ALSF-2 displays some anomalies such as the centerline bars that should appear to be a straight line aligned with the runway centerline, but instead appear to be irregularly spaced and in some cases overlapped. This could lead to confusion for the pilot on a low-visibility approach in which he might not identify the lights as the ALSF-2 and would have to abort the approach.



**Figure 3. KIAD Runway 04 ALSF-2 as modeled by Ohio University**

Following the visit to Dulles, the Airport Lighting Model was developed to assist with correcting these issues. The installation schematics for the ALSF-2 were referenced and the following modeling of the system was made in the OU Lighting Model (Figure 3):

The anomalies discovered during the flight evaluation are clearly evident in the modeling results in which a couple of the systems centerline bars appear to almost coincide instead of contributing to a nearly constant plane. Multiple iterations of adjustments to heights were evaluated on the model given certain restraints on the heights and locations of the lighting towers. The final modeling result is seen in Figure 3. The installed system was re-configured with the data from the modeling results and a new flight evaluation was conducted to confirm the improvement (Figure 4). The system can be seen to be markedly improved over the initial installation. This will lead to less pilot confusion, especially in an extremely low-visibility situation for a pilot. Again, the intermediate steps were all done without adjustment to the existing system and without costly flight evaluation, thus potentially saving thousands of dollars. Following this implementation of the Lighting Model, it has been used to assist other sites with difficult lighting situations.



**Figure 4. Final KIAD Runway 04 ALSF-2 Configuration as modeled by Ohio University**



**Figure 5. ALSF-2 As Re-configured on Runway 04 at KIAD**

### **Features of the Airport Lighting Model**

The Airport Lighting model was designed to provide a moderately realistic real-time 3-dimensional simulation of what a pilot would see on approach to a lighted runway in the daytime or nighttime. Frames from this simulation can be captured, or output as a movie in Microsoft Audio Video Interleave, or AVI file. The systems can also be viewed on a 2-dimensional plot, viewed side-by-side with previous iterations, and exported to Google Earth to be superimposed over satellite photographic data of the installation site.

Some of the features of the Airport Lighting Model are:

#### 1) Lighted features:

- A typical runway edge lighting installation
- Runway centerline lighting
- Touchdown zone lighting
- Vertical-slope indicator lighting (VASI and PAPI),
- Runway End Indicator Lighting (REIL),



- Random off-airport lights to provide depth cues.
- Approach Lighting Systems (ALS)

All of these light sources may be turned on or off as needed to improve simulation times.

2) FAA and ICAO standard light-plane Approach Lighting Systems:

- MALSR and MALSF
- ALSF and ALSF-2
- SSALR
- ODALS
- ICAO Simple Approach Lighting System
- ICAO Precision Approach Cat. I Lighting System
- ICAO Precision Approach Cat II and Cat III Lighting System

Each of the lighting systems is fully modifiable and new ones can easily be generated. The model allows extensive input of these systems including different light arrangements, intensities, colors, and flash times, as well as multi-mode system capability.

3) Non-Lighted Objects included for realism and blockage analysis:

- Runway surface
- Ground surface
- Tree lines,
- Static and dynamic traffic lines
- Solid plates

The solid plates can be used to represent walls of buildings, retaining walls, etc. The traffic lines can be used to represent typical traffic represented as a car, a Sport-Utility Vehicle, and a semi-tractor trailer following a road. The user specifies the location, length, and height of each object.

4) Ambient Weather Conditions

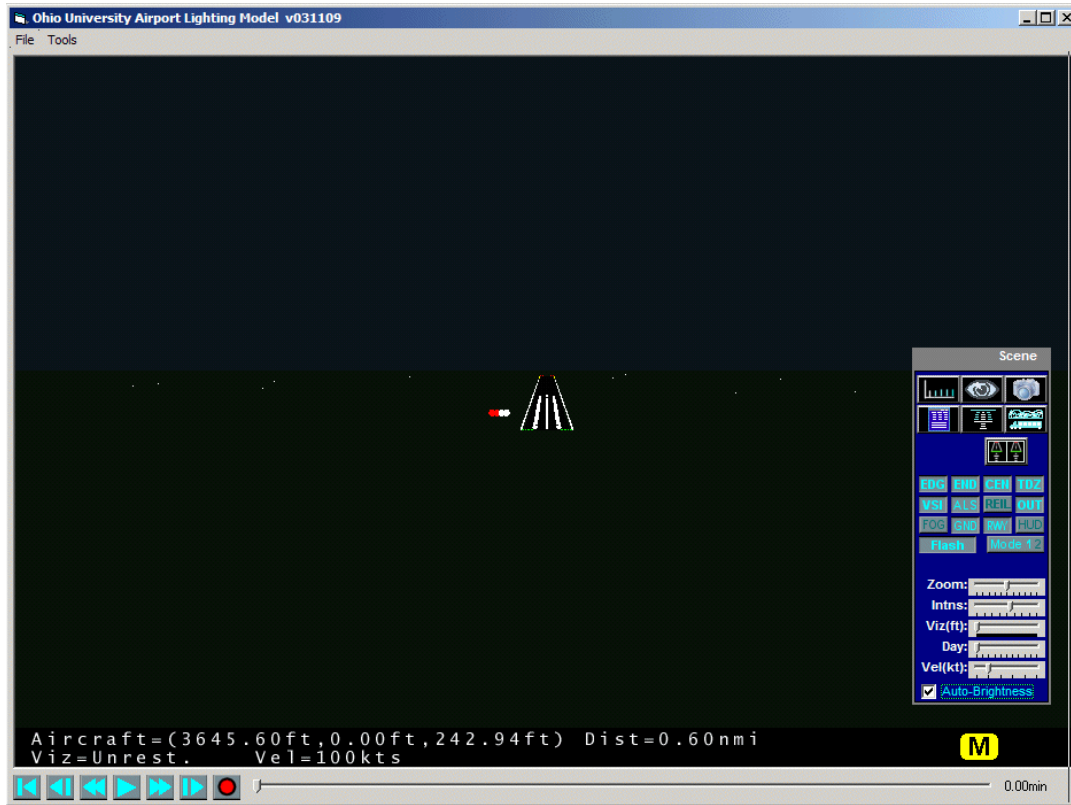
- Daylight
- Visibility,
- Cloud Layer.

These allow the approach to be viewed under degraded ambient conditions

### **Layout of the Model**

On initial startup, the main simulation window is displayed (see Figure 6). It presents a view from an aircraft on approach to a typically lighted runway at night with no obstructions or weather features. A scene parameter window is set to the right side, while an approach frame control bar and buttons are at the bottom. These do not appear

in screen captures, or any movie outputs. Current data about the approach are superimposed over the scene in the lower left, while marker beacon lights are superimposed on the scene in the right corner. These two features are part of the scene and appear in all output media. Along with the marker beacon light indications, an aural indication is given when a beacon is passed that is not currently captured in the AVI.



**Figure 6. Airport Lighting Model Simulation start-up Window**

The scene parameter window is where the parameter controls for the simulation are located. Every aspect of the scene may be turned on or off from the small toggle buttons in the middle of this window. Sliders in the bottom portion of the scene parameter window control the amount of daylight, speed of the aircraft, and visibility. Finally, control buttons at the top give access to frame capture, 2-D plots, aircraft location control, approach lighting system design, blocking plate editing, and other features. This window can be moved around within the main window for optimal viewing of the simulation. This window does not appear in screen captures, or movie captures.

### **Simulation Time/Frame Control**

The frame control bar and buttons (Figure 7) are the primary controls for running the simulation. They allow the user to run the simulation in real time, fast-forward, reverse, and step through the approach. Recording the simulation to a windows AVI movie is accessed from this bar as well.

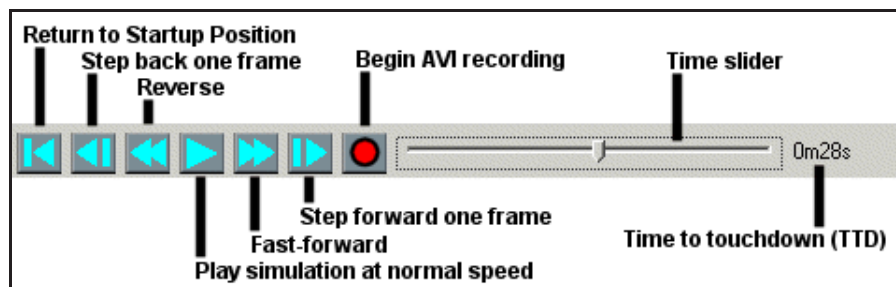


Figure 7. Frame Control Bar and Buttons


### Simulation View Control

The model uses two points to define the view: the camera, and the target. The camera represents the eye of the pilot, and the target is the point at which the pilot is looking. When a simulation is run, the camera location progresses along the vector defined by the starting camera location and the target location. The camera location can be modified using the mouse to pan, tilt, and move. It can also be modified, along with the target location, using the keyboard to enter absolute Cartesian coordinates(see Figure 8)

The mouse can be used to move the camera location around the target location simulating pitch and yaw of the aircraft. There is currently no functionality for roll of the aircraft. The mouse operates in two modes dependent upon the button pressed when the mouse is moved. If the left mouse button is depressed and the mouse moved around the simulation window, the view will rotate and tilt around the target point. If the right mouse button is depressed and the mouse moved forward or backward, the camera will move in towards, or out away from the target point, respectively.



Figure 8. Window for manual entry of camera and target parameters

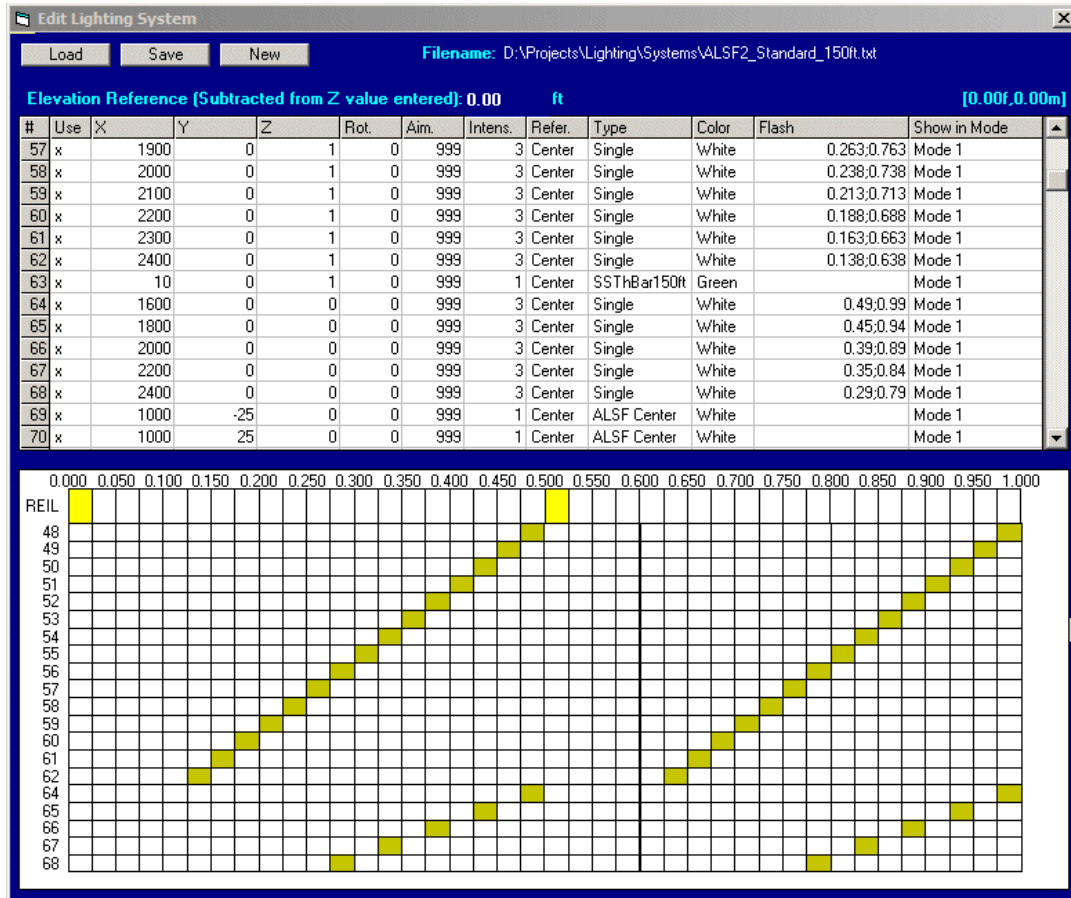
To adjust the camera and target parameters by keyboard entry, the  button on the Scene window is used. The window that opens is seen in Figure 8. From this window, the user can enter Cartesian coordinates for the camera and target, or can implement one of four point calculators that can determine a point based on distance, azimuth, and elevation angle from the target, or the threshold.

### Editing the Approach Lighting System

Clicking the Lighting System editing control button



opens up the window in Figure 9.



**Figure 9. Lighting System Editing Window**

The text grid at the top of the editing window allows input of up to 499 lighting elements and their parameters. A lighting element consists of a small grouping of lights that will be used repeatedly. Examples of these elements are a single bulb, and an ALSF centerline light with 5 bulbs. There are other presets, and since the lighting elements are currently stored as preset files, they are expandable as needed.

The graphical grid at the bottom of the window shows which lights will flash, and how often. The grid represents one second divided into 40 steps of 0.025 seconds each. The current maximum frame rate in for the AVI movie file is 30 frames per second so it is possible that some flashes may not be seen. The ID number of the light is given at the left, a white background indicates the light is off during that period, and a yellow background indicates the light is on.

In addition to choosing the x, y, and z coordinates of the light element relative to the threshold at centerline, the element can be intensified, and its' color changed. An element can also be restricted to use in just one of two available system modes. This is useful for representing systems such as the ALSF-2 that has both a normal mode, and a

reduced power consumption mode called a Simplified Short Approach Lighting System, or SSALR.

The system shown in the example data in Figure 8 is a standard ALSF-2 with the SSALR mode included. Returning to the main window and increasing the daylight to full, we see the ALS shown in Figure 10.

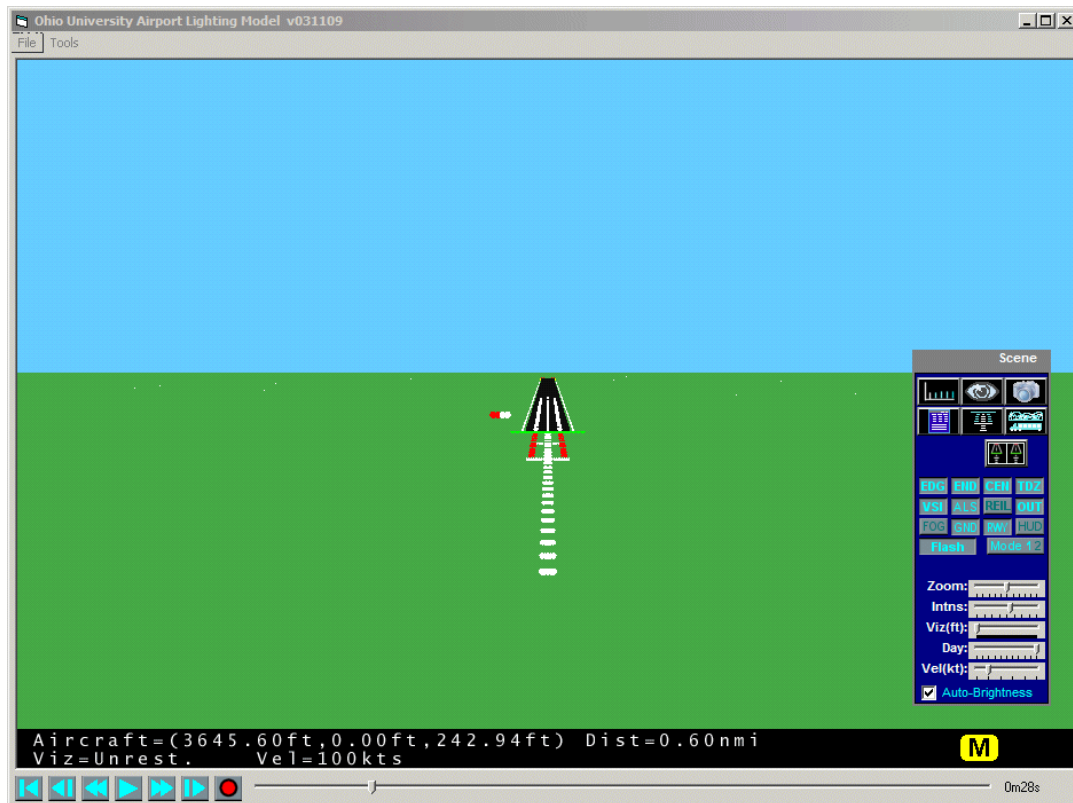

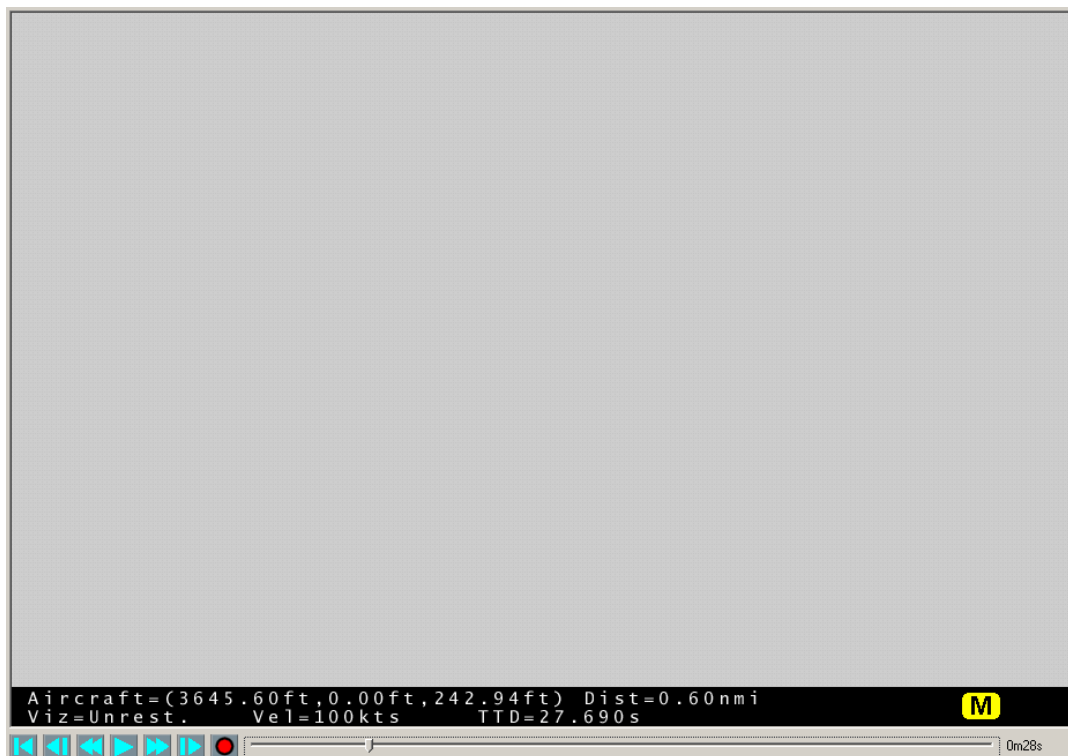


Figure 10. Simulation of a standard ALSF-2 for a 150-ft wide runway in daylight

### Simulating Adverse Weather

While an approach lighting system definitely improves the visibility of the runway while conditions are clear, it is when the weather conditions degrade that the system becomes absolutely critical. Ground fog, haze, and cloud layers will all make an unlit runway surface very difficult, and often impossible to see. The Airport Lighting Model is able to simulate two types of adverse weather: A zero-visibility cloud layer, and fog.

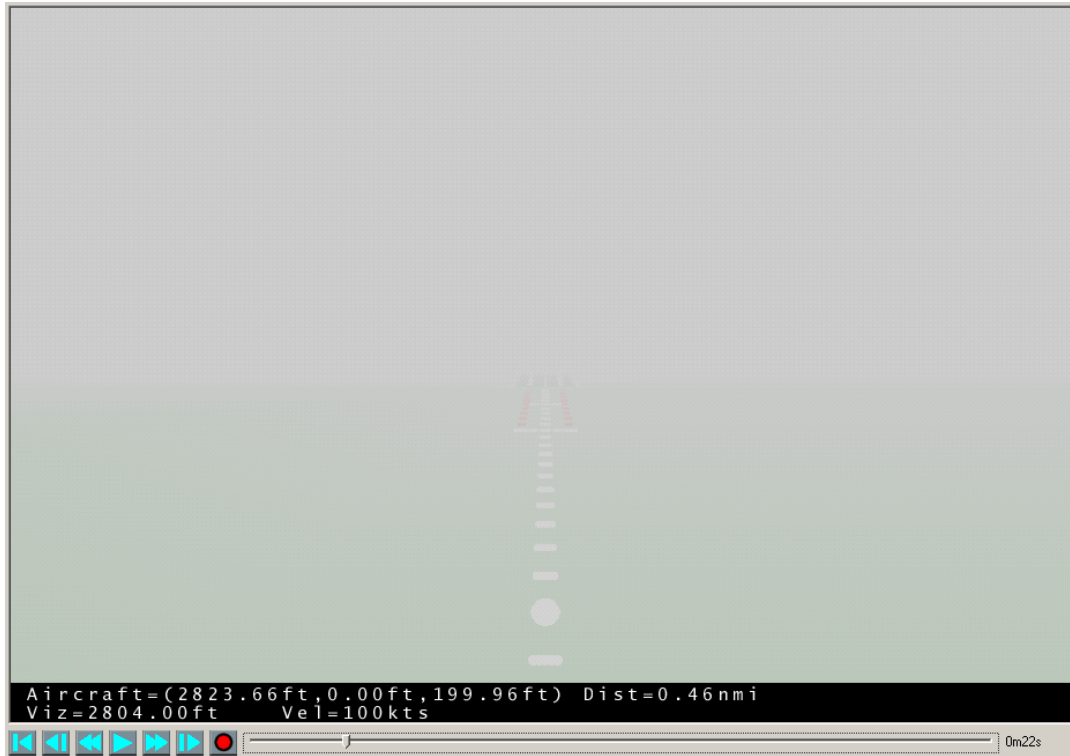
A cloud layer can be activated by accessing the Other Parameters menu with the  button on the 'Scene' window. Setting the cloud tops to 500 feet and the bottoms to 200 feet the simulation result at the aircrafts current position is seen in Figure 10.



**Figure 11. Aircraft inside cloud layer**

Because the cloud layer is zero-visibility, there is nothing of interest to be seen when the aircraft is between 200 feet and 500 feet of altitude.

Fog is activated and controlled from the Scene window using the ‘FOG’ button and the Visibility slider to set the visibility in feet. After setting the visibility to roughly 2800 feet, turning the fog on, and shuttling the aircraft forward to just under the cloud layer, the result is Figure 12.




**Figure 12. Simulation showing fog underneath a cloud layer**

The current method of producing fog does not allow interaction of the lights with individual water droplets, and therefore, there is no reflection or refraction to produce haloes and illumination of the surrounding area.

### **Simulating Potential Blockage Issues**

In an ideal airport environment, all structures, trees, and roads would be excluded from the entire airport environment and thus would not affect the approach lights. As is generally the case, though, airports are simply unable to acquire all the real estate to make this possible. Quite often, a drive around an airport's perimeter will take a person right through the center of an approach light lane. It is often times necessary to identify objects in and around the lighting system's envelope that could potentially block a light signal from reaching an aircraft attempting to locate the system

There are three types of blockage hazards that are implemented in this model: Tree lines, traffic lines (Both static and dynamic), and rectangular plates that can be used generically to represent buildings or other structures. Entry of these objects is done using

the 'Place Objects' window which is accessed by pressing the  button on the Scene window (see Figure 13).



#	Use	Type	X1	Y1	Z1	X2	Y2	Z2	Color
1	Yes	Treeline	1175.00	-5000.00	0.00	1175.00	5000.00	20.00	White
2	Yes	Road (Stat)	1050.00	-5000.00	0.00	1050.00	5000.00	12.00	White
3	Yes	Road (Stat)	1070.00	5000.00	0.00	1070.00	-5000.00	12.00	White
4	Yes	Generic	1000.00	-45.00	15.00	1030.00	-50.00	30.00	White
5									
6									
7									
8									
9									
10									
11									
12									
13									
14									

**Treeline** : Row of deciduous trees; Z2 can be any height

**Road (Stat)** : Creates a row of Static Vehicles (Semi, SUV, car)  
 - Height of Semi is 12ft. Z2 MUST EQUAL Z1 + 12 feet for correct scale

**Road (Dyn)** : Creates a row of Moving Vehicles (Semi, SUV, car)  
 - Height of Semi is 12ft. Z2 MUST EQUAL Z1 + 12 feet for correct scale  
 - Traffic Speed is 35 mph

**Generic** : Creates a single static and untextured plate

**Note:** Swap (X1,Y1) and (X2,Y2) to flip image (ie. traffic dir.)

**Important!** - Input objects from farthest to nearest for best display.



Figure 13. The Place Objects window for implementing tree lines, traffic lines, and generic rectangular plates

For this example, we have modeled a 20-foot tall tree line running perpendicular to runway centerline at a distance of 1175 feet from threshold. We have also included a highway represented by two static traffic lines going in opposite directions. By choosing the dynamic traffic line type, the vehicles would move in a straight line at a speed of 35 mph.

Finally, we have added a plate to represent a billboard on this roadway that is 15 feet tall and starts at 15 feet above the ground. When we now view the simulation and shuttle the aircraft in a bit closer we see the output of Figure 14. The image has been annotated to point out the billboard.


In this arbitrary example, we can already see a potential blockage issue caused by the highway. And although the tree line is not quite a problem at this instant, as the trees grow, they will probably block the 1100-foot station of the lighting system. The billboard is not seen to be a blockage candidate while the aircraft is on centerline where it should be, but an aircraft that is off the localizer to the left might see light elements blink in and out as they pass behind the sign.




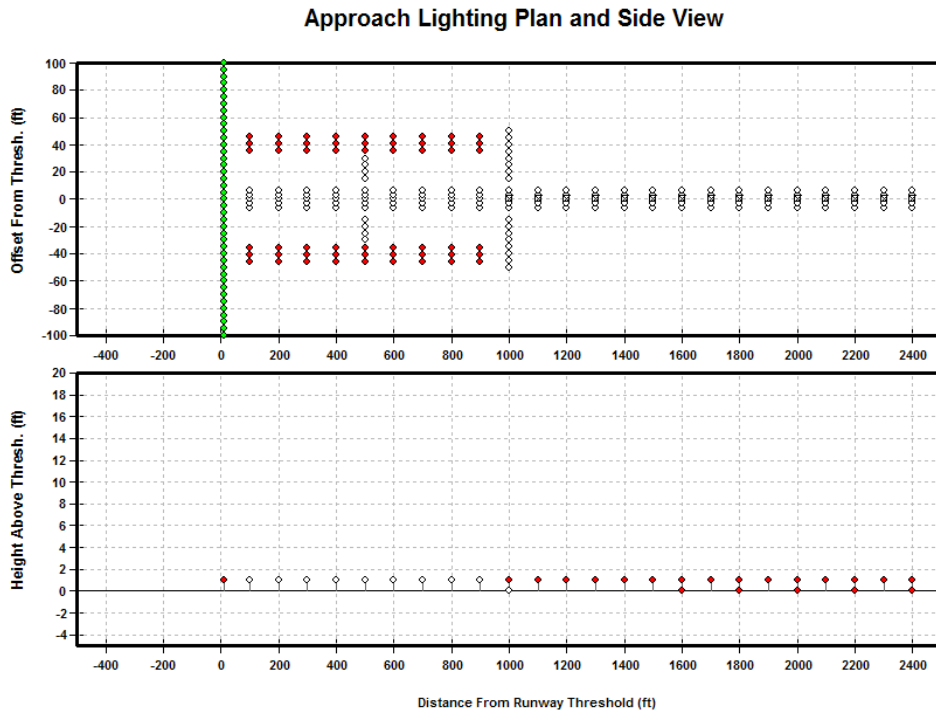
**Figure 14. Pictorial showing the various object types which could potentially block the light plane.**

### Simulation Output

Once all of the simulation parameters have been input, the model provides a number of methods of output:

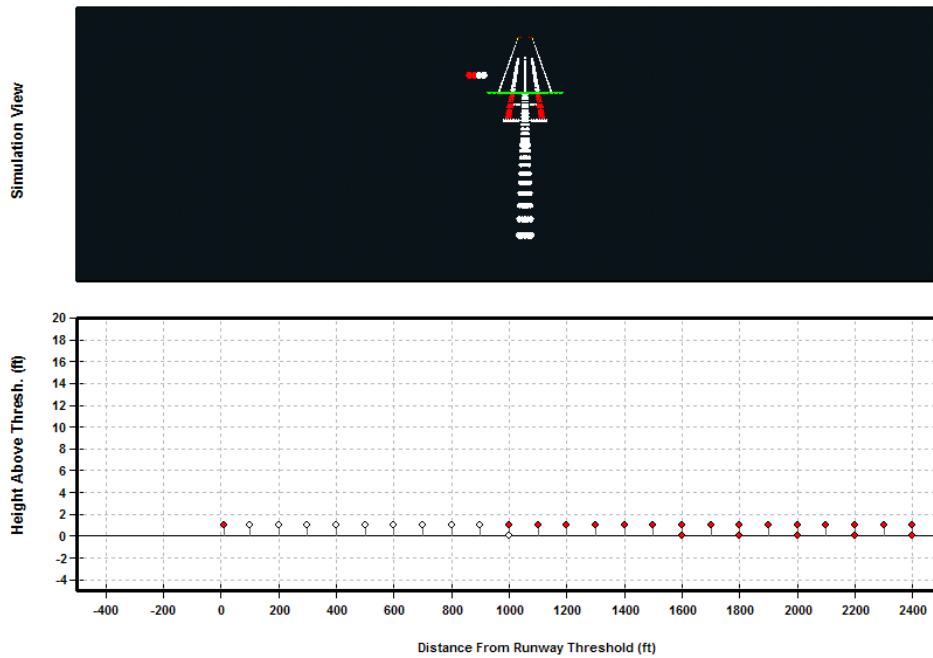
- 1) Screen Capture – Captures a single frame and sends the image to a Windows Bitmap File (BMP). This is accessed by clicking the  button on the Scene window.
- 2) Movie Capture – Save an entire simulation at 30 frames-per-second to a Microsoft Audio Video Interleave (AVI) file that can be replayed in Windows Media Player. The playback is in real time and is started by clicking the record button in the frame controls at the bottom of the main window. Once a filename has been selected, the option for the data to be compressed to reduce disk space is offered. Applying compression to video comes with a decrease in the quality of the output.
- 3) Two-Dimensional Plot Data –Two-dimensional graphs of the plan view, and the profile view of the system can be output to a Windows Bitmap File (BMP) . Figure 15 is an example with the plan and profile views together. In place of the plan view,

a smaller version of the simulation window can be used (see Figure 16). The 2-D plotting is accessed by clicking the  button on the Scene window.



**Figure 15. Two-Dimensional plan and profile graph of an example ALSF-2 system**

### Approach Lighting Simulation and Side View



**Figure 16. Simulation and profile views drawn together on 2-D graph**

- 4) Export System to Google Earth – If Google Earth is present on the simulation computer, the locations of the lighting system bulbs are output as KML features to it. To correctly position the bulbs, the model takes as input the latitude and longitude of the runway threshold and stop end. It is possible to get these values straight from Google Earth, or enter them manually.

This feature can be used to recognize potential collocation of lights with existing terrain features such as roads. An example of exporting a standard ALSF-2 system positioned at the Ohio University Airport Runway 7 Is shown in Figure 17.

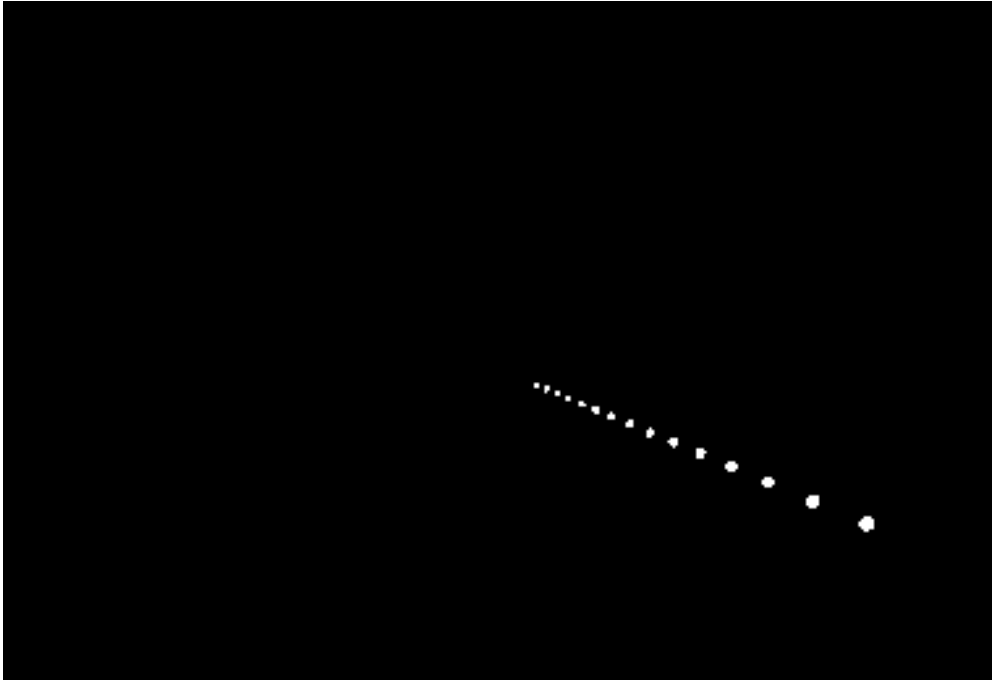


**Figure 17. ALSF-2 system exported from the model to Google Earth**

### **ALS Design Considerations**

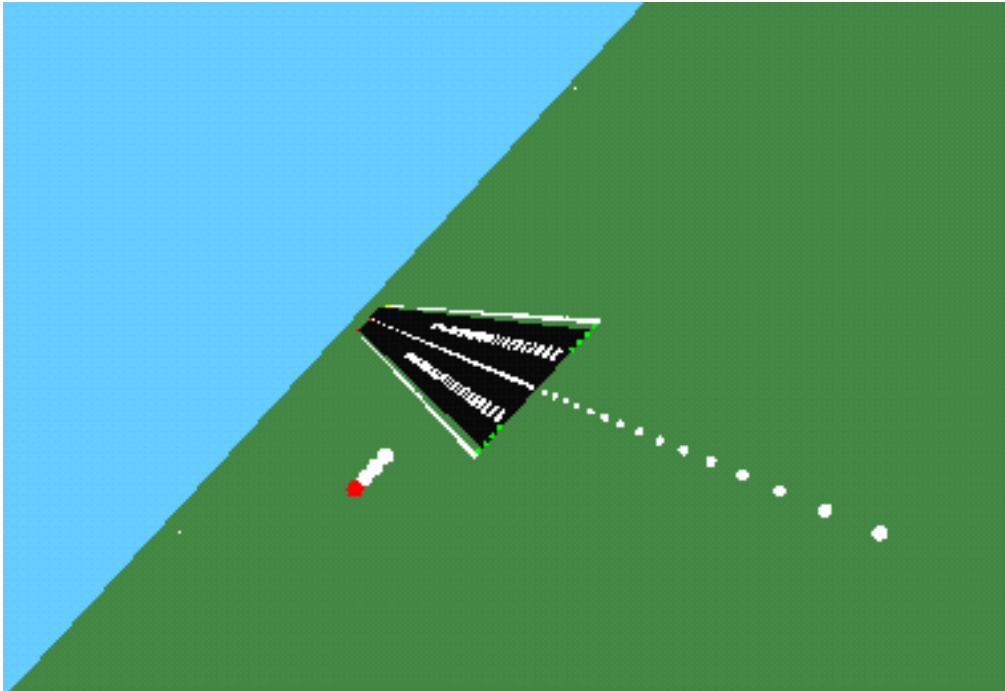
The Approach Lighting System (ALS) has the responsibility of providing as much information about the location of the runway as possible before the pilot ever has the chance to see it. The ALS does not reduce landing minimums but credit can be achieved for visibility requirements. Three key data points that are vital to the approaching aircraft are the location of the runway threshold, the direction that the runway extends from that point, and the orientation of the plane that includes the runway.

As an example of how the system provides this information, we start with a very simplistic approach system: a line of single lights with equal spacing between them positioned starting near the threshold and extending down the extended runway centerline. Figure 18 illustrates how this arrangement would appear to a pilot on approach. Assuming that the lighting system is always aligned with the runway centerline, the only thing known is that the pilot is NOT on the centerline. We have no indication of where the runway threshold is, or of the orientation of the runway plane.

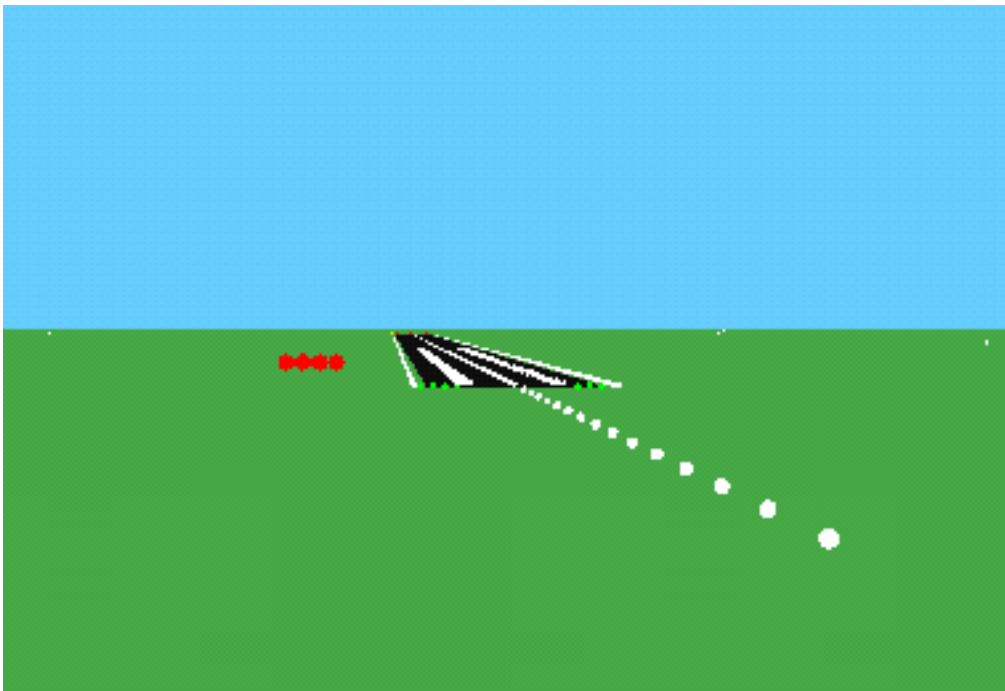


**Figure 18. Simulation of aircraft approaching a simplified approach light system at night**

One assumption that could be made is that the aircraft is in a level attitude and is off the runway centerline to the left. However, as Figure 19 and 20 demonstrate, there are many (infinite, actually) possible orientations of the aircraft that would produce the same orientation of the lighting system. It becomes clear that the only piece of information the pilot has from the lighting system alone is the location of the runway centerline. There is no data to support where the runway is, or the orientation of the plane containing the runway threshold.



**Figure 19. Simulation of aircraft approaching simplified light system revealing a miss-orientation of the aircraft**

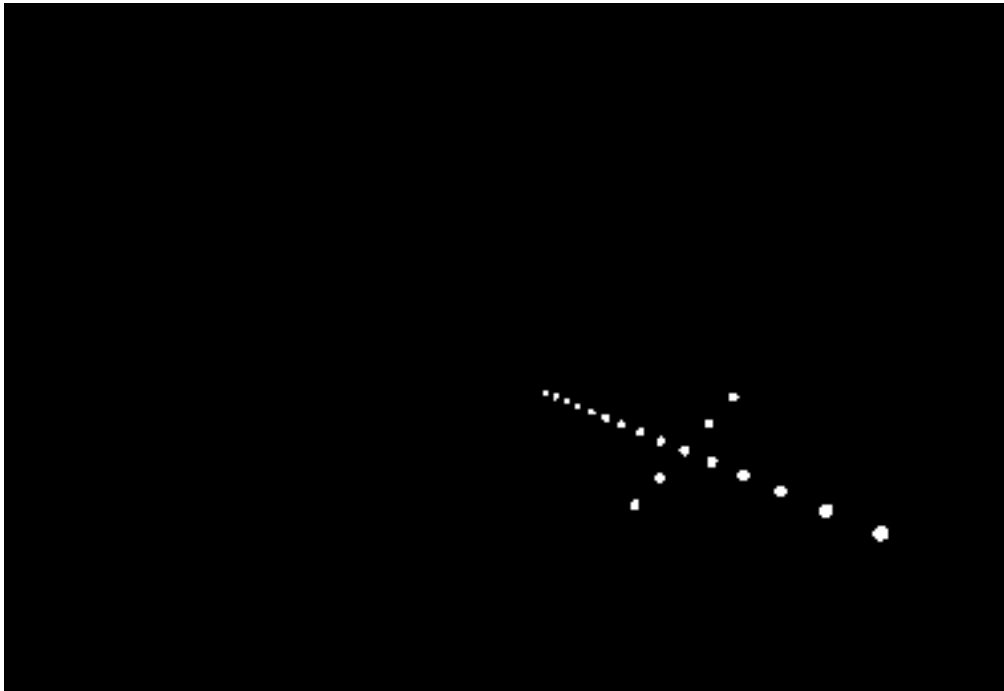


**Figure 20. A second possibility for the orientation of the aircraft with the simplified light system**

To give the pilot a better image of how the runway plane is oriented, a second grouping of lights can be placed in a line orthogonal to the first, but also falling in the same plane as the runway threshold. Generally this bar is placed also as a distance marker at, for example 500 feet or 1000ft, to give the pilot an indication of the distance to the threshold. Figure 21 shows the aircraft in the same location and orientation as before, but with this modified lighting system in place. As can be seen by comparing with Figure 22, we have a better idea of where the runway is and its' orientation relative to the aircraft. This second grouping solves the problem of the orientation of the runway plane, but gives us no real information as to the exact location of the runway threshold. It is extremely difficult to tell if the aircraft is flying towards the runway, or is beside it and flying away.

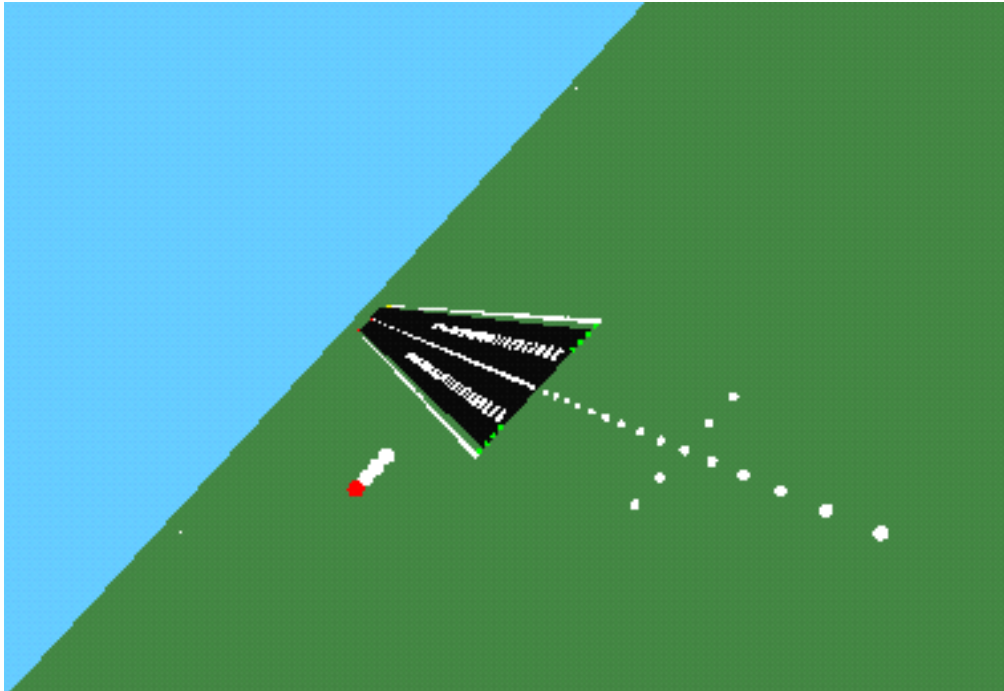
This final vital information can be provided in many ways, for example a third grouping of lights running parallel to the runway threshold and placed a known distance from the threshold. This grouping is often colored differently from the white lights of the rest of the system. Another method is to provide a group of sequenced flashers that indicate to the pilot the direction the aircraft should travel over the lighting system. The sequenced flashers also make the system stand out even when the airport itself is difficult to locate.

Another method employed by the ALSF-1 and ALSF-2 systems is by using red terminating bars spaced on each side of the runway centerline and extending from the threshold bar out to the 1000 foot bar. These bars actually allow the pilot to descend below 100 feet from touchdown elevation if they are clearly in sight.



**Figure 21. Aircraft located as before, but with lighting system amended to better illustrate the plane in which the runway threshold falls**





**Figure 22. Simulation shown in Figure X3, but in daylight revealing how much more information we have about the runway**

### **Examples of Implementation**

The best example of the implementation of this model is its first use in modeling done for Washington Dulles International Airport (KIAD) Runway 01L. This example was discussed in the opening section of this paper.

Since that first implementation, the model has been used to assist with siting a proposed MALSR at Ohio University Snyder Field (KUNI). This implementation was done before the addition of the Google Earth connectivity, and thus the 2-D output plot shown in Figure 23 was composited with an aerial photograph using a drawing program.



**Figure 23. KUNI MALSR Output Plot Overlaying Aerial Photograph**

A third use of the model involved siting an ALSF-2 that would have to contend with a pipeline that ran across the centerline of the runway around 1800 feet in front of the threshold. In lieu of a cylinder, a plate was used to represent the pipeline and the simulation executed revealing no blockage (Figure 24) when the aircraft was on a reasonable approach vector.



**Figure 24. Simulation of Kukaruk ALSF-2 and Pipeline**

### Summary

The Ohio University Airport Lighting Model was developed to assist personnel with siting approach lighting systems in non-standard applications. It has already assisted with the adjustment of an ALSF-2 serving on Runway 04 at Washington Dulles International Airport (KIAD), as well as a few other sites.

With the current interest in energy conservation has come the need to re-evaluate current approach lighting systems to see where any energy savings can be gained by reducing lighting system footprints, or reducing the numbers of lights, while still providing optimal safety for the pilot. It is hoped that this model will lend further assistance to that end.

## References

1. [http://www.nbpcorp.com/assets/alsf2\\_opspecs.html](http://www.nbpcorp.com/assets/alsf2_opspecs.html)
2. Federal Aviation Administration Order 6850.5C, “Maintenance of Lighted Navigational Aids”
3. Federal Aviation Administration Code of Federal Regulations Section 91

# The Investigation of the Influence of Snow upon Glide Slope

## Yutaka. OIKAWA

Flight Inspector  
Japan Civil Aviation Bureau  
Ota-ku, Tokyo, Japan  
Fax: +81 3 3747 0568  
E-mail: oikawa-y09ra@cab.mlit.go.jp



## Hisashi. YOKOYAMA

Research engineer  
Electronic Navigation Research Institute  
Chouhu city, Tokyo, Japan  
Fax: +81 422 41 3175  
E-mail: yokoyama@enri.go.jp



## 1. ABSTRACT

The snow in the Glide Slope (GS) reflection area has brought in a very burdensome task for Aeronautical Navigation Service Provider (ANSP) who needs to maintain GS in normal operation in snowy region.

Japan Civil Aviation Bureau (JCAB) made a flight investigation with the cooperation of Japan Electronic Navigation Research Institute (ENRI) at Aomori airport located in a heavy snowy region, concerning how depths and characteristics of snow at GS reflection area could affect GS signals.

In this presentation we would like to present a method of measurement for actual dielectric constants of snow layer, analysis of reflections of radio waves in snow condition, and the comparison of the result between actual flight investigations and a simulation, and introduce criteria of the snow removal at GS reflection area.

## 2. INTRODUCTION

In Japan a lot of ILS facilities in snowy region including Aomori airport are existing and are operated.

It is needed to pay attention to conditions in GS reflection area in order to continue stable operation service because general GS systems utilize reflection radio wave from the ground in front of GS antenna. Especially during snowfall season, it is important to pay attention to depths and

unevenness of snow, furthermore to even its characteristics of snow.

In Japan, Air Traffic Service Engineer in charge of ILS operation executes snow removal of the GS front area in accordance with the snow removal criteria which have been established by JCAB in order to apply to all ILS facilities in the country. This criteria is paying attention to depth and unevenness of the snow in the reflection area, also it is very strict.

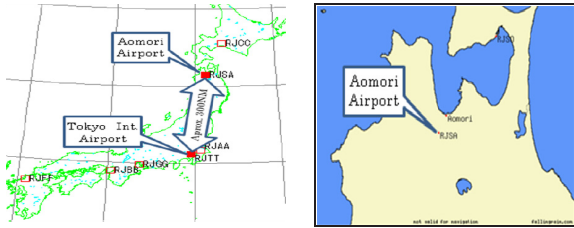
Because not only execution of the frequent snow removal according to this criteria becomes a big burden for an ATS Engineer, but also actual operation of airline aircraft might be affected, this influence investigation was planned by Air Traffic Services Engineering Division in JCAB headquarter for the purpose of easing of this snow removal criteria.

This investigation was conducted in Aomori airport which is one of the heaviest snowfall areas in Japan under cooperation of the researcher who is tackling research of ILS for years in the ENRI by flight inspection result and by comparing the simulation result with the data which was acquired by the flight inspection aircraft in the actual snow situation.

## 3. CHARACTERISTIC OF AOMORI AIRPORT

Aomori airport (RJSA), located in the northernmost of Japan's main island, has severe climate. The yearly

average temperature is around 10 degrees Celsius and a seasonal wind blows from the Sea of Japan in winter, and a large quantity of wet snow falls with it. The maximum depth of snow could be reaching over than 1,500mm in case of heavy snow year. Moreover, because the airport is located close to the sea, they had been afflicted by the cancellation of flights due to poor visibility caused by a dense sea fog especially in summer season, so that installation of high category ILS had been desired.



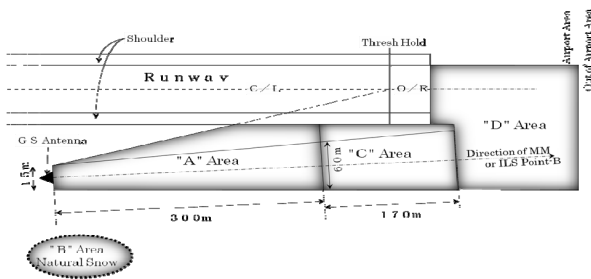
**Fig 3.1: Location of Aomori Airport**

ILS of Aomori airport was commissioned as CAT-I in July, 1987, afterward equipment was renewed in October, 2005 due to aging and aiming at CAT-III-izing for the purpose of reducing the cancellation of flights, and then CAT-III operation was commenced in March, 2007 after the operational evaluation of CAT-III. However, because it was the first experience for JCAB to install high category ILS in heavy snowy region in Japan, the easing review of the snow removal criteria for CAT-III that was stricter than for CAT-I became pressing needed.

Location: 40 44 00N / 140 41 19E (ARP)  
 Runway: 3,000m (RWY 06/24)  
 Height of ARP 650ft  
 ILS (CAT-III): 1 set (RWY 24)  
 LOC, GP, T-DME, IM

**4. THE FORMER SNOW REMOVAL CRITERIA**

The outline of the snow removal criteria for CAT-III ILS for each reflection area at the time of having installed the new ILS in Aomori airport is shown as follows.



**Fig 4.1: JCAB's Former Definition of Snow Removal Area**

In the above figure,

- “A” Area: Depth of snow should be 10cm or less. In addition, unevenness should be ±10cm or less.
- “C” Area: Depth of snow should be 60cm or less.
- “D” Area: There must not be snow bank more than 2m from an average snow cover surface caused by the snowfall.

These criteria are very strict, and it is hard for a heavy snowfall airport to maintain the criteria especially for “A” area. So the frequent snow removal and an out-of-service situation with it were assumed.

**5. EXECUTION OF FLIGHT INVESTIGATION**

Because it was necessary to create the snow condition required for the investigation, it was difficult to maintain CAT-III operation during winter. Therefore, operational category was changed from CAT-III to CAT-I from the time when the snowfall began to be observed to the time when the investigation was completed. Then flight investigation was carried out. By doing so, it was possible to create a snow condition required for the investigation, which is exceeding the existing snow removal criteria demanded to CAT-III.

This flight investigation was conducted as follows using Global Express (BD-700) flight inspection aircraft.

	Y / M / D	Level Run	Low Apch
2005-06 winter season	2006 / 1 / 20	0	1
	2006 / 1 / 25	1	1
	2006 / 2 / 14	2	1
	2006 / 2 / 15	2	1
	2006 / 3 / 15	1	1
2006-07 winter season	2007 / 1 / 15	0	1
2007-08 winter season	2008 / 2 / 6	1	3
	2008 / 2 / 18	1	3
	2008 / 2 / 19	1	3
	2008 / 2 / 20	2	3
	2008 / 3 / 6	3	3
	2008 / 3 / 7	4	1
	2008 / 3 / 10	4	1
	2008 / 3 / 12	7	2
	2008 / 3 / 13	6	1

**Table 5.1: Number of Investigation Flight**

In the 2005-06 wintertime 6 Level-Runs and 5 Low-Approaches, in the 2006-07 wintertime 1 Low-Approach and in the 2007-08 wintertime 29 Level-Runs and 20 Low-Approaches were repeatedly conducted in various snow conditions respectively. Although flight investigation had been meant to continue also in the 2008-09 wintertime, unfortunately we could not execute it due

to bad weather and because of no opportunity to have become an appropriate snow condition expected.

We acquired various data such as Path-Angle, Path-Width, Path Structure, Structure Below Path (SBP), Modulation Level and so on, which was calculated by AFIS. In order to contribute to the detailed analysis in ENRI simultaneously, the raw data outputted from AFIS was acquired and saved by the electronic file (ASCII format), and it was provided to ENRI later.

Fortunately, it is convenient to provide the data to the organization that does a detailed investigation and research such as ENRI because AFIS system on Global Express (BD-700) flight inspection aircraft can acquire the raw data of various parameters in ASCII format. The typical parameter contained in the submitted electronic data (ASCII format) is as follows, and was recorded every 0.1 second.

Aircraft Latitude / Longitude	in Degrees
Aircraft Altitude	in Feet
GP Average Deviation	in Micro Amp
Aircraft – GP Distance	in Nautical Miles
Aircraft – Threshold Distance	in Nautical Miles

, etc.

In addition, when we acquired the data we used DGPS as a position sensor basically. But in order to use DGPS, we had to land at Aomori airport and set up DGPS Ground Station, so when we were pressed for time, there was a case that we used TVPS, Laser ALT and Radio ALT for a position update, too.

## **6. DIFFICULTY IN DATA ACQUISITION**

There were various difficulties in this mission. One of these is that it did not readily become suitable snow condition for the investigation we expected. The snow condition to be expected is the condition of boundary of whether ATS Engineer has to make snow removal or not. In reviewing the snow removal criteria, it is necessary to confirm that the signal received in the space is satisfactory even in the most critical condition. Moreover, in order to establish new snow removal criteria which enable CAT-III operation to continue as long as possible, it is preferable to be able to confirm that signal in space is satisfactory even in every conceivable bad condition. However, snow condition was extremely changing year by year. There were hardly snowfall in one winter due to a mild winter; on the other hand there were extremely much snowfall in one winter due to the abnormal weather of recent years. In addition, there was a case also that the flight itself could not be done because we were not able to maintain VMC by a heavy snowfall even if there was adequate fallen snow. Furthermore, if it had continued to snow, the depth of snow increased too much and if it had been sunny, snow began to melt by solar radiation, so the

timing of the mission was very difficult even if it was in the adequate snow condition expected.

These are reason why we were able to do it only once for the winter season of 2006-07 and were not able to do at all for the winter season of 2008-09.

## **7. RESULT OF FLIGHT INVESTIGATION**

Flight investigation was conducted by changing the snow condition of “A” area into various conditions. Because the ATS Engineer thought that if all of data required for CAT-III had been within tolerance under such a condition, so many snow removal would not necessarily be required even if it is CAT-III.

From the result of the Level Run in February, 2008, Path Width of 0.85 degrees which was out of tolerance for CAT-III GS (0.62 - 0.82 degrees) was obtained (However, it was within tolerance for CAT-I).

The snow condition in “A” area at this time was that there were some snow bank of about 50cm and was uneven like wave (depth of snow in all other area in the “A” area was less than 30cm). Path angle was 2.99 degrees and path width was 0.72 degrees at the time of “Commissioning flight inspection” of Aomori ILS. Path angle was 2.99 degrees and path width was 0.75 degrees at the time of “Periodic Flight Inspection” under the condition without snow in December, 2007 2 months ago. The path width was within tolerance when the reflection area was not comparatively uneven even if it was covered by snow.

Taking every above thing into consideration, it is supposed that unevenness in the reflection area affected the path width.

In addition, it was confirmed that all of other parameter such as path angle, SBP and path structure were within tolerance for CAT-III in any snow conditions which we carried out this time.

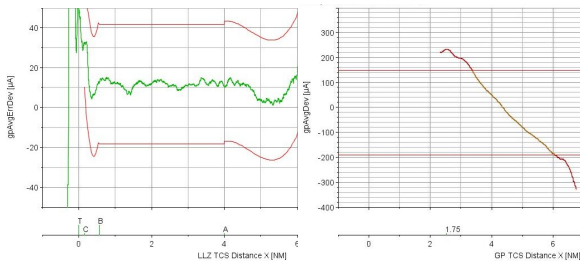
Although the “snow removal criteria” defined by JCAB has been defined paying attention to the depth of snow and the unevenness in the reflection area, generally speaking it is considered that the snow quality which might affect GS signal in space cannot be ignored, either.

Month / Date	Path Angle	Path Width
Jan. 25 <sup>th</sup>	3.05 °	0.82 °
Feb. 14 <sup>th</sup>	3.07 °	0.77 °
Feb. 15 <sup>th</sup>	3.06 °	0.78 °
Mar. 15 <sup>th</sup>	3.03 °	0.75 °

**Table 7.1: Result of Flight Investigation in 2006**

Month / Date	Path Angle	Path Width
Feb. 6 <sup>th</sup>	2.95	0.84
Feb. 18 <sup>th</sup>	3.05	0.85
Feb. 19 <sup>th</sup>	3.06	0.85
Feb. 20 <sup>th</sup>	3.08	0.84
Mar. 6 <sup>th</sup>	3.02	0.81
Mar. 7 <sup>th</sup>	3.02	0.78
Mar. 10 <sup>th</sup>	3.02	0.76
Mar. 12 <sup>th</sup>	3.00	0.77
Mar. 13 <sup>th</sup>	2.99	0.78

**Table 7.2: Result of Flight Investigation in 2008**



**Fig 7.1: Example of Path Structure and Displacement Sensitivity (on February 15<sup>th</sup>, 2006)**

## **8. TYPE OF GS ANTENNA AND THE SNOW CONDITION OF REFLECTION AREA**

The type of GS antenna in Aomori airport is M-Array antenna with dual frequency and 3 elements, which has been adopted as standard type in Japan. The GS antenna position is offset from the runway by 120m.



**Fig 8.1: GS Antenna with Dual Frequency and 3 Elements in Snow Condition**

### **8.1 Change of Snowfall during Snow Season**

Although the snow condition in Aomori airport is complicated, it can be roughly classified by the period into three states as shown in Table 8.1.

Oct. ~ Nov.	The beginnings of a snowfall. It will gradually become lingering snows. Snow condition is natural snow condition by one layer.
Jan. ~ Feb.	The heavy snowfall period. As for the lower layer, it becomes compacted snow by snow removal. The snow sectional structure of 2 or 3 layers is formed by a fresh snowfall above the lower layer.
Mar. ~ Apr.	The snowfalls decrease, the temperature rises and the snow becomes in a wet snow condition. Especially the snow of the lower layer becomes slush and becomes sectional structures of 1 or 2 layer.

**Table 8.1: Change of Snowfall during Snow Season in Aomori Region**

### **8.2 Snowfall Change and Snowfall Condition**

The method of snow removing on GS reflection surfaces is that, as being shown in Figure 8.2, treading on natural snow with a bulldozer is carried out when the depth of accumulation is close to the set value. After that, those operations are conducted to keep the set value of the depth of snow in front of GS site at every snowfall. Mostly, those operations are carried out during a snowfall in dark time before the airport is opened. And it is often that those operations lead the GS reflection surfaces into unevenness, because the snow removing by the bulldozer has to be done as avoiding 5 instruments which are being set on GS reflection surfaces to measure the depth of snow.



**(a) Snow Removal (b) Surface after Snow Removal**  
**Fig 8.2: Scenery of Snow Removal by Bulldozer**

### **8.3 GS Reflection Surface and Flight Investigation Method**

The Figure 8.3 shows the method of flight investigation and the condition of snow on GS reflection surfaces.



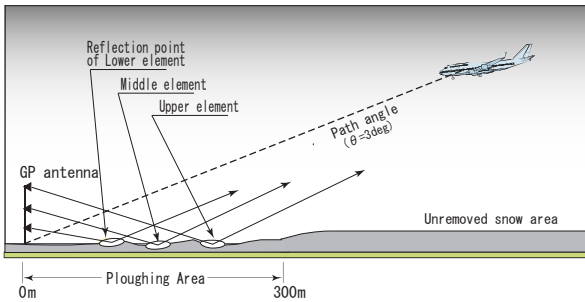


Fig.8.3 Flight check test under the condition of filed snow condition on the reflection plane

The GS angle is measured by low approach flight on GP and the path width is measured by level flight at 2,200feet MSL (1,500feet AGL). When the GS angle is assumed to be  $\theta_{3deg}$  and the path width is assumed to be  $\theta_{wid}$ , those answers are as follows;

$$\theta_{3deg} = \tan^{-1}\left(\frac{H}{X_s}\right) \quad (1)$$

$$\theta_{wid} = \tan^{-1}\left(\frac{H}{X_{s-high}}\right) - \tan^{-1}\left(\frac{H}{X_{s-low}}\right)$$

GS path is made up of direct waves and reflected waves. As Figure 8.3 shows, 3 reflected points are formed on GS reflection surfaces. And, as snow removing by machine is done for the accumulated snow within 300m area in front of GS site, the reflection surfaces become layer structure and unevenness. The area beyond 300m is nature snow area not removed.

## 9. ANALYSIS METHOD

### 9.1 Development of Measurement Instrument for a Dielectric Constant

The layer structure on the sectional structure of accumulated snow changes depending on the weather condition. Therefore, ENRI developed a measurement instrument for a dielectric constant. Figure 9.1 shows its block diagram.

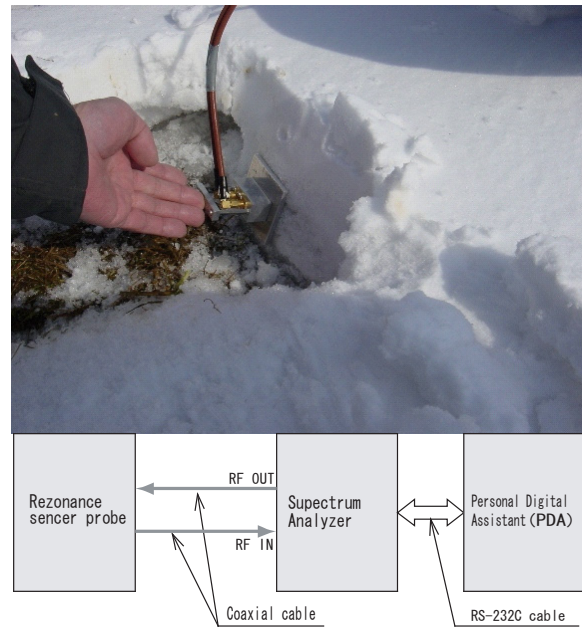


Fig.9.1 measurement method of dielectric constant of snow

A sensor, “transmission-type electromagnetic open resonator probe” shown in Figure 9.1, is inserted into the sectional structure of accumulated snow to measure the dielectric constant. The change in the resonant characteristics of probe sensor depending on quality of snow is measured with spectrum analyzer and the dielectric constant is calculated by a portable terminal (PDA). As being compact and light, this instrument is suitable to calculate the dielectric constant in a field by amplitude measurement.

Figure 9.2 shows the result of measurement on the dielectric constant of snow in the frequency band of GS. The Figure 9.2 shows the measurement result of the dielectric constant when a water component in a fresh snow or compacted snow changed depending on outside temperature.

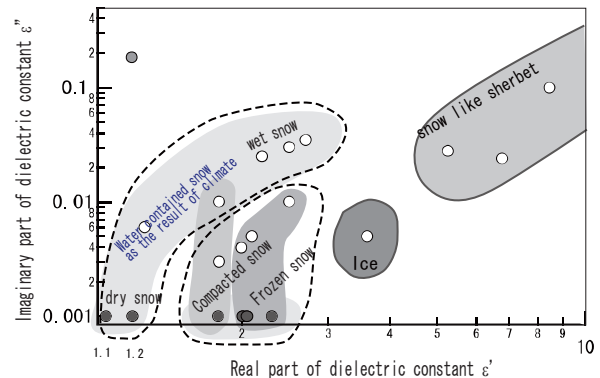


Fig.9.2 Measurement result of snow quality as the result of climate

## 9.2 Prediction Method of Snow Surface Configuration

A snow removal area on the GS reflection area is within 300m from GS antenna. The fresnel zone beyond it is a natural snow area where the snow removal is not executed. Since GS reflection area was within a restricted area, the depth of snow, the snow layer and the dielectric constants were measured at intervals of 20m. As a result, it was confirmed that the snow layer and the depth of snow were various at each measurement point as shown in Figure 9.3.

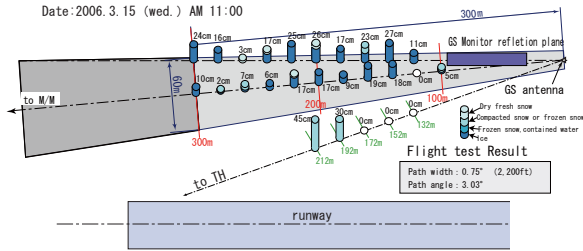


Fig. 9.3 Snow Roughness of GS reflection plane  
2006. 03. 15

The rotating laser level meter was used to measure the depth of snow. The rotating laser level meter is a device which compensates the level by itself automatically at the time of power-on and then emits laser beam to the measuring direction when the vertical elevation for emission is set to 0.3% as same as the vertical slope of the reflection ground surface. This device was set up beside the GP antenna as shown in Figure 9.4.

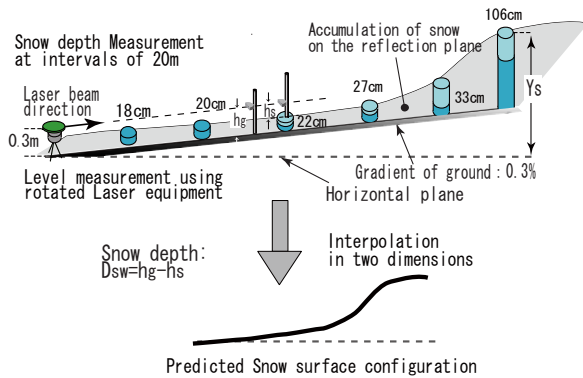


Fig. 9.4 Snow Depth Measurement on the GS reflection plane

A surveyor stands the surveying pole that attached the laser detector on the top of it at the measurement point on the snow surface or the ground. Then a surveyor makes a laser detector slide up and down, and looks for the height that the laser detector gleams. This height is the height that we need in order to calculate the depth of snow. By measuring the height from the ground ( $h_g$  m) and the snow surface ( $h_s$  m) to the gleaming point by this method, the height from the horizontal plane to the surface of snow ( $Y_s$  m) can be calculated from the following formula.

$$Y_s = a_{grd} \cdot X_s + 0.3 - h_g + D_{sw}$$

$$D_{sw} = h_g - h_s \quad (2)$$

Here,  $X_s$  (m) is horizontal distance between the rotating laser level meter and the measurement point, 0.3 is the height (m) from the ground to the laser emission point of the rotating level meter, and  $D_{sw} = h_g - h_s$  (m) is the depth of snow from the ground.

The snow data measured at intervals of 20m can be converted into the predicted snow surface configuration of 20cm intervals by using interpolation in two dimensions.

The example of snow surface configuration presumed from the snow data measured on January 25<sup>th</sup>, 2006 is shown in Figure 9.5.

There are convex portion ( $D_{max}$ ) and concave portion ( $D_{min}$ ) on the snow surface.

Figure 9.6 shows the relation between the path width and a difference between the maximum snow depth and the minimum snow depth ( $D_{max} - D_{min}$ ). This was led from the result of the flight investigation. Refer to Figure 9.5 for a difference between the maximum snow depth and the minimum snow depth.

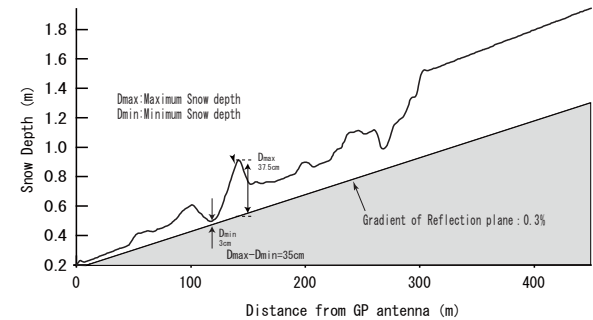


Fig. 9.5 Predicted Snow surface Configuration at 2006. Jan. 25<sup>th</sup>

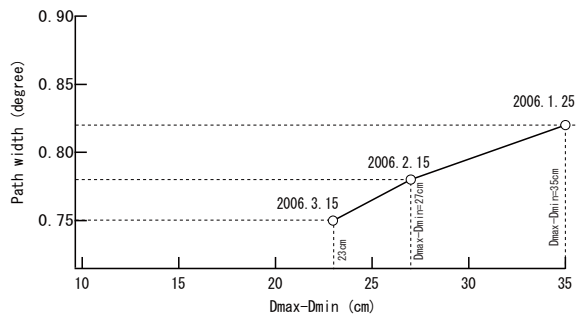


Fig. 9.6 The Relationship between Path width and difference of Snow depth ( $D_{max} - D_{min}$ ) on the reflection plane with 300m range.

Although there were a few samples, it was confirmed that the path width was changing almost linearly in proportion to ( $D_{max} - D_{min}$ ) of snow surface configuration. The key

factor of a widened path width is the unevenness of snow surface by snow removal. In order to maintain path width within tolerance limit, it is necessary to make snow surface configuration as flat as possible.

### 9.3 Analysis Methods Applied to GS Reflected Wave

The coordinate origin is set on the ground surface of GS antenna and GS antenna is 120m offset from runway center line. The vertical slope of reflecting ground surface is set to 0.3%, and cross slope is set to 1%. As described in Figure 9.5, the arbitrary point of the surface profile, 20cm interval, of snow covering is assumed as an imaginary reflecting point ( $X_f, Y_f, H_f$ ). We analyze the crossing point ( $H_0$ ) of the tangential plane of ideal reflecting point and the Z axis (GS antenna) of coordinate origin. Additionally, measured unidirectional data row is used as substitute for the asperity of Y axis of the surface of snow covering, and cross slope is set to 1%.

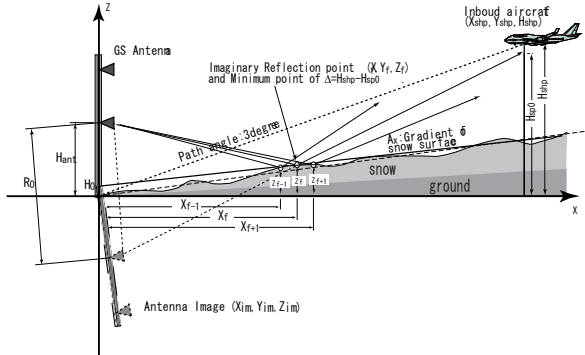


Fig. 9.7 Estimation of reflection point on rough surface of snow

To set up the reflecting point, the coordinate of antenna image ( $X_{im}, Y_{im}, Z_{im}$ ) from GS antenna becomes symmetry to the tangential plane.

$$\begin{aligned} (X_{im}, Y_{im}, Z_{im}) &= \left( R_0 \sin \theta_x \cos \theta_y, R_0 \sin \theta_y \cos \theta_x, (2H_0 - H_{ant}) + R_0 (\sin^2 \theta_x + \sin^2 \theta_y) \right) \\ H_0 &= -a_x J_x + H_{gd}(n) + H_{sw}(n) \\ R_0 &= 2 \cdot (H_{ant} - H_0) \end{aligned} \quad (3)$$

To set up the reflecting point of electrical wave, at first, the height ( $H_{sp0}$ ) of aircraft position ( $X_{shp}, Y_{shp}$ ), which deduce a straight line connects with the GS antenna image and imaginary reflecting point, then real reflecting point should be deduced by minimize delta ( $\Delta = H_{shp} - H_{sp0}$ ,  $H_{shp}$  is known aircraft position).

Secondly, reflection coefficient  $\Gamma_{01}$  should be set up when the cross section structure of snow is single layer. The incident angle into the snow surface is  $\phi_{in}$  and the complex dielectric constant is  $\epsilon_g$ , then these come out reflection coefficient  $\Gamma_{01}$  by the theory of distributed constant, calculating equation-(4).

$$\begin{aligned} \Gamma_{01} &= \frac{(Z_1 \cos \phi_{in} - Z_0)}{(Z_1 \cos \phi_{in} + Z_0)} \\ Z_1 &= Z_{s1} \cdot \frac{(Z_{gd} + Z_{s1} \tanh \gamma_{gd})}{(Z_{s1} + Z_{gd} \tanh \gamma_{gd})} \\ \gamma_{gd} &= 2 \cdot C_j \pi D_{sw} \sqrt{\epsilon_{s1} - \sin^2 \phi_{in}} / \lambda \\ Z_{s1} &= Z_0 / \sqrt{\epsilon_{s1} - \sin^2 \phi_{in}} \\ Z_{gd} &= Z_0 / \sqrt{\epsilon_g - \sin^2 \phi_{in}} \\ \epsilon_1 &= \epsilon'_1 - j \epsilon''_1 \\ \epsilon_g &= \epsilon'_g - j \epsilon''_g \\ Z_0 &= 120\pi \end{aligned} \quad (4)$$

In this equation,  $Z_1$  means incident impedance as seen ground from surface of snow covering,  $Z_{s1}$  means characteristic impedance of snow cross section,  $\gamma_{gd}$  means propagation constant,  $Z_0$  means characteristic impedance of air,  $\epsilon_1$  means complex dielectric constant of snow, and  $\epsilon_g$  means complex dielectric constant of ground.

From  $\Gamma_{01}$  and the distance between GS image antenna and aircraft position ( $\gamma_d$ ), reflected wave ( $E_{ref}$ ) can be calculated as follows.

$$\begin{aligned} E_{ref} &= \frac{\Gamma_{01} \cdot E_{amp} \epsilon^{-jA r_d}}{r_d} \\ r_d &= \sqrt{(D_{shp} - D_{im})^2 + (H_{shp} - H_{im})^2} \\ D_{shp} &= \sqrt{X_{shp}^2 + Y_{shp}^2} \\ D_{im} &= \sqrt{X_{im}^2 + Y_{im}^2} \end{aligned} \quad (5)$$

In this equation, ( $X_{shp}, Y_{shp}, H_{shp}$ ) is the coordinate of aircraft position.

Figure 9.8 describes the analysis result of  $\Gamma_{01}$ , when the structure of snow cross section is made into single layer and its snow depth ( $D_{sw}$ ) varies between 0.0m and 1.0m. In this figure, imaginary part ( $\epsilon''$ ) of snow is fixed to 0.001. In the case that real part ( $\epsilon'$ ) of the complex dielectric constant of snow is set to 1.1 or 1.3, reflection coefficient is markedly decreased when  $D_{sw}$  is 68cm or 40cm. In the case of fresh snow, electrical wave is especially absorbed.

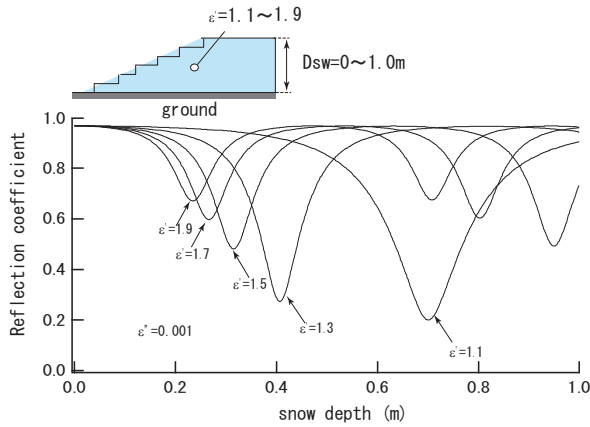


Fig.9.8 Reflection Coefficient of snow surface in case of one layer of snow cross section

#### 9.4 The up-and-down Shifting of Path Angle by Snow

Figure 9.9 describes DDM property when the structure of snow cross section is set to single layer. DDM is observed to change to  $147\mu A$  (path angle;  $0.7$  degrees below) when  $\epsilon'$  is  $1.1$  in fresh snow conditions. When the water content of snow increases and  $\epsilon'$  becomes  $4\sim 10$ , DDM change by snow decreases and becomes asymptotic straight line ( $0.0027^\circ/cm$ ).

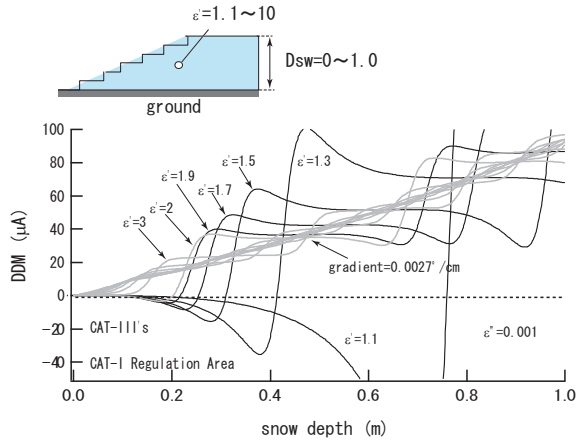


Fig.9.9 DDM variation of snow in case of one layer of snow cross section

Figure 9.10 describes DDM property in the case of double layers of snow where lower layer is made a pressed snow condition and fresh snow is piled on it. In this figure, horizontal axis is set to the depth of upper layer with fresh snow ( $D_{sw2}$ ), and lower layer is fixed to  $D_{sw1} = 15cm$  and  $\epsilon_1 = 2 - j0.003$ . If a lower layer is made a pressed snow condition like this, a change in DDM by depth of snow would be restrained compared with Figure 9.9.

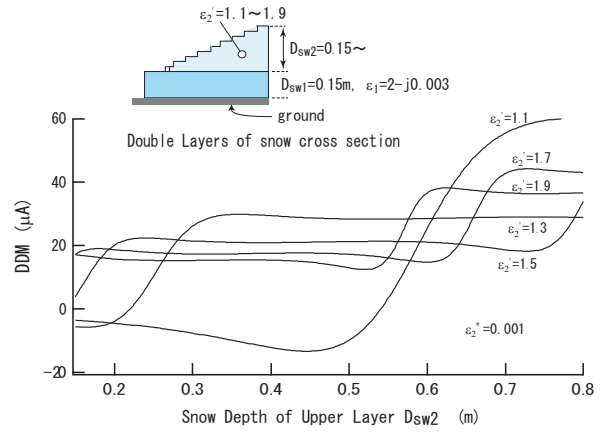


Fig.9.10 Snow variation of DDM in case of double layers of snow cross section

### 10. DELIBERATION OF SNOW REMOVAL CRITERIA

#### 10.1 The Range of DDM Variation of Single Layer of Snow

Figure 10.1 shows analysis results in the condition that the reflection surfaces were covered with the snow of one layer structure flatly.

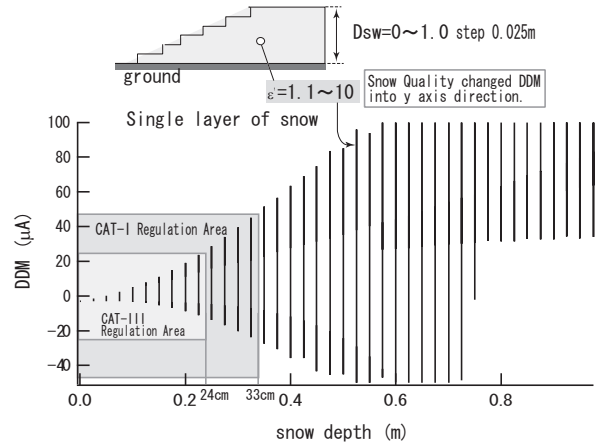


Fig.10.1 Snow Quality variation of DDM at single layer of snow cross section

In the Figure 10.1, the horizontal axis (X-axis) shows the changes in snow depth ( $D_{sw}$ ) and the vertical axis (Y-axis) shows DDM variation. When the snow depth ( $D_{sw}$ ) was changed at  $2.5cm$  intervals ranging from  $0$  to  $1m$ , and also when the quality of snow in each snow depth ( $\epsilon'$ ) was changed between  $1.1$  and  $10$ , DDM could vary between bottom and top on each vertical line (Y-axis) according to those depth and quality as shown in the Figure 10.1.

In the case of the quality of snow being fresh, DDM varies toward either end of each vertical line in the Figure

10.1. In the meantime, in the case of the water content included in snow ( $\epsilon'$ ) being increased from 3 to 10, DDM variation is shown on the almost straight trend line depicted in the Figure 9.9. The rate of inclination in the Figure 9.9 is  $0.0027^\circ/\text{cm}$ .

Additionally, the light shaded part in this figure means the region within defined value of CAT-I and the dark shaded part means the region within defined value of CAT-III. When  $D_{sw}$  of single layer was more than 33cm defined in CAT-I or more than 24cm defined in CAT-III, each condition could be out of tolerance, so snow removal shall be done.

### 10.2 The Range of DDM Variation of Double Layers of Snow

Figure 10.2 shows analysis results in the condition that reflection surface is assumed to be covered with the snow of double layers. In that case, the snow depth of lower layer is changed such as  $D_{sw1} = 15\text{cm}, 20\text{cm}, 25\text{cm}$ , but the quality of snow is unchanged. In the Figure 10.2, the horizontal axis (X-axis) shows the change in snow depth of upper layer and the vertical axis (Y-axis) shows the changes in snow quality of upper layer. As a result, the ranges of DDM variation were decreased compared to the result of single layer shown in Figure 10.1. As shown in Table 2.1, the condition of double snow layers occurs at when snow removal is carried out from January to April.

When the  $D_{sw}$  was more than 32cm in CAT-III criteria (dark shaded part) or more than 56cm in CAT-I criteria (light shaded part), each condition could be out of tolerance.

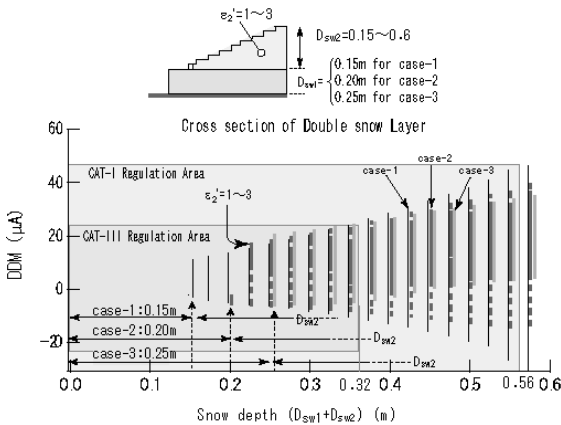


Fig.10.2 Snow variation of DDM in case of double snow layer

### 10.3 The Range of DDM Variation with Unevenness on the Reflection Surface

As described in Figure 10.3, we assessed DDM property when the snow cross section is composed of two layers with an asperity of snow surface

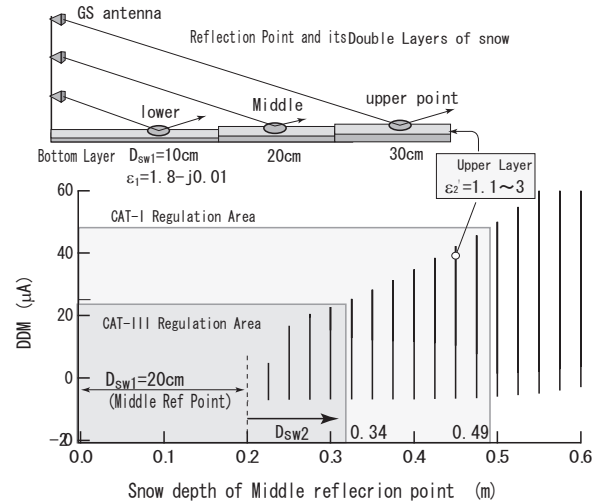


Fig.10.3 Snow Depth Variation of DDM due to double layers of snow cross section at 5nm on path

In this figure, as for lower layer, the depth of lower layer in each point is fixed to  $D_{sw1} = 10\text{cm}$  at lower antenna reflection point, fixed to  $D_{sw1} = 20\text{cm}$  at middle antenna reflection point and fixed to  $D_{sw1} = 30\text{cm}$  at upper antenna reflection point, also the quality of snow is fixed to  $\epsilon_1 = 1.8 - j0.01$ . In this case, unevenness ( $D_{max} - D_{min}$ ) becomes  $\pm 10\text{cm}$ . Hereupon, when dielectric constant of upper layer ( $\epsilon_2'$ ) was changed from 1.1 to 3.0 and also the depth of upper snow layer was changed, DDM varies according to those depth and quality as shown in Figure 10.3. In this case the ranges of DDM variation of both CAT-I and CAT-III are decreased slightly in comparison with Figure 10.2.

## 11. PROPOSAL OF SNOW REMOVAL CRITERIA

In this paper, the snow removal criteria was studied in consideration of various conditions, such as dielectric constant of the snow layer measured by the dielectric constant measuring device, depth of snow, unevenness of snow surface and so on.

➤ Table 11.1 shows the present snow removal criteria of FAA and JCAB.

The proposal of the snow removal criteria based on this simulation calculation result is shown in Table 11.2.

As shown in the Table 11.2, the snow depth is deviated from criteria at 33cm in case of CAT-I and at 24cm in case of CAT-III because DDM is extremely changeable by snow in case of the fresh snow condition.

➤ If the lower layer is trod down and a snow cross section is made into two layers the depth of snow

can be allowed up to 56cm in case of CAT-I and can be allowed up to 32cm in case of CAT-III. As a result the remarkable relaxation of criteria is enabled.

- Although at Aomori airport there is a case that unevenness of snow depth at the GS reflection point becomes  $\pm 10\text{cm} \sim \pm 20\text{cm}$ , the snow depth that is thought to be deviated from criteria can be slightly reduced compared with the above paragraph from the result of analysis considering  $\pm 10\text{cm}$  unevenness. In this case the depth of snow can be allowed up to 49cm in case of CAT-I and can be allowed up to 34cm in case of CAT-III.

By the above study, DDM is extremely changeable by snow in case of the fresh snow condition, and there is a possibility to deviate from the ICAO tolerance.

However, the remarkable relaxation of criteria is enabled even if unevenness occurs on the snow surface if snow cross section is managed to two layers.

	CAT I	CAT III
JCAB	30cm	10cm
FAA	60cm	28cm

**Table 11.1: Present Snow Removal Criteria of FAA and JCAB**

	CAT-I	CAT-III
In case of one layer of Fresh Snow	33cm	24cm
In case of lower layer of Pressed Snow	56cm	32cm
In case of unevenness of $\pm 10\text{cm}$	49cm	34cm

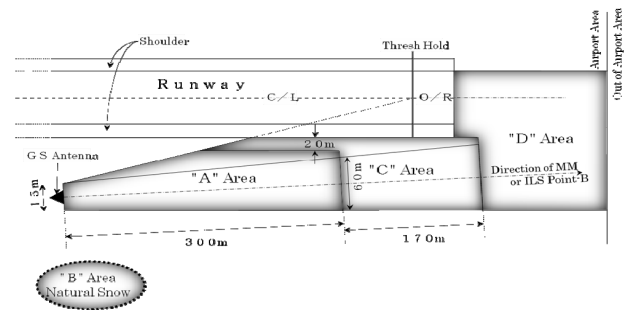
**Table 11.2: Proposal of Snow Removal Criteria based on the Result of Simulation**

$DDM \leq \pm 46.8\mu\text{A}$  for CAT-I & CAT-II

$DDM \leq \pm 24\mu\text{A}$  for CAT-III

## 12. FUTURE WORK

As for the JCAB snow removal criteria in the present, a part of the "A" area only had been changed to the "C" area in 2006 from the result of the simulation / experiment, and to our regret it has not reached its drastic easing due to the fewness of basic and evaluation data under the expected snow condition.



**Fig 12.1: JCAB's Present Definition of Snow Removal Area**

In the future, the JCAB Air Traffic Services Engineering Division intends to continue to make further investigation and evaluation if suitable snow condition for the investigation was expected, and JCAB Flight Inspection also intend to work together towards snow removal criteria relaxation of the high category ILS.

On the other hand, now JCAB is studying the pavement of the whole of "A" area in some snow airports. Its purpose is the improvement in workability of snow removal work and the saving time/cost for its work accompanying it.

However, when selecting the airport which will be implemented, it is necessary to decide with the greatest care and with taking cost-benefit into account, because to pave the whole of "A" area needs a large expense.

## 13. REFERENCES

- [1] ICAO, July 1996, International Standards and Recommended Practices, Annex 10 to the Convention on International Civil Aviation, Volume 1, Radio Navigation Aids, 5th Edition
- [2] ICAO, 2000, Manual on Testing of Radio Navigation Aids, Doc 8071 Volume 1, Testing of Ground Based Radio Navigation Systems, Fourth Edition
- [3] FAA, October 2005, United States Standard Flight Inspection Manual, Order 8200.1C
- [4] FAA, October 2005, Maintenance of Instrument Landing System (ILS) Facilities, Order 6750.49A
- [5] Hisashi Yokoyama, October 10-20, 2006, An Installation Method of Glide Path Near Field Monitor for All Weather Operation, NSP WGW WPXX
- [6] Hisashi Yokoyama, November 10-20, 2009, ILS Glide Slope (GS) Path Characteristics Analysis for Paved GS Reflection Area, NSP WGW IP16

# THE ANALYSIS AND SOLUTIONS ABOUT GP STRUCTURE PROBLEM IN ILS FLIGHT INSPECTION ON HIGH ELEVATION PLATEAU AIRPORTS

## Mr. Ge Mao

Inspection Engineer  
Safety and Tech Department  
Flight Inspection Center of CAAC  
23#, Tianzhu Road,  
Tianzhu Airport Industry Zone,  
Capital International Airport,  
Beijing,  
People's Republic of China  
E-mail:simone\_10031@yahoo.co  
m.cn



## ABSTRACT

During the flight inspection for image type glide slope in high elevation plateau airports, the structure of the glide path is often out of tolerance, this article will deeply analyze the major reasons leading to the phenomenon and then propose the solutions.

## KEYWORDS

High elevation plateau airports, flight inspection, the structure of glide path, out of tolerance, solutions.

## BACKGROUND

CAAC defined the airports in which the altitude is +2560 m sea level and above as the high elevation plateau airports. Currently China has nine high elevation plateau airports in total, these airports are mainly located in China's southwest and northwest, and respectively are: Jiuzhaigou / Huanglong, Lhasa / Gonggar, Qamdo / Banda, Nyingchi / Millington, Ali, Kangding, Yushu / Pakistan Tong, Diqing / Shangri-La and the Golmud Airports. In addition to Nyingchi and Golmud airports, there are seven airports elevation more than +3000 m, in which Ali, Banda and Kangding airports elevation more than +4000 m. Most high elevation plateau airports are mountainous, and these airports have complex natural and geographical environment, significantly the terrain change around the airports, complex field geological conditions, bad weather conditions, and big difficulty in airports construction. These factors have often effected on the design of flight procedures, scheduled flights normal operations, the installation of ground radio navigation equipment and cause flight inspection tremendous

difficulties.

ILS (Instrument Landing System) as a Precision Approach Guidance Device is widely used in China's high elevation plateau airports. The localizer and glide slope respectively supply the precise guidance for approaching aircraft in horizontal direction and vertical direction. The data of Glide path structure obtained from flight inspection is used to assess the bend of glide path, which directly affects the attitude of the aircraft and landing security. Simultaneously it effects the calculations of the glide path angle and reference datum height, and becomes one of the important parameters to assess the quality of the glide slope in flight inspection.

Good glide path structure data is crucial to the approaching aircrafts near the space of high elevation plateau airports. It is of great significance to ensure the safety of the approaching aircrafts in complex topography conditions. For the aircraft approaching under complex terrain and obstacle clearance conditions, bad glide path structure may lead to dramatic attitude change in approaching, when using the autopilot capturing the glide path. This will affect the establishment of final phase landing configuration for approaching aircraft. Especially for the high elevation plateau airports which runway's end close to a steep slope or a valley, the dramatic changes in altitude can lead aircraft to excessive undulation, it is very dangerous, because in extreme cases, excessive undulation may result in the situation that the actual altitude of the aircraft below the runway threshold level and leading to the occurrence of fatal accident.

During actual flight inspection in high elevation plateau airports, flight inspectors often encounter glide path structure data out of tolerance; it is more difficult than the low-altitude airports to solve the problems. In some high elevation plateau airports, the problem of glide path structure out of tolerance is still not satisfactorily resolved. As the glide path structure data express the bend of the glide path, many factors can affect the bend of the glide path. Through years of flight inspection practice, experience and analysis on design factors, site factors, equipment factors, clearance factors, the antenna factors, and so on, **we deemed: Insufficiency on the length of glide slope reflection area and unsatisfactory flatness are the important reasons leading to glide path structure data out of tolerance in high elevation plateau airports.**

# 1. The introduction of glide slope image radiation principle and Huygens-Fresnel principle and the formation of the glide slope first Fresnel zone

## 1.1 Glide slope image radiation principle

In China most high elevation plateau airports use capture effect type glide slope system, which is the most tolerant to far-field reflectors and rising terrain, especially suitable for poor site conditions, poor clearance conditions and limited reflecting field airports. Capture effect type glide slope system is the image-type beacon system, according to FAA Order 6750.16D, the image radiation principle is: If the radiation from a located antenna above the reflecting surface, the reflected signal appears to emanate from an image antenna along the same vertical plane as the real antenna and the distance below the reflecting surface equal to the distance of real antenna above the surface. The signals from the real and image antenna combine vectorially in space. (See Figure 1 Schematic From FAA Order 6750.16D)

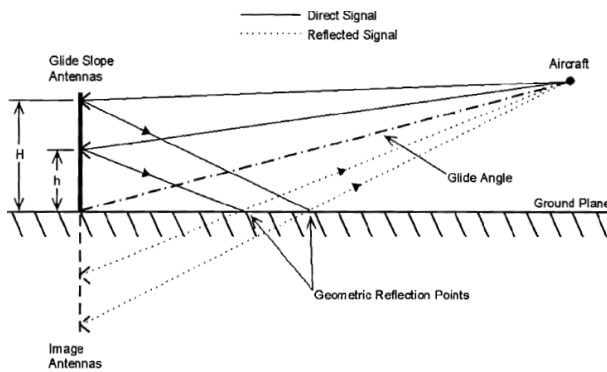


Figure 1 Schematic of the image antenna

Glide path actually is produced by the vector sum of four different signals includes: the direct and reflected signals from the carrier antenna and the direct and reflected signals from the sideband antenna. Theoretically, if you want to get a good glide path, the signal aberration from the image antennas should be as small as possible, so the reflecting field surface should be smooth, uniform and large enough. But it is difficult to achieve in practice, for limitation by the factors of the terrain, clearance, buildings or obstacles, the ideal reflecting field surface is almost impossible to exist.

## 1.2 Introduction of Huygens-Fresnel principle and the formation of the glide slope first Fresnel zone

### (1) Introduction of Huygens-Fresnel principle

Huygens-Fresnel principle: During the propagation of electromagnetic waves, every point on wave front surface will be considered as the secondary radiation wave source

radiating spherical wave, this wave source is called the secondary wave source. Because any point on closed surfaces which enclosing the wave surface can be considered as the secondary radiation wave source, so the radiation field of any point in space is the result of mutual interference and superposition from the secondary radiation wave source. As shown in Figure 2.

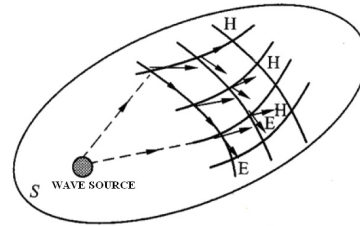


Figure 2 Huygens-Fresnel Principle

### (2) Space and the first Fresnel zone

The secondary radiation wave sources on closed surface is near or far to the reception point, which makes the signal field strength changes at the reception point. Figure 3, Q is the wave source in free space, P is the reception point, Q and P is the focus of rotational ellipsoid, we called the space area enclosed by rotational ellipsoid Fresnel zone.

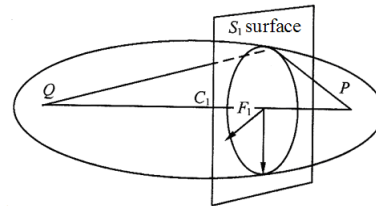


Figure 3 Schematic Of Space Fresnel Zone And The First Fresnel Zone

As shown in Figure 3, S1 is a point in space, the surface vertical to line QP contained S1 cut the Fresnel area a circle C1, the radius of the circle:

$$F1 = \sqrt{\lambda d_1 d_2 / d}$$

Where d is the distance between the point Q and P, d1 and d2 is the distance from point Q and point P to the center of the circle C1, the Fresnel region formed by circle C1 is the first Fresnel zone.

In free space, the electromagnetic energy radiating from the wave source point Q to the point P is mainly propagated through first Fresnel zone, as long as the first Fresnel zone will not be blocked, you can obtain approximate propagation conditions of free space. To ensure the normal wave propagation, effect or block on first Fresnel zone does not exceed 20%. Otherwise, wave multipath propagation will have a negative impact to the quality of received signals.

### (3) The formation of the first Fresnel Zone on glide



### slope reflection site

If we combine the Huygens - Fresnel principle and the glide slope image radiation principle, we can know, between the image antenna radiation point and aircraft received point will be formed a rotational ellipsoid (DEFG) shown in Figure 4 ,in which the image antenna point (A ' ) and the aircraft received point (B point) is the focus of the rotational ellipsoid, the glide slope reflection surface cut the Fresnel zone space a ellipsoid surface (MSNT).For any point on this ellipsoid surface, the projection in horizontal plane of the first Fresnel zone relative to image point A ' are included in the ellipse surface (MSNT), generally we considered the ellipse surface (MSNT) as first Fresnel Zone of glide slope reflection surface.

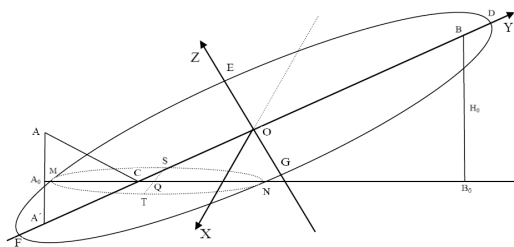


Figure 4 Formation Of The First Fresnel Zone Of Glide Slope

In figure 4, we can see: The lower glide path angle and the farther distance of the aircraft can result in the larger first Fresnel zone on glide slope reflection surface; the higher glide path angle and the closer distance of the aircraft can result in the smaller first Fresnel zone on glide slope reflection surface.

### (4) Features of the first Fresnel zone on glide slope reflection surface

The size of the first Fresnel zone on glide slope reflection surface is relative to the distance to reception point. Generally glide slope antenna located beside the runway, for approaching aircrafts, the first Fresnel zone is not only changing in size, but also changing in direction. We reference the contents of FAA Order 6750.16D to show the first Fresnel Zone changes relative to approaching aircraft on glide slope reflection surface:

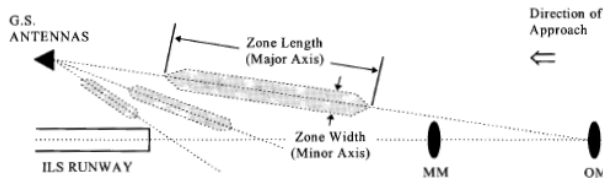


Figure 5 The First Fresnel Zone For ILS Glide Slope

The size and position of the glide slope first Fresnel zone is affected by the glide path angle and aircraft's elevation and distance from the facility. When an aircraft is over

the outer marker, the Fresnel zone appears as a long narrow ellipse. As the aircraft approaches the runway, the ellipse becomes continuously smaller and gradually migrates as figure 5.

The signal radiated from image antenna mainly propagate through the first Fresnel Zone on glide slope reflection surface, so the quality of the first Fresnel Zone including size, flatness and consistency and uniformity of the reflection medium is crucial to the vector sum of glide slope signals in space. If the first Fresnel Zone on glide slope reflection surface is flatness, consistency and uniformity, we can get the ideal glide slope path and good structure. In practice it is difficult to achieve ideal requirements for the first Fresnel zone on glide slope reflection surface, uneven or rough sites may lead to a scattering or phase shift on reflected signals, affecting the signal vector sum in space, causing bend on glide path. Practice shows that this influence is more direct and serious than other factors impacting the glide path.

### 2. The analysis of glide slope structure out of tolerance due to insufficiency of length of glide slope reflection area

In China, the site design of glide slope is based on the industry standard MH/T4003-1996 "The Specification Of Site Setting For Radio Navigation Stations And Radar Stations" or the requirements provided by the manufacturer of ILS. As shown in Figure 6, we can see the criteria about the reflection protected area for image-type glide slope in MH/T4003-1996.

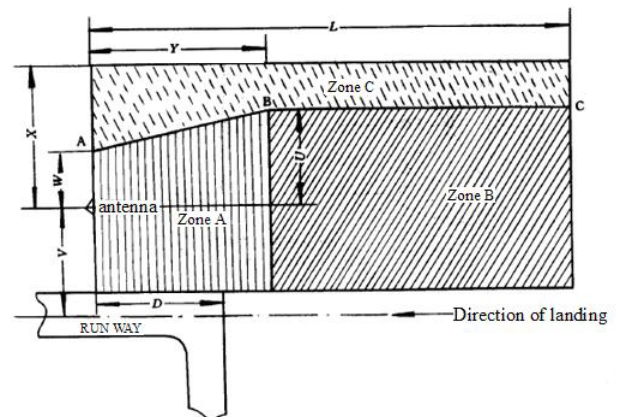


Figure 6 The Reflection Protected Area For Image-Type Glide Slope In MH/T4003-1996

- D—the distance from glide slope antenna to threshold , m ;
- U=60m ;
- V—the distance from glide slope antenna to the centerline of runway, m ;
- W=30m ;
- X=120m ;
- Y=360m or the distance to D (select which is longer);
- L=900m or the distance to the airports property line or the distance to where smooth terrain terminated (select which is shorter) .

From the specification above, the distance parameter related to protected areas are clearly defined, but it is not clearly defined the distance to the airports property line or the distance to where smooth terrain is terminated. Practice shows, in circumstances which constraints in the protected areas total length  $L$  is less than 900m, if the distance to the airports property line or the distance to where smooth terrain is terminated is not clearly defined, it is possible to meet the situation that the glide path structure is worse due to insufficient in the reflection area.

Most of the high elevation plateau airports in China were built on a ridge, hillside or valley, the airport's boundaries or properties is often close to the steep slopes, or valleys. For the terrain constraints, it is difficult to meet the length requirements of 900m of protected areas, in some circumstance distance to the airports property line or the distance to where smooth terrain is terminated is very short, in some high elevation plateau airports, this distance is about or less than 400m. Though shorter length of  $L$  does not violate the specification, but it will seriously affect the quality of the glide path and structure of the glide path.

As mentioned in the preamble, the quality of the first Fresnel Zone including size, flatness and the consistency and uniformity of the reflection medium is crucial to the vector sum of the glide slope signals in space. If the first Fresnel Zone on glide slope reflection surface is flatness, consistency and uniformity, we can get the ideal glide slope path and good structure. So before we consider the affect to the glide path for shorter length of  $L$ , the first thing is to calculate the length of the first Fresnel Zone. Theoretically the length of  $L$  should be longer than the length of the first Fresnel Zone, if the length of  $L$  is shorter than the length of the first Fresnel Zone, the quality of the glide path and structure data of the glide path will be affected seriously.

In the below, we will use Figure 7 as well as Figure 8 and Figure 9 provided in the FAA order 6750.16D to roughly calculate the distance from the glide slope antenna to the far end of the first Fresnel zone and define the smallest length of  $L$ .



Figure 7 The Distance From Glide Slope Antenna To The Far End Of The First Fresnel

Because the first Fresnel zone on the glide slope reflection area is relevant to the glide path angle, the

altitude of the aircraft and the distance between aircraft and the glide slope antenna, in high elevation plateau airports, the designed glide path angle generally may not be less than  $3^\circ$ , and the glide path structure is out of tolerance always does occur within 4 NM to the threshold of the runway, so we will calculate the length from the glide slope antenna to the far end of the first Fresnel zone, at the glide path angle of  $3^\circ$  and at the position of 4 NM to the threshold of the runway.

From figure 7 the distance from the glide slope antenna to the far end of first Fresnel zone is roughly as follows:

$$L1 = L2 + L3/2$$

$L1$  ---the distance from glide slope antenna to the far end of the first Fresnel zone

$L2$  ---the distance from glide slope antenna to the centre of the first Fresnel zone

$L3$  ---the length of the first Fresnel zone

From Figure 8, we can know, when aircraft approach at the glide path angle of  $3^\circ$  and at 4NM(about 24305ft) to threshold ,the distance from the glide slope antenna to the centre of first Fresnel zone is about 1000ft (about 305m), i.e.  $L2 = 305m$

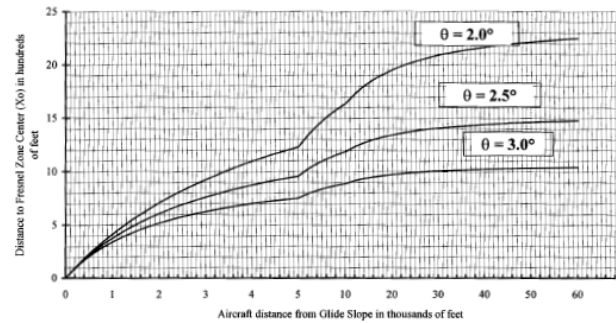


Figure 8 Location Of Glide Slope Fresnel Zone Center

From Figure 9, we can know, when the aircraft approach at the glide path angle of  $3^\circ$  and at 4NM(about 24305ft) to the threshold, the length of the first Fresnel zone is about 1700ft (about 518m), i.e.  $L3 = 518m$

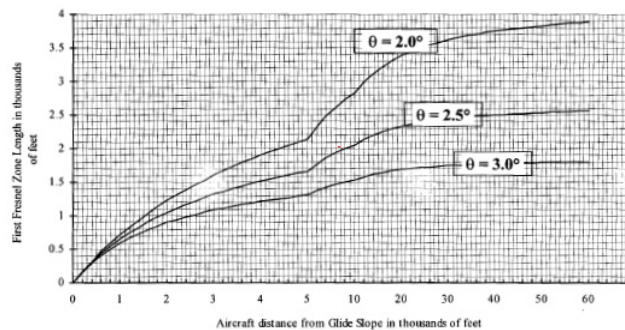


Figure 9 First Fresnel Zone Length As Function Of Glide Angle And Aircraft Distance From Glide Slope

Therefore, the distance from the glide slope antenna to the far end of first Fresnel zone is:

$$L1 = L2 + L3/2 = 305 + 518/2 = 564\text{m}$$

Namely, when the aircraft approach is at the glide path angle of  $3^\circ$  and at the 4NM to the threshold, the length of L should be more than 564m, otherwise the integrity of the first Fresnel zone will be damaged, and make it possible to affect the quality of the glide path as well as structure of the glide path.

Similarly, we can calculate the length from the glide slope antenna to the far end of the first Fresnel zone, at the glide path angle of  $3^\circ$  and at the position of 2 NM to the threshold of the runway, the length of L1 is 527m. Namely, when the aircraft approach is at the glide path angle of  $3^\circ$  and at the 2NM to threshold, the length of L should be more than 527m, otherwise the integrity of first Fresnel zone will be damaged, and make it possible to affect the quality of glide path as well as the structure of the glide path.

In the actual flight inspection, in some high elevation plateau airports the problem exist of the glide path structure being out of tolerance, and has not being solved until today. In this airport, glide slope adopt capture effect system, and the designed glide slope is  $3^\circ$ , the runway threshold and end is close to a steep slopes or valleys, the distance from the glide slope antenna to airports property line or the distance to where smooth terrain is terminated is about 400m. Namely, the length of L is about 400m. The flight inspection report shows the glide slope structure is out of tolerance seriously within 2NM to the threshold of the runway. According to the calculation result above, when the aircraft approach at  $3^\circ$  of the glide path angle and at 2NM to the threshold, the length of L should be more than 527m. Namely, in this circumstance the first Fresnel zone is damaged about 127m, accounted for 24% of required first Fresnel zone, however, this is a fairly large proportion.

So it is very important to image-type glide slope to protect the integrity of the first Fresnel zone, shorter length of L may damage the integrity of the first Fresnel zone, and make it possible to affect the quality of the glide path as well as the structure of the glide path.

### 3. The analysis of glide path structure out of tolerance caused by uneven or bumpy flatness of the reflection area.

If you want to get a good glide path structure data, it is not only to ensure the length of the first Fresnel zone and size, but also ensure the flatness, consistency and uniformity of the first Fresnel zone. For the approaching aircraft, the first Fresnel zone is not only changing in size, but also changing in direction, so the glide slope reflection area including the first Fresnel zone should be

fairly large. in practice it is difficult to ensure so large area to meet all the requirements for the first Fresnel zone in high elevation plateau airports

In china, most high elevation plateau airports are built on a ridge, a hillside or a valley, and generally have the features of complex geological conditions. Most of these airports are high-filled airports, and construction works are very difficult. The glide slope reflection area is lived in the surface of embankment body on soil surface area which is close to the embankment body of the runway tank area, the material of the filling bed is artificial sand and gravel, covered with thin soil layer on the surface of the embankment body.

The actual situation shows that it is difficult to maintain the flatness of the glide slope reflection area in high elevation plateau airports for the following reasons:

(1) High-filled airports have features more prone to instability and deformation (i.e., settlement and differential settlement) on the foundation or embankment body, and may cause great changes of the flatness of the glide slope reflection area.

(2) The excretion of rains is mainly the cause of surface flooding in High elevation plateau airports, it is likely to cause a loss of surface soil, destruction of soil surface of the glide slope reflection area, and damage the flatness of the glide slope reflection area.

(3) In high elevation plateau airports, Geological conditions, climatic conditions and thin soil layer on the surface of the glide slope reflection area make it difficult to form a scale of grass land with flatness, consistency and uniformity, it is also difficult to use the grass land to prevent soil erosion.

For some high elevation plateau airports it is almost impossible to overcome the above-mentioned factors, so to ensure the flatness of the glide slope reflection area is very difficult. In actual flight inspection, flight inspectors have encountered the situation that the glide path structure out of tolerance caused by uneven or bumpy flatness on the glide slope reflection areas. In a period flight inspection on 20 # ILS in Jiuzhaigou Airport, the flight inspector found the structure of glide path is out of tolerance, especially in zone2 and zone3, but on commissioning flight inspection, all the structure data is good. The ground maintenance personnel finally found the glide slope reflection area was uneven and bumpy, in some areas the uneven or bumpy degrees is more than 30cm and far exceeds the requirements on the specification, then the ground maintenance personnel suspected it was the reason causing the glide slope out of tolerance, after leveling off the glide slope reflection area, the structure problem was solved successfully.

Thus, the features of geography, geology and characteristics of constructions in high elevation plateau airports will lead to a difficulty in maintaining a good flatness in Fresnel zone on the glide slope reflection area causing a image distortion in space and impacting the

vector sum, finally resulting in the glide slope structure out of tolerance.

#### 4. The solutions for the problem of the glide path structure out of tolerance in high elevation plateau airports

In high elevation plateau airports, if constrained by the terrain conditions, the glide slope reflection area may not be long enough to contain the first Fresnel zone. In theory, it should be best to adopt the non image-type glide slope system rather than image-type glide slope system, thus, the signals radiated from the glide slope system can get rid of the dependence on length and flatness of the glide slope reflection area.

For high elevation plateau airports, if there is no conditions to use non-image type system and uneven or bumpy flatness of the glide slope reflection area is the main reason to affect the glide path structure result, then we can adopt methods that can decrease the foundation settlement or differential settlement and reduce rainfall erosion damage to keep the flatness of the glide slope reflection area.

##### 4.1 Use End-Fire glide slope systems to solve the problem of the glide path structure out of tolerance caused by insufficient length and uneven or bumpy flatness on glide slope reflection area

End-Fire type glide slope system is non image-type system, it is different from capture effect system in principle, unlike image-type glide slope system, the End-Fire system does not use the ground reflection plane or surface, the glide path angle is determined by the relative phase of the signals radiated by the front main antennas and rear main antennas. End-Fire has the features of strong orientation levels in horizontal radiation, lower demand on sensitive areas and little influence by the ground conditions and clearance. At present, End-Fire glide slope system has not been widely used in China.

The only set of End-Fire type glide slope system in China is 02 # ILS glide slope system in Jiuzhaigou airports, from the statistical results in Table 1, we can see the End-Fire type glide slope system can supply ideal and stable flight inspection data under the complex terrain and geological conditions. In Table 1, glide path structure data are all less than 20 microamps, it is very satisfactory. This fully illustrate the adaptability and availability of End-Fire type glide slope system in high elevation plateau airports, and provided strong theoretical basis and practical basis on solving the problem of the glide slope structure out of tolerance in high elevation plateau airports.

**Table 1 Statistics Of Main Flight Inspection Data Of 02#ILS Glide Slope In Jiuzhaigou Airports**

Time Of Flight Inspection	Transmitter	Glide Path Angle	Reference Datum Height	Structure Of Glide Slope		
				Zone 1	Zone 2	Zone 3
2007.08.24	TX1	3.00	16.0	5	9	12
Commissioning	TX2	3.01	15.5	4	8	12
2008.08.19 Period	TX1	3.01	16.2	4	7	17
	TX2	3.01	15.8	4	8	13
2009.05.18 Period	TX1	2.99	17.1	5	16	17
	TX2	2.99	17.7	4	7	14
2010.01.20 Period	TX1	3.00	16.1	6	10	9
	TX2	3.01	16.1	4	6	11

Although End-Fire type glide slope systems has higher cost, but it has lower demand on the length and flatness of the glide slope reflection area, it has prominent advantages than capture effect glide slope systems in high elevation plateau airports. In addition to strong adaptability and availability, End-Fire type glide slope system is very worthwhile to be used by the high elevation plateau airports with poor terrain and geological conditions. End-Fire type glide slope systems will supply stable, reliable glide path signal and provide security guarantee for the approaching or landing aircraft in high elevation plateau airports.

Therefore, if conditions permitting, we recommend to use End-Fire type systems to solve the problem of glide path structure out of tolerance caused by insufficient length and uneven or bumpy flatness on glide slope reflection area.

##### 4.2 Using concrete reflection surface to solve the problem of glide path structure out of tolerance only caused by uneven or bumpy flatness on glide slope reflection area

For the high elevation plateau airports, if the length of glide slope reflection area can completely contain the first Fresnel zone, then uneven or bumpy flatness is most likely to be the major reason of the glide path structure out of tolerance. For some high elevation plateau airports, it is almost inevitable to avoid the occurrence of foundation settlement or differential settlement and soil erosion. If there is no conditions to use non-image type glide slope systems, how to solve this problem? We recommend using concrete reflection surface to solve this problem, the reason as follows:

(1) Using concrete reflection surface can ensure the flatness of the glide slope reflection area in long term. The concrete reflection surface can produce better image radiation; get rid of the signal distortion caused by uneven or bumpy flatness.

(2) Using concrete reflection surface can effectively prevent settlement and differential settlement in glide slope reflection areas.

(3) Using concrete reflection surface can prevent soil erosion caused by rainfall.

While in theory concrete reflection surface may cause effects in reflection coefficient and medium consistency, but in practice the effects is not obvious in the vector sum and coverage distance of the glide slope signals.

Because capture effect glide slope systems has strong anti-interference ability for far-field terrain, so it is enough to laying concrete reflection surface on zone A for capture effect glide slope systems. In some circumstance, concrete reflection surface also can be laid in specific area according to the actual situation of the glide slope reflection area and the actual flight inspection results. Although using concrete surface may cost higher, but it is worthwhile to use it.

Therefore, if the length of glide slope reflection area can completely contain the first Fresnel zone and have no condition to use non-image type glide slope system, we recommend using concrete reflection surface to solve the problem of glide path structure out of tolerance caused by uneven and bumpy flatness on glide slope reflection area.

### **Epilogue:**

Insufficiency on length of glide slope reflection area and unsatisfactory flatness are the important reasons leading to the glide path structure data out of tolerance in high elevation plateau airports. In order to prevent similar problems and ensure flight safety, the effect caused by length and flatness of the glide slope reflection area should be considered carefully at the beginning of design and equipment installation. Appropriate glide slope type selection, reasonable construction scheme will lay a good foundation to effectively keep glide slope signals normal and stable in long term.

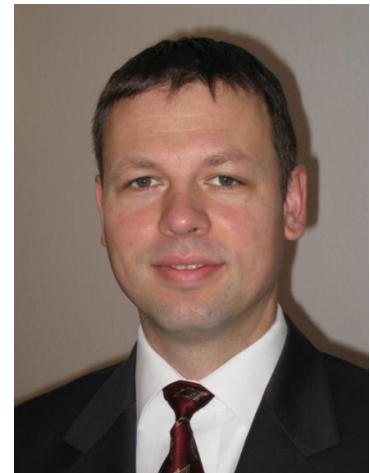
### **REFERENCES**

1. *MANUAL ON TESTING OF RADIO NAVIGATION AIDS, ICAO Doc.8071*
2. *AERONAUTICAL TELECOMMUNICATIONS (RADIO NAVIGATION AIDS), ICAO Annex 10 Volume 1*
3. *SITING CRITERIA FOR INSTRUMENT LANDING SYSTEM, FAA ORDER 6750.16*



# Flight Inspecting Ground Based Augmentation Systems (GBAS)

**Dipl.-Ing. Thorsten Heinke**  
Program Manager  
Aerodata AG  
38108 Braunschweig Germany  
Fax: +49 531 2359 222  
E-mail: [heinke@aerodata.de](mailto:heinke@aerodata.de)



## **Abstract**

The civil air traffic has increased tremendously during the last decade and a break of this steady rise is not foreseeable. The capacities on the main hubs are exhausted due to geographic restraints or through separation minima required by the instrument landing procedures based on conventional ILS. The discrepancy between the escalating traffic and the limitations at the airports initiates the search for other applicable navigation systems.

Ground based augmentation systems are one of those navigation systems, which shall help the global traffic solving those conflicts. Nearly all new multimode receivers installed in new cockpits of the commercial air transport have the capability to perform GBAS approaches. Those navigation devices are certified and the standards are set. The ground segment for GBAS is still in its infancy. Just a few ground stations are operational and certified for commercial air transport. Those

ground systems have been flight inspected with flight inspection systems providing GBAS capability to show that the systems fulfill their dedicated specification.

This paper summarizes results, experiences and common practices regarding the flight inspection of ground based augmentation systems. Several flight inspection tasks are presented, explained and analyzed. Procedures and necessary hardware is examined and evaluated. Overall the paper identifies and explores the upcoming necessity to upgrade the current flight inspection system with the capability to perform GBAS measurements

## **Introduction**

GBAS flight trials and flight inspection tasks have been performed in the past on several airports on which different GBAS ground stations were installed. Most of those ground stations were prototypes and revisions of those. Only a few GBAS ground stations have been commissioned so far. The

commissioning of the first certified GBAS station in Germany is ongoing meanwhile. This long developing phase has certainly more than just one reason; but defining the rules to flight inspecting these ground stations, defining the procedures to flight inspect them and developing the body structure of flight inspection systems for GBAS inspection are some of those reasons. But finally it is about to come to an end.

This paper evaluates the latest trials and flight inspection tasks in Europe, displays their highlights and summarizes their findings. These flight inspection missions were performed on research bases and airports with an flight inspection aircraft equipped with the latest and state of the art flight inspection. The requirements for flight inspection systems in the future for GBAS calibration are explained and explored. Examples from flight inspection systems, which are capable to perform those inspections, are shown.

### **Flight Inspecting GBAS stations**

The latest flight inspection tasks were flown at the research airport in Braunschweig, Germany. At the site a GBAS ground station was installed temporarily and flight checked accordingly with a suitable flight inspection aircraft. The aircraft was a Beechcraft King Air 350 equipped with an AeroFIS<sup>®</sup> state of the art flight inspection system.



### **Figure 1: AeroFIS<sup>®</sup> capable to perform GBAS flight inspection missions**

The flight inspection system included a Rockwell Collins MMR GLNU-935 supports the use of the ILS and GBAS guidance systems. This equipment is connected via an ARINC429 interface to the flight inspection computer. The latest windows based flight inspection software enables the operator to record and re-process the gathered online evaluated data from the GBAS.

The aircraft was equipped with an additional VOR / LOC-antenna. It is also possible via a suitable connection method to share an existing VOR / LOC antenna, if there is no space for an additional antenna. With this additional or shared antenna it is possible to receive the VDB data of a GBAS ground station without getting into problems with the standard ILS antenna. Furthermore the aircraft was equipped with Aerodata information display on which the pilot is informed about the flight inspection track and flight inspection procedure. The system was coupled to the autopilot to assure highest accuracy during flight inspecting of GBAS.

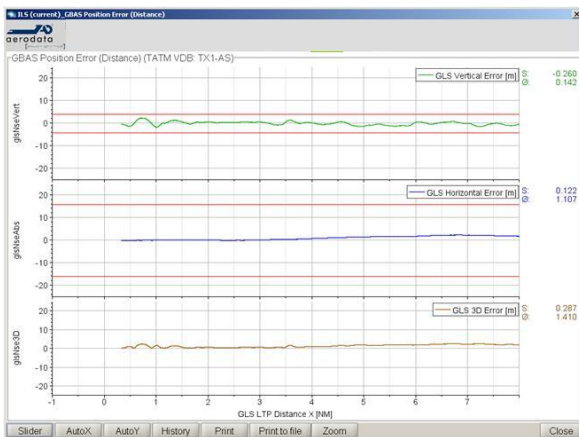


**Figure 2: Cockpit of Flight Inspection Aircraft highlighting the Cockpit information Display**



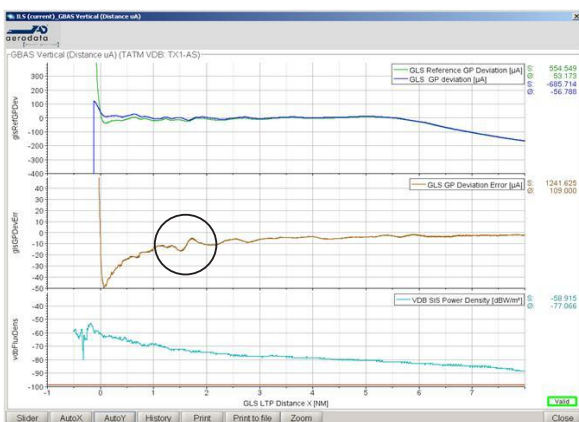
## Data evaluation

For data evaluation the flight inspection system evaluates by comparison with its high accurate reference position results as know from ILS flight inspection tasks. The reference position was determined by a hybrid position algorithm using PDGPS, INS, Baro etc. as sensors. The vertical and horizontal deviation error is calculated by the flight inspection system and displayed online with its tolerance lines (Figure 3).



**Figure 1: Deviation Error**

The time constant of the GBAS receiver has to be elaborated thoroughly and implemented in the flight inspection system to achieve accurate results. The bends caused by the time delay of the GNLU are clearly visible on the graphs (Figure 4).



**Figure 4: GP Deviation Error**

## Requirements of a Flight Inspection System for GBAS calibration

The research flight trails and flight inspection missions, the ICAO documentation and regulation and the experience from flight inspection systems already equipped with GBAS capability has constituted the requirements and recommendations for flight inspection mentioned in this paper.

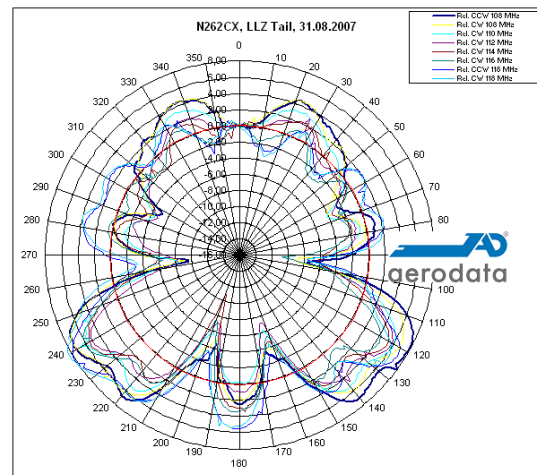
From the flight trails previously completed, it has been found necessary that the flying pilot have a visualization of the GBAS signal. This is obtainable through a cockpit which is equipped with a modern multi mode receiver, which you will find in the avionic of nearly all new large aeroplanes. But unfortunately most flight inspection aircraft - also new ones - are equipped with neither such an avionic nor with such a multi mode receiver. Therefore either the avionic has to be upgraded or the flight inspection system has to be coupled to the cockpit displays to visualize the GBAS data. This can be achieved either through a separate display or through the EFIS itself interfaced to the flight inspection system. Otherwise the pilot is not able to follow the GBAS approach and to deliver its necessary impression of fly-ability. To obtain an accurate flight track and thus the desired positions for the measurement, a flight guidance on the EFIS or the separate display from the flight inspection system is recommended.

To assure the continuity of the GBAS signal the message types 1, 2, and 4 have to be decoded, analyzed, displayed, and recorded by the flight inspection system. The recording will prove the necessity of availability for the flight track during inspection. Interference of the VDB signal has to be investigated with a capable spectrum analyzer connected to a suitable antenna. This can be achieved with an automatic spectrum analyzer program,

which displays and records the spectrum in parallel to the GBAS data. If interference is observed, this can be analyzed in detail during replay, or even in multiple replays from different approaches on this particular airfield. Therefore, it is very important that the GBAS data and the spectrum are recorded simultaneously in one common recording file. Otherwise an exact and detailed investigation in the office is difficult, due to the fact that the data has to be time synchronized.

The space segment of these approach techniques has to be checked during flight inspection as well. All satellites and their individual information especially their signal to noise ratio, has to be displayed and recorded to assure the mandatory availability. Interference from the ground should be examined with a downward looking GPS antenna or with another there for suitable antenna connected to the spectrum analyzer input. Airborne interference can be investigated with the GPS receiver in combination with the spectrum analyzer. The necessary synchronized recording of the GPS data and the spectrum data is applicable here as well.

Some effort has to be spent to confirm the correct coverage of the VDB signal according to the published tolerances. The field strength tolerances according to ICAO of 3dB are only achievable with a calibrated antenna and the compensation of the antenna characteristic by the flight inspection software.



**Figure 5: Antenna Pattern Correction**

The flight trails in the past detected that the measurements with GBAS receivers are not as accurate as with a spectrum analyzer. Therefore a connection of the spectrum analyzer to the GBAS antenna and the accurate measurement of the internal signal loss are recommended.

The flight inspection system of course has to be equipped with a GBAS device to receive and decode the message types of the GBAS data. The receiver has to be tuned to the appropriate function on the dedicated frequency of the ground station.

**Examples of GBAS Flight Inspection Systems**

The Telerad VDB receiver has been used in flight inspection systems for years and is well known in the flight inspection community. It is basically used to decode the dedicated message types. It also allows field strength measurements through its AGC output.



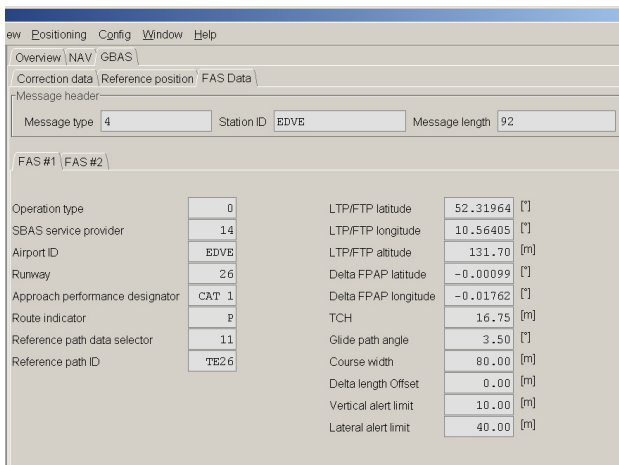
**Figure 6: Telerad VDB Receiver**

The Rockwell Collins MMR GNLU 930 has been flying in some flight inspection systems since a couple of years. Upgrades and new MMR's are being developed by the manufacturer. A special software version has to be implemented in the GNLU 930 which provides additional useful AGC information.



**Figure 7: Rockwell Collins GNLU 930**

A few systems have been equipped with the necessary GBAS hard- and software as mentioned above for a couple of years. A screenshot of the GBAS capable AeroFIS<sup>®</sup> software is shown below. Exemplarily, the alphanumeric page of the decoded message type 4 (FAS) is displayed.



**Figure 8: FAS Data Viewer in AeroFIS<sup>®</sup>**

The calibration of GBAS ground stations with an AeroFIS<sup>®</sup> equipped aircraft is feasible and performable without additional enhancements.

### Conclusions

GBAS is a suitable technique for performing ILS look-a-like approaches for the therefore equipped aircraft. The accuracies are on all tasks according to their requirements although some anomalies have been found at certain prototype ground stations. Those were corrected on the newer revisions.

Flight inspection of GBAS ground stations can be performed with an aircraft which is equipped with a flight inspection system with the following implemented enhancements:

- GBAS receiver
- GBAS flight guidance in the cockpit by primary equipment or from the flight inspection system
- Suitable spectrum analyzer for GPS and VDB
- Calibrated VDB antenna system.
- An adjusted capable software with correct delay values.

These mandatory main aspects have to be controlled and managed by a capable software, which has to be very sensitive regarding the parallel recording of these necessary signal data.

### References

[1] ICAO Doc 8071, Vol. II - Manual on Testing of Radio Navigation Aids, Testing of Satellite-based Radio Navigation Systems, Fifth Edition, 2007



# Current Issues in Flight Inspection Measurements June, 2010

## **Dr.-Ing. Gerhard GREVING**

NAVCOM Consult  
Ziegelstr. 43, 71672 Marbach, Germany  
Fax: +49 7144 862561  
E-mail: [navcom.consult@t-online.de](mailto:navcom.consult@t-online.de)



## **L. Nelson Spohnheimer**

Spohnheimer Consulting  
Auburn, WA 98001, USA  
Fax: +1 508 526 8273  
E-mail: [Nelson@SpohnheimerConsulting.com](mailto:Nelson@SpohnheimerConsulting.com)



## **ABSTRACT**

This is a continuation from previous International Flight Inspection Symposia of a series of discussions and papers by the authors on demanding flight inspection measurements. It presents investigations into current technical problems encountered during simulations and ground/airborne measurements.

We have experienced decades of development and application of traditional ground-based navigational aids. Several generations of Automatic Flight Inspection System (AFIS) have been fielded. Yet a variety of signal-in-space characteristics actively used to disqualify procedural uses (e.g., airways and approaches) of navaids continues to need definition or standardization. As the use of advanced simulations becomes more prevalent to approve or disapprove proposed development near the navaids, the missing or insufficient definitions become even more evident.

This paper addresses two classes of such definition and standardization issues – the “pseudo-problems” of VOR filtering and ILS Glide Path (GP) structure tolerances, and some measurement challenges related to DVOR with nearby Wind Turbines (WTs) and the airborne measurement of radio field strength. Recent experiences during flight inspections on a variety of

ground-based navaids, using several current Flight Inspection Systems are presented.

While maintaining neutrality by not mentioning location or equipment manufacturers, the paper contrasts results between simulation predictions (e.g., for Wind Turbine effects) and actual measurements, and analyzes calculation, presentation, and potential misapplication errors experienced with modern flight inspection systems. The paper concludes with recommendations in areas such as improved international policy recommendations, more detailed guidance material, and further harmonization of flight inspection practices and measurements.

## **DISCLAIMER**

In general, measurement locations and methods are intentionally kept anonymous. The authors intend only the constructive use of the examples included in this paper.

## **“PSEUDO-PROBLEMS”**

### **VOR Error Analysis**

The increased pressure on enroute navigational aids, in particular on the VOR by proposals for construction of Wind Turbines (WTs), continues to highlight the need for re-assessment of the application

of VOR tolerances. ICAO’s Annex 10 [1] defines in paragraph 3.3.3.2 the VOR bearing error performance only in terms of the ground station’s contribution being limited to  $\pm 2$  degrees of alignment error. ICAO’s 2002 Doc 8071 Manual on Testing [2] elaborates on tolerances for the received signal as follows:

**Alignment - 2.3.10** (excerpt) The alignment of the VOR is determined by averaging the error throughout the orbit.

**Bends - 2.3.12** A bend is determined by flying a radial pattern [underlining added] and comparing the indicated course against a position reference system. The error is measured against the correct magnetic azimuth of the radial. Deviations of the course due to bends should not exceed  $3.5^\circ$  from the computed average course alignment and should remain within  $3.5^\circ$  of the correct magnetic azimuth.

**Roughness and scalloping error - 2.3.13** Scalloping is a cyclic deviation of the course line. The frequency is high enough so that the deviation is averaged out and will not cause aircraft displacement. Roughness is a ragged irregular series of deviations. Momentary deviations of the course due to roughness, scalloping or combinations thereof should not exceed  $3.0^\circ$  from the average course.

The 1972 version of Doc 8071 allowed slightly larger limits on alignment and roughness/scalloping ( $3.5$  degrees maximum for each). However, neither version of Doc 8071 defines quantitatively the characteristics of alignment (A), bends (B), and roughness and scalloping (R/S), but instead uses descriptions such as “average throughout the orbit” and “momentary deviations”. It is generally recognized that A and B errors displace the aircraft from the desired course, while R/S errors do not. With today’s modern automated flight inspection systems (AFIS) equipment, individual manufacturers or service organizations are forced to define the frequency characteristics of these terms, and to implement filters to determine the magnitude of each component.

We have previously presented [3] how A, B, and R/S errors are separated and measured in one AFIS. Figure 1 is repeated here from that earlier paper, and shows a conceptual version of the error processing. The receiver’s 2-second filter eliminates highest-

frequency (“don’t care”) errors, while four-pole computational filters in the AFIS separate the remaining components. In this AFIS, alignment error is a “longer than 34 seconds” moving average, bends have periods 10 to 34 seconds long, and R/S errors have periods 2 to 10 seconds long. The 10-second definition for Bends is based on an aircraft speed of 120 knots. Faster aircraft will see the same spatially-fixed errors as higher frequencies – ie, bends will tend to become R/S, and R/S will tend to be eliminated by the receiver filter as aircraft speeds increase. Note that the time period definitions in this implementation are somewhat arbitrary.

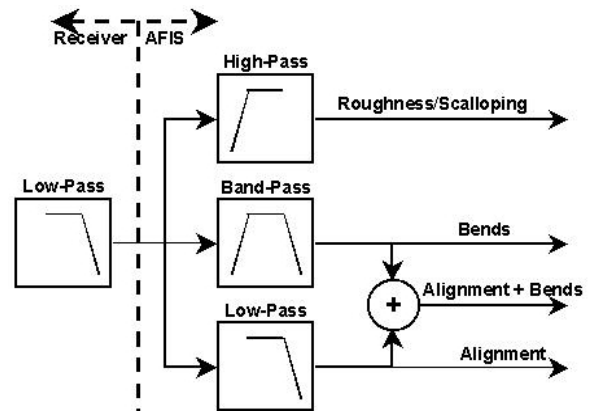


Figure 1. AFIS VOR Crosspointer Filtering

Even if an international standard were available for the frequency content of A, B, and R/S, the specific filter implementation (number of poles, ripple characteristics, etc.) will result in varying results according to the AFIS and flight inspection organization. This lack of definition first affects proposals for development (e.g., WTs, power lines, buildings) near VORs, because mathematical simulations predicting the effects of the development may prevent some construction. As physical construction occurs for the surviving proposals, some VOR airways and approach procedures will be removed from service after failing flight inspection criteria. It is often the R/S parameter that is used to disqualify either a proposal or a VOR procedural application after construction of a proposal.

Since R/S is widely agreed to have frequency characteristics sufficiently high that the aircraft path is not altered by the pilot or the autopilot, the application of an arbitrarily-defined R/S tolerance is effectively a “pseudo-problem” – i.e., it is not necessary to restrict construction proposals or VOR

instrument procedures and applications due to R/S. The operational effects of R/S are typically only a nuisance to the pilot. The result of omitting the R/S tolerance would be the same as changing the receiver filter to eliminate these frequencies from being presented to the AFIS or pilot/autopilot altogether.

### ILS GP Structure

Standards and Guidance Material for ILS Glide Path (GP) structure are defined in ICAO Annex 10, as follows:

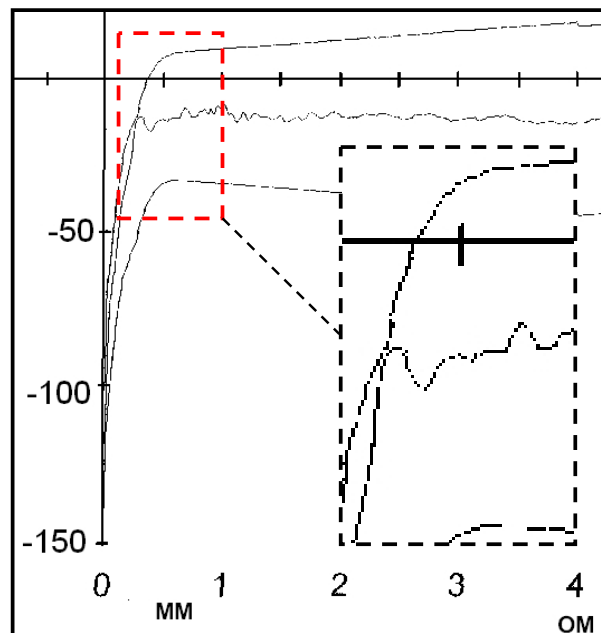
**3.1.5.4.2 [Bends]:** For Facility Performance Categories II and III — ILS glide paths, bends in the glide path shall not have amplitudes which exceed the following: [30  $\mu$ A at Point A, decreasing to 20  $\mu$ A at Point B, and 20 uA to the reference datum].

*Attachment C, 2.1.5, Application of localizer course/glide path bend amplitude Standard.* If the bend amplitudes are to be evaluated in any region of the approach, the flight recordings, corrected for aircraft angular position error, should be analysed for a time interval of plus or minus 20 seconds about the midpoint of the region to be evaluated. . . . Analysis of ILS glide path bends should be made using as a datum the mean glide path and not the downward extended straight line. The extent of curvature is governed by the offset displacement of the ground equipment glide path antenna system, the distance of this antenna system from the threshold, and the relative heights of the ground along the final approach route and at the glide path site . . . [underlining added]

Note that both sections of Annex 10 are for Bends (B) only, and that Roughness and Scalloping (R/S) are not mentioned. The guidance material focuses on how to apply the 95% “in-tolerance criterion”. Similar to the VOR situation, neither the frequency content nor the length of a bend is specified, although additional guidance material defines the intention of the B tolerances to limit [CAT II/III aircraft] deviations “...at the 15 m (50 ft) height, to less than 2 degrees of roll and pitch attitude and to vertical displacements of less than 1.2 m (4 ft)...”

Once again, individual flight inspection designers and manufacturers must define a method of applying the

B tolerance. However, for a GP signal close to the runway threshold, this is more challenging because of the changing nature of the GP signal – the “mean glide path and not the downward extended straight line.” The guidance material suggests (but does not define) that the mean GP in this area is a smooth curve, since it is governed mainly by the GP mast offset and geometrical relationships.

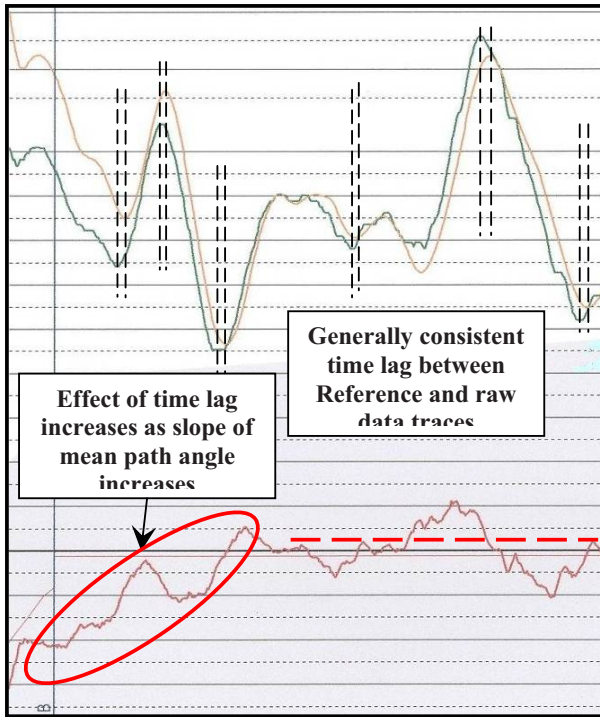


**Figure 2. GP Bend Tolerance Application**

Generally, current FI system implementations of the structure measurement do not actually take into account the installation’s physical parameters, but instead apply B tolerance limits roughly matching the zero difference-in-depth-of-modulation (DDM) trend line. This requires a very low-pass filter to any high frequencies. An example is shown in Figure 2, a GP recording between Points A and T, in which the crosspointer at first glance appears to exceed the plotted B tolerance limits within a half mile of Threshold. However, close examination reveals that the tolerance line has a bend in it, with the parameter trace nearly but not quite reaching the tolerance line.

Filtering of the crosspointer trace is somewhat defined in ICAO documents, and has been discussed in previous papers [3, 5]. If the filtering applied to determine the “mean glide path” for purposes of B tolerance application is any different from that applied to the crosspointer, or has a different time lag, then apparent out-of-tolerance conditions can appear.

These may be merely artifacts of the measurement, and not a GP problem – i.e., a “pseudo-problem.” In Figure 2, it is likely that the filtering is indeed different, because the limits curves contain little of the higher crosspointer frequencies. However, the limits are also not smoothly drawn lines.



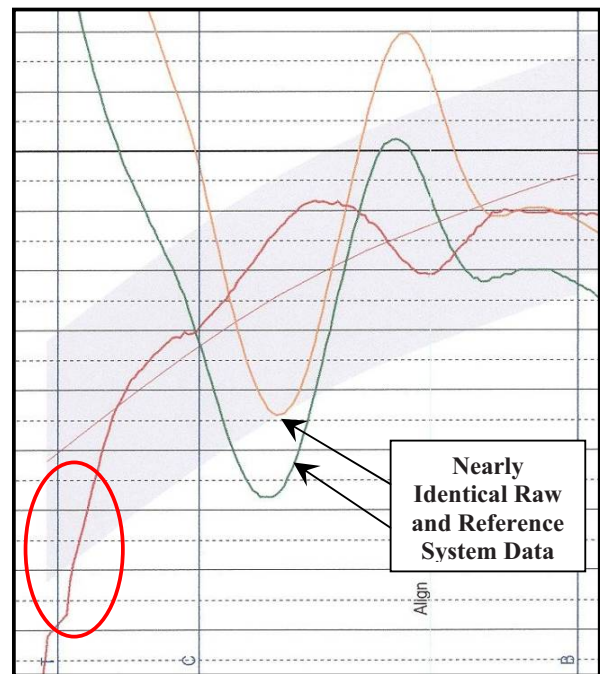
**Figure 3. Aircraft Dynamics With Time Lag**

Another example is shown in Figure 3, which covers approximately the last two miles of an approach. Here the raw data and the reference system traces are both visible in addition to the difference or corrected trace at the bottom. On this run, there were substantial aircraft dynamics, and the general shape of raw data matches quite closely the reference system trace. This suggests, but does not directly prove, that the GP is quite straight – this is confirmed in the (magnified) difference trace in the right half of the Figure, showing a reasonably straight GP as approximated with the dashed line.

However, there is a noticeable time lag between the two traces. If this time lag is constant and the GP straight, it results in a bias error (i.e., GP angle error) in the difference trace. However, as the aircraft nears threshold and the location of the “mean path angle” curves due to the site-peculiar geometry, the time lag results in an increasing error in the difference trace.

This increasing error adds to the mean path curvature produced by siting conditions, making it look even more curved. This increasing curvature DDM trace is filtered to produce the B tolerance limits on the recording. As the curve steepness increases, the time lag effects become accentuated.

As shown in the measurements between Points B and T of Figure 4, which is another example of high measurement dynamics with nearly identical raw and reference system data, this can produce an apparent out-of-tolerance condition without the GP necessarily having substantial real errors – another “pseudo-problem.”



**Figure 4. High Dynamics on Curved Mean Path**

A final GP example is shown in Figure 5, which shows a 9-mile approach on a GP known to be installed abnormally far (by approximately 50m) inside threshold. Zone 1 and most of Zone 2 of the approach should be expected to be reasonably straight, while the abnormally-large setback distance intuitively should result in a high threshold crossing height. This was confirmed by high-quality simulations using the actual reflection surface terrain. However, the recording shows a gradually but continually changing path angle and a substantial flare near the threshold. In spite of these characteristics, the announced TCH was surprisingly nominal at about 15m. Since it is not physically



realistic to have a constantly-changing path angle and a nominally-correct TCH value [4] at a site with a known large setback distance, it is extremely likely

that this measurement suffers from some type of data problem, and is not representative of the actual GP performance.

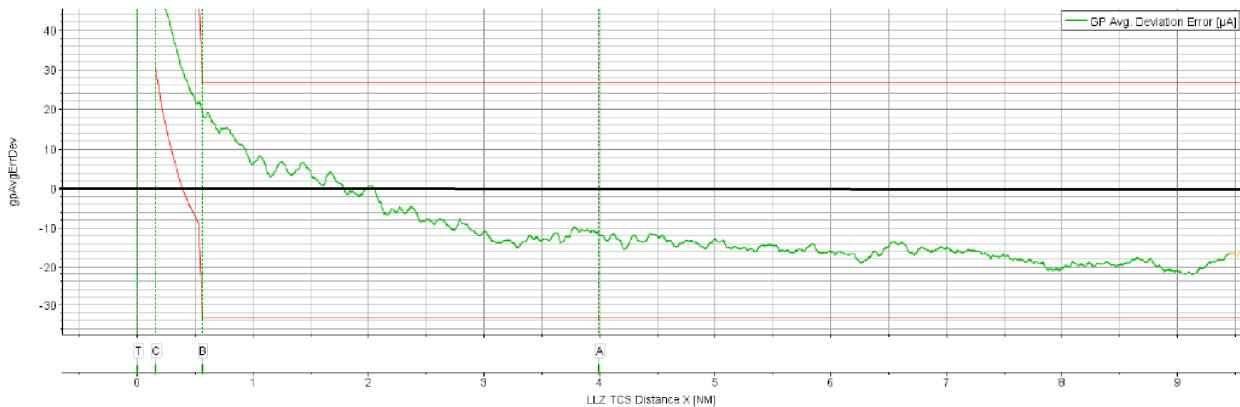


Figure 5. Continually-Changing Mean Path Angle with Known-Incorrect TCH Announcement

## SIMULATIONS AND MEASUREMENTS

### DVOR and Wind Turbines (WTs)

A recent study effort involved approximately 65 existing wind turbines which have been installed for some years within 5 km of a ground-mounted DVOR. Up to an additional ten are new or planned. Figure 6 shows the location of the WTs with respect to the facility. It also shows an abnormally close complex of agricultural storage silos approximately 300m distant. The silos are up to 50m in height (nearly 10 degrees!) and are located on ground approximately 8 meters lower than the DVOR site, as shown in Figure 7.

To assess the effects of the proposed turbines by mathematical simulation, it was first necessary to deal with the challenging silos, which are essentially in the mutual near-field of the DVOR and the silos. A new spectral analysis method of simulation was applied to the four silos (one rectangular, three cylindrical), with excellent resulting correlation to flight inspection measurements [6]. Figure 8 shows the modeled silos in mesh format, the prediction for their effect (without any WTs) near 135 degrees azimuth in the top graphic of crosspointer error, and the actual flight inspection measurements in the bottom graphic. Note that the flight measurements at approximately 1000m altitude and 10 NM radius include the effects of the existing ~65 turbines. Their effect is difficult to distinctly identify, although they undoubtedly raise slightly the noise floor on the bearing error measurement.

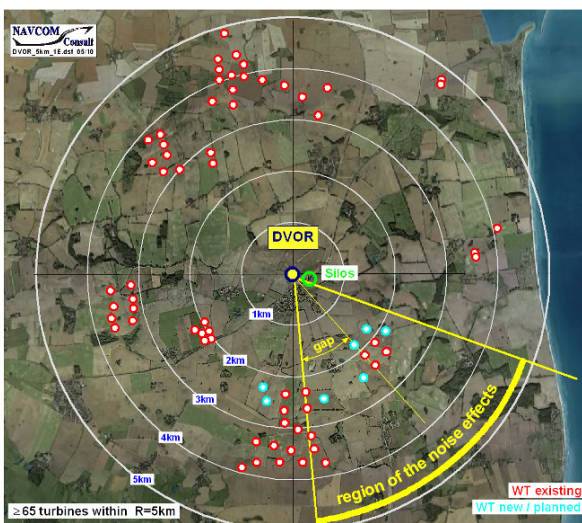


Figure 6. DVOR and Existing/Planned WTs

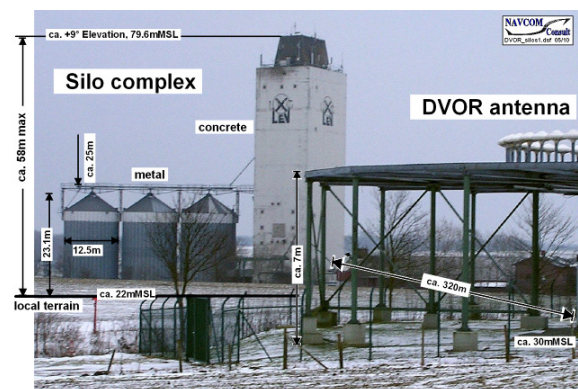


Figure 7. DVOR and Abnormally-Close Silos

## DVOR - Simulations vs Measurements

### Bearing error on orbit 10nm, 3400ft MSL by 4 silos

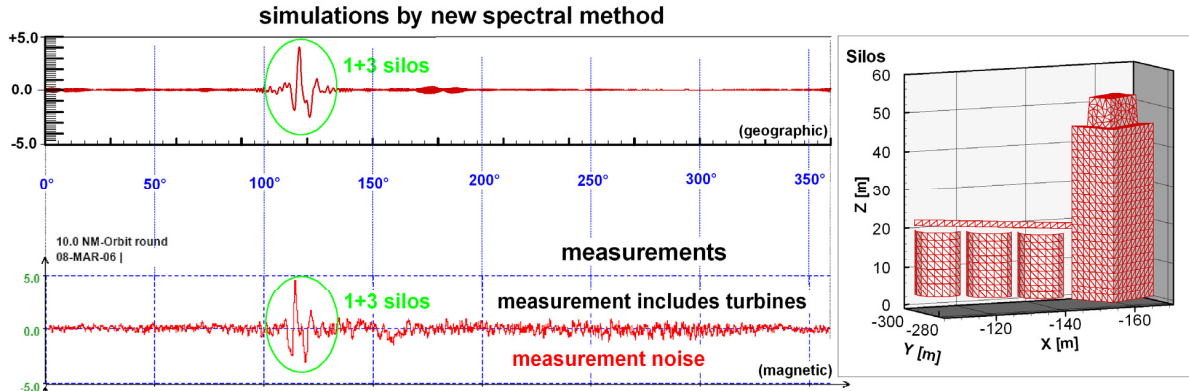


Figure 8. Modeled Silos, Simulated (Silos only) and Actual Flight Inspection (with ~65 WTs) Results

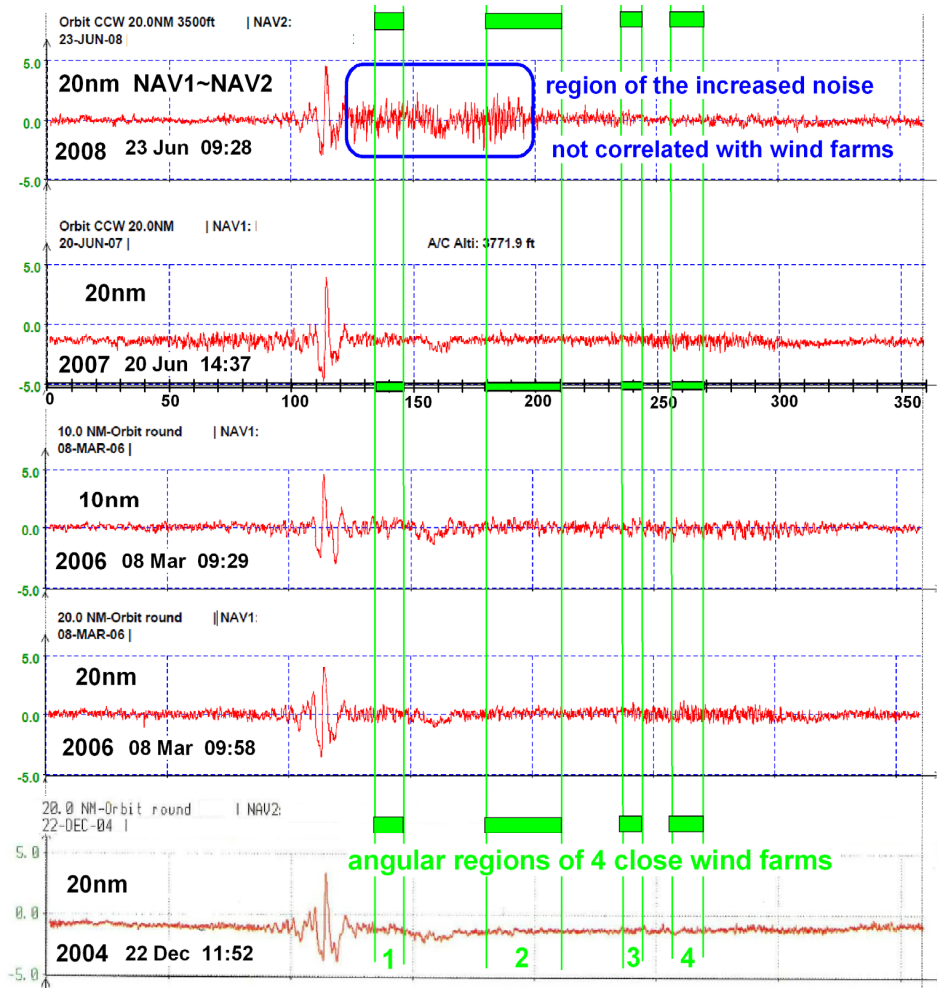


Figure 9. Five Years of DVOR Flight Inspection Measurements, Silos and Existing WTs

With excellent correlation achieved between silo simulations and flight measurements, additional simulations were carried out for the proposed new WTs. Although the simulations predicted fully benign results, the provider rejected the construction on the basis of existing errors in the DVOR orbit recordings.

Figure 9 shows five years of orbit recordings on the existing WT environment (with the silos), from 2004 through 2008. Four of the five results were taken at 20 NM, and one at 10 NM. Starting at the bottom for late 2004, the effects of the silos are clearly evident, with only a noisy baseline for the effects of the WTs. In the 20 NM measurements for 2006, the baseline noise is elevated somewhat, but the noise level is  $\pm 1$  degree or less. The 10 NM measurement in 2006 is nearly identical to that for 20 NM, as expected. The 2007 results are again nearly identical to the previous results. [It is unknown if all of these measurements were made with the same flight inspection system, the same filtering, etc.]

In Figure 9, only the top graphic for the 2008 results shows any difference in overall performance, with substantially elevated noise levels only in the  $\sim 120$  to  $\sim 200$  degree azimuth range. This elevated noise level was the basis of the regulatory denial for the newly-planned WTs. The expected areas of interference from the WTs are shown by green bands at the top of the graphic and by vertical lines throughout all the measurements. The potential effects of the WTs are expected in these angular areas from basic DVOR theory. It is evident that the potential areas of effect from the existing WT's do not correlate at all with this elevated noise level. This in turn suggests that there is no evident basis for disapproval of the additional WTs on the basis of the measured increased noise level in orbital measurements (Doc 8071 applies bends tolerances in radial flight).

The technical reason for the increased noise effect between  $\sim 120$  and  $\sim 200$  degrees is unresolved. Repeated measurements in 2009 confirmed the earlier measurements (2004 – 2007) without the increased noise. Simulations of the effects of the 21 existing WTs show that the noise-like bearing distortions have peaks in the order of about 0.2 degree, which is a value generally not visible in flight check measurements. It is concluded technically that

the increased noise floor is definitively not caused by the WTs.

### Field Strength Measurements

ICAO Annex 10 and Doc 8071 define navigational aid coverage on the basis of field strength, in general units of Volts/Meter, or alternately in units of Power Density such as Watts/square meter. (Signal strength at the receiver input is a different parameter, typically measured as a conducted signal on a coaxial cable, and has units of volts, or of power if the measurement impedance is known – typically 50 ohms.) Field strengths are independent of measurement equipment (e.g., antenna, receivers), which is a primary advantage of their use. An example of a defined field strength requirement is found in Annex 10:

*3.1.3.3.2 [Localizer] In all parts of the coverage volume specified in 3.1.3.3.1, . . . , the field strength shall be not less than 40 microvolts per metre (minus 114 dBW/m<sup>2</sup>).*

Until recently, despite ICAO's Standards and Recommendations being expressed in terms of field strength and/or power density, flight inspection measurements have typically been made in the signal strength domain. Conversion between field and signal strength is mathematically straight-forward, but requires knowledge of the correct "antenna factor", which includes system losses and is related to the effective capture area of the antenna – ie, the ability of the antenna to recover power from the received field. This received field is considered to have a horizontally-polarized, locally-planar wavefront.

Antenna factors of an antenna above a reference ground plane can be defined by careful measurements on a test range. However, a horizontally-polarized wave always has a field minimum at the ground level, and this makes even range testing of antennas by themselves challenging, and a planar wavefront is difficult to achieve near the ground. However, the same antenna in its operating environment (e.g., an airframe) will usually have a very different factor that varies in azimuth and elevation due to the proximity of irregular surfaces such as movable wing surfaces, rounded fuselages, engine nacelles, etc. The aircraft has to be treated as a part of the antenna due to mutual coupling. Figure 10 illustrates a typical airborne antenna pattern in free space, with large variations in response. In this particular example, the

antenna response at negative vertical angles, from which ground station signals will be received, is of very low gain and with highly irregular shape. Even when extreme care is taken, the differences between the aircraft on the ground and away from the earth surface can introduce large differences in effective antenna factor and antenna pattern shape [4, 5], which result finally in measurement errors.

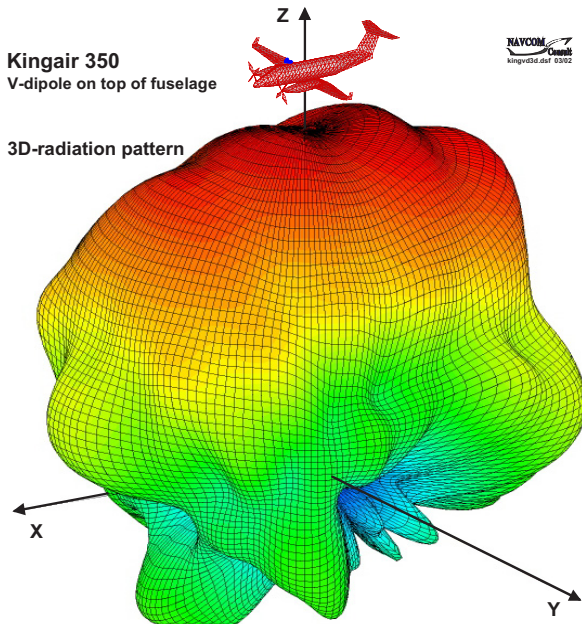


Figure 10. Three-Dimensional Antenna Pattern

Recent efforts by some flight inspection organizations to increase the accuracy of field strength measurements, by determining the installed antenna factor(s), have resulted in initial measurements of insufficient field strength. This in turn caused the development of an advanced simulation capability [6] for predicting field strengths, taking into account the curved earth. An example is for the ILS Localizer, for which the general problem is shown in Figure 11. It shows that the generation of the required plane wave for the total illumination of the aircraft and airborne antennas as a whole above ground is a major part of the problem.

Field strength requirements were used to calculate for curved earth the minimum required Effective Radiated Power (ERP) of the ground station to meet the field strength specification. This minimum ERP in turn defines the maximum tolerable loss in the cabling and distribution networks. Specifically, this

was for a given clearance antenna pattern at 35°, 17 NM distance, and 2000' altitude [6].

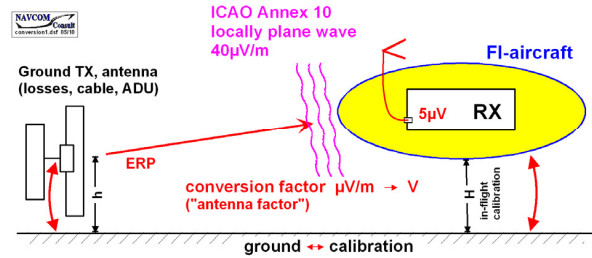


Figure 11. Field Strength Calculation Issues

The results indicate that a substantial power margin of up to approximately 10 dB exists for acceptable total losses for the particular Localizer. This matches our collective experience that modern ILS equipments have sufficient transmitter power margin and antenna gain to meet all operational requirements at reasonable sites. However, the predictions and experience are in contrast to the initial measurements of field strength which showed a relatively high negative margin of up to 6 dB.

The problem in the lack of correlation is likely to be found in use of the "correct" antenna factor (a "calibration" activity) when highly irregular antenna pattern shapes [4, 5] exist. Since the appropriate 3-D "calibration pattern" is therefore irregular as well, the activity also requires a highly precise determination of the spatial geometry and orientation between the ground-based radiating system and the actual flight inspection aircraft in space. It is as-yet unproven if this is reliably possible, given the naturally-expected tolerances of perhaps ±3 dB, or even necessary, given today's modern receivers with consistently better sensitivity performance than required.

## CONCLUSIONS

1. The frequency content of alignment, bends, and roughness/scalloping for VOR and ILS are not quantitatively defined in international documents.
2. Methods for determining average alignment (in orbital or radial flight), mean glide path alignment, and bends are not commonly defined or applied.
3. It may be completely unnecessary to measure and apply tolerances to roughness/scalloping, since by definition R/S cannot displace the aircraft.

4. Disqualification of ground-based procedural uses on the basis of R/S is unnecessary and deprives the user of many ground-based services.
5. Application of GP bends tolerances to a changing mean path angle is challenging and often problematic. The methods are not standardized.
6. Measurements taken under high aircraft dynamics conditions are generally very suspect.
7. Roughness and Scalloping, for VOR and GP in particular, are not mentioned in Annex 10 Standards and Recommendations. It may be unnecessary and inappropriate to disqualify these applications on that basis.
8. Disqualification of ground-based services and proposals for new construction sometimes occurs based on measurement errors that do not spatially correlate with the expected effects. The expected results are readily available based on sound experience and advanced simulations.
9. Disqualification of ground systems or structures such as buildings and WTs should not be based solely on orbital flights or simulations.
10. Measurement of field strength in flight to a reasonable uncertainty is extremely challenging due to the highly irregular antenna factors involved.

### **RECOMMENDATIONS**

1. ICAO should define the spectral content of alignment and bends for ILS and VOR, and other navaids as appropriate.
2. ICAO and the flight inspection community should consider carefully whether R/S tolerances are necessary or should be used as the basis for navaid services disqualification.
3. Flight inspectors should be vigilant that high-dynamics measurements are questioned and repeated several times for consistency, before using them to disqualify navaids services.
4. Flight inspectors should treat as suspicious any GP measurements with continually-changing path angles. (In these cases, suspect a data problem.)
5. Flight inspectors and engineering personnel should corroborate on challenging measurements, to ensure measurement results match physical expectations, before disqualifying navaids services.
6. In-flight measurement of field strength may be unnecessary, given today's modern receivers with high sensitivity.

### **ACKNOWLEDGEMENTS**

The authors gratefully acknowledge the contributions and assistance with the numerical calculations provided by Mr. W.D. Biermann, Mr. R. Mundt, and Mr. H. Müller, all of NAVCOM Consult.

### **REFERENCES**

- [1] International Civil Aviation Organization, July, 2006, Annex 10, Aeronautical Telecommunications, Volume 1, Radio Navigation Aids
- [2] International Civil Aviation Organization, 2000, Manual on Testing of Radio Navigation Aids [Doc 8071], Volume 1, Testing of Ground-Based Radio Navigation Systems (10/02 version)
- [3] G. Greving and N. Spohnheimer, Recent Issues in Demanding ILS Ground and Flight Measurement Environments, 14<sup>th</sup> International Flight Inspection Symposium, Toulouse, France, June, 2006
- [4] G. Greving and N. Spohnheimer, Problems and Solutions for Navaids Airborne and Ground Measurements – Focus on Receiver Sampling and TCH, 12<sup>th</sup> International Flight Inspection Symposium, Rome, Italy, June 2002
- [5] G. Greving and N. Spohnheimer, Problems and Solutions for ILS CAT III Airborne and Ground Measurements – European and U.S. Views and Perspectives, 11<sup>th</sup> International Flight Inspection Symposium, Santiago, Chile, June 2000
- [6] G. Greving, Latest Achievements of Complex System Simulations for ATC Systems – Actual Examples and Flight Inspection, 16<sup>th</sup> International Flight Inspection Symposium, Beijing, China, June 2010
- [7] G. Greving and N. Spohnheimer, Current Issues in Demanding Flight Measurement



Environments; 15<sup>th</sup> International Flight Inspection  
Symposium, Oklahoma City, USA, June 2008

## *Portable Calibration System for Air Traffic Control Surveillance Radar*

Xiaofeng Shi

Department of Electronic and Information Engineering  
Beihang University  
Beijing, China  
E-mail: [shixiaofeng@buaa.edu.cn](mailto:shixiaofeng@buaa.edu.cn)



XiaoQiang Lee

Department of Electronic and Information Engineering  
Beihang University  
Beijing, China  
E-mail: [xqli552@gmail.com](mailto:xqli552@gmail.com)



***Abstract***—In this article, we design a portable calibration system for air traffic control surveillance radar. This system realizes the automatic flight calibration for Secondary Surveillance Radar (SSR), and also can provide a simple flight calibration capability for any aircraft without standard equipment onboard. On the basis of high-precision GPS technology, this system is composed of a portable dual-frequency & dual-antenna GPS receiver, a portable PC and a software system by our own R&D. By analyzing the position accuracy of GPS and dual-antenna, the portable calibration system has the ability of providing automatically conversion arithmetic of coordinate system between WGS-84 and radar station center. A ground dynamic test for this system has been finished, and an actual flight data processing mission for an airport has been accomplished.

***Keywords***—Air Traffic Control Surveillance Radar, Flight Calibration, GPS, Calibration.

### I. INTRODUCTION

Secondary Surveillance Radar (SSR) is a radar system to locate air crafts through the inquiry by a ground interrogator and responders onboard. SSR is one of the basic systems of Air Traffic Control (ATC). In China, the current civil flight calibration by radar is as follows: first, an aircraft reaches the designated check point, a flight calibration operator receives in-flight radar distance and azimuth from the radar controller; second, the operator presses the event button and input the distance into the calibration system instantly; at last, with the help of distance or direction provided by radar, the computer analyzes if there is no error or not. This radar flight calibration method can be done only by aircraft with

airborne flight calibration system. The data source is obtained through the radio voice communication between a flight calibration operator and SSR controllers. Apparently, an uncertain time delay is also caused by the radio voice communication, which brings some errors to the calibration system. With the business development of airfields, air traffic has become much busier. Current calibration system can no longer meet the demand of flight calibration.

GPS (Global Position System) is satellite navigation and position system, which established by the United States in the 1970s. By using this system, its customers can realize all-weather, continuous, real-time and three-dimensional navigation, positioning and speed-measuring. In addition, its customers can realize high-accurate time transfer and precision positioning.

Based on GPS technology and by using a module structure and a combination of hardware and self-R&D software, we design a portable calibration system for air traffic control surveillance radar. Without any aircraft modification and connection with aircraft electric equipment, this portable system can expand the capability of specific calibration aircrafts and also supply simple function of flight calibration to any aircraft with this system onboard. In this way, the problem of short flight calibration resources should be alleviated. Besides, this system analyzes data resources with real-time flight GPS data and radar positioning data of ground radar recorder and aligns and analyzes data with a unified UTC time so as to realize automatic radar calibration and prevent the shortcoming of the traditional artificial calibration method.

### II. ANALYSIS OF POSITIONING ACCURACY

#### *A. Analysis of GPS Positioning Accuracy*

Due to the changes of satellite geometric figures and measuring errors, GPS performance is dynamic and it changes with time and location. A global positioning

function should be defined by some statistic terminology based on satellite constellation and the capability of receivers. For example, RMS error or 95% error distribution, the latter is often known as 95% error. Chart 1 provides SPS (Standard Positioning Service) of [SPS (2001)] and the approximate accuracy which can usually be obtained. This index only considers space signal errors while the performance obtained by the majority of customers is much better than the index, which is listed in the TABLE I below.

TABLE I.

Error (95%)	Index	Measured Data
Horizontal Position (m)	13	10
Vertical Position (m)	22	15
Time (ns)	44	30

### B. Dual Antenna

The working principle of dual antenna is to receive GPS signals by two antennas, integrate the two-way signal into one by a frequency synthesizer and then send it to GPS receiver. The application requires that there should be no common-vision satellite among the satellites which are searched by the two antennas. Tests have proved that the accuracy of dual antenna is a little bit less than the positioning accuracy of a single antenna due to multi-path attenuation. However, its error will not exceed the baseline length and will not have big impact on the positioning error of this system.

The application of dual antenna is as simple as to stick two small GPS antenna on aircraft porthole without any aircraft modification or connection to electric equipment.

## III. RESEARCH ON COORDINATE TRANSFORMATION ARITHMETIC

Because the calibration is to be done for calibration radar, the data measured by ground radar station is the aircraft flight coordinates based on the coordinates of ground radar center while GPS receiver, as airborne equipment, outputs the location of aircraft in flight based on WGS-84 coordinates. Therefore, the following transformation needs to

$$\begin{bmatrix} xg \\ yg \\ zg \end{bmatrix} = \begin{bmatrix} \cos(lon) * (ye - yu) - \sin(lon) * (xe - xu) \\ \cos(lat) * (ze - zu) - \sin(lat) * \cos(lon) * (xe - xu) - \sin(lat) * \sin(lon) * (ye - yu) \\ \cos(lat) * \cos(lon) * (xe - xu) + \cos(lat) * \sin(lon) * (ye - yu) + \sin(lat) * (ze - zu) \end{bmatrix}$$

be done according to the system requirement.

### A. Transformation from BLH to ECEF (x, y, z.)

The formula of coordinate conversion is as follows:

$$\begin{bmatrix} x \\ y \\ z \end{bmatrix} = \begin{bmatrix} (r_n + alt) * \cos(lat) * \cos(lon) \\ (r_n + alt) * \cos(lat) * \sin(lon) \\ [(r_n * (1 - NAV\_E2) + alt)] * \cos(lat) \end{bmatrix}$$

Among them:

$$r_n = \frac{A\_EARTH}{\sqrt{1 - NAV\_E2 * (\sin(lat))^2}}$$

$$NAV\_E2 = (2 - flattening) * flattening$$

$$A\_EARTH = 6378137$$

$$flattening = 1 / 298.2572235$$

### B. Transformation from ECEF (x, y, z.) the customer coordinate system

Among them, **(xg, yg, zg)** is the converted target coordinated under customer coordinate system. **(xe, ye, ze)** is the target coordinates under ECEF coordinate system and **(lon, lat)** is the customer longitude and latitude under WGS-84 coordinate system.

### C. Transformation from Space Right-Angle coordinates to Radar Polar Coordinates

$$\begin{bmatrix} R \\ A \\ E \end{bmatrix} = \begin{bmatrix} \sqrt{x^2 + y^2 + z^2} \\ \arctan\left(\frac{x}{y}\right) \\ \arcsin\left(\frac{z}{R}\right) \end{bmatrix}$$

**(R, A, E)** are target slant distance, azimuth and elevation measured by radar and **(x, y, z)** is the target coordinates on the center coordinates of radar station.

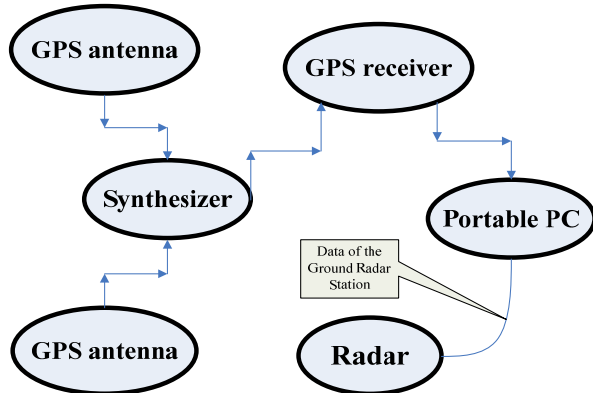
## IV. REALIZATION OF THE CALIBRATION SYSTEM

### A. Principles of the System

Considering that the positioning accuracy of radar is about 300 meters while the positioning accuracy of GPS receiver is 10 meters or even less than that, it is reasonable to use high-accurate GPS technology to verify air traffic control surveillance radar. Small antenna can be stuck on aircraft porthole to receive GPS signal which can be used as a benchmark to verify the positioning data of air traffic control surveillance radar. The sticking of an antenna on the porthole of both sides can both maintain balance and expand the search scope of satellite and improve GPS positioning accuracy. This calibration system requires neither aircraft modification nor connection to aircraft electric equipment, and its application needs no airworthiness certificate.



### B. System Composition

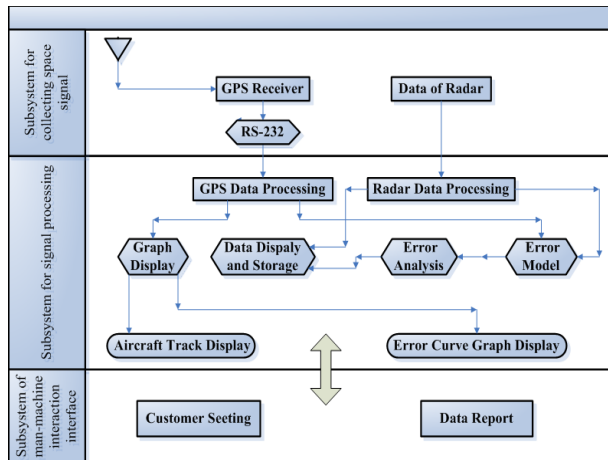


GRAPH I. Hardware Structure of The System

The connection of the calibration system to airborne equipment shown as GRAPH I is that one small GPS receiver is to be stuck on the symmetric porthole of an aircraft and connect them by two cables into a synthesizer which combines the two-way signal into one and inputs it into a portable GPS receiver. The single-way signal will be sent, through RS-232, to PC software for processing.

This system can collect GPS positioning data in a real-time manner. After flight calibration, it obtains in-flight radar positioning data from ground radar station and processes register data of time and space and assess radar ranging distance error and radar measured angle error.

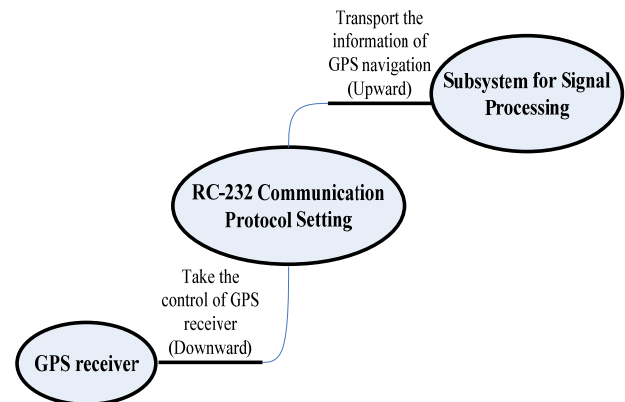
### C. Analysis of GPS Positioning Accuracy



GRAPH II. System Function Module

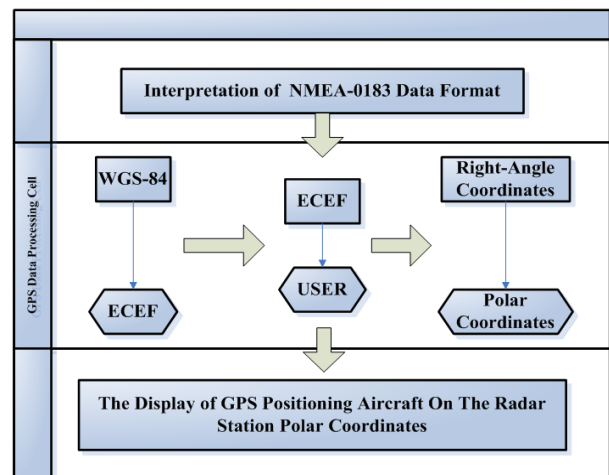
The calibration system is composed of the following three parts according to its functions: subsystem for collecting space signal, subsystem for signal processing and subsystem of man-machine interaction interface.

The subsystem for collecting space signal is mainly to collect GPS space signal, establish a collection module of space signal. This model is involved with antenna, receiver, interface, communication protocol etc. The realization process is shown in GRAPH III.

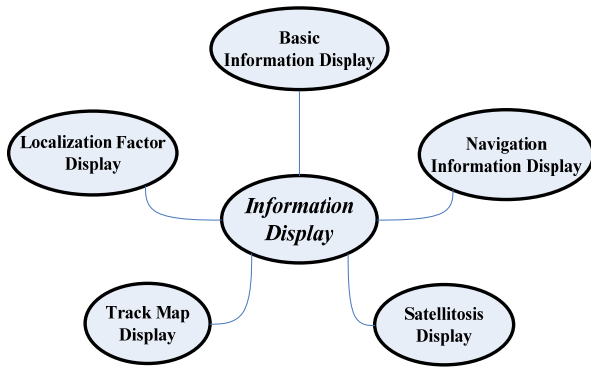


GRAPH III. The Realization Process of GPS Signal Collection

The subsystem for signal processing calculates and interprets GPS data to obtain GPS-positioned aircraft information with the data from the subsystem for space signal gathering. Besides, it compares the information from the two sources so as to obtain the error value. With this value, the subsystem establishes an error analysis model and realizes the calibration of radar signals. At the same time, the system needs to show necessary information including GPS data processing cell, information display cell and data storage cell. It can monitor satellite status in a real-time way and describe aircraft track figure and error curve graph.



GRAPH IV. The Function Module Graph of GPS Data Processing Cell



GRAPH V. The Function Module Graph of Information Display

The subsystem of man-machine interaction interface is the operating platform of the whole system. In the context of Windows XP, it can provide diversified man-machine interaction modes for customers to have different settings and control of equipment. It can also create data forms according to customer demand. The system software has module design and has good operation ability, stability and expandability.

#### D. System Validation

This program adopts a portable Javad dual-frequency, dual-antenna GPS receivers. In order to validate its dynamic positioning accuracy, insure its criterion for the calibration of ATC surveillance radar and get it ready for airborne test, we have conducted a dynamic GPS test on a moving vehicle in Beiqing Road. With the high-accurate RTK technology as the reference, we have tested dynamic positioning accuracy of the dual-frequency, dual-antenna Prego receiver.

The specific process of the dynamic test is as follows: We set a NovAtel dual-frequency receiver and Prego dual-frequency and dual-antenna receiver in the vehicle. A Prego receiver antenna was stuck on the corresponding side of the window. As a RTK moving station, NovAtel receiver antenna was fixed on the top the car. The benchmark station of RTK was set up in a landmark in Beijing which transferred difference information with the moving station through a wireless network. The communication rate was 115200bps.

By using relevant software, we processed the data stored by Prego and NovAtel and the data result is shown in TABLE II.

TABLE II. DYNAMIC POSITIONING ACCURACY

	Comprehensive Standard Deviation	Horizontal Standard Deviation	Vertical Standard Deviation
NovAtel	0.143	0.075	0.122
Javad	2.026	1.354	1.480

After further processing, the dynamic positioning accuracy of dual-frequency receiver can reach 2.03 meters.

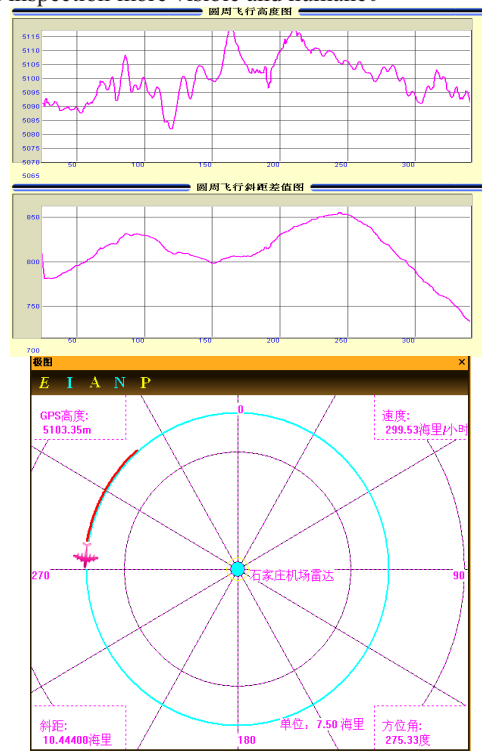
Although it is less good than the RTK dynamic positioning accuracy of NovAtel, it can fully meet the demand of radar calibration.

#### V. SYSTEM APPLICATION

This system has successfully finished three practical flight inspection tasks in Beijing International Airport, Taiyuan Wusu Airport and Hebei Shijiazhuang Airport respectively. The results are proved to be excellent.

##### A. Real-Time Flight Inspection Graphics Display

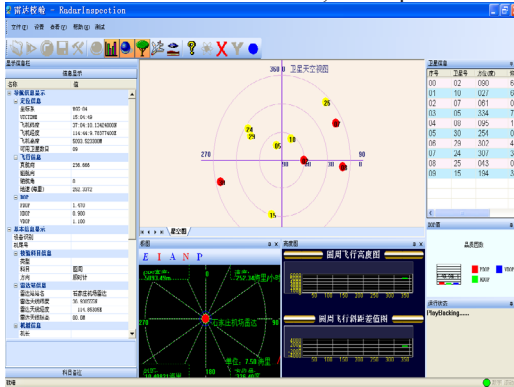
As flight goes on, system software presents real-time graphics display including stars chart, polar diagram, slant distance and azimuth curve chart, which would make the flight inspection more visible and humane.



GRAPH VI-1 and GRAPH VI-2

The star chart demonstrates the locations and signal intensity of current visible GPS satellites; the polar diagram displays the aircraft position in polar coordinates with the radar station being inspected as the origin; the azimuth in the diagram means the relative azimuth with respect to the radar station, and the distance means the slant range between the aircraft and the radar station; the polar diagram also give out the aircraft's current altitude, speed, path and other information. The graphics can also be displayed in two modes -- enroute Mode and inspection Mode and the diagram can be easily zoomed by mouse wheel; The altitude, azimuth and cross-track error and other information plotted by real-time flight error chart in curve lines is illustrated as GRAPH VI.

Besides, the system software offers a friendly and a beautiful GUI. Every View of the software can be docked to another or docked to the edge of the mainframe or auto-hidden when the view was not used, as Graph xx shows..

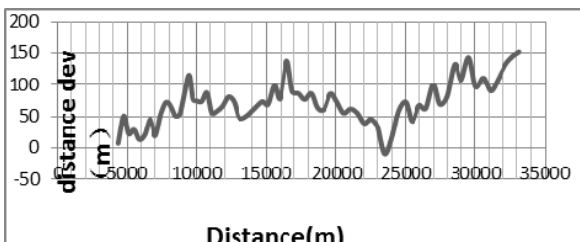
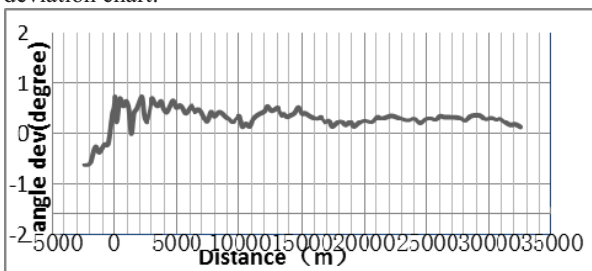


GRAPH VII System Software

It's convenient for inspector to operate and the inspector get more information compared with the traditional way.

### B. Post-Processing

Post-processing calculates the deviations by comparing the radar positioning data and the GPS positioning data which were got from the GPS receiver on board at the same UTC. However, the radar records a positioning data every 3.8 seconds, while the GPS receiver records data per second, so it's a position projection. Using an interpolation algorithm which applies several data around the current data to calculate the GPS positioning data at the radar timestamp, the system got the inspection result. Graph X shows the inspection result of Shijiazhuang Radar Inspection, including slant distance deviation chart and azimuth deviation chart.



GRAPH VIII Deviations

From the graph, with better signal, the deviation of slant distance arrives at 78.82m, and the deviation of azimuth arrives at 0.30 degree, the maximum difference values are 150m and 0.65 degree, both used the GPS calibration radar.

## VI. CONCLUSION

The portable calibration system for air traffic control surveillance radar designed in this article can improve radar flight calibration procedure and realize automatic calibration of air traffic control surveillance radar. This system needs no aircraft modification and equipment and no airworthiness certificate. It provides GNSS application and a simple flight calibration capability for non-calibration aircraft and also provides an option for alleviating the lack of flight calibration resources in China right now.

### References

- [1] (US)Pratap Misra (US)Per Enge, Ming Luo Translated.Global Positioning System, Signals, Measurements, and Performance [M].2<sup>nd</sup> Edition. Beijing: Publishing House of Electronics Industry, 2008.
- [2] Qiushi Keji, Xianyong Li. Serial Port Communication Technology and Engineering Practice of Visual C++ [M].2<sup>nd</sup> Edition Beijing: Posts & Telecom Press, 2004
- [3] Hua Liu, Cunliang Wang. The Application of GPS in the Detection Accuracy Evaluation of Aero-Radar [J] GNSS WORLD OF CHINA, 2008, (4):49-52.
- [4] Zhigang Huang, Guoliang Sun, Wenquan Feng, Jinping Chen, Yugui Zheng. The Principle and System of Radio Navigation, [M].Beijing: BUAA Press [M], 2007
- [5] Biliang Gu, Liming Wang, Yan Han. Data Collection and Processing Based On VC++ [J]. Information of Microprocessor and Computer 2008, (13):203-204+311.
- [6] DOC-8071[S].
- [7] Annex 10 Volumn I [S].
- [8] Schuchman L, Elrod B.D, Van Dierendonck A.J. Applicability of an augmented GPS for navigation in the National Airspace System [J]. Proceedings of the IEEE, 1989, 77(11):1709-1727.
- [9] Besada Portas J.A, Garcia Herrero J, de Miguel Vela, G.Radar bias correction based on GPS measurement for ATC applications. Radar, Sonar and Navigation, IEE Proceedings', 2002, 149(3):137-1



# Method of Signal Assessment and Flight Inspection for DME/DME RNAV

## Shi Dongwei

Junior Navigation Engineer

Technology Support Center, Middle South Regional ATMB of China

3# NanYun East Street, Airport Road, Guangzhou, China

Fax: +86 20 861 35607

Mail: shidongwei@atmb.org

## Lu Yongdong

Navigation Engineer

Technology Support Center, Middle South Regional ATMB of China

3# NanYun East Street, Airport Road, Guangzhou, China

Fax: +86 20 861 37124

Mail: whister@atmb.org

## ABSTRACT

DME/DME RNAV is one of the primary technologies of Area Navigation system. The DME/DME infrastructure should be checked prior to provide navigation services to RNAV. The workload of flight inspection is very heavy when a number of DMEs involved in the region. To solve this problem, the paper proposes a method of signal assessment and flight inspection for DME/DME infrastructure. Firstly, a assessment software has been developed, which simulates the terrain without projection and analyzes signal coverage of DME, then calculates the available DME/DME coverage based on the guidance and standard of ICAO PBN Manual. Before flight inspection, parts of the prior DMEs which can generate the available pair coverage without critical DME are selected according to the assessment tool. Then these DMEs will be evaluated during the flight inspection. When the result is consistent with what the software estimated, other DMEs is not necessary to check, and the inspection cost can be reduced.

The method has been applied to the flight inspection of terminal RNAV procedures in Guangzhou Baiyun Airport, which proves that the assessment method has high accuracy and the inspection work is reduced tremendously.

**Keywords:** DME/DME RNAV, Flight Inspection, Area Navigation

## 1 INTRODUCTION

### 1.1 DME/DME RNAV System

DME (Distance Measure Equipment) /DME RNAV is one of the main systems of Area Navigation. Many RNAV aircrafts use two DMEs or above to determine their positions<sup>[3]</sup>. ICAO has provides guidance and standardization for DME/DME RNAV system<sup>[1]</sup>. There is a minimum standard for DME/DME infrastructure evaluation in support of Area Navigation routes and procedures<sup>[2, 3]</sup>. The DME facilities should satisfy this minimum standard to provide RNAV services.

DME/DME coverage exists where the availability of DME facilities permits the baseline for RNAV system to achieve better than certain navigation accuracy <sup>[3]</sup>. If one DME becomes unavailable resulting in inadequate DME/DME RNAV system performance to sustain operations along a specific route or procedure, it is critical DME to this route or procedure.

### **1.2 Flight Inspection for RNAV Procedure and Route**

Before the RNAV routes and procedures are released, they must be checked, as part of the safety assurance process, to specify which navigation sensor may be used <sup>[4]</sup>. These checks can be carried out by flight inspection with suitably equipped aircraft. ICAO Doc 8071 <sup>[6]</sup> provides general guidance on the extent of testing and inspection. It also provides guidance on the flight inspection of instrument flight procedures.

The flight inspection is required to measure the actual coverage, accuracy and suitability of signals received from one or a number of navigation aids along the entire instrument flight procedure.

DME/DME RNAV flight inspection is quite different from traditional route or procedure. For a specified route or procedure, multi DMEs should be evaluated and the inspection data should be analyzed and computed according to DME/DME RNAV criteria. At last, redundant coverage or available coverage with critical DME and area navigation gaps should be calculated and listed.

### **1.3 The Problem and Motivation**

With aircraft equipped with no RNAV system for flight inspection, DME should be

evaluated individually. In order to determine redundant available DME/DME coverage, the flight inspection must check DMEs for specified route or procedure as more as possible. According to capability of existing technology, the equipment of inspection aircraft can follow limited number of DMEs at the same time. Generally, there are large numbers of DME facilities in the area where RNAV is implemented, so one route or procedure may be checked for more than one time. Sequentially, the flight inspection will be a heavy workload.

As signal of navaid can't reach some airspace because of its capacity and the geographical factors, it isn't necessary to be checked for the RNAV route or procedure through this airspace. Even if the DME is available, it may be not necessary to be checked because of its failure of generating available DME/DME coverage. If these unusable DMEs can be found beforehand, the number of DMEs for checking during flight inspection can be reduced.

In order to anticipate the performance, a software tool for DME/DME RNAV assessment is designed and developed. The tool can determine the coverage of one single DME and DME pairs. Beforehand, prior DMEs facilities are selected by the assessment tool to be checked during the inspection. If the inspection result indicates that these DMEs are available and can generate DME/DME pairs without critical DME, other DMEs can be ignored, or additional inspection will carry out for the alternative DMEs. As result, the cost of the flight inspection can be saved.

## **2 DME/DME RNAV ASSESSMENT AND FLIGHT INSPECTION**

This chapter presents the principle for

DME/DME infrastructure assessment and method for operational implementation of flight inspection.

### 2.1 Geographical Model

The coverage of the DME signal is influenced by the geographical factors, including terrain, obstacle and curvature of ground. Construction of geographical model is essential for analyzing signal coverage.

Geographical model is created using the SRTM [7], a DEM (Digital Elevation Model) database, and the shielding angle data of DME station. The model based on WGS-84 coordination simulates the authentic earth in three-dimensional Cartesian coordinate system without any projection. As the suitability of frequency, DME signal can be seen as linear transmission. The signal coverage analysis is computed on this model with visual analysis, whose principle is show by the following figure.

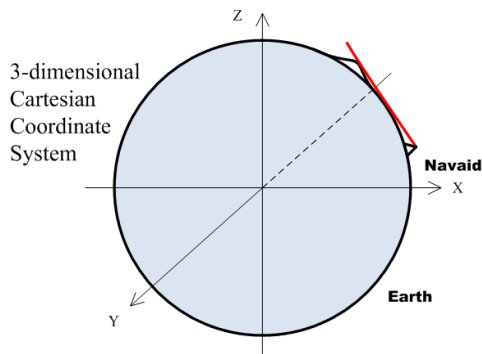


Figure 1 Principle of Coverage Analysis

### 2.2 Criteria for DME/DME RNAV

ICAO PBN Manual [1] has defined minimum DME/DME RNAV system baseline performance. The assessment tool determines the available DME/DME coverage according to those criteria that can be evaluated by the

software. The following outlines these criteria.

(1) DME facility relative angles. When needing to generate a DME/DME position, the RNAV system must use DMEs with a relative include angle between  $30^\circ$  and  $150^\circ$ . This requirement generates the area as the shadow of the following figure shown.

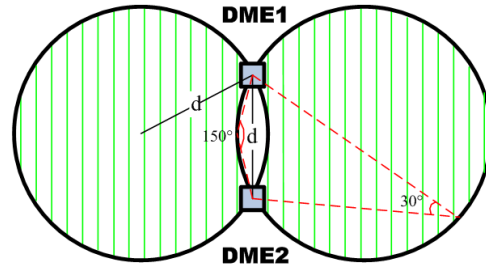


Figure 2 Area Generated by 2 DME with Required Angle

(2) RNAV system use of DMEs. The RNAV system must use an available DME anywhere within the following region around the DME facility: i) Greater than or equal to 3 NM from the facility; and ii) Less than  $40^\circ$  above the horizon when viewed from the DME facility and out to 160 NM.

(3) Position Estimation Error (PEE). When using a minimum of two DMEs facilities satisfying the criteria in (2), and any other DME facilities not meeting that criteria, the 95% position estimation error must be better than or equal to the following equation:

$$2\sigma_{DME/DME} \leq 2 \frac{\sqrt{(\sigma_{1,air}^2 + \sigma_{1,sis}^2) + (\sigma_{2,air}^2 + \sigma_{2,sis}^2)}}{\sin(\alpha)}$$

Where:  $\sigma_{sis} = 0.05NM$

$\sigma_{air} = \text{Max}\{0.085NM, 0.125\% \text{ of distance}\}$

$\alpha = \text{inclusion angle } 30^\circ \leq \alpha \leq 150^\circ$

The overall RNAV-1 system accuracy (Total System Error, TSE) <sup>[2]</sup> is required to be equal or less than +/-1 NM during 95% of flight time. This includes the Navigation System Error (NSE) due to path definition error and Position Estimation Error (PEE) and display error as well as the Flight Technical Error (FTE). While path definition error and display error have been assumed negligible, NSE is decided by FEE. While the use of flight director or autopilot is recommended, 0.5NM FTE is achievable in manual flight. As FTE and NSE are treated as independent errors, this FTE allocation provides for a maximum permissible NSE of +/-0.866 NM (95%) using the root sum square formula.

Thus, the maximum  $2\sigma_{DME/DME}$  result for DME/DME navigation is evaluated against the maximum NSE of 0.866NM derived above.

The maximum  $2\sigma_{DME/DME}$  result should be equal or less than 0.866 NM, or RNAV-1 services can't be provided.

### 2.3 Assessment for DME Infrastructure

Basic data, including DEM terrain database, navaid properties and flight routes, should be configured for the tool running the assessing function. Three coverage functions are realized. The following describes each function in detail.

(1) Coverage Analysis for Single DME: Analyze the coverage of the DME at a specified level. As mentioned above, the terrain and obstacle will affect the analysis result. The following example shows the coverage scope for LMN DME at 1000 Meters.

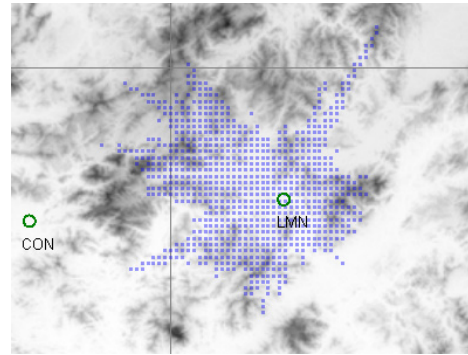


Figure 3 Coverage of Single DME

(2) Coverage Analysis for Area: Analyze the coverage of multiple DMEs or DME/DME in an area at a specified level. The coverage of multi DMEs shows how many and which DMEs are available at the selected area. The coverage of DME/DME pair can be computed based on these available DMEs according to the criteria presented in 2.2.

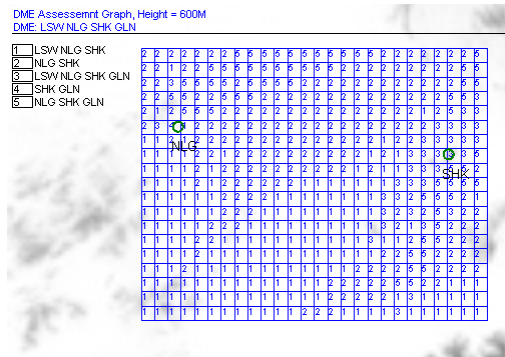


Figure 4 Coverage of Multi DMEs

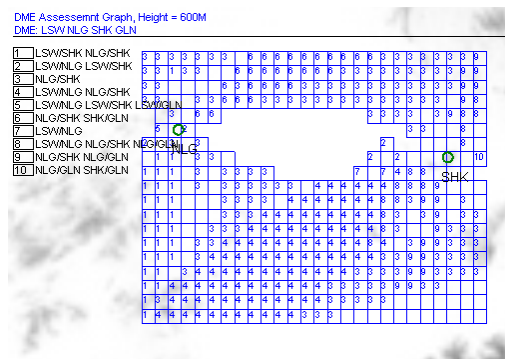


Figure 5 Coverage of DME/DME

(3) Coverage Analysis for Route or Procedure: Analyze the coverage of multiple DMEs and



the DME/DME for a specified route or procedure of RNAV. The route and procedure consists of way points with minimum flight level. For every route or procedure, prior DMEs can be determined by the assessment function.

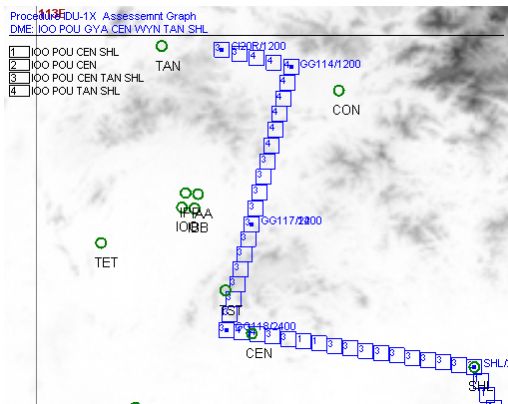


Figure 6 Coverage of Multi DMEs

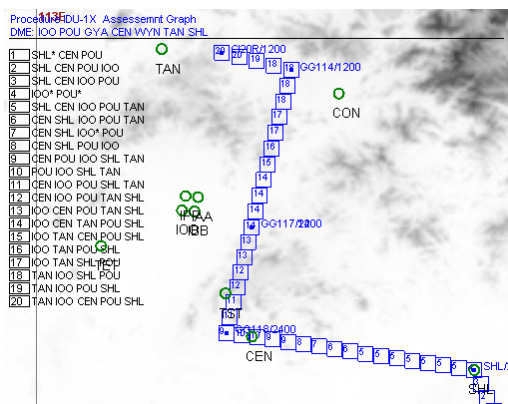


Figure 7 Coverage of DME/DME

## 2.4 Flight Inspection Method

Procedure and route relying on DME/DME RNAV require flight inspection to determine if the DME/DME coverage provides adequate support. It is the responsibility of the procedure owner to use the results of the flight inspection to confirm that the infrastructure along the nominal track is valid.

Flight inspection validates the reception and performance of individual DME facility.

Before conducting the evaluation, the routes and procedures should be determined by the assessment tool. The route or procedure is divided to segments by way points. After the tool evaluating, every segment has certain number of DMEs which are the best choose to generate adequate coverage for DME/DME.

During the flight inspection, these prior DMEs will be evaluated. If the result is consistent with what the tool anticipates, other DMEs are not necessary to be evaluated, or alternative should be evaluated by additional inspection. The data gathered during the flight inspection should be used to support the subsequent analysis:

- (1) Identification of available DME/DME coverage: DMEs which can provide adequate DME/DME coverage and required accuracy over the procedure and route.
- (2) Identification of critical facilities: DME which is critical to ensure adequate DME/DME coverage. When the DME is unavailable, there is no DME/DME navigation service for the correlative route or procedure.
- (3) Identification of coverage gaps: No DMEs generate effective coverage. The critical DME and coverage gaps with specified route or procedure should be promulgated in the Notice to Airmen (NOTAM).

## 3 EXPERIMENTATION

The method proposed by this paper has been implemented in the flight inspection of terminal RNAV procedures for Guangzhou Baiyun Airport in South China. There were 29 procedures, including 14 STARs and 15 SIDs for this inspection, and 18 DMEs facilities to be evaluated.

The equipped aircraft evaluated the accuracy and coverage for each DME. Figure 8 is one example of curve graph for range error of DME. Figure 9 is the curve graph for the AGC. The tolerance of range error is 0.866NM while the minimum AGC should be -89 dbm.

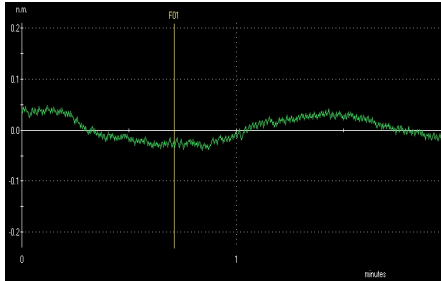


Figure 8 Range Error for DME signal

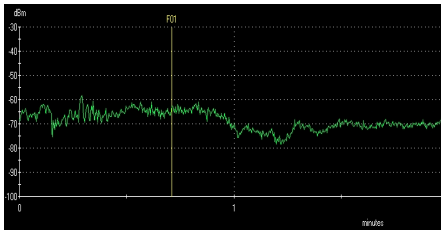


Figure 9 AGC for DME signal

The following evaluates the accuracy of assessment and inspection workload based on the data collected at this flight inspection.

### 3.1 Evaluation for Accuracy of Assessment

The accuracy of assessment result evaluated by the software tool can be identified by comparing with the actual result of flight inspection. Comparison between assessment and inspection is shown in the table 1. The statistic data is the total DME-times appearing in every segment of procedure for no signal, discontinuity and continuity. Continuity means the signal is received all the time and satisfies the conditions that  $AGC \geq -89\text{dbm}$  and  $0.2\text{ NM} \geq \text{Range Error} \geq -0.2\text{NM}$ . Discontinuity means the signal is usable, but unusable sometimes.

Table 1 Comparison between Inspection and Assessment

	Flight Inspection	Assessment of Success	Accuracy Rate
DME-Times of No Signal	67	43	64.3%
DME-Times of Discontinuity	92	63	68.4%
DME-Times of Continuity	343	309	90.1%

Table 2 Comparison between Traditional and Improved Inspection

	Traditional Inspection	Improved Inspection
Times of Flight for All Procedures	87	46
Average Times of Flight per Procedure	3	1.59
Average DME-Times per Segment of Procedure	18	8.9

Inspection result is assumed as accurate ignoring external factor, such as weather, disturbance, and flight error. The table shows that the accuracy of assessment can reach 60% or above, especially 90% for continuity. In the first row, most of flight inspection results are

continuity, so it can be derived that most of anticipated results are what we wanted.

### 3.2 Evaluation for Inspection Workload

Traditionally, all DMEs for checking should

be evaluated for every procedure. If preferential DMEs are selected for flight inspection beforehand, the number can be reduced. Table 2 shows the comparison result between traditional and improved inspection of this paper.

According to the result, the times of inspection flight and number of DMEs followed are all reduced. As a result the workload is saved, ensuring the DME/DME coverage analysis is sufficient.

#### **4 FUTURE WORK**

The coverage assessment is based on visualization without analysis of intensity. Therefore the result of theoretical analysis is available while it's not sure to satisfy the needs of application. The range calculated theoretically is larger than it is in reality, but it's ok to use it as primary analysis. Future work will be the consideration for the physical characteristic of specific equipment and the consummating related calculation models.

Although this method aims at DME/DME RNAV1, the basic theory can be applied to other area navigation systems. Future work can be the extend application to other navigation technologies and standards.

#### **5 CONCLUSIONS**

The method of signal analysis in this paper simulates the real geographical space without processing of projection, so the calculation error has been decreased. The result has been compared with that in flight inspection and proved to be of high precision, which proves the reliability and feasibility of this method. What's more, the related evaluating method of area navigation has also gained some achievement that the cost and workload can be

reduced.

With the development of area navigation technology, the ground-based need to be quality and safe. This method can provide service for signal evaluation, area navigation evaluation and flight inspection. Thus the performance evaluation of supporting area navigation has important meanings and a bright application future.

#### **6 REFERENCES**

- [1] ICAO, Performance Based Navigation Manual, Working Draft 5.1 Final, Mar, 2007.
- [2] ICAO, Navigation Infrastructure Assessment in Support of PBN.
- [3] FAA ORDER 7470.1, DME/DME Infrastructure Evaluation for RNAV Routes and Procedures, 2004.
- [4] Guidance Material for the Flight Inspection of RNAV Procedures: <http://www.flightcalibration.de>
- [5] ICAO Doc 8168, PANS-OPS, Aircraft Operations, Volume I Flight Procedures. Amendment No.3, Fifth Edition, 2006.
- [6] ICAO Doc 8071, Manual on Testing of Radio Navigation Aids, fourth Edition, 2003.
- [7] DEM Data: <http://srtm.csi.cgiar.org>.



## Investigation of Terminal Area Distance Measuring Equipment Signal Interference A Case Study

### Todd Bigham

Electronics Engineer  
Aircraft Maintenance and Engineering Group  
Oklahoma City, Oklahoma USA  
Tele : +1 405 954 7329  
E-mail: [todd.bigham@faa.gov](mailto:todd.bigham@faa.gov)



### Brad Snelling

Airspace System Inspection Pilot  
Flight Inspection Operations Group  
Oklahoma City, Oklahoma USA  
Tele: +1 405 954 9060  
E-mail: [brad.snelling@faa.gov](mailto:brad.snelling@faa.gov)



## 1. ABSTRACT

Routine flight inspection of the Dulles International Airport discovered several places around the terminal area where the Distance Measuring Equipment (DME) signal was not useable. Especially bothersome was consistently unusable signal along the approach to one of the runways. What was the cause of this problem?

Our FAA Beech King Air outfitted with flight inspection antennas and avionics made a great tool for investigating the problem. With a minor wiring modification to feed the DME video signal to our troubleshooting instruments we were ready to go hunting for some signal trouble.

After collecting some signals on the oscilloscope it was apparent that multi-path was the problem. But what structure was causing the multi-path? With the aid of basic mathematics and computer mapping software, the location of the multi-path structure was found.

The results of the investigation have taught the author with firsthand experience the importance of the multi-path phenomenon and an effective method in finding the location of the multi-path structure. In addition, considerations for construction projects in the terminal area can be learned as well.

## 2. RELEVANCE FOR NEXTGEN

Why is a DME interference case study relevant to improving flight inspection for NextGen? The United States Federal Aviation Administration (FAA) defines NextGen as "an umbrella term for the ongoing, wide-ranging transformation of the National Airspace System (NAS)"<sup>1</sup>. The United States DME infrastructure is in fact growing under this umbrella as evidenced by pending contracts to acquire new DME systems in 2010. Whereas DME/DME positioning is considered a top candidate for backup to the susceptible GNSS, maintaining technical and flight inspection expertise of DME issues is necessary. In

addition, the topographical and RF environment is growing in complexity resulting in DME susceptibility to interference and multi-path issues. As long as DME is relied upon as a primary or backup positioning sensor for RNAV, improving flight inspection capabilities and techniques for DME facilities is a worthwhile endeavor. This paper provides a complex case study of the Arnel (AML) DME multi-path issue and builds on the results to discuss methods we might employ to improve future DME flight inspection under the NextGen umbrella.

### 3. DME PROBLEM DISCOVERY

Flight inspection recordings during a routine flight inspection of the Dulles International Airport revealed a problem with the Distance Measuring Equipment (DME) signals.

Figure 1 shows part of the flight recording during an in-bound approach flight profile

on a 300 degree radial. Notice the DME status trace at point “A” in Figure 1. The DME status trace can indicate one of three values: locked, coast, and unlock. At point ‘A’ the DME status went from the baseline locked status to coast briefly and then to unlock. Simultaneously, the DME range error trace indicated a sudden large increase in range error at point ‘B’ in Figure 1. Notice similar conditions re-occur a bit later in this recording.

Additional clues to the DME problem were measured on a 17 mile orbit flight profile. At a bearing of approximately 315 degrees the DME coasts and loses lock with an associated increase in DME range error. A similar situation occurs at a bearing between 146 and 150 degrees.

Figure 2 illustrates on an aerial photo the bearing direction from the ground station to each of these DME problem areas.

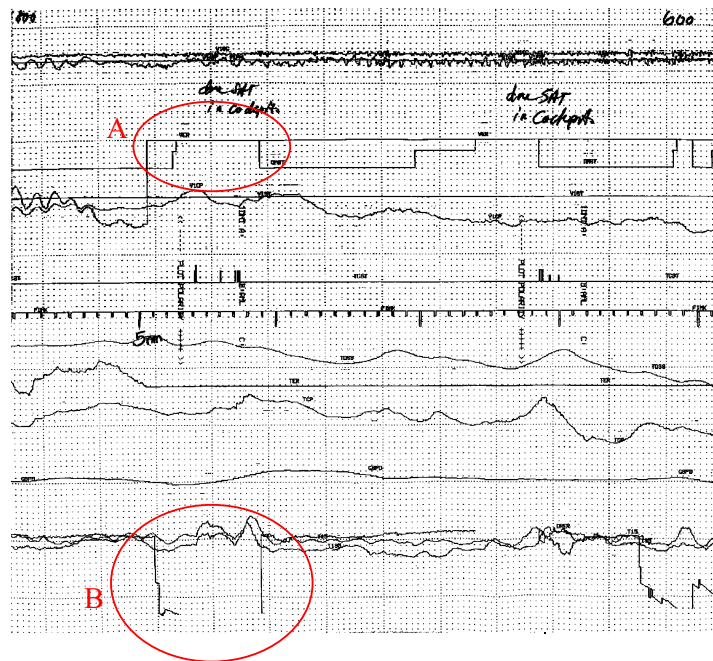


Figure 1

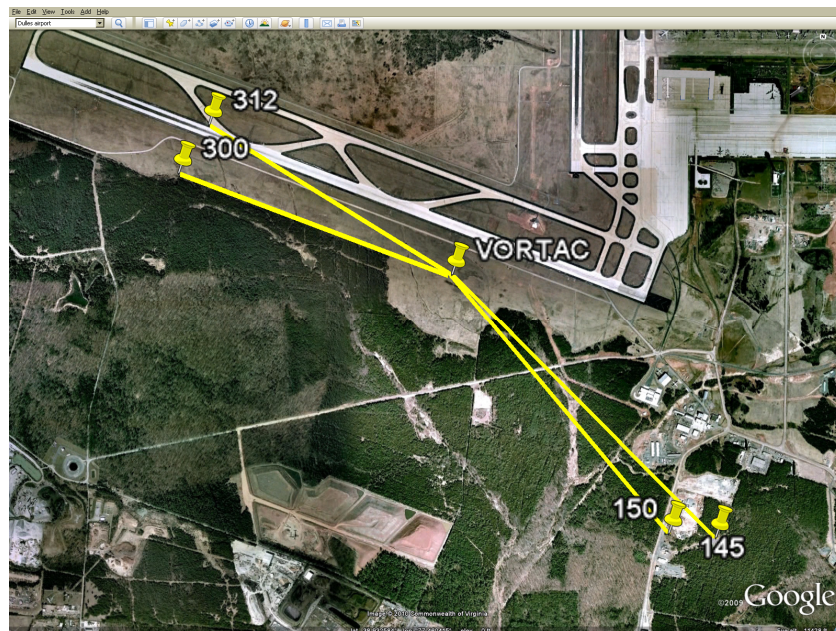


Figure 2

#### 4. A Brief Review of DME

Distance measuring equipment (DME) utilizes a receiver-transmitter in the aircraft and a transponder at the ground station. The term ‘transponder’ is short for *Transmitter-responder* and is defined as a receiver-transmitter that will generate a reply signal upon proper electronic interrogation<sup>2</sup>.

During flight, the aircraft’s DME receiver-transmitter sends an interrogation signal on the frequency corresponding to the desired ground station. After receiving the interrogation, the ground station transponder delays a pre-defined time,  $T_0$ , and replies on a “paired” frequency. The round trip distance can be calculated by subtracting the ground station delay time from the total elapsed time and dividing by the speed of the radio waves.

The formula to calculate the one way distance in terms of nautical miles is:

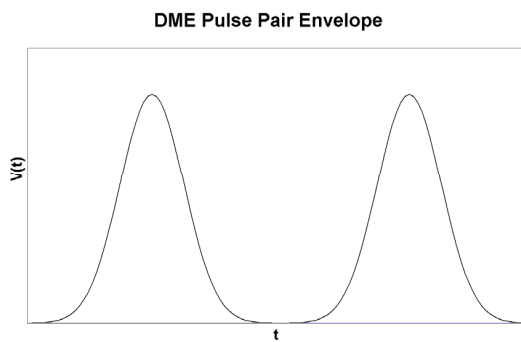
$$D = (\Delta t - T_0) / 12.35 \mu\text{s}/\text{NM} \quad [3]$$

Where  $\Delta t$  is the total elapsed time,  $T_0$  is the time delay of the transponder equipment, and 12.35  $\mu\text{s}$  is the time for radio waves to travel one nautical mile and back, also known as the radar mile.

Carrier frequencies for the DME system are assigned the range of 915 to 1213 MHz. The ground station reply carrier frequency is either 63 MHz higher or lower than the interrogation carrier frequency, depending on the channel type (X or Y). Simple pulse pair modulation is used to distinguish valid interrogations from noise pulses. Gaussian shaped pulses reduce the bandwidth of the emitted signal. Figure 3 illustrates the modulation envelope of a Gaussian pulse

pair used for aircraft interrogations and ground station replies.

The spacing between pulses determines the type of channel. For X channels the time delay between pulses, measured at the 50% leading edge point, is 12 us for both interrogations and transponder replies. For Y channels the time delay between pulses is 36 us for interrogations and 30 us for transponder replies.



**Figure 3**

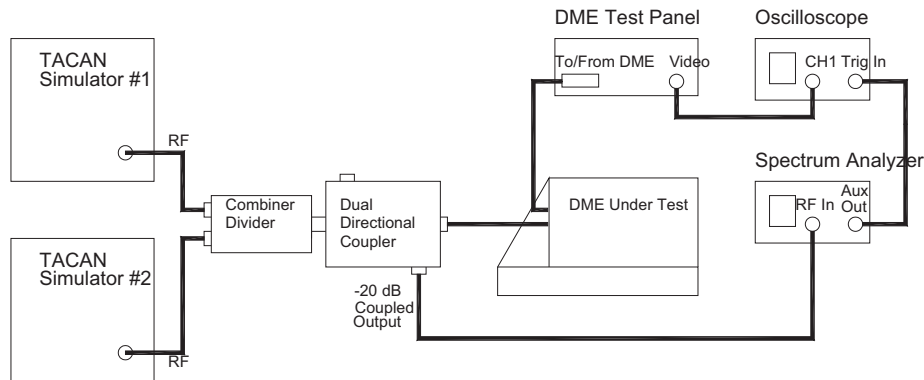
The last significant point to remember in DME system operation is how to distinguish

ground station replies to other aircraft from your own reply. The aircraft DME transceiver uses a time correlation technique along with random intervals of interrogations to isolate the desired ground station reply from all other replies<sup>4</sup>.

## 5. DME Problem Investigation

### 5.1. Preparation

Some preparation was in order prior to the actual visit to Dulles and airborne investigation. Two objectives were in mind during the preparation. First, practice with the oscilloscope was needed in finding and tracking the DME ground station replies to our interrogations. Second, since we were guessing that the problem may be multi-path, we wanted to simulate a multi-path scenario for the DME instrument we use in our flight inspection aircraft to obtain some preliminary idea about how the DME behaves in the presence of a multi-path signal. Figure 4 illustrates the equipment setup in the lab for this testing.



**Figure 4**

To capture ground station replies we needed to use the oscilloscope in an externally

triggered mode. The trigger signal needed to be our DME pulse pair interrogation. This signal was obtained by connecting to

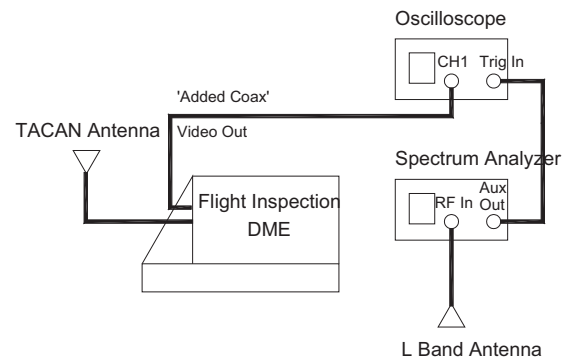


the coupled port of the directional coupler and routing this signal to the spectrum analyzer RF input. The spectrum analyzer was setup for a span of 0 Hz and a center frequency corresponding to the carrier frequency of the DME interrogation pulse pair. By using the 0 Hz span setting the spectrum analyzer is put into a time domain mode and the video signal output on the Aux Out connector serves as the oscilloscope trigger input.

The demodulated ground station reply was supplied by connecting CH1 of the scope to the video connector of the DME Test Panel. Since the ground station reply signal is delayed, use of an oscilloscope with a time base delay feature is essential in observing these range replies.

Despite using varying amplitudes and delays for the simulated multi-path signal, we could not duplicate any DME coast or unlock status conditions with our test setup when TACAN Simulator #2 was added as a multi-path source.

With instrument familiarization complete, the final item of preparation required was a slight modification of the flight inspection aircraft. One coax cable was added to access the DME video signal for connection to the oscilloscope that would be used during the airborne investigation. Figure 5 illustrates the functional block diagram of the aircraft troubleshooting setup.



**Figure 5**

## 5.2. Day 1 Investigation Activities

On September 10, 2009, a flight inspection plane and crew were scheduled to help investigate the DME problems at Dulles Airport associated with the ARMEL VORTAC. The investigation strategy consisted of eight in-bound approach flight profile runs, each run testing a different ground station configuration. Different antennas and echo suppression settings were tested for effect on the DME problem. During each run, an engineer on the flight inspection plane monitored ground station replies on the oscilloscope for abnormalities.

The first approach profile run confirmed the same DME problems areas without any parameter changes to the ground station using the standard VORTAC antenna.

During the second approach profile run the echo suppression settings were changed. The original settings for that ground station were a gate width of 150uS and a power threshold of -30 dBm. Echo suppression is a technique used by ground stations to prevent a multi-path interrogation signal from triggering a second ground station reply. The gate width is the length of time the ground station 'looks' for a multi-path signal

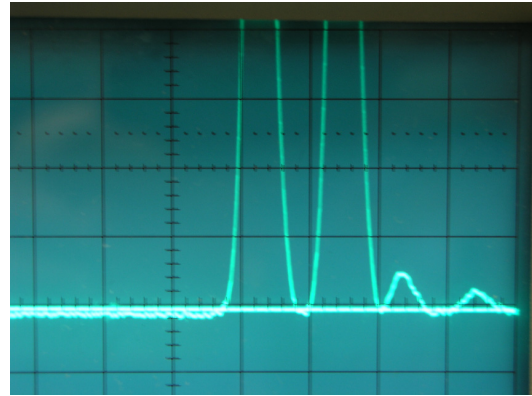
after a valid interrogation pulse pair, and the threshold setting is the level during the gate time that a signal must exceed to be considered multi-path. So for normal settings the ground station will suppress the reply for any multi-path that arrives within 150 us after the direct interrogation signal arrives with a signal strength exceeding -30 dBm.

With echo suppression settings of 400uS and -70dBm, DME coast and unlock conditions continued to be observed on the flight recordings during the second approach flight profile run.

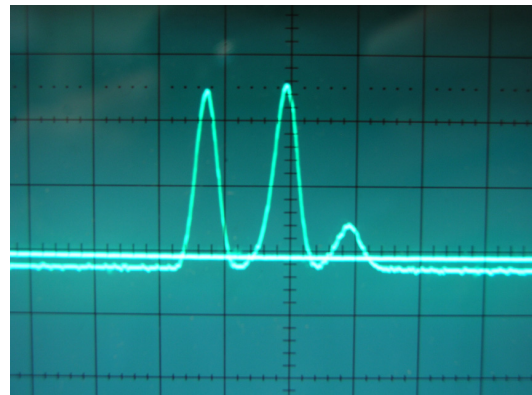
Likewise, DME problem areas did not improve during the third and subsequent approach flight profile runs with different antenna types mounted outside the VORTAC structure.

During all these runs, however, some interesting oscilloscope results were captured and saved to the oscilloscope memory for later review. Signal stability was an issue for most of the day, complicating the tracking of the ground station replies, until it was realized that the DME automatic scan mode of six ground stations was causing the problem. The stability problem was eliminated after putting the DME in manual mode and looking at just the ground station of interest.

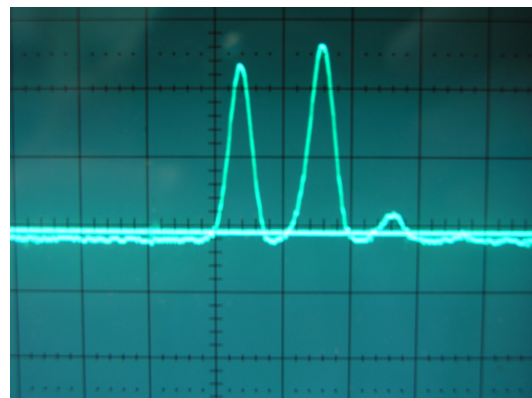
The following waveforms were captured. The oscilloscope setting for each waveform capture was 10us/div and 0.5 V/div. Unfortunately, the ground configuration for waveform captures for memory locations 3 – 6 were not recorded due to the pre-occupation of trying to find and track the ground signals - a detail we would correct on day 2.



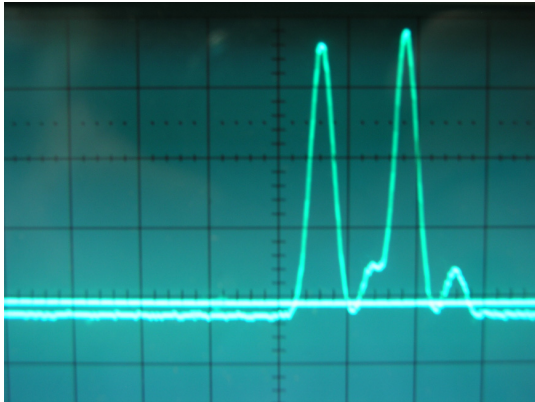
**Figure 6, Memory Location 3**



**Figure 7, Memory Location 4**



**Figure 8, Memory Location 5**



**Figure 9, Memory Location 7**

Memory location 7 was captured at a range of 28 miles and an altitude of 4000 feet.

The last interesting piece of data observed during the flights was the performance of the cockpit DME during the approach flight profile runs. Unlike the flight inspection DME that would coast or unlock, the cockpit DME would appear normal or sometimes, during its range countdown on the approach, suddenly jump back to a higher range by approximately 0.5 – 0.75 nm.

### 5.3. Analysis of Day 1 Activities

After seeing the captured ground station reply waveforms, it was evident that, indeed, a multi-path problem existed. Was it an aircraft interrogation multi-path or a ground station reply multi-path problem? If the ground station was producing two replies, one from the direct path and one from the multi-path signal from the aircraft, we would expect to see two equal amplitude sets of pulse pairs, one delayed by the additional multi-path distance. However, the captured waveforms show a strong reply from the direct path and a delayed weaker reply. The conclusion is that this must be multi-path from the ground station to the aircraft.

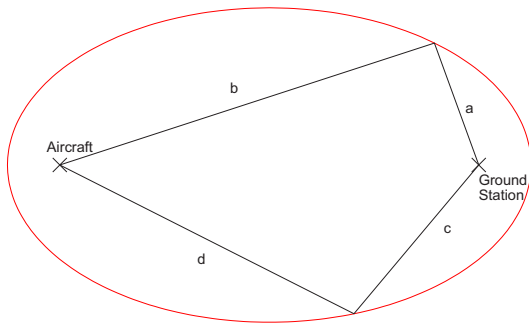
The second observation was that the multi-path delay time was such that the first pulse of the multi-path signal occurred in the vicinity of the second pulse of the direct path signal.

Ground maintenance engineers designed some of their corrective measures on the hunch that the airfield was the multi-path reflector. Thus, some different antennas were brought to the sight and mounted on monitor poles. It was hoped that the increased radiation angle of these antennas would prevent the reflections off the airfield. These corrective measures did not effect any improvement of the DME problem areas on this day.

Nonetheless, day one was productive. We had conclusively identified a multi-path problem with the ground station replies, and the multi-path signal was occurring at a time that could be corrupting the second pulse of the direct path pulse pair. From this data some questions naturally came to mind. What is the structure that is causing the multi-path? How does our Flight Inspection DME instrument process reply signals; in particular, what role does the second pulse of the pulse pair play in processing range replies and could deformity of that pulse cause the status problems that we have been seeing?

After digging into the documentation for our DME instrument and reading the theory of operation, this question was answered. A five microsecond window is used to receive the second pulse after reception of the first pulse. If the second pulse is not detected the first pulse is discarded as invalid. Reading between the lines it seemed plausible that if the second pulse was corrupted, especially the leading edge, it could also cause the pulse pair to be rejected. Missing too many replies could cause the DME to coast and unlock.

What structure could be causing the multi-path signal? We had some guesses after visiting the site: the airstrip and some metal buildings not far from the end of Runway 12. However, after calculating the additional distance the delayed pulses represented, the air strip theory did not fit the data. I discussed this investigation with one of my co-workers at the FAA in Oklahoma City. He came to the realization that the locus of all points where the multi-path structure could be located is defined by an ellipse. The foci of the ellipse would be the position of the flight inspection aircraft and the position of the ground station. The geometry is illustrated in Figure 10.



**Figure 10**

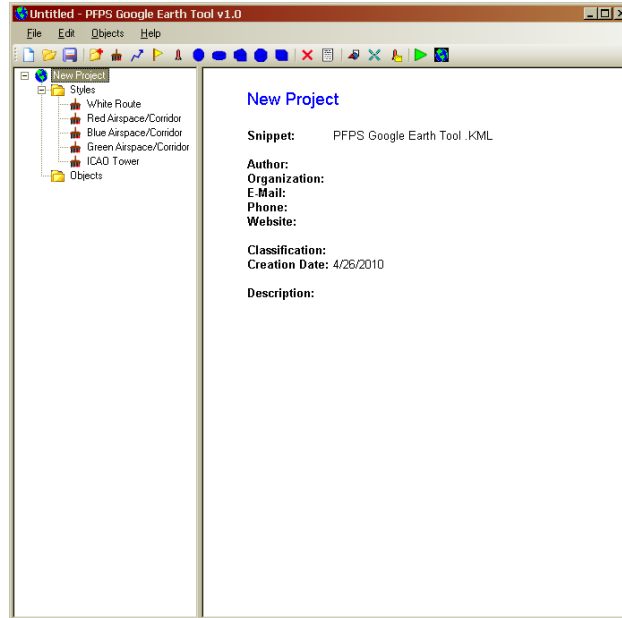
For an ellipse any path from one foci to the ellipse and to the other foci represents a constant distance. For example, in Figure 10 the two paths defined by  $ab$  and  $cd$  are equal in length. This realization allows us to focus our search for the multi-path structure knowing the distance between the aircraft and the ground station and the additional multi-path distance. Fortunately, we had one oscilloscope capture for which we knew the approximate aircraft position; which we could use to plot a real world example.

In addition, a tool exists, created by pilots to help visualize flight plans, which could be used with Google Earth<sup>5</sup> to overlay certain geometric shapes onto a Google aerial map. The tool is called PFPS Google Earth Tool v1.0<sup>6</sup>.

#### 5.4. PFPS Google Earth Tool Tutorial

The next few paragraphs will give a short tutorial on how to use the PFPS Google Earth Tool to generate an ellipse object using the stored waveform and import it into Google Earth.

Figure 11 illustrates the PFPS Google Earth Tool v1.0 after starting the application.



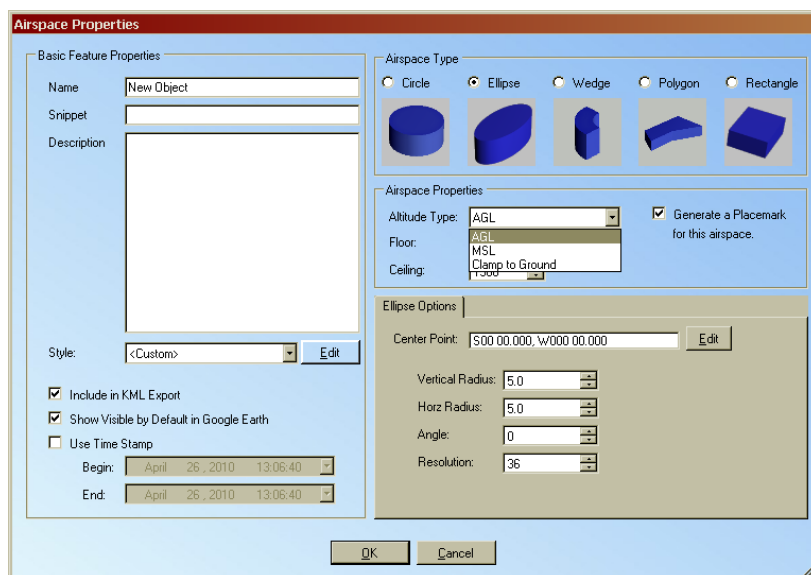
**Figure 11**

To generate an ellipse object click on Objects > New Airspace > Ellipse, or click the ellipse on the toolbar. Figure 12 is the Airspace Properties window that appears.

Give the airspace object a name. In the Airspace Properties section of this window

choose Clamp to Ground for the Altitude Type.

Under the tab Ellipse Options we need to determine the ellipse center point. We will have to do some preliminary work in Google Earth to find the ellipse center point.



**Figure 12**

Start Google Earth and use the Find Businesses tab to fly to Dulles Airport. Find the AML VORTAC beside Runway 12.

Use the Ruler tool and click on the Line tab of the Ruler dialog box. Since distances collected in our Flight Inspection equipment are in nautical miles, select the Nautical Miles option for the Length field. Now click on the AML VORTAC to start the line measurement and extend it 14 nautical miles on a 300 degree magnetic heading (the waveform was captured when the aircraft was approximately 28 NM from the ground station). Google displays headings referenced to true north, requiring conversion of our magnetic heading by using the declination value of the area. One way to find the declination value is using the magnetic declination calculator at the National Geophysical Data Center web site (<http://www.ngdc.noaa.gov/geomagmodels/truts/calcDeclination>). Entering the AML VORTAC coordinates and September 10, 2009 for the date we obtain a declination value of 10.30 W. The converted heading, then, is 289.70°.

After measuring 14 nautical miles on a heading 289.70 from the VORTAC, put a placemark at this location. Right clicking on the placemark and selecting properties will show latitude and longitude information as well as other items. After obtaining the latitude and longitude information for the center of the ellipse, return to the PFPS Google Earth Tool.

In the PFPS Google Earth Tool, click the Edit button beside the Center Point field. Select the correct format and input the coordinates obtained from Google Earth and click OK.

The vertical and horizontal radius of our ellipse will have to be calculated. The

length of the minor axis of an ellipse is given by:

$$\text{Minor axis} = \sqrt{(a+b)^2 - f^2} \quad [7]$$

Where a and b are illustrated in Figure 10 and f is the distance between the foci. We know a+b, in our case, as the multi-path length. This is the actual range noted when the waveform was captured plus the distance the delayed signal represents.

The extra distance represented by the delayed signal is:

$$D = (.75 \text{ div})(10\text{us/div})(3 \times 10^8 \text{ m/s}) / (1852 \text{ meters/nautical mile}) = 1.21 \text{ nautical miles.}$$

The minor axis, then, is:

$$\text{Minor axis} = \sqrt{(29.21)^2 - (28)^2} = 8.32 \text{ nautical miles.}$$

The vertical radius will be half this, or 4.16 nautical miles.

The major axis is a+b. [7]

From the work above a+b = 29.21 nautical miles.

Before entering in this information into the PFPS Google Earth Tool, we need to know how this ellipse will be imported into Google Earth. First, the radius information entered into PFPS should be in nautical mile units. Secondly, the ellipse will be placed with the vertical axis pointing true north in Google Earth when the angle entered in the PFPS tool is 0. Positive values of angles entered into the PFPS tool will rotate the ellipse placement clockwise.

For this example, enter 4.16 nautical miles for the vertical radius, and 29.21/2 (14.6) nautical miles for the horizontal radius. Since the horizontal axis of the ellipse will

be pointing at 90 and 270 degrees with 0 rotation, we need to enter 19.70 for the rotation to achieve our bearing of 289.70 degrees from the VORTAC. Figure 13 shows the completed Airspace Property for our ellipse. Click OK. With the newly created object selected use File>Export to KML file or the green button on the toolbar to export the KML file.

After launching Google Earth, click File>Open and browse/select the file exported from PFPS. Figure 14 illustrates the resulting display in Google Earth after the ellipse import. Figure 15 shows a close-up of the terminal area with the imported ellipse present.

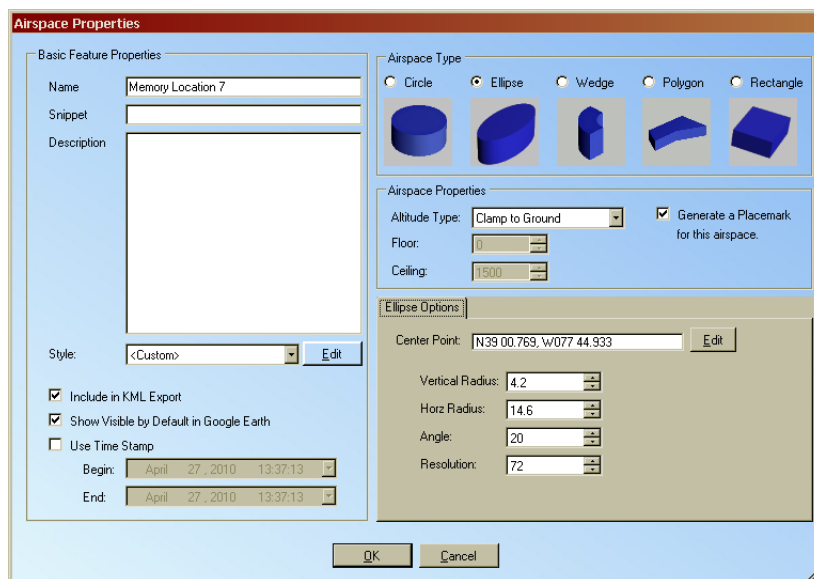
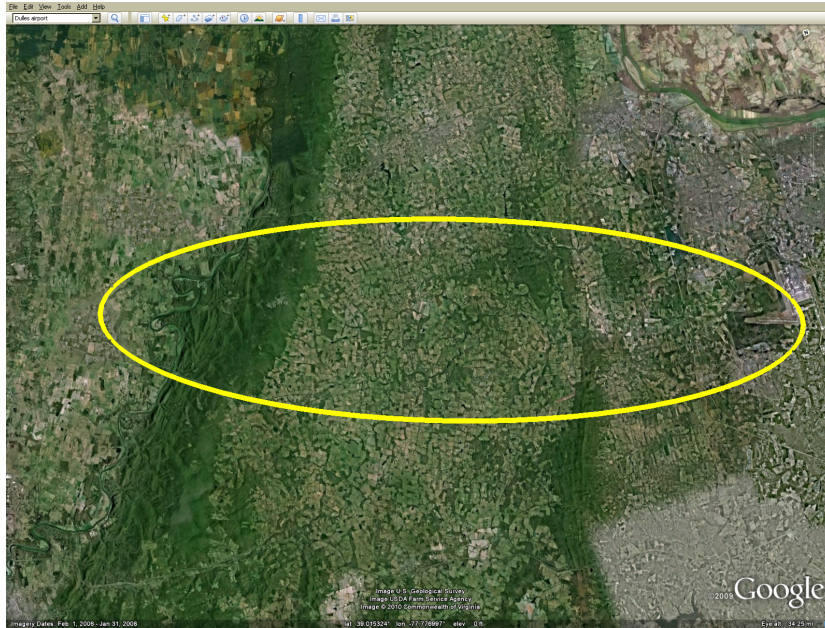
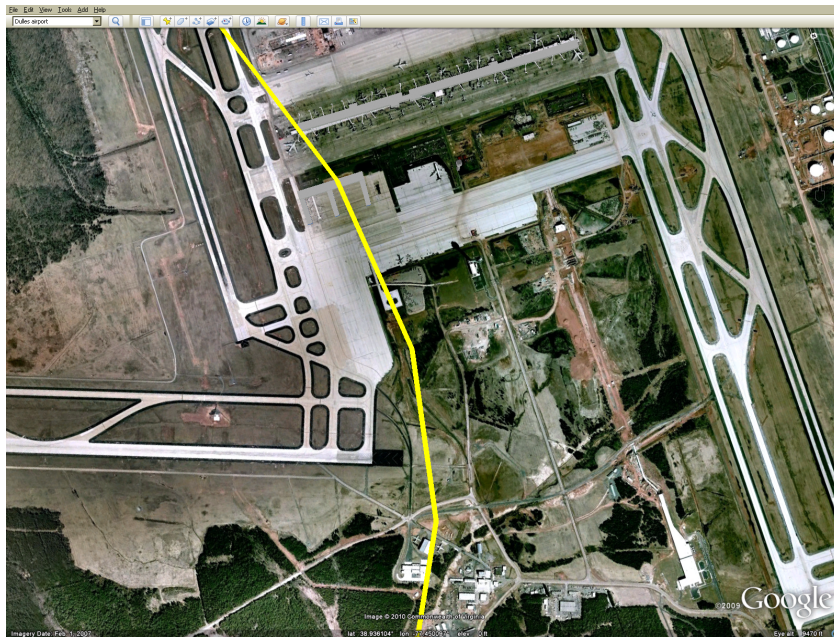


Figure 13



**Figure 14**



**Figure 15**

During the next flight inspection opportunity, our plan was to collect accurate data about

the aircraft position by obtaining GPS latitude/longitude coordinates at the instant the oscilloscope signal was captured. In



addition, we hoped to obtain enough data to plot at least two ellipses, the intersection of these pinpointing the multi-path structure.

#### 5.5. Day 2 Investigation Activities

On day 2 we added a 7 mile orbit flight profile and an approach flight profile to one of the other Dulles runways with the hope of obtaining multi-path signals on the oscilloscope from different angles. This was in addition to many approach flight profile runs on Runway 12.

During these flight runs ground maintenance was busy configuring equipment between runs to identify possible solutions. The first change tested a DME antenna located at the top of the TACR monitor pole. This antenna had a main beam of radiation angled up at  $3^\circ \pm 1^\circ$ . Echo suppression was used in conjunction with this antenna. Flight recordings showed some improvement, but unlocks were still occurring.

The next change tested an antenna that provides vertically polarized, omnidirectional coverage with a main beam of radiation angled up at  $7^\circ \pm 1^\circ$  to minimize the effects of ground reflections. This antenna showed the most promise to resolve the issue of multi-path. Flight check made several runs to confirm DME coverage with both approach and coverage orbit flight profiles. Flight check reported seeing reflections but no DME unlocks.

As an additional refinement, this antenna was fitted with a full length pattern shaping element to further reduce the RF energy from the air traffic control (ATC) tower, the suspected multi-path structure at the time. The element reduces the RF energy in a pattern of approximately  $50^\circ$  in a pie shape. The element was aligned on the radial of the ATC tower. Flight inspection aircraft reported some improvement with a decrease of the reflected signal during approaches. When a coverage orbit was flown the  $50^\circ$  area around the ATC Tower was unsatisfactory with DME loss in the cockpit and some loss with the flight inspection DME.

The last ground station configuration change was to use a Y channel DME configuration. The ground station was configured to be 82Y instead of 82X. Permission from the spectrum manager was obtained prior to the re-configuration. The flight inspection DME never experienced a DME status problem during this run.

A total of 46 waveforms were captured during these flights. Figure 16 shows the printout, hand labeled by the flight inspection technician as Mk4, from the flight inspection system at the same time that memory location 4 was captured on the oscilloscope, shown in Figure 17.

```

-----
                                DME/FIX UPDATE CONTROL
DME GATE 01.1
NAU MODE MN-DME ID ERR      RNG/BRG  FREQ  CHNL

          AML  0.0  007.1/031^ 113.50
          AML  0.0  007.1/031^ 113.50
          AML  0.0  007.1/031^ 113.50
          AML  0.0  * 007.1/031^ 113.50
          AML  0.0  007.1/031^ 113.50
          AML  0.0  007.1/031^ 113.50 002X

IDME FREQ 113.50      CHNL 002X      IDME RNG 007.10

          LAT      LONG
RNU POS N030^49'34.7 W077^31'37.9  BALT-F 01501FT
FI FAC  N030^49'04.5 W077^28'00.1  A/C HDG 124.07^
GND STN N000^00'00.00 W000^00'00.00  00000FT

          IRU  N030^49'25.7 W077^31'31.3
          GPS  N030^49'30.0 W077^31'43.0
          HYBRID N030^49'30.0 W077^31'41.2
          DGPS  N***^**^***.**

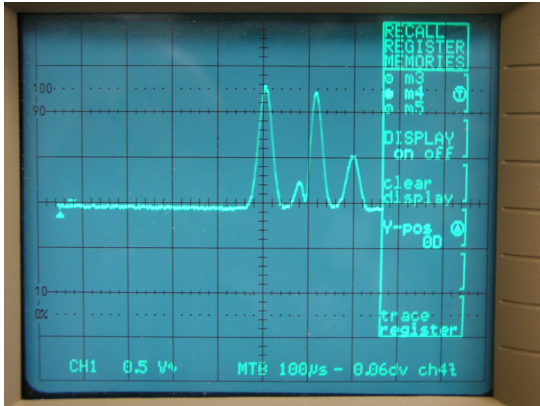
          HDOP 001.0      UTC 11:44:17  ST 08
          UDOP 001.5      DATE 10/07/09  SU 08
          VFCM 181M      MODE NAU
          HFQM 150M
          FINAV MODE: RNAV      DR VELOCITY 1SS
-----

```

*Handwritten notes:*  
 217  
 MK 4

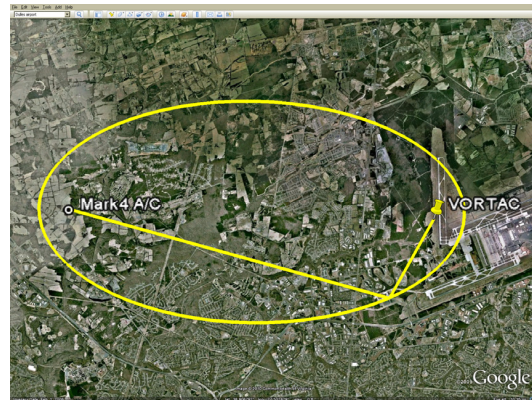
**Figure 16**

profile and it was hoped that collecting the multi-path signal from a different angle would help narrow down the location of the structure causing the multi-path and causing the DME status problems on approach to Runway 12. Figure 18 shows the resulting ellipse in Google Earth.



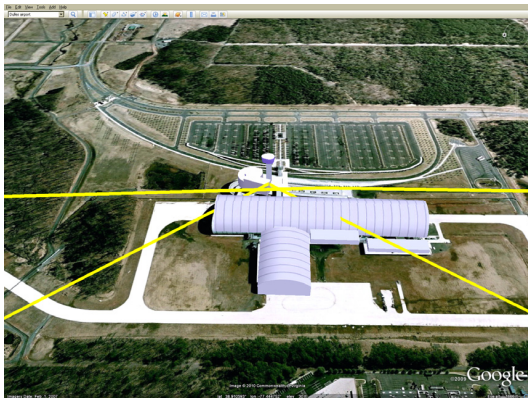
**Figure 17**

Using the signal delay of the multi-path shown in the scope capture and the aircraft hybrid coordinates shown in Figure 16, an ellipse airspace object was created using the procedures discussed earlier and imported into Google Earth. Memory location 4 was captured during the seven mile orbit flight



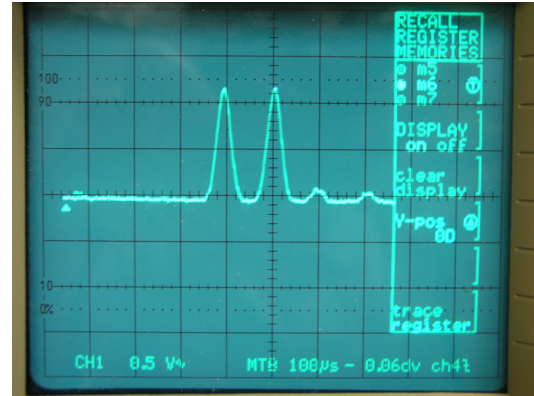
**Figure 18**

Interestingly, it looked like the only structure on this plotted ellipse that could be causing multi-path is illustrated by the white lines in this figure. After zooming and panning in from a different angle in Google Earth and making sure that the 3D buildings layer is enabled in Google Earth, we get the image in Figure 19. The tower or associated buildings at the National Air and Space Museum appear to be the structure causing this multi-path signal.



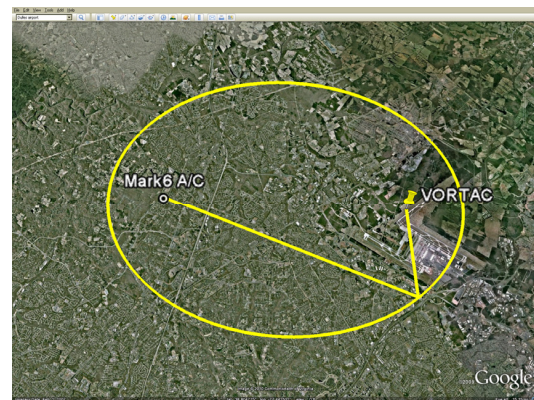
**Figure 19**

The next multi-path signal that looked interesting, due to the much longer signal delay, was the signal captured at Mark6 during the seven mile orbit. Figure 20 shows the multi-path signal capture.



**Figure 20**

The location fix and the signal delay obtained resulted in the ellipse pictured in Figure 21. A close-up view of the probable multi-path structure along the ellipse path is illustrated in Figure 22.



**Figure 21**

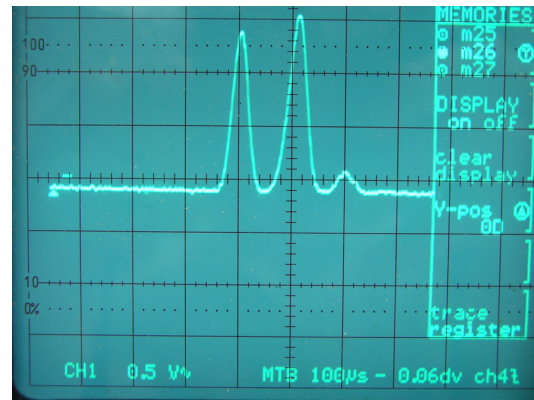


**Figure 22**

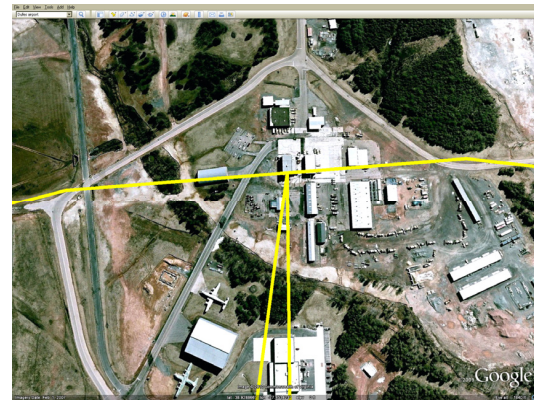
After plotting these ellipses and identifying probable multi-path structures, two realizations started to come into focus. First, the multi-path structure not only has to be located at the right distance represented by the additional signal path length, but the structure must also have a surface angled correctly to produce a reflection from the ground station to the aircraft. Consequently, our strategy of trying to obtain a multi-path signal captured on the oscilloscope from a different angle than the approach to Runway 12 would probably not be successful. The second realization, interesting to a developing signal interference sleuth, is that there is no lack of multi-path signals in the terminal area, especially in a city area like this with many taller buildings. Unfortunately for the AML VORTAC ground station, there is a structure located just the right distance and has a surface at just the right angle to corrupt the second pulse of the DME pulse pair.

Thus, we turned our evaluation to the day 2 oscilloscope data collected on approach to Runway 12. The waveform shown in Figure 23 was captured 13 nautical miles from the ground station on approach to Runway 12 during a DME coast indication. This type of waveform was observed quite often (as on

day 1) but mostly ignored due to the apparent absence of the second multi-path signal. We later realized there actually was a second multi-path signal present, disguised as the second, larger amplitude direct path pulse. From this waveform it appears the multi-path is delayed 9 uS. Figure 24 shows a close-up of the resulting ellipse plotted in Google Earth. The complex of buildings near the east of Runway 12 seems to be the likely structures causing the multi-path on this oscilloscope waveform capture.



**Figure 23**

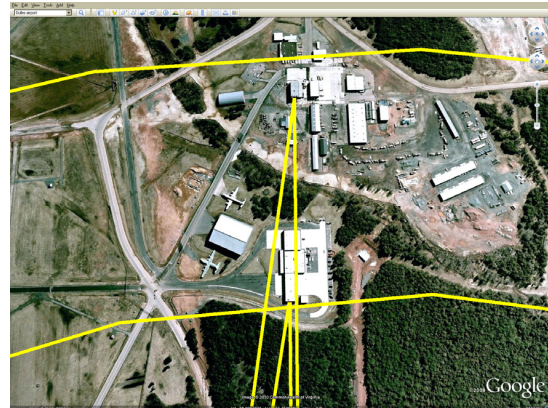


**Figure 24**

Oscilloscope memory location 27, shown in Figure 25, was also captured at about the time the DME indicated coast on the flight recording. This scope capture is interesting due to all the multi-path present. Not only is there a multi-path return on the trailing edge of the direct path return, but there is also another multi-path signal visible approximately 8-9  $\mu\text{s}$  after the second pulse of the direct path return. Apparently, the corresponding multi-path signal from the first pulse of the direct return is occurring when the second pulse of the direct return is developing. See how the leading edge of the second, direct pulse is widened some and the overall pulse amplitude is higher. Notice also the shape of the multi-path signal occurring 8-9  $\mu\text{s}$  after the second pulse of the direct path return. It is wider and has a flatter peak. Perhaps this is a composite waveform of two different multi-path signals from slightly different distances. Figure 26 shows the resulting ellipses when multi-path delays of 7 and 9.5  $\mu\text{s}$  are used to plot two ellipses in Google Earth.



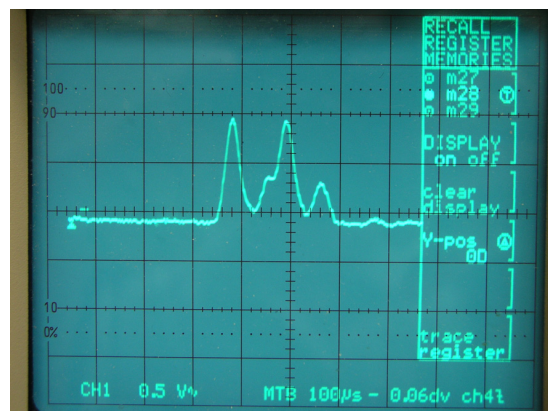
**Figure 25**



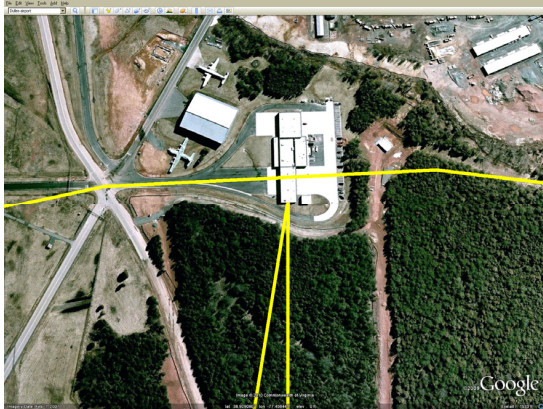
**Figure 26**

Again, the complex of buildings near the east end of the runway seems to be the best candidate for causing the multi-path signal captured in Figure 25.

The last oscilloscope capture that will be discussed is shown in Figure 27. The aircraft was on approach to runway 12 and was 7.43 nautical miles from the ground station when the waveform was captured. The multi-path signal is fairly strong on this waveform and appears to be delayed by 7  $\mu\text{s}$ . The resulting ellipse imported in Google Earth is shown in Figure 28.



**Figure 27**



**Figure 28**

Again, the complex of buildings near the east end of the runway seems to be the best candidate for causing the multi-path signal captured in Figure 27.

#### 5.6. DME Problem Solution Options

During the course of the investigation several alternate ground station configurations were tested by ground maintenance engineers: various echo suppression settings with the standard VORTAC antenna, antenna with 3° radiation angle mounted on a monitor pole, antenna with 7° radiation angle mounted on a monitor pole, antenna with 7° radiation angle plus a pattern shaping element designed to notch out the area toward the air traffic control tower, and a Y channel configuration using the standard VORTAC antenna. The omni-directional 7° antenna configuration and the Y channel configuration proved the best solutions.

Due to numerous VORTAC stations in the eastern part of the U.S., the Y channel solution was not readily implemented. This station re-assignment would require frequency re-assignments in other nearby VORTAC stations causing a ripple effect for

VORTAC frequency assignments. Therefore, the omni-directional 7° antenna configuration was put into operation.

## 6. Case Study Results and Current Flight Inspection Policy

Current flight inspection policy in the U.S. evaluates a DME on each procedural leg and on a flight inspection service volume coverage orbit. Unless restrictions are identified, this policy assumes the DME is operational everywhere else. Considering the amount of multi-path discovered in this case study, the probability of an undetected DME multi-path problem seems likely. If RNAV provides aircraft capability to navigate at any location along any path, we need to guarantee DME availability for users requiring DME as a primary or backup positioning sensor. How do we improve flight inspection procedures so that all DME problems can be identified without flying every square mile of the coverage area? If possible we would like to make an analysis in advance of the flight inspection that flight inspection crews could use to focus their efforts. The authors are investigating a software tool that could generate a report showing possible DME signal loss areas due to multi-path. The use of such a tool would add value to flight inspection by providing a manageable process of identifying theoretical areas where DME signal loss could occur, thus limiting additional flight inspection to the few, if any, theoretical problem areas.

The authors propose the flight inspection community consider predictive DME multi-path analysis as a requirement on all new DMEs considered critical for RNAV in the NAS. This predictive analysis would recommend flight inspection paths in addition to those currently required to

determine if any areas of DME loss are significant enough to pose navigation solution issues for aircraft relying on DME as a primary or backup navigation sensor.

## 7. Conclusion/Lessons Learned

This DME case study was rich in lessons learned for the authors. Setting up and using lab equipment to test the DME for multi-path and familiarization with equipment prior to the flight inspection proved invaluable, especially at the pace at which things happen during flight. Flying in the Dulles airport area and monitoring the range replies revealed that DME multi-path signals are not uncommon. For the DME system, multi-path becomes a problem when the multi-path structure is located at just the right distance and has a structural surface angled at just the right angle to reflect the range reply to the airplane. This multi-path corrupts the second pulse of the direct path pulse pair, causing rejection of these replies and eventual coast and unlock conditions due to the rejected replies. For DME signals, multi-path can be analyzed using simple geometric ‘ray analysis’: straight lines and incident angles approximately equaling reflected angles. Terminal area construction projects would do well to guard against constructing a building surface that would allow reflections from DME ground stations to reflect down the path of a runway approach. The realization that the locus of multi-path structure locations could be defined as an ellipse was groundbreaking for us. Using the PFPS Google Earth Tool to generate the ellipse air space and importing into Google Earth made for a very practical tool in locating the possible multi-path structures. The relevance of this paper for NextGen is the concern for ensuring DME signal integrity in the expanded NextGen airspace.

## REFERENCES

- [1] “What is NextGen?” 3 May 2010. <[http://www.faa.gov/about/initiatives/nextgen/why\\_nextgen\\_matters/what/](http://www.faa.gov/about/initiatives/nextgen/why_nextgen_matters/what/)>.
- [2] “Transponder.” Wikipedia. 20 April 2010. <<http://en.wikipedia.org/wiki/Transponder>>.
- [3] Helfrick, Alfred: “Principles of Avionics,” 5<sup>th</sup> Edition, Avionics Communications Inc., 2009
- [4] Helfrick, Alfred: “Principles of Avionics,” 5<sup>th</sup> Edition, Avionics Communications Inc., 2009
- [5] “Google Earth.” 27 April 2010. <<http://earth.google.com/>>.
- [6] “PFPS Google Earth Tool.” 27 April 2010. <<http://www.googleearthpilot.com/>>.
- [7] “Major / Minor axis of an ellipse.” Math Open Reference. 27 April 2010. <<http://www.mathopenref.com/ellipses.html>>.

## ACKNOWLEDGEMENTS

The AML DME problem investigation was truly a team effort and I would like to acknowledge that fact. I would like to thank the flight inspection crews from Atlantic City that patiently flew the many flight profiles while engineers collected data to find solutions. I would like to acknowledge the ground maintenance engineers that expertly reconfigured the ground station between flight profiles: Donald Reiss, Frank Floteron, and Wayne Bullock. Finally, I would like to acknowledge and thank Dale Rhoads for passing on his

knowledge from his past DME troubleshooting experiences. Dale is a Supervisor in the Aircraft Maintenance and Engineering Group at the FAA's Mike Monroney Aeronautical Center.

#### **ABOUT THE AUTHORS**

Todd Bigham is an Electronics Engineer in the Aircraft Maintenance and Engineering Group at Mike Monroney Aeronautical Center. Mr. Bigham has been with the FAA since 2009. Mr. Bigham graduated with a B.S. in Applied Mathematics and a B.S. in Electrical Engineering. Mr. Bigham worked

for the Air Force for 20 years in the automated test equipment field developing automated tests for avionics prior to coming to the FAA.

Brad Snelling is a graduate of the United States Air Force Academy and The George Washington University with a B.S. and M.S. in Aeronautical Engineering. He is an Airspace System Inspection Pilot and Test Pilot conducting certification and operational flight tests for the FAA. Brad has over 4,500 hours in multiple aircraft types flying for the United States Air Force, Northwest Airlines, and the FAA.



## Airborne RFI Detection For China Civil Aviation

### Mr. Pan Yi

Deputy Director  
Flight Inspection Center of CAAC  
23#, Tianzhu Road,  
Tianzhu Airport Industry Zone,  
Capital International Airport,  
Beijing,  
People's Republic of China  
E-mail: Pany@chinacfi.net



### Mr. Liu Tong

Deputy Director  
Development & Research  
Department  
Flight Inspection Center of CAAC  
23#, Tianzhu Road,  
Tianzhu Airport Industry Zone,  
Capital International Airport,  
Beijing,  
People's Republic of China  
E-mail: ltzhism@sina.com



### ABSTRACT

Facing to more and more radio frequency interference (RFI) hazards to civil aviation, many flight inspection organizations are appointed to establish airborne RFI detection capability based on their airborne equipment superiority. Airborne RFI detection technology research becomes a hot topic of Flight Inspection Symposium. This paper describes the configuration of airborne RFI detection equipments installed in flight inspection aircrafts of CFI, and how CFI implement airborne RFI detection.

### BACKGROUND

With the continuous and rapid development of China's economy, more and more radio and television stations have been set up, of which some district and county radio or television stations not only occupied a lot of frequency resources, but also resulted in the frequency band spreading or shifting due to rush construction, immature technology or insufficient filtering, and furthermore

frequently invading into civil aviation bands, leading to aviation radio interference events frequently. For the treatment of harmful radio interference, the national radio frequency management department had invested a lot of manpower and resources into setting up ground detection capabilities of radio frequency interference which consists of ground stations, terrestrial radio frequency interference detection vehicles and portable detection equipments, etc. However, due to the screening feature of radio frequency interference signals traveling along the surface of ground, by these means of radio detection, in most cases, it is very difficult to find the interference signal, almost the same as looking for a needle in a bottle of hay, in Chinese sayings, looking for a pin in the sea.

In order to effectively deal with the hazards to the civil aviation caused by radio interference, reduce the range of ground detections and improve the detection efficiency, China's civil aviation authorities decided to establish an air force, which makes use of the direct characteristic of radio frequency interference signals in the air, and thus quickly identify the region of the source of interference. Like other countries in the world Civil Aviation Administration of China also chooses flight inspection organization to implement this mission, it is because one of the prerequisites for realizing this capability is to own appropriate aircraft, and the exact positioning of the aircraft itself, as well as to own the orientation equipment equipped in ground detection vehicle, in the same time in order to increase the utilization of the aircrafts, reduce the comprehensive flight cost, and make the aircrafts taking other work into account

Next, we'd like to introduce what equipments the Flight Inspection Center of CAAC (CFI) installed and used for radio frequency interference detection. We hope to share our experience and make discussion with worldwide professionals, to improve detection technologies, so as to ensure a cleaner radio frequency environment for civil aviation security.

### What capabilities and equipments should be configured for airborne RFI detection?

To set up the airborne RFI detection capability, the following equipments were considered to be installed into our aircraft:

#### **-Spectrum Analyzer**

This equipment is used for observing and recording the information of frequency band which being interfered and determining the central frequency of the interference signal.

Upon the regular features, following key features of

Spectrum Analyzer should be highly concentrated on:  
 Frequency Range: should cover the whole Aviation Frequency Bands, including HF, VHF, UHF and L bands.  
 Marker functions which allows us to mark exact interference signals and display their information such as frequency, amplitude, etc.,

Spectrogram: a three dimensional representation of frequency, time and power is being used for identifying intermittent interference. The power levels are represented by different colors. With this function, we can record the spectrum during detection and replay it for re-analysis.

AM/FM/SSB should be able to be demodulated and output the audio.

The spectrum analyzer should be controllable by computer, and all the spectrum can be recorded and stored into computer hard disk or USB disk.

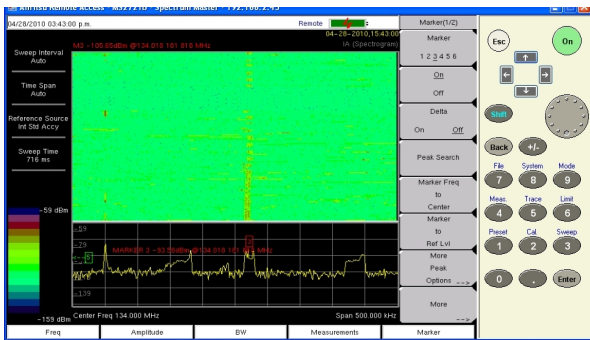


Figure 1 Spectrum display

### -Direction Finder

This equipment is used for detecting the bearing of interference source relative to the aircraft. Two Direction Finder Systems should be installed, one for VHF band and another for L band.

The direction finder should be able provide the relative angle of interference source against aircraft heading. The accuracy of detected direction should be within following:

±5 Degrees RMS

for VHF band

±10 Degrees RMS for VHF band

The direction finder could be controlled through computer software. And all the lobes can be recorded and displayed on a moving map.

Different demodulations allows customer to demodulate all kind of signal modulations.

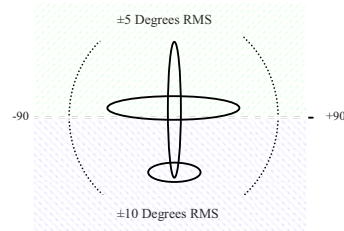


Figure 2 Error requirement of DF

### -Positioning System.

This system should combine by following:

A GPS/DGPS device can provide real time latitude and longitude of the aircraft. The existing GPS/DGPS system of flight inspection system can be utilized for this work.

Magnetic heading and attitude of the aircraft, they are very important for RFI source position calculation and screen display.

### -Voice Recorder

A voice recorder is installed into system for interference voice recording. It can help technicians analyze and identify the interference radio station, further more, provide evidence to relative authority when deal with problems.

### -VHF Communication

If the air-ground co-ordination is set up for rapid searching for a harmful interference source, VHF communication is very important for real time air to ground information exchange, with which better cooperation could be realized.

### -Audio panel

Through this equipment, operator can control the communications or choose any audio for listening, such as spectrum audio, DF audio, VHF audio. For an inspection system, this can be realized by improving the existing audio panel.

### -Computer

Different with other institutes and ground vehicle DF systems, our system was developed interference position calculation function based on DF lobes and real time aircraft position through multi-lobe intersections.

Normally, the performance of existing flight inspection computer is completely able to competent for the remote operation of spectrum analyzer and DF, collection of GPS and aircraft information, calculation of RFI source position, generation of detection results or reports, therefore, additional computer will not be necessary.

### -Antennas

Two antenna arrays, each of them consists of four elements, are needed separately for VHF band and L band DF.

Another two independent antennas should be installed for frequency monitoring separately for each band.

When choosing VHF antennas, stick-shape antenna is not suitable for jet aircraft since they would be very possible being broken during high speed flight.

Additionally, the system should also include an antenna switching capability to switch spectrum analyzer onto any inspection system antennas including monitoring antennas for better analysis through Antenna Switching Unit and software switching control.



Figure 3 DF antennas

### The types of airborne RFI detection

We prepared to separate airborne RFI detection missions into three types, they are:

#### -emergency airborne RFI detection

This is a rapid responsive detection in order to find out the serious radio interference which significantly impacting civil aviation radio works and provide most helpful information, including interference frequency spectrum, detected interference source position together with error range estimation, and necessary audio recording, to the related department in time.

#### -periodic airborne RFI monitoring

A detection being carried out in some period on the frequency serving for important en-route control, busy airport control, in order to monitoring the spectrum situation and find out any potential trend of interference to operation of civil aviation radio frequencies.

Normally only spectrum analyzer is used to accomplish this work. Once there is any interference occurs during monitoring, DF and Recorder is normally necessary to be used to make a deep investigation.

#### -special required detection

If any interference is under suspicion during a normal flight inspection or normal civil aviation radio operation

and the problem is existing continuously or occurs frequently, special detection could be required by local operation unit or local Radio Frequency Office.

New airport site evaluation and some other requirements on airborne radio detection can also be defined as this type of detection.

During this type of detection, frequency spectrum, DF results should be recorded and reported to local Radio Frequency Office.

### Common procedure for implement of airborne RFI detection

This procedure is applicable to emergency, normal airborne RFI detection and special required detection.

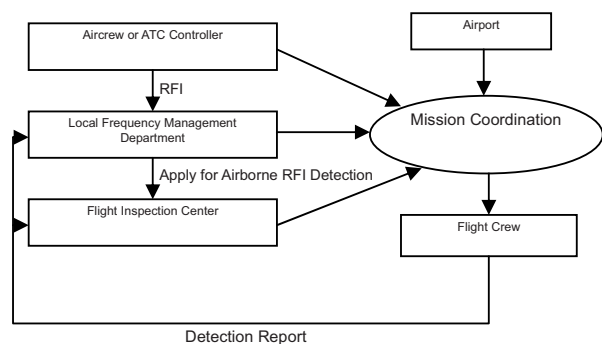


Figure 4 Procedures of RFI detection

#### -apply for airborne FRI detection

Normally when the local civil aviation frequency is suffered RFI and it is very difficult to be found by ground measures, local radio frequency management office shall weigh and determine whether airborne measure should be put into RFI detection. When CAAC radio frequency management office decided to utilize airborne RFI detection, an order should be sent to Flight inspection center of CAAC in time. Once the order is received by CFI, the whole program of airborne RFI detection would be initiated.

All the detection mission should be applied for by some frequency control department or by some air traffic management directly. The application materials should be provided to CFI and includes the following information:

The frequency being interfered

The area being interfered

Whether interference is continuous, intermittent or accidental, and the time interval description

Voice or indication description

Interference reported crew, aircraft type, reported time

Other interference features

#### -Mission Coordination

As soon as being informed by CFI about the mission

initiated, Local frequency management office should make mission coordination of airborne interference detection flight crew, local ground detection personal, airports, ATC, or even air force, through a preparation meeting, and define the following during the meeting:

Detail flight plan

Air-ground communication method and frequency

Logistics issues such as mobiles, airport pass, etc

#### **-Carry Out Mission**

During the mission, detection flight crew should collect and analyze frequency spectrum first, find out the main frequency point of interference signal, then make direction finding and calculate the position of interference source. If it is possible, the interference audio should be recorded.

Depends on different requirement level, when there is a very emergent situation, flight crew should establish the contact with ground detection mobile through the communication frequency pre-defined, and inform the interference source position as soon as it is obtained, in order to implement fast capture of the interference.

#### **-Detection Report**

An airborne detection report and evidence information should be provided to local frequency management office by flight crew after mission, which shows the following information:

Detection date

Detection airport/region

Aircraft tail number

Crew members

Interference source coordination and estimated error range

Recorded spectrum code (if recorded)

Recorded audio code (if recorded)

#### **Certification for Equipments and personnel**

There should be a certification procedure to ensure the airborne detection equipments are qualified for both airworthiness and specification of detection requirements. Whole detection system as part of the aircraft, especially the antenna should not affect the performance of flight. And the capability should be accepted through flight test.

In order to make the airborne RFI detection more efficient and more accurate, the personnel operating the detection system should go through strict training. They should master the operation skills of spectrum analyzer, DF and locating, audio recorder, etc, as well as detection reports filling and equipment maintenance.

## **REFERENCES**

## How to make the airborne detection of RFI more efficient and more accurate

### Mr. Liu Tong

Deputy Director  
Development & Research  
Department  
Flight Inspection Center of CAAC  
23#, Tianzhu Road,  
Tianzhu Airport Industry Zone,  
Capital International Airport,  
Beijing,  
People's Republic of China  
E-mail: ltzhsm@sina.com



### ABSTRACT

The rapid and accurate detection and locating of RFI which threatens civil aviation, is the key precondition of resolving and administer RFI. This puts forward higher requirements on airborne RFI detection devices, capabilities and performances. Based on research airborne RFI detection in current years, Flight Inspection Center of CAAC had accumulated certain of experience on functional principles and applications. We would like to introduce our concepts and methods on airborne RFI detection, exchange ideas and share our experience with coteries all over the flight inspection domain.

Coincidentally, the current airborne RFI detection equipments employed by most of flight inspection institutions basically consist of spectrum analyzer and direction finder, as well as voice recorder of some other equipments being installed by some part of institutions. Whether can these equipments fully come into play depends on application methods and farther development of their functions and accuracy. For example, a normal direction finder installed on the aircraft would be not very accurate due to various factors such as aircraft body reflections. Research on error statistics and certain

compensation, will be a very practicable way to promote detection accuracy and efficiency.

Let's talk about each step of airborne RFI detection, looking for every feasibility of promoting detection efficiency and accuracy.

### Identify RFI through spectrum analysis and determine the central frequency of RFI

One of the important characteristics of Radio-Frequency Interference (RFI) is that most of the interference sources or the basic frequencies of their harmonic wave are usually not located at the frequency points interfered, i.e. the frequency point to which the maximum power corresponds may lie on another position; The another characteristic of RFI is that the modification methods for the interference sources may be diverse. Consequently, if it is necessary to detect interference sources spectrum analysis should be conducted first so as to enhance the detection effectiveness.

In the aerial detection of RFI, the tasks of a frequency spectrum analyzer include spectrum analysis and spectrum recording. The spectrum analysis of the frequency range interfered is to determine the spectrum features of the interference sources, including the central frequency, bandwidth, modulation schemes or modulation characteristics, so as to find out the frequency points where the interference signal has the most strong and steady power, which will facilitate to determine optimum orientation frequency, know the modulation scheme of the interference sources, and help us choose optimum de-modulation scheme for the orientation device, in the same time the audio information de-modulated may make the detection become very simple if the detection clues, such as station names, talking contents, etc., can be read out.

In our preliminary attempts we have found some characteristics for the frequency spectrum of various

interference sources. These characteristics can help us find out these typical interference frequencies easily in the spectrum patrol from the useful frequency signals. The examples are described as follows:

Figure 1 shows a typical spectrum of normal ATC control frequency and Automatic Terminal Information Service frequency. The most obvious characteristic of ATC control signal on spectrum display is that it consists of long dashes, however, the terminal information service signal spectrum is displayed as a long line.

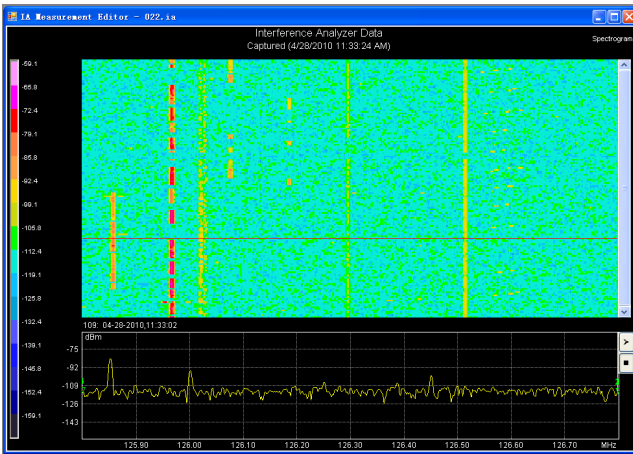


Figure 1 Typical spectrum of normal ATC control frequency and Automatic Terminal Information Service frequency

Figure 2 shows a typical spectrum of an FM radio station signal which harmonic component fell in Aviation VHF band. Compared with normal ATC control frequency signals, the spectrum range of FM radio signal is normally very wide and not very stable. As shown in this figure, the central frequency of FM radio signal is very clear and could be defined as the best detection frequency point for DF.

Other than FM radio station signals, VHF data link signals are another kind of threats which is possible to affect aviation radio frequencies. As shown in figure 3, the spectrum characteristic is that they present as short dash line.

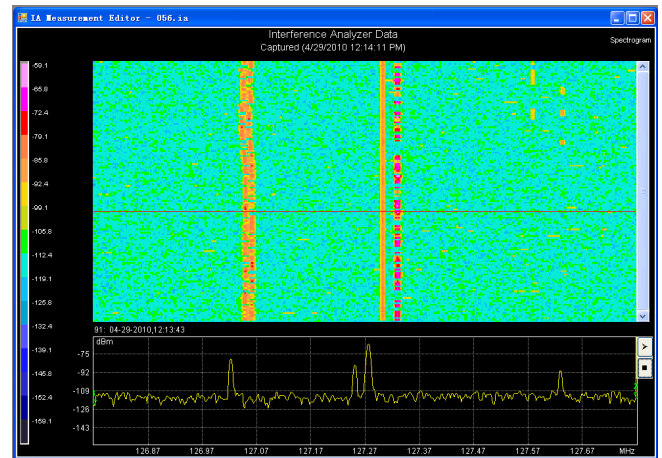


Figure 3 Typical spectrum of VHF data link signals

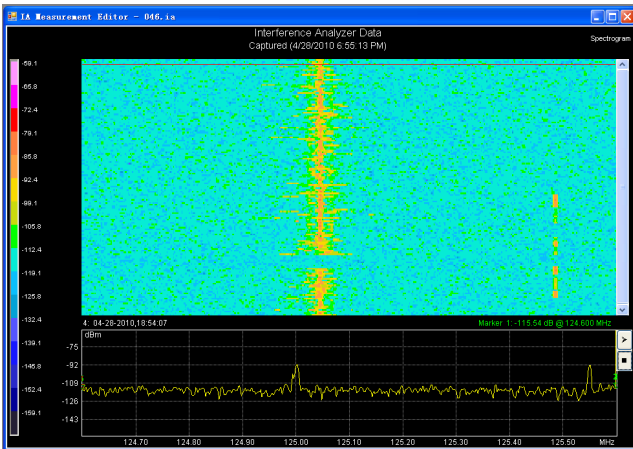


Figure 2 Typical spectrum of an FM radio station signal which harmonic component fell in Aviation VHF band.

Some of the interference signals are caused by unstable frequency which means the interference resource transmitter are very old or poor. Figure 3 also shows a typical unstable interference signal spectrum.

The recording of interference spectrum can provide ground radio frequency management and monitoring personnel with very helpful information after flight, which makes the ground monitoring corresponding to the real interference source according to the frequency features of the interference source, meanwhile, the frequency spectrum records are able to be the powerful evidence for the frequency governance work.

### Listening and audio recording

It is well known that most of the institute in charge of aviation airborne RFI detection all equipped spectrum

analyzer and DF onboard, but few of them installed audio recorder. The function of listening was ignored. However, listening and audio recording is very helpful for detection mission and sometimes can play an important role and give a greater action than what we expected. During an actual mission, we directly heard from the interference audio of the FM station name at the beginning of detection through proper demodulation and recorded it. With this information, the local frequency management officer got hold of the interference resource without any difficulty. Another very important role of listening is to separate interference signal from useful signal during DF or identify an important interference from clutter. Audio recording is also a very important evidence for the interference investigation and treatment.

### How to determine the position of interference resource

Same with many other flight inspection institutes in charge of RFI detection, CFI also use DF to detect interference resource position, farther more, CFI put a concept of airborne position calculation by multi-LOB intersection of DF into actual detection utilizing the rapid positions change of aircraft in the space, in order to provide possible and more accurate coordination of RFI resource. Figure 4 shows how to make multi-LOB intersection. (LOB=Line of Bearing)

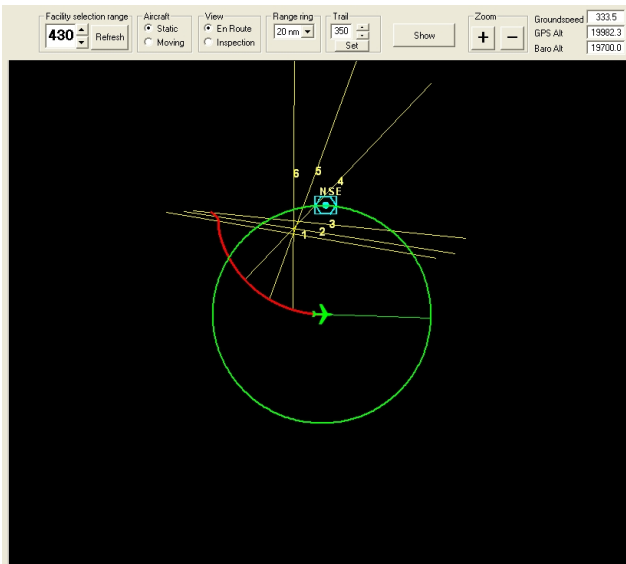


Figure 4 Multi-LOB intersection

### How to make DF more accurate

Since the antenna system is composed of merely four fixed antenna elements, which detect the direction of signal by amplitude comparison, the accuracy of direction finder is not very high. After they are installed at the bottom of aircraft body, the direction finder error caused by the reflection from fuselage, wings, and other antennas could lead to the increase of the orienting error in some azimuths multiplied. figure 5 and 6 shows different estimated range of resource against different direction finder errors.

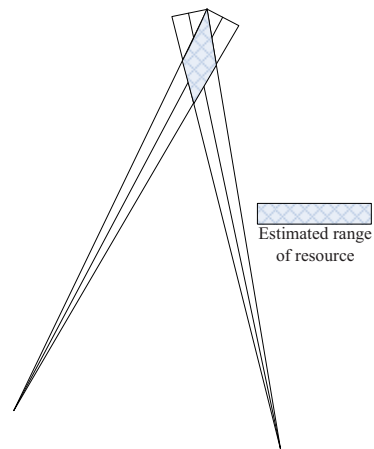


Figure 5 Intersection error based on smaller DF error

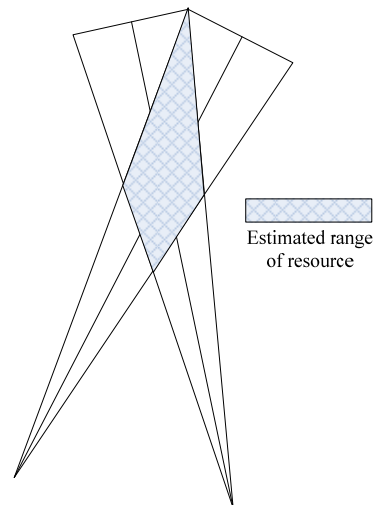


Figure 5 Intersection error based on larger DF error

### How to make the direction finder bearing error compensation

Based on the knowledge of orientation principles and the discussion on the factors affecting orientation accuracy, we hold that the error distribution principle of the direction finder is very similar with that of ADF, the airborne receiver of NDB. In order to reduce orienting error, ADF can be compensated through the compensation of errors in various quadrants, and based on this principle we hold that If we can measure and plot a diagram showing error distribution as a function of various azimuths of the radio interference direction finder, and set up an error compensation table for compensating the errors, the orienting errors will be reduced considerably, thereby enhancing the orienting accuracy.

An actual flight test should be carried out to obtain the distribution of the bearing error of direction finder, however, the ground test would be more difficult to get these numbers due to the released landing gear and surrounding reflection objects on the ground. Before the test flight, following things should be prepared ahead of schedule:

A flat terrain environment for flight

A VHF radio or L-band radio, which frequency could be adjusted

An accurate surveyed point for placing the radio

Test flight profile designed before flight and coordinated with pilots

Recording sheet

Communication between ground radio operator and airborne test technician

The error distribution test could be measured in each degree or in every other certain degree. Table 1 shows a typical distribution test result of our DF. Based on this information, we can make software compensation of DF LOBs based on the line relationship from this table during the calculation.

A confirmation flight with same procedure of distribution test was conducted to confirm compensation; results are shown in table 2.

From this table, we can consult following:

The bearing error caused by aircraft body could be compensated, and errors could be decreased obviously.

Bearing	Error	Bearing	Error
0	0	0	0
-15	-2	15	-2
-30	-8	30	-8
-45	-15	45	-14
-60	-8	60	-9
-75	-3	75	-3
-90	0	90	0
-105	-3	105	-3
-120	-8	120	-9
-135	-16	135	-18
-150	-9	150	-6
-165	-3	165	-4
-180	0	180	0

Table 1 Typical distribution test result of DF

Bearing	Error	Bearing	Error
0	0	0	0
-15	0	15	+1
-30	+1	30	+1
-45	+3	45	+2
-60	-2	60	-3
-75	+2	75	-1
-90	0	90	0
-105	-1	105	-2
-120	+2	120	+2
-135	-3	135	-2
-150	+4	150	+2
-165	+1	165	0
-180	0	180	0

Table 2 Distribution test result of DF after compensation

### What should be paid attention for accurate DF during flight?

-The importance of maintaining a level attitude of aircraft  
 Maintaining aircraft at a level attitude is very important for accurate direction finding during whatever detection flight or error test flight. The antenna relative position change caused by attitude change could lead to errors for DF. The larger degrees of attitude, the larger errors



generated.

#### **-Flight altitude**

The accuracy of DF could be affected by slant angle of antenna elements layout relative to signal resource if the detection aircraft altitude is too high, especially when aircraft is almost above the resource. On the other hand, the lower altitude, the more chaotic reflections or screening will cause wrong direction indication of interference resource. Based on our experience, the best altitude range for RFI detection we thought is from 2100m to 6000m above the site.

#### **-Flight method**

Two flight methods are normally used by us to detection interference resource: Fly-by method and Fly-over method.

In China, or some other countries, it is difficult to fly freely for RFI detection, so before carry out the RFI detection flight, flight crew and relevant people should make a predetermined flight plan depending on the area interference was reported happened and carry out the detection according to the plan at the beginning. Therefore, only fly-by method can be used to obtain direction LOBs and determined an approximate position of resource. A shorter DF time constant setting such as 0.5 or one seconds is normally suitable for this method in order to get a more real indication.

As soon as the approximate position of resource is determined, if the free flight clearance was approved, flight crew could fly directly to the resource through fly-over method and make two events during station passage, and get a more accurate position of interference resource. From our experience, the lower altitude of this flight, the better results we can get. A longer DF time constant setting of 2 or 4 seconds is normally suitable for this method in order to get a more stable direction indication to pilot for their tracking.

No matter which flight method is chosen for RFI position detection, the aircraft movement should be considered and corrected based on aircraft speed and half of receiver time constant.

#### **-Demodulation settings**

Demodulation of DF is very important to the quality of

DF lobs. We should set it correctly based on spectrum analysis. For example, if the frequency bandwidth of interference signal is very narrow, and very close to the interfered frequency, we should set a AM demodulation for DF receiver, however, if the frequency of interference signal is not stable and signal strength is very strong, or it is a FM radio station, we should better set the demodulation to FMW so as to get a more stable indication of direction.

#### **-the judgment of multi-paths**

The direction indications of DF are normally very unstable when we make the detection above some big city or mountain area due to multi-path reflections. So we must accumulate the experiences on how to judge which lobe is believable and which one has been affected by multi-reflection. Some obvious outliers should be deleted for more accurate position calculation to decrease error.



# Flight Validation Data Gathering and Evaluation Capabilities

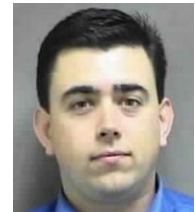
## Timothy J. Lovell

Multi Discipline Systems Engineer, Senior  
 The MITRE Corporation's Center for Advanced Aviation  
 System Development  
 Oklahoma City, Oklahoma, USA  
 Fax: +1 405 954 5270  
 E-mail: [tlovell@mitre.org](mailto:tlovell@mitre.org)



## Jeremy P. Irish

Multi Discipline Systems Engineer, Senior  
 The MITRE Corporation's Center for Advanced Aviation  
 System Development  
 Oklahoma City, Oklahoma, USA  
 Fax: +1 405 954 5270  
 E-mail: [jirish@mitre.org](mailto:jirish@mitre.org)



## ABSTRACT

Traditional flight inspection evaluates terrestrial navigation signals and ensures obstacle/terrain clearance is maintained throughout the instrument flight procedure. In order to validate satellite-based Performance Based Navigation (PBN) procedures, the US flight inspection model has been supplemented. This new process, referred to as Flight Validation (FV), has been defined in regulatory guidance published by the United States Federal Aviation Administration (FAA). Additionally guidance for FV is being developed by the International Civil Aviation Organization. The FAA FV process requires that aircraft performance and obstacle locations be verified to ensure that the Instrument Flight Procedure (IFP) works as expected operationally.

The MITRE Corporation's Center for Advanced Aviation System Development (CAASD), in cooperation with the FAA, has developed and tested new data capture processes that allow users to accomplish FV while satisfying FAA regulatory requirements. CAASD has integrated commercial-off-the-shelf (COTS) equipment with prototype software, enabling users to independently record aircraft flight tracks and complete required obstacle assessments.

This paper describes FV capabilities developed and prototyped by CAASD. It provides a summary of the equipment tested and proven to work for airborne and ground obstacle assessment and the real time display/recording of aircraft flight track information. It also describes data analysis techniques that enable cost effective obstacle surveys, demonstrating that horizontal and vertical survey accuracies of 10 feet can be achieved.

## INTRODUCTION

IFPs using satellite-based navigation provided by a Global Navigation Satellite System (GNSS) are the foundation of the FAA Next Generation Air Transportation System (NextGen) and will become the predominant method by which most air transport turbojet aircraft navigate. The most advanced and accurate method of satellite navigation employs PBN. PBN is defined as "area navigation based on performance requirements for aircraft operating along an Air Traffic Service (ATS) route, on an instrument approach procedure or in a designated airspace".<sup>1</sup>

The FV of PBN IFPs encompasses both ground and airborne activities. The ground portion of FV is the evaluation of the instrument procedure design and documentation; if feasible, a ground obstacle assessment; and, if required, flight simulation of the IFP. The airborne portion of FV includes an infrastructure assessment and at least one on-course/on-path flight evaluation of the proposed procedure in an appropriately equipped PBN aircraft. If performed from the air, the obstacle assessment should be accomplished prior to the on-course/on-path evaluation. An Autonomous Global Position Satellite Recording System (AGRS) must record the obstacle assessment and validation flight. These recordings then become part of the IFP documentation and can be used by the FAA to recreate those portions of the FV. This capability allows governmental oversight of FV activities even if the FV was performed without government participation. The FV process provides significant benefits to operators and other capable nongovernmental entities by empowering them to perform their own validation flights.

This allows state agencies to concentrate on governmental activities such as IFP oversight and the flight inspection of terrestrial navigation aids and their associated IFPs. Additionally the FV of IFPs by non-governmental entities allows the costs associated with PBN IFP development to be contained and controlled by the proponent. This allows full inclusion of FV into the proponent's business model.

This paper describes the processes and equipment that leverage advanced cost effective portable measuring and recording equipment, including GNSS receivers and laser rangefinders. This equipment can be used to record, and playback, aircraft flight tracks thus verifying aircraft flight track to IFP Obstacle Evaluation Area (OEA) relationships. It also enables non-specialized trained personnel to conduct obstacle assessments that achieve a high level of accuracy and repeatability. Data enhancement techniques for synthesizing information from multiple measurements to minimize errors are also described.

### **SCOPE**

This paper provides some background and a description of the processes involved in the application of GNSS technologies to the recording and real time display of aircraft flight tracks and ground obstacle surveys in support of FV. The intended audience is aviation specialists with a background in and understanding of instrument procedures and the application of obstacle accuracies in their construction and validation. The equipment required to perform a FV ground obstacle survey and record a FV is described, with more detail, in Appendix 1.

These processes are intended to be used by individuals with proper training and an understanding of the equipment employed and a comprehension of the correct use of that equipment. Even though this equipment is relatively easy to operate and use, failure to do so correctly could result in unsatisfactory results and incorrect interpretations.

### **PROCESS DEVELOPMENT**

Initial process development was derived from the requirements defined by the FAA's Flight Procedure Implementation and Oversight Branch. The first data was gathered using equipment identical to that owned by the FAA and defined in FAAN 8260.67<sup>2</sup> as meeting AGRS requirements; Magellan Mobile Mapper CX GNSS receivers.

An initial feasibility study was undertaken to test the capabilities and limitations of this equipment. The AGRS units were evaluated during two dimensional ground movement tests. These tests consisted of AGRS units mounted on multiple vehicle dashboards being driven on roads at varying speeds and under conditions of acceleration, deceleration and differing turn rates. These initial ground tests were made to determine the accuracy

and efficiency of AGRS units in moving vehicles. Multiple routes were driven, recorded and analyzed. This recorded data was processed and geo-referenced against satellite imagery to validate initial track keeping capabilities and potential limitations of the AGRS units. As can be seen from Figure 1 below, the ground tracks (shown in blue) driven and recorded were very similar, suggesting that the tested AGRS units are capable of providing accurate and recordable track data.

Testing was performed by driving on roads with a standard road lane width of 12 feet. This testing revealed that the data tracks obtained were always within the 12 foot road width and on the correct side of the road.



**Figure 1. Geo-referenced vehicle derived ground tracks**

The previous figure, figure 1, and multiple other ground recorded routes indicated that no gross deviations had occurred. The results of this research indicated that no significant track deviation should be expected during airborne FV recordings.

Airborne tests were performed to demonstrate that these AGRS units reliably provide accurate position data. Initial airborne testing was made in a twin turboprop aircraft at speeds between ground taxi and 250 knots to include approach and departure speeds. Altitudes involved in this testing ranged from a field elevation of 1,295 feet at Oklahoma City Will Rogers World Airport to 15,000 feet during cruise. At no time during these initial tests was any GNSS track difference noticed between planned and flown track as recorded by the AGRS. Also, no loss of signal or unlock was experienced by the AGRS units during this flight.

Further tests at higher airspeeds and altitudes were made in a turbojet aircraft from a field elevation of 341 feet at Memphis International Airport to a cruise altitude of 16,000 feet. Speeds during this test ranged from ground taxi to more than 320 knots during cruise. These tests revealed that the AGRS units sometimes fail to acquire a GNSS position in flight. The units in question are designed for high accuracy ground surveying, and are not intended for

high speed use. As expected, the AGRS unit was able to re-acquire a position after the aircraft had slowed down for landing.

Additional airborne tests were conducted of Satellite Based Augmentation System (SBAS) capable GNSS receivers with both SiRFstarIII chipsets and MTK chipsets. These receivers do not incorporate any internal calculation capabilities but purely output point in space speed, altitude and other standard data included in National Marine Electronics Association (NMEA) 0183 data sentences. These GNSS units (hereafter referred to as “GNSS mouse receivers” due to their size and shape), are much more compact, require less power, and are significantly less expensive than the other AGRS units tested. The GNSS mouse receivers, combined with the CAASD FV Toolset software, provided consistent and repeatable results for airborne applications.

The FV Toolset receives the NMEA 0183 data output from GNSS mouse receivers via a Universal Serial Bus (USB) port. This NMEA 0183 data is used to establish a GNSS position, which can be displayed in the software’s Graphical User Interface (GUI). This additional functionality, when combined with the existing software capability to display geo referenced satellite imagery provides a real time position solution.

This real time position solution is used in conjunction with existing aeronautical, obstacle and geo-referenced image data to provide an accurate depiction of the aeronautical environment surrounding the GNSS derived position. Provided with this situational awareness it is possible to determine positions accurately relative to database defined obstacles, IFP OEAs depicted in the FV Toolset GUI, and other aspects of IFPs.

### **FLIGHT APPLICATION**

The FV Toolset simultaneously receives and displays data from multiple USB GNSS mouse receivers and, if desired, can average these positions. Additionally data from the NMEA 0183 data string outputs can be set to display speed and altitude in real time at 1 to 60 second intervals and when recorded is available for playback at any time. Though output from numerous USB GNSS mouse receivers can be accomplished by the addition of USB hubs to laptops, this was found to cause system degradation and slow processing significantly. For optimum computer and FV Toolset performance the ideal number of USB GNSS mouse receivers was determined to be two.

The real time position information and display of geo-referenced aeronautical information allow for in flight data analysis. This also facilitates the correction of identified IFP discrepancies while airborne. This capability of real time analysis and IFP modification could have significant

cost saving benefits by alleviating the need for additional flights by FV operators.

In this study, the GNSS receivers were connected to a laptop using USB extension cords. They were mounted to aircraft side windows using suction cups to provide a clear view of the sky and GNSS constellation. In order to ensure reception of an adequate number of GNSS satellites and maintain an acceptable level of Position Dilution of Precision (PDOP), at least two GNSS mouse receivers are used, mounted in windows on either side of the aircraft. This configuration has been demonstrated to provide adequate track data reception regardless of aircraft attitude.

In figure 2 below the dual GNSS data tracks from an aircraft departing parking at Boeing Field, Seattle, Washington, USA are depicted in black. Two GNSS mouse receivers, one on either side of the aircraft, provided the GNSS data tracks. The initial positional “jitter” seen around the aircraft is typical of this type of GNSS receiver outputting raw NMEA data sentences. However, once moving this “jitter” disappears and the real time accuracy of multiple GNSS receivers and the FV Toolset is evident.

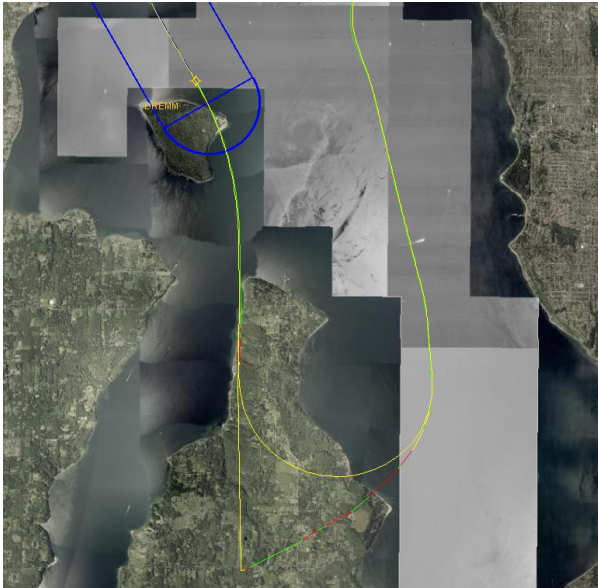


**Figure 2 Taxi Operations at KBFI Using Two GNSS Mouse Receivers, Connected to the FV Toolset**

Note the signal degradation and possible multipathing caused by the proximity of the large hangar in the middle of the picture. This signal degradation is localized, and restricted to the GNSS mouse receiver in the right side window. The GNSS mouse receiver on the left side of the aircraft was not impacted by the multipathing.

A typical example of signal retention by one GNSS mouse receiver and signal loss by the other side GNSS mouse receiver, in a high bank angle situation, is depicted in figure

3 below. In this case the aircraft was flying from top center to the south and banked hard right to turn to the DREMM waypoint. During this maneuver the GNSS receiver on the right side was turned toward the ground and suffered signal degradation. This is depicted by the straight-line GNSS track and differing colors of degraded PDOP reports from the NMEA data stream. However, the opposite side receiver maintained signal reception and continued to transmit position data throughout the turn. This continuity of data is essential to a complete and accurate analysis and record of FV flights.



**Figure 3 GNSS Mouse Receiver Signal Loss During High Bank Angle Turn**

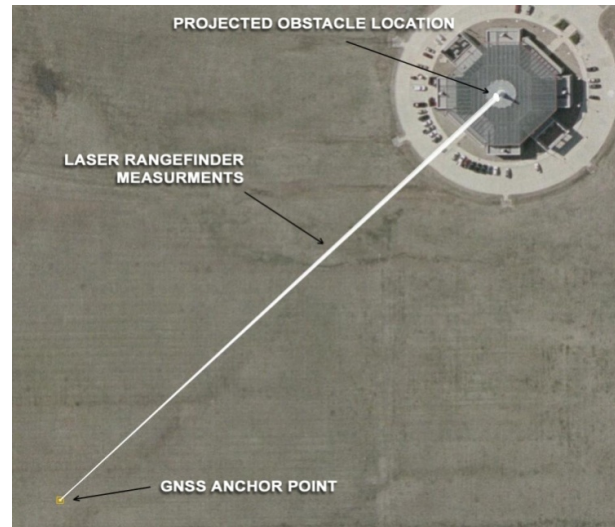
Post flight analysis is facilitated by the immediate availability of recorded flight track data that includes aircraft speed and altitude from any given time and place on the flight. This recording can become an integral part of the IFP package.

**GROUND APPLICATIONS**

The same technologies that allow the accurate real time depiction of aircraft positions can be used to support the ground obstacle assessment portion of the FV process. Processing and displaying the derived positions from GNSS receivers it is possible to determine the positions of obstacles and obstructions to air navigation. This is most easily accomplished when access to the base of those structures is available. However, since most obstacles are not easily accessible, a means of accurately determining the position of these obstacles relative to a separate GNSS-derived position was needed. An effective method for combining GNSS-computed positions with range and azimuth data from handheld laser rangefinders is described

below. These methods enable the measurement of obstruction locations and heights to ensure that they are properly accounted for in procedure design and evaluation. The FV Toolset, using information from the laser rangefinder and the GNSS receiver, computes the location of a given obstacle. The laser rangefinder equipment also has the capability to measure the height of obstacles. The combination of range, azimuth, and height data is automatically tied to any GNSS anchor point as defined by a mouse receiver. Each anchor point can contain multiple range, azimuth, and height measurements for an obstacle that is surveyed. The FV Toolset averages these measurements and depicts on a map the individual computed locations as well as the average overall location. Figure 4, below, shows an FV Toolset depiction of laser rangefinder data projected from a recorded GNSS anchor point.

In addition to the laser rangefinder and GNSS mouse receiver data, geo-referenced digital images from a GNSS/SBAS enabled camera can also be recorded with the obstacle survey. This provides the ability to photograph obstacles and have the images correctly positioned at the camera coordinates or at the obstacle’s location to aid in future obstacle identification and analysis. This can be of significant benefit for obstacle identification during validation flights.



**Figure 4. CAASD Toolset Depiction of Laser Rangefinder Measurement from Anchor Point**

Testing of the hardware and its integration with the FV Toolset revealed that an accurate, repeatable and cost effective method of obstacle location identification was achievable. In order to reach this goal, further testing and process definition was conducted.

## GROUND OBSTACLE SURVEY PROCESS

Historically, obstacles must be surveyed by a professional surveyor, which takes a significant amount of time and resources. In order to determine the accuracy attainable using the FV Toolset and readily available equipment, the process was tested against known reliable data. The FAA's Aviation Systems Standards Information System (AVNIS) database contains data for obstacles on and around airports within the United States. This data defines obstacles with varying degrees of accuracy in accordance with FAA Order 8260.19D. Therefore, to determine the accuracy of the surveying process described here, results were compared with data from known AVNIS obstacles. Survey results were also compared against National Geospatial System (NGS) benchmarks. These benchmarks have been surveyed and defined to centimeter accuracy by the NGS, and were used to provide high-resolution comparisons to survey results. An NGS benchmark is pictured in Figure 5, below.



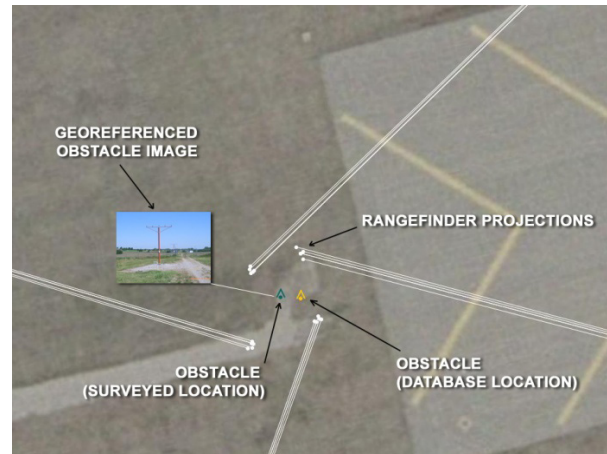
**Figure 5 NGS Benchmark – Secondary Airport Control Station (SACS), Westheimer Airport, Norman, OK, USA (KOUN)**

## FIELD SURVEY PROTOCOL

A protocol was developed to follow at each survey location in order to ensure repeatable survey results. Based upon initial research and standard survey techniques, it was determined that GNSS data needed to be gathered for at least 20 minutes for each obstacle/benchmark to be surveyed. Two different methods of conducting a survey were employed.

If the obstacle's base was accessible, then its position was obtained directly. In this case, a 20-minute GNSS position average was taken. This GNSS data is processed by The FV Toolset and averaged to provide a computed obstacle location. In this case, the laser rangefinder is not needed to compute the obstacle's location.

If the obstacle's base was not accessible, then at least three nearby "anchor point" locations were selected. At each anchor point, a five-minute GNSS average was obtained. For best results, these five-minute GNSS averages should be evenly distributed around the obstacle. Each anchor point must provide an unobstructed view of the entire obstacle to allow for laser rangefinder use. An example of an FV Toolset depiction of 4 anchor points with laser rangefinder projections can be seen in figure 6 below.



**Figure 6 CAASD Toolset Depiction of Laser Rangefinder Measurements from Anchor Points**

In order to use the location averaging method the laser rangefinder must be used exactly over the anchor point. This laser rangefinder measurement can be stored with the other anchor point data in the FV Toolset. Laser rangefinder measurements from several anchor points are combined by the software to compute a location for the obstacle or benchmark being surveyed. As shown in Figure 6 above significant gains in accuracy are obtained in making at least five measurements. However, after more than five measurements the incremental increase in accuracy diminishes.

Regardless of whether five minutes of data was gathered to establish an anchor point, or 20 minutes of data was gathered to survey the location of an obstacle/benchmark the equipment was always set up in the same manner. Five independent GNSS units were mounted on a tripod located directly over the point to be surveyed. This tripod height was recorded and used in the post survey analysis to derive correct GNSS heights. Examples of the GNSS equipment setup and the tripod height measurement can be seen in figure 7 below.



**Figure 7 Tripod Height Measurement**

### **Field Survey Steps**

The following two sections describe the steps that were followed to conduct obstacle surveys. The first section lists the steps to be followed when the base of the obstacle is accessible. The second section lists the steps for the case where the obstacle must be measured remotely. A working knowledge and complete understanding of the equipment to be employed and how to use it is required and assumed prior to applying the below steps.

#### **Obstacle Base Accessible**

1. Set up GNSS receivers at base of obstacle. Determine GNSS signal suitability. If unsuitable consider applying the obstacle base inaccessible process below
2. Configure recording software and ensure connectivity to GNSS receivers and laser rangefinder
3. Record 20 minutes of data from GNSS receivers
4. Measure height of the obstacle using the laser rangefinder. Repeat five times

#### **Obstacle Base Inaccessible**

1. Determine optimal location to establish the anchor point and mark it. Optimal location has an unobstructed view of the obstacle
2. Photograph obstacle for documentation purposes
3. Set up tripod and GNSS receivers directly over marked anchor point (use plum bob)
4. Configure recording software and ensure connectivity to GNSS receivers and laser rangefinder

5. Measure and record antenna height (mounted on tripod)
6. Record five minutes of data from GNSS receivers. Compute an average to determine anchor point location
7. Calibrate azimuth of laser rangefinder
8. Remove GNSS receivers from tripod and replace with laser rangefinder over marked anchor point
9. Measure distance and azimuth to obstacle. Repeat five times, aiming at same point
10. Measure height of the obstacle using the laser rangefinder. Repeat five times

### **LIMITATIONS AND RESOLUTIONS**

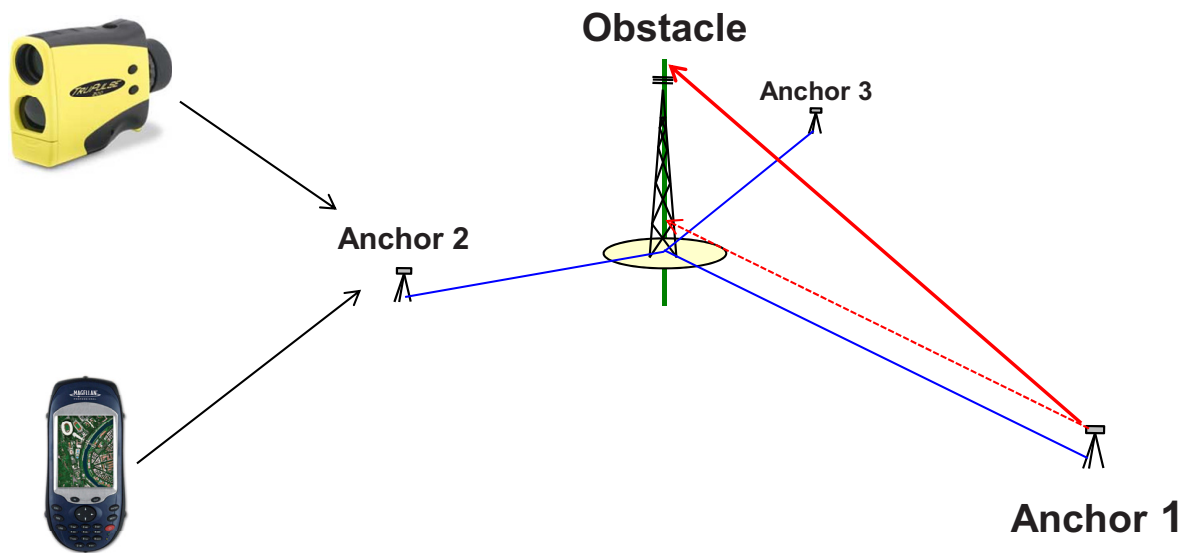
There are certain obstacle locations that could preclude ground obstacle surveys such as remote locations with limited ground infrastructure and challenging terrain areas. Locations like these with limited access would make using the above methods and equipment difficult, if not impossible. However, such locations do not normally have airports and obstacle environments that would require ground obstacle surveys. Therefore, this limitation is not anticipated to be a significant impact.

Azimuth measurements generated by the laser rangefinder are subject to magnetic interference from a variety of different sources. These include, but are not limited to, electromagnetic interference from overhead and underground power lines and telephone lines. Also of concern was the rangefinder's proximity to moving and stationary vehicles, electronic equipment (laptops, etc), ferromagnetic materials such as watches, fences, water lines, tripods and other metal structures.

Post field survey analysis suggests that range trilateration is a more accurate method of determining an obstacle's lateral position than rangefinder azimuth data. In order for trilateration to be of benefit, at least three distance measurements must be taken from different anchor points. However, the more distance measurements that are made, the more accurate the trilateration solution will be.

As the laser rangefinder relies on reflected light in order to measure distance, target reflectivity is a significant issue. Larger objects, especially those with greater surface area, are much easier to measure. For example, over the same distance, a water tower is much easier to survey using a range finder than an antenna tower. This is because some of the lasers light passes through the metal structure and is not strongly reflected from the tower itself. Objects with less surface area, such as antenna towers, need to be surveyed from smaller distances, typically less than one thousand feet, in order to obtain a measurement.





**Figure 8. Diagram of GNSS Survey Components**

Highly reflective targets such as water towers can be surveyed from greater distances, typically up to three thousand feet.

**Trilateration Resolution**

Since the rangefinder’s error in range was found to be much smaller than its error in azimuth, it was determined that using only the range measurements to estimate the location of an obstacle was the most applicable methodology to use. Trilateration is a method whereby a set of range measurements from different locations is used to estimate the location of an obstacle at the intersection of each measurement’s range ring. When there are more than three points, a least squares solution can provide a very good estimate of the location point.

Both GNSS mouse receivers output NMEA 0183 data sentences that contain one-second position updates. When a receiver is stationary, the latitude and longitude reported in these one-second position updates varies and is rarely the same location. A two dimensional plot of these positions suggests the GNSS is moving. This is obviously not the case as during this study all of the recordings were completed over at least a five-minute period in one location. This inherent characteristic of these GNSS receivers does not allow the use of this data to establish an accurate anchor point without further processing.

In order to overcome this problem, the FV Toolset averages a specified number of NMEA 0183 data sentences. This number of data sentences can be defined by time and allows users to select the duration of the NMEA data to be

averaged. Averaging is completed by dividing the actual latitude and longitude by the number of values received. Once averaged, the resulting position information has been found to be reliable enough to be used as an anchor point for performing surveys to support ground obstacle assessment.

**GROUND OBSTACLE SURVEY ACCURACIES**

An in-depth analysis of measurements has demonstrated that with the tested COTS equipment, ground based obstacle surveys are capable of repeatedly achieving obstacle accuracy codes of "1B", corresponding to a 20 ft lateral and 10 ft vertical accuracy<sup>3</sup>.

Examination of the measured errors suggest that the highest lateral accuracy code of 20 ft ("1" lateral code) is easily achievable with any of the GNSS units. However, the lateral accuracy of 20 ft is not guaranteed for all surveys. When an insufficient number of anchor points are recorded, or when the anchors are poorly distributed, larger accuracy codes would be required. These errors can be monitored for any survey using a lateral error model. Provided the basic process of ground based obstacle evaluation is followed, this 20 ft accuracy can be assumed.

Table 1, below, is an example of the accuracy obtainable using the FV Toolset for a 250ft obstacle surveyed from 4 anchor points, with 5 rangefinder measurements made at each. These anchor points are located at 90 degree intervals around the obstacle at distances of 1000 ft from the obstacle.

<u>GNSS Type</u>	<u>Lateral (ft)</u>	<u>Vertical (ft)</u>
Magellan MobileMapper With Antenna Post Processed Data	4.4	2.8
Magellan MobileMapper Without Antenna Post Processed Data	4.3	1.7
Magellan MobileMapper With Antenna Raw Data	5.8	4.9
Magellan MobileMapper Without Antenna Raw Data	7	5.2
Magellan MobileMapper NMEA 0183 Stream	6.4	5.2
GlobalSat	10.7	12.2
GlobalTop	18.9	11.7

**Table 1 An Example of Total Survey Errors**

These accuracy values obtained will vary depending upon **the following parameters:**

1. Height of obstacle
2. Number of anchor points
3. Distance from anchor points to obstacle
4. Number of range finder measurements taken at each anchor point

#### **Vertical Accuracy**

The vertical accuracy of the survey is primarily constrained by the vertical accuracy of the GNSS units (unless surveyed near the range limit of the laser rangefinder). With only a single anchor point, vertical accuracies of the GlobalTop and GlobalSat units were observed within the 50 ft accuracy code ("D" vertical code). The three raw Magellan GNSS units fall within the 20 ft vertical limit ("C" vertical code). The two Magellan units, from which the data was post-processed against Continually Operating Reference Stations (CORS), have the highest accuracy of the examined units at 10 ft ("B" vertical code). However, they are not accurate enough with a single measurement to achieve the highest vertical accuracy code (3 ft, "A" vertical code).

By averaging the height measurements over multiple anchor points, it is theoretically possible to meet the highest level of vertical accuracy (3 ft, "A" vertical code). However, this was not provided by the benchmark validations undertaken. Therefore, it is unknown how averaging these measurements will reduce the vertical error (GNSS measurements at multiple anchors may be slightly correlated, through which averaging could not reduce the error). Without further validation, these surveys can only be said to achieve vertical accuracies of 10 ft, which

requires the use of the Magellan MobileMapper CX GNSS units and post processing against CORS.

#### **SUMMARY**

This paper has defined and demonstrated the methodologies and application of cost effective COTS equipment that allow operators to perform, efficiently, FAA required FV actions. It is important to remember that any tool is only as good as its user; therefore, a complete and full understanding of the technologies discussed is necessary to achieve consistent accurate repeatable results. Given that, these technologies and capabilities should help further the implementation of PBN satellite based IFPs within the United States National Airspace System and beyond.

#### **ACKNOWLEDGMENTS**

This paper is presented as the work of the two primary authors. However, this work, and this paper, would not have been possible without the unending support of fellow CAASD employees; Dr. Michael Mills, Project Team Manager, Steven Chase, Software Applications Development Engineer and the concise, accurate and in-depth analysis of Adric Eckstein, Systems Engineer.

#### **REFERENCES**

- [1] International Civil Aviation Organization, *CAR/SAM Roadmap for Performance-Based Navigation*, 2008.
- [2] Federal Aviation Administration, *Notice 8260.67, Flight Validation (FV) of Satellite-Based Performance-Based Navigation (PBN) and Special Wide Area Augmentation System (WAAS) Instrument Flight Procedures (IFP)*.
- [3] Federal Aviation Administration, *Order 8260.19D, Flight Procedures and Airspace, appendix 3, paragraph 101, August 2007*.

## APPENDIX 1

### EQUIPMENT

Below is a complete list of all of the equipment that was used to develop the obstacle survey process with a brief description of each item's function and capabilities. This list is specific to the types of equipment used to conduct the study; however comparable equipment could be used and similar results would be expected.

#### Dell 620 Laptop Computer laptop computer

A laptop computer was used to run the FV Toolset and process inputs from other COTS hardware. Additional batteries, vehicle power supplies and inverters were utilized to provide laptop power while in the field. Laptop computer configuration as tested is as follows:

- Intel® Core™2 central processing unit T7400 at 2.16 gigahertz
- 2 gigabytes of random access memory
- Microsoft Windows XP Professional Version 2002 Service Pack 3

#### CAASD FV Toolset

CAASD-developed software was modified to support FV requirements. Modifications include the capability to receive and process laser rangefinder signals, GNSS signals, and digital camera images. These inputs are geo referenced to existing aviation data to provide real time on the fly survey capabilities.

#### Rocketfish™ - Micro Bluetooth® USB Adapter

The Rocketfish™ Bluetooth® USB adaptor is used to receive data from the laser rangefinders and GNSS enabled camera.

#### Verizon Wireless PC5750 WAN Card

Used to import FAA Aviation Systems Standard Information System (AVNIS) referenced aeronautical data and aerial photography into the laptop running FV Toolset while in the field. It was also used to save data while in the field to protect against loss of data.

#### GlobalSat BU-353 USB Cable GNSS SBAS Enabled Receiver

Uses a SiRFstarIII processor. Receives L1 frequency at 1575.42 MHz. Outputs National Maritime Electronic Association (NMEA) 0183 messages: GGA, GSA, GSV, RMC, VTG and GLL. Baud Rate = 4800bps, update rate =

1Hz. Provides raw NMEA data to a laptop via USB cable for processing by FV Toolset.

#### GlobalTop GMR75 USB Cable GNSS SBAS Enabled Receiver

Uses a Media Technology Inc. (MTK) processor. Receives L1 frequency at 1575.42 MHz. Outputs NMEA 0183 messages: GGA, GSV, RMC and VTG. Baud Rate = 9600bps, update rate = 1Hz. Provides raw NMEA data to a laptop via USB cable for processing by FV software.

#### Magellan Mobile Mapper CX GNSS SBAS Capable Receiver (Self Contained AGRS Unit)

The MobileMapper CX is a complete GNSS receiver and data processor with built in display. The MobileMapper CX GNSS receiver is integrated into a pocket computer running Microsoft Windows CE. Receives L1 frequency at 1575.42 MHz. Outputs NMEA 0183 messages: GGA, GLL, GSA, GSV, RMC, RRE, VTG, and ZDA. Update rate = 1Hz. Provides raw NMEA data to a laptop via USB, Serial cable or Bluetooth® for processing by FV Toolset. Additional FV Toolset processing of Magellan proprietary data must be accomplished via manual inputs.

#### Magellan MobileMapper Office Software

MobileMapper Office is proprietary Magellan software installed on the laptop. When combined with the MobileMapper field software, MobileMapper Office software enables the display and post processing of data downloaded from the MobileMapper CX GNSS receiver.

#### Magellan MobileMapper Field Software

Field Software is a proprietary Magellan add-on that will process NMEA data sentences and provide average GNSS position information and other proprietary capabilities. This software is a required component of the capability to post process field survey data.

#### Magellan NAP 100 Professional Antenna

Can be used with the MobileMapper CX GNSS unit in order to achieve sub-foot accuracies via post processing can also provide greater accuracies for raw data when properly used. Receives L1 frequency at 1575.42 MHz.

### **Laser Technology Incorporated - TruPulse 360B Laser Rangefinder**

A handheld unit that uses a reflected laser beam to determine the distance to an object. The unit also incorporates an electronic compass and inclinometer to measure azimuth and inclination thus providing bearing and height. Provides range, bearing and height data to a laptop via serial cable or Bluetooth® for processing by FV Toolset. The manufacturer's accuracy specification for the TruPulse 360B is as follows:

- Distance +/- 1ft (30cm) – High Quality Targets, +/- 1 yd (1 meter)– Low Quality Targets
- Inclination +/- 0.25°
- Azimuth +/- 1.0°

### **Ricoh Caplio 500SE Digital Camera**

An 8 Mega Pixel digital camera with an integrated GNSS/SBAS receiver. Provides geo referenced digital photographs to a laptop via Bluetooth® or WiFi™ for processing by FV Toolset.

### **Brunton Nomad V2 Pro Digital Compass**

A handheld digital compass used for calibration of the TruPulse 360B range finder.

### **Manfrotto 715B Digi Tripod with Integrated Ball Head with Dove Tail Plate**

Used to provide a stable mounting platform for the TruPulse 360B range finder.

### **Seco Prism Pole Tripod, Thumb Release**

Used to provide a stable mounting platform for the GNSS units.

### **Stanley Measuring Tape**

300-foot measuring tape used to verify distances and heights.

### **Plum Bob**

Used to precisely locate Seco Prism Pole Tripod, supporting GNSS units and laser rangefinder target, over NGS benchmarks.

### **Fifteen foot USB Extension Cables**

Used to allow survey locations to be located an applicable distance away from the vehicle. Also used to facilitate remote GNSS receiver mounting in aircraft windows.

## QA Document 9906, Volume 5, Flight Validation of Instrument Flight Procedures

By Fabrizio Maracich  
Crew Training Manager and Flight  
Inspection Pilot  
ENAV S.p.A. - Radiomisure  
Hangar 127 Ciampino Airport  
00040 Ciampino (Rome)  
Italy  
e-mail: [fabrizio.maracich@enav.it](mailto:fabrizio.maracich@enav.it)



&

Glenn Bissonnette  
FAA Manager, Flight Inspection  
Policy  
Aviation System Standards  
Oklahoma City, OK USA 73125  
e-mail: [glenn.r.bissonnette@faa.gov](mailto:glenn.r.bissonnette@faa.gov)



**BACKGROUND:** The International Committee for Airspace Standards and Calibration (ICASC) was created following the 8<sup>th</sup> International Flight Inspection Symposium (IFIS) and exists to supplement the biennial (every two years) formal symposiums by promoting continuity in the exchange of regulatory, technical, operational and commercial information in flight inspection. The committee functions as an advisory group that researches topics of interest to the flight inspection and aviation community and provides technical input to the International Civil Aviation Organization (ICAO). Membership of the committee is intended to represent the worldwide flight inspection community, and is a reflection of industry, academia, and government interests. At the eighth meeting of its 186<sup>th</sup> Session, on March 9 2009, Representatives of the Council to the International Civil Aviation Organization included ICASC in the list of international organizations that may

be invited to attend suitable ICAO meetings.

Following this recognition, ICAO tasked ICASC with defining the competency framework for flight validation pilots. During the initial workgroup meetings held in Montreal in June 2009 the need arose to actually describe the PROCESS that is associated with the work that a flight validation pilot will have to perform prior to developing pilot competencies and training requirements. The “flying aircraft components” of it was relatively clear, but we needed to identify (by defining a process) what additional qualifications would be required. This resulted in a decision to expand the project by developing two new volumes to the Quality Assurance Procedure Design Series of guidance material. Volume 5 would describe the Flight validation of Instrument Flight Procedures and Volume 6 would address the Flight Validation Pilot

Training and Evaluation. This is the reason why the manual Volume 5 only addresses the activities that are performed by the Flight Validation Experts.

**Difference Between Flight Inspection and Flight Validation:** For the purpose of quality assurance in the procedure design process, flight inspection, and flight validation are separate activities that may or may not be accomplished by the same entity. “Flight Inspection” is used in reference to an in-flight evaluation of a navigation system or ground-based navigation aid(s) to ascertain or confirm the ability of the navigation aid/system upon which the procedure is based to support the procedure in accordance with the standards in Annex 10 – Aeronautical Telecommunications and guidance in the Manual on the Testing of Radio Navigation Aids (Doc 8071). Flight inspection is not meant to verify the accuracy of space-based navigation systems, but provides a means to evaluate signals in space for local degradation and interference. The term “Flight Validation” is part of the Procedure Validation process and is concerned with factors other than the performance of the navigation aid or system that may affect the suitability of the procedure for publication. Flight Validation is a flight assessment of a new or revised instrument flight procedure to confirm that the procedure is operationally acceptable for safety, including required obstacle clearance, flyability, navigation database ARINC-424 coding, design accuracy, and required infrastructure (i.e., runway markings, approach lights, communications, runway lights, charting, etc.) with all supporting documentation. A procedure design organization may not have the expertise necessary to determine under which conditions flight inspection and/or flight validation may be necessary. For this reason, it is

recommended that a review of the procedure by the flight inspection and flight validation organizations be included in the States procedure design process flow, following ground validation.

**The Need for Flight Validation –** Aviation is transitioning from ground-based NAVAID(s) and analog signals in space to computer-derived flight guidance completely dependant on accurate data. Flight Validation completes an End-to-End Process that connects the Virtual World to the Real World. Flight management System (FMS) and Simulator databases have varying degrees of accuracy and integrity to represent the real world environment. Flight validation verifies that the:

- Flight path clears obstacles and terrain safely,
- There is no significant local interference to the Global Positioning System (GPS) or SBAS signal
- The achieved flight path is the same as the one intended by the designer
- All data to be published are correct

**Data Accuracy and Integrity.** Procedural data accuracy is extremely important. Flight procedures utilizing ground-based NAVAIDS(s) (e.g., Instrument Landing System (ILS), Very High Frequency Omnidirectional Range (VOR), Nondirection Beacon (NDB)) can be referenced to a surveyed terrestrial fixed antenna location. In contrast, satellite based Area Navigation (RNAV) procedures deliver the aircraft to a point in spaced based on the WGS-84 geodetic datum. RNAV procedures consist of sequenced ARINC 424 coded

path and terminators and waypoints. The combination of different ARINC 424 leg path and terminators provides the desired ground track and vertical path of a procedure. This requires very high integrity and accuracy of the survey data used in the flight procedure and the aircraft navigation database. It is mandatory that an appropriate quality assurance system covering all domains of data collection (surveys), processing, publication, and navigation database development be maintained (Ref. ICAO Annexes 4, 11, 14, and 15).

Data errors have several sources and can have critical effects to the procedure design process. Survey data is a common source of error in many countries. Terrain and obstacle data may be incomplete or just plain wrong. Ground-Based Augmentation System (GBAS) uses an earth-centered, earth-fixed (ECEF) reference system based on WGS-84. Conversions between geodetic data can also induce errors. Vertical datum difference between NAD-83 and WGS-84, for example, can result in positioning errors causing the actual Threshold Crossing Height (TCH) for SBAS LPV procedures being higher or lower than designed. Input errors, especially to the Final Approach Segment (FAS) Data Block, can result in significant changes to the flight path in relation to the runway. Additionally, data errors can be introduced by not using the appropriate “pending” data (e.g., when future changes to the airport will be realized by the time the procedure is actually published).

Particular attention should be paid to data accuracy in the precision FAS Data Block for Space-Based Augmentation System (SBAS) and GBAS flight procedures. Corruption of ellipsoid height data can have disastrous effects on the location of a glide path by displacing the glide path forward or aft along track of the intended design. All of

these examples of data errors indicate a need to actually connect the virtual world of databases to the real world environment to assure safety of flight.

#### **The Validation Process Overview–**

The validation of instrument flight procedures must be carried out as part of the initial certification of the procedure, or when an amendment is made to the procedure that has the potential to significantly affect the lateral or vertical flight path. The purpose of Validation is the verification of all obstacle and navigation data, and to provide an assessment of the flyability of the procedure. Validation and verification procedures are established which ensure that quality requirements (accuracy, resolution, and integrity) and traceability of aeronautical data are met. Validation normally consists of Pre-flight Validation, Flight Validation and Post flight analysis and documentation.

Prior to leaving the design phase, the instrument flight procedure should undergo a Ground Validation within the procedure design quality assurance process. It should encompass a systematic review of the steps and calculations involved in the procedure design.

Pre-flight Validation begins when the procedure package is received. In this phase of the process, the information provided is validated and potential errors in the procedure design are identified. Pre-flight Validation may include both a simulator evaluation and obstacle assessment.

Flight Validation requires a flight assessment in a properly equipped aircraft to confirm the procedure is operationally acceptable for safety, flyability, and design. The procedure must be flown in the relevant navigation mode required by the design. The objectives of flight validation include:

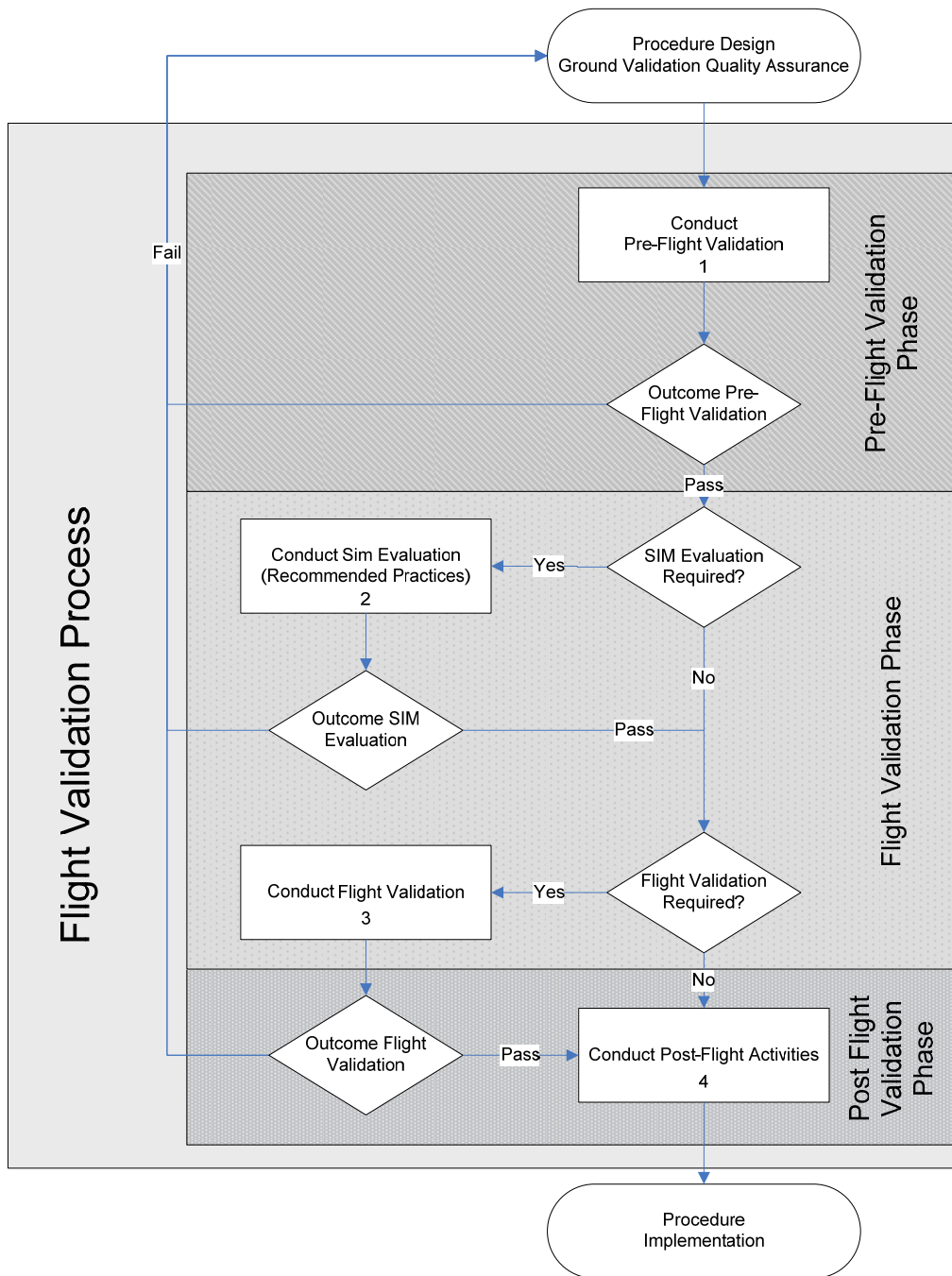
flyability and overall safety; final assurance of adequate obstacle clearance; verification that the navigation data is correct and results in the designed flight path; verification that all required infrastructure is in place and operative; and the necessary signals in space are present and support the procedure. For complex procedures, additional flyability checks may be required in the proponent's aircraft or simulator.

Post Flight analysis and documentation finishes out the Validation process.

Certain types of flight and navigational data must be recorded during the Flight Validation. Some of this data must undergo post-flight analysis to verify navigation data accuracy and integrity, as well as proper flight track performance, both laterally and vertically. A determination of satisfactory or unsatisfactory results should be made, along with ensuring the completeness and correctness of the procedure package. All recorded electronic data and the final report should be archived.

The validation process flow diagram





**Pre-flight Validation Steps:**

A Pre-flight validation review of the entire instrument flight procedure package should be completed by a person(s) familiar with procedure design concepts (see Doc 9906 Volume 6 for Flight Validation Pilot Competencies and Training) and with appropriate knowledge of flight validation issues. It is meant to identify deviations from criteria and documentation and evaluate prior to flight, to the extent possible, those elements that will be evaluated in the flight validation phase. Issues identified during the pre-flight validation phase should be addressed prior to the flight validation phase. Pre-flight validation determines the necessary subsequent steps in the flight validation process.

Before proceeding to the next step, it is recommended to resolve any known discrepancies with the designer.

#### Step 1: Conduct Inventory and Review Instrument Flight Procedures (IFP) Package

The Flight Validation Pilot must ensure that the IFP is complete and all necessary charts, data and forms are available. The goal is to familiarize and identify potential errors in the procedure design. The following minimum tasks should be performed:

- Ensure completeness of package (all forms, files and data included).
- Determine charts and maps are available in sufficient details to assess IFP during the Flight Validation (FV).
- Familiarize with procedure design constraints, requirements and intended users to determine the acceptability and geographical context to assist in the validation process.

- Discuss the procedure package with the procedure designer, as necessary.
- Verify procedure graphics and data from forms match.
- Compare the IFP design, coding and relevant charting information against the navigation database used for flight validation.
- Verify governing and secondary obstacles are properly identified (location, description, height).
- Determine need for flight simulator evaluation, especially where there are special or unique design considerations.
- Evaluate information provided concerning runway environment, airport markings and/or special local operations procedures (e.g., non-standard traffic patterns, lighting activation, airport lighting, noise abatement) in order to prepare for the FV.
- Review pertinent flight inspection and flight validation reports. Confirm that the applicable navigation systems support the intended instrument procedure. Check NAVAIDS, Global Navigation Satellite System (GNSS) availability and assess if flight inspection is required.
- Identify items that require flight inspection, such as new or amended fixes using ground-based navigation aids and Visual Glide Slope Indicator (BGSI) and other lighting systems requiring angle evaluations.

#### Step 2: Evaluate data and coding

For RNAV IFP, verify true course to next waypoint, distances, and altitudes reflect the flight procedure design. Leg segment data accuracy must be evaluated by comparison of the procedural waypoint data to the flight plan waypoint data. When evaluating RNAV Course to Fix (CF) legs, including holding lets, compare aircraft navigation performance with the instrument procedure design. Do not apply any tolerance to course-to-fix values. Confirmation of proper ARINC coding will be accomplished with either an appropriately equipped aircraft, or by a desktop evaluation of the current navigation database. Out-of-tolerance values or questionable ARINC 424 coding must be resolved.

For ground-based IFP, it is recommended to verify course, distances, and the Flight Path Angle (FPA) indicated on the IFP depiction and submission form of the procedure design. Where positive course guidance is required by the IFP design, confirm NAVAIDS performance meets all required flight inspection tolerances in conjunction with the Flight Validation.

Steps to evaluate data and coding:

- Prepare loadable data and coding.
- Compare true courses and distances for segments between data file and procedural data.
- Compare ARINC-424 coding for legs and path terminators between data file and procedural data.

Where the flight procedure design involves a complex new procedure or a significant change to existing procedures/ routes in a complex airspace, the State is strongly advised to

liaise with the major commercial navigation data houses prior to promulgation. This liaison should provide the data houses with additional advance notice of the proposed changes and should allow them to review the proposed procedures, clarify any outstanding questions, and advise the state of any technical issues that may be identified. Advance notification of procedures should contain the following elements:

- Graphical layout of the procedure
- Textual description of the procedure
- Coding advice, when applicable
- Coordinates of fixes used in the procedure

Step 3: Review special operational and training requirements

- Review deviations from criteria and equivalent level of safety provided by waivers.
- Review safety case supporting the waver.
- Assess restricted procedures for special training and equipment requirements.

Step 4: Coordinate operational issues

- Consideration should be given to temperature and wind limitations, air speeds, bank, angles, climb/descent gradients, etc.
- Determine aircraft and equipment required to

complete flight validation phase of the IFP.

- Determine airport infrastructure and NAVAID availability
- Check weather minima and visibility required for the flight validation phase. Initial assessment must be conducted in daylight conditions in Visual Meteorological Conditions (VMC) in each segment with visibility requirements sufficient to determine obstacle assessment.

Step 5: Conduct the night evaluation in the following circumstances:

- IFP developed for airport with no prior Instrument Flight Rules (IFR) services
- IFP to newly constructed runways or to runways lengthened or shortened
- Addition or reconfiguration of lights to an existing system already approved for IFR

Step 6: Coordinate with Air Traffic Services (ATS) and other stakeholders.

Step 7: Document the results of the pre-flight validation phase

- Assess whether the IFP is ready for further processing for simulator (optional) or flight validation.
- Provide a detailed written report of the results of the pre-flight validation phase (See Appendix C for fixed wing sample report forms.

See Appendix XX for helicopter sample report forms)

### Flight Validation

This step should always be carried out as part of the validation of initial and amended procedures. The state may determine that an actual flight with an aircraft may not be necessary under certain circumstances, such as (but not limited to) editorial changes to a published procedure or overlay to published procedures. However, a validation flight with an aircraft is required in the following cases:

- New procedures where there are no published procedures to the same RWY
- Procedures that contain non-standard design elements (deviation from criteria e.g. non-standard approach angles/steep approach, non-standard segment lengths, speeds, bank angles, etc.)
- When accuracy/integrity of data used in the IFP design and/or the Aerodrome environment is not assured.

This list is not all inclusive and may be expanded as appropriate by the state authority.

Flight validation should be included as part of the periodic quality assurance program as established by the individual States to ensure the procedure design process and its output, including the quality of aeronautical information/data, meet the requirements of Annex 15. It must be accomplished by a qualified and experienced flight validation pilot, certified or approved by the State.

The flight validation pilot must occupy a seat in the cockpit with visibility adequate to conduct the flight validation, and additional crew members must be briefed on FV requirements. Ground track path error performance varies with mode of flight guidance system coupling. It is recommended to evaluate new procedures coupled to the flight director and autopilot (when not prohibited). Evaluate for lateral and vertical disconnects from the autopilot/ flight director. Procedures design is based on TRUE altitudes. In-flight evaluation should be conducted at true altitudes with consideration for temperature variations from standard day. Lateral and vertical transitions from departure, en route, descent, and approach must produce a seamless path that ensures flyability in a consistent, smooth, predictable, and repeatable manner.

FV should be performed for all types of IFP described in PAN OPS. The procedure must be flown in the relevant navigation mode required by the design. For example, for RNAV (GNSS) IFP, ensure that only the GNSS sensor is utilized during the FV. All following required steps should be adapted to the specifics of each design and IFP.

The objectives of the flight validation of instrument procedures are to:

- Conduct an assessment of flyability to determine that the procedure can be safely flown.
- Provide the final assurance that adequate obstacle clearance has been provided.
- Verify that the navigation data to be published is correct.

- Verify that all required infrastructure, such as runway markings, lighting, and communications and navigation sources are in place and operative.
- Ensure the documentation of navigation systems confirms the applicable navigation system(s) (NAVAID, GNSS, RADAR, etc.) supports the procedure.
- Evaluate other operation factors, such as charting, required infrastructure, visibility, intended aircraft category, etc.
- Verify that waivers to standard design do not compromise safety.

Step 1: Verify data

It is essential that the data used in the procedure design compares to the charts, FMS data, or suitable navigation system data. The validation flights (simulator or aircraft) should be recorded with a collection/recording device that archives the procedure and aircraft positioning data (see Paragraph 7.3.6 Record flight validation). The procedure development package, charts, and airport data must match. It is recommended that RNAV/RNP procedures are packed and loaded electronically into the FMS or suitable navigation system without manually coding the ARINC 424 path/terminator data. Integrity measures such as Cyclic Redundancy Check (CRC) should be used to assure that data are not corrupted. This allows the flight validation process to evaluate the data as it was developed, without manipulation. If the procedure waypoint data must be manually entered into the FMS, it must be compared to the procedure data to ensure the data points match.

*Steps to data verification:*

- Ensure the data from the flight validation database matches that used in the procedure design.
- Ensure the data produces the desired flight track.
- Ensure that the final approach course/glide path deliver the aircraft to the desired point in space.

*SBAS/GBAS FAS Data Requirements:*

For SBAS and GBAS FAS data, the LTP/FTP latitude and longitude, the LTP/FTP ellipsoid height, glide path angle, DCH, and the FPAP latitude and longitude contribute directly to the final

approach alignment. Corrupted data will skew lateral, vertical, and along track alignment from the intended design. Flight validation using a flight inspection system or post process analysis that can perform the necessary evaluations in a documented, quantitative fashion is required. It is recommended that at least the following IFP characteristics be evaluated as means of validating the FAS data elements defining LTP Lat/Long, LTP Ellipsoid Height, FPAP Lat/Long.

*Horizontal Course Characteristics:*

- Misalignment type, linear or angular
- Measure angular alignment error in degrees (when applicable) and linear course error/offset at the physical runway threshold or decision altitude point.

*Vertical Path Characteristics:*

- Achieved/measured DCH
- Glide path angle

**Step 2: Assess obstacles**

Detailed guidance regarding obstacle assessment is contained in Appendix A. In general, obstacles should be visually assessed to the lateral limits of the procedure design segment. The aircrafts should be positioned in a manner that provides a good view of the obstacle environment that is under consideration. This may require flying the lateral limits of the procedure protection areas in order to detect if unaccounted obstacles exist. The controlling obstacle should be verified for each segment of the IFP. Should unaccounted obstacles be observed, further investigation by the Flight Validation Pilot is required.

### Step 3: Assess Flyability and Human Factor

Fly at least one on-course/on-path flight evaluation of the proposed procedure in an appropriate aircraft capable of conducting the procedure. See Appendix B for more detailed human factors information. The objectives of flyability assessment of instrument flight procedures are:

- Evaluate aircraft manoeuvring areas for safe operations for each category of aircraft for which the procedure is intended.
- Review the flyability of the instrument procedure as follows:
  - Fly each segment of the IFP on-course and on-path.
  - Validate the intended use of IFP as defined by

Stakeholders and described in the conceptual design.

- Evaluate other operational factors, such as charting, required infrastructure, visibility, intended aircraft categories, etc.
- Evaluate the aircraft manoeuvring area for safe operations for each category of aircraft to use the IFP.
- Evaluate turn anticipation and the relationship to standard rate turns and bank angle limits.
- Evaluate the IFP complexity, required cockpit workload, and any unique requirements.
- Check that waypoint spacing and segment length are suitable for aircraft performance.
- Check distance to runway at Decision Height/Decision Altitude/Minimum Descent Altitude that are likely to be applied by operators and evaluate the ability to execute a landing with normal manoeuvring.
- Evaluate required climb or descent gradients, if any.
- Evaluate the proposed charting for correctness, clarity, and ease of interpretation.

### Step 4: Evaluate Ground Proximity Warning System (GPWS) warnings.

The flyability assessment must be flown at speeds and aircraft configurations consistent with the normal IFR operations and meet the design intent (Aircraft Category). The Final Approach Fix to Threshold of an instrument approach procedure must be flown in the landing configuration, on profile, on speed with the GPWS active. Flyability should be evaluated with the aircraft coupled to the autopilot (to the extent allowed by the aircraft flight manual or SOP(s)) and may require additional evaluation by hand flying.

Aircraft category restrictions might be published and must be confirmed acceptable. In every case, the pilot is required to pay particular attention to the general safe conduct of the procedure and efficiency of the flight for the intended aircraft category.

*Note: It is recommended that if different minima are provided for the same final segment (e.g. LNAV, LNAV/VNAV, LPV), that the evaluation of the final segment is accomplished on separate runs.*

Step 5: Conduct associated validation tasks

The following associated flight validation tasks may be performed in conjunction with the obstacle or flyability assessment as required:

- Verify that all required runway markings, lighting, and communications are in place and operative.
- Verify that any required NAVAID(s) have been satisfactorily flight inspected to support the procedure design.
- Ensure the VGSI angles appear as intended or charted when

evaluating vertically guided procedures.

- Air/ground communications with Air Traffic Control (ATC) must be satisfactory at the initial approach fix or intermediate fix minimum altitude and at the holding fix. Satisfactory communications coverage over the entire Minimum Vectoring Altitude, airway or route segment (in controlled airspace) at the minimum en route IFR altitude must be available with an ATS facility.
- Ensure radar coverage is available for all portions of the procedure, where required.
- Indicate any GPWS warnings or alerts. Record details of the alert to include lat/long, aircraft configuration, speed, and altitude.
- If night evaluation is required, determine the adequacy of airport lighting systems prior to authorizing night operation. Conduct night evaluations during VMC following appropriate daytime evaluation.

Step 6: Evaluate the light system for:

- Correct light pattern as charted
- Local lighting pattern in the area surrounding the airport to ensure they do not distract, confuse, or incorrectly identify the runway environment.

Step 7: Verify that waivers to standard design do not compromise safety.

Step 8: Verify chart depiction and details



- Check to ensure the chart has sufficient detail to safely navigate and identify significant terrain or obstacles.
  - Ensure that the chart accurately portrays the procedure and is easily interpreted. Ensure flight track matches chart and takes aircraft to designated point.
  - Verify true and magnetic course to next waypoint indicated on the FMS or GPS accurately reflects the procedure design. (Magnetic courses displayed by the FMS/GPS navigator may be dependent upon the manufacturer's software processing of magnetic variation.)
  - Verify segment distances indicated by the aircraft navigation system accurately reflect the procedure design.
  - Verify the FPA indicated on the FMS or GPS accurately reflects the procedure design.
  - Check that waypoint spacing and segment length are sufficient to allow the aircraft to decelerate or change altitude on each leg without bypassing.
- c. Minimum number of satellites
  - d. Average Position Dilution of Precisions (PDOP)
  - e. Maximum Observed Horizontal Dilution of Precision (HDOP) [SBAS Procedures only]
  - f. Vertical Protection Level (VPL) [SBAS/GBAS Procedures only]
  - g. Horizontal Protection Level (HPL) [SBAS/GBAS Procedures only]
  - h. Maximum Observed Vertical Dilution of Precision (VDOP) [SBAS Procedures only]
  - i. For each segment, the maximum and minimum altitude, ground speed, climb rate, and climb gradient
  - j. A printed graphic or an electronic file of sufficient detail that depicts the flight track flown referenced to the desired track of the approach procedure, including procedure fixes

#### Step 9: Record flight validation

A recording device should be used that is capable of the following: IFP storage, time and 3-dimensional position in space with an acceptable sampling rate (not less than 1 Hz), and ability to post-process recorded data.

Record and save the minimum following flight data:

- a. Processing date and time
- b. Maximum number of satellites

#### Post Flight Validation

Post Flight analysis and documentation finished out the Validation process. Certain types of flight and navigational data must be recorded during the Flight Validation. Some of this data must undergo post-flight analysis to verify navigation data accuracy and integrity, as well as proper flight track performance, both laterally and vertically. A determination of satisfactory or unsatisfactory results should be made, along with ensuring the completeness and correctness of the procedure package. All recorded electronic data and the final report should be archived.

Step 1: Assess the results of the flight validation:

- Review all aspects of the flight validation process to complete the assessment.
- Make a determination of satisfactory or unsatisfactory results based on criteria established by the State.
- For satisfactory flight validations, complete the IFP processing:
  - Ensure the completeness and correctness of the IFP package to be forwarded.
  - Confirm that required flight inspection of navigation aids and/or lighting, if any, has been completed.
- For unsatisfactory flight validations, return the IFP to the procedure designer(s) for corrections.
  - Provide detailed feedback to the procedure designer(s) and other stake holders.
  - Suggest mitigation and/or corrections for unsatisfactory results
- Complete a detailed written report of the results of the flight validation.
- Ensure any findings and operational mitigations are documented
- Forward uncharted controlling obstacle position and elevation data to procedure designer(s).
- Ensure recorded data is processed and made available for archiving.

**Next Steps to ICAO Implementation –** QA document 9906 Vol. V is now finalized and ready for final deliberation during the next International Flight Procedure Panel (IFPP) meeting to be held at the ICAO headquarters in Montreal in October 2010. Adjustments and fine tuning of details are expected to keep this volume consistent with the others in the 9906 series. Publication is expected by mid 2011.

Step 2: Document the results of flight validation

# Flight Validation of Performance Based Navigation (PBN) Procedures

**Donald P. Pate**  
Consultant/FAA  
Aviation Airspace Consulting, Inc.  
Edmond, OK, USA  
E-mail: donppate1@yahoo.com

AUTHOR  
PHOTO  
HERE

## ABSTRACT

Instrument flight procedures (IFPs) constructed under the criteria contained in *Procedures for Air Navigation Services – Aircraft Operations* (PANS-OPS, Doc 8168) using conventional ground-based navigational aids have always required the exercise of a high level of quality control during development and publication. However, with the implementation of Performance Based Navigation (PBN) procedures with their associated airborne databases, even small errors in data could lead to catastrophic effects during instrument flight operations. This significant increase in the criticality of airborne data, including coding, accuracy, resolution and integrity, has led to additional requirements in the quality assurance process and may also be included as part of a State Safety Management System. The PANS-OPS, Volume II, Part 1, Section 2, Chapter 4, *Quality Assurance*, refers to Doc 9906 specifying that a State take measures to ‘control’ the quality of the processes associated with the construction of instrument flight procedures. To this end, *The Quality Assurance Manual for Flight Procedure Design, Volume 5 and 6*, is being assembled to provide guidance in attaining these stringent requirements for quality assurance in the PBN procedure design process. There are six volumes in this draft manual which address crucial areas related to the attainment, maintenance and continual improvement of procedure design quality. Volume 5, *Flight Validation of Instrument Flight Procedures*, provides guidance for conducting the flight validation process for PBN instrument flight procedures, to assess their safety, flyability and design accuracy. This paper addresses the inherent improvement in quality and safety of implementation of newly developed or revised PBN procedures.

## INTRODUCTION

Instrument flight procedures based on conventional ground-based navigational aids have always demanded a high level of quality control. However, with the implementation of area navigation (RNAV) and the associated airborne databases, even small errors in data could lead to catastrophic effects. This significant increase in data quality requirements (accuracy, resolution and integrity) has led to the need for a systemic quality assurance process (often part of a State Safety Management System). The *Procedures for Air Navigation Services – Aircraft Operations* (PANS-OPS, Doc 8168 Volume II, Part 1, Section 2, Chapter 4, *Quality Assurance*), refers to Doc 9906 and specifies that a State take measures to ‘control’ the quality of the processes associated with the construction of instrument flight procedures. To this end, *The Quality Assurance Manual for Flight Procedure Design* is under revision to provide the guidance for attaining these stringent quality assurance requirements for the Performance Based Navigation (PBN) procedure design process. All six volumes of Doc 9906 address crucial areas related to the attainment, maintenance and continual improvement of procedure design quality. Data quality management, procedure designer training, and validation of software are all integral elements of a quality assurance program

This paper addresses two volumes of the manual:

**Volume 5** – *Flight Validation of Instrument Flight Procedures*, which provides guidance for conducting the flight validation process of PBN based instrument flight procedures, including safety, flyability and design accuracy.

**Volume 6** – *Flight Validation Pilot Training and Evaluation*, which provides guidance for the establishment of a flight procedure validation pilot training program. Training is the starting point for any quality assurance program.

Some new terminology has been introduced into the process for evaluating an IFP which should be clarified:

**Flight Validation.** Flight assessment of a new or revised instrument flight procedure to verify the procedure is operationally acceptable for safety, flyability and design, including obstacle assessment and database verification, and supporting documentation.

**Validation.** Confirmation through the provision of objective evidence that the requirements for a specific intended use or application have been fulfilled (Annex 15). The activity whereby a data element is checked as having a value that is fully applicable to the identity given to the data element, or a set of data elements that is checked as being acceptable for their purpose.

For the purposes of quality assurance in the procedure design process, flight inspection and flight validation are separate activities that may or may not be accomplished by the same organizational entity. Traditionally, flight inspection has been conducted for the purpose of confirming the ability of a navigational aid(s) to support IFPs based on the navaid, in accordance with the standards specified in Annex 10 — *Aeronautical Telecommunications* and guidance in the *Manual on the Testing of Radio Navigation Aids* (Doc 8071).

Flight validation is concerned with factors other than the performance of the navigational aid that may affect the suitability of the procedure for publication, as detailed in PANS-OPS, Volume II, Part I, Section 2, Chapter 4, *Quality Assurance*. Currently, the procedure design or flight inspection organizations may not be trained to determine the conditions requiring flight validation. However, ICAO expects the State to provide for the overall performance of a procedure, as well as the quality and suitability of the procedure prior to publication. For this reason it is recommended that a review of PBN procedures by the flight inspection and/or flight validation organizations be included in the State's procedure design process flow, following ground validation.

Implementation of instrument flight procedures is the responsibility of Contracting States, and state authorities have final responsibility for the procedures published within their territory. There is no ICAO limitation on either a state performing flight validation or delegating the function under state oversight to a third party (ATS providers, private companies, other State, etc.).

The *Procedures for Air Navigation Services— Aircraft Operations* (PANS-OPS, Doc 8168) specifies that the State take measures to perform ground and flight validation of instrument flight procedures. This process validates the quality and safety of the procedure design before publication. In all cases, including third party delegation, the State retains the ultimate responsibility for the procedures published in their national Aeronautical Information Publication (AIP).

*The Quality Assurance Manual for Flight Procedure Design*, Volumes 5 and 6 are being developed by an Instrument Flight Procedure (IFPP) Working Group to provide guidance to states for establishing a flight validation process that will ensure the quality of the PBN flight procedures they publish. The manual provides an acceptable means for developing a flight validation program. This paper reviews the currently drafted ICAO Flight Validation requirements and the recently released FAA Notice 8260.67 which provides US guidance for implementing the ICAO requirement.

### **Volume 5 – Flight Validation of Instrument Flight Procedures**

The Integrated Aeronautical Information Package should be thoroughly checked and coordinated with the responsible services to make certain that all necessary information has been included and that it is correct in detail prior to distribution. Validation and verification procedures must be established which ensure that quality requirements (accuracy, resolution, and integrity) and traceability of aeronautical data are met.

Flight Validation is one of the final quality assurance steps in the procedure design process for instrument flight procedures (IFP). The purpose of validation is to verify all obstacle and navigation data, and assess flyability of the procedure.

Flight validation encompasses both ground and flight elements. The flight validation process includes pre-flight, in-flight and post flight activities required for evaluating the IFP. Flight validation of IFP(s) must be carried out as part of the initial certification and for amendments to an existing IFP that significantly affects the lateral or vertical flight path. It must be accomplished by a qualified flight validation pilot (FVP) trained and approved in accordance with Volume 6 of the manual.

A flight validation report must be provided but it is the responsibility of the State to determine the method of documentation. Minimum requirements are name and signature of the FVP, date, type of aircraft, findings, validation pilot comments and operational recommendations. It is recommended that a printed graphic and/or electronic file of sufficient detail be archived that depicts the flight track flown referenced to the desired track of the instrument flight procedure, including procedure fixes, and that the maximum and minimum altitude, ground speed, climb rate and climb gradient.

To provide an initial evaluation of database coding, flyability, and to provide feedback to the procedure designer, a simulator assessment may be necessary. Preparation for a simulator evaluation should include a comprehensive plan with a description of the conditions to be evaluated, profiles to be flown and objectives to be achieved.

For complex Required Navigation Performance Authorization Required (RNP AR) and special procedures, a simulator

evaluation is necessary. The evaluation must be flown in a simulator which meets all procedure requirements. If the procedure is designed for a make/ model/ series or specific FMS or software, the evaluation should be flown in a simulator with the same configuration as used by the operator in daily operations.

Flight validation of instrument procedures should be carried out as part of the validation of initial and amended procedures. Flight validation should be included as part of the periodic quality assurance program established by States to ensure the procedure design process and its output, including the quality of aeronautical information/data, meet the requirements of Annex 15. It must be accomplished by a qualified flight validation pilot, certified or approved by the State.

Ground track path error performance varies with mode of flight guidance system coupling. It is imperative to evaluate new procedures coupled to the flight director and autopilot (when not prohibited). Evaluate lateral and vertical disconnects from both the autopilot and the flight director. Procedure design is based on TRUE altitudes, so in-flight evaluation should be conducted at true altitudes with consideration for temperature variations from standard day. Lateral and vertical transitions from departure, en route, descent, and approach must produce a seamless path that ensures flyability in a consistent, smooth, predictable, and repeatable manner.

FV is required for PBN procedures and recommended for 1 other types of IFPs described in PAN OPS. The procedure must be flown in the relevant navigation mode required by the design. For example, for RNAV (GNSS) IFP, one must ensure that only the GNSS sensor is utilized during the FV. The objectives of a flight validation are to:

- Conduct an assessment of flyability to determine that the procedure can be safely flown.
- Provide the final assurance that adequate obstacle clearance has been determined.
- Verify that the navigation data to be published is correct.
- Verify that all required infrastructure, such as runway markings, lighting, and communications and navigation sources are in place and operative.
- Ensure that documentation of navigation systems confirms the applicable navigation system(s) (NAVAID, GNSS, RADAR, etc.) support the procedure.
- Evaluate other operation factors, such as charting, required infrastructure, visibility, intended aircraft category, etc.
- Verify that waivers to standard design do not compromise safety.

It is essential that the data used in the procedure design is compared to the chart, flight management system (FMS) data, or other suitable navigation system databases. Load and verify the IFP into a data collection/recording device that archives the procedure and aircraft positioning data. The procedure development package, charts, and airport data must all agree.

It is recommended that RNAV procedures be packed, Cyclic Redundancy Check (CRC) be used, and the data be loaded electronically into the FMS or suitable navigation system without manually coding the ARINC 424 path/ terminator data. This allows the flight validation process to evaluate the data as it was developed, without manipulation. If the procedure waypoint data must be manually entered into the FMS, it must be compared to the procedure data to ensure the data points match.

Steps to verify data:

- Ensure the data from the flight validation database matches that used in the procedure design.
- Ensure the data produces the desired flight track.
- Ensure that the final approach course/ glide path deliver the aircraft to the desired point in space.

Detailed guidance regarding obstacle and infrastructure assessment is contained in Appendix A of the manual. In general, obstacle assessment should be evaluated to the lateral limits of the procedure design segment.

Sloping surfaces, such as the missed approach and departure procedures, should be flown at the standard minimum performance gradient, or that depicted on the IFP. It is recommended that vertically guided approach procedures be flown on path to assess obstacle clearance.

To assess obstacle and infrastructure:

- Verify the listed controlling obstacle for each segment of the IFP.
- Conduct obstacle assessment to the lateral limits off each segment.
- Document any uncharted obstacles with position and an evaluation.

To assess flyability and human factors, fly at least one on-course/ on-path flight evaluation of the proposed procedure. See Appendix B of the manual for more detailed human factors information. The objectives of a flyability assessment are to:

- Evaluate aircraft manoeuvring areas for safe operations for each category of aircraft for which the procedure was designed.

- The flyability of the instrument procedure can be evaluated as follows:
  - Fly each segment of the IFP on-course and on-path.
  - Validate the intended use of IFP as defined by Stakeholders and described in the conceptual design.
  - Evaluate other operational factors, such as charting, required infrastructure, visibility, intended aircraft categories, etc.
  - Evaluate the aircraft manoeuvring area for safe operations for each category of aircraft to use the IFP.
  - Evaluate turn anticipation and the relationship to standard rate turns and bank angle limits.
  - Evaluate the IFP complexity, required cockpit workload, and any unique requirements.
  - Check waypoint spacing and segment length as suitable for aircraft performance.
  - Check distance to runway at Decision Height/ Decision Altitude/ Minimum Descent Altitude likely to be applied by operators and evaluate the ability to execute a landing with normal maneuvering.
  - Evaluate required climb or descent gradients, if any.
  - Evaluate the proposed charting for correctness, clarity, and ease of interpretation.
  - Evaluate GPWS warnings.
- Verify that any required NAVAID(s) have been satisfactorily flight inspected to support the procedure design.
- Confirm waypoint/ fixes cross reference to coordinate values used in the IFP design.
- Ensure the Visual Glide Slope Indicator (VGSI) angles appear as intended or charted when evaluating vertically guided procedures.
- Confirm that Air/ ground communications with ATC are satisfactory at the initial approach fix or intermediate fix minimum altitude and at the holding fix. Verify satisfactory communications coverage over the entire Minimum Vectoring Altitude, airway or route segment (in controlled airspace) at the minimum en route IFR altitude.
- Ensure radar coverage is available for all portions of the procedure, where required.
- Indicate any GPWS warnings or alerts. Record details of the alert to include lat/ long, aircraft configuration, speed, and altitude.
- Confirm that the final approach segment of the procedure follows the intended track and takes the aircraft to the intended point in space.
- If night evaluation is required, determine the adequacy of airport lighting systems prior to authorizing night minimums. Conduct night evaluations during VMC following appropriate daytime evaluation

Evaluate the lighting system for:

- Correct lighting pattern as charted
- Local lighting pattern in the area surrounding the airport to ensure they do not distract, confuse, or incorrectly identify the runway environment

Verify that waivers to standard design do not compromise safety.

Verify chart depiction and chart notes:

- Check to ensure the chart has sufficient detail to safely navigate and identify significant terrain or obstacles.
- Ensure that the chart accurately portrays the procedure and is easily interpreted. Ensure flight track matches chart and takes aircraft to designed point.
- Verify true and magnetic course to next waypoint indicated on the FMS or GPS accurately reflects the procedure design. (Magnetic courses displayed by the FMS/ GPS navigator may be dependent upon the manufacturer's software processing of magnetic variation.)
- Verify segment distances indicated by the aircraft navigation system accurately reflect the procedure design.

The flyability assessment must be flown at speeds and aircraft configurations consistent with normal instrument flight rules (IFR) operations and meet the design intent (Aircraft Category). The Final Approach Fix to Threshold of an instrument approach procedure must be flown in the landing configuration, on profile, on speed with the Ground Proximity Warning System (GPWS) active. Flyability should be evaluated with the aircraft coupled to the autopilot (to the extent allowed by the aircraft flight manual or SOP(s)) and may require additional evaluation by hand flying.

Aircraft category restrictions might be published and must be confirmed acceptable. In every case, the pilot is required to pay particular attention to the general safe conduct of the procedure and efficiency of the flight for the intended aircraft category.

Other validation tasks may be performed in conjunction with the obstacle or flyability assessment:

- Verify that all required runway markings, lighting, and communications are in place and operative.

- Verify the Flight Path Angle (FPA) indicated on the FMS or GPS accurately reflects the procedure design.
- Check that waypoint spacing and segment length are sufficient to allow the aircraft to decelerate or change altitude on each leg without bypassing.

A recording device must be used that is capable of the following: IFP storage, time and 3-dimensional position in space with a sampling of not less than 1 Hz, and ability to post-process recorded data. The recording device must be compliant with reference to the applicable minimum operational performance specification for the GNSS or ground-based navigation.

A printed graphic or an electronic file of sufficient detail that depicts the flight track flown referenced to the desired track off the approach procedure, including procedure fixes should be developed.

Ground Proximity Warning Systems (GPWS) may alert while flying over irregular or rapidly rising terrain at altitudes providing standard obstacle clearance. If GPWS alerts are received while validating a procedure, repeat the maneuver, ensuring flight at the designed true altitude using Temperature Compensation at the maximum design speed for the procedure. If an alert is repeated, record the information in the report, including sufficient details for resolution by the designer. Do not hesitate to provide potential operational solutions such as speed restrictions, altitude restrictions or waypoint relocation. A false GPWS alert may be generated when approaching an airport runway that is not in the GPWS's database. The GPWS check should be performed with proper aircraft configuration to reflect a scenario during the on-course on-path evaluation of an instrument flight procedure (IFP).

#### **FAA NOTICE 8260.67/ FLIGHT VALIDATION OF PBN IFPS**

This notice establishes FAA policy and guidance for conducting Flight Validation (FV) of Performance-Based Navigation (Satellite) and Special Wide Area Augmentation Systems (WAAS) Instrument Flight Procedures (IFP). This notice supplements the requirements of FAA Order 8200.1, United States Flight Inspection Manual and also describes the requirement for simulator evaluations and obstacle assessments. This paper summarizes key concepts of the FAA notice and correlates those requirements to those given in ICAO Doc 9906-AN/472 Volume 5.

This notice defines *validation* as the final quality assurance step in the procedure design process of performance-based navigation (PBN) and WAAS instrument flight procedures (IFP). The purpose is to verify obstacle and navigation data, and assess the flyability of an IFP. The notice states that *validation* consists of both ground and flight validation. PBN procedures containing FAS data require an approved system to validate FAS data elements for course alignment, approach

angle, threshold crossing height (TCH) and the Cyclic Redundancy Check (CRC).

PBN procedures such as RNAV (GPS) RNAV (RNP) and WAAS IFPs require highly accurate data based on the WGS-84 geodetic datum. They require a quality assurance system that will cover all domains of data collection (surveys), processing, publication and navigation database be established and maintained consistent with ICAO Annexes 4, 11, 14, and 15.

The FAA Notice defines a Ground Validation (GV) phase in the review of an IFP package by a trained Flight Validation (FV) specialist prior to the FV. GV is meant to identify deviations from criteria, documentation; and verify those elements to be evaluated in the FV phase. Ground Validation includes both the simulator evaluation and obstacle assessment.

The FAA Notice requires a Flight Validation of all PBN IFPs as part of their initial certification. FV must be accomplished by a qualified flight validation pilot/evaluator approved in accordance with the Notice.

The FAA Notice states that the objectives of Flight Validation are to:

- (1) Conduct an assessment of flyability to determine that the procedure can be safely flown
- (2) Provide final assurance that adequate obstacle clearance has been provided
- (3) Verify that all published navigation data to be is correct
- (4) Verify that FAS data elements provide navigation guidance, as designed, to the physical runway threshold or required point-in-space. (WAAS only)
- (4) Verify that all required infrastructure, such as runway markings, lighting and communications and other navigation sources are in place and operative.
- (5) Evaluate other operational factors, such as charting, required infrastructure, visibility.

The FAA Notice requires Flight Validation ensure that the lateral and vertical path achieves the design objective and database functions in flight as intended. The FV flight crew should note and document any anomalies with regard to the flight procedure, flight management system (FMS) operation, obstructions, communications, surveillance, airport infrastructure. Obstacle assessments, as outlined in Order 8200.1 may be completed before or after the simulator evaluation.

Service providers conducting development and/or Flight

Validation of WAAS IFP must have an FAA Flight Standards-approved system to evaluate and confirm the integrity of the FAS data including course alignment, threshold crossing height, and glide path angle.

Ground Validation includes the following:

- (1) Review of the PBN IFP Package
- (2) Review of operational issues such as temperature and wind limitations, air speeds, bank angles, climb/descent gradients
- (3) Verification of the PBN or WAAS IFP design, coding, and relevant charting information against the FMS Navigation Database
- (4) Review of any special operational and training requirements
- (5) Discuss the procedure package with the procedure designer, as necessary. If organizational structure permits, include the procedure designer in the simulator evaluation
- (6) Conduct a desktop simulator evaluation (recommended) of database coding & flyability
- (7) Plan the simulator evaluation (if required)

Required Navigation Performance (RNP) Special Aircraft and Aircrew Authorization Required (SAAAR) IFPs are required to have a simulator evaluation prior to Flight Validation. This requirement can be waived at the discretion of the Flight Procedure Implementation and Oversight Branch (AFS-460). A simulator evaluation of IFPs other than PBN may be conducted to evaluate a special design or determine any special operational conditions that may be required.

Simulator Requirements:

- (a) For a public PBN IFP, the simulator evaluation should be conducted in an FAA-qualified Level “C” or Level “D” flight simulator capable of flying the procedure under normal operations.
- (b) For a Special PBN IFP designed for a specific operator, conduct the simulator evaluation in an FAA-qualified Level “C” or Level “D” flight simulator. If the procedure is designed for a specific make/model/series or specified FMS, software part number, software version, or revision, the initial simulator GV should be flown in a simulator with the same configuration as used by the operator for this operation. If the procedure is considered a Special for other reasons, i.e., climb performance, The GV will be flown in a simulator matching the procedure requirements.

- (c) Simulator evaluations must be accomplished by appropriately qualified flight crew and evaluators as specified by the Notice.
- (d) All items listed on FAA Form 8260-30A, Simulator Evaluation Checklist described in the Notice must be evaluated.
- (e) Simulator evaluation records must be maintained. Organizations performing simulator evaluations retain the original FAA Form 8260-30A and forward a copy to Flight Standards (AFS-460).

The FV must be recorded using an Autonomous Global Positioning System Recording System (AGRS) or other suitable systems approved by Flight Standards (AFS-460).

The flight crews and evaluators of PBN, Special and WAAS IFPs must be approved by Flight Standards and meet specific requirements outlined in the Notice.

### CONCLUSION

The increased flexibility of IFP RNAV tracks based on a high integrity airborne database has added new requirements to the flight inspection and IFP design functions. This paper has provided an overview of the draft ICAO Flight Validation Manual and the FAA Flight Validation Notice which highlights these new requirements.

Due to the high interaction between aircraft/equipment performance, flight crew procedures, airborne databases and the advanced procedure design it is necessary to verify the integrity of this interaction prior to publication of the IFP. This verification process is described in the new set of flight simulator, obstacle validation and flight validation requirements published by the FAA and under development by the ICAO.

### REFERENCES

- [1] ICAO, Third Edition, 2008, Performance Based Navigation Manual, Volumes I and II, Doc 9613-AN/937
- [2] FAA, December 2005, Approval Guidance for RNP Procedures with Special Aircraft and Aircrew Authorization Required, AC 90-101
- [3] ICAO, Procedures Design for RNP(AR) Approach Procedures, PANS Ops Manual
- [4] FAA, U.S. Standard for Required Navigation Performance (RNP) Approach Procedures with SAAAR, FAA Order 8260.52
- [5] ICAO, Procedures for Air Navigation Services — Aircraft Operations, PANS-OPS, Volume I & II, PANS-OPS, Doc 8168



[6] ICAO, The Quality Assurance Manual for Flight Procedure Design, Volume 5 (Draft), Flight Validation of Instrument Flight Procedures, Doc 9906-AN/472

[7] FAA, Flight Validation (FV) of Satellite-Based Performance-Based Navigation (PBN) Instrument Flight Procedures (IFP)-Current Guidance and Criteria, FAA Notice N8260.67

[8] FAA, United States Flight Inspection Manual, FAA Order 8200.1



## Measurement sampling rates based on aircraft speed to accurately measure and characterize the guidance quality

### Simbo A. Odunaiya, Ph.D.

Senior Research Engineer  
Ohio University  
Athens, Ohio 45701  
Fax: (740) 593-1604  
Email: [odunaiya@ohio.edu](mailto:odunaiya@ohio.edu)



### David Quinet

Senior Research Program Engineer  
Ohio University  
Athens, Ohio 45701  
Fax: (740) 593-1604  
Email: [quinet@ohio.edu](mailto:quinet@ohio.edu)



### ABSTRACT

Recent developments have shown that when analyzing the performance of navigation systems, the agreement of flight check results with modeling results depend largely on the sampling intervals used in the modeling exercise. This is of course expected as the replication of flight measurements depend on the filtering which in turn depends on the sampling intervals. What has been noticed recently is the issue of under sampling especially when measurements are made over the runway using vehicles at speeds that are much lower than that of a typical flight inspection aircraft. The effect of under sampling are also amplified or pronounced when scattering aircraft is located in the so called ILS sensitive areas.

ICAO Annex 10 documents currently requires that measured DDM values for ILS be filtered at a time constant  $T_f$  seconds of  $50/V$  where  $V$  is the velocity of the aircraft in knots. This speed based requirement is expected to make it easy to correlate measurements made with slower moving vehicles over the runway with data received in the aircraft. A similar filter is required in modeling analysis so that modeling results can be conveniently compared with flight measurements. In order to avoid aliasing or signal distortions the data samples in the modeling analysis must be done at a rate that is consistent with the Nyquist theorem. This requires that there is a proper understanding of the nature or characteristics of the bends, scalloping, and the roughness of the ILS signal due to multipath.

In addition, the characteristic of the reflected signal (diffraction) can cause very short disturbances which may or not be seen by the flight inspection aircraft depending on the aircraft approach speed and the flight inspection systems data sampling rate.

This paper presents several considerations in determining the appropriate sampling rates. Several results will also be

presented that shows correlations between flight data and modeled results.

### INTRODUCTION AND BACKGROUND

This paper is in response to recent developments in the analysis of navigation and landing systems. Issues pertaining to under sampling when simulating approach flights have been reported. These issues are more pronounced in CAT III simulation especially if there are objects positioned to cause significant errors in zone 5. When simulating approach flights for navigation systems, the agreement of flight check results with simulation results will depend greatly on the sampling intervals used in the simulation exercise. The sampling interval that must be used depends on the speed of the aircraft/data collection vehicle and the filter used in the analysis of the collected data.

The constraints to keep in mind when analyzing Instrument Landing System localizer and glide slope is that ICAO Annex 10, Attachment C documents [1] state as follows:

*“Owing to the complex frequency components present in the ILS beam bend structures, measured values of beam bends are dependent on the frequency response of the airborne receiving and recording equipment. It is intended that beam bend measurements be obtained by using a total time constant (in seconds) for the receiver DDM output circuits and associated recording equipment of  $92.6/V$ , where  $V$  is the velocity in km/h of the aircraft or ground vehicle as appropriate.”*

Since this specified time constant is speed based, it is still easy to correlate data measured using slower moving vehicles over the runway when all the parameters have been considered.

The intent of this paper is to consider the various parameters that affect the sampling rates

### ILS SIGNAL SAMPLING IN MULTIPATH ENVIRONMENT

In order to avoid signal distortions or what is also known as aliasing the ILS signal must be sampled at a sufficient rate to reproduce the actual effect of the source of multipath. This means that the sampling frequency must be at least twice the bandwidth of the signal to be reproduced.

$f_s = \frac{1}{T_s}$  where  $f_s$  is the sampling frequency and  $T_s$  is the sampling rate. Bredemeyer, Kleinmann, and Kraemer [2] have shown that for ILS signal sampling the sample rates can be computed as follows:

$$f_s [Hz] = 6.75 * \frac{V[knots]}{\lambda[feet]}$$

Using the Bredemeyer et. al. formula above the sampling rate for a localizer maximum frequency of 111.95 Mhz and an assumed aircraft speed of 118 knots will be about 90 Hz. This paper will show the implications of the sampling rate in practical terms.

### **Ohio University Landing and Performance Prediction Model (OUNPPM)**

In the Ohio University Navigation and Landing Performance Prediction Model (OUNPPM), bilinear transformation is used in the development of the filter to avoid aliasing. The resulting filter equation is [3]

$$H(z) = \frac{T_s * \omega(z+1)}{2 * (z-1) + T_s * \omega(z+1)}$$

In this equation  $\omega$  is the corner frequency for the filter. Figure 1 and Figure 2 compares a filtered modeled result with unfiltered modeled result.

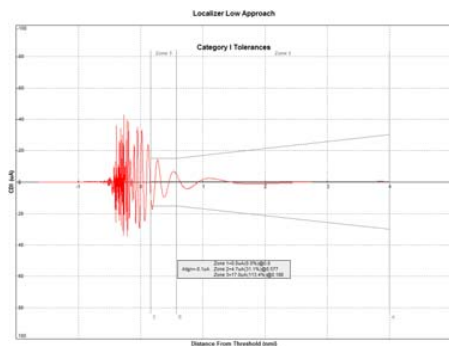


Figure 1. Unfiltered output from OUNPPM

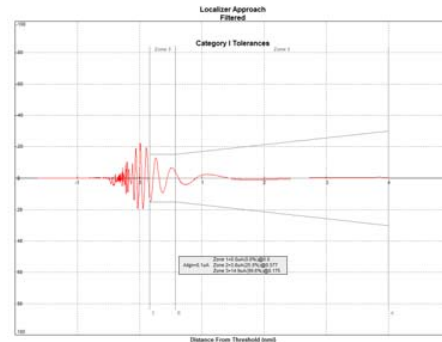


Figure 2. Filtered output from OUNPPM

### Analysis using Simulation Tool

The Ohio University Performance Prediction Model (OUNPPM) was run to demonstrate various forms of degradations and sampling rates based on the location, orientation, and length of reflecting objects. Figures 3 shows the different multipath signatures based on the parameters. Note the similar trends that high frequency abeam the object with the scallop frequency slowly decreasing. Results for other parameters like length and orientation are shown in Figure 4 and 5. Changes to these parameters will change the scalloping frequency. Simulations were run to determine how sensitive each parameter is. See result i

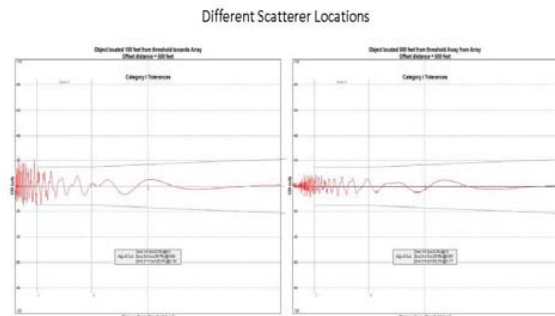


Figure 3. Scalloping as a function of location. As the object is located farther away from the radiating source the frequency is reduced.

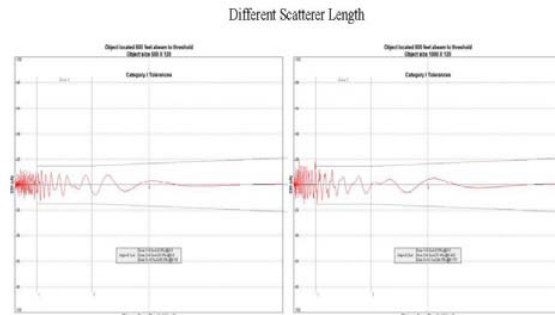


Figure 4. Scalloping as a function of scatterer length. Longer length results in lower the scalloping frequency

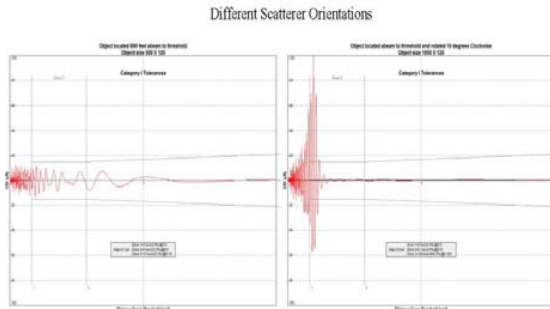


Figure 5. Scalloping as a function of scatterer orientation. Scalloping increases as angle of incidence tends towards oblique incidence.

If objects are placed on either side of the runway in a symmetrical manner, the degradation from both objects will cancel each other. Since the information is contained in the 90- and 150-Hz AM signals; under sampling of either signal will result in incomplete cancellation. Figure 5 shows the degradation from an identical object on the 90- and 150-Hz sides. Note that the amplitude and scalloping are identical but the disturbance sign is opposite. Figure 6 shows the result when both objects are considered at the same time.

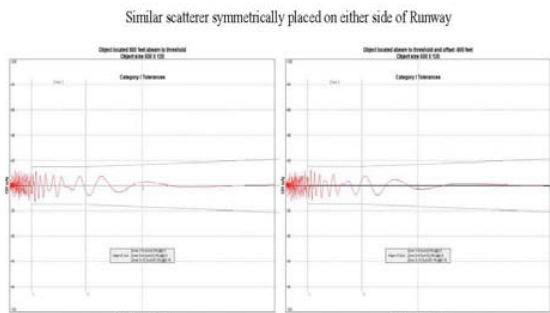


Figure 5. Symmetrical objects on either side of runway showing out of phase scalloping.

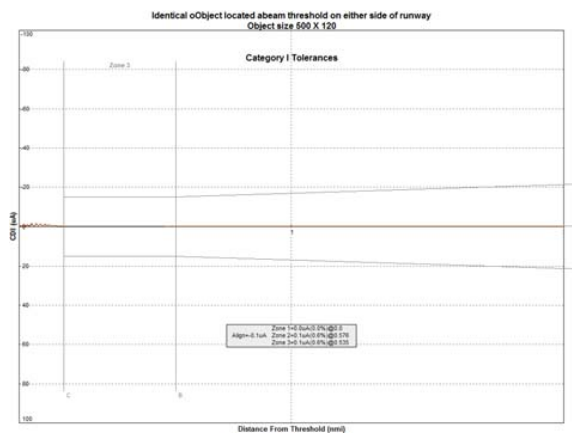


Figure 6. Result showing cancellation when identical objects are on both sides of the runway

**Various Locations:** Simulations were performed with the location of an object located at the same offset from centerline but at various setback and sampling rate. A summary of the results are contained in Table 1. These results indicate that the reflecting source location has some

effect on the sampling rate when the scalloping or roughness falls in zone 5. The result also shows that in this instance the sampling frequency required increases with closer proximity to the array.

**Length of reflecting objects:** For the simulations to ascertain the effect of the scatterer length on the sampling rate the scatterers used are oriented parallel to the runway centerline and the simulations were done at different sampling rates. The results in this case suggest that the shorter the length of the scatterer the higher the sampling frequency required to accurately represent the scalloping due to the scatterer. This effect is also mostly noticed in ILS zone 5. In the summary of the results shown in Table 2, the results indicate for example that a 4Hz sampling will not be adequate to reproduce the errors for a 250 feet long plate scatterer, this sampling rate is however adequate for a 1000 feet long plate scatterer. It is also noted that the calculated 100 Hz sampling rate from Bredemeyer et. al. is more than required in this scenario. This indicates that the length of a reflecting object should be considered in determining the sampling rate when modeling the object, especially if it is determined a priori that the scalloping from the object will fall within ILS zone 5.

**Orientation:** Several rotations of the same object have also been checked against the sampling rate. The summary of the results are as presented Table 3. These results indicate that the orientation of the object also has some effect on the sampling frequency. In fact the results obtained indicate that this is the most sensitive parameter with respect to sampling rate.

**Conclusions**

The results presented have shown that there are several parameters including location, length, and orientation of scatterers that do affect the choice of sampling frequency in the simulation of the ILS multipath environment. The results also indicate that the theoretically calculated value of 90Hz sampling frequency for the ILS is not necessary in many situations. In particular, a long, non-parallel reflecting object closer to the threshold will require a much higher sampling rate. In determining the scalloping frequency the engineer is advised to evaluate the scenario before making a decision. It is safer to just use the theoretically evaluated sampling frequency but when doing calculations to determine the size of critical or sensitive areas the overhead can be avoided if the sampling frequency is judiciously determined. In addition, to verify the rate is appropriate, mirror the object on the other side of the runway and verify the resulting simulation produces negligible error.

Table1. Summary of simulation results for object location versus sampling rate.

Sampling Rates (Hz)	CDI Error (uA) for Different Scatterer Distances to threshold (ft)											
	Zone 2			Zone 3			Zone 4			Zone 5		
	-4000	-5000	-6000	-4000	-5000	-6000	-4000	-5000	-6000	-4000	-5000	-6000
4	1.0	0.5	0.3	4.8	2.3	1.2	7.5	6.4	3.5	4.1	5.1	3.9
10	1.0	0.5	0.3	4.8	2.3	1.2	7.9	6.6	3.6	2.3	2.9	3.9
50	1.0	0.5	0.3	4.9	2.4	1.2	7.9	6.6	3.6	1.8	2.8	4.2
100	1.0	0.5	0.3	4.9	2.4	1.2	7.9	6.6	3.6	1.9	2.9	4.2
200	1.0	0.5	0.3	4.9	2.4	1.2	7.9	6.6	3.6	1.9	3.0	4.2

Table2. Summary of simulation results for object length versus sampling rate.

Sampling Rates (Hz)	CDI Error (uA) for Different Scatterer Lengths (ft)											
	Zone 2			Zone 3			Zone 4			Zone 5		
	250	500	1000	250	500	1000	250	500	1000	250	500	1000
4	0.5	1.0	2.0	2.3	4.7	9.2	6.4	9.1	11.5	5.1	3.7	4.5
10	0.5	1.0	2.0	2.3	4.7	9.2	6.6	9.1	11.5	2.9	4.1	4.2
50	0.5	1.0	2.0	2.4	4.7	9.2	6.6	9.1	11.5	2.8	4.2	4.3
100	0.5	1.1	2.0	2.4	4.7	9.2	6.6	9.1	11.5	2.9	4.2	4.3
200	0.5	1.1	2.0	2.4	4.7	9.2	6.6	9.1	11.5	3.0	4.2	4.3

Table2. Summary of simulation results for object orientation versus sampling rate.

Sampling Rates (Hz)	CDI Error (uA) for Different Scatterer Rotations (degrees)											
	Zone 2			Zone 3			Zone 4			Zone 5		
	10 deg CW	0 deg	10 deg CCW	10 deg CW	0 deg	10 deg CCW	10 deg CW	0 deg	10 deg CCW	10 deg CW	0 deg	10 deg CCW
4	0.5	0.5	1.2	0.8	2.3	2.1	0.6	6.4	3.2	12.5	5.1	3.3
10	0.5	0.5	1.2	0.8	2.3	2.1	0.7	6.6	3.3	8.5	2.9	2.6
50	0.5	0.5	1.2	0.8	2.4	2.1	0.7	6.6	3.3	10.2	2.8	2.6
100	0.5	0.5	1.2	0.8	2.4	2.1	0.7	6.6	3.3	10.2	2.9	2.6
200	0.5	0.5	1.2	0.8	2.4	2.1	0.7	6.6	3.3	10.2	3.0	2.6

Table4. Summary of simulation results for audio tones versus sampling rate.

Sampling Rates (Hz)	CDI Error (uA) for Audio Tone Cancellations											
	Zone 2			Zone 3			Zone 4			Zone 5		
	0 deg	10 deg	20 deg	0 deg	10 deg	20 deg	0 deg	10 deg	20 deg	0 deg	10 deg	20 deg
4	0.0	0.0	0.0	0.0	0.0	0.0	0.0	0.0	0.0	0.1	0.9	4.8
10	0.0	0.0	0.0	0.0	0.0	0.0	0.0	0.0	0.0	0.1	0.8	4.6
50	0.0	0.0	0.0	0.0	0.0	0.0	0.0	0.0	0.0	0.1	0.8	5.4
100	0.0	0.0	0.0	0.0	0.0	0.0	0.0	0.0	0.0	0.1	0.8	5.5
200	0.0	0.0	0.0	0.0	0.0	0.0	0.0	0.0	0.0	0.1	0.8	5.6

**REFERENCES**

1. ICAO: "Annex 10 to the Convention of International Civil Aviation, Volume I, Radio Navigation Aids," Montreal 2001
2. J. Bredemeyer, T. Kleinmann, and H. Kraemer; "ILS Interference Measurements and Dynamic Receiver Behaviour," Proceedings of the 14<sup>th</sup> International Flight Inspection Symposium (IFIS 2006).
3. Simbo Odunaiya and David Quinet, "Calculations and Analysis of Signal Processing by Various Navigation Receiver Architectures," Digital Aviation Systems Conference, 2004

# Improving Flight Inspection by process automation

## **Sileno. Godicke**

FI New Systems & Technology Manager  
ENAV S.p.A.  
Hangar 127, Aeroporto di Ciampino, Roma, 00040, Italy  
E-mail: [sileno.godicke@enav.it](mailto:sileno.godicke@enav.it)

## **Marcello D. Mannino**

Area Manager  
IDS Ingegneria Dei Sistemi S.p.A.  
Rome, Italy  
E-mail: [m.mannino@ids-spa.it](mailto:m.mannino@ids-spa.it)

## **Cristiana Cafiero**

Program Manager  
IDS Ingegneria Dei Sistemi S.p.A.  
Rome, Italy  
E-mail: [c.cafiero@ids-spa.it](mailto:c.cafiero@ids-spa.it)

## **Alessandro Nobiletti**

EMACS Product Manager  
IDS Ingegneria Dei Sistemi S.p.A.  
Rome, Italy  
Fax: +39 06 33217456  
E-mail: [a.nobiletti@ids-spa.it](mailto:a.nobiletti@ids-spa.it)

## **ABSTRACT**

Performance Based Navigation is challenging the flight inspection team capabilities due to a near and medium term increase in instrument flight procedures and routes validation and signal in space verification, but is not likely to assist in an equivalent increase in aircraft and personnel dedicated to flight inspections goals. The only means to achieve the required workload to ensure a safe flight environment is to increase the flight inspection team efficiency and proficiency.

Until today instrument flight navigation procedures rely upon fixed ground Nav aids, but this cannot be taken for granted anymore. The current Area Navigation and the potential to apply GNSS together depend ENTIRELY upon data quality and AIS/AIM team of ANSP department is responsible for it.

Interoperability and collaboration is a key to the future AIS to AIM and involve actively Flight inspection department. All this is reliant on data of the required content, quality & timeliness to reach “The right digital info, right place, right time” across the ANSP.

Additional challenges come from quality and safety requirements to adopt a standardized and certified workflow.

This paper will highlight the features of a Flight Inspection Planning and Post-processing tool (FLIPP-TMS) which has been designed to:

1. Managing flight checks requests coming from C/N/S infrastructure managers (for commissioning and special flight inspections)

and automatically generating the periodic flight checks requests

2. Support the strategic and tactical flight inspection mission planning to cope with the requested workload
3. Track all the activities from their initial request up to the final archiving and post-mission analysis.
4. Ensure Flight Inspection data integrity consistency and certification , both for nav aids and procedures data uploaded in the Flight Inspection System and Flight Check results downloaded from the FIS
5. Flight Inspection data results archiving and dissemination to all involved parties.
6. Web based interface allowing flight crew to access all the information needed with an ordinary PC wherever they are.

## **INTRODUCTION**

Flight Inspection is an activity which is continuously changing its means and its goals to face the new challenges coming of air navigation.

In these latest years all Flight Inspection organizations started to consider efficiency and control of costs as one of the leading parts of their managing variables.

The present leading edge of air navigation is moving faster and faster every year from the classical radio-navigation aids based navigation to Area-Navigation.

Introduction of GBAS and SBAS precision approach system, where one ground subsystem can serve several

approaches, potentially at different airports and potentially with multiple approaches to the same runway end imply the needs to promulgate accurate information for each individual approach.

Other services that may be provided by a GBAS ground subsystem are a regional augmentation service (GRAS) and/or a local Differentially Corrected Positioning Service (DCPS) require ANSP's that some information relative to the location of the ground subsystem be published consistently in the AIP as well the data requirements that shall be included in the States publication for GLS Instrument Approach procedure and to facilitate the encoding of such procedures in an ARINC 424 Navigation Data Base.

Finally the process to transfer the FAS data block information to industry still needs to be standardized. FAS data block information is to be uploaded by the ground station or a simulator.

In this evolutionary path Performance Based Navigation is only the latest challenge for the F.I. community.

In this climate States and/or regions working to implement PBN navigation: all instrument runway ends should have an approach procedure with vertical guidance (APV), either as the primary approach or as a back-up for precision approaches by 2016.

While ISO 9001 specifies the requirements for quality management systems, it does not specify the requirements for products and services. These remain to be specified according to the particularities of each organization.

IDS in design and implement the QMS for ENAV AIS by mapping all the process, instead of simply comply with the Standards and Recommended Practices (SARPs) in Annex 15, understand and revealed the opportunities to enhance performance, productivity and coordination, and to eliminate redundancies, inconsistencies and wasted efforts. This would likely result in significant improvements in the quality of products delivered as well as savings in operating costs. The quality-improved products and services offered with a system in place that produces predictable and repeatable results, expansion of or changes to activities by an easier plan and control.

The main goal is translating all the needs in the automation of aeronautical information management, by simplifying the day to day activities of the AIS organization. Keywords are:

- Maintain and improve quality levels of the products produced.
- Provide the flexibility to produce new and improved products.

- Increase efficiency by realizing shorter turnaround times for production, printing and distribution of aeronautical information products.
- Provide management with a tool for tracking the status of the many phases of the aeronautical information publication and maintenance workflow.
- Provide access to new and/or changed information early in the cycle of chart and document production and maintenance.
- Decrease chance of errors in transmission or exchange of aeronautical data.
- The capability to exchange aeronautical data in many standard aeronautical formats (ARINC, DAFIF, DTED, AICM).
- The capability to interactively design flight procedures (Standard, RNAV, etc.)
- The capability to simulate performance of radio navigation aids (bearing error, coverage, etc.)

All this considerations have brought ENAV with IDS to analyze all the AIS process and extend the ICAO QMS concept for the first time also to the FI unit with the development of the Flight Inspection Planning & Post-processing (FLIPP-TMS) tool, to cover these main goals:

- Mission planning support. This task is accomplished through the selection of the aircraft, the crew and the radio navigation aids to be flight checked during a flight checking mission (the latter are selected from the central AIS/Design database),
- Repository for the data collected during the flight check. At the return from the flight checking mission it is possible to store the data that is collected from the ground based equipment and from the GNSS satellites in the FLIPP-TMS database
- Post-processing tool. FLIPP-TMS is able to show the variation of the performance parameters collected during the flight checking mission of ground based equipments. The post-processing of the GNSS data is executed by means of the PEGASUS tool from Eurocontrol

#### **THE REFERENCE ENVIRONMENT**

Introduction of Area Navigation and PBN let the activity of a modern Flight Inspection department become more and more challenging, because the instrument flight procedures validation effort, which brings changes and workload, has been added to the well known commissioning and periodic flight checking activity.



This environment has become more and more difficult to fulfill due to the nowadays economic crisis which is asking to give a top level service with a view also to the cost of performed activity.

One of item on which it is possible to act, is the flight inspection process organization, in order to increase as much as possible the probability of success of a flight inspection mission.

In order to increase this probability, ENAV decided to update its Flight Inspection Planning and Post-processing tool (FLIPP) introducing task management capabilities and having increased planning capabilities.

This update program produced the FLIPP-TMS tool.

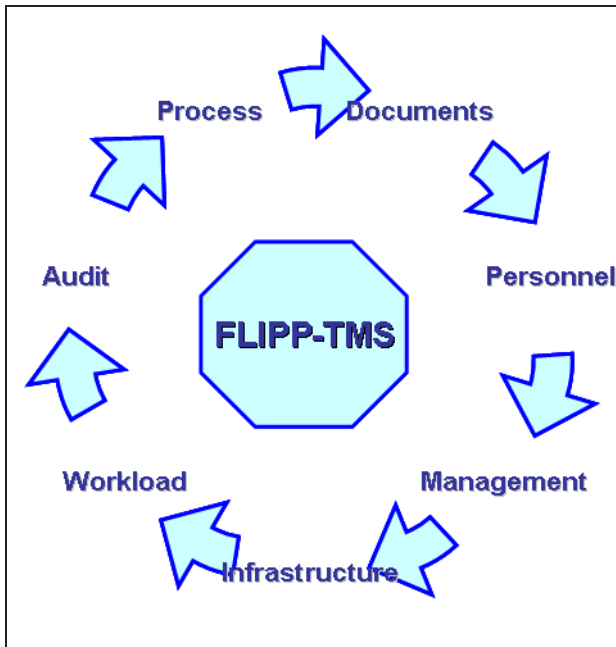
The flight inspection planning process in ENAV (as in many other similar organizations) is a quite complex task requiring:

1. The cooperation of two separate offices: the CET and RM departments. The CET department is in charge of C/N/S equipment maintenance and acts as the collection point for all the flight inspection needs from any internal and external bodies. This department is responsible for the periodic and non periodic flight inspection planning.
2. RM acts in ENAV as a small air operator specialized in flight inspections. RM is responsible for the technical execution of the flight inspections according the national and international regulations.

### **THE BENEFITS OF PROCESS AUTOMATION**

The major ENAV goals which were set-up at the base of the FLIPP-TMS development were:

1. define the Company Flight Inspection Process:
  - a. Support the personnel involved in this process to work according to the official standards and tracing the progress of their activity, even when you don't know what steps may happen in what order.
  - b. support the collaboration between workers across ENAV organization
2. give an update picture of the overall process to ENAV management which needs to
  - a. Analyze activities and performance of users and cases within the process.
  - b. Track the state of each case and where it is in the enterprise.
  - c. Account for documents, decisions, and changes (who, what, and when) at the data, content, task, and virtual folder levels to meet audit and compliance requirements.
3. act as a document management tool in support to flight inspection:
  - a. Easily link unstructured information into structured process. It's of paramount importance aggregate all necessary data, document, files, tasks or other critical information into a single virtual folder making it easier for users to collect all relevant documents related to the 'case',
  - b. Give complete transparency to any change in enterprise documents to meet audit and compliance requirements.
  - c. Access to documents regardless of location or archive in a seamless, "single view" of all case information.
  - d. Establish and maintain the relationships between documents through intuitive document linking that includes versioning, access control, assignments, deadlines, and other metadata.
4. Discuss and manage cases and their supporting documents and tasks in the context of the overall process via threaded discussions and annotations.
5. Comprehensive tracking, auditing and monitoring



**Figure 1: ENAV goals at the base of the FLIPP-TMS**

The first step of this the FLIPP-TMS process development was the analysis of the current workflow for the Flight inspection activity (the so called “as is” scenario) which was analyzed and the upgraded to the so called “to be” scenario.

The “to be” scenario is a business model which describes how the Flight Inspection shall be executed in ENAV near future taking into account the following features and constraints:

1. the present infrastructure and how it is expected to evolve in the near future
2. The “to be” scenario should be a step forward to a better way of working avoiding a jump in a totally unknown world: it will represent for the management and personnel involved an optimization of their present *modus operandi* not a total change.

### **”AS IS” AND “TO BE” SCENARIOS**

In order to identify the optimal workflows for ENAV flight inspection activities, a Business Process Modeling Analysis has been carried out.

First of all, ENAV current flight inspection workflows have been analyzed through interviews to flight inspection operational personnel, in order to collect information about actual processes (“who is doing what”) and supporting tools, and in order to identify the so called “as is” Scenario.

In parallel, all international standards and regulations have been collected and analyzed, in order to create the *Flight Inspection Regulation Framework*.

Afterwards, a *Gap Analysis* has been carried out, through the comparison between “as is” Scenario and the Flight Inspection Regulation Framework, in order identify possible discrepancies between Regulation requirements and current processes. The output of the Gap Analysis was a list of critical elements associated to a level of criticality and a priority.

At the end, the Gap Analysis was used as an input for the so called “to be” Scenario definition. The “to be” Scenario represents optimal ENAV flight inspection workflows, and includes both regulations and processes optimization aspects. “to be” Scenario describes ENAV future processes, including some of the possible optimizations in the flight inspection request processing, starting from its origin up to the final posting of the flight inspection report.

As previously described, the main objective of the “to be” Scenario was the optimization of ENAV flight inspection activities, focusing the attention on activities supporting tool into account, in order to identify tool users, interfaces and requirements.

In this sense, the “to be” Scenario can be considered the environment where the supporting tool will be used to automate most of flight inspection processes, with the aim of reducing planning time and costs and increasing safety.

Major ENAV flight inspection processes have been described in order to identify the boundaries of the flight inspection supporting tool. To easily represent workflows, actors, users, tools, etc., a Business Modeling tool was used: Casewise.

Processes listed in the “to be” Scenario is (see picture below):

- Strategic mission organization and planning
- Tactical mission organization and planning
- Flight inspection
- Flight inspection output evaluation
- Flight inspection output dissemination

In the picture below, it is possible to identify process originators, core processes and their interactions, and final users.

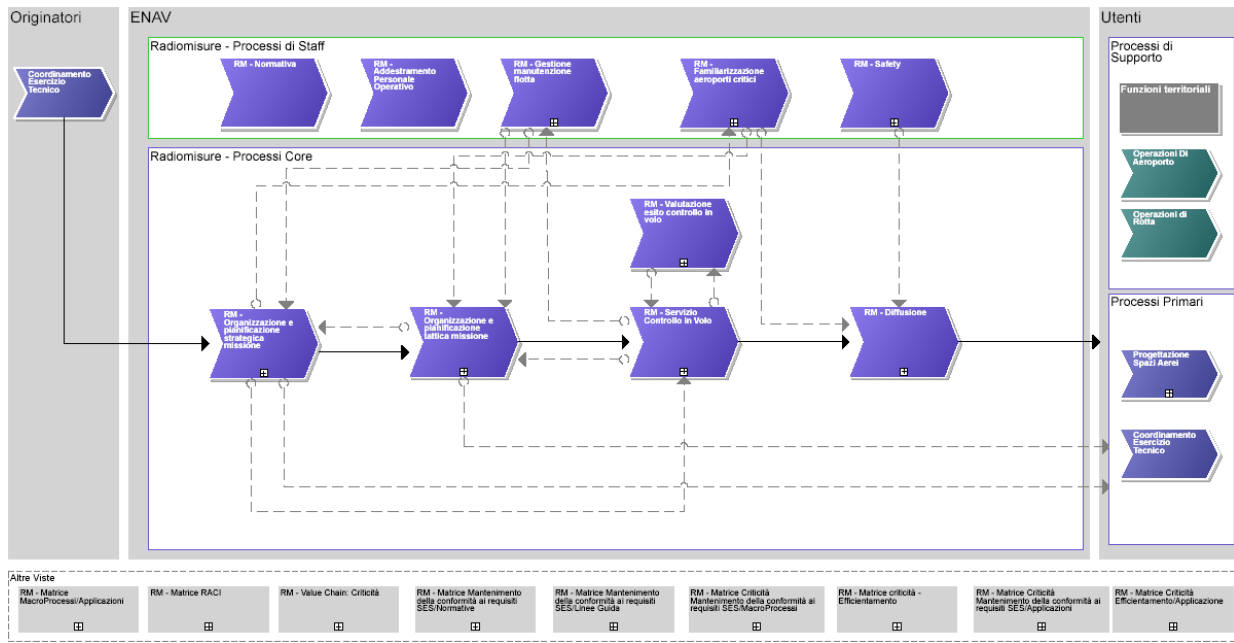


Figure 2: "To be" business model process originators, core processes and their interactions, and final users

FLIPP-TMS has been identified within the “to be” Scenario, as the supporting tool for all ENAV Flight Inspection activities, from the flight inspection request collection, to the post processing analysis and dissemination. This means that FLIPP-TMS unifies both processes and data management system.

**PLANNING AND POST-PROCESSING**

The “to be” business scenario identified and described in the previous section was one of the input data to the design of FLIPP-TMS.

The other strong requirement for FLIPP-TMS is that it has to be integrated in the ENAV AIS workflow, as matter of fact this tool shall:

- use the facility data stored in the ENAV centralized ATS DB;
- allow to different users different operations according to their duties in the flight inspection department
- makes available the data collected to all the trusted and interested system users
- store all the document processed (in input and in output) during the flight inspection programming process

- track all the changes in the mission planning in order to have a complete logging of the events which produced perturbations on the normal flight inspection workflow

This tool has been designed in order to have a human-machine interface which gives an easy access to functions and data.

The main human-machine interface was conceived subdivided in 4 sections as shown in fig 3, 4, 5:

- The one along the left hand side give the access to all the possible activities and queries available to the trusted user
- The remaining part of the human machine interface is subdivided in three rectangular sections:
  - The central one is reserved to messages and new activities in charge to the trusted user or to a group of users,
  - The one on the top one is reserved to the activities which are closer than 7 days to they due date
  - The one on the bottom is reserved to the overdue activities

In each window of the MMI is always shown the name of the logged user and its role in the organization.

The screenshot shows the FLIPP-TMS interface for user Valerio (Operator CET). The interface includes a menu on the left and three tables of activities on the right.

**Menu:**

- Visualizza Notifiche
- Apparati
- Controllo in Volo
  - Inserisci Richieste Controlli in Volo
  - Modifica CV inviati a RM
  - Modifica/Richiedi Approvazione CV
  - Visualizza Calendario Controlli
  - Visualizza Controlli in Volo
- Gestione Account
- Missione
  - Visualizza Piano Strategico

**Allarmi:**

Oggetto in carico	Nome Oggetto	Stato	Data Scadenza	Data assegnazione	Nuova
<input checked="" type="checkbox"/>	ARA-VOR-Araxos	Controllo da inviare per approvazione	5/17/2010	5/7/2010	Si
<input checked="" type="checkbox"/>	BRD-VOR-BRINDISI	Controllo da inviare per approvazione	5/16/2010	5/7/2010	Si

**Attività da svolgere:**

Oggetto in carico	Nome Oggetto	Stato	Data Scadenza	Data assegnazione	Nuova
<input checked="" type="checkbox"/>	LI-VOR-BRINDISI	Controllo da inviare per approvazione	4/30/2011	4/29/2010	Si
<input checked="" type="checkbox"/>	LI-VOR-BRINDISI	Controllo da inviare per approvazione	4/30/2012	4/29/2010	Si
<input checked="" type="checkbox"/>	LI-VOR-CARAFFA DI CATANZARO	Controllo da inviare per approvazione	5/11/2011	4/29/2010	Si
<input checked="" type="checkbox"/>	LI-VOR-CARAFFA DI CATANZARO	Controllo da inviare per approvazione	5/11/2012	4/29/2010	Si
<input checked="" type="checkbox"/>	LI-VOR-CAMPAGNANO	Controllo da inviare per approvazione	6/23/2011	4/29/2010	Si
<input checked="" type="checkbox"/>	LI-VOR-CAMPAGNANO	Controllo da inviare per approvazione	6/23/2012	4/29/2010	Si

Attività da svolgere (6 di 6)

**Attività Scadute:**

Oggetto in carico	Nome Oggetto	Stato	Data Scadenza	Data assegnazione	Nuova
<input checked="" type="checkbox"/>	IPR-DME-PARMA	Controllo da inviare per approvazione	5/4/2010	5/3/2010	Si
<input checked="" type="checkbox"/>	LIPR-PAPI-RIMINI/Miramare	Controllo da inviare per approvazione	5/4/2010	5/3/2010	Si

Figure 3: example of typical layout of the FLIPP-TMS user interface

The FLIPP-TMS tool takes into account automatically for all the recurrent activities, such as the scheduling of periodic flight checks: the human interventions are needed only for the non recurring activities (commissioning and special flight checks).

The systems allows the responsible of one activity to give or deny its clearance to a flight check or to a mission, then the task will proceed to the next step according to the ENAV working procedure: all the events are tracked and logged by the system.

As soon as the flight checks have been cleared, they are processed by the planning department, which will arrange the

- strategic mission planning (i.e. a mission planning with a time span of one month in advance with the due date)
- Tactic (i.e. weekly) mission planning.

These two plans differ for the level of detail available: at strategic level (see Figure 5) only the mission starting and ending dates, and the list of flight checks to be executed during the mission (i.e. the task list) must be mandatory specified,

In the tactical planning the other details such as the aircraft ID, the crew ... are specified, as shown in Figure 6.

Between the implicit goals of tactical planning there is also the resolution of possible changes in priorities and the allocation of unscheduled urgent FI tasks.

If it's not possible to absorb ad tactical phase these unscheduled changes, is always possible to ask for a modification a strategic level.

All the actors involved in this process share the same information in form of FI lists and FI calendar (see Figure 4).

As soon as a network connection is available, it's possible to connect a laptop to the headquarter facility to upload the collected data.

FLIPP-TMS enables:

- the automated production of final flight check reports loading data collected from the automated flight inspection system,
- The post-processing of GNSS data with the support of PEGASUS functionalities for processing and post-processing GNSS data collected from receivers. It is able to compute the receiver position and features of the GNSS navigation system such as accuracy, reliability and availability. Furthermore Pegasus is able to compute positioning errors along trajectories and to compute the accuracy and availability with the required integrity.

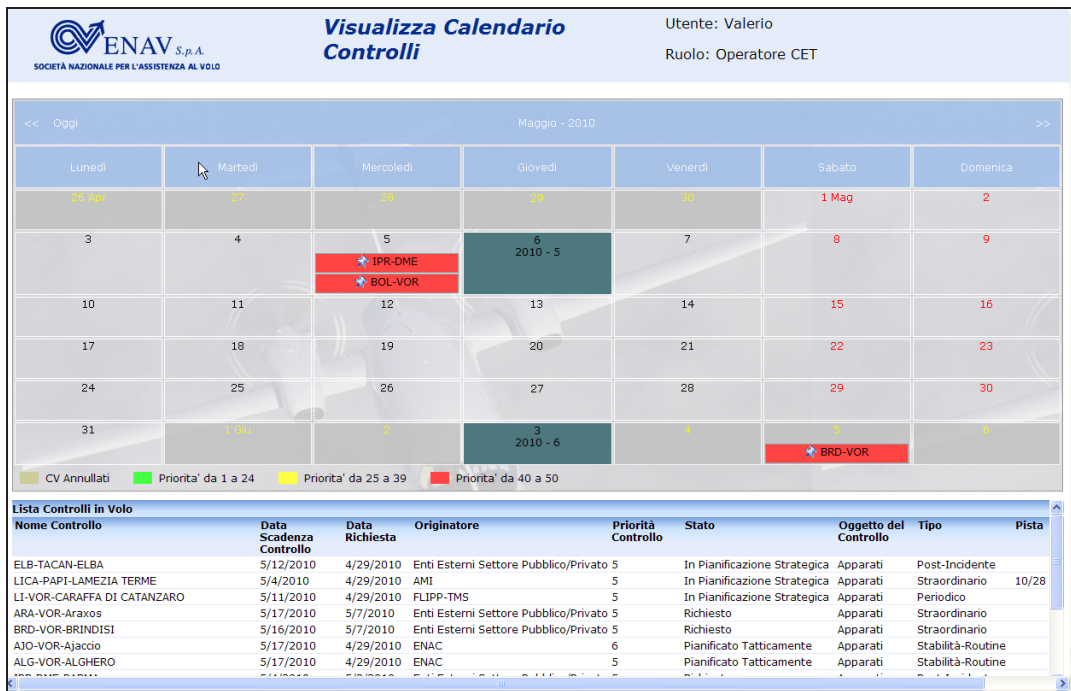


Figure 4: an example of FI calendar



Figure 5: an example of FI Strategic plan

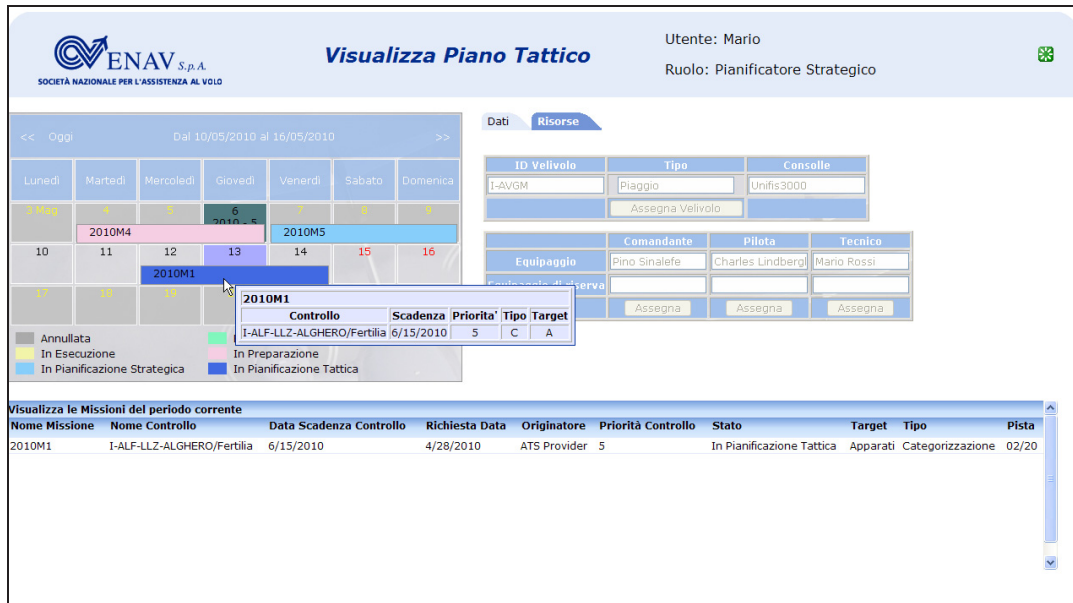


Figure 6: an example of Tactical plan

and execution topics.

## CONCLUSIONS

In order to face the challenges coming from the advent of the RNAV and PBN navigation, and from the AIS to AIM requirements on data management ENAV has decided to invest in the identification of its flight inspection business model, and in its implementation.

In order to achieve efficiency, managerial control and traceability of the flight inspection activities it was decided to empower the ENAV FI team of a task management system and of a post-processing tool: FLIPP-TMS.

This tool is in charge of FI requests collection, management, planning and for related data storage and post-processing.

Efficiency is gained because FLIPP-TMS:

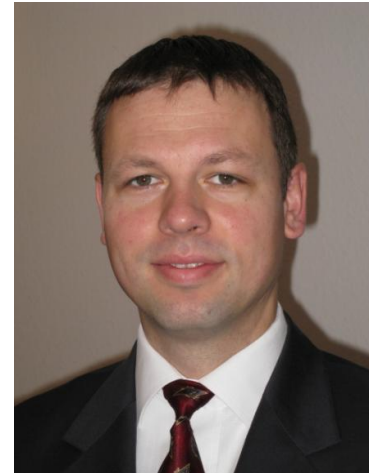
- all FI activities are executed according to the "To Be" business model
- takes into account automatically for all the recurrent activities,
- manage all the input and output documents,
- trace all the FI inspection activities, giving a complete overview of what has happened during the planning process
- Ease the team discussion about the FI planning

## REFERENCES

- [1] ICAO, PANS OPS-Doc 8168, "Procedures for Air Navigation Services - Aircraft Operations", Volume II Construction of Visual and Instrument Flight Procedures, <http://www.icao.int>
  - [2] ICAO, International Standards and Recommended Practices, Annex 10 to the Convention on International Civil Aviation, Volume 1, Radio Navigation Aids, 6th Edition, AMDT 84 <http://www.icao.int>
  - [3] ICAO Manual on Testing Radionavigation Aids doc. 8071, <http://www.icao.int>
  - [4] Eurocontrol "Guidance material for the Flight Inspection of RNAV Procedures" ed. 3 May 2005
  - [5] ICAO, Doc. 9613, "Performance-based Navigation (PBN) Manual", <http://www.icao.int>
  - [6] ICAO, Doc. 9906, "The Quality Assurance Manual For Flight Procedure Design" ", <http://www.icao.int>
- Eurocontrol Pegasus Prototype EGNOS and GBAS Analysis Using SAPPHIRE, <http://www.ecacnav.com/Tools/PEGASUS>
- [7] ICAO "ANNEX 15 " [www.icao.int](http://www.icao.int)
  - [8] ICAO "Draft Guidance material for Quality Management System QMS", <http://www.icao.int>

# Necessities for Flight Inspecting ADS-B Signals

**Dipl.-Ing. Thorsten Heinke**  
 Program Manager  
 Aerodata AG  
 38108 Braunschweig Germany  
 Fax: +49 531 2359 222  
 E-mail: [heinke@aerodata.de](mailto:heinke@aerodata.de)



## Abstract

The demand for increasing safety due to expanding capacity in civil air traffic is generating several new surveillance techniques for commercial airplanes. ADS-B (Automatic Dependent Surveillance Broadcast) is such a technique and used in all new commercial air transport and most general aviation aircraft. This safety relevant signal regarding flight information for each individual aircraft is transmitted through different data links. The level of implementation of ADS-B ground stations for area-wide coverage is steadily increasing. What are the requirements to flight inspect such data derived from ADS-B stations in accordance to its sensitivity for flight safety during surveillance? What kind of flight checks have to be performed to uphold the accuracy and integrity of this signal?

This paper summarizes experiences, practices and requirements regarding the flight inspection of ADS-B systems. It evaluates the hard- and software requirements to flight inspect the ADS-B

service. Examples of flight inspection of existing ground stations using modern flight inspection systems with ADS-B capability are presented and explained. By ADS-B flight check it can be verified that the systems fulfill their dedicated specification. The corresponding procedures are analyzed and evaluated in regard to accuracy and integrity.

## Introduction

All modern commercial airplanes are equipped with capable transponders using the ADS-B transmission. In the past three different techniques were followed, explored and analyzed in regard to its advantages and disadvantages.

One technique is the transmission via a separate VHF data link, which requires special equipped VHF radios to fulfill the requirements according to MOPS ED108A. The second technique focuses on the dedicated Universal Access Transceiver (UAT) working in the 978 MHz band. Each aircraft has to be equipped with such unit which complies with RTCA DO 282B and

TSO C154c. This technique is mainly used for the lower airspace in the United States and Australia. The third method for transmitting ADS-B signals is the extended squitter technique in the 1090 MHz Band. It complies with RTCA DO 260A and TSO C166a. The extended squitter method is suitable for the lower and upper airspace and used by all commercial airplanes.

This paper focuses on the extended squitter method. It highlights the type of transmitted data and evaluates reason for flight checking such data. The requirements for flight inspection systems for ADS-B calibration are explained. Examples from flight inspection systems, which are capable to perform such inspections, are shown.

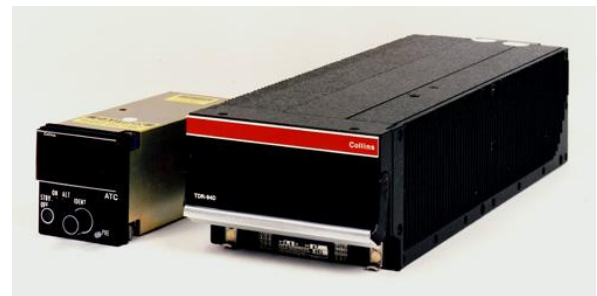
### **Requirements for ADS-B Flight Inspection**

The general requirement to establish an ADS-B link is to have an airborne segment, which transmits and decodes the necessary data in a special format and a ground segment which receives the data and encodes it. The newest flight inspection systems, like the AeroFIS<sup>®</sup>, are equipped with state of the art transponders, which are capable to transmit the required data for the ground station. The ground stations are normally equipped with ADS-B receivers to encrypt the data and display such data to the radar or ADS-B display operator.



### **Figure 1: AeroFIS<sup>®</sup> capable to perform ADS-B flight inspection missions**

The flight inspection system included a Rockwell Collins TDR 94 latest revision supporting the transmission of elementary and enhanced surveillance and ADS-B messages. Therefore the aircraft is equipped with an additional L-Band antenna for the transponder transmission. Only the newest revision of this transponder complies with TSO C166a capable for the transmission of ADS-B.



### **Figure 2: Suitable ADS-B Transponder latest revision**

To operate a non primary transponder on an airborne system special rules according to airworthiness standards have to be followed. The special and advance design of the certified aircraft installation has to make sure that not two targets are visible for the ATC controller. The airborne flight inspection transponder is fully controlled by the flight inspection operator, which enables him to submit via the data-link special test data. This assures proper decoding at the ground segment and/or allows the ground station to perform fully autonomous checks with such specialized data. The AFIS computer is connected to the transponder via a digital data link. The computer submits automatically the necessary dataset required by the transponder to transmit the desired and requested ADS-B data.

The flight inspection mission of a receiving ADS-B ground segment has to focus on three main tasks:



- Coverage Checks
- Interference Checks
- Data Continuity and Integrity Checks

The coverage checks are performed together or in accordance with the regular radar flight inspection missions. The data continuity and integrity has to be monitored at the ground segment continuously. The time stamped data recordings from the flight inspection system will be compared fully automatically to those recordings from the ground segment. The format of such data is customized and adaptable to the dedicated ground station. During commissioning customized special datasets can be transferred to ease the ground facility installation.

### Data transmission

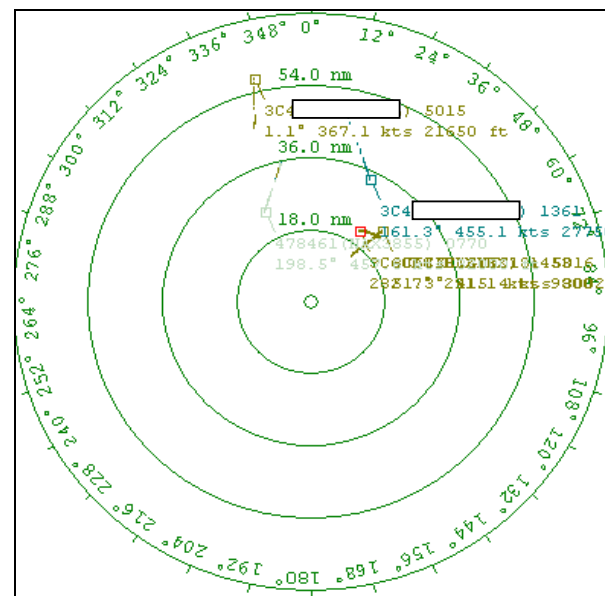
Nowadays a dataset with below listed information is able to be transmitted via the ADS-B link.

- Time
- Altitude
- Track Angle
- Ground Speed
- Position (including horizontal and vertical integrity limits with its accuracy)
- Vertical Velocity
- N/S and E/W Velocity
- Estimated Position Uncertainty
- Radio Height
- True Track Angle
- Selected Heading
- Magnetic Heading

- Wind Speed
- Wind Direction
- Inertial Vertical Speed
- Height above the Ellipsoid
- A/C Registry
- GPS Status

Not all aircrafts are capably to transmit the complete information. This is caused on the one hand due to missing sensors connected to the extended squitter transmitter or on the other hand due to an old standard of the transponder itself. Nowadays only a few of such transponder are fully certified according to TSO C166a, but of course also the availability of such units is growing.

An example picture for a visualization of such received ADS-B data at the ground station is shown in Figure 3. (The mode S code and the call sign is masked on this paper)



**Figure 3: ADS-B information on a polar diagram received on ground**

It is generated by a simple commercial of the shelf ADS-B receiver connected to a commercial of the shelf antenna and controlled by Windows based PC. The information of the DAS-B link is decoded on alpha pages and can be recorded for further data evaluation.

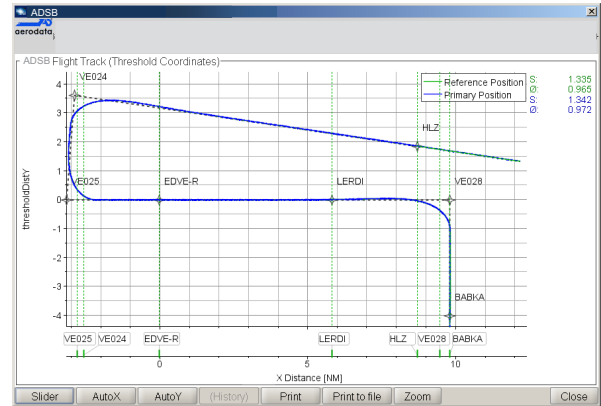
Flag	Code	Callsign	Country	Altitude	Speed	Track	Vert Rate	Squawk	Latitude
	3C	H	Germany	9,800 ft	291.1 kts	282.7°	-512	1453	52.396°
	3C	G	Germany	30,025 ft	415.4 kts	51.3°	-1088	5015	52.395°
	3C	L	Germany	21,650 ft	367.1 kts	1.1°	-3072	5015	53.020°
	3C	B	Germany	27,750 ft	455.1 kts	161.3°	1472	1361	52.609°
	47	N	Norway	32,000 ft	457.6 kts	198.5°	0	0770	52.471°
	47	N	Norway	36,975 ft	483.1 kts	178.7°	0	2535	52.333°

**Figure 4: Alpha page of the ground receiver with ADS-B information**

It is recognizable at this real data example that not all information is transmitted. This can be caused by reasons mentioned earlier in this paper or by intention from the aircraft operator.

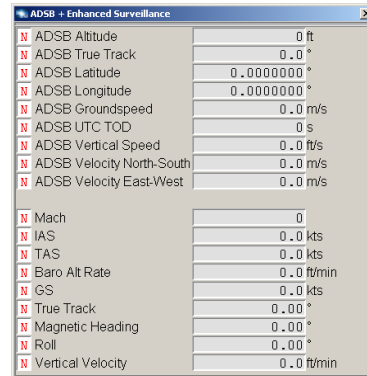
**Flight Inspection of ADS-B facilities**

The main aspect for flight inspection nowadays of course is to fulfill the requirement of the stipulated and announced coverage. Interference in those regions of coverage has to be precluded. The full announced observed sector has to rely on the displayed ADS-B data. This is only manageable from the airborne segment. Interference is easily detected by advanced flight inspection systems and can be eliminated once traced. In addition modern flight inspection system can modify the data transferred to the ground station to assure correct decoding of the signal and to adjust settings during commissioning. An example to show the flight track on which the desired ADS-B check is monitored and recorded is shown in Figure 5. This graphic and its alphanumeric values are compared automatically to the graphics and recordings of the ground station.



**Figure 5: Flight track of flight inspection mission with monitored ADS-B information**

An example of alpha pages modifiable by the flight inspection operator is shown in Figure 6. For testing purposes all values a set to zero for transmission.



**Figure 6: Alpha page of flight inspection system with ADS-B information**

Of course such modified ADS-B transmission has to be communicated with ATC and has to follow such regulations of each country.

**Conclusion**

Taking into account the required and intended improvements for the surveillance of aircrafts in regard to air traffic control, and the growing capability of the ADS-B link, it is found to be mandatory to flight inspect such ADS-B reception. If ATC has

to relay on these ADS-B data the coverage has to be maintained and interference in these stipulated areas has to be avoided or announced.

The development in future for this surveillance, situation awareness and information technique is not easily foreseeable yet, but its growing capacity in conjunction with possibilities for ATC improvement will definitely require flight inspection of these techniques in the future.

### **References**

- [1] ICAO Annex 10, Vol IV – Surveillance and Collision Avoidance Systems, Fourth Edition, 2007
- [2] ICAO Doc 9871 – Technical Provisions for Mode S Services and Extended Squitter, First Edition, 2008



# ADS-B data evaluation supported by the flight tests in western China

*Liu Wei, Zhu Yanbo, Zhang Jun, Wang Yongchun,  
Aviation Data Communication Corporation*

## BIOGRAPHY

Liu Wei. Work in Aviation Data Communication Corporation as the CNS Division Manager.

Zhu Yanbo. Work in Aviation Data Communication Corporation as the deputy manager.

Zhang Jun. Work in Aviation Data Communication Corporation as the director.

Wang Yongchun. Work in Aviation Data Communication Corporation as the programmer.



## ABSTRACT

Automatic Dependent Surveillance-Broadcast (ADS-B) is an up-to-date data-link-based surveillance technology which can be used for both air-ground and air-air application. ADS-B technology can provide more timely, accuracy and abundant information about aircraft. ADS-B is a totally new surveillance method, so that before practically applied and operated in China, abundant tests and evaluations are necessary to validate the performance of ADS-B and guarantee the operational security. Based on this background, we will evaluate performance of the ADS-B system through comparing with baseline data from the flight inspection in western China. With the evaluation results, it would be much easier for CAAC and airlines to determine whether and how to use ADS-B in China. In this paper, we will present the ADS-B data evaluation content and results of the flight tests. In addition, the latest progress of ADS-B development in western China is introduced.

## INTRODUCTION

ADS-B is a surveillance technology that uses position information broadcast by aircraft as a basis for surveillance. Currently, the Civil Aviation Administration of China (CAAC) is developing ADS-B in western China, with the aim of solving the lack of surveillance methods there caused by the complex terrain and costly maintenance. CAAC installed one ADS-B ground station

at Chengdu and one at Jiuzhai in Apr. 2007, which monitored the targets of opportunity equipped with ADS-B equipments and collected the ADS-B data output from these aircraft continuously. Till now, three flight tests have been made and the inspect aircraft were equipped with real-time kinematic (RTK) equipment to collect high accuracy position as the baseline position data. Meanwhile, both radar and ADS-B data were collected to evaluate ADS-B data. The first flight test was executed in Dec. 2008. A319 aircraft flying from Chengdu to Jiuzhai was used for this test, which took about one and a half hour. The second flight test was executed at Mianyang in Feb. 2009. The third was executed at Chengdu in Aug. 2009, flying from Chengdu to Jiuzhai.



Figure 1 the inspection aircraft

## THE ADS-B EVALUATION SYSTEM

The framework of ADS-B evaluation system is shown in Figure 2.

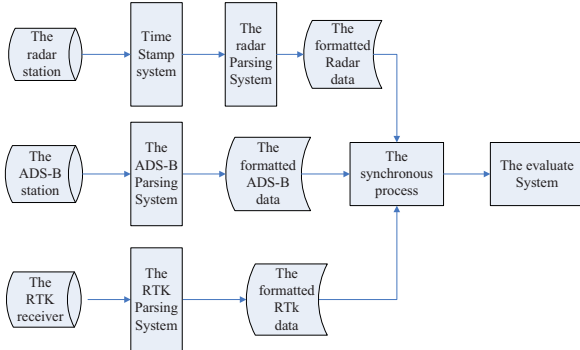


Figure 2 the framework of ADS-B evaluation system

The true locations of the aircraft are obtained by onboard real-time kinematic (RTK) receiver. The raw data of radar is from the radar ground station manufactured by Raytheon Corporation and the raw data of ADS-B is from the ADS-B ground station manufactured by Sensis Corporation. First, the raw data should be processed to satisfy the data format requirements of the ADS-B evaluate system. For the radar data, we need the real time information but the radar messages don't contain the real time information, so the time stamp system is added to provide the time of radar data by getting the Network Time Protocol (NTP) time and adding to the radar messages. For the ADS-B data, we will get the formatted data by parsing the raw data of ADS-B according to the Interface Control Document (ICD) of Sensis. For the RTK data, it is made up of raw observed data and accuracy difference data. The former is the raw GPS data collected from GPS Receiver. The latter is obtained from the internet and post-processed with the former data. We will extract the required data items and constitute the formatted data for the evaluation system. Second, the different data source has different update rate. As we know, the update rate of radar data is one message for 4 seconds, ADS-B is 0.5 second and RTK is 0.2 second. We need the synchronous data to get the accuracy of radar and ADS-B and compare the performance of radar and ADS-B, so we use the synchronous process to synchronize the data of ADS-B, RTK and radar data. Finally, the evaluation system will use the synchronous data to evaluate the performance of ADS-B technology.

### THE RESULTS OF THE ADS-B INTEGRITY EVALUATION

Integrity of ADS-B reports is characterized by NUC (Navigation Uncertainty Category), which ranges from the integers of 0 to 9. According to relating ICAO standards, only if the NUC value of the ADS-B report is

greater than 4, the report can meet the requirements of radar-like service. The number of ADS-B reports falling into different NUC values is counted to obtain the distribution of NUC. By collecting ADS-B reports from Chengdu ADS-B ground station for about 40 days, we can get the distribution of NUC as shown in Figure 3.

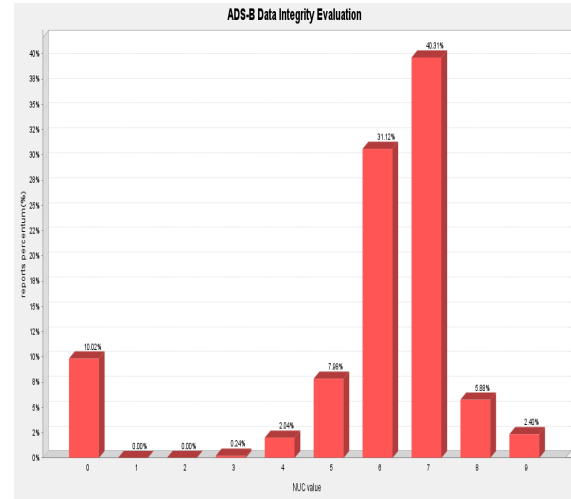


Figure 3 ADS-B data integrity evaluation

The x-coordinate is NUC value and y-coordinate is reports percentage. The number of the reports collected from Chengdu ADS-B ground station is 41,776,974. We can see that a majority of reports (88%) with NUC greater than 4 can meet the requirement of radar-like service, and most of these reports (31.12% and 40.31%) with NUC equal to 6 and 7 are high quality reports.

### THE RESULTS OF THE ADS-B ACCURACY EVALUATION

By comparing ADS-B, radar and baseline position data at the same time, we can get the distance between synchronized ADS-B and baseline position data and the distance between synchronized radar and baseline position data.

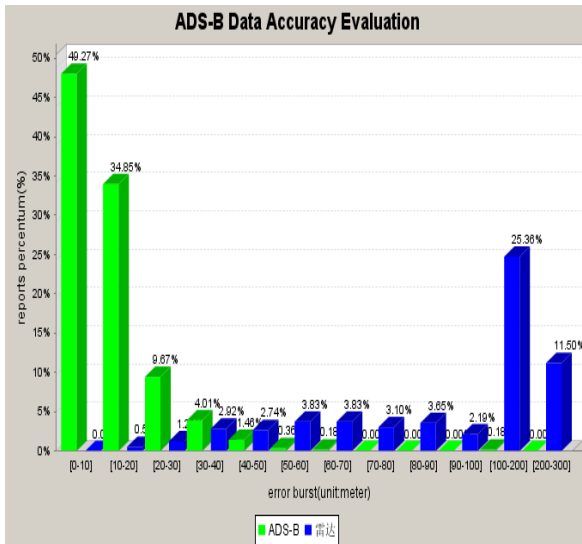


Figure 4 ADS-B data accuracy evaluation

The x-coordinate is error burst and y-coordinate is reports percentum. ADS-B data is shown in green and radar in blue. It is obvious that ADS-B messages are more than radar in the small error burst and less in the big error burst. Through counting, we get that the accuracy of ADS-B data (95% sample point) is 33m, the accuracy of radar data (95% sample point) is 248m.

### THE RESULTS OF THE ADS-B POSITION EVALUATION

By collecting the ADS-B data ,baseline position data and the radar data at the same time interval, we get the track of the airplane used for the test as shown in Figure 5

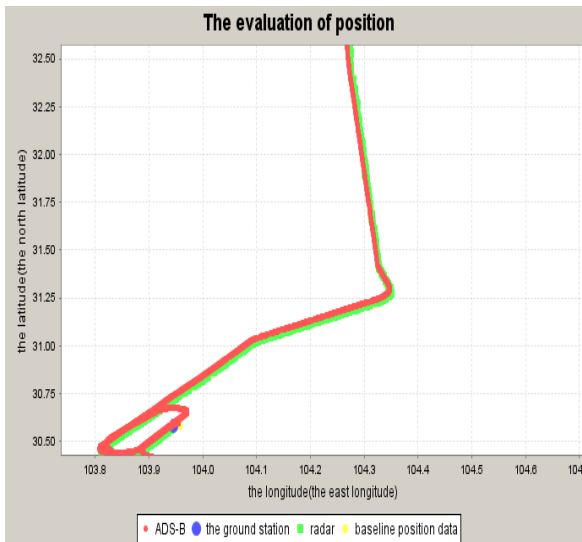


Figure 5 the evaluation of position

The x-coordinate is the east longitude and y-coordinate is the north latitude. ADS-B data is shown in red, the ground station in blue, radar in green and baseline position data in yellow. The Figure 6 is the detailed view.

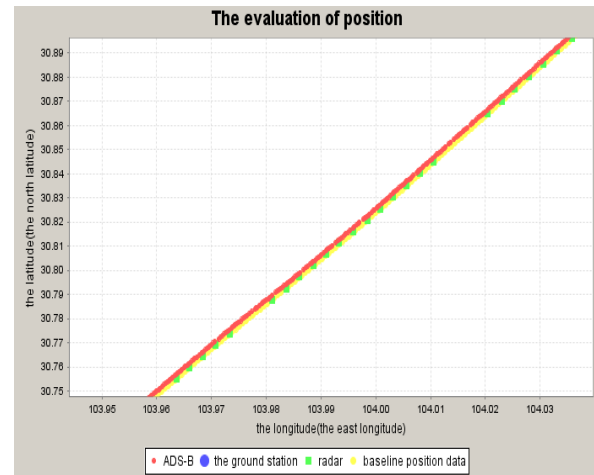


Figure 6 the detailed view of the evaluation of position

From figure 6 we can see that the ADS-B flight path and the radar flight path coincide with the one formed from the baseline position data. Compared with radar flight path, ADS-B is more consistent and denser.

### PROSPECT

The Civil Aviation Administration of China (CAAC) is conducting the communication and surveillance project on the Chengdu- Lhasa route. It programmed to build 5 ADS-B stations to solve the problem of insufficient surveillance methods on Chengdu-Lhasa route caused by the severe geographical situation and promote the development of civil aviation of Tibet region. At the beginning of 2009, the feasibility report has been finished and the bidding works has been accomplished at the end of the same year. Now the project has been launched and will be accomplished at the last half of 2010. This project will improve the surveillance condition on Chengdu-Lhasa route and improve the utility ratio of the airline and promote the social and economic development in the Tibet region.

### CONCLUSION

In this paper, we introduce the three flight tests of ADS-B in western China and show the results of the ADS-B evaluation. By collecting the data from Chengdu ADS-B ground station, we can count that the majority of reports of ADS-B can meet the requirements of radar-like service. Based on baseline data, we compare the accuracy of ADS-B data with radar data and conclude that the accuracy of ADS-B is better than radar. Then we evaluate the position of ADS-B and radar, we can get that the

flight path derived from ADS-B data is more consistent and denser than radar data. So, we can conclude that the performance of ADS-B data is much better than radar data.

#### ACKNOWLEDGMENTS

This work is supported in part by the National High-Tech Research and Development Program of China (863 program, No.2006AA12A103) and the National High-Tech Research and Development Program of China (863 program, No.2009AA12Z329) and the National Science Fund for Distinguished Young Scholars (No.60625102).

#### REFERENCES

- [1] “Minimum Aviation System Performance Standards for Automatic Dependent Surveillance Broadcast (ADS-B)”, DO-242A, RTCA, Inc., June 25, 2002.
- [2] “Minimum Operational Performance Standards for 1090 MHz Extended Squitter Automatic Dependent Surveillance – Broadcast (ADS-B) and Traffic Information Services – Broadcast (TIS-B)” DO-260A, RTCA, Inc., Dec. 2006.
- [3] Andrew D. Zeitlin, Robert C. Strain, Augmenting ADS-B with traffic information service-broadcast - Aerospace and Electronic Systems Magazine [J]. IEEE, 2003
- [4] The modern air traffic management, Beijing University of Aeronautics and Astronautics press, Sep. 2005.
- [5] “Assessment of ADS-B to Support Air Traffic Services and Guidelines for Implementation”, 2006, ICAO.

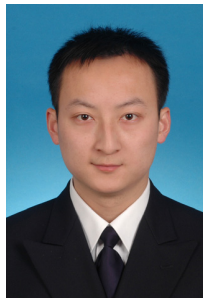


# The Research of How to Reduce the Collision between Inspection

## Flight and Transportation Flight at the Busiest Airports

### Mr. Zhang Jiayi

Safety and Tech Department  
 Flight Inspection Center of  
 CAAC. 23#, Tianzhu Road,  
 Airport Industry Zone  
 Beijing,  
 People's Republic of China  
 E-mail: zhangjy@chinacfi.net



### Abstract

The conflicts between inspection flight and transportation flights at busiest airports have made the flight inspection organizations and the Air Traffic Controller (ATC) departments in many countries very nerve wracking. With the rapid growth of the busiest airports in China, this problem is also placed in front of Civil Aviation Administration of China. Based on the study on all the co-ordinate links of flight inspection, this paper will describes how to employ a certain means to strengthen the understanding for the controllers on flight inspection thereby enhancing the flight efficiency, reducing the influence of flight inspection on scheduled flights.

### 1. Introduction

With the rapid development of civil aviation in China, the flights flow in hub airports has increased so fast. However ATC did not understand the flight inspection deeply, so there are more and more collisions between inspection flight and transportation flight. It mainly shows that the descending of flight inspection efficiency because the waiting and avoiding time of inspection flight has

increased in the air which is for the whole flight safety of airports. It also happened that the delay of scheduled flight and the descending of airport operational efficiency because the ATC should increase the flight distance for avoid the inspection flight. At Beijing Capital International Airport, Shanghai Pudong International Airport and Chengdu Shuangliu International Airport, the inspection flight hardly operated at the daytime but use the morning time which has low density flight. These problems have disturbed the flight inspection center of CAAC and the ATC departments many years. They are also the urgent problems for the flight inspection organization and the ATC departments around the world.

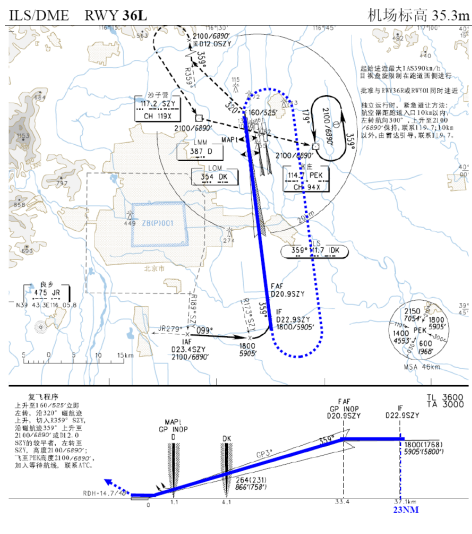
This paper is based on many years practical working experience of flight inspection and research the cooperation phases of flight inspection. It advanced three methods to improve the efficiency of flight inspection and reduce the influence between inspection flight and transportation flight. (1) Provide flight inspection theory training deeply for ATC based on active flight inspection procedure manual; (2) Show the inspection flight route to radar display to assist controllers based on calculating the key points' coordinate; (3) Suggest to establish the special control for inspection flight area.

### 2. Flight inspection training according to air traffic controllers

Civil Aviation Administration of China (CAAC) carried out flight inspection work just 20 years. After 10 years of practical work,

we found that most of ATC of the domestic airport don't understand the flight inspection and the differences between inspection flight and transportation flight. Most of the flight distance increasing and the waiting and avoiding time of flight inspection aircraft is largely due to controllers or other personnel didn't understand flight inspection, especially for flight inspection route and purpose. If we can make these people understand flight route accurately and understand the flight inspection purpose fully, we will reduce distance largely and reduce the influence between transportation flight and inspection flight. Based on this discussion, flight inspection center of CAAC researched the airport flight procedures and airport terrain at every airport in China from 2006. We designed the inspection flight procedure manual for each airport around China, which standardized the flight inspection route as pictures and added the explanation with words and data.

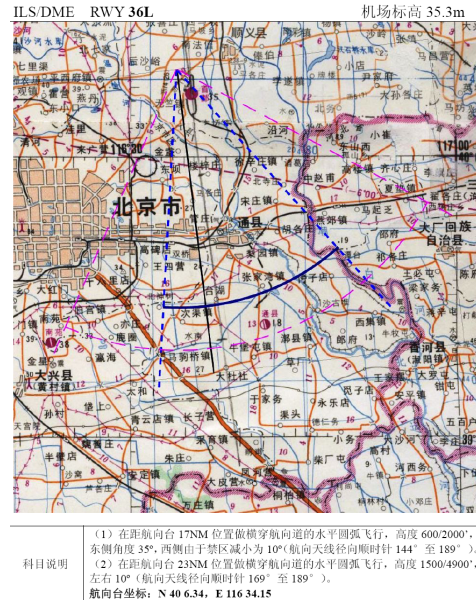
on the map with a scale of 1:500,000 and figure 3 is VYK VOR profile based on Beijing district figure. After three years using in the domestic airports, this method has played a certain role and relax the conflict between transportation flight and inspection flight.



科目说明 按 ILS 进近程序进近，三边高度 1800/5900'，五边起始距离 23NM，高度 1800/5900'，到跑道入口后平飞进场。

Figure 1: ILS approach procedure profile

As the inspection flight procedure manual of Beijing capital international airport an instance, figure 1 is ILS approach procedure profile, figure 2 is ILS coverage profile based



科目说明 (1) 在距航向台 17NM 位置做横穿航向道的水平圆弧飞行，高度 600/2000'，东侧角度 35°，西侧由于禁区减小为 10°航向天线径向前时针 144°至 189°。(2) 在距航向台 23NM 位置做横穿航向道的水平圆弧飞行，高度 1500/4900'，左右 10°(航向天线径向前时针 169°至 189°)。航向台坐标：N 40 6.34, E 116 34.15

Figure 2: ILS coverage profile based on the map with a scale of 1:500,000

However, through the method of promotion the procedure manuals still have some problems. The ATC is difficult to take the initiative of studying the procedure manuals because of work pressure. The present situation is that most controllers understand the inspection flight routes and profiles by communicating with pilots using radio.

So, it is hard to solve the conflict between transportation flight and inspection flight effectively. According to this problem, we suggest the CAAC cooperate with the Air Traffic Management Bureau of China training ATC around the country deeply by explaining the flight inspection purpose, each profile's flight routes and each figure and words in the procedure manuals. We believe that it will improve the efficiency of the flight inspection effectively and reduce the influence between

transportation flight and inspection flight.



Figure 3: VYK VOR profile based on Beijing district Figure

### 3. Show the inspection flight on the controllers' radar display

Nowadays, the control modes of most domestic hub airports are radar control or procedure control under radar surveillance. In another way, radar plays an important role in the air traffic control. Because controllers controlling planes mainly based on the radar display, so we consider show the inspection flight route to help controllers by calculating the coordinates of key points objectively except improve controllers command ability subjectively. It will enhance the flight inspection efficiency and reduce the influence between transportation flight and inspection flight.

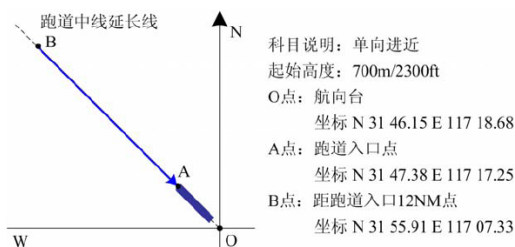


Figure 4: ILS inspection flight procedure 1 (Approach)

Then, make the Hefei Luogang International Airport as an example to introduce how to show the inspection flight route on the radar display by calculating the coordinates of key points. Figure 4 is the key coordinates and radar displaying of ILS inspection flight procedure 1 on runway 14 in Hefei Luogang airport. We can calculate the coordinates of the Localizer O point, the runway entry A point and the point distanced 12NM with runway entry based on Luogang airport database. If we import the three points to control radar, we will show the BA line on radar display. And with simple profile and flight height explanation, controllers will understand this profile's inspection flight route distinctly.

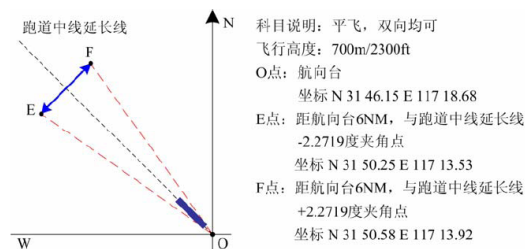


Figure 5: ILS inspection flight procedure 3 (Localizer width)

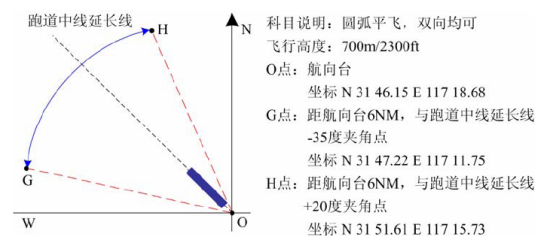


Figure 6: ILS inspection flight procedure 4 (Localizer clearance)

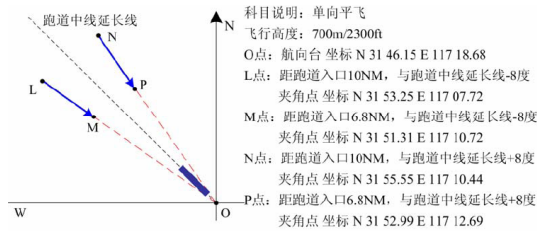


Figure 7: ILS inspection flight procedure 7  
(Glidepath coverage)

Figure 5, figure 6 and figure 7 are Localizer width profile, Localizer clearance profile and Glidepath coverage profile. These figures and profiles are corresponding to each other. After showing the flight route on radar display, the ATC who were trained will understand the purpose of flight inspection and the route of inspection flight. By this way, we can avoid the meaningless waiting, improve the flight inspection efficiency consumedly and reduce the scheduled flight's delay effectively which is caused by inspection flight.

#### 4. Establish the special control for inspection flight area

Nowadays, the air traffic control of domestic hub airports is not only divide sectors to control but also divide as approach control, tower control, ground control, deliver control etc. In Beijing Capital International Airport, the control area is further divided final control between approach control and tower control which have different controllers to control the planes and whose controllers will change of shift on time. This control mode is very good at control, ensure the safety and improve the operating efficiency, but it will be some problems for inspection flight. As the former paper said, a profile of inspection flight will always occupy many control areas at the airport terminal and change the frequency frequently between approach control area and tower control area. It also happened that we will explication repeatedly because of some

control area changing of shift. These problems not only make influence on controlling but also reduce the flight inspection efficiency deeply.

Based on the existence of this problem, we propose to establish the special control for inspection flight area in each busy airport. It means that we can assign one or two controllers who were trained about flight inspection theory control the inspection plane specifically. It will reduce the influence between transportation flight and inspection flight and improve the flight inspection efficiency by reducing talking between flight crew and controller and improving communication between controller and controllers.

#### Conclusions

With rapid development of civil aviation of China, the conflict between transportation flight and inspection flight has bigger and bigger. We have developed three methods based on many years' practical working experiences which are providing flight inspection theory training deeply for ATC based on active flight inspection procedure manual, showing the inspection flight route to radar display to assist controllers based on computing the key points' coordinate and suggesting establishing the special control for inspection flight area. These methods have operated in domestic airports step-by-step and have got good results. After combining these three methods, it must be high-efficiency operation and high-efficiency flight inspection in each busy airport in China.

## Field Strength Versus Signal Strength

**Dale M. Rhoads, P.E.**

Manager, Avionics Engineering  
 FAA Aviation Systems Standards  
 Oklahoma City, OK, USA 73125  
 Tel: 1.405.954.4208  
 E-mail: [dale.rhoads@faa.gov](mailto:dale.rhoads@faa.gov)



**Abstract**

Radio navigation aids transmit signals into space for use by airborne receivers. The signals leave a ground-based antenna, travel through space, arrive at the aircraft antenna, and are routed to the navigation receiver by means of a transmission line. Flight Inspection is tasked with ensuring that those signals-in-space arrive with sufficient energy to be used by the receiver.

The signal-in-space specifications in ICAO Annex 10 are expressed in field strength units of microvolts per meter (uV/m) and power density units of decibel-Watts per meter squared (dBW/m<sup>2</sup>). Flight Inspection in the United States verifies that radio signals arriving at the aircraft receiver are greater than a specified signal level, expressed in units of microvolts (uV). Is this equivalent to measuring field strength or power density? If not, how are the quantities related?

This paper will attempt to answer these questions. In the process, field strength,

power density, and signal strength will each be explained in easily understandable terms.

**Introduction**

The motivation for writing this paper was to develop an intuition of how signals in space can be measured. The relationship between field strength and signal strength, or power density and signal strength will be investigated. Attempts to classify one method of measurement as better than another will not be attempted. The goal is to gain a better understanding.

To explain field strength, power density, and signal strength, a certain amount of background information is necessary. Mathematical equations and relationships will be given along with an explanation. Every attempt will be made to keep explanations easily understandable. After all, the objective of this paper is to build intuition, not to confuse. Tables 1 and 2 provide a list of physical quantities and constants that will be used throughout the paper.

Table 1. Physical Quantities and Associated Units

Physical Quantity	Units	Equivalent Units (if applicable)
Electric Charge (Q)	Coulombs (C)	
Force (F)	Newtons (N)	
Potential (V)	Volts (V)	Newton-meter per Coulomb (N·m/C)
Field Strength (E)	Volts per meter (V/m)	Newtons per Coulomb (N/C)
Power Density(P)	Watts per meter squared (W/m <sup>2</sup> )	
Effective Aperture (A <sub>eff</sub> )	Meters squared (m <sup>2</sup> )	

Table 2. Physical Constants and Associated Units

Physical Constant	Value	Units
Permittivity of free space ( $\epsilon_0$ )	$8.8542 \cdot 10^{-12}$	Farads per meter (F/m)
Intrinsic impedance of free space ( $\eta_0$ )	377	Ohms ( $\Omega$ )
Ratio of Circle's Circumference to Diameter ( $\pi$ )	3.14159	

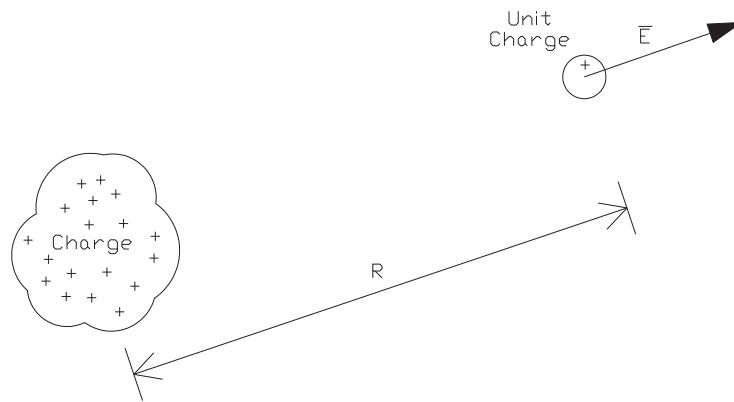


Figure 1. Basic Field Strength

### **Field Strength**

Field strength is commonly expressed in units of volts per meter (V/m). However, field strength can also be expressed in equivalent units of Newtons per Coulomb (N/C). To show that V/m is equivalent to N/C, first rearrange the equivalent units for potential ( $V=N \cdot m/C$ ) and substitute into N/C to arrive at V/m.

Field strength is probably more easily understood in terms of N/C. A Newton (N) is a unit of force, a Coulomb (C) is a unit of charge, and N/C is the measure of force per unit of positive charge. This means that if a quantity of charge exists in space, and a single positive charge is placed some distance away, the force exerted on the single charge by the quantity of charge is its

field strength in N/C (or V/m)<sup>1</sup>.

Additionally, since force is applied in a particular direction, field strength is appropriately represented as a vector. The direction of the vector will be from the positive to the negative (or less positive) as illustrated in Figure 1. The mathematical equation for calculating the magnitude of the field strength vector (E) is given in Equation 1, where Q is the quantity of charge in coulombs and R is the distance in meters.

$$E = \frac{Q}{4\pi\epsilon_0 R^2} \quad (1)^2$$

It's a bit more complicated trying to understand field strength in terms of V/m. This is probably best explained by example. Take a dipole antenna transmitting a signal

with an amplitude of 10 V. If time could be frozen at the instant the transmitted signal is at its peak amplitude, there would be a 10 V difference of potential between the dipole elements. It's probably safe to say that maximum field strength exists at the antenna feed point, shown in Figure 2. If, as shown in this example, the dipole elements are spaced one centimeter apart at the feed point and the potential difference is 10 V, the field strength at the feed point would be 1000 V/m and can be obtained by dividing the voltage by the distance as shown in Equation 4.

$$V = -\int \vec{E} \cdot d\vec{L} \quad (2)^3$$

$$\left. \frac{dV}{dL} \right|_{\max} = E \quad (3)^4$$

$$E = \frac{\Delta V}{\Delta L} \quad (4)$$

Moving away from the dipole feed point changes things somewhat. The electric field is no longer linear between the dipole elements. It bends through space. Figure 3 shows the dipole antenna of the previous example, with the field now being examined at a distance 32 kilometers from the feed point. The circles represented by solid lines show the electric field, and the dashed lines are equipotential lines, or lines of equal voltage. At 32 kilometers from the antenna, the path between dipole elements, around one of the solid circles, is 100 kilometers and the voltage between the elements remains at 10 Volts. Using Equation 4 once

again, the field strength at 32 kilometers from the antenna is 100 uV/m. This is much less than 1000 V/m experienced at the feed point and makes sense since the field strength is now being examined at a point 32 kilometers away. Equation 4 can be used here, but the distance is now the entire path shown as one of the circles represented by a solid line in Figure 3. A point worth noting is that when tracing the field line (solid) from one dipole element to the other, the equipotential lines (dashed) are evenly spaced, and are always at a right angle to the field. This is true for any value of field strength.

Equation 2 states that the voltage difference between two points in the field is the integration of the electric field between the two points and along the line between them. Equation 3 states that the magnitude of field is the maximum voltage gradient. The maximum voltage gradient always occurs along a line at a right angle to the equipotential lines. Equation 4 is a rewrite of Equation 3 as long as the length, L, is the length of the line formed by intersecting the equipotential lines at right angles keeping the equipotential lines equally spaced.

One final point worth noting is that the pattern resulting from the line of constant field strength, for a given field strength value (i.e. the solid lines shown in Figure 3), is the radiation pattern for that antenna<sup>5</sup>. In other words, the constant field line is the radiation pattern.

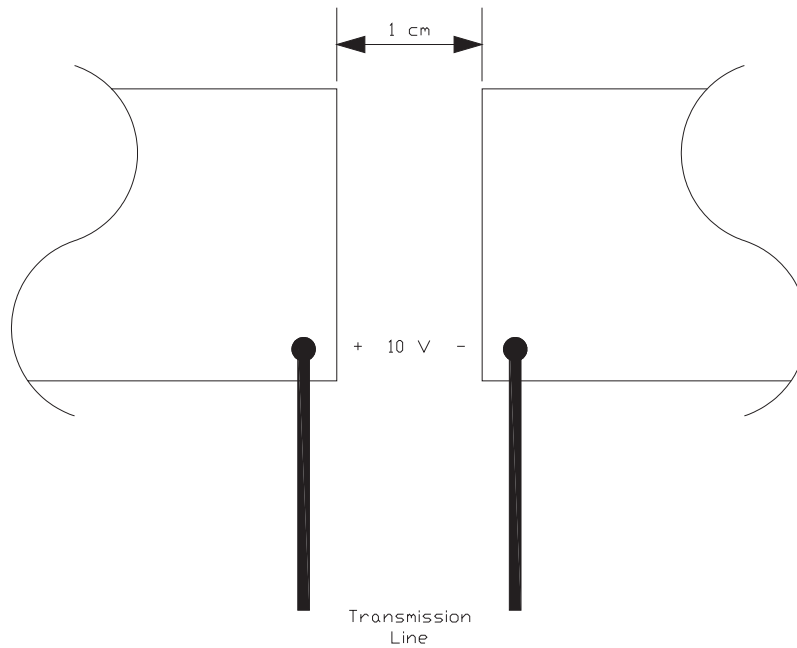


Figure 2. Field Strength Between Dipole Elements at Feed Point

### Power Density

Between field strength and power density, power density is by far the easier quantity to understand. Power density is the distribution of power passing through a surface. For example, take an antenna transmitting 100 Watts in an omnidirectional pattern near ground level. The radiation pattern would appear as a hemisphere at a distance of ten kilometers, similar to that shown in Figure 4. The surface area of the hemisphere formed by the radiation pattern at a distance of 10 kilometers from the antenna would be 628.32 million square meters. If power is

evenly distributed, the power passing through one square meter of the hemisphere would be approximately 160 nanowatts (nW). This is obtained by dividing the total transmitted power by the surface area formed by the radiation pattern, as shown in Equation 5. Therefore the power density at 10 kilometers would be 160 nanowatts per square meter ( $\text{nW}/\text{m}^2$ ), which is equal to  $-68 \text{ dBW}/\text{m}^2$  using Equation 6 to convert to decibel-Watts per square meter ( $\text{dBW}/\text{m}^2$ ).

$$P = \frac{P}{A} \quad (5)$$

$$\text{dBW} / \text{m}^2 = 10 \log_{10}(P) \quad (6)$$



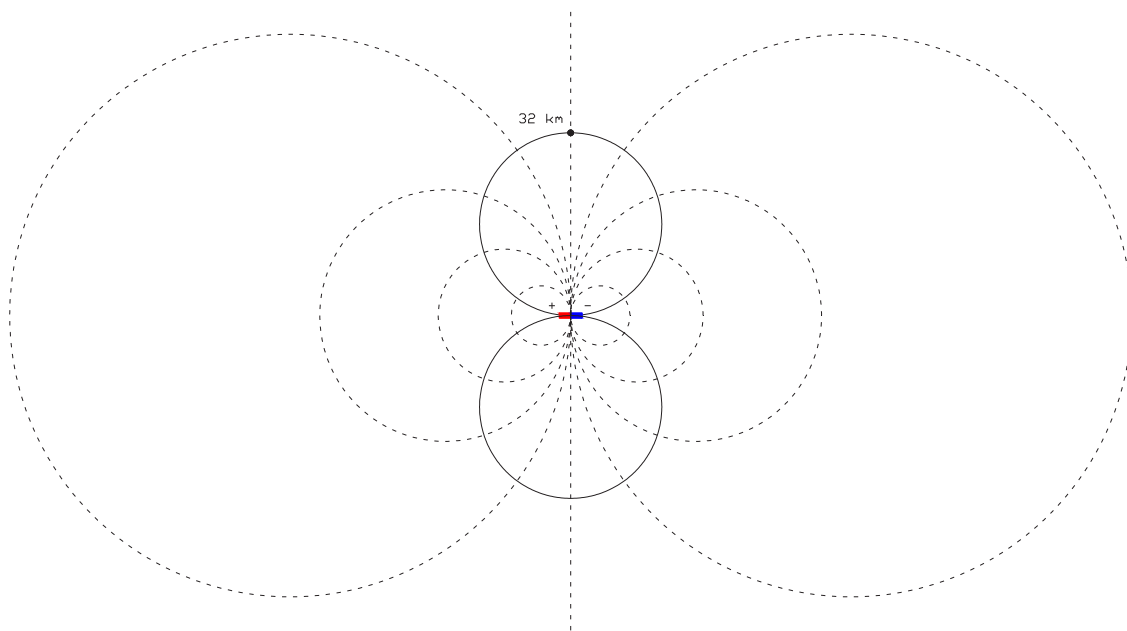


Figure 3. Field and Voltage Lines for a Dipole Antenna

### **Field Strength and Power Density Relationship**

Obtaining power density from field strength and field strength from power density is merely a matter of knowing the intrinsic impedance of the medium through which the energy is traveling, and substituting values into Equation 7 or 8, as appropriate. In this case the medium is free space and the intrinsic impedance of free space ( $\eta_0$ ) equals  $377 \Omega$ .

$$P = \frac{E^2}{\eta_0} \quad (7)^6$$

$$E = \sqrt{P\eta_0} \quad (8)$$

From the earlier example of the dipole shown in Figure 3, the power density at 32 kilometers would be  $26.5 \text{ pW/m}^2$  ( $-106 \text{ dBW/m}^2$ ) using Equation 7, where E equals  $100 \text{ uV/m}$  at 32 kilometers from the antenna feed point.

### Signal Strength

Signal strength, which is commonly expressed in units of volts, is the measurement of the effects of an electric field on a receiving antenna placed in that field. As shown in a previous example, for an antenna to transmit a signal through space, a voltage is applied to the transmitting antenna at its feed point, which sets up an electric field in space. If a receiving antenna is placed within that field, a voltage develops across its terminals. The voltage will also appear at the other end of the coaxial transmission line and would be present at the input to the radio receiver. The amount of voltage present at the receiver input is dependent upon the magnitude of the electric field present and the antenna's ability to convert field strength to voltage.

The parameter responsible for an antenna's ability to convert field strength to signal strength is its effective aperture. Effective

aperture, as the name might imply, is expressed in units of square meters ( $m^2$ ). The equation for effective aperture is given in Equation 9, where  $G$  is the antenna gain factor, and  $\lambda$  is the wavelength of the signal. The effective aperture can be thought of as a window. A large gain equates to a large effective aperture, ie. a large window.

$$A_{eff} = \frac{G\lambda^2}{4\pi} \quad (9)^7$$

Eliminating the gain factor from Equation 9 would make an antenna's effective aperture very predictable and easy to deal with. However, the gain factor can be frequency dependent and directional. This means that the effective aperture of a receiver antenna will vary based on frequency and angle of exposure to the field. To fully understand an antenna's ability to convert field strength to signal level, its effective aperture would have to be known over the intended frequency range and at all angles of exposure to the electric field.

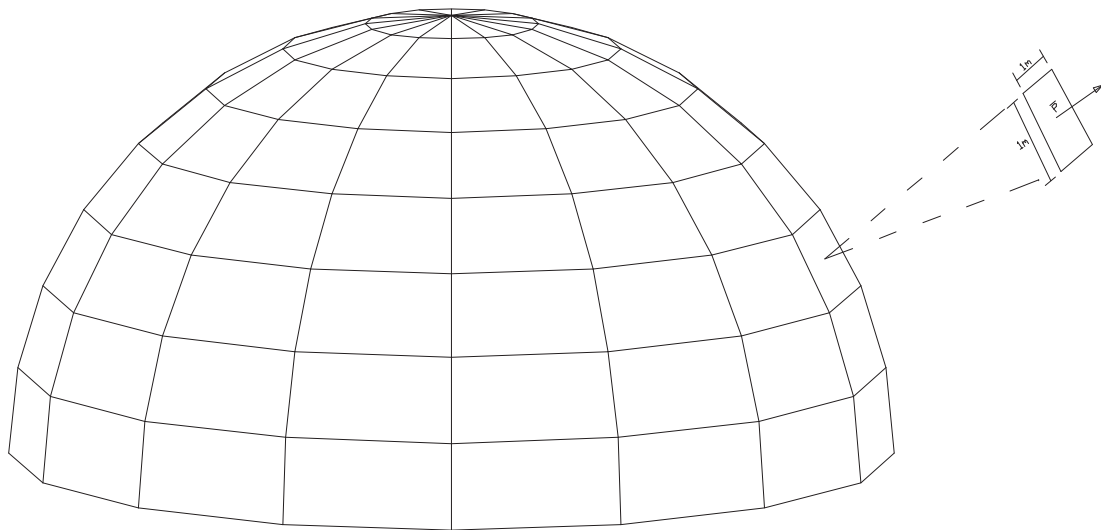


Figure 4. Power Density of a Signal Transmitted by an Omni-Directional Antenna

### **Field Strength and Signal Strength Relationship**

The goal of this paper has been to characterize the relationship between field strength and signal strength, but now there's the parameter of effective aperture to deal with. Equation 10 shows that signal power delivered to a receiver is the product of the power density and the receiving antenna's effective aperture. If the power delivered to the receiver is known, then Equation 11 shows the relationship between receiver power and voltage, where  $Z_r$  is the receiver's input impedance, usually equal to  $50 \Omega$ . Rearranging Equation 11 to solve for  $V$  will produce a signal strength value, however, the ability to solve for signal strength still relies on knowing the receiving antenna's effective aperture. In other words, to calibrate the flight inspection system to produce a field strength result when signal strength is measured, effective aperture of the receiving antenna is critical.

$$P_r = PA_{eff} \quad (10)^8$$

$$P_r = \frac{V^2}{Z_r} \quad (11)^9$$

At this point, the question is how to find effective aperture if it's critical in determining signal level from field strength and vice versa. One method of finding effective aperture would be to get it from the antenna manufacturer. Unfortunately, this is not a specification typically found on an antenna datasheet. Quite often a polar plot of gain versus exposure angle is available, but these plots are usually idealized for a single frequency and do not fully represent and actual installation. Most antenna

installations on flight inspection aircraft are less than ideal due to the large number of antennas installed and limited space.

A better method would be to measure effective aperture by exposing the antenna to a known electric field and measuring the voltage developed across its terminals.

Effective aperture can be found mathematically by substituting Equations 7 and 11 into Equation 10 to get Equation 12, which can be rearranged to get Equation 13, and further reduced by replacing  $Z_r$  and  $\eta_0$  with their respective values.

$$\frac{V^2}{Z_r} = \frac{E^2}{\eta_0} A_{eff} \quad (12)^{10}$$

$$A_{eff} = \frac{V^2 \eta_0}{E^2 Z_r} \quad (13)$$

$$A_{eff} = \frac{V^2}{E^2} \times 7.54 \quad (14)$$

To make things more complicated, measurement of effective aperture should be accomplished with the antenna installed on the aircraft, with the aircraft rotated through all exposure angles, and away from anything that may skew measurement results – this includes the ground (airborne would be best). Ignoring any of these factors could introduce error.

In summary, if an antenna's effective aperture is known, field strength can be derived from signal strength measurements using Equation 15.

$$E = V \sqrt{\frac{\eta_0}{A_{eff} Z_r}} \quad (15)$$

## **Conclusion**

Antenna design is an exercise in compromise. Antennas with large effective apertures are more sensitive than antennas with small effective apertures. However, a large effective aperture usually means a physically large antenna. Antenna manufacturers strive to design antennas with acceptable sensitivity levels while keeping physical sizes as small as possible. For this reason there's not much difference in antenna performance between manufacturers.

Assuming antennas of the same type will all perform about the same, all will produce about the same signal level when exposed to a given field strength. In practice, it should be sufficient for Flight Inspection to verify minimum signal strength<sup>11</sup>, especially when using commercially available, off-the-shelf antennas.

## **About the Author**

Dale Rhoads is an Avionics Engineer in the Engineering Branch of the Office of Aviation Systems Standards. Mr. Rhoads has been with the FAA since 1988 and has held positions of Avionics Technician, Avionics Instructor, Avionics Engineer, and Avionics Engineering Supervisor. Mr. Rhoads holds a Bachelors Degree in Electrical Engineering from the University of Oklahoma and is a Licensed Professional Engineer

## **References**

---

<sup>1</sup> Hayt, William H. and John A. Buck: "Engineering Electromagnetics," 6<sup>th</sup> ed., McGraw-Hill, New York, 2001

<sup>2</sup> Hayt, William H. and John A. Buck: "Engineering Electromagnetics," 6<sup>th</sup> ed., McGraw-Hill, New York, 2001

<sup>3</sup> Hayt, William H. and John A. Buck: "Engineering Electromagnetics," 6<sup>th</sup> ed., McGraw-Hill, New York, 2001

<sup>4</sup> Hayt, William H. and John A. Buck: "Engineering Electromagnetics," 6<sup>th</sup> ed., McGraw-Hill, New York, 2001

<sup>5</sup> Laport, Edmund A.: "Radio Antenna Engineering," McGraw-Hill, New York, 1952

<sup>6</sup> Laport, Edmund A.: "Radio Antenna Engineering," McGraw-Hill, New York, 1952

<sup>7</sup> Semtech Advanced Comms & Sensing: "TN1200.04, Calculating Radiated Power and Field Strength for Conducted Power Measurements," [http://www.semtech.com/images/datasheet/semtech\\_acs\\_rad\\_pwr\\_field\\_strength.pdf](http://www.semtech.com/images/datasheet/semtech_acs_rad_pwr_field_strength.pdf), 2007

<sup>8</sup> Semtech Advanced Comms & Sensing: "TN1200.04, Calculating Radiated Power and Field Strength for Conducted Power Measurements," [http://www.semtech.com/images/datasheet/semtech\\_acs\\_rad\\_pwr\\_field\\_strength.pdf](http://www.semtech.com/images/datasheet/semtech_acs_rad_pwr_field_strength.pdf), 2007

<sup>9</sup> Semtech Advanced Comms & Sensing: "TN1200.04, Calculating Radiated Power and Field Strength for Conducted Power Measurements," [http://www.semtech.com/images/datasheet/semtech\\_acs\\_rad\\_pwr\\_field\\_strength.pdf](http://www.semtech.com/images/datasheet/semtech_acs_rad_pwr_field_strength.pdf), 2007

<sup>10</sup> Semtech Advanced Comms & Sensing: "TN1200.04, Calculating Radiated Power and Field Strength for Conducted Power Measurements," [http://www.semtech.com/images/datasheet/semtech\\_acs\\_rad\\_pwr\\_field\\_strength.pdf](http://www.semtech.com/images/datasheet/semtech_acs_rad_pwr_field_strength.pdf), 2007

<sup>11</sup> Spohnheimer, Nelson: "Flight Inspection Guidance Comparison Study," and "Differences Report of Flight Inspection Guidance Comparison Study," Spohnheimer Consulting, 2007

# How to save time and money on ILS flight inspection using correct methods and input data

## Alf W. Bakken

Systems Engineer/Product Adv., Navigation  
Northrop Grumman Park Air Systems  
PO Box 150 Oppsal  
NO-0619 Oslo, Norway

Phone: +47 900 50 425, Fax: +47 23 18 02 10

E-mail: [a.bakken@no.parkairsystems.com](mailto:a.bakken@no.parkairsystems.com)



## ABSTRACT

As a supplier of ILS ground systems Northrop Grumman Park Air Systems have had an extensive experience with many Flight Inspection units, which have made us aware that several incorrect methods and data handling are quite often used.

It is not uncommon that errors that are easy to correct are not detected, leading to hours and sometime days of unnecessary flight time, imposing large extra cost on the end user and the equipment supplier. In a few cases we have experienced that ILS equipment has been turned off as a consequence of flight inspection errors, with possible large income loss for the airport due to lost traffic.

The purpose of this paper is to give flight inspectors and ground technicians a simple tool to fast detect errors that can be corrected so unnecessary flight time can be avoided and money saved.

Typical “foot-print” graphs of the various error possibilities described, as well as the characteristics of how bends/scalloping caused by reflected/diffracted signal looks like is supplied, to make it easy for the flight inspector or ground technician to determine if a problem is caused by the ILS equipment, or if it is due to some error with the flight inspection.

## ILS BENDS CAUSED BY MULTIPATH SIGNAL

A bend or scalloping on an ILS signal caused by reflected and or diffracted signal has a very distinct “foot-print”, caused by the laws of physics;

- Flying towards the runway (or ILS installation), the bend starts with a low frequency
- The bend frequency increases as the distance between the aircraft and the reflecting object decreases
- When the aircraft passes the reflecting object, the bend disappear

This is shown for a computer simulation of a Localizer approach in Figure 1.

Also when there is more than one scattering object present, with partly overlapping bend patterns, it is usually easy to see the typical ILS bend “foot-print” with increasing bend frequency as the aircraft approaches the runway. An example of this is shown in Figure 2.

Bends on Glide Path systems will have similar characteristics.

Real ILS bends (e.g. bends caused by reflections/diffractions from scattering objects or terrain formations) will always have this characteristic structure; starting with low frequency and the bend frequency increases as the aircraft approaches the runway, and the bend(s) disappear when the aircraft passes the scattering object.

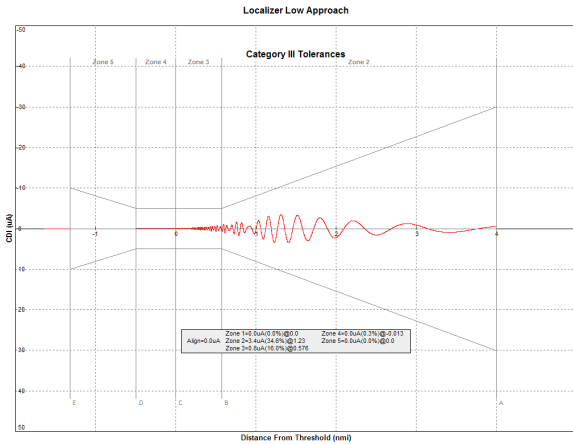


Figure 1

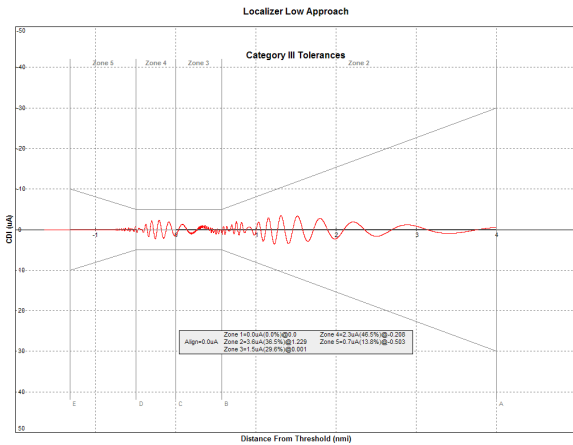


Figure 2

### AN EASY RELIABILITY TEST FOR FLIGHT INSPECTION EQUIPMENT

When the flight inspection aircraft reports a large structure problem on an ILS, there is an easy test that can be performed immediately to determine if there is a problem with the flight inspection equipment or not. Test the repeatability of the structure by flying repeated approach flights.

Bends on ILS signals caused by scattering from fixed objects do not change. When performing a number of approach flights on the same ILS, without any change to the ground installation, the recorded structure in the flight inspection aircraft should remain the same from one flight to another. Since it is impossible to fly at the exact same position each time, there will always be some small differences between the recorded structure from different approach flights, but the structure pattern should basically be the same, with a good correlation from flight to flight.

If there is little or no correlation from flight to flight, this is a proof of a problem with the flight inspection equipment, and to continue “burning fuel” is a waste of time and money; the resources should be used to figure out what the problem with the flight inspection equipment is.

(Figure 3 to Figure 6) below illustrate this. This are four consecutive approach flights on the same localizer without any change to the ground installation.

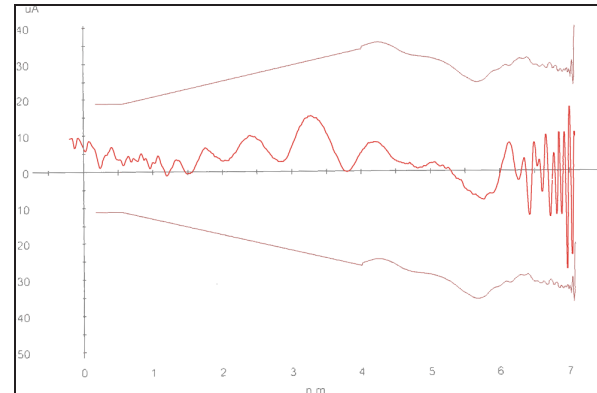


Figure 3

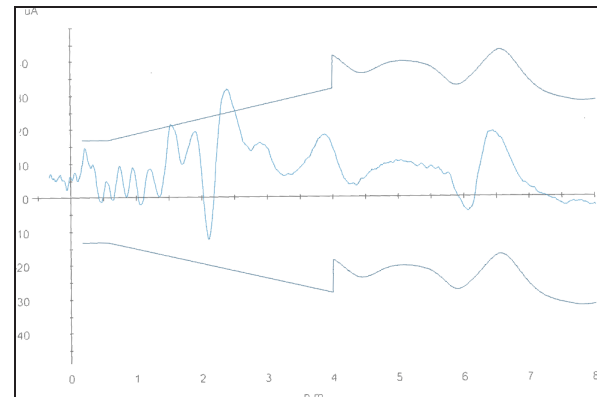


Figure 4

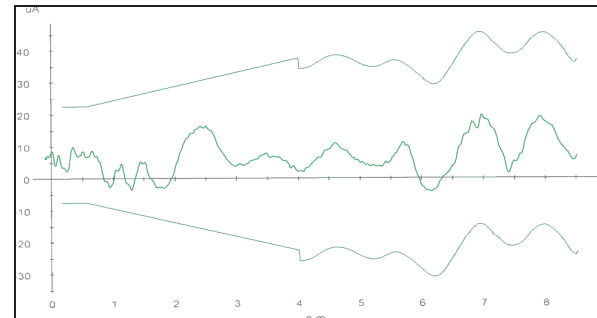
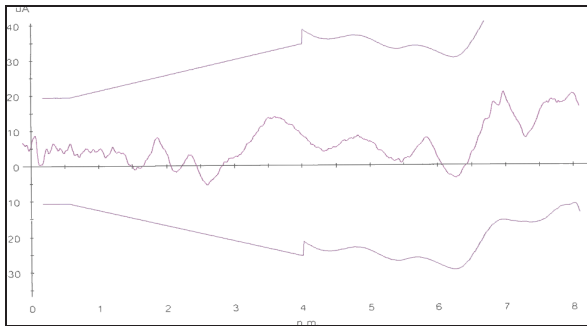


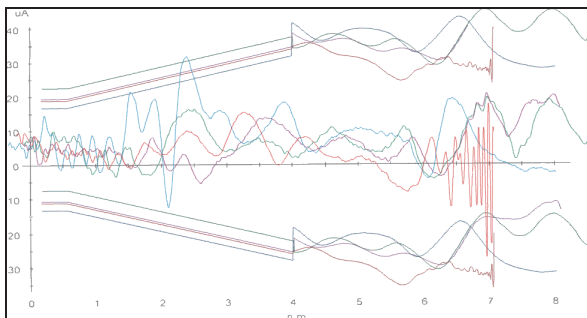
Figure 5



**Figure 6**

To better compare the results, all four flights are overlaid in the same figure (Figure 7).

Inspecting and comparing the structure (bend pattern) from the four flights reveal that for the structure there is no correlation at all, proving that in this case there is a large problem with the flight inspection equipment. None of these flights can be used to tell us anything about the structure of the Localizer, but it is possible to conclude that there is an alignment error of approx.  $5\mu A$ .



**Figure 7**

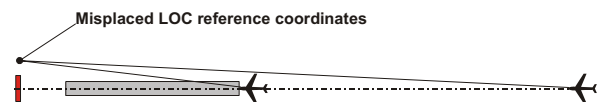
### PARALLAX ERROR

A quite common flight inspection error we have experienced is parallax error caused primarily by coordinate errors in the Flight Inspection System (FIS) database (e.g. wrong coordinates entered), or misplaced reference station for DGPS based tracking systems. Parallax errors produce a quite significant pattern on the flight recording that can easily be spotted. This type of errors result in an incorrect reference signal that produces an increasing angle error as the aircraft approaches the runway.

The most common errors we have experienced with FIS systems based on DGPS are the following:

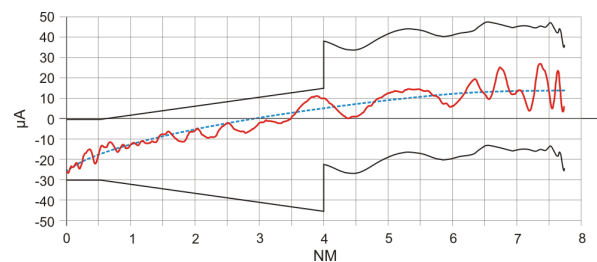
- Error in Threshold coordinates, both lat long errors and height errors
- For Localizer, lat long errors for the coordinates for the facility (e.g. the antenna phase center)
- For Glide Path, lat long and height errors for the Glide Path flight inspection aiming point
- Misplaced DGPS ground station (e.g. the DGPS ground station sited differently than the surveyed position)

The principle on how the parallax error works is shown in Figure 8 for a Localizer with the phase centre coordinates misplaced to the side of the Localizer antenna. For the misplaced reference point 20m to the side of the centerline and an aircraft position far out (e.g. at 10NM), the angular error in the reference signal is very small,  $0.06^\circ$ . As the aircraft approaches the runway, the angular error increases, at a distance of 1.5NM from the Localizer the angular error in the reference signal is now  $0.41^\circ$  producing a significant DDM error in corrected recorded Localizer structure.



**Figure 8**

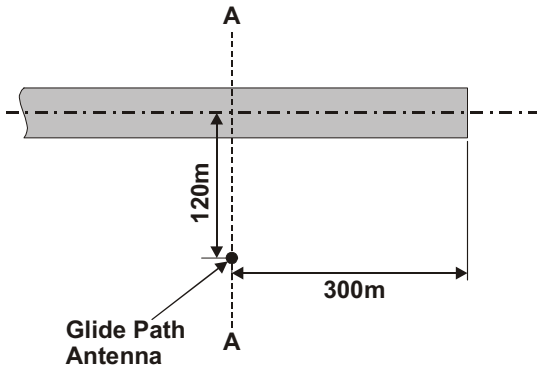
An actual recording of this phenomenon on a Localizer approach flight is shown in Figure 9.



**Figure 9**

It is important to stress that there is no error originating from a Localizer installation that could produce an error on the structure and alignment like this, so whenever a result like this is seen, check that all reference coordinates in the FIS system are correctly programmed.

The probably most common error seen on flight inspection recordings of Glide Path structure is parallax error caused by error in the coordinates of the flight inspection aiming point for Glide Path. Most of these errors are based on a common misunderstanding of how image Glide Path systems work. A quite normal situation for a Glide Path installation is shown in Figure 10.



Cross section A - A

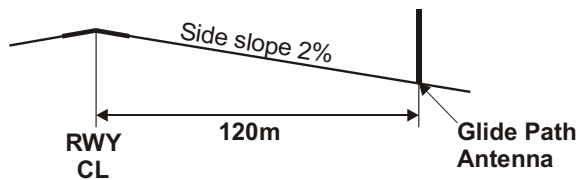


Figure 10

In most cases the Glide Path flight inspection aiming point lat long coordinates are correctly positioned abeam the Glide Path antenna mast on the runway centerline, *but for the height of the aiming point, the height of the base of the Glide Path antenna mast is used, which in this example is 2.4m below the surface of the runway centerline.*

To demonstrate the effect of using this Glide Path aiming point, a 3D computer model with a perfect Glide Path Beam Forming Area (BFA) with no scattering objects present, but with a side slope of 2%, was constructed. A Glide Path approach flight was computer simulated with an M-Array (Capture effect) Glide Path adjusted to theoretical correct antenna feeds and alignment for a 3.00° Glide Path angle.

The resulting computer simulated graph is shown in Figure 11.

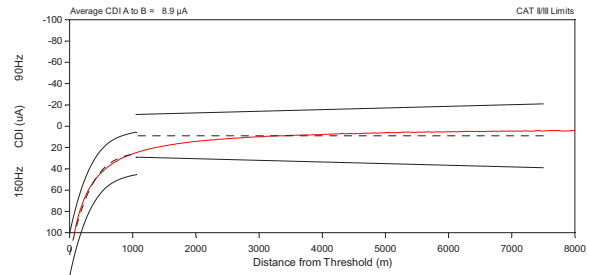


Figure 11

The large “skew” on the recording between ILS point A and B (zone 3) is not caused by an error in the Glide Path signal or any antenna alignment errors, but only caused by the wrongly chosen height for the Glide Path flight inspection aiming point. The FIS system would report a bend close to 20µA in this case, but in reality there is no bend present.

So what is then the correct height of the aiming point? Well, with a nice perfect Glide Path BFA as in this case, and in a majority of airports, a good value would be at the height of the runway centerline abeam the Glide Path antenna mast, or one foot above this.

The mathematical explanation for this is that the whole Glide Path cone tilts sideways with the side slope of the BFA, and the height of the aiming point must also follow the side slope towards the runway centerline, (a line perpendicular to the z-axis of the tilted Glide Path cone) and because we are moving away sideways from the centre of the Glide Path cone, the aiming point must be elevated slightly more.

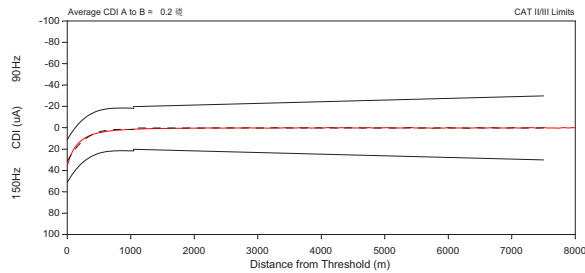
The computer simulated approach flight, now with the aiming point one foot above the level of the runway centerline abeam the Glide Path mast is shown in Figure 12.

As can be seen the “skew” between ILS point A and B has disappeared, and the FIS system would report correctly close to 0µA structure in zone 3.

More important is that if there is a “skew” present on the Glide Path recording between ILS point A and B, the Glide Path angle is not computed correctly, and neither is the RDH (TCH). With the aiming point used for the recording presented in Figure 11, the error on the calculated Glide Path angle would be 0.04°, which is more than the commissioning tolerance for a CAT III Glide Path. Also the RDH would be calculated with a gross error. *With the aiming point used for the example in Figure 11, the calculated RDH (TCH) would be 13.3m, which is below ICAO tolerances, while the correct RDH*

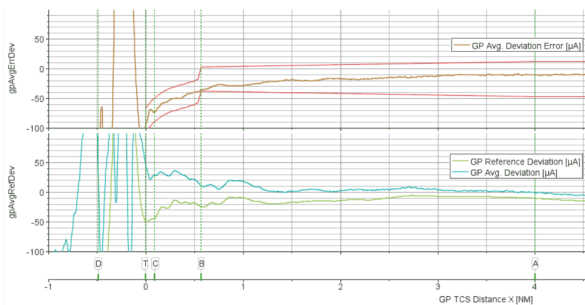


(TCH) based on the correct aiming point used for the example in Figure 12 is **16.0m**.



**Figure 12**

Figure 13 shows an actual approach flight on GP with error in the height of the Glide Path aiming point.



**Figure 13**

If the Glide Path aiming point is misplaced along the runway centerline, the effect on the flight inspection error will have the same characteristics as with height error, but the error must be much larger to produce the same “skew” on the Glide Path recording between ILS point A and B.

For a Glide Path installation with BFA that is not so perfect and that may have a bad structure, the only way to find the correct Glide Path flight inspection aiming point is to follow a simple procedure, which should be done during the commissioning flight check:

- Start with a initial value for the aiming point positioned abeam the Glide Path antenna mast on the runway centerline, with the height of the runway surface at this point as the height value
- Fly a normal approach on the Glide Path angle
- If there is no “skew” on the recorded Glide Path between ILS point A and B, everything is fine, the used aiming point coordinates should be used for all following flight inspections
- If there is a “skew” on the recorded Glide Path between ILS point A and B, adjust the height value of the aiming point accordingly, and repeat

the approach flight. This should be done repeatedly to the “skew” between ILS point A and B is reduced to the minimum value. Some flight inspection equipment allows you to do this on a “re-run” of the existing approach data, some not

- The final height that gives the minimum “skew” should then be fixed and used for later flight inspections on that specific Glide Path installation

Normally finding the correct height of the Glide Path flight inspection aiming point should not take more than two or three approach flights during the commissioning flight inspection.

### **INCORRECT DISPLACEMENT SENSITIVITY IN THE FIS EQUIPMENT**

For the flight inspection equipment to calculate the correction for aircraft deviations from the nominal ILS path, the displacement sensitivity parameter in the flight inspection system must be the same as the actual displacement sensitivity for the Localizer or Glide Path under test.

Usually this is not a problem, but for some rear occasions we have experienced that incorrect value for displacement sensitivity has been used.

The effect of using incorrect value for the displacement sensitivity is that the FIS will either over- or under-compensate for aircraft movements and then produce “phantom” bends. However, this is very easy to detect, since this will show up on the recording of an approach flight as a bend pattern overlaid the real ILS bends that follows the recording of the aircraft movement (the reference signal).

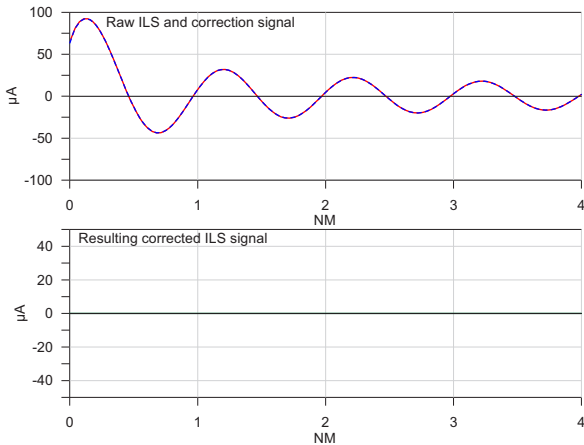
### **TIME SYNCRONISATION ERROR BETWEEN REFERENCE SIGNAL AND ILS SIGNAL**

One of the most complicated parameters to handle correctly in the flight inspection equipment, especially for DGPS based reference systems, are the handling of time synchronization between the ILS signal and the DGPS position data.

Both processing of the DGPS signal and the ILS signal introduce some time delay, that may not be identical for the two signals. For the flight inspection system to compute the correct correction signal for the reference system, the difference in time delay for the two signals must be compensated so the ILS signal and the position data for the aircraft are perfectly synchronized.

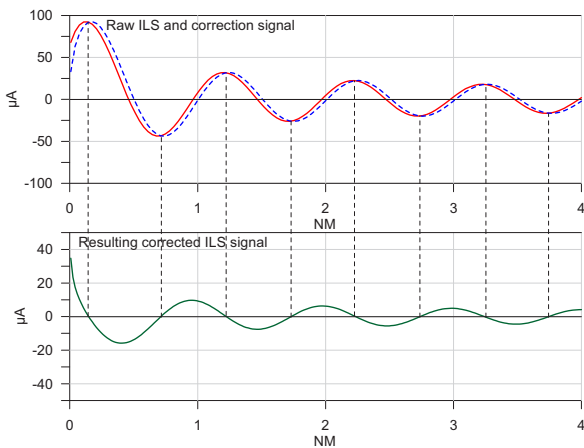
To illustrate the problem we have generated aircraft deviations from a nominal perfect Glide Path with linear

displacement sensitivity. When there are no time synchronization error between the raw ILS signal and the reference system, the two signals perfectly overlap, and the corrected ILS signal will be a straight line, as shown in Figure 14.



**Figure 14**

Introducing a small time synchronization error between the ILS signal and reference signal, the two signals will not overlap. The difference between the two signals will actually produce “phantom” bends caused by the aircraft movements instead of correcting for them, as shown in Figure 15.



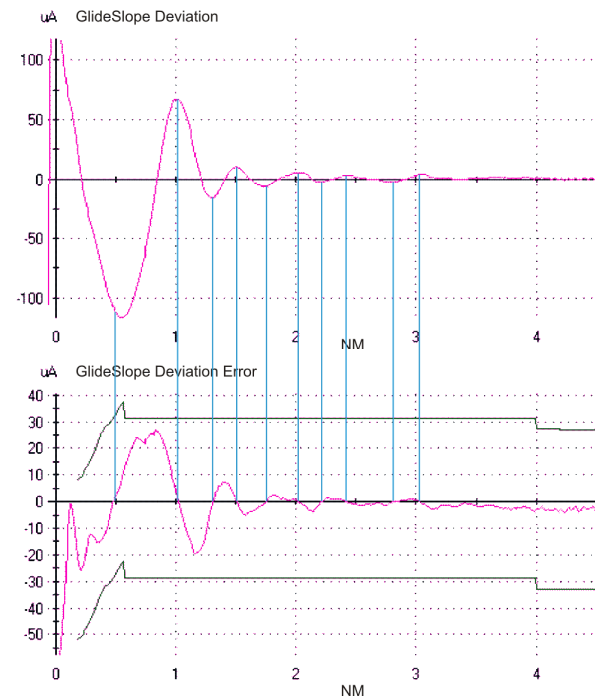
**Figure 15**

Fortunately, the bends caused by the combination of aircraft movements and time synchronization error between the raw ILS signal and the reference signal are easy to detect since it produce a very distinct bend pattern on the corrected ILS signal. As can be seen from Figure

15, the corrected ILS signal will pass through zero at the same time as the uncorrected (raw) ILS signal has a maximum or very close to a maximum. This happens of course at the points where the raw ILS signal and the reference signal have the same value, which will always be close to a maximum value when there is a small time synchronization error between the two signals.

A real recording from an approach flight on a Glide Path illustrating this is shown in Figure 16. In this example, the flight inspection aircraft flew auto coupled. By inspecting the bend patterns on the corrected ILS signal, it is obvious that the largest bends are not real bends on the ILS signal, since the bend frequency decreases as the aircraft approaches the runway. On the other side, the raw ILS signal follows a pattern that is typical for an auto coupled aircraft that doesn't manage to follow the ILS signal due to turbulence.

As can be seen, the maxima on the raw ILS signal coincide with zeros on the corrected ILS signal, the typical foot-print for a time synchronization problem between the reference signal and the ILS signal.



**Figure 16**

For this type of flight inspection problem there is probably not an easy cure. It could be a calibration issue with the flight inspection equipment, but more probably it is a built-in problem that must be solved by the manufacturer of the equipment.

## BEING INTOLERANT OF TOLERANCES

**Abstract-**The US flight inspection manual, specifically FAA Order 8200.1, is replete with the term tolerances. Almost every section has a listing titled “tolerances”. Interestingly, though, Section 1 of the Appendix 1 containing a glossary does not include a definition of the term tolerance.

Presumably then one can assume that the writers believe that we all know precisely what is meant by the term tolerance. As a try for a definition, let us define tolerance as a bound in quantitative terms that is applied to numerical values derived from observations of system performance. Beyond this bound or tolerance the system is considered unacceptable for the prospective user. This is very neat. Once the numerical values for performance are produced, then even a school boy can make a determination as to whether the system is acceptable and presumably safe for the user by referring to published tolerances. The astute reader will readily point to the importance of having the right tolerance value published. The term right must be couched in terms of flight safety. Right implies that a safe operation with the system will be consistently possible.

This paper addresses the establishment of tolerances. History seems to point to several items related to tolerances. First, many tolerance values have been in place for decades usually having been established long before the involvement of those concerned with flight inspection today. Records apparently have not been kept or have been lost concerning the rationale for specifying the tolerance values. We have been comfortable in using numbers from the past, probably sometimes the results of committee votes, because they have resulted in safe operations. In particular speaking in terms of ILS operations we have not had an aircraft accident in nearly sixty five years due to a system being at or near tolerance limits. On the other hand, we have accidents due to facilities being unavailable because tolerances could not be met. The author’s 1994 IFIS paper titled “The Exigency of the Aviator” serves as background.

We seem to be very willing to accept published tolerance values no matter the basis for determining the values. The contention presented in this paper is that we should be intolerant of tolerances that have been in existence for decades. Today we have means for identifying appropriate, precise tolerances, tolerances that can be justified based not only on good experience, but also, on computer simulations and on motion-based, sophisticated flight simulators. We need to provide maximum facility availability for maximum safety. Motivation should come, too, from economics by satisfying only needed values of system parameters. We don’t need to chase million dollar microamperes we have found occupying our time in the past. Identifying the optimum tolerances to protect the flight and provide maximum availability ought to be made a serious goal for the flight inspection community.

## INTRODUUCTION

The term tolerance has many facets according to Webster, however, the one of interest for this paper is “TOLERANCE -, the allowable deviation from a standard”. One does not have to search far to find standards for flight inspection in the FAA Order 8200.1 or ICAO Doc 8071, for example, Along with the standards there are specified allowable deviations called tolerances. Workers have most always bowed in respect to published tolerances. The title of this paper may seem to imply some heresy, but in reality its purpose is fundamentally to increase flight safety.

The assertion is made that absence of a guidance signal can be more dangerous than one just outside of published tolerance limits. This brings up the term HMI, i.e., hazardous misleading information. It is very important to protect absolutely against providing the pilot with HMI. It is generally known that there are but a very few times when HMI exists and the monitor does not shut down the facility.

For example, for many years after image glide slopes were well established facility shut-downs were common due to the image ground plane being disturbed by snow cover covering the ground. Field monitors located some 250 feet in front of the transmitting antenna mast receive the radiated signals but with vastly different grazing (incident) angles. The ground-reflected signal for the monitor has a greater grazing angle than the signal received at the aircraft in flight. The fact is significant because the difference in angles makes a difference in observed angles of the glide path. As a result

After careful study the monitor signals were found to be uncorrelated with those received by the aircraft. These field monitors were replaced by integral monitor coupled to the antennas and visual observations by maintenance technicians. My facility outages have been prevented with no HMI found.

Monitors are typically linear in character meaning that the monitor tracks deviation from a standard in unit by unit terms compared to what the aircraft sees. Creating alerts as the monitor progresses towards its alarm limit is probably good; however it would be good to have a study and reports of this

behavior of the monitor in saving outages. Again, remembering that one of the most unsafe conditions is to have the facility off the air.

## THE LAWYER

Once an accident occurs it is highly probable that a lawyer or lawyers will enter the scene because if there is a fault in the operation, design, performance of maintenance personnel, it is likely that a suit will be filed against the government (the FAA). The government with its deep pockets is always a good target for litigation. The discovery phase of the litigation has a good chance of uncovering any deficiencies. The very conservative nature of the operation and monitoring tends to make it very difficult for lawyers to find significant defects and win cases. In fact history shows there is no known cause of an accident with ILS operations that has allowed a judicial decision in favor of a claimant.

The reader may ask why raise the issue of tolerances if they have been so protecting. And preventing of losses in court cases. The answer is that lives have been lost because of systems being absent when executive monitors have removed the system from service all the while the signal in space is perfectly satisfactory. {Re: Exigency of the Aviator}. This is presently a penalty we pay for having monitors that are not representative.

Fortunately lawyers are not schooled and experienced in navigation technology to allow them to challenge the deficiencies in monitor design and operation. We as engineers in the field of air navigation can point to needs to make the monitoring more representative. Over the past decades changes have been made by the government to make monitoring of VOR, glide slopes, and localizers more representative. An example of this is the removal of the near-field monitors from the ground plane in front of the antenna mast.

The establishing of tolerance values is very important. They, in effect, place a bound around the standard value. When dealing with a navigation signal in space this bound or tolerance is well documented in the flight inspection manuals. Unfortunately for the purpose of this paper and other uses we do not have documentation on the rationale that went into establishing the quantitative values of the tolerances. Because the course structures that are acceptable and having heard that they may have come from committee votes in the early years of aviation, the suggestion is made that motion-based

flight simulators now be used to validate the values for current tolerance values of the navigation aids.

It may be instructive to consider a syllogism and some deductive reasoning. For example, assume, the proposition all A is B. This can be represented pictorially with a circle A inside of a circle B. B then becomes a necessary condition for the proposition to be true. The converse statement is not true.

For application to flight inspection let A be “Safety standards are met”. Let B equal flight inspection tolerances are met and A equal flight safety is achieved. It is true that flight inspection tolerances must be met but the converse, if flight safety conditions are met, the flight inspection tolerances will be met. This points to the illustrative geometries and the desirability of the two circles being congruent. The greater the disparity between the two circles, the greater the probability of your having conditions where the system has resulted in the facility being removed from service due to the executive monitor.

## THE AVIONICS

The avionics on board an aircraft are certified to meet particular requirements for guidance accuracy under various conditions. These requirements are derived from RTCA Minimum Operating Performance Specification (MOPS); These performance requirements are derived from the ground equipment specifications and the airspace protection surfaces to ensure safe flight.

Typically flight inspection performs a validation of certain parameters which consist of received signal level, modulation levels and guidance accuracy. The guidance accuracy is the most critical parameter to ensure safety. In many cases, a flight inspect system measures many parameters; which are bound by tolerance limits and have no bearing on the critical component as guidance accuracy. For example; there are tight tolerances on the FM modulation limit for Doppler VORs even though the variation in this parameter does not degrade the guidance accuracy. In recent years, many countries have relaxed this tolerance. Multipath from objects close to a DVOR can cause significant variation in this parameter but does not translate to bearing error.

## CONCLUSIONS AND REOMENDATIONS

We should continue to be intolerant of lack of perfection in monitoring of air navigation electromagnetic signals because lives can be lost, in particular due to navigation facilities being sometimes removed from service when they are needed most.

Consider redesign of systems with the tolerances bounds being established with the aid of motion-based, modern flight simulators.

Allow for greater congruence of the illustrative, circular geometries discussed in this paper.

## REFERENCES

McFarland. R. H., “The Exigency of the Aviator”, Paper presented at the 8<sup>th</sup> International Flight Inspection Symposium, Denver, CO ,June 7, 1994.

McFarland, R. H., “Initial Assessment of Appropriateness of Quantitative Tolerance Values used to Qualify Glide Slope Structures,” Technical Memorandum G-3, Avionics Engineering Center, Ohio University Athens, OH, July 1984.

Richard H. McFarland, Ph.D., P.E., ATP  
Dr. Michael Braasch,  
David Quinet  
Avionics Engineering Center  
Ohio University  
Athens, Ohio

